ANALYSES OF ARTICULAR CARTILAGE-DERIVED STEM CELLS:

IDENTIFICATION OF CELLULAR MARKERS FOR STEM CELLS WITHIN THE HEALTHY AND OSTEOARTHRITIC KNEE ARTICULAR CARTILAGE

A thesis submitted to Cardiff University for the degree of Doctor of Philosophy

Christopher Fellows B.Sc. (Hons.)

Cardiff School of Biosciences,
Sir Martin Evans Building,
Cardiff University

October 2014

Declaration

This work has not been submitted in substance for any other degree or award at this or any other university or place of learning, nor is being submitted concurrently in candidature for any degree or other award.

Signed …….. (candidate) Date ……..

STATEMENT 1

This thesis is being submitted in partial fulfilment of the requirements for the degree of PhD.

Signed …….. (candidate) Date ……..

STATEMENT 2

This thesis is the result of my own independent work/investigation, except where otherwise stated.
Other sources are acknowledged by explicit references. The views expressed are my own.

Signed …….. (candidate) Date ……..

STATEMENT 3

I hereby give consent for my thesis, if accepted, to be available for photocopying and for inter-library loan, and for the title and summary to be made available to outside organisations.

Signed …….. (candidate) Date ……..

STATEMENT 4: PREVIOUSLY APPROVED BAR ON ACCESS

I hereby give consent for my thesis, if accepted, to be available for photocopying and for inter-library loans **after expiry of a bar on access previously approved by the Academic Standards & Quality Committee.**

Signed …….. (candidate) Date ……..

Abstract

Previous studies have identified stem cell populations in articular cartilage using colony forming assays and mesenchymal stem cell (MSC) marker expression. The specificity of classical MSC markers for isolation of stem cells within articular cartilage is insufficient, with large and highly variable quantities being reported in the literature. This study has demonstrated, for the first time, a panel of stem cell markers specific for articular cartilage-derived stem cells (ACSC).

ACSCs were isolated, quantified and cultured from healthy and OA joints. Stem cells were clonally-derived cell lines that proliferated beyond 50 population doublings whilst maintaining a phenotype, and demonstrated tri-lineage potential. We discovered that OA cartilage had a two-fold increase in stem cell number, consisting of two divergent stem cell sub-populations. These divergent populations varied in proliferative capacity with only 50% of stem cells from the OA joint capable of extended proliferation *in vitro*.

Using transcriptomic next generation sequencing of culture-expanded chondrocytes and ACSCs we successfully identified differentially expressed genes and a panel of novel markers of cartilage-specific stem cells. Novel markers were validated using qPCR and protein labelling and, were specifically expressed in ACSCs, with no expression in the culture-expanded full-depth chondrocytes. Using immunofluorescence for novel stem cell markers we found articular cartilage-derived stem cells are localised within the transitional zone in normal cartilage and the superficial zone in OA cartilage. OA cartilage was found to contain a 2-fold increase in stem cells using immunofluorescence.

Subsequently, we used the panel of novel markers and fluorescent active cell sorting to isolate a sub-population from full-depth cartilage with stem cell characteristics. These cells were plastic adherent, clonogenic, with proliferative capacity greater than 50PD and displayed tri-lineage potential, therefore meeting all criteria for classification as a MSC population. The use of specific markers to isolate ACSCs will allow for further characterisation of stem cells, including a more in-depth understanding of the mechanisms of proliferation, differentiation and degeneration within articular cartilage.

Acknowledgements

I would like to thank my academic supervisors Professor Charles Archer and Associate Professor Ilyas Khan for their assistance, guidance and advice during the course of my PhD studies. Sincere appreciation is also due to all my friends and colleagues in Cardiff and Swansea Universities, in particular Dr Rebecca Williams, Dr Kristy Richardson, Dr Helen McCarthy, Dr Larissa Nelson, Dr Yadan Zhang and Mr Ben Morgan for their help and support over the years. Special gratitude to Dr Kirsty Richardson for her invaluable assistance with flow-cytometry, helping to make some of this work possible. Additional, thanks must also be given to Larissa Nelson for making the commute to Swansea bearable after the laboratory relocation.

I would also like to thank previous CTBL colleagues, whose skills and prior work built the foundation for my study. I would also like to thank all my friends both within, and outside of Cardiff University who helped, motivated and encouraged me throughout the course of my PhD. In particular, I would like to mention the support from Christopher Gwilliams, Laura Easter and Amie Doidge.

Finally, I would like to thank my family who have supported me throughout my studies and Juliette for her encouragement, support and patience during, what seemed like, endless hours of writing.

The Medical Research Council (MRC) funded this work.

Contents

DECLARATION ..... **II**

ABSTRACT ..... **III**

ACKNOWLEDGEMENTS ..... **IV**

CONTENTS ..... **V**

LIST OF FIGURES ..... **XI**

LIST OF TABLES ..... **XV**

ABBREVIATIONS ..... **XVII**

CHAPTER 1: **1**

GENERAL INTRODUCTION **1**

1.1 JOINTS **2**
1.1.1 SYNOVIAL JOINTS 3
1.1.1.1 Synovial joint development 4
1.1.1.2 Synovial joint maturation 8
1.2 ARTICULAR CARTILAGE **9**
1.2.1 PRENATAL ARTICULAR CARTILAGE FORMATION 10
1.2.2 ARTICULAR CARTILAGE MATURATION 13
1.2.3 ARTICULAR CARTILAGE HOMEOSTASIS 15
1.3 STRUCTURE OF ARTICULAR CARTILAGE **15**
1.3.1 ZONES OF ARTICULAR CARTILAGE 16
1.3.1.1 Superficial zone 18
1.3.1.2 Middle zone 18
1.3.1.3 Deep zone 19
1.3.1.4 Calcified zone 19
1.3.2 EXTRACELLULAR MATRIX REGIONS 19
1.3.2.1 Pericellular matrix 20
1.3.2.2 Territorial matrix 20
1.3.2.3 Interterritorial matrix 20
1.3.3 COMPOSITION OF ARTICULAR CARTILAGE 22
1.3.3.1 The chondrocyte 22
1.3.3.2 The cartilage collagens 23
1.3.3.2.1 Type I collagen 24
1.3.3.2.2 Type II collagen 24
1.3.3.2.3 Type III collagen 24
1.3.3.2.4 Type V collagen 25
1.3.3.2.5 Type VI collagen 25
1.3.3.2.6 Type IX collagen 25
1.3.3.2.7 Type X collagen 26
1.3.3.2.8 Type XI collagen 26
1.3.3.3 Cartilage proteoglycans 28
1.3.3.3.1 Hyaluronic acid 29
1.3.3.3.2 Aggrecan 29
1.3.3.3.3 Perlecan 30
1.3.3.3.4 Small leucine rich proteoglycans 30
Class I 30
Class II 31

1.3.3.3.5 Cells surface proteoglycans 31
1.3.3.3.6 Surface Zone protein 31
1.3.3.4 Other macromolecules 31
1.3.3.5 Interstitial fluid (water) 33
1.3.4 CARTILAGE MATRIX TURNOVER 33
1.3.5 CHONDROCYTE-MATRIX INTERACTIONS 33
1.4 DAMAGE AND DEGRADATION OF ARTICULAR CARTILAGE 35
1.4.1 AGE-RELATED CHANGES 35
1.4.2 INFLAMMATORY DAMAGE 36
1.5 OSTEOARTHRITIS 36
1.5.1 CLINICAL SIGNS OF OA 37
1.5.2 CARTILAGE CHANGES IN OA 38
1.5.3 METALLOPROTEINASES IN OA 39
1.5.4 OTHER TISSUES AFFECTED IN OA 39
1.5.5 MECHANISMS 41
1.6 REPAIR 41
1.6.1 SURGICAL INTERVENTIONS 41
1.6.1.1 Arthroscopic repair 41
1.6.1.2 Microfracture 42
1.6.1.3 Osteotomy 42
1.6.1.4 Osteochondral autograft transfer system (OATS) 42
1.6.1.5 Repair of articular cartilage using tissue engineering 43
1.6.1.5.1 Autologous chondrocyte implantation (ACI) 43
1.6.1.5.1.1 Scaffold-free repair 45
1.6.1.5.1.2 Scaffold matrix-assisted repair 45
1.7 STEM AND PROGENITOR CELLS 46
1.7.1.1 Induced pluripotent stem cells 47
1.7.2 MULTIPOTENT ADULT STEM CELLS 48
1.7.2.1 Mesenchymal stem cells (MSC) 50
1.8 RESIDENT MESENCHYMAL PROGENITOR CELLS IN SYNOVIAL JOINT TISSUES 51
1.9 STEM CELLS IN ARTICULAR CARTILAGE 52
1.9.1 CHONDROGENIC DIFFERENTIATION OF MSCS 53
1.9.2 STEM CELL DEFINITIONS WITHIN THIS THESIS 54
1.10 AIMS OF THIS THESIS 55
1.11 HYPOTHESIS 55

CHAPTER 2: 56

GENERAL METHODS 56

2.1 TISSUE ISOLATION 57
2.2 CELL ISOLATION AND CULTURE 57
2.2.1 PRONASE AND COLLAGENASE DIGESTION 57
2.3 SELECTION OF STEM CELLS 58
2.3.1 FIBRONECTIN ADHESION 58
2.3.2 COLONY ISOLATION 58
2.4 CULTURE MEDIA 58
2.4.1 MONOLAYER EXPANSION 58
2.4.2 POPULATION DOUBLINGS 59
2.5 COLONY FORMING EFFICIENCIES 59
2.6 DIFFERENTIATION 59
2.6.1 MEDIA 59
2.6.1.1 Chondrogenic 59
2.6.1.2 Osteogenic 60
2.6.1.3 Adipogenic 60
2.6.2 MONOLAYER 60
2.6.3 PELLET CULTURES 60

2.7 RNA EXTRACTION 61
2.7.1 RNA FROM CELLS 61
2.7.2 RNA FROM TISSUE 61
2.7.3 RNA FROM PELLETS 61
2.7.4 QIAGEN RNEASY KIT 61
2.7.5 ESTIMATION OF RNA QUANTIFICATION AND PURITY 62
2.8 COMPLEMENTARY DNA (CDNA) SYNTHESIS 62
2.9 POLYMERASE CHAIN REACTION (PCR) 62
2.10 AGAROSE GEL ELECTROPHORESIS 63
2.11 MOLECULAR CLONING 63
2.12 QUANTITATIVE POLYMERASE CHAIN REACTION (QPCR) 63
2.13 TISSUE PROCESSING 64
2.14 PELLET PROCESSING 64
2.15 TISSUE PROCESSING 64
2.16 PARAFFIN WAX SECTIONING 64
2.17 CRYOSECTIONING 65
2.18 IMMUNOFLUORESCENCE OPTIMISATION 65
2.19 ANTIGEN UNMASKING 66
2.20 IMMUNOSTAINING 66
2.20.1 IMMUNOCYTOCHEMISTRY 66
2.20.2 IMMUNOFLUORESCENCE 66
2.21 HISTOLOGY 67
2.21.1 ALCIAN BLUE 67
2.21.2 TOLUIDINE BLUE 67
2.21.3 SAFRANIN –O 68
2.21.4 ALIZARIN RED 68
2.21.5 VON KOSSA 68
2.21.6 OIL RED –O 68
2.21.7 CRYSTAL VIOLET 69
2.22 STATISTICS 69

CHAPTER 3: 70

WHOLE TRANSCRIPTOME NEXT GENERATION SEQUENCING OF CARTILAGE STEM CELLS 70

3.1 INTRODUCTION 71
3.2 METHODOLOGY 76
3.2.1 CELL ISOLATION AND CULTURE 77
3.2.2 RNA EXTRACTION AND PURIFICATION 77
3.2.3 NEXT GENERATION TRANSCRIPTOMIC SEQUENCING (NGS) 77
3.2.4 PIPELINE 78
3.2.5 SEQUENCE ALIGNMENT 79
3.2.5.1 'Tophat' alignment 79
3.2.5.2 'Cufflinks' alignment 79
3.2.6 NORMALISATION 79
3.2.7 'HTSEQ' – GENERATING TRANSCRIPT COUNTS 80
3.2.8 DIFFERENTIATION GENE EXPRESSION ANALYSIS 80
3.2.8.1 Gene count based methods 80
3.2.8.1.1 Negative binomial modals 80
3.2.8.1.1.1 'DESeq' 80
3.2.8.1.1.2 'edgeR' 81
3.2.8.1.2 Bayesian model 81
3.2.8.1.2.1 'Bayseq' 81
3.2.8.2 Transformation-based method 82
3.2.8.2.1 'Cuffdiff' 82
3.3 RESULTS 83

3.3.1 QUALITY AND NORMALISATION CONTROL 83
3.3.2 DIFFERENTIAL EXPRESSION 85
3.3.2.1 'DESeq' analysis 85
3.3.2.2 'edgeR' analysis 89
3.3.2.3 'Bayseq' analysis 96
3.3.2.4 'Cuffdiff' analysis 96
3.3.2.5 Comparative analysis 101
3.3.3 CANDIDATE STEM CELLS MARKERS 101
3.4 DISCUSSION 104
3.4.1 IDENTIFICATION OF POTENTIAL STEM CELL MARKERS 105
3.4.2 COMPARISON OF DIFFERENTIAL EXPRESSION METHODS 108
3.4.3 LIMITATIONS 110
3.4.4 CONCLUSIONS 111

CHAPTER 4: 112

AN IMMUNOHISTOCHEMICAL AND QUANTITATIVE ANALYSIS OF NOVEL STEM CELL MARKERS IN PRIMARY MONOLAYER CUTURES 112

4.1 INTRODUCTION 113
4.2 METHODOLOGY 115
4.2.1 CELL ISOLATION AND CULTURE 117
4.2.2 RNA EXTRACTION AND PURIFICATION 117
4.2.3 CDNA SYNTHESIS 117
4.2.4 QPCR ANALYSIS 117
4.2.5 IMMUNOCYTOCHEMISTRY 119
4.2.6 QUANTIFICATION OF POSITIVE LABELLING THROUGH IMMUNOCYTOCHEMISTRY 120
4.2.7 BROMODEOXYURIDINE LABELLING (BRDU) 121
4.2.8 PHENOTYPE PLASTICITY 121
4.2.9 HISTOLOGY 122
4.2.10 STATISTICS 122
4.3 RESULTS 123
4.3.1 PERCENTAGE STEM CELLS 123
4.3.2 PROLIFERATION ANALYSIS 123
4.3.3 PHENOTYPE PLASTICITY 125
4.3.3.1 Chondrogenic pellet differentiation 125
4.3.3.2 Osteogenic pellet differentiation 125
4.3.3.3 Adipogenic differentiation 126
4.3.4 IDENTIFICATION OF ACSC MARKERS 134
4.3.4.1 qPCR analysis 134
4.3.4.2 Immunocytochemical analyses of potential stem cell markers 143
4.4 DISCUSSION 153
4.4.1 CHARACTERISATION OF ACSC 153
4.4.2 CHARACTERISATION OF POTENTIAL STEM CELL MARKERS 158
4.4.3 CONCLUSIONS 162

CHAPTER 5: 163

GENE EXPRESSION ANALYSIS AND LOCALISATION OF NOVEL STEM CELL MARKERS IN NORMAL AND OSTEOARTHRITIC CARTILAGE 163

5.1 INTRODUCTION 164
5.2 METHODOLOGY 167
5.2.1 TISSUE PROCESSING 168
5.2.2 RNA EXTRACTION AND PURIFICATION 168
5.2.3 CDNA SYNTHESIS 168
5.2.4 QPCR ANALYSIS 168
5.2.5 IMMUNOFLUORESCENCE 169

5.2.6 QUANTIFICATION OF POSITIVE LABELLING IN TISSUE THROUGH IMMUNOFLUORESCENCE..170
5.2.7 STATISTICS....170
5.3 RESULTS....171
5.3.1 NESTIN....171
5.3.2 FRMD5....172
5.3.3 C11ORF41....172
5.3.4 EMBIGIN....173
5.3.5 EAAT1....173
5.3.6 OTHER MARKERS....174
5.4 DISCUSSION....194

CHAPTER 6:....197

FLUORESCENCE ACTIVATED CELL SORTING OF EMBIGIN AND FERM DOMAIN CONTAINING 5-POSITIVE CELLS – ISOLATION OF A SPECIFIC CHONDROCYTE SUB-POPULATION WITH STEM CELL PROPERTIES....197

6.1 INTRODUCTION....198
6.2 METHODOLOGY....201
6.2.1 CELL ISOLATION....GO OUTG203
6.2.2 ANTIBODY PURIFICATION AND CONJUGATION....203
6.2.3 FACS – DIRECTLY CONJUGATED ANTIBODIES....204
6.2.4 FLOW-CYTOMETRY ANALYSIS....204
6.2.5 CELL CULTURE....206
6.2.6 RNA EXTRACTION AND PURIFICATION....207
6.2.7 CDNA SYNTHESIS....207
6.2.8 QPCR ANALYSIS....207
6.2.9 IMMUNOCYTOCHEMISTRY....209
6.2.10 PHENOTYPIC PLASTICITY....209
6.2.11 PAPAIN DIGESTION....209
6.2.12 DMMB....210
6.2.13 HISTOLOGY....210
6.2.14 STATISTICS....210
6.3 RESULTS....211
6.3.1 FLOW-CYTOMETRY....211
6.3.2 PERCENTAGE COLONY FORMING CELLS....219
6.3.3 PROLIFERATION ANALYSIS....219
6.3.3.1 Immunocytochemical analyses of ACSC markers....222
6.3.3.2 qPCR analysis....229
6.3.4 PHENOTYPE PLASTICITY....234
6.3.4.1 Monolayer differentiation....234
6.3.4.1.1 Chondrogenic differentiation....234
6.3.4.1.2 Osteogenic differentiation....234
6.3.4.1.3 Adipogenic differentiation....234
6.3.4.2 3D-pellet culture differentiation....235
6.3.4.2.1 3D chondrogenic differentiation....235
6.3.4.2.2 Osteogenic differentiation....237
6.4 DISCUSSION....255
6.4.1 CHARACTERISATION OF FRMD5/EMBIGIN DUAL-POSITIVE CELLS....255
6.4.2 ACSC STEM CELL MARKER LABELLING IN FRMD5/EMBIGIN DUAL-POSITIVE CELLS....260

CHAPTER 7:....263

GENERAL DISCUSSION....263

7.1 GENERAL DISCUSSION....264
7.2 FUTURE WORK....268
7.3 CONCLUSION....270

CHAPTER 8: **271**

BIBLIOGRAPHY **271**

CHAPTER 9: **296**

APPENDICES **296**

List of Figures

CHAPTER 1

Figure 1.1: Classification of joints. 2
Figure 1.2: A schematic diagram of a synovial joint (knee). 4
Figure 1.3: Schematic diagram of endochondral ossification. 5
Figure 1.4: Normal human articular cartilage of the femur and tibia. 10
Figure 1.5: Diagram summarising the hypothesis for articular cartilage cellular lineage. 13
Figure 1.6: Human knee articular cartilage morphology. 16
Figure 1.7: Diagrammatic summary of the zonal macromolecular and cellular organisation of mature articular cartilage. 17
Figure 1.8: The organisation of normal articular cartilage matrix. 21
Figure 1.9: Collagen fibre formation. 27
Figure 1.10: Schematic representation of an Aggrecan aggregate. 30
Figure 1.11: Schematic diagram of the stages involved in ACI . 44
Figure 1.12: Alternate models of stem cells maintenance and differentiation. 47
Figure 1.13: The epigenetic landscape of reprogramming differentiated cells. 49
Figure 1.14: The transcriptional control of pluripotency 49
Figure 1.15: Schematic representation summarizing mesenchymal differentiation pathways 51

CHAPTER 2

Figure 2.1 – Labelled photograph of the human tibial plateaux excised from a total knee replacement 57

CHAPTER 3

Figure 3.1 – RNA-seq pipeline and workflow 78
Figure 3.2 – Representative images of normal and osteoarthritic cartilage and stem cell colonies. 84
Figure 3.3 – Histogram showing the distribution of p-values for differentially expressed genes. 86
Figure 3.4 – Scatter plot of changes in gene expression between full-depth chondrocytes (FD) and the average expression across all articular cartilage stem cells. 87
Figure 3.5 – Scatterplot of direct log fold-change (lfc) versus moderated log-ratios (mod_lfc). 88
Figure 3.6 – Heatmap of next generation sequencing (NGS) of normal and osteoarthritic cartilage cell lines. 90
Figure 3.7 – Venn diagram showing a comparison in differentially regulated genes between 'DESeq', 'edgeR', 'Bayseq' and 'Cuffdiff' 102

CHAPTER 4

Figure 4.1 – Percentage stem cells within healthy normal and osteoarthritic cartilage and growth kinetics of articular cartilage-derived cells lines. 127
Figure 4.2 – Number of day to reach 10, 20, 30 and 40 population doublings (PD) of articular cartilage-derived cell lines. 128
Figure 4.3 – Bromodeoxyuridine (BrdU) labelling of normal and osteoarthritic articular cartilage-derived stem cell lines. 129
Figure 4.4 – Donor age does not correlate with proliferative capacity of cartilage stem cells. 130
Figure 4.5 – Representative images of toluidine blue stained chondrogenic differentiated pellet cultures showing glycosaminoglycan accumulation. .131
Figure 4.6 – Representative images of Alizarin red(A,B,D,E,F) and Von Kossa (C,D,G,H) stained osteogenic differentiated pellet cultures, showing mineral deposits. 132
Figure 4.7 – Adipogenic differentiation of cartilage stem cells. 133
Figure 4.8 – Gene expression of novel cartilage stem cell specific genes in full-depth chondrocytes, normal cartilage-derived stem cells and osteoarthritic cartilage-derived stem cells. 137
Figure 4.9 – Gene expression of cartilage specific genes in full-depth chondrocytes, normal cartilage-derived stem cells and osteoarthritic cartilage-derived stem cells. 138
Figure 4.10 – Gene expression of the progenitor cell markers Notch-1 and Jagged-1 in full- depth chondrocytes, normal cartilage-derived stem cells and osteoarthritic cartilage-derived stem cells. 139
Figure 4.11 – Principal components analysis (PCA) of gene expression within full-depth chondrocytes, normal cartilage-derived stem cells and osteoarthritic cartilage-derived stem cells. 140
Figure 4.12 – Heatmap of gene expression within full-depth chondrocytes, normal cartilage-derived stem cells and osteoarthritic cartilage-derived stem cells. 141
Figure 4.13 –Scatter graphs showing correlations between proliferative capacity and stem cell marker gene expression in normal cartilage-derived and osteoarthritic cartilage-derived cartilage stem cells. 142
Figure 4.14 – Immunocytochemistry of NESTIN protein labelling within culture-expanded full-depth chondrocytes, normal cartilage-derived stem cells and osteoarthritic cartilage-derived stem cells. 145
Figure 4.15 –Immunocytochemistry of FRMD5 protein labelling within culture-expanded full-depth chondrocytes, normal cartilage-derived stem cells and osteoarthritic cartilage-derived stem cells. 146
Figure 4.16 –Immunocytochemistry of C11ORF41 protein labelling within culture-expanded full-depth chondrocytes, normal cartilage-derived stem cells and osteoarthritic cartilage-derived stem cells. 147
Figure 4.17 –Immunocytochemistry of EMBIGIN protein labelling within culture-expanded full-depth chondrocytes, normal cartilage-derived stem cells and osteoarthritic cartilage-derived stem cells. 148
Figure 4.18 –Immunocytochemistry of EAAT1 protein labelling within culture-expanded full-depth chondrocytes, normal cartilage-derived stem cells and osteoarthritic cartilage-derived stem cells. 149
Figure 4.19 –Bar graphs showing the percentage cells exhibiting positive antibody labelling for stem cell markers in culture-expanded normal and osteoarthritic cartilage-derived stem cells. 150

Figure 4.20 –Immunocytochemistry of stem cell marker protein labelling within human bone marrow stromal cells (mesenchymal stem cells) (MSCs). 151
Figure 4.21 – Immunocytochemistry of stem cell marker protein labelling within initial colonies of cartilage-derived stem cells. 152

CHAPTER 5

Figure 5.1– Gene expression of cartilage stem cell specific genes in normal and osteoarthritic tissue. 175
Figure 5.2–Immunofluorescence of NESTIN in normal articular cartilage 176
Figure 5.3–Immunofluorescence of NESTIN in OA articular cartilage 177
Figure 5.4–No primary control for NESTIN in normal articular cartilage 178
Figure 5.5–No primary control for NESTIN in OA articular cartilage 179
Figure 5.6–Immunofluorescence of FRMD5 in normal articular cartilage 180
Figure 5.7–Immunofluorescence of FRMD5 in OA articular cartilage 181
Figure 5.8–Immunofluorescence of C11ORF41 in normal articular cartilage 182
Figure 5.9–Immunofluorescence of C11ORF41 in OA articular cartilage 183
Figure 5.10– No primary antibody control for FRMD5 and C11ORF41 in normal articular cartilage 184
Figure 5.11– No primary antibody control for FRMD5 and C11ORF41 in OA articular cartilage 185
Figure 5.12– Immunofluorescence of EMBIGIN in normal articular cartilage....186
Figure 5.13– Immunofluorescence of EMBIGIN in OA articular cartilage 187
Figure 5.14– Immunofluorescence of EAAT1 in normal articular cartilage 188
Figure 5.15– Immunofluorescence of EAAT1 in OA articular cartilage 189
Figure 5.16– No primary control from EMBIGIN and EAAT1 in normal articular cartilage 190
Figure 5.17– No primary control from EMBIGIN and EAAT1 in OA articular cartilage 191
Figure 5.18– Percentage positively labelled cells within each zone of normal and OA articular cartilage.....193

CHAPTER 6

Figure 6. 1 – A schematic of conventional fluorescence activated cell-sorting (FACS) 200
Figure 6.2 – Fluorophore spectra 205
Figure 6.3 – Diagram illustrating gating and voltage adjustments 206
Figure 6.4 – Flow-cytometry analysis of normal sample 1 (CF01N) 212
Figure 6.5 – Flow-cytometry analysis of normal sample 2 (CF02N) 213
Figure 6.6 – Flow-cytometry analysis of normal sample 3 (CF03N) 214
Figure 6.7 – Flow-cytometry analysis of normal sample 4 (CF04N) 215
Figure 6.8 – Flow-cytometry analysis of OA sample 1 (CF01OA) 216
Figure 6.9 – Flow-cytometry analysis of OA sample 2 (CF02OA) 217
Figure 6.10 – Flow-cytometry analysis of OA sample 3 (CF03OA) 218
Figure 6.11 – Percentage dual-labelled and colony forming cells in normal and OA cartilage.....220
Figure 6.12 – Growth kinetics of dual FRDM5 and EMBIGIN-positive and dual FRDM5 and EMBIGIN-negative cells.....221
Figure 6.13 – Immunocytochemistry of NESTIN in FACS cells 224
Figure 6.14 – Immunocytochemistry of FRMD5 in FACS cells 225

Figure 6.15 – Immunocytochemistry of C11ORF41 in FACS cells 226
Figure 6.16 – Immunocytochemistry of EMBIGIN in FACS cells 227
Figure 6.17 – Immunocytochemistry of EAAT1 in FACS cells 228
Figure 6.18 – qPCR of stem cell markers in FAC sorted cells isolated from normal cartilage 231
Figure 6.19 – qPCR of stem cell markers in FAC sorted cells isolated from OA cartilage 232
Figure 6.20 – qPCR of Basigin, EMBIGIN and Monocarboxylate transporter (MCT) -1, -2, -3 and -4 in FAC sorted cells 233
Figure 6.21 – Monolayer chondrogenic differentiation of FACS cells. 239
Figure 6.22 – Monolayer osteogenic differentiation of FACS cells. 240
Figure 6.23 – Monolayer adipogenic differentiation of FACS cells 241
Figure 6.24 – PCR for adipogenic genes in adipogenic induced cultures. 242
Figure 6.25 – Three dimensional chondrogenic differentiation of FACS cells. 243
Figure 6.26 – Three dimensional chondrogenic differentiation of FAC sorted cells. 244
Figure 6. 27 – DMMB assay quantifying glycosaminoglycan (GAG) content of chondrogenic pellets 245
Figure 6.28 – qPCR for chondrogenic genes in 3D chondrogenic pellet culture differentiation of FACS cells from normal tissue 246
Figure 6.29 – qPCR for chondrogenic genes in 3D chondrogenic pellet culture differentiation of FACS cells from OA tissue. 247
Figure 6.30 – Immunofluorescence for Collagen Type II in 3D chondrogenic pellet culture differentiation of FACS cells. 248
Figure 6.31 – Immunofluorescence for Aggrecan in 3D chondrogenic pellet culture differentiation of FACS cells. 249
Figure 6.32 – qPCR for stem cell marker genes in 3D chondrogenic pellet culture differentiation of FACS cells from normal tissue 250
Figure 6.33 – qPCR for stem cell marker genes in 3D chondrogenic pellet culture differentiation of FACS cells from OA tissue. 251
Figure 6.34 – Three dimensional osteogenic differentiation of FAC sorted cells. 252
Figure 6.35 – qPCR for osteogenic genes in 3D chondrogenic pellet culture differentiation of FACS cells from normal tissue 253
Figure 6.36 – qPCR for osteogenic genes in 3D chondrogenic pellet culture differentiation of FAC sorted cells from normal tissue 254

APPENDICES

Figure S1.1 – NGS – Bio-analyser data 297
Figure S1.2 – qPCR melt curves 302
Figure S1.3 – qPCR standard curves 306

List of tables

CHAPTER 1

Table 1.1: Major collagens of articular cartilage. 27
Table 1.2: The molecular composition of glycosaminoglycans. 28
Table 1.3: Morphological changes in OA. 38

CHAPTER 3

Table 3.1 – Materials and suppliers 76
Table 3.2 – Table showing uniform expression of house-keeping genes in RNA-seq experiment. 85
Table 3.3 – The 50 most significantly up-regulated genes between full-depth differentiated chondrocytes and articular cartilage derived stem cells lines using 'DESeq' analysis. 91
Table 3.4 – The 50 most significantly down-regulated genes between full-depth differentiated chondrocytes and articular cartilage derived stem cell lines using 'DESeq'. 92
Table 3.5 – Gene expression of cartilaginous genes between full-depth differentiated chondrocytes and articular cartilage derived stem cells. 93
Table 3.6 – The 50 most significantly up-regulated genes between full-depth differentiated chondrocytes and articular cartilage derived stem cells lines using 'edgeR' analysis. 94
Table 3.7 – The 50 most significantly down-regulated genes between full-depth differentiated chondrocytes and articular cartilage derived stem cells lines using 'edgeR' analysis. 95
Table 3.8 – The 50 most significantly up-regulated genes between full-depth differentiated chondrocytes and articular cartilage derived stem cells lines using ''Bayseq' analysis. 97
Table 3.9 – The 50 most significantly down-regulated genes between full-depth differentiated chondrocytes and articular cartilage derived stem cells lines using ''Bayseq' analysis. 98
Table 3.10 – The 50 most significantly up-regulated genes between full-depth differentiated chondrocytes and articular cartilage derived stem cells lines using ''Cuffdiff' analysis. 99
Table 3.11 – The 50 most significantly down-regulated genes between full-depth differentiated chondrocytes and articular cartilage derived stem cells lines using ''Cuffdiff' analysis. 100
Table 3.12 – Comparison of expression levels of genes selected as potential stem cell markers or full-depth differentiated chondrocyte markers using 'DESeq', 'edgeR', 'Bayseq' and 'Cuffdiff'. 103

CHAPTER 4

Table 4.1– Materials and suppliers 116
Table 4.2 – NormFinder results and primer sequences for house-keeping genes. 118
Table 4.3 – Primer sequences and annealing temperature for primers used in this study. 119

Table 4.4 – Primary antibody optimal concentrations. 120
Table 4.5 – Secondary antibody optimal concentrations. 120

CHAPTER 5

Table 5.1 – Materials and suppliers 167
Table 5.2– NormFinder results and primer sequences for house-keeping genes. 169

CHAPTER 6

Table 6.1 – Materials and suppliers 202
Table 6.2 – Table showing conjugated antibodies used in flow-cytometry experiments 204
Table 6.3 – NormFinder results and primer sequences for house-keeping genes. 208
Table 6.4 – Primer sequences and annealing temperature for primers used in this study. 208

APPENDICES

Table S1.1 – qPCR efficiency and R^2 values 307

Abbreviations

AC	Articular cartilage
ACI	Autologous chondrocyte implantation
ACSC	Articular cartilage-derived stem cell
ACT	Autologous chondrocyte transplantation
ADAMTS	A disintegrin and metalloproteinase domain with thrombospondin motifs
BMP	Bone morphogenetic protein
BMSC	Bone marrow-derived stromal cell
BrdU	Bromodeoxyuridine
BSA	Bovine serum albumin
C11ORF41	Chromosome 11 open reading frame 41
CD	Cluster of differentiation
CD29	beta 1 integrin
CD44	Hyaluronan receptor
CD49e	alpha 5 integrin (fibronectin receptor, alpha polypeptide)
CD51	Integrin alpha V
CD73	Ecto-5'-nucleotidase
CD90	Thy-1 (thymocyte differentiation antigen-1)
CD105	Endoglin
CD106	Vascular cell adhesion protein 1 (VCAM-1)
CD117	c-kit
CD166	activated cell adhesion molecule (ALCAM)
CDU	Collagen digestion units
COMP	Cartilage oligomeric matrix protein
CS	Chondroitin sulphate
DAPI	4',6-Diamidino-2-phenylindole
DAPT	N-[N-(3,5-difluorophenacetyl)-1-alanyl]-S-phenylglycine t-butyl ester
DEX	Dexamethasone
DMEM	Dulbecco's modified Eagle's medium
DMMB	Dimethyl methylene blue
DMSO	Dimethyl sulfoxide
dNTP	Deoxyribonucleotide triphosphate
DS	Dermatan sulphate
DTT	DL-Dithiothreitol
DZ	Deep zone
EAAT1	Excitatory amino acid transporter 1 (GLAST, SLC1A3)
ECM	Extracellular matrix
EDTA	Ethylenediaminetetraacetic acid
EGF	Epidermal growth factor
ERCC	External RNA Controls Consortium
ES	Embryonic stem cell
ETOH	Ethanol

FACIT	Fibril-associated collagen with an interrupted triple helix
FACS	Fluorescent activated cell sorting
FBS	Foetal bovine serum
FD	Full-depth chondrocytes
FGF	Fibroblast growth factor
FRMD5	FERM domain containing 5
GAGs	Glycosaminoglycans
GDF	Growth and differentiation factor
GTF	Gene transfer file
HA	Hyaluronic acid
HIF-2α	Hypoxia inducible factor-2α
HS	Heparan sulphate
HSC	Hematopoietic stem cells
IGF	Insulin-like growth factor
IgSF	Immunoglobulin superfamily
IL-1	Interleukin-1
Ihh	Indian hedgehog
iPSC	Induced pluripotent stem cell
ITS	Insulin-transferrin-selenium
KIF26B	Kinesin family member 28B
KS	Keratan sulphate
LB	Luria broth
MACI	Matrix-assisted autologous chondrocyte implantation
MCT	Monocarboxylate transporter
MFI	Mean fluorescence intensity
MMP	Matrix metalloproteinase
MRI	Magnetic resonance imaging
MSCs	Mesenchymal stem cells
MZ	Mid zone
NB	Negative binomial
NBFS	Neutral buffered formal saline
NF-kB	Nuclear factor kappo B
N-SC	Normal cartilage-derived stem cell
OA	Osteoarthritis
OA-SC	OA cartilage-derived stem cell
OCP	Osteochondral plug
PBS	Phosphate buffered saline
PBST	PBS containing tween 20 (polyethylenesorbitan monolaurate)
PCNA	Proliferation cell nuclear antigen
PCR	Polymerase chain reaction
PD	Population doubling
PFA	Paraformaldehyde
PRDM1	PR domain zinc finger protein 1 (BLIMP-1)
PTHrP	Parathyroid hormone-related peptide

qPCR	Quantitative polymerase chain reaction
RA	Rheumatoid arthritis
ROS	Reactive oxygen species
RPKM	Reads *per* kilobase of exon model *per* million mapped reads
RT-PCR	Reverse transcriptase polymerase chain reaction
SB	Subchondral bone
SD	Standard deviation
SEM	Standard error of the mean
SLRP	Small leucine-rich proteoglycan family
SLC1A3	Solute carrier family 1 (glial high-affinity glutamate transporter), member 3 (EAAT1, GLAST)
SOC	Super optimal with catabolite repression
ST6GAL2	ST6 beta-galactosamide alpha-2,6-sialyltranferase 2
SZ	Superficial zone
SZP	Surface zone protein
TBE	Tris Borate EDTA
TGF-β	Transforming growth factor–β
TIMP	Tissue inhibitors of metalloproteinases
TMEM132B	Transmembrane protein 132B
TNF-α	Tumor necrosis factor–α
TP	Tibial plateau
TRI	Trizol
VCAM-1	Vascular cell adhesion protein–1
X-Gal	5-bromo-4-chloro-3-indolyl- β -D-galactopyranoside

CHAPTER 1:

GENERAL INTRODUCTION

1.1 Joints

A joint or articulation is the structure formed when two or more parts of the skeleton intersect. There are several types of joints within the body, with two major methods of classification (Figure 1.1). Joints can be classified based on their structure and their function (Wooley et al., 2005). The structural classification is based on the presence or absence of a synovial cavity between the articulating bones. Fibrous joints have no synovial cavity; bones are held together by fibrous, collagenous connective tissue. Cartilaginous joints also have no synovial cavity, bones are held together by cartilage tissue. Finally, synovial joints are enclosed within a fibrous capsule with opposing bones lined with cartilage, separated by a cavity and connected by ligaments. Joints are categorized into functional classes dependent on their degree of movement. Synarthroses are immovable joints, ampiarthoses are marginally movable joints and diarthoses joints are capable of free-movement (Tortora and Grabowski, 1996). Examples of synarthroses include the skull and the epiphyseal joints of developing long bones. Examples of ampiarthoses include the joints of the cervical and lumbar vertebrae and the tibiofibular joint. Diathroses joints include the joints of the shoulder, elbow and knee (Gray, 1989).

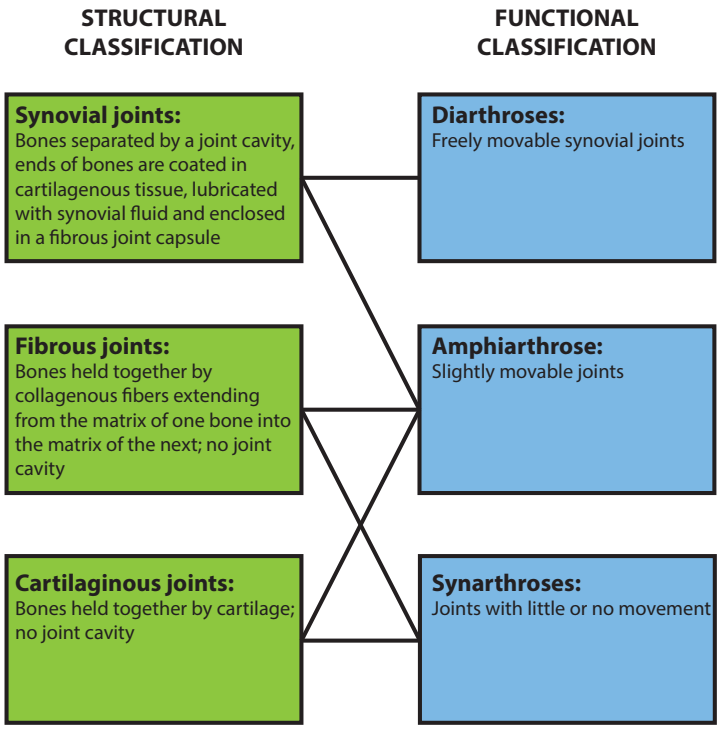


Figure 1.1: Classification of joints.

1.1.1 Synovial Joints

Synovial joints account for most of the body's articulations and are evolutionarily the most advanced joint. Synovial joints allow for efficient force transfer, have low friction surfaces, and shock absorption capacity which consequently provides the capacity for the high-level of mobility seen in vertebrates (Wooley et al., 2005). The structure of healthy synovial joints enables high tensile forces to be absorbed whilst providing a low frictional coefficient, permitting smooth, pain-free movement. During normal daily activity the synovial joint undergoes approximately 5,000 loading cycles and endures over 10^8 loading cycles in an 80-year lifespan. Even during simple daily activities, such as walking, the mechanical forces endured are several times higher than body weight. Joint forces within the human knee have been shown to range from 1.2 to 7.2 times body-weight, with synovial joints able to endure loads of up to ten times the body weight without failure (Neu et al., 2009).

The synovial joint can be viewed as on organ as it comprises many different tissues including bone, meniscus, ligament, synovium, hyaline cartilage (that is commonly referred to as articular cartilage), and the fibrous joint capsule (Figure 1.2). The size and range of movement of the synovial joint varies throughout the body (Tortora and Grabowski, 1996, Martini, 2006). The articulating bone surfaces are usually rounded, occasionally flattened cancellous bone, encapsulated within a thin covering of dense cortical bone forming the subchondral bone plate. A thin layer of articular cartilage, with an intermediate layer of calcified cartilage coats the subchondral bone. Below the subchondral bone plate lies cancellous bone. In adults, this contains the bone marrow and, in children, it represents the most distal segment of the epiphysis (Wooley et al., 2005). The articular cartilage is a specialized tissue providing a smooth, low friction and resilient connective tissue that serves as the weight-bearing and gliding surface required to mediate normal function and painless movement of synovial joints (Buckwalter and Hunziker, 1999). The synovial joint has a tissue space called the joint cavity enclosed by a fibrous capsule that is continuous with the periosteum and links the articulating bones enclosed in the cavity. The joint capsule also integrates ligaments, meniscus and synovium and the structure is stabilised by muscles and tendons. The synovial membrane that secretes

synovial fluid lines the inner surface of the joint capsule. Synovial fluid is essential for nutrition, lubrication and shock absorption (Martini, 2006).

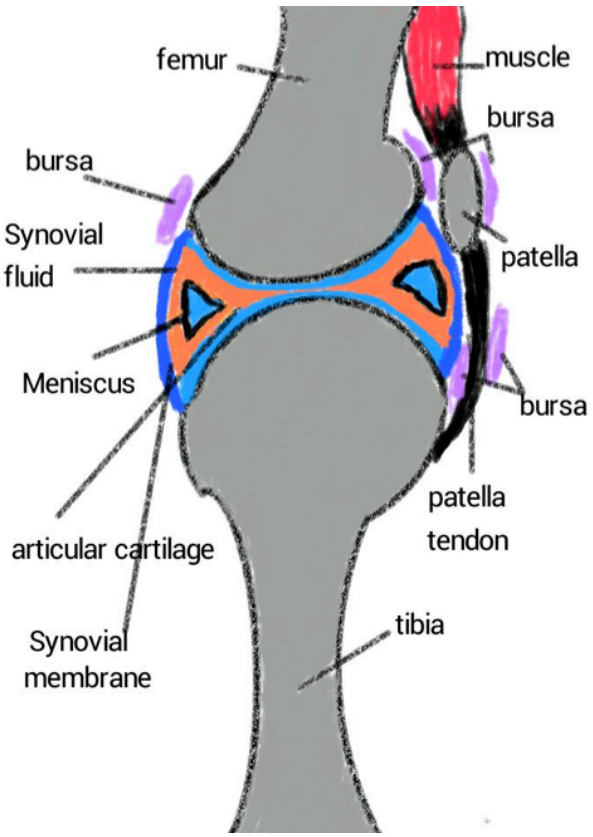


Figure 1.2: A schematic diagram of a synovial joint (knee).

Articular cartilage covers the ends of opposing bones.

1.1.1.1 Synovial joint development

During embryonic growth, cartilage and bone development are closely related and interconnected. Bones can form through two mechanisms, intramembranous ossification and endochondral ossification. Intramembranous ossification forms the bones of the skull by direct osteoblast differentiation from mesenchymal stem cells. The long bone of the synovial joints are formed by endochondral ossification of condensations of mesenchymal cells at specified sites mediated by cell adhesion molecules and matrix receptors (Archer et al., 2003). The mesenchymal condensations differentiate into chondrocytes, which secrete cartilage extracellular matrix proteins forming a template for bone formation composed of hyaline cartilage. The cartilaginous template subsequently undergoes a process of endochondral ossification, there is migration of cells first into the centre and secondly at either end establishing the primary metaphyseal

and, secondary epiphyseal, centres of ossification. The chondrocytes stop expressing Collagen Type II, switching to secrete Collagen Type I and Type X and become hypertrophic. These centres of ossification gradually replace the cartilage with mineralized bone, driven by osteoblasts and osteoclasts, ultimately replacing the entire template except for the articular surfaces (Figure 1.3) (Mackie et al., 2008, Kronenberg, 2003). Growth of bones during endochondral ossification is co-ordinated by a cartilaginous growth plate. The growth-plate comprises of four zones, resting cartilage, proliferating cartilage, maturing cartilage and calcified cartilage (Kronenberg, 2003). The steroid hormone oestrogen induces VEGF; oestrogen combined with the androgens increases the growth of the long bones by inducing increased expression of growth factors such as insulin-like growth factor (IGF).

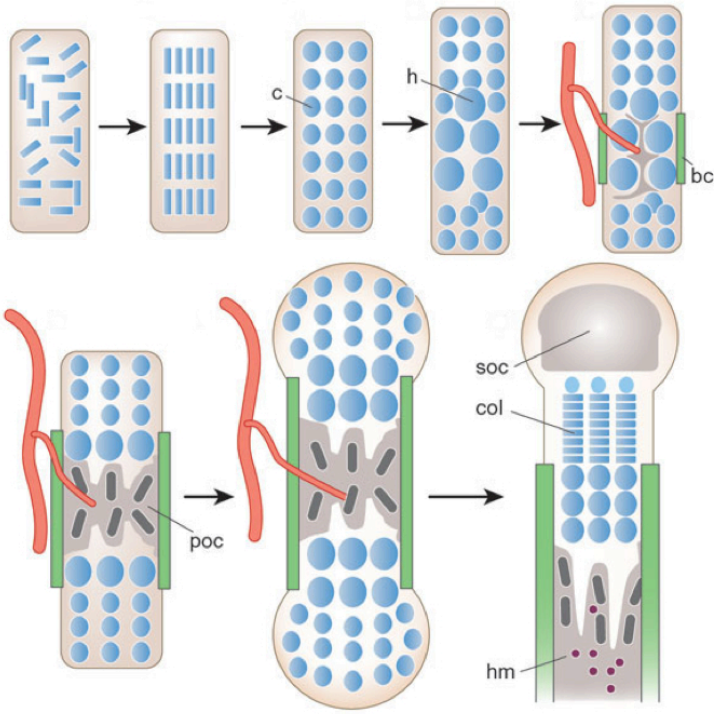


Figure 1.3: Schematic diagram of endochondral ossification.

Mesenchymal cells condense and differentiate to form rounded chondrocytes (c) and the cartilaginous template. The chondrocytes, at the centre of the template cease proliferating and become hypertrophic (h). Perichondrial cells become osteoblasts, migrate and form the bone collar (bc). Hypertrophic chondrocytes direct the formation of mineralized matrix, attract blood vessels, and undergo apoptosis. Osteoblasts form in the primary centre of ossification (poc). Chondrocytes continue to proliferate, lengthening the bone. At the end of the bone, the secondary ossification centre (soc) forms. The growth-plate is established below the secondary centre of ossification in orderly columns of proliferating chondrocytes (col). Haematopoietic marrow (hm) develops in the marrow cavity along with stromal cells. Adapted from (Kronenberg, 2003).

Initially, in the creation of the joint of opposing long bones, the mesenchymal condensation develops as a continuous structure with uninterrupted cartilaginous template tissue spanning across the future joint location (Craig et al., 1987, Pacifici et al., 2005). The majority of cells within these condensations commit to the growth-plate epiphyseal chondrocyte fate; however, at prospective joint locations sub-populations of cells differentiate to adopt an articular phenotype (Dy et al., 2010). The developing joint is first recognised histologically by a densely packed flattening of cells in the presumptive joint region. These cells lose type II collagen expression and acquire type I collagen expression, the region becomes non-cartilaginous and is defined as the interzone (Archer et al., 2003, Archer et al., 1994, Craig et al., 1987, Khan et al., 2007). The formation of the interzone and joint specification is a secondary segmentation event (Khan et al., 2007), with the tissues of the joint to be derived from the interzone (Mitrovic, 1977). The mechanisms that determine the joint site are species-dependent. In the chick embryo, a distinct three layered structure forms, comprising two chondrogenous layers separated by flattened cells (Craig et al., 1987). In mammalian embryos, a thin flattened layer of 2-3 cell layers forms (Edwards et al., 1994). As the interzone thickens, the external mesenchyme starts to form the joint capsule, tendons, ligaments and the intermediate layer of the interzone develops joint associated structures such as the synovial membrane and meniscus. The outer cell layer of the interzone proliferates and differentiates into chondrocytes that go on to form the articular surfaces of the synovial joint. Appositional growth of the chondrocytes at each of the epiphyses contributes to the growth of the articular surface (Khan et al., 2007, Wooley et al., 2005).

Discoveries over the last decade have demonstrated that several signalling pathways work to specify the fate of joint cells. Positioning and patterning of limbs involve cellular interactions between the mesenchymal limb bud core and the surrounding ectoderm (Khan et al., 2007). This process is controlled by three main signalling centres, which drive patterned limb growth along each of the proximal-distal, anterior-posterior and dorsal-ventral axes (Niswander, 2002). Transforming growth factor beta (TGF-β) signalling, mainly triggered by the TGF-β2 receptor, act upstream of canonical Wnt/beta-catenin signalling initiated by Wnt9a (formally Wnt14), Wnt4 and Wnt6 (Seo and Serra, 2007, Spagnoli et

al., 2007). TGF-β signalling subsequently activates expression of growth differentiation factor-5 (GDF-5) a member of the transforming growth factor-β (TGF-β) family, that functions in the specification of synovial joints (Settle et al., 2003, Storm and Kingsley, 1999). It has been shown that TGF-β is essential and without the TGF-β signalling pathway, the interzone fails to form and joint cavitation is inhibited (Spagnoli et al., 2007). Formation of the interzone is prompted by the down-regulation of the chondrogenic transcription factor SOX-9 combined with specific expression of GDF-5 (Archer et al., 2003). Mutations in the GDF-5 gene have been shown to cause skeletal abnormalities (Francis-West et al., 1999, Storm and Kingsley, 1999). It is thought that GDF-5 does not directly specify the joint; Wnt9a has been shown as a key synovial developmental factor that acts to induce GDF-5 expression (Khan et al., 2007). Homeodomain-containing transcription factors (Hox genes) have been shown to be critical for the specification and patterning of vertebrate embryo, with mutations causing numerous developmental abnormalities (Pacifici et al., 2005).

Joint morphogenesis follows the formation of the joint interzones; this process comprises joint cavitation and differentiation into articular components. In humans cavitation occurs after around week 8 of development, separating the two opposing cartilaginous elements (Wooley et al., 2005). The mechanism of cavitation is not conclusively known; it is thought that skeletal movement, hyaluronan secretion, and shifts in extracellular matrix composition all contribute to inducing joint cavitation (Dowthwaite et al., 2003). Cavitation occurs through the differential synthesis and secretion of glycosaminoglycans (GAGs), in particular, hyaluronan (HA) by the cells of the chondrogenic layer in both chicken and human joints (Archer, 1994, Edwards et al., 1994, Pitsillides et al., 1999, Pitsillides, 1999). Although the initiation of cavitation is not dependent on motion, formation of the synovial cavity appears to depend on mechanical input (Dowthwaite et al., 1999, Pitsillides et al., 1999). Paralysis of the embryo results in the failure to cavitate or fusion of previously cavitated joints. It has also been shown that Notch and TGF-β signalling specify and initiate differentiation of articular chondrocytes, with insulin-like growth factor 1 (IGF1) promoting chondrogenesis through stimulation of matrix secretion (Hardingham et al., 2006, Serra and Chang, 2003). Basic fibroblast growth factor (bFGF) promotes proliferation of chondrocytes; proliferation prevents terminal differentiation to

hypertrophic cells. *SOX-9,* the master chondrogenic transcription factor is initially expressed in the mesenchymal condensation; expression is essential for conversion of these cells into chondrocytes and expression is critical at every stage of chondrocyte differentiation (Kronenberg, 2003, Hayes et al., 2001). *SOX-9* stimulates transcription of a number of cartilage matrix genes, including *COL2A1*, *COL11A2* and *ACAN*. *SOX-5* and *SOX-6* have been shown to define the fate and ensure proper differentiation of chondrocytes in both growth-plate and articular cartilage. It is thought that they most likely work in combination with *SOX-9* (Dy et al., 2010). The homeobox family protein barx-1, Wnt-4, GDF-5, hepatocyte growth factor (HGF) and parathyroid hormone-related peptide (PTHrP) all act to stop the articular chondrocytes from ossifying.

1.1.1.2 Synovial joint maturation

During skeletal growth, bones grow by the process of endochondral ossification; proliferation, matrix production, hypertrophy and mineralization of the epiphyseal growth-plate occurs. The thin layer of cartilage entrapped between the epiphyseal and metaphyseal bone contains immature cells at the proximal epiphysis in a region called the resting zone, more mature chondrocytes are present below the resting zone in the proliferating zone and, large chondrocytes are found in the hypertrophic zone adjacent to this. During childhood, the growth-plate matures, its size decreases and, eventually, at the end of puberty, is completely replaced by bone, thus, ceasing longitudinal growth (Emons et al., 2011).

There are many proposed mechanisms for growth-plate fusion; it has been shown that numerous growth factors and hormones are key mediators of this maturation process. Bone morphogenetic proteins (BMPs), FGF and Wnt proteins engage in autocrine and paracrine signalling between the perichondral cells and epiphyseal chondrocytes that are thought to be essential in the temporal control and progression of growth-plate maturation (Emons et al., 2011). Paracrine feedback signalling of PTHrP and Indian hedgehog (ihh) regulate longitudinal growth through chondrocyte proliferation, endochondral ossification and osteoblast differentiation. It has been shown that mutations in the ihh gene causes premature fusion of the epiphyseal plate in humans and

over-expression of PTHrP in mice delays growth-plate closure and results in an abrupt closure (Chiang et al., 1996, Hellemans et al., 2003, Jobert et al., 1998). Vascular endothelial growth factor (VEGF) and vitamin D levels increase with puberty and are also thought to be important in the growth-plate fusion. Currently, there are four accepted hypotheses for the mechanism of fusion; the most widely accepted is apoptosis of hypertrophic chondrocytes, the others comprise of autophagy, trans-differentiation of chondrocytes into osteoblasts and hypoxia-induced necrosis (Emons et al., 2011). After skeletal epiphyseal growth-plate fusion, the only cartilaginous tissue remaining is the articular cartilage at the ends of the bones, hence its designation as permanent cartilage.

1.2 Articular cartilage

Within the adult, there are three main types of cartilage: fibrocartilage, elastic cartilage and hyaline cartilage. Fibrocartilage is located at the enthesis attachment sites between tendon, ligaments and bone. The collagen fibres of fibrocartilage form thick bundles comprising predominately Collagen Type I (Benjamin and Ralphs, 1998). Elastic cartilage has a matrix that contains a high proportion of elastin fibres, it can be found at the outer ear, eustachian tube and epiglottis. The most frequent cartilage found in the body is hyaline cartilage, of which the tracheal rings are comprised, along with the ventral surfaces of the ribs and the ends of bones. (Martini, 2006).

Articular cartilage is a thin layer of hyaline cartilage that covers the surface of bones of diarthrodial joints. Articular cartilage is an avascular and aneural tissue, it is smooth, glassy and white in appearance, with the avascular nature preventing pain or bleeding if the surface is penetrated (Figure 1.4) (Benjamin, 1999). It is a highly organised and specialised tissue capable of free articulation, painless movement and transmission of force through the skeleton. Compared to other tissues, articular cartilage has a low rate of metabolic activity (Pearle et al., 2005). The tissue is maintained by a single specialised cell, the chondrocyte (Buckwalter and Hunziker, 1999). Articular cartilage comprises a highly organised matrix with a large matrix to cell volume ratio, the basic structure is composed of a 3D collagen scaffold and proteoglycans (Jeffery et al., 1991). The arrangement, direction and location of these collagen fibrils vary, along with the

cell density, matrix composition and overall thickness throughout the tissue, providing different mechanical properties across the joint. The different arrangements and properties are divided into 4 zones; the superficial (tangential), transitional, radial and calcified zones (Eyre, 2002). The physical and biochemical differences between the zones are important to allow the cartilage to resist both extrinsic and intrinsic forces due mechanical stress, and swelling in the proteoglycans-rich areas (Knudson and Knudson, 2001). Cartilage tissue contains a large proportion of water (65-80% by wet weight). Chondrocytes comprise approximately 5%-10% of the tissues total volume, collagens form 10-30%, whilst proteoglycans and other molecules consist of 5-10% of the tissues wet weight (Archer et al., 2003, Bhosale and Richardson, 2008, Eyre, 2002, Hunziker et al., 2007). The depth of articular cartilage remains for the most part unchanged throughout adult life, allowing normal joint function for around 80 years. Articular cartilage does, however, exhibit an inadequate ability to undergo self-repair. Traumatic injuries and tears to cartilage can result in degradation and degenerative conditions such as osteoarthritis (OA).

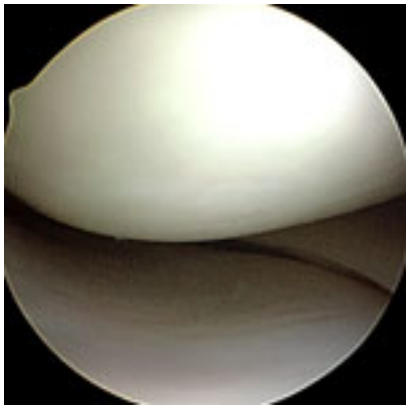


Figure 1.4: Normal human articular cartilage of the femur and tibia.

Arthroscopy of a healthy human knee: hyaline cartilage and the fibrocartilagenous meniscus between the articulating surfaces can be seen (Struh, 2013).

1.2.1 Prenatal articular cartilage formation

The mechanisms specifying which mesenchymal cells differentiate into articular cartilage and resist endochondral ossification are not fully understood (Pacifici et al., 1999).

It is believed phenotype stability is partially achieved through intrinsic signalling within the extracellular environment of cells in articular cartilage. Work by multiple groups has aimed to elucidate the roles of extracellular macromolecules in joint development (Koyama et al., 1995, Pacifici, 1995, Pacifici et al., 1993). The ECM macromolecule tenascin-C and one of its cell surface receptors syndecan-3 were identified to have a role in developing synovial joints, specifically within articular cartilage (Pacifici et al., 1999). This work was supported by previous developmental studies by Chiquet and colleagues who identified tenascin-C as a factor involved in joint development of the chick embryo. Within the synovial joint, they showed an enrichment within the interzone, forming the boundary which leads to the creation of the opposing skeletal bones (Chiquet-Ehrismann et al., 1988). Exogenous tenascin-C expression has also been found to stimulate prechondrogenic mesenchymal cells in *in vitro* micromass cultures to undergo chondrogenic differentiation and maintain a rounded cell shape (Mackie et al., 1987). As the limb develops and separation of the skeletal elements occurs, tenascin-C levels increase, especially in the epiphyses, forming a barrier (Pacifici, 1995). Within the chick embryo, by day 18 of incubation, tenascin-C is strongly expressed, localization is restricted to the articular chondrocytes of the epiphysis and is not found in the growth-plate. Tenascin-C maintains the chondrogenic phenotype through interactions with cell surface receptors (including syndecan) and decreases the proliferative ability by maintaining the rounded shape of the cells (Pacifici et al., 1999). Syndecan-3 may have a role in regulating chondrocyte proliferation. Early in development of the chick embryo, syndecan-3 is strongly expressed by dividing perichondral cells around the diaphysis and epiphysis with tenascin-C expression low (Koyama et al., 1995, Siczkowski and Watt, 1990).

There are two proliferative bands within immature articular cartilage; one below the articular surface and one located above the secondary centre of ossification. Mankin showed through tritiated thymidine incorporation in immature rabbit knees that immature cartilage grows by both apposition from the articular surface and interstitial growth from the band above the subchondral bone (Mankin, 1962b, Mankin, 1963, Mankin, 1962a). A study by Archer et al., (1994) in the marsupial (*Monodelphis domestica*) showed cellular proliferation by antibody labelling of the proliferating cell nuclear antigen (PCNA). Proliferating

cells during early development were initially extensive in the epiphyses; however, once the secondary centre of ossification had formed, the distribution was restricted to the surface of articular cartilage, becoming increasingly restricted to the surface layers of articular cartilage with maturity, indicative of appositional growth. The proliferative cells of the surface of articular cartilage were also shown to have an increased expression of IGF, and other growth factors and receptors, implying this is a potentially important signalling centre (Archer, 1994). A further study within the immature joint of the South American opossum utilised bromodeoxyuridine (BrdU) to identify cycling cells. BrdU is incorporated into replicating DNA during S-phase of the cell cycle but blocks proliferation after incorporation. This study identified a slow cycling cell population within the superficial zone of immature cartilage. The flattened cells of the superficial zone incorporated BrdU after 10 days compared with 4 days for the cells of the transitional zone. The long cycling time of the superficial zone cells was characteristic of a progenitor or stem cell population while the faster cycling time of the transitional zone cells could imply a transit amplifying population (Figure 1.5) (Hayes et al., 2001).

Hayes and colleagues have shown that members of the Notch signalling pathway are expressed in the surface of immature mouse articular cartilage. This family of signalling molecules and receptors are able to regulate cell fate decisions and are involved in regulating the elongation of the growth-plate and ossification (Hayes et al., 2001). Dowthwaite et al., showed a sub-population of chondrocytes in immature bovine articular surface that expressed Notch-1, and potentially contained a progenitor population. Their work suggests that Notch-1 signalling acts to control proliferation in cartilage; inhibition of Notch-1 signalling using N-[N-(3,5-difluorophenacetyl)-1-alanyl]-S-phenylglycine t-butyl ester (DAPT) prevented the formation of colonies by the cartilage progenitor cells (Dowthwaite et al., 2004).

In the late embryo, the immature articular cartilage chondrocytes are rounded in shape and randomly arranged throughout the tissue. The mitotic activity is low and the tissue is relatively more cellular compared to mature tissue (Howlett, 1979, Takechi and Itakura, 1995).

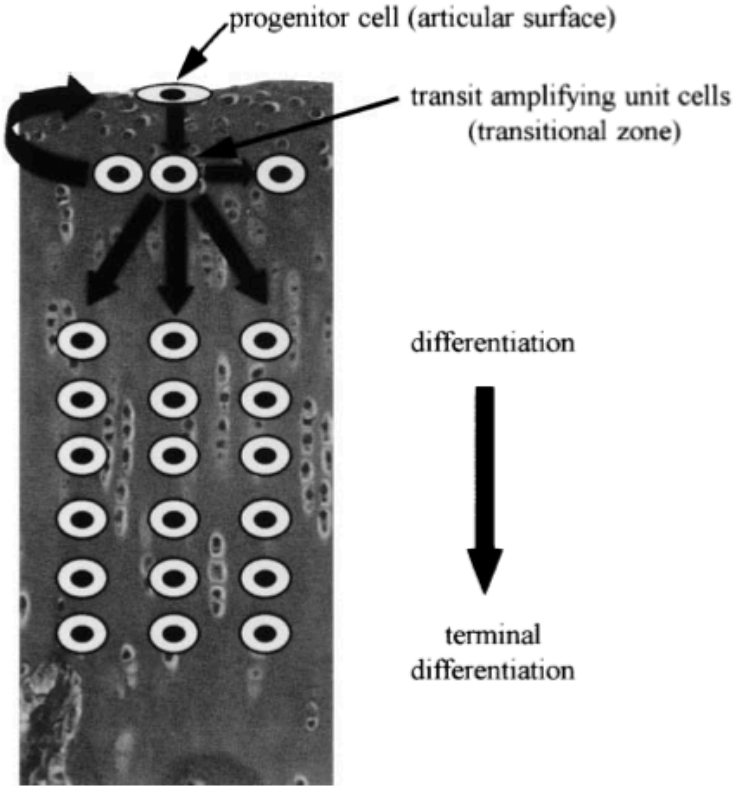


Figure 1.5: Diagram summarising the hypothesis for articular cartilage cellular lineage.

Progenitor cells in the articular surface divide asymmetrically to give two daughter cells, one being another progenitor cell and the second being a transit-amplifying cell within the transitional zone. The transit-amplifying cell can then undergo further cell divisions along the chondrocyte differentiation pathway. Adapted from (Hayes et al., 2001).

1.2.2 Articular cartilage maturation

At birth articular cartilage is relatively unstructured; the density of chondrocytes is high, with the cells distributed randomly throughout the full-depth of the tissue. The time-span for the maturation process varies with species from around 4 months in the rabbit, 18 months in the horse to 15-18 years in the human (Hunziker et al., 2007, Khan et al., 2011). In a series of developmental transitions leading to adulthood, articular cartilage undergoes significant structural, compositional, and morphologic changes in response to the biomechanical demands placed on the tissue (Williams et al., 2008). In the months following birth, the articular cartilage reduces in thickness, develops its distinct zonal stratification and the high matrix to cell volume (Lotz and Loeser, 2012). Chondrocytes become arranged in 4 layers: a thin superficial zone with flattened cells, a transitional layer with rounded cells, a thicker deep layer where

chondrocytes are aligned in columns, and a calcified zone, that interdigitates between the hyaline cartilage and the subchondral bone plate. The arrangement, direction and types of collagen fibrils start to vary through the zonal structure of the maturing tissue. Morphologic changes of maturation occur concurrently with the reorganisation of the collagen network. This leads to alignment of chondrocytes in the longitudinal plane of collagen fibrils (Benninghoff, 1925) as cited in (Khan et al., 2011). Furthermore, the extracellular matrix (ECM) is organized into pericellular, territorial, and interterritorial matrices, each of which has specific biochemical and biomechanical functions (Guilak et al., 2006).

The reorganisation of articular cartilage during maturation has been investigated using the immature rabbit knee joint. One month postnatal, the superficial zone cells were arranged perpendicular to the joint surface with disorganisation within the deeper layers and the collagen fibrils randomly arranged. By two months, cell density decreases and the cells appear more anisotropic. At three months, the cellular organisation is comparable to mature tissue, the depth of the tissue has decreased 50% and the collagen scaffold is arranged in an arcade-like manner (Hunziker, 2009, Hunziker et al., 2007). The widely accepted hypothesis for the mechanism of cartilage maturation is a gradual process of resorption from the lower zones and appositional growth from the surface of the tissue. This growth is thought to be directed by tissue-specific stem cells situated within niches in the tissue (Dowthwaite et al., 2004). However, until recently the metabolic and biochemical stimuli that induce these progressive changes have not been fully identified and many remain elusive.

Studies by Khan et al. (2011, 2013) have shown that a combination of FGF-2 and TGF-β1 induces profound morphologic changes in immature articular cartilage, consistent with a highly accelerated maturational response. Growth factor stimulation induced apoptosis and resorption from the basal aspect and cellular proliferation in the surface chondrocytes. The tissue dramatically reduces in thickness, the total percentage of water is reduced to that of mature tissue and, the dry weight increases to become identical to a mature articular cartilage. The total collagen content is increased as a proportion of the dry weight, with the collagen network being remodelled, manifested by the formation of mature covalent cross-links, leading to increased mechanical stiffness and the formation of pericellular matrix around chondrocytes. The production of keratan sulphate

containing proteoglycans increases, which is characteristic of the mature tissue (Khan et al., 2011, Khan et al., 2013). This result indicates that FGF and TGF signalling pathways may be key mediators of postnatal cartilage maturation.

1.2.3 Articular cartilage homeostasis

Adult articular cartilage chondrocytes are considered post-mitotic; they have a low metabolic activity, maintaining the ECM by low-rate turnover of certain matrix proteins (Goldring and Marcu, 2009). Cartilage was traditionally thought of as an inert tissue, however, it is now known to respond to extrinsic factors that regulate gene expression and protein synthesis within the chondrocytes. The balance between catabolism and anabolism of the ECM maintains the healthy cartilage structure; deregulation in either of these processes can lead to degeneration. Several studies have used a range of approaches both *in vivo* and *in vitro* to examine the effect of moderate exercise and loading in maintaining cartilage homeostasis (Bader et al., 2011, Goldring and Marcu, 2009). These studies have confirmed that articular chondrocytes are able to directly respond to mechanical stimuli by release of cytokines, chemokines and growth and differentiation factors that cause structural changes in the surrounding matrix. It has also been shown that both overloading and immobilization of articular cartilage both lead to degradation of cartilage, loss of ECM components and cell death (Jeffrey et al., 1995, Kim et al., 1996, Palmoski et al., 1979). The mechanical stimuli imposed on the joint are essential in ensuring equilibrium within the tissue, maintaining normal homeostasis. Dynamic compression is thought to be required to increase matrix synthesis and to maintain healthy joint activity (Bader et al., 2011). During ageing and disease, there is a deregulation and the equilibrium is disrupted, the rate of loss of ECM both collagen and proteoglycan exceeds the rate of deposition of newly synthesized molecules (Goldring and Marcu, 2009).

1.3 Structure of articular cartilage

The structure of articular cartilage varies with the depth from the surface in terms of ECM composition, organisation and mechanical properties, as well as cell morphology and function (Bhosale and Richardson, 2008, Buckwalter et al.,

1988). This variation with depth leads to the distinct zonal stratification characteristic of the mature articular cartilage (Figure 1.6). The structure and mechanics of each zone has been shown to vary between species, and between different synovial joints of the same species (Smyth et al., 2012). The morphology of articular tissue is affected by age and pathology, thus altering the structure leading to decomposition.

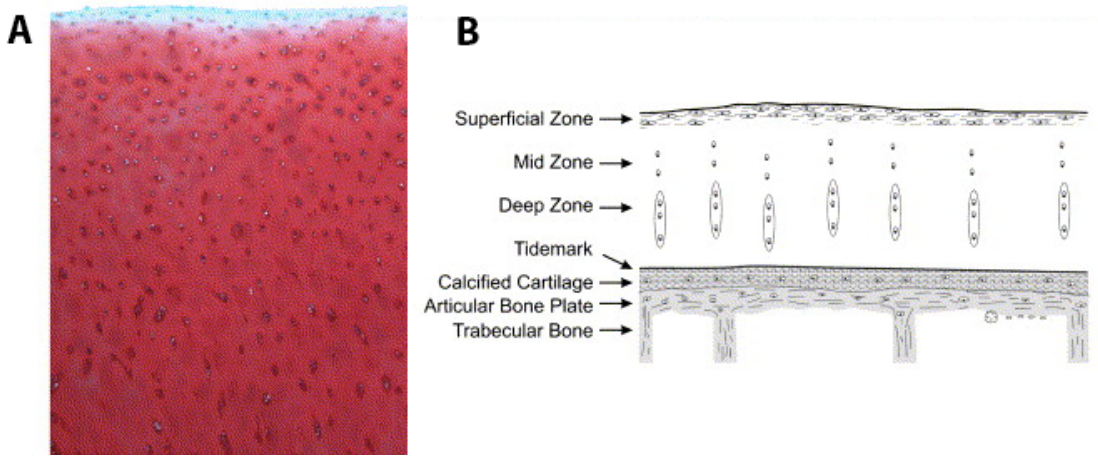


Figure 1.6: Human knee articular cartilage morphology.

A) Normal articular cartilage stained with safranin-O and fast green. The surface is smooth with flattened cells, the intermediate and radial zones have rounded cells are arranged in columns. **B)** Schematic diagram of the cellular arrangement in the zones of articular cartilage. Adapted from (Pritzker et al., 2006).

1.3.1 Zones of articular cartilage

As previously mentioned, mature articular cartilage is segregated into 4 pseudo-stratified zones. The shape and arrangement of the chondrocytes differ within these four regions, as does the composition and organisation of collagens and other glycosaminoglycans (GAGs) (Figure 1.7). Approximately 10 – 20% of the cartilage thickness comprises the superficial zone, 60% of the cartilage thickness is the middle zone and, the deep zone constitutes 30% (Bhosale and Richardson, 2008). The superficial zone has flattened chondrocytes and the collagen fibrils run parallel to the apical surface of the cartilage. The collagen content is high, around 85% of the dry mass and this allows cartilage to withstand sheer forces and prevents excessive water from leaving the tissue under compression. The collagen content decreases with increasing tissue depth. (Hunziker et al., 2007), (Eyre, 2002). The deep zone has the least collagen, the fibrils are varied in size

and vary in orientation but with the tendency to be arranged perpendicular to the apical surface (Eyre et al., 2006). The transitional and radial zones (mid and deep zones) act like a 'sponge' and are able to expand and swell with the intake of water; this allows forces to be spread evenly over the cartilage when it is compressed. The chondrocytes have a more spherical shaped in appearance and are arranged in distinct columns within the deep zone. The middle zone acts as an intermediate between the superficial and deep zones with the oblique collagen fibres randomly orientated and with rounded chondrocytes (Jeffery et al., 1991). The calcified zone is a mineralized matrix; it acts as an interface between the cartilage and bone (Eyre, 2002). There are no distinct boundaries between the upper three zones with the morphological changes occurring gradually and through development.

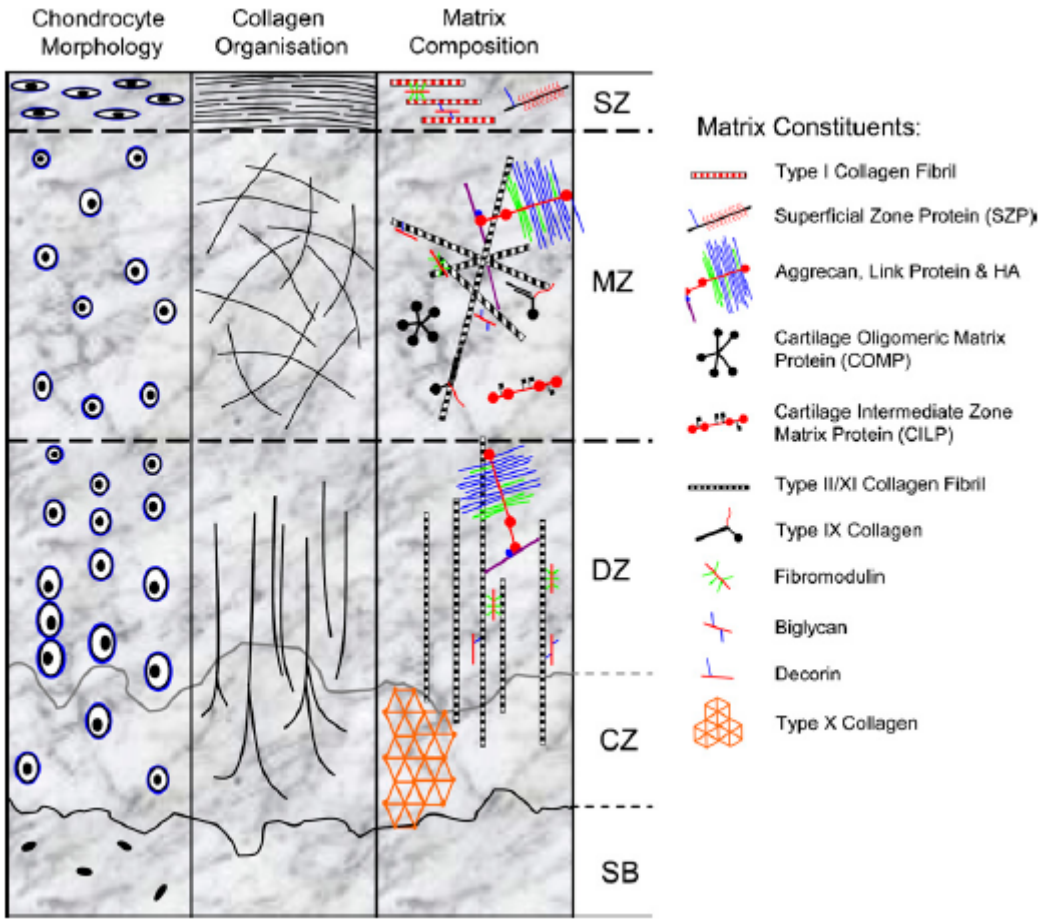


Figure 1.7: Diagrammatic summary of the zonal macromolecular and cellular organisation of mature articular cartilage.

Articular cartilage contains 4 zones: superficial (SZ); middle (MZ), deep (DZ), and a zone of calcified cartilage matrix (CZ) sitting above the subchondral bone (SB). Each zone has a distinctive cellular morphology, collagen fibril organisation and molecular composition of its extracellular matrix (ECM) (Hayes et al., 2007).

1.3.1.1 Superficial zone

The superficial, surface or tangential zone is adjacent to the joint cavity. It comprises two regions, an acellular region and a deeper cellular layer (Wu et al., 2008). An overlying matrix known as the lamina splendens is thought to be a fibrous membrane-like structure, acting as a barrier to enzymes and large molecules such as hyaluronic acid (HA), while allowing small molecules such as glucose to permeate into cartilage. It is a few microns thick and merges gradually into the middle zone; however, work has suggested that this barrier-like structure was just an artefact observed in phase-contrast microscopy (Aspden and Hukins, 1979, Martin et al., 1998). The superficial zone is the thinnest zone, the structure and composition gives this region specialised mechanical resistance to sheer stress. The cells are flattened and elliptical in shape, arranged so that their major axes are parallel to the articular surface. The matrix contains the highest collagen content of the zones with a low proteoglycan concentration. There is also increased fibronectin and surface zone protein (lubricin) and HA content in this zone which, together lubricate and protect the surface (Flannery et al., 1999, Nishida et al., 1995). The parallel arrangement of collagen fibrils in the superficial zone provides the region with a high tensile stiffness and strength, to resist shearing forces. The dense collagen network also regulates the movement of molecules in and out of the cartilage (Eyre, 2002, Eyre et al., 2006). Disruption in this zone alters the forces exerted on the lower zones of the tissue and contributes to the onset of osteoarthritis.

1.3.1.2 Middle zone

The middle zone or transitional zone of articular cartilage is located between the superficial and deep zones, with an intermediary tissue morphology and matrix composition. As previously mentioned, this is the largest region of the cartilage occupying approximately 60% of the tissue. The chondrocytes in this zone are rounded in shape and equally spaced, occurring singularly or in doublets (Hunziker, 2010). Mid zone chondrocytes have a higher concentration of synthetic organelles, endoplasmic reticulum and Golgi complex membranes than the superficial zone chondrocytes. The proteoglycan (PG) content is higher than the superficial zone but the water and collagen concentrations are lower when compared. Collagen fibrils in the middle zone have a larger diameter relative to

the fibrils of the superficial zone and are arranged randomly as shown by polarised light microscopy of pico-sirius red stained sections (Buckwalter and Hunziker, 1999).

1.3.1.3 Deep zone

The deep or radial zone contains large circular shaped cells arranged into columns aligned perpendicular to the joint surface. This pattern is maintained by the collagen fibre organisation and there is a gradual increase in cell size with depth. In the upper regions of the deep zone, chondrocytes are rich in organelles such as endoplasmic reticulum and Golgi apparatus. The cells in the deeper regions are commonly arranged in groups of three to four within a single chondron as chondrocyte columns (Hunziker, 2010). The diameter of the collagen fibrils is largest in this region, in an arrangement perpendicular to the joint surface, that penetrate into the calcified cartilage beneath (Eyre, 2002). The deep zone has the highest concentration of PGs and the lowest concentration of water (Buckwalter and Mankin, 1997).

1.3.1.4 Calcified zone

The calcified zone is the region that separates the non-calcified cartilage from the subchondral bone. The chondrocytes are smaller, rounded and fewer in abundance than the zones above. This region has a lower metabolic rate, therefore, containing smaller amounts of endoplasmic reticulum and Golgi apparatus (Morrison et al., 1996). The calcified cartilage/subchondral bone interface is known as the osteochondral junction. During postnatal growth of the skeletal bones, this zone advances and the matrix compartment becomes actively mineralised and ossifies.

1.3.2 Extracellular matrix regions

The ECM within articular cartilage can be divided into various histological regions depending on their distance from the cell. The pericellular matrix is localised immediately around the cell, a distinct territorial matrix surrounds the pericellular matrix and farthest from the cell is the interterritorial matrix (Figure 1.8). Each matrix zone is characterized by different distributions and densities of matrix constituents (García-Carvajal et al., 2013). These matrices protect the

cells from damage during loading and deformation of the tissue. The principal function of the interterritorial matrix is to provide mechanical support for the tissue (Buckwalter and Hunziker, 1999, Hunziker, 2010).

1.3.2.1 Pericellular matrix

The pericellular matrix is a region surrounding chondrocytes in articular cartilage where signalling molecules such as growth factors interact with the receptors expressed on the membrane cell of chondrocyte. It is approximately 1μm thick region rich in proteoglycans such as aggrecan, hyaluronan and decorin, with a network of thin fibrils of fibronectin and type VI and type IX collagen (García-Carvajal et al., 2013). The term chondron is used to define the chondrocyte and its surrounding pericellular matrix, this matrix is free of fibrillar collagens, but rich in PGs and non-fibrillar collagens that form a fine meshwork (Poole et al., 1992). The pericellular matrix shields the cells from damage during loading and deformation of the tissue, the chondron forms a unit able to absorb load and provide protection for the chondrocyte (Buckwalter and Hunziker, 1999, Poole et al., 1987). Collagen Type VI is thought to aid the chondrocytes in attachment to the macromolecular framework of rest of the matrix (García-Carvajal et al., 2013).

1.3.2.2 Territorial matrix

The territorial matrix, like the pericellular matrix contains type VI collagen microfibrils but little or no fibrillar collagen (García-Carvajal et al., 2013). Collagen fibrils that form a basket-like arrangement, enveloping individual pairs or, in the deep zone, whole chondron clusters of chondrocytes and their pericellular matrices (Hunziker, 2010). The thin collagen fibrils of the territorial matrix adhere to the pericellular matrix, giving this basket-like arrangement. The function of this matrix is similar to the pericellular matrix and, may provide mechanical protection for the chondrocytes during loading and deformation of the tissue (Buckwalter and Hunziker, 1999).

1.3.2.3 Interterritorial matrix

The interterritorial matrix constitutes the main bulk of the extracellular space. This matrix is composed of Collagen Type II, Collagen Type XI and Collagen Type

IX containing a non-collagenous domain, permitting association with other matrix components and retention of proteoglycans. These collagens exhibit a marked increase in fibril diameter and give the cartilage structure, tensile stiffness and strength (García-Carvajal et al., 2013). There is a high concentration of proteoglycans, with the concentration of PGs in the interfibrillar space between the collagens varying with cartilage zone. The interterritorial matrix collagen fibrils do not surround the chondrocyte; instead the interterritorial matrix contains fibrils and fibril bundles with the arrangement and orientation varying with the zone of articular cartilage (Buckwalter and Hunziker, 1999). The collagen orientation is initially perpendicular to the surface within the deep zone, and transition becoming more oblique until, in the superficial zone, the fibrils orientate parallel to the joint surface (Eyre et al., 2006).

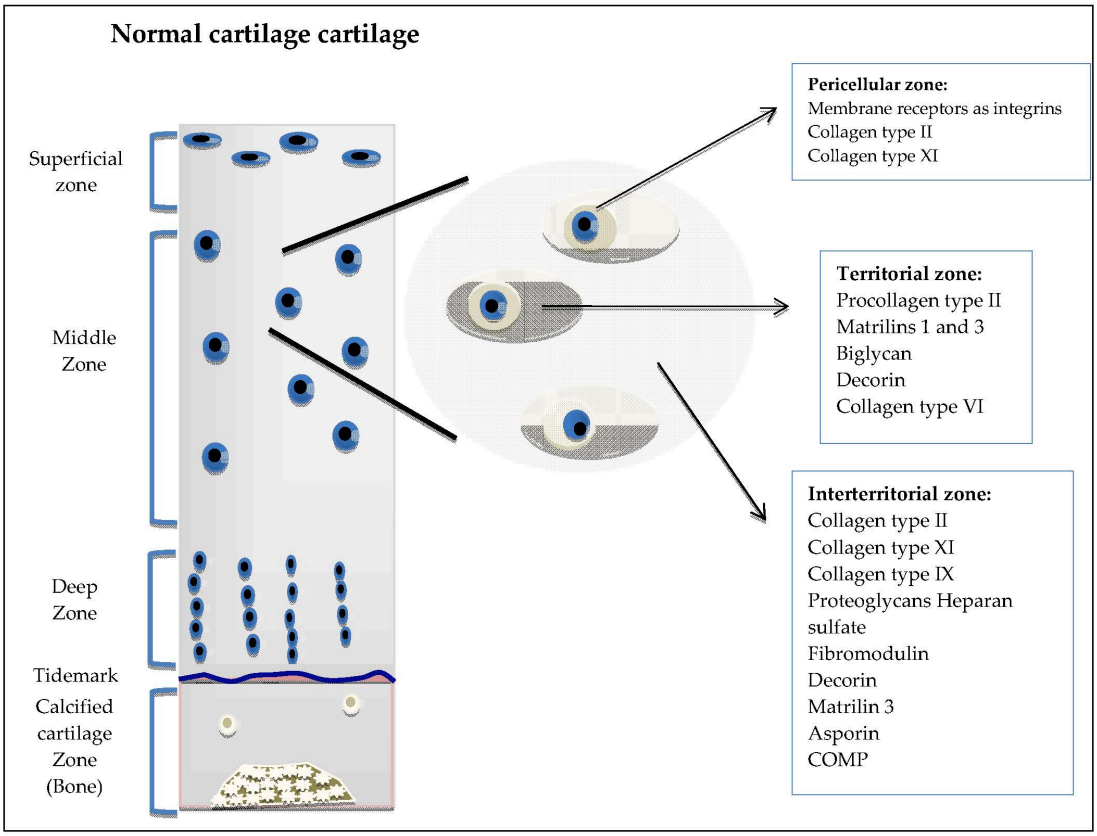


Figure 1.8: The organisation of normal articular cartilage matrix.

The extracellular matrix is divided on distance from the chondrocytes. The pericellular matrix is immediately surrounding the chondrocytes. The territorial matrix is adjacent to pericellular zone and the interterritorial zone is the most distant. Every zone has specific functions, molecular structures and affects the activity and the expression of different molecules by the chondrocyte (García-Carvajal et al., 2013).

1.3.3 Composition of articular cartilage

1.3.3.1 The chondrocyte

The chondrocyte is the only cellular component of cartilage. It has evolved to withstand compressive forces and is able to survive in a low oxygen environment (Muir, 1995). Nutrition and excretions occurs *via* diffusion due to the avascular nature, this gives the tissue a low metabolic rate and poor reparative ability, making cartilage vulnerable to degeneration. The cellular component only constitutes approximately 10% by volume in the superficial zone reducing to around 1% in the deep-zone of mammalian articular cartilage (Archer and Francis-West, 2003). It has been proposed that the higher cell density at the articular surface is due to the proximity to the synovial fluid and, therefore, short diffusion of nutrients (Stockwell, 1978). Chondrocytes are approximately 10μm in diameter and are generally spheroidal in shape, with the exception of chondrocytes within the superficial zone that are more flattened. In mature articular cartilage, apart from cells within the superficial and middle zones, chondrocytes are arranged roughly into vertical columns, with varying morphologies depending on the zone in which they reside (Hunziker et al., 2007). Mature chondrocytes are located in lacunae and their cell membranes adhere directly to the pericellular matrix, which contains PGs, non-collagenous proteins and glycoproteins (James and Uhl, 2001). Adult articular chondrocytes do not normally divide, but contribute to the maintenance and integrity of the cartilage through a combination of synthetic and catabolic activities (García-Carvajal et al., 2013). When compared to other anatomical tissues, the chondrocytes primarily rely on anaerobic metabolism. Consequently, chondrocytes usually have relatively low numbers of mitochondria as cell energy requirements come from glycolysis (Archer et al., 2003, Buckwalter and Hunziker, 1999). Despite the low metabolic activity of the chondrocyte, the cells must remain active as maintaining the articular surface requires a turnover of matrix macromolecules, including synthesising type II collagen, large aggregating proteoglycans and other lower abundance matrix proteins. Chondrocytes are also able to sense there mechanical environment through short microvilli extending from the cell into the matrix, they can then modify the ECM accordingly (Buckwalter and Hunziker, 1999).

1.3.3.2 The cartilage collagens

There are 29 genetically distinct collagens present in animal tissues; they are large triple-helical proteins that form fibres or large sheet networks as part of the ECM (Heino et al., 2009, Cilla et al., 2007). Cartilage contains a complex arrangement of collagens, providing scaffolding to ensure the integrity of the ECM (Table 1.1). The collagen network gives cartilage its form and tensile strength, and accounts for approximately two-thirds of the dry weight of mature tissue. The collagens constituting articular cartilage include types I, II, III, V, VI, IX, X, XI, XII and XIV (Eyre et al., 2006).

The main collagen of cartilage is the fibrillar type II collagen, which constitutes about 80-90% of adult cartilage collagens (Gelse et al., 2003, Eyre et al., 1987). Collagens all consist of a triple helix formed by 3 α polypeptide chains containing Gly-X-Y amino acid allowing formation of a tight triple helix with glycine residues in the centre. The (X) and (Y) can consist of any amino acids however, proline (Pro) and hydroxyproline (Hyp) are the most prominent. Proline and hydroxyproline permit the sharp twisting of the helix and increase stability; therefore, the collagen α chain normally contains repeating Gly-Pro-Hyp (GPO) motifs (Heino et al., 2009).

Filamentous collagens aggregate into large fibrils providing the tensile strength of the tissue. The fibrils aggregate and join together in a quarter-staggered arrangement creating the banded look of the fibre (Figure 1.9). Fibril associated collagens (FACITs) are often, but not always, associated with fibrillar collagens (Figure 1.9), they control fibril diameter and allow the fibrils to interact with the other ECM components and chondrocyte receptor molecules (Vanderrest and Garrone, 1991). Collagen Type II and III and XI are fibrillar collagens of cartilage. Collagen Type II and III are both homotrimers and Type XI is a heterotrimer. Collagen Type XI is incorporated into the fibre in order to limit the fibril diameters to ~15–50nm (Gelse et al., 2003). Collagen Type IX is the major FACIT collagen of articular cartilage, it functions to control fibre diameter. The functions of many of the FACITs are still yet to be identified; the other FACIT collagens in cartilage are type XII, XIV and XX (Heino et al., 2009). Some collagens form beaded filaments; these have short triple helical domains and large NC

domains. In cartilage, the heterotrimer type VI collagen is the major beaded filament (Eyre, 2002). Collagen Type VI is the major pericellular collagen surrounding the chondrocyte.

1.3.3.2.1 Type I collagen

Type I collagen, a heterotrimer comprising two α1(I) chains and an α2(I) chain, is a fibrillar collagen that is present at the onset of chondrogenesis early in development. Type I collagen is gradually replace by type II collagen in articular cartilage (Gelse et al., 2003). However, during endochondral ossification within the forming bone, type II collagen is replaced by type I collagen, secreted by hypertrophic chondrocytes (von der Mark et al., 1976). It is also present at the articular surface during development and in repair.

1.3.3.2.2 Type II collagen

Type II collagen is the most abundant collagen and it contains large amounts of hydroxylysine, glucosyl and galactosyl residues to interact with ECM proteoglycans (Gelse et al., 2003). It is synthesised as a homotrimer; consisting of 3 identical polypeptide α1(II) chains and differential splicing results in two variants, collagen IIA and IIB (Ryan and Sandell, 1990). The type II collagen α chains are synthesised as pro-collagens, with non-collagenous N- and C-propeptide domains. Through extracellular post-translational modification, proteinases cleave the N- and C- terminal domains and produce mature triple helices Type II collagen supports chondrocyte adhesion by binding through its helical domain with specific cell surface integrins (Holmvall et al., 1995).

1.3.3.2.3 Type III collagen

Type III collagen, is another fibrillar collagen and a minor collagenous component of articular cartilage. Type III is copolymerised and covalently linked to the same fibres as type II collagen (Eyre et al., 2006). It also interacts with type I collagen to regulate fibril formation and fibril growth (Duance V. C., 1999). Its function is not currently known, however, it is thought to be synthesised in response to injury.

1.3.3.2.4 Type V collagen

Type V collagen is a fibrillar collagen with a high homology to type XI collagen and, is thought to aid in the control of the size of forming fibres (Duance V. C., 1999).

1.3.3.2.5 Type VI collagen

Type VI collagen is a microfibrillar collagen synthesised as a heterotrimer of three distinct chains. Type VI monomers assemble into anti-parallel dimers, these dimers then form tetramers; the tetramers aggregate into a large microfilament network which is separate from the other collagens and fill gaps within the matrix (Gelse et al., 2003). Type VI collagen is located in the pericellular matrix of chondrocytes, where the microfibrils are stabilised by interaction with hyaluronan (Eyre et al., 2006, Vanderrest and Garrone, 1991). Increased expression during osteoarthritis has led to the implication that it may be involved in a reparative reaction (Chang and Poole, 1996).

1.3.3.2.6 Type IX collagen

Collagen Type IX is the major FACIT in cartilage and it is located on the outside of the collagen fibril and helps control the fibril diameter. It is heterotrimeric molecule comprised of three different chains [α1(IX) α2(IX) α3(IX)], each consisting of three collagenous triple-helical domains (COL1-3) separated by 4 globular non-collagenous (NC) domains, which provide a 'hinge' region that allows the molecule to protrude from the edge of the Collagen Type II fibril. This allows interactions with proteoglycans and prevents further type II molecules aggregating (Gelse et al., 2003). It accounts for at least 10% of the collagen in foetal cartilage, but only around 1% of the collagenous protein in adults (Eyre, 2002). Collagen Type IX is sometimes also classed as a PG due to attachment sites for chondroitin-sulphate at the non-collagenous NC3 domain (Eyre et al., 1987). Type IX collagen is always found in combination with type II collagen through covalent links, modulating fibril formation by preventing close parallel alignment of the Collagen Type II fibrils (Wotton et al., 1988). The covalent crosslinks to type II contributes to the stability of the collagen network and aids to resist the swelling pressure of the proteoglycans (Eyre, 1991).

1.3.3.2.7 Type X collagen

Type X collagen is a cartilage-specific short non-fibrillar helical homotrimer, consisting of three α1(X) chains, with a short non-helical amino terminus, a single triple-helical domain and a globular C- terminal domain (Eyre, 1991). It is considerably shorter in length than types II, IX and XI and is expressed in low abundance in normal adult articular cartilage. It may have a role in the mineralisation of cartilage, as its expression is highly restricted to the ECM of the deep calcified hypertrophic zone following synthesis by terminally differentiating chondrocytes (Kwan et al., 1991, Schmid and Linsenmayer, 1985). Due to the localisation specifically within hypertrophic chondrocytes and at the growth-plate, it is believed that it is important in endochondral ossification (Eyre, 2002). During OA, the chondrocytes nearer to the superficial zone, near the articular surface, synthesise Collagen Type X.

1.3.3.2.8 Type XI collagen

Collagen Type XI is a heterotrimeric procollagen comprising three distinct proα1-3(XI) chains. Its main function is to control fibrillogenesis of type II collagen (Gelse et al., 2003). It contains two collagenous domains (COL1-2) and three non-collagenous domains (NC1-3). Collagen XI in combination with Collagen Type II and IX form a heteropolymer fibre by covalent interactions (Figure 1.9) (Eyre et al., 2006). Glycosylation of the triple helix makes Collagen Type XI a bulky molecule that alters spacing within heterogenic fibrils. Type XI collagen interacts with proteoglycans and the chondrocytes and may have a role in cell matrix intercommunication (Vaughan-Thomas et al., 2001). Alternative splicing of the N-terminal domains may influence interactions with other matrix molecules (Duance V. C., 1999).

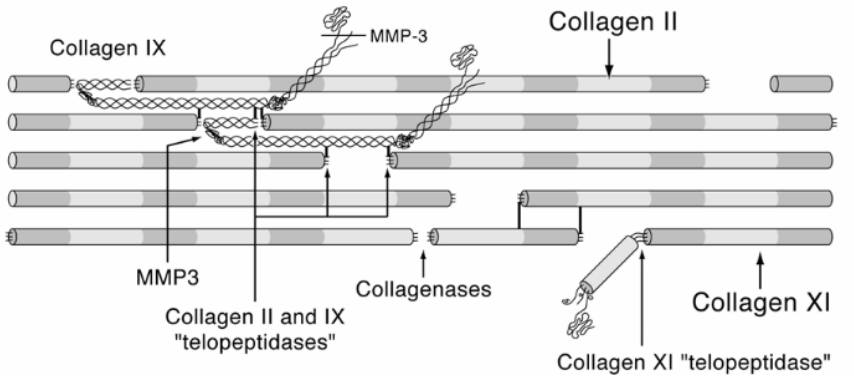


Figure 1.9: Collagen fibre formation.

Collagen Type II fibrils form covalent bonds between each other to create the larger fibre. Collagen Type XI fibrils are incorporated within the fibre and Collagen Type IX is bound to the outside, thereby controlling the fibre diameter by preventing further aggregation (Eyre et al., 2006).

Collagen	**Collagen Type**	**Molecular composition**	**Genes**	**Percentage of total collagen**
Collagen II	Fibril forming	$[a1(II)]_3$	COL2A1	~ 80-90%
Collagen III		$[a1(III)]_3$	COL3A1	~ 10%
Collagen XI		a1(XI)a2(XI)a3(XI)	COL11A1 COL11A2 COL11A3	~ 3%
Collagen VI	Microfibrillar (beaded filaments)	a1(VI),a2(VI),a3(VI)	COL6A1 COL6A2 COL6A3	<1%
Collagen IX	FACIT	a1(IX)a2(IX)a3(IX)	COL9A1 COL9A2	~ 1%
Collagen XII		$[a1(XII)]_3$	COL12A1	
Collagen XIV		$[a1(XIV)]_3$	COL14A1	
Collagen XX		$[a1(XX)]_3$	COL20A1	
Collagen x (hypertrophic cartilage only)	Hexagonal network forming collagens	$[a3(X)]_3$	COL10A1	

Table 1.1: Major collagens of articular cartilage.

The collagens are categorized into groups of similar properties and function. The molecular composition of the fibrils and the genes that encode the filaments are shown (Eyre et al., 2006, Gelse et al., 2003, Vanderrest and Garrone, 1991).

1.3.3.3 Cartilage proteoglycans

Proteoglycans (PGs) are protein cores with covalently attached glycosaminoglycan (GAG) chains (Bayliss et al., 1983). GAGs are long unbranching polysaccharide chains of repeating disaccharide units. Each disaccharide unit contains a hexosamine joined to a hexuronic acid (Sasisekharan et al., 2006). The GAGs are acidic and contain a negative charge due to covalently attached sulphate groups. There are many different GAGs, the most important being, chondroitin sulphate (CS), dermatan sulphate (DS), keratan sulphate (KS), heparan sulphate (HS) and hyaluronic acid (HA). The dominant GAG in cartilage is CS but KS is also extensively found (Knudson and Knudson, 2001). Proteoglycan content is greatest in the transitional and upper radial zones, this produces the large negative charge that draws in water (Bayliss et al., 1983). The molecular compositions of the different GAGs are shown in Table 1.2.

Glycosaminoglycan	Hexuronic acid	Hexosamine
Chondroitin-4-sulphate	D-glucuronic acid	N-acetyl-D-galactosamine-4-sulphate
Chondroitin-6-sulphate	D-glucuronic acid	N-acetyl-D-galactosamine-6-sulphate
Dermatan sulphate	L – iduronic acid	N-acetyl-D-galactosamine-4-sulphate
Hyaluronic acid	D – glucuronic acid	N-acetyl-D-glucosamine
Keratan sulphate	D-galactose	N-acetyl-D-galactosamine-6-sulphate
Heparan Sulphate	L – iduronate-2-sulphate	N-sulpho- D-glucosamine-6-sulphate

Table 1.2: The molecular composition of glycosaminoglycans.

Chondroitin sulphate and dermatan sulphate have very similar structures; the only difference is the isomerisation of the hexuronic acid. Hyaluronic acid is shown to be the only GAG without sulphate groups. (Sasisekharan et al., 2006).

There are 3 categories of proteoglycans in articular cartilage; these are, large aggregating proteoglycans, small leucine rich proteoglycans (SLRPs) and cell surface proteoglycans (Knudson and Knudson, 2001). The most abundant proteoglycan in cartilage is the large aggregating proteoglycan, aggrecan. The SLRPs can be subdivided into 3 categories. Class 1 SLRPs bind the TGF-β growth factors, these include decorin and biglycan. Class 2 SLRPs in cartilage are fibromodulin, lumican and PRELP. Finally, class 3 SLRPs are only found in epiphyseal cartilage. The cell surface proteoglycans syndecans and glypican act as transmembrane signalling receptors.

1.3.3.3.1 Hyaluronic acid

Hyaluronic acid is a nonsulphated GAG that is composed of repeating disaccharide units of D-glucuronic acid linked to N-acetyl-D-glucosamine that form large, negatively charged molecules (Atkins and Sheehan, 1971). As mentioned earlier, it is essential during development for cavitation of diarthrodial joints and forms an integral component of articular cartilage ECM. Through interactions with Aggrecan and link proteins, it forms large molecular aggregates that function to draw water into the tissue (Roughley, 2006). The interaction between Aggrecan and HA is non-covalent, stabilised by the small glycoprotein link protein. Chondrocytes and HA interact through the CD44 family of surface receptors, facilitating organization of the tissue, cell adhesion, migration, differentiation and anchor PG aggregates within the articular cartilage (Ishida et al., 1997).

1.3.3.3.2 Aggrecan

Aggrecan is the predominant PG in articular cartilage; a large aggregating PG, with a core protein of ~250kDa, it consists of three globular domains (G1, G2 and G3) and three extended domains (interglobular domain [IGD], KS and CS). KS and CS chains are attached between the G2 and G3 domains, the core molecule binds approximately one hundred CS chains and thirty KS chains *per* molecule (Knudson and Knudson, 2001, Roughley, 2006). The G1 domain is at the N-terminus, it has a link protein-like structural motif and interacts with HA and link protein to facilitate aggregation. The Aggrecan aggregates form a macromolecule of greater than ~3000kDa with more than 300 Aggrecan molecules in a bottle brush like conformation (Figure 1.10) (Pitsillides et al., 1999). This macromolecule has a large negative charge, which draws water into cartilage providing resistance to compressive forces (Karp, 2008, Knudson and Knudson, 2001, Roughley, 2006). The G3 domain contains EGF binding regions and a calcium dependent lectin module that bind sugar molecules (Iozzo, 1998, Knudson and Knudson, 2001). Loss and break down of Aggrecan is a major aspect of cartilage degradation and disease (Buckwalter and Hunziker, 1999). Aggrecan is broken down by ADAMTS metalloproteinases (a disintegrin and metalloproteinase with a thrombospondin motif), specifically ADAMTS4 and ADAMTS5 (aggrecanase -1 and -2 respectively) (Huang and Wu, 2008).

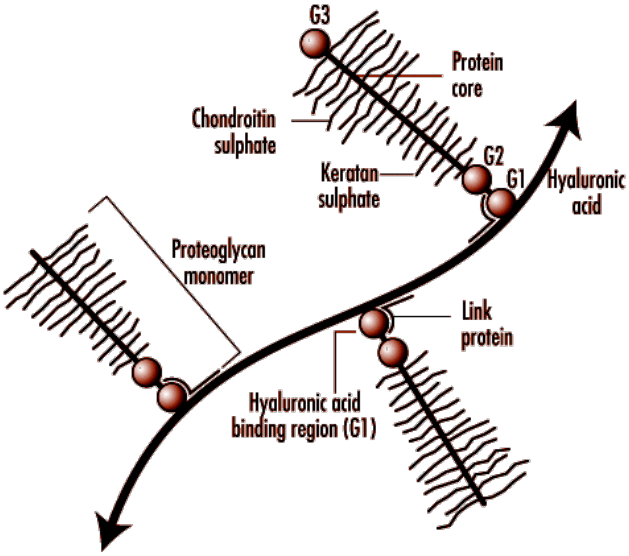


Figure 1.10: Schematic representation of an Aggrecan aggregate.

Diagram of Aggrecan structure showing the GAG chains and the aggregation of proteoglycans on a hyaluronan core. G1, G2 and G3 are globular, folded regions forming link proteins of the central core protein (Robert and Urban, 2013).

1.3.3.3.3 Perlecan

Perlecan is found in the pericellular matrix of articular cartilage. It is a large non-aggregating PG with a large protein core of ~400 kDa with two or three HS-GAG chains and several structural domains that facilitate interaction with cells, other matrix macromolecules and growth factors (Knudson and Knudson, 2001).

1.3.3.3.4 Small leucine rich proteoglycans

SLRPs are ubiquitous in connective tissues. They have small core proteins that contain leucine-rich domain repeats for protein-protein interactions. This allows interaction with fibrillar collagens, assisting in the control of fibril diameter during fibrillogenesis and, also, protects the fibrils from proteolytic damage by preventing collagenases from accessing cleavage sites (Roughley, 2006).

Class I

Decorin and biglycan are classified as DS PGs. Decorin is an ECM PG, it is a horseshoe shaped proteoglycan containing 1 CS or DS GAG; it joins to collagen fibrils in the gap regions and controls fibril spacing. Biglycan is also in the pericellular matrix, it contains either 2 CS or DS GAGs and is thought to be involved in bone formation (Knudson and Knudson, 2001)

Class II

Fibromodulin and lumican are classified as KS PGs. Fibromodulin contains 4 KS GAGs, it joins onto collagen fibres like decorin and controls fibril diameter. Lumican is another KS proteoglycan, it also controls fibril diameter and can delay fibrogenesis (Iozzo, 1998). PRELP has 4 N- linked glycosylation sites, showing importance in protein folding and matrix organization (Knudson and Knudson, 2001).

1.3.3.3.5 Cells surface proteoglycans

Cell surface proteoglycans act as transmembrane signalling receptors. They include the syndecans and glypican and contain 1 CS and 2 or more HS GAG chains. These proteoglycans act as receptors for bFGF and TGF-β, increasing cell proliferation and inhibiting differentiation (Knudson and Knudson, 2001).

1.3.3.3.6 Surface Zone protein

Surface zone protein (SZP, lubricin) is a proteoglycan expressed by the surface zone chondrocytes (Flannery et al., 1999, Schumacher et al., 1994). SZP is not exclusively entrapped in the matrix and so is also present in the synovial fluid. It is believed that it is secreted into the synovial fluid. SZP is involved in protecting the articular surface and providing lubrication to the joint. It is a boundary lubricant of synovial joints, that reduces friction at the articular surface maintaining articular cartilage integrity during movement (Becerra et al., 2010, Rhee et al., 2005).

1.3.3.4 Other macromolecules

There many proteins within articular cartilage that are neither collagenous nor proteoglycans but aid the organization, structure and function of the matrix, while assisting matrix-cell signalling.

Fibronectin is a large glycoprotein that binds to integrins and other matrix components, playing a major role in cell adhesion, attachment, migration and

development. It is also involved in wound healing, and in the regulation of cell growth, differentiation and homeostasis (Hayashi et al., 1996). The integrin α5β1 is a receptor for fibronectin and is expressed at the surface of articular cartilage (Dowthwaite et al., 2004). In articular cartilage, fibronectin is synthesised by chondrocytes and present in the ECM and in the synovial fluid (Heinegard and Oldberg, 1989). Expression is up-regulated in OA and fragments of fibronectin are generated that signal through the α5β1 integrin to activate inflammatory and catabolic responses (Homandberg et al., 1998). Foetal knee articular chondrocytes has strong expression of β1, αVβ5 dimer, α5 and α6 integrins throughout the tissue. Like adult cartilage, foetal articular cartilage preferentially expresses (α5β1) fibronectin receptor, but also the (α6β1) laminin and (αVβ5) vitronectin receptors (Salter et al., 1995).

Tenascin-C is a hexameric ECM glycoprotein with disulphide sub-units with domains that have structural homology to fibronectin. It is predominantly expressed in the condensing mesenchyme during development and during repair (Gluhak et al., 1996). It has also been shown to be expressed in the ECM of mature articular chondrocytes (Patel et al., 2011). Increased expression of tenascin-C in the cartilage matrix and the synovial fluid is considered a marker of osteoarthritis disease progression (Sofat et al., 2012). Unlike fibronectin, tenascin-C has anti-adhesion and anti-spreading properties, the inhibition of cell attachment favours a rounded cell shape that promotes the differentiation of chondrocytes from mesenchyme progenitors (Mackie and Ramsey, 1996, Spring et al., 1989). It has been shown to function through cell-surface receptors, including integrins and syndecans (Salmivirta et al., 1991).

Cartilage oligomeric protein (COMP) (thrombospondin-5) is a pentameric protein (Lohmander et al., 1994). Initially, in developing cartilage, it is localised to the territorial matrix, however, localisation in mature cartilage is within the inter-territorial matrix. COMP binding to collagens I, II and IX, fibronectin and aggrecan, mediates chondrocyte attachment to the ECM (Murray et al., 2001). It is thought to have a role in endochondral ossification and there is an increase in COMP within the synovial fluid in OA; it is unknown whether this is a reparative process or part of disease progression (Murray et al., 2001, Tseng et al., 2009).

1.3.3.5 Interstitial fluid (water)

The largest component of cartilage is water, accounting for up to 80% of the wet weight of articular cartilage. The interactions between water and the macromolecules are required to maintain the mechanical properties of the tissue. A portion of the water is able to move in and out of the tissue aiding joint lubrication and supplying nutrients to the chondrocytes. The movement of the water in an out of the tissue is dependent on the large macromolecules, principally the large aggregating proteoglycans due to their large negative charge (Bollet and Nance, 1966, Buckwalter and Hunziker, 1999). The interstitial fluid consists of water and inorganic salts and the high concentration of cations within the fluid interact with the negatively charged proteoglycans. The interstitial flow allows the exchange of gases, small proteins, metabolites and cations from the synovial fluid to the chondrocytes (Buckwalter and Mankin, 1997).

1.3.4 Cartilage matrix turnover

The chondrocyte controls synthesis and catabolism within articular cartilage. Matrix metalloproteinases (MMPs) are the main enzymes responsible for degradation of proteoglycans and collagens in cartilage. The chondrocytes precisely control synthesis and degradation to maintain a balance. Increased levels of MMPs leads to degeneration and the development of pathology, including osteoarthritis (OA) and rheumatoid arthritis (RA) (Tetlow et al., 2001, Li et al., 2011). In articular cartilage, the enzymes principally involved in Aggrecan turnover are ADAMTS -4 and -5. Collagens have a slow rate of turnover due to resistance to degradation, a result of the tightly arranged fibrils and, interactions, with glycoproteins. It has also been shown, however, that matrix turnover can occur more rapidly in response to mechanical signals (Eyre, 2002, Grodzinsky et al., 2000). The major collagenase in articular cartilage is collagenase -3 (MMP13), expressed by the chondrocytes; its main substrate is type II collagen. The collagen fibril degradation occurs by digesting into two fragments, a three- quarter and one-quarter length fragments (Eyre, 2002).

1.3.5 Chondrocyte-matrix interactions

The interaction between chondrocytes and the ECM is partly mediated by integrins, whose internal cytoplasmic domains are attached to the cytoskeleton. This signalling through integrins is bidirectional; interactions providing a means of exchanging signals between the cell and the ECM (Loeser, 2002, van der Kraan et al., 2002). Chondrocytes are able to adhere to fibronectin, and Collagen Types I, II, V, IX and XI and studies have suggested that integrins mediate attachments to these proteins. Integrins are heterodimeric proteins that are composed of α and β subunits; each subunit has an extracellular and cytoplasmic domain (Reid et al., 2000). Integrins recognize and bind to the Arg-Gly-Asp (RGD) motif mediating cell adhesion. The binding of integrins with ligands within the ECM can induce cellular responses and promote cytoskeletal and ECM reorganisation (García-Carvajal et al., 2013, Kim et al., 2003). The most abundant integrin expressed on chondrocytes is the fibronectin receptor α5β1 (Woods et al., 1994).

Annexins are another group of transmembrane molecules that act as receptors for the ECM; annexin II, V and VI are all expressed in articular cartilage (Reid et al., 2000). Annexin V (Anchorin CII) is present on the surface of chondrocytes, is the most abundant annexin within articular cartilage and has various functions including anti-inflammatory responses, signal transduction, and cell-matrix interactions and plays a vital role in cartilage metabolism (Mollenhauer et al., 1999, van der Kraan et al., 2002). In cartilage, it is believed to bind chondrocytes to Collagen Type II and type X. As previously discussed, cartilage also expresses the HA receptor CD44 whose interactions are essential for cartilage homeostasis.

The ECM also acts as a mechanical signal transducer for the chondrocytes acting through a positive feedback mechanism. The matrix can transmit signals that result from mechanical loading to the chondrocytes, which as a result, respond to these signals by altering their matrix. As mentioned earlier, studies have shown that static loading, overloading or immobilizing articular cartilage all lead to breakdown of the cartilage ECM (Jeffrey et al., 1995, Kim et al., 1996, Palmoski et al., 1979) and that dynamic compression increases matrix synthesis (Bader et al., 2011). The physicochemical, mechanical and electrical signals induced by loading, stimulate chondrocyte responses that may cause persistent changes in the molecular organisation of the matrix (Martin and Buckwalter, 2000). The exact mechanisms of the changes caused by chondrocyte matrix interactions are

unknown; however, it is thought that growth factors and cytokines play a key role. Interleukin-1 (IL-1) induces the expression of MMPs resulting in degradation of matrix molecules, while TGF-β stimulates matrix synthesis and FGF-2 induces cell division (Khan et al., 2010, Mengshol et al., 2001, van Osch et al., 1998).

1.4 Damage and degradation of articular cartilage

The superficial zone of articular provides the smooth low friction surface that resists the high tensile forces and ensures normal function and structure is retained by cartilage. Trauma to joints often occurs and the superficial layer begins to show signs of damage. Damage to this layer exposes the deeper cartilage zones, propagating forces to the lower layers when loaded, triggering further degeneration (Martin and Buckwalter, 2002). If traumatic injury or imbalance in ECM catabolism and anabolism occurs, cartilage tissue lacks the ability to actively respond to damage and, is therefore, limited in its reparative response (Redman et al., 2005). Partial thickness chondral defects that are contained within the cartilaginous regions are incapable of spontaneous repair. Full-thickness or osteochondral defects <3mm that extend down to the vascularised subchondral bone, are able to repair, possibly due to the release of bone marrow stem cells that fill the defect (Shapiro et al., 1993). However, larger osteochondral lesions of more than 6mm do not heal and lead to progressive degeneration as demonstrated in a goat defect model (Jackson et al., 2001). The repair tissue formed in small osteochondral defects is fibrocartilagenous and does not integrate into the surrounding articular cartilage. The mechanical properties of fibrocartilage is inferior to hyaline cartilage and, therefore, prone to future injury (Hunziker, 2009, Redman et al., 2005). Damage to articular cartilage ultimately leads to the debilitating condition of osteoarthritis (OA).

1.4.1 Age-related changes

As cartilage ages, there are morphological changes that occur within the tissue that alter the mechanical properties (Martin and Buckwalter, 2002). Superficial fibrillation and softening can be seen in the surface however, in most instances, these do not penetrate into the deeper zones (Buckwalter and Lane, 1996, Horton et al., 2006). The total cell number appears to decline with age, each

chondrocyte exhibits a reduced mitotic index and decreased synthetic metabolism. The water content declines and both ECM undergo age-related remodelling of the PGs and collagens (Armstrong and Mow, 1982, Horton et al., 2006). Aggrecans become smaller along with the size of the aggregates (Martin and Buckwalter, 2002). HA also decreases in size but increases in abundance; however, fragmented proteins from proteolysis bind HA inhibiting normal functionality (Thonar et al., 1986). The KS content within Aggrecan increases and the CS content decreases. Collagens are more cross-linked and reductions in type XI collagen content increase within the fibril, both these modifications reduce flexibility and make the cartilage more rigid (Eyre et al., 1988). These changes make articular cartilage more prone to damage with age.

1.4.2 Inflammatory damage

Oxidative stress is caused by an imbalance in the equilibrium between reactive oxygen species (ROS) and antioxidant species (Finkel and Holbrook, 2000) and can cause tissue damage and cell death (Wijeratne et al., 2005). ROS can be produced endogenously in chondrocytes by mitochondria, peroxisomes, lipoxygenases, NADPH oxidase and cytochrome P450 enzymes but can also be released by many exogenous sources such as during inflammation by macrophages and neutrophils (Finkel and Holbrook, 2000). ROS have also been shown to be involved in degeneration of articular cartilage; hydrogen peroxide causes apoptotic cell death through up-regulation of Caspase-3 and induction of genomic instability (Asada et al., 2001). Hydrogen peroxide has also been shown to inhibit PG production and cause PG degradation reducing matrix stability (Bates et al., 1985, Tiku et al., 1999, Tiku et al., 2000). Studies have shown ROS increases expression of early markers of OA; these include 3B3(-), procollagen IIA and chondrocyte hypertrophy (Khan et al., 2008a, Aigner et al., 1999). During OA, there is an increase in ROS due to transient inflammatory responses. Macrophages release inflammatory cytokines inducing ROS release, that assists cartilage degeneration (Bonnet and Walsh, 2005, Mackie et al., 2008)

1.5 Osteoarthritis

OA is the most common disease affecting articular cartilage and most often occurs in the knee, hip and shoulder joints, but any synovial joint can be affected.

Symptoms include joint pain, restricted movement, deformity and inflammation (Buckwalter and Lane, 1996). Of the chronic disease conditions, OA places the biggest economic burden on medical and social services in the developed world due to healthcare costs and working days lost; with an ageing population this is expected to only increase (Bitton, 2009). Most commonly, OA occurs as primary or idiopathic OA, risk factors include obesity, overuse, joint instability, genetics or anatomical irregularities. OA arising as a result of injury is secondary OA (Buckwalter and Martin, 2006). OA results in deterioration and loss of articular cartilage. The disease progresses in 3 stages; firstly there are changes in or loss of the ECM, then chondrocytes attempt to remodel and repair the tissue and finally, the degeneration occurs faster than synthesis causing incremental loss of cartilage (Hendren and Beeson, 2009).

1.5.1 Clinical signs of OA

During OA, articular cartilage loses its firmness and white glossy appearance discolouring to a yellowy off-white colour. The damage varies with each patient and even within different regions of the same joint. Pathological changes can be detected with arthroscopy or radiology, the joint space narrowing, fibrillation or lesions can been seen in the joint surface and osteophytes form (Le Graverand et al., 2010). In areas close to lesions, there is a reduced cell density, while adjacent unaffected sites show chondrocyte clustering and proliferation (Poole et al., 1987, Poole et al., 1991, Rothwell and Bentley, 1973). There are also changes to the subchondral bone including sclerosis, osteonecrosis and fractures that are visible through x-rays or magnetic resonance imaging (MRI) (Lajeunesse et al., 2003, Yamada et al., 2002). Morphological changes exhibited by OA cartilage are outlined in Table 1.3.

Grade	Definition
0	Normal Cartilage
1	Destruction of the superficial zone cartilage, confined to the high load bearing areas. Superficial flaking, early fibrillation and shallow pitting or grooves can be seen
2	More extensive damage, still in the load bearing areas, damage does not penetrate into the subchondral bone. Deep fibrillations are evident and there is a notable loss of cartilage

3	Total loss of cartilage in one or more high pressure areas with exposure of the subchondral bone. Wide-spread fibrillation and flaking of the remaining cartilage. Damage evident on non-load bearing regions
4	Complete loss of articular cartilage from large regions of the joint. Eburnation of the subchondral bone

Table 1.3: Morphological changes in OA.

Arthroscopic classification of knee osteoarthritis. Table adapted from the modified Collins classification (Brismar et al., 2002).

1.5.2 Cartilage changes in OA

Progressive loss of the structure and function of articular cartilage is one of the typical features of OA. Initially, the imbalance between anabolic and catabolic processes leads to the over-expression of MMPs and ADAMTSs resulting in a loss of collagen and PGs from the matrix (Pritzker et al., 2006). Delamination or fibrillation of the superficial zone extends into the middle zone of the articular cartilage and there is a loss of PGs initially in the surface, fibrillated regions and chondrocytes clusters, progressing into the deeper zones as the disease progresses. During osteoarthritis, the increased permeability of the tissue results in a gain in water content, combined with reductions in Aggrecan concentration and shortening of GAG chains, stiffness of the ECM is reduced (Martin and Buckwalter, 2002). In a reparative attempt, chondrocytes proliferate and synthesise increased quantities of matrix molecules, however, MMPs and cytokines are also produced; further increasing the overall enzymatic degradation of the matrix (Tetlow et al., 2001).

Cell clusters are formed as a result of chondrocyte proliferation and the hyaline cartilage is replaced by a repair tissue resembling fibrocartilage (Poole et al., 1991, Rothwell and Bentley, 1973). Collagen Types II, IX and XI are broken down, increasing the stresses on the remaining collagen-fibril network and type X collagen starts to be expressed outside of the calcified zone (van der Kraan et al., 2001). Collagen Type I expression is also induced in the surface replacing the original Collagen Type II network (Miosge et al., 2004, Miosge et al., 1998). In some cases, the unsuccessful repair response leads to the formation of osteophytes. Fragments of cartilage can also detach from the articular surface

and become trapped within the joint space causing obstruction and inflammation as well as further structural damage (Nelson et al., 2010). As the fissures extend deeper, they eventually reach the subchondral bone, this is often accompanied by an increase in matrix synthesis and duplication of the tidemark (Revell et al., 1990). The continued degradation results in further loss of the superficial zone cells, which are responsible for cell regeneration. There is a progressive continuation of degradation with cartilage loss and decreases in chondrocyte proliferation, eventually cumulating in the complete loss of the articular cartilage and thickening of the subchondral bone (Lorenz and Richter, 2006).

1.5.3 Metalloproteinases in OA

The gradual loss of proteoglycans and type II collagen is due to increased production of the degrading metalloproteinase enzymes. These include the collagenases MMP-1, -2, -8 and -13; each collagenase is specific to a certain collagen and digests at a particular structural epitope (Chu et al., 2002). Other up-regulated MMPs include: MMP-3, MMP-9, and MMP-14, these enzymes degrade Collagen Types II, III, IV, IX, and X, PGs, fibronectin, laminin, and elastin (Naito et al., 1999, Masuhara et al., 2002). MMP-9 is selectively expressed in the fibrillated cartilage and, therefore, believed to be responsible for the progressive degeneration of OA (Aigner et al., 2003). The MMPs in combination with the aggrecanases ADAMTS-4 and -5 degrade the matrix macromolecules, decreasing the cartilage structural integrity (Bondeson et al., 2008, Huang and Wu, 2008). Tissue inhibitor of metalloproteinase (TIMPs) are also found to be elevated in OA (Naito et al., 1999).

1.5.4 Other tissues affected in OA

Osteoarthritis also affects other tissues within the synovial joint including the subchondral bone, synovial membrane and the meniscus.

The subchondral bone secretes catabolic enzymes that can affect the neighbouring cartilage; promoting abnormal cartilage metabolism and destruction (Lajeunesse and Reboul, 2003). Osteocalcin and osteopontin, which promote bone formation, increases in the synovial fluid of patients with early OA

implying that bone cell changes occurs early during disease progression (Sharif et al., 1995). Alterations in the subchondral bone include, trabecular architecture, the formation of boney osteophytes at the joint margins and the development of subchondral cysts (Martel-Pelletier and Pelletier, 2010). Histologically, there is also evidence of tidemark advancements and duplications (Revell et al., 1990).

In OA, pro-inflammatory cytokines are activated in the synovial membrane and other surrounding tissue and increase gene expression levels and activities of MMPs and ADAMTS in chondrocytes. IL-1β and TNF-α production by the synovial membrane are key perpetrators in the development of OA (Smith et al., 1997). IL-1β is released and stimulates catabolic enzymes in the ECM, whilst also suppressing the anabolic pathways. Therefore, production of ECM proteins are reduced and enzymatic degradation is increased (Goldring et al., 1988, Goldring et al., 2008).

Meniscal protrusion is frequently associated with knee OA; this decreases joint stability and changes the load distribution, causing the femoral and tibial bone surfaces to suffer an increased susceptibility to OA (Berthiaume et al., 2005).

1.5.5 Mechanisms

Osteoarthritis is considered a multi-factorial disease, however, the exact mechanisms in the disease process are not fully understood. It is thought that many of the changes occurring during OA are recapitulation of developmental processes. Development signalling pathways are induced, including FGF, Wnt, BMP, TGF-β and Hedgehog signalling during OA (Blom et al., 2009, Dell'Accio et al., 2006, Chia et al., 2009, van den Berg, 1995).

1.6 Repair

As mentioned previously cartilage has a poor intrinsic repair capacity, tears and defects are unable to be successfully restored and often lead to OA. Therefore, intervention is often necessary to repair damaged tissue and to prevent further damage. The most effective treatment for end-stage OA is arthroplasic prosthetic replacement. However, due to the finite lifespan of prostheses, this is unsuitable for patients younger than 45 years. A variety of treatment methods have been used to repair defects and stimulate the formation of new articular cartilage. These include microfracture, lavage, osteochondral allographs, cell transplantation and osteotomy. Each procedure has varied success and many factors have to be considered in the selection of the correct method. Considerations include the size of the defect and age of the patient (Bhosale and Richardson, 2008).

1.6.1 Surgical interventions

1.6.1.1 Arthroscopic repair

Arthroscopic repair procedures represent the most cost-efficient and least invasive treatments for damaged cartilage. Lavage and debridement are used to alleviate pain, however, they do not induce any repair of the damaged tissue (Redman et al., 2005). Lavage is a washing procedure that removes cartilage debris and inflammatory factors from the joint temporarily eliminating some of the pain (Livesley et al., 1991). Debridement involves shaving the delaminating cartilage in order to smooth the surface and reduce friction (Chang et al., 1993).

1.6.1.2 Microfracture

The most widely used method that surgeons adopt for cartilage repair involves penetration of the subchondral bone causing the release of multipotent mesenchymal stem cells in a process defined as marrow stimulation. Previous methods have included Pridie drilling, spongialisation and abrasion, though the most popular modern method is microfracture (Ronn et al., 2011). Under arthroscopy, tiny fractures are made using an awl in the subchondral bone, inducing bleeding and a fibrin clot that is infiltrated with stem cells from the bone marrow. Stem cells fill the defect and differentiate and form a repair tissue (Yen et al., 2008). It has been shown that this repair tissue is fibrocartilage and not hyaline cartilage. Fibrocartilage does not have the same mechanical properties as articular cartilage, and is less suited to withstand the demands of everyday activities, thus, it is at higher risk of future breakdown (Redman et al., 2005). However, microfracture does offer symptomatic relief; in a follow up study it was reported that pain was decreased and function improved in 95% of the study population after up to 17 years post-surgery (Steadman et al., 2003).

1.6.1.3 Osteotomy

Osteotomy is a technique that in used in combination with debridement and lavage. It is generally conducted on joints with unilateral arthritic damage. The bone is cut in order to change joint alignment and redistribute load, reducing pressure on the damaged cartilage surface. It has been reported that osteotomies lead to the formation of a new articular cartilage surface, however, results are highly variable (Buckwalter, 1999).

1.6.1.4 Osteochondral autograft transfer system (OATS)

Osteochondral transfer can be performed as an autologous therapy. Autologous osteochondral transplantation, or mosaicplasty is employed mainly for smaller sized cartilage defects because, like with ACI, there is a shortage of harvestable tissue (Jakob et al., 2002). Osteochondral plugs are harvested from low weight-bearing areas within the knee joint, and inserted into the debrided defects. Plugs are poorly integrated with the surrounding tissue and viability of the chondrocytes within the plugs is uncertain (Hangody et al., 1998, Hangody et al., 2004). The damage of large areas of healthy tissue to repair defects can result in

subsequent degradation in this area (Redman et al., 2005). Results have shown only short-term benefits, reducing pain and increased joint function (Jakob et al., 2002). Allogeneic transfers use tissue derived from cadavers in an attempt to repair large osteochondral defects, as large quantities of tissue can be retrieved and no damage to healthy cartilage occurs (Gomoll et al., 2012).

1.6.1.5 Repair of articular cartilage using tissue engineering

Hunziker has described tissue engineering "the art of reconstituting mammalian tissues both structurally and functionally" (Hunziker, 2002). The predominate aim is to create a functional repair tissue *ex vivo* and to intergrate this repair tissue into the body. Tissue engineering generally requires an appropriate cell type, bioactive factors and can be performed with or without supporting scaffolds.

1.6.1.5.1 Autologous chondrocyte implantation (ACI)

Autologous chondrocyte implantation was first developed for use in humans by Brittberg and colleagues in 1994 and is currently regarded as the 'gold standard' for cartilage repair (Brittberg et al., 1994). This procedure involves harvesting the patient's own cartilage from a low weight-bearing region, extracting the cells and expanding them *in vitro*. Once a sufficient cell number is achieved in monolayer culture, the chondrocytes are injected into a full-thickness articular defect. A periosteal membrane patch in placed over the defect and sealed with fibrin glue, encapsulating the cells within the defect (Figure 1.11) (Brittberg et al., 1994, Brittberg et al., 2003, Redman et al., 2005). The implanted chondrocytes produce matrix and start to replace the cartilaginous tissue. There are drawbacks to this procedure however, initially this is a multi-stage procedure and it is more invasive than microfracture requiring multiple surgeries. Secondly, defect size limits the efficacy of ACI, a finite number amount of tissue can be harvested and since extensive *in vitro* expansion of harvested chondrocytes results in progressive de-differentiation, larger defects cannot be effectively repaired (Barbero et al., 2003). It has been shown that human chondrocytes lose their chondrogenic phenotype beyond 5-7 population doublings (PDs) (Benya and Shaffer, 1982, Cournil-Henrionnet et al., 2008). ACI has been shown to produce effective and durable repair tissue in full-thickness

cartilage defects, relieving symptoms and, with clinical success remaining high, even after 20 years post-implantation (Peterson et al., 2010). The repair tissue produced by ACI has been shown to be varied but often more hyaline-like than microfracture. However, it is rich in type I collagen which is a characteristic of fibrocartilage (Roberts et al., 2002). A number of modifications have been made to improve the outcome of ACI; synthetic collagen membranes have replaced the periosteal flap, and several synthetic and natural scaffolds have been developed into which the cells are seeded (Redman et al., 2005). In follow-up studies, it has been shown that initially, a year post-operatively, ACI offers significantly improved repair than microfracture (Visna et al., 2004); however, after 2 - 5 years post-surgery, randomised trials show no significant difference in repair efficiency between ACI and microfracture (Knutsen et al., 2007, Van Assche et al., 2010).

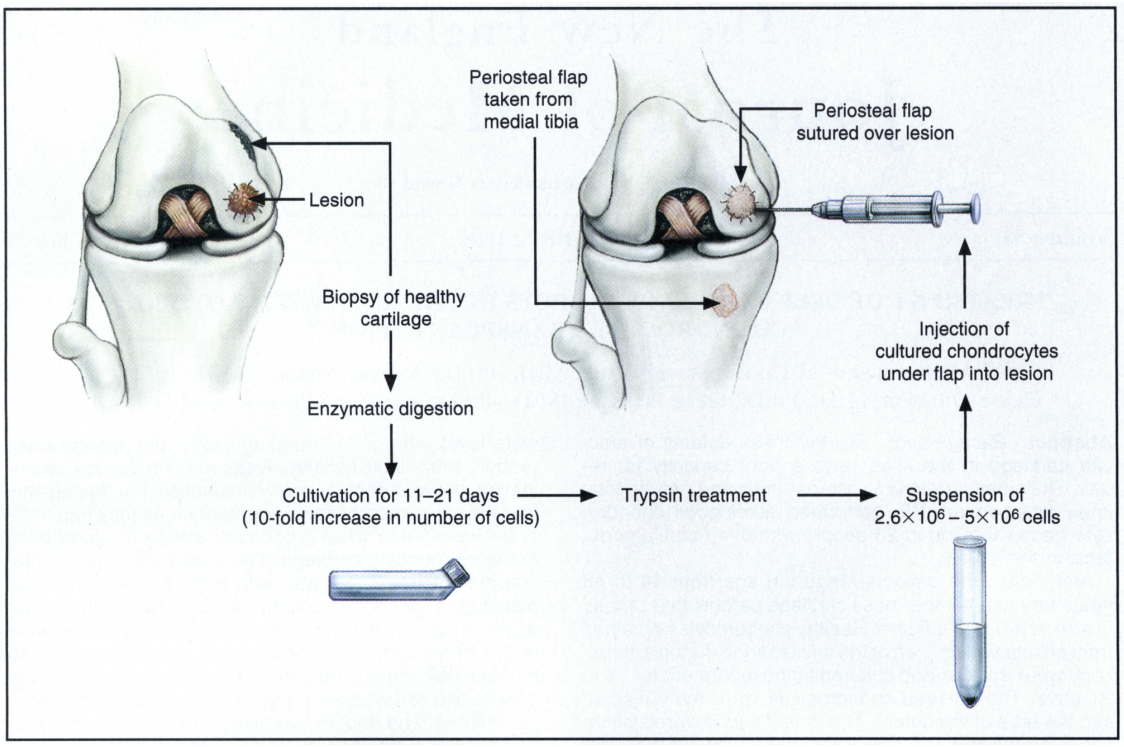


Figure 1.11: Schematic diagram of the stages involved in ACI .

Adapted from (Brittberg et al., 1994).

1.6.1.5.1.1 Scaffold-free repair

Cartilage tissue has been produced *in vitro* using scaffold free three-dimensional culture methods. Hayes and colleagues showed that bovine primary chondrocytes cultured for 8 weeks in transwell culture could form a cartilage of hyaline appearance with identifiable zonal stratification, discernible through cellular morphology, matrix organization, and immunohistochemical matrix composition. The study went on to show monolayer expansion of the cells prior to transwell culture resulted in reduced thickness, loss of zonal arrangement and fibrocartilagenous histology, indicating the importance of the correct cell type in tissue engineering (Hayes et al., 2007). This study is supported by a subsequent publication where transwell inserts were used to culture human bone marrow mesenchymal stems cells, differentiating them and forming a hyaline cartilaginous tissue *in vitro* (Murdoch et al., 2007). An early pilot study in the rabbit, has shown that scaffold-free cartilage grown *in vitro* is capable of surviving surgical transplantation and is viable post-operatively (Kandel et al., 1995). Scaffold-free growth of cartilage, therefore, offers a valuable future clinical option as well as an important experimental platform for research into cartilage repair.

1.6.1.5.1.2 Scaffold matrix-assisted repair

Numerous different scaffolds have been utilized in tissue engineering articular cartilage. A scaffold is designed to mimic the three-dimensional environment in which the chondrocytes naturally reside. The scaffold has to be biocompatible and bioresorbable, this ensures that the scaffold can be physiologically remodelled, with neither the scaffold nor the products of degradation causing inflammation or an immunogenic response (Hutmacher, 2000, Chapekar, 2000). Ideally, the rate at which the scaffold is broken down should be comparable to the rate of synthesis of repair tissue. The porosity and cellular attachment of the scaffold is essential to enable seeding of cells and cellular migration and to allow for the diffusion of nutrients into the graft (LeBaron and Athanasiou, 2000). The seeded cells need to be able to migrate in order to allow tissue organisation and native cells must be able to migrate into the defect to facilitate integration (Agrawal and Ray, 2001). Finally, the scaffold must have sufficient mechanical

integrity to survive surgical implantation and the loading of the synovial joint, while retaining its location in the defect. A scaffold can be derived from natural materials or be entirely synthetic. Scaffolds utilized in articular cartilage have been produced from fibrin, collagen, hyaluronan, alginate, agarose, polyurethane and polylactic acid (Stoddart et al., 2009, Hutmacher, 2000, Caterson et al., 2001). Scaffolds are frequently used in combination with ACI in order to attempt to achieve a more natural three-dimensional structure. This technique is termed matrix-induced chondrocyte implantations (MACI), with results that are comparable to the original ACI therapy (Bartlett et al., 2005).

1.7 Stem and progenitor cells

Stem cells are cells from eukaryotic organisms that are capable of self-renewal; these cells can differentiate into more specific specialised cell types of the body (Figure 1.12). There are different types of stem cells that have varying degrees of plasticity. The cells can be totipotent, pluripotent, multipotent or progenitor cells. Totipotent cells are from the blastomere and are capable of differentiating into all of the cells of the placenta and the embryo; however, they are not widely used in research. Pluripotent stem cells are capable of differentiation into all of the cell types of the body but not the placenta, these include embryonic stem cells (ES) and induced pluripotent stem cells (iPS). Adult stem cells such as neural stem cells, hematopoietic stem cells and mesenchymal stem cells reside within stem cell niches in the adult body. These cells are multipotent, they are further down the differentiation pathways and, therefore, have a more limited number of lineages into which they can differentiate. Progenitor cells are lineage-specific adult stem cells that can only differentiate into specific cell types. These cells reside in specific niches within a tissue. An example is the chondroprogenitor cells found in the surface zone of articular cartilage (Dowthwaite et al., 2004). Under specific culture conditions, stem cells can be differentiated into different cell types *in vitro*. These cells can then be used in regenerative therapies (through the production of grafts), disease modelling, drug design and toxicity testing.

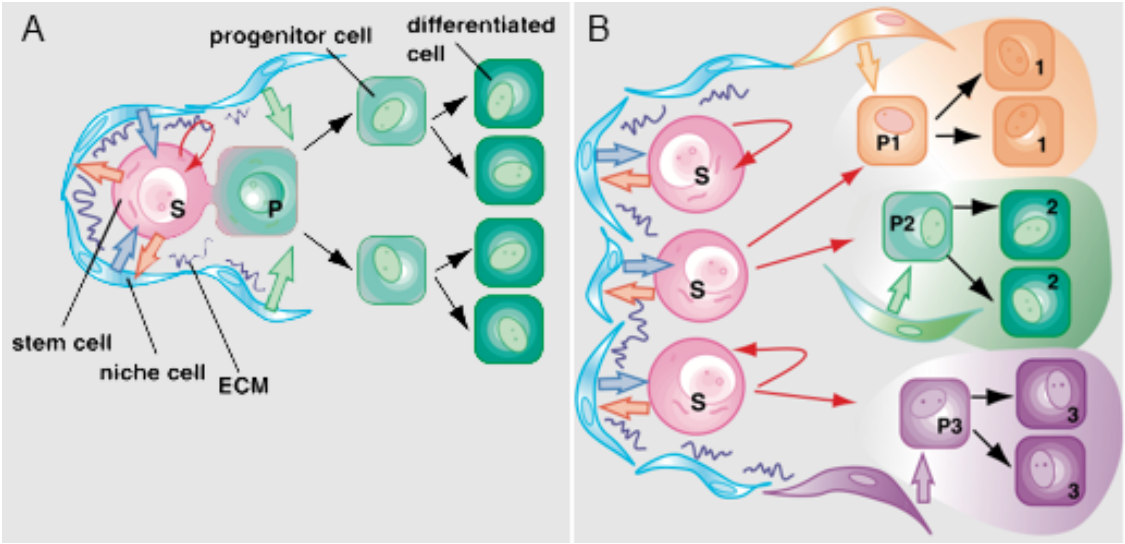


Figure 1.12: Alternate models of stem cells maintenance and differentiation.

A) Asymmetry division. A stem cell (S) forms a progenitor (P) with a more restricted proliferation potential by asymmetric division. The progenitor differentiates in response to extrinsic signals. The stem cell phenotype is maintained by reciprocal short and/or long-range signalling (thick coloured arrows). **B)** Populational asymmetry. Stem cells give rise to daughter cells that can be either stem cells or else progenitors that differentiate along different pathways (1, 2, and 3) depending on the combination of extrinsic factors to which they are exposed (Watt and Hogan, 2000).

1.7.1.1 Induced pluripotent stem cells

Recently, a method of returning terminally differentiated cells to an early developmental stage has been developed. This allows somatic cells to have pluripotency re-induced into them, producing an embryonic-like phenotype. These cells are called induced pluripotent stem cells (iPSC) and are now widely used in drug development and disease modelling (Yamanaka, 2007). An advantage of iPSCs over ES cells is that there are no ethical restraints associated with their use.

Production of autologous pluripotent cells from patients is a major goal in regenerative medicine. It provides a large cell source, which is required for treatment of the larger defects and removes the ethical complications associated with the use of embryonic cells. As these cells are produced autologously from the patient, there are no immune tolerance issues and, therefore, rejection of the graft is not a problem. This offers a benefit over ES cells, as it has recently been shown that these cells are not immune privileged; and therefore, strategies to

prevent graft rejection would need to be devised (Chidgey and Boyd, 2008). Reprogramming pushes differentiated cells back up the differentiation pathway to earlier developmental and epigenetic states (Figure 1.13) (Hochedlinger and Plath, 2009). Originally, reprogramming differentiated cells was performed by nuclear transfer. The nucleus of the differentiated cell is transplanted into an oocyte. The differentiated cell could also be reprogrammed by ES cell fusion where the somatic cell and an embryonic stem cell are fused. These methods although functional, have the major drawback of still requiring embryonic or oocyte cells (Pfannkuche et al., 2010). iPSCs can be produced by the introduction of different factors into the differentiated cell, completely removing the dependence on embryonic tissue sources (Yamanaka, 2007). Reprogramming by fusion suggested that ES cells contained factors that reprogrammed the somatic cell, twenty-four genes were tested but a combination of just 4 different genes were required. Reprogramming achieved with the transcription factors, c-Myc, Klf-4, Oct-3/4 and SOX-2; these are retrovirally introduced into differentiated cells to induce pluripotency (Figure 1.14) (Hochedlinger and Plath, 2009). iPS cells are not currently clinically utilized for transplantation as tumorgenicity is a concern due to the use of retroviruses (Yamanaka, 2007). However, more recent methods to produce iPSCs without the need for viral vectors have been developed, offering a valuable new resource for regenerative medicine and drug design (Webb, 2009). Reprogramming has also been achieved in the absence of c-Myc by instead introducing Lim28, this is beneficial for future iPS cell therapies as c-Myc is a known oncogene (Pfannkuche et al., 2010, Shi, 2009).

1.7.2 Multipotent adult stem cells

Once stem cells are confined in a certain tissue, they become multipotent adult stem cells. Adult stem cells undergo asymmetric self-renewing but have a more limited self-renewal ability, in part, because of the lack of high levels of telomerase. The array of differentiated cell phenotypes that can be generated from adult stem cells is limited, daughter cells can differentiate into cells of a specific tissue of origin but not into all the other cell types (Diez Villanueva et al., 2012). Adult stem cells include, but not limited to, mesenchymal stem cells (MSC), haematopoietic stem cells (HSC), neural stem cells and endothelial stem cells.

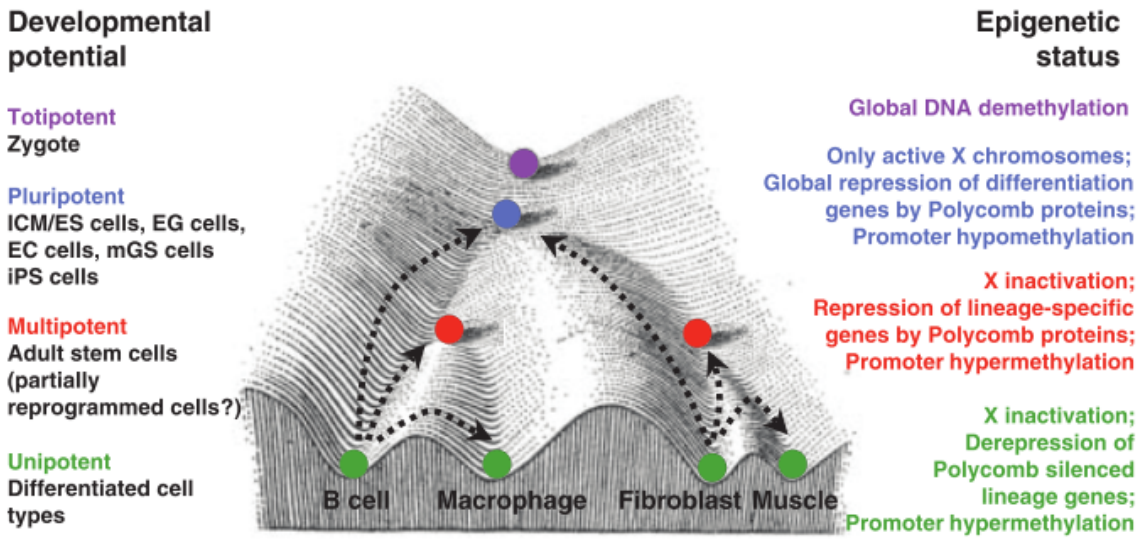


Figure 1.13: The epigenetic landscape of reprogramming differentiated cells.

(Hochedlinger and Plath, 2009).

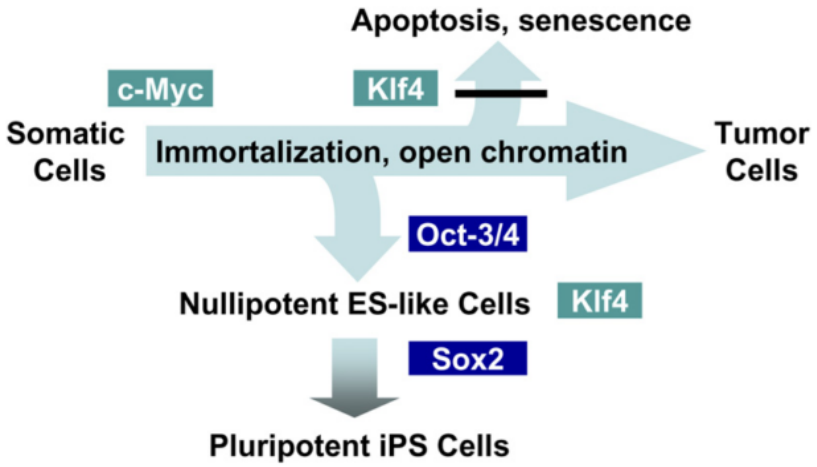


Figure 1.14: The transcriptional control of pluripotency

Reprogramming of differentiated cells requires 4 factors. C-Myc induces immortality and opens and activates the chromatin structure. Klf4 inhibits Apoptosis and senescence, normally associated with c-Myc expression. Oct-3/4 changes the cell fate from a tumorigenic cell to ES-like cell. Finally pluripotency is established by SOX-2 (Yamanaka, 2007).

1.7.2.1 Mesenchymal stem cells (MSC)

Friedenstein and co-workers first reported clonogenic fibroblast-like cells extracted from bone marrow *via* attachment to tissue culture plastic. These marrow-derived stromal cells (MSC) were found to be inherently osteogenic (Prockop, 1997, Friedenstein et al., 1976). It was soon discovered that these cells were capable of differentiating into multiple lineages, therefore, MSCs are typically defined as adherent, fibroblastoid-like cells that differentiate to osteoblasts, adipocytes, and chondrocytes *in vitro* (Figure 1.15) (Phinney and Prockop, 2007).

Since the initial isolation and characterisation of bone marrow-derived MSCs, MSCs have been found in numerous cells types including skeletal muscle, adipose tissue, synovium, dental pulp and the circulatory system as well as many other tissue types (Phinney and Prockop, 2007). The cells from different tissue types vary in their differentiation potential and efficiency. Unlike HSC, there is no singular marker for identification and extraction of MSCs and a panel of positive and negative selection marker criteria must be used. MSC populations commonly express surface proteins including CD29, CD44, CD49a-f, CD51, CD73, CD90, CD105, CD106, CD166, and Stro1 and must be negative for hematopoietic lineage markers including CD11b, CD14, and CD45 (Halfon et al., 2011). The panels of marker that should be used are frequently debated and numerous other markers are available in the literature, while specificity of other markers are often challenged. The International Society of Cellular Therapy recommended that MSCs must meet a minimum criteria including: adhesion to plastic, expression of surface markers CD73, CD90, CD105 and tripotent differentiation into chondrogenic, osteogenic and adipogenic phenotypes (Horwitz et al., 2005).

Johnstone and colleagues described a defined media for directed MSC differentiation into the chondrogenic lineage *in vitro*. This media included dexamethasone and TGF-β1 in the absence of foetal bovine serum (FBS) (Johnstone et al., 1998, Yoo et al., 1998). However, the utility of MSCs in chondrogenic repair still faces numerous issues; firstly the quantity and proliferative capacity of MSC are heavily reduced by age and degenerative changes in the joint are associated with aberrant differentiation of MSCs leading

to loss of chondrogenic potential and acquisition of a fibrogenic phenotype (Caplan, 2007, Barry and Murphy, 2013). Secondly, the purity of MSCs isolation is poor with only a fraction of these isolated cells capable of chondrogenic differentiation (Caplan, 2007). Finally, after undergoing chondrogenesis, the chondrocytes continue on to terminally differentiate, undergoing hypertrophy, reducing Collagen Type II expression and increasing the expression of Collagen Type I and X as well as the alkaline phosphatase enzyme required for calcification (Pelttari et al., 2008).

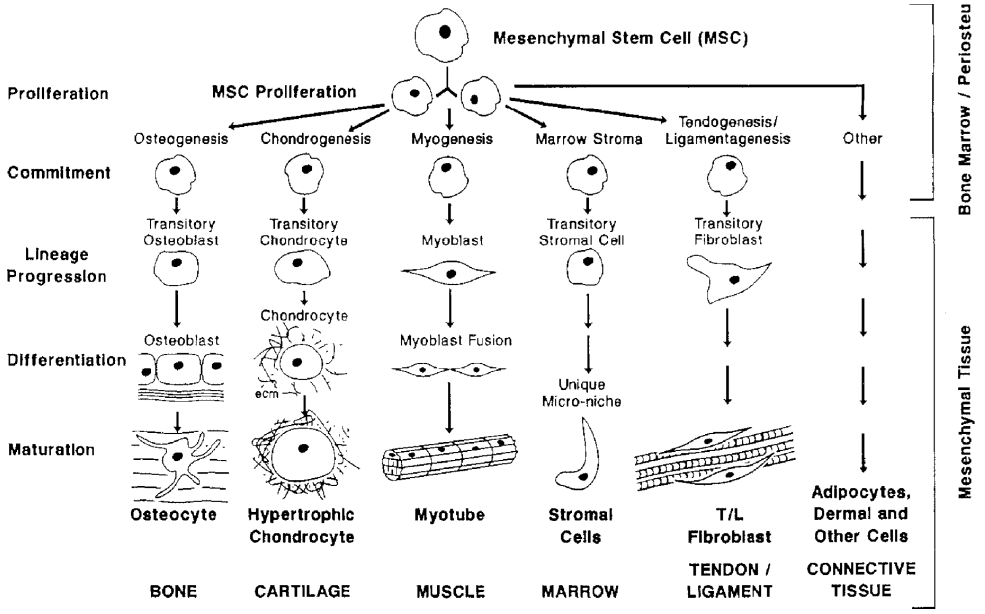


Figure 1.15: Schematic representation summarizing mesenchymal differentiation pathways.

MSCs can differentiate into multiple cell types of the mesenchymal lineage including bone, cartilage, muscle and fat (Caplan, 2009).

1.8 Resident mesenchymal progenitor cells in synovial joint tissues

Multiple MSC niches have been described in the synovial joint. These niches have been observed in tendons, bone marrow, the nodes of Ranvier at the periphery of articular cartilage, within the synovial fluid and membrane, the intra-articular fat pads and the articular cartilage itself (Dowthwaite et al., 2004, Jones et al., 2008, Karlsson et al., 2009, Khan et al., 2008b, Kurth et al., 2011). These stem cells offer potential cell sources for articular cartilage tissue engineering each have different differentiation potentials and have been utilized with varied success.

1.9 Stem cells in articular cartilage

Adult articular cartilage was thought to be devoid of stem cells or progenitors but recent work by multiple groups has demonstrated their presence *in vivo* and *in vitro* (Alsalameh et al., 2004, Dowthwaite et al., 2004, Fickert et al., 2004, Grogan et al., 2009, Pretzel et al., 2011, Williams et al., 2010, Nelson et al., 2014).

In vivo, chondrocytes demonstrate a slow or limited capacity for self-repair; this is assumed to be due to poor vascularisation, restricted cellular mobility and a lack of progenitor cells. It is generally accepted that articular cartilage grows through appositional growth from the joint surface and that, in immature tissue, progenitor cells are located at the articular surface (Dowthwaite et al., 2004, Hayes et al., 2001). The surface zone chondroprogenitors were isolated by Dowthwaite et al (2004) from immature bovine articular cartilage. These cells expressed the cell fate marker, Notch1 and preferentially adhered to fibronectin mediated by high α5β1 integrin (CD29 and CD49e respectively) expression. Under *in vitro* culture, this sub-population of cells exhibited a high colony forming efficiency and were able to undergo multiple population doublings while maintaining chondrogenic phenotype (Dowthwaite et al., 2004).

Tissue specific MSCs have also been isolated from healthy human adult articular cartilage. These cells are capable of multipotent differentiation, preferentially bind fibronectin and exhibit a high colony forming efficiency. It has been shown these cells are capable of over 70 population doublings *in vitro* (Williams et al., 2010). More recently, analysis of stem cell numbers in OA cartilage show that the number of stem cells doubles in diseased cartilage (Nelson et al., 2014). Alsalameh and colleagues identified a stem cell population expressing cell surface markers CD105 and CD166 in human cartilage. The majority of chondrocytes were found to express CD105 and a minority CD166. In combination, it was shown that approximately 3% of cells co-express the markers and these, when isolated and cultured, define a multipotent stem cell population. The number of CD105/CD166-positive cells was found to increase in OA, possibly in a reparative attempt (Alsalameh et al., 2004). Further work by Pretzel et al., (2011) separated cartilage cells using flow-cytometry for co-expression of CD105 and CD166. This study found approximately 15% of cells

were positive in normal cartilage and 17% in OA cartilage with expression confined to the mid- and surface zones. This is a high percentage for a stem cell population and, therefore, the specificity of CD105 and CD166 for isolation of cartilage stem cells could be insufficient (Pretzel et al., 2011). The assumption that current surface markers do not isolate specific cell populations is supported by the isolation of CD9/CD90/CD166-positive co-expressing cell population identified in osteoarthritic joints. These were multipotent and present at between 2-12% abundance (Fickert et al., 2004). Fickert et al., (2004) also identified a CD9/CD54/CD90-positive population at 13.6-19% of the total cells. The expression and distribution of stem cell markers Notch-1, Stro-1 and VCAM-1 identified a sub-population of cells in articular cartilage, 45% of cells labelled, therefore, the specificity of this combination is thought to be insufficient for selection of articular cartilage stem cells (Grogan et al., 2009).

Stem cell populations within articular cartilage offer a potentially novel and promising cell source for tissue engineering. Identification of markers and isolation methods are essential in ensuring the most effective repair. The use of specific markers to isolate chondroprogenitors will allow for further characterisation, including a more in-depth understanding of the mechanisms of proliferation, differentiation and disease within articular cartilage. This has the potential to lead to an improved understanding of the role of these markers and, as such, may provide us with a more beneficial cell type that could significantly contribute to the field of articular cartilage repair.

1.9.1 Chondrogenic differentiation of MSCs

Adult stem cells reside in their niche in an undifferentiated state, in order to form cartilage the cells must be induced to undergo chondrogenic differentiation. In culture, chondrogenic differentiation has been shown to require a 3D environment and a combination of growth factors. The TGF-β superfamily are the most common and most potent growth factors used for chondrogenesis. However, others including BMPs, FGF-2 and IGF-1 have been utilised (Johnstone et al., 1998, Longobardi et al., 2006). The synthetic drug dexamethasone (DEX) has been shown to be a powerful supplement, inducing chondrogenesis, it acts *via* the glucocorticoid receptor, synergistically increasing activation by TGF-β. Stimulation with TGF-β and DEX induces Collagen Type II, SOX-9 and Aggrecan

expression (Shintani and Hunziker, 2011, Sekiya et al., 2001). The addition of FGF-2 to MSCs has also been shown to induce cartilage-specific PGs expression and chondrogenic differentiation by inducing TGF-β signalling (Ito et al., 2008).

1.9.2 Stem cell definitions within this thesis

Embryonic stem cells are undifferentiated cells with infinite self-renewal capacity and pluripotent potential. Mesenchymal stem cells represent a multipotent adult stem cell with a reduced differentiation and proliferative potential than ES cells. MSC are defined by: a) plastic adherent, b) colony forming, c) immunophenotype, d) multipotential *in vitro* differentiation and e) extended proliferative capacity *in vitro* (Wagner et al., 2008). MSCs have a finite lifespan *in-vitro,* after around 40±10 population doublings MSCs enter senescence, morphologically characterized by enlarged and irregular cell shapes and a stop of proliferation (Stenderup et al., 2003). The maximum population doublings a cell can undergo before senescence is defined as the Hayflick limit (Hayflick, 1965). In this study a stem cell is defined as a plastic adherent, colony-forming cell with a Hayflick limit greater than 30 population doubling and the capacity for multipotential differentiation *in vitro*.

1.10 Aims of this thesis

Articular cartilage specific MSCs have been isolated from normal and osteoarthritic cartilage. These stem cells are required for tissue engineering; however, specific isolation of these cells has been problematic. Classical MSC stem cell markers are variable, unreliable and non-specific in articular cartilage. Using full-depth de-differentiated chondrocytes and clonally-derived stem cell lines from human articular cartilage, this study attempted to use transcriptomics to discover novel stem cell markers for use in localising, identifying and isolating stem cells. Detection of markers for a pure stem cell population will allow lineage tracing of stem cells during cartilage development and disease, and enhance tissue engineering strategies through the isolation of potent, chondrogenic and proliferative cell-lines.

This study used Next Generation Sequencing (NGS) transcriptomic techniques to discover differentially expressed stem cell specific genes using culture-expanded cell populations. We further investigated the expression of novel stem cell markers in cultured-expanded chondrocytes to determine whether sub-populations of stem cells could be identified and efficiently isolated. Stem cell markers were used to determine the abundance and location of articular cartilage stem cells within healthy and osteoarthritic tissue. Fluorescence activated cell sorting was employed with the aim to reliably isolate a stem cell population and assess the potential as a cell source for regenerative therapies.

This will be achieved by:

- Next generation transcriptomic sequencing and computational analysis
- Real time polymerase chain reaction
- Histological analysis by immunofluorescence of stem cell markers
- Immunocytochemistry of stem cell markers *in vitro*
- Fluorescence activated cell sorting

1.11 Hypothesis

Transcriptomics will identify novel biomarkers of articular cartilage-derived stem cells. These novel markers will allow for the identification, localisation and isolation of a stem cell population for use in regenerative therapies.

CHAPTER 2:

GENERAL METHODS

2.1 Tissue isolation

Human tissue was acquired from healthy normal donors (NHS Blood and Tissue Bank, Liverpool, UK) and patients diagnosed with OA, who had undergone total knee replacement surgery. All tissue was obtained under institutional and local NHS Research Ethics Committee and patient consent. OA was diagnosed following physical, radiographic and biochemical examination. The full-depth articular cartilage biopsies were obtained from the tibial plateaux of males and females for both the normal donors (n = 12; mean age 49.4yrs, range 25-75) and OA donors (n = 7; mean age 56.4yrs, range 50-85). Only tissues from the tibial plateaux were used for this study; cartilage and bone obtained from the femoral condyles were omitted in this analysis in order to maintain consistency. Biopsies from OA donors were taken from a region adjacent to the lesion site that showed macroscopic roughening but not degraded cartilage. Following surgery or post-mortem, tissue was immediately transported from the hospital to the laboratory in sterile saline solution.

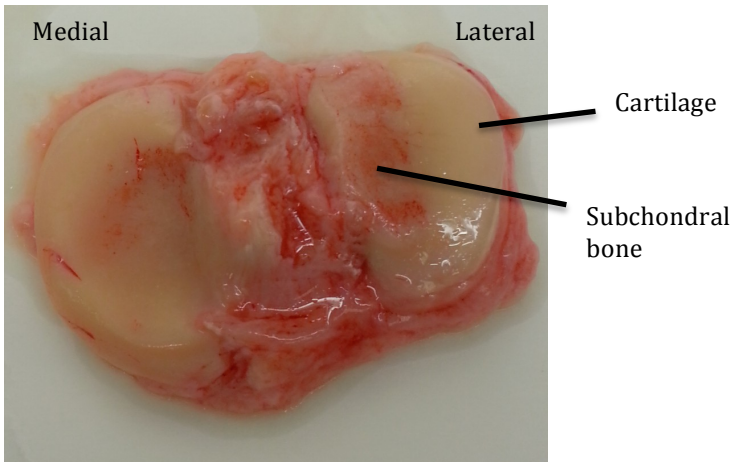


Figure 2.1 – Labelled photograph of the human tibial plateaux excised from a total knee replacement

2.2 Cell isolation and culture

2.2.1 Pronase and collagenase digestion

Chondrocytes were isolated by sequential pronase (70U ml^{-1}, 1 hour at 37°C) and collagenase (300CDU ml^{-1}, 3 hours at 37°C) digests. Isolated cells were either plated as a full-depth chondrocyte control populations or articular cartilage-derived stem cell populations were selected by differential adhesion to fibronectin as described by Dowthwaite et al., (Dowthwaite et al., 2004).

2.3 Selection of stem cells

2.3.1 Fibronectin adhesion

Six well plates were coated with 10µg ml^{-1} fibronectin (FN; Sigma, UK) in 0.1M phosphate buffered saline (PBS, pH7.4) containing 1mM $MgCl_2$ and 1mM $CaCl_2$ (PBS+) overnight at 4°C. The isolated full-depth chondrocytes (500 cells in 1ml) were seeded onto the fibronectin coated plates for 20 minutes at 37°C in Dulbecco's modified Eagle's medium (DMEM). After 20 minutes, media and non-adherent cells were removed. Fresh DMEM containing Penicillin 100µg ml^{-1}/Streptomycin 100U ml^{-1}, 0.1mM ascorbic acid, 0.5mg ml^{-1} L-glucose, 10mM HEPES, 1mM sodium pyruvate, 2mM L-glutamine and 10% irradiated foetal bovine serum (FBS) (DMEM+) were added to the remaining adherent cells which were maintained in culture for up to 12 days.

2.3.2 Colony isolation

At day 12, colonies of 32 cells or more, derived from more than 5 population doublings (PD) of a single cell, were counted and isolated using sterile cloning rings (Sigma, UK). Cloning rings were placed over the colony and 100µl of trypsin was added to detach the cells from the plate. After 5 minutes at 37°C, the cell suspension was removed and transferred to 24 well plate containing culture media

2.4 Culture media

Dulbecco's modified Eagle's medium (DMEM) containing Penicillin 100µg ml^{-1} /Streptomycin 100U ml^{-1}, 0.1mM ascorbic acid, 0.5mg ml^{-1} L-glucose, 100mM HEPES, 1mM sodium pyruvate, 2mM L-glutamine and 10% irradiated foetal bovine serum (FBS) (DMEM+) plus 1ng ml^{-1} TGF–β2 (PeproTech, UK) and 5ng ml^{-1} FGF-2 (PeproTech, UK).

2.4.1 Monolayer expansion

Once the cells reached confluence, they were washed in serum-free media and incubated in trypsin-EDTA for 5-8 minutes at 37˚C. The lifted cells were transferred to a 50ml centrifuge tube and an equal volume of DMEM + 10% FCS was added to the tube to deactivate the trypsin. The cell suspension was then

centrifuged at 2000 rpm for 5 minutes. The supernatant was removed and the pellet was re-suspended in DMEM+ plus 1ng ml^{-1} TGF–β2 and 5ng ml^{-1} FGF-2.

2.4.2 Population doublings

At each passage, the number of cells obtained and the number of cells re-plated was recorded; this was used to calculate population doublings using the equation:

$$PD = X + 3.322 (\log Y - \log I)$$

Where: X = The previous population doublings
Y = The number of cells harvested
I = The inoculation number

2.5 Colony forming efficiencies

Twenty-four hours after plating cells by the fibronectin adhesion assay, the number of adhered cells was counted in both OA and normal cultures. After 14 days of culture, clusters of more than 32 cells (clonal) were counted. Colony forming efficiencies were calculated as a percentage of the initial seeding density. Colonies of thirty two cells after 14 days in culture was chosen as the threshold as this number represents a population of cells derived from more than 5PD of a single cell, thereby discounting a transient amplifying cell cohort.

2.6 Differentiation

Differentiation studies were undertaken to determine phenotypic plasticity of cells. Both monolayer and 3D differentiation protocols were utilised throughout this study.

2.6.1 Media

2.6.1.1 Chondrogenic

Chondrogenic media contained DMEM/F12 + Glutamax with 10% heat-inactivated FCS (FBS was placed at 56^{o}C for 30 minutes to degrade complement and most labile proteins), Penicillin 100µg ml^{-1}/Streptomycin 100U ml^{-1}, 100µg ml^{-1} ascorbic acid, 1mg ml^{-1} L-glucose, 2mM L-glutamine, 1% HEPES, and

supplemented with 1% insulin transferring selenium (ITS), 0.1μM dexamethasone and 10ng ml^{-1} TGF-β1)

2.6.1.2 Osteogenic

Osteogenic differentiation medium contained DMEM + 10% FCS, 10mM β-glycerophosphate, 10nM dexamethasone and 0.1mM L-ascorbic-acid-2-phosphate), Penicillin 100μg ml^{-1}/Streptomycin 100U ml^{-1} and 1% Hepes.

2.6.1.3 Adipogenic

Adipogenic differentiation media contained DMEM + 10% FCS containing 10μg ml^{-1} insulin, 1μM dexamethasone, 100μM indomethacin, 500μM 3- isobutyl-1-methyl xanthine (IBMX) and 15% normal rabbit serum.

2.6.2 Monolayer

Chondrogenic, osteogenic and adipogenic differentiation was undertaken in monolayer. Six-well plates were seeded at $5x10^4$ cells *per* well and cultured in DMEM+ plus 1ng ml^{-1} TGF–β2 and 5ng ml^{-1} FGF-2 until 70-80% confluence. At this point the culture media was changed to the appropriate differentiation media detailed previously, control samples were maintained in the usual culture media. Cultures were maintained for 10 days with the media changed every 2 days.

2.6.3 Pellet cultures

For chondrogenic and osteogenic differentiation, 3D-pellet cultures were also employed. Confluent culture flasks were trypsinised as described in 2.4.1. Total cell number was counted and half a million cells were placed in a 1.5ml Eppendorf tube containing 1ml of either chondrogenic or osteogenic media. The Eppendorf tube containing cells was then centrifuged at 2000 rpm for 10 minutes and incubated at 37˚C. Pellets were fed every second day for 3 weeks.

2.7 RNA extraction

2.7.1 RNA from cells

RNA was extracted from monoclonal cell lines using RNeasy™ kit and a DNase1 column digest (Qiagen, UK). One million cells were used for RNA isolation for each cell line

2.7.2 RNA from tissue

Tissue was weighed and 100mg was placed in a shaking flask containing a grinding ball and 1ml of trizol (TRI) reagent. The sealed shaking flask containing tissue, TRI reagent and the grinding ball were snap-frozen in liquid nitrogen. Tissue was homogenised by shaking at 2000 rpm for 1 minute using a micro-dismembranator (B. Braun Biotech). The powdered material was collected and stored at -80^{o}C until needed. RNA was then extracted and purified from the TRI reagent using RNeasy™ kit with a DNase1 column digest (Qiagen, UK). Between each sample isolation, the shaking flasks and grinding balls were cleaned, initially using a detergent in tap-water, and then they are rinsed in distilled water 3 times and finally placed in 5M NaOH for 5 minutes and rinsed 3 times in distilled water.

2.7.3 RNA from pellets

After 3 weeks, pellets were placed in three hundred and fifty microlitres of Buffer RLT (Qiagen, UK) with 10µl ml^{-1} β-mercaptoethanol. The pellet was disrupted and lysed by gentle pipetting and snap-frozen at -80°C Pellet lysates were stored at -80^{o}C until needed. RNA was isolate and purified using the Qiagen RNeasy™ Mini Kit and DNase1 column digest (Qiagen, UK).

2.7.4 Qiagen RNeasy kit

Outlined is the protocol utilised to extract RNA using the RNeasy kit. The lysate was transferred into a RNeasy spin column in a 2ml collection tube and centrifuged for 15 seconds at maximum speed (10,000 rpm) and the flow through discarded. To eliminate genomic DNA contamination, additional on-column DNase digestion steps were carried out. Three hundred and fifty microlitres of Buffer RW1 was added to the spin column and centrifuged for 15

seconds at 10,000 rpm. Ten microlitres of DNase I stock solution was added to 70µl Buffer RDD and placed directly on the RNeasy spin column membrane and left for 15 minutes at room temperature. Subsequently, 350µl Buffer RW1 was added to the spin column and centrifuged for 15 seconds at 10,000 rpm. Five hundred microlitres of Buffer RPE were then placed onto the RNeasy column and centrifuged for 15 seconds at 10,000 rpm. Another 500µl of Buffer RPE was added to the RNeasy column and centrifuged for a further 2 minutes at 10,000 rpm. After every step, the flow-through was discarded. To elute the total RNA, the RNeasy column was transferred to a new 1.5ml collection tube, and 50µl of RNase-free water was placed onto the RNeasy membrane and centrifuged for 1 minute at 10,000 rpm. The total RNA was stored at -80°C.

2.7.5 Estimation of RNA quantification and purity

Total RNA was quantified by measuring the absorbance at 260nm and 280nm using a NanoDrop ND-100 Spectrophotometer (NanoDrop Technologies, UK) against a blank of molecular biology grade water. The shape of the absorbance curve and the ratio of absorbance provides an indication of the purity of the RNA with respect to contaminants that absorb in the UV spectrum such as proteins and phenol. Pure RNA has an A_{260}/A_{280} ratio of ~2.0.

2.8 Complementary DNA (cDNA) synthesis

cDNA was produced from the extracted RNA. The amount of RNA was standardised to 1µg *per* reaction. Reactions were performed in 50µl containing, 400µM dNTPs, 0.4µg of random hexameric primers (Promega), 0.2U/µl avian myeloblastoma virus (AMV) reverse transcriptase (RT) enzyme (Promega) and 0.5U/µl RNasin (Promega). Samples were incubated at 25^{o}C for 10 minutes, 48^{o}C for 1 hour and then 95^{o}C for 2 minutes in a thermocycler.

2.9 Polymerase chain reaction (PCR)

PCR amplification of genes of interest were carried out using cDNAs. Reactions were performed in 100µl volumes containing 2.5mM $MgCl_2$, 200nM of each forward and reverse primer, Go*Taq* Flexi buffer, pH8.5 and 1 unit of Go*Taq* Hot start DNA polymerase in the presence of 200µM dNTPs (Promega, UK). The

following thermocycler protocol was used; initially denature at 95˚C for 3 minutes and then amplified for 40 cycles at 95˚C for 30 seconds, primer specific annealing temperature (Tm) for 30 seconds, and the extension phase was held for 30 seconds at 72˚C (refer to Table 4.3 for annealing temperatures). A final extension was held at 72˚C for 10 minutes.

2.10 Agarose gel electrophoresis

Nucleic acid was resolved on 2% (w/v) agarose gels containing SafeView nucleic acid stain at 5µl *per* 50ml prepared in 1x Tris Borate EDTA (TBE) buffer. DNA ladders were run alongside the products. Gels were visualised using a transilluminator on a Bio-Rad ChemiDoc.

2.11 Molecular cloning

PCR products were purified using QIAquick PCR clean up kit (Qiagen, UK). Purified PCR products were ligated into the vector pBSTA at a 1:3 molar ratio (insert: plasmid) using T4 ligase (NEB, UK), 4^{o}C overnight. Ligated vectors were transformed into competent cells. In brief, competent cells were defrosted on ice; 1µl of 1M dithiothreitol (DTT) was added *per* 100µl competent cells. Vector was added at a 1:10 ratio (vector:cells) and incubated on ice for 20 minutes. Competent cells were heat-shocked at 45^{o}C for 1 minute and then 100µl of SOC media added. Ten microliters of 1M Isopropyl β-D-1-thiogalactopyranoside (IPTG) and 20ml 5-bromo-4-chloro-3-indolyl-β-D-galactopyranoside (X-Gal) (Promega, UK) were added before spreading on Luria broth (LB) agar plate containing ampicillin (50µg ml^{-1}). Plates were left to absorb and incubated at 37^{o}C overnight. White colonies were selected and cultured in 2ml of 2-YT broth at 37^{o}C overnight in a shaker incubator. Plasmids were extracted and purified using Wizard® Plus SV miniprep DNA purification kit (Promega, UK). Purified plasmids were sequenced to ensure the correct identity of the insert.

2.12 Quantitative polymerase chain reaction (qPCR)

Quantitative polymerase chain reaction (qPCR) was completed using the ABI 7700 and the Biorad CFX96 detection systems. The fluorescent dye SYBR Green was used to determine the absolute expression levels of potential stem cell

markers. Real-time PCR reactions were carried out in 25 µl volumes in a 96-well plate (Agilent Technologies™) containing 3.5 mM $MgCl_2$, 200 µM dNTPs, 0.3 µM of sense and antisense primers, 0.025 U/µl enzyme and 1:66000 SYBR Green. All reactions were made using GoTaq qPCR Master Mix (Promega, UK). Absolute values for the gene of interest were calculated from standard curves generated using serially diluted plasmid templates cloned and the sequence verified.

2.13 Tissue processing

Tissue biopsies were fixed to prevent antigen loss or degradation and to preserve antigen position to allow for possible detection by antibodies. For this study, three predominant fixation methods were used, 10% neutral buffered formalin (NBFS), ice cold 95% ETOH and snap-freezing by immersion in a pre-cooled n-hexane/ETOH/dry ice bath.

2.14 Pellet processing

Following the incubation period, the pellets were washed in PBS and then fixed in 4% paraformaldehyde (PFA) for 20 minutes. The pellets were dehydrated in graded alcohols (70%, 95% and 100% x 2) with changes of 20 minutes each before being cleared in xylene (one change of 20 minutes), infiltrated with paraffin wax at 56˚C for one hour and finally embedded in paraffin wax. Following embedding, the pellets were sectioned as outlined in Section 2.15.

2.15 Tissue processing

Tissue fixed in 10% NBFS or 95% ETOH overnight were dehydrated in graded alcohols (70%, 95% and 100% x 2) with changes of 20 minutes each before being cleared in xylene (one change of 20 minutes), and paraffin wax embedded at 60°C for 1 hour twice.

2.16 Paraffin wax sectioning

The embedded tissue biopsies and pellets were sectioned at a thickness of 10µm using a microtome (Leitz 1512, UK) and placed in a water bath at 45°C to flatten. Sections were removed on poly-l-lysine histology slides and dried in an

incubator for 24hrs at 45^{0}C. Prior to use slides were deparaffinised in xylene (2x2 minutes) and rehydrated in graded alcohol for 2 minutes at each concentration; concentrations of ethanol were 100% (x2), 95% and 70% followed by 2 minutes in tap water.

2.17 Cryosectioning

Tissue was snap-frozen in n-hexane using dry ice and ethanol. The frozen, unfixed tissue was embedded in OCT embedding media (R.A. Lamb, UK). Tissue was sectioned at a thickness of 10μm using a cryostat (Bright OT5000, UK) and mounted on poly-l-lysine histology slides. Slides not used immediately were stored at -80°C until required.

2.18 Immunofluorescence optimisation

Primary antibody concentrations were optimised by titration. Secondary antibodies were used at 10μg ml^{-1} and primary antibodies were titrated at 2.5, 5 and 10μg ml^{-1}.

An enzymatic pre-treatment is often necessary in cartilage due to large amounts of glycosaminoglycans and proteoglycans present in the tissue result in masking of antigens. Each antibody was tested on tissue fixed with 10% NBFS and 95% ETOH and snap-frozen cryosections. Both cryosections and paraffin wax sections were tested without enzymatic treatment, with a hyaluronidase digest, with a chondroitinase ABC digest and a combination of both enzymes. Wax embedded sections were also tested with and without antigen retrieval through boiling sections for 1 minute in an unmasking solution (Vectorlab). For all antibodies used in this study, optimum staining was found using 10% NBFS fixed tissue after the unmasking procedure and a combination of hyaluronidase and chondroitinase ABC digests.

Background fluorescence can be a problem in articular cartilage and to reduce this where possible, far-red (Alexa Fluor 633, 647) fluorophores were used.

2.19 Antigen unmasking

Paraffin-wax embedded tissue sections were rehydrated as described in section 2.15 and boiled for 1 minute in antigen unmasking solution (Vectorlab). Sections were washed with PBS and incubated with hyaluronidase (Sigma-Aldrich; 2U ml-1) and chondroitinase ABC (Sigma C3667 0.1U ml^{-1}) in PBS 0.2% Triton-X-100. Sections were incubated at 37°C for 1 hour and then washed for 5 minutes in PBS before proceeding to block with relevant sera to secondary antibodies.

2.20 Immunostaining

2.20.1 Immunocytochemistry

Immunofluorescence detection of stem cell markers was performed on culture-expanded cell lines. Primary and secondary antibody concentrations were optimised for each protein. All antibodies and immunoglobulin matched (IgG-matched) controls were prepared in PBS (Sigma-Aldrich) containing 0.2% Triton-X-100 (Sigma-Aldrich) and 5% blocking serum (serum was species matched to the secondary antibody). Samples were washed 3 times in PBS/0.1% Tween-20 (PBST) and blocked in 10% relevant sera for 1 hour. Excess serum was removed and cells were incubated with primary antibodies for 1 hour at room temperature. The slides were washed 3 times in PBST and then incubated with fluorescence 10μg ml^{-1} conjugated secondary antibodies for 1 hour at room temperature. Samples were washed a further 3 times in PBST before being mounted in Vector shield ™ containing DAPI.

2.20.2 Immunofluorescence

Immunofluorescence detection (of wax or frozen sections) of primary antibodies was used to detect the presence of stem cell markers in articular cartilage tissue. Primary and secondary antibody concentrations were optimised for each protein. All washes and incubations steps were performed at room temperature and in a darkened humidified chamber unless otherwise stated. All antibodies and immunoglobulin matched (IgG-matched) controls were prepared in PBS (Sigma-Aldrich) containing 0.2% Triton-X-100 (Sigma-Aldrich) and 1% blocking serum (serum was species matched to the secondary antibody).

Wax embedded sections were unmasked and rehydrated as described previously (Section 2.15 and 2.17) and cryosections were hydrated for 5 minutes in PBS before fixation in fresh 95% ETOH for 2 minutes at 4°C. Sections were circled with a water-repellent marker (Dako pen; Vectorlab, UK), washed 3 times in PBS/0.2% Triton-X-100 and blocked in 10% relevant sera for 1 hour. Excess serum was removed by blotting and sections were incubated with primary antibodies overnight at 4^{o}C. The slides were washed 3 times in PBST and then incubated with 10μg ml^{-1} fluorescence conjugated secondary antibodies for 1 hour at room temperature. Samples were washed a further 3 times in PBST before being mounted in Vector shield ™ containing DAPI. Control sections were identically processed with either omission of primary antibody or incubation with IgG-matched controls.

2.21 Histology

Sections were rehydrated through xylene and graded alcohols to distilled water as described in Section 2.15 prior to staining. Subsequent imaging of histological staining was performed with the Leica BX51 brightfield microscope.

2.21.1 Alcian blue

To detect sulphated GAGs alcian blue staining was carried out. Alcian blue solution (1%) was made by dissolving 1g in 100ml acetic acid; the pH was adjusted to pH2.5 on the day of use. Rehydrated slides or cells stained in Alcian blue solution for 30 minutes and washed in running tap water for 2 minutes. Samples were dehydrated with 2 changes of 95% ethanol (3 minutes) and cleared in xylene, 3 minutes. Samples were mounted using DPX under a cover slip.

2.21.2 Toluidine blue

To detect sulphated GAGs toludine blue staining was carried out. Rehydrated slides were stained in 0.04% toluidine blue for 10 minutes. Following staining, sections were washed in running water for 2 minutes (or until water was clear). Slides were then counterstained in 0.02% Fast Green solution for 3 minutes and

then rinsed in 2 changes of distilled water. Toluidine blue stained sections were air-dried overnight and mounted under coverslips using DPX the following day.

2.21.3 Safranin –O

To detect sulphated GAGs safranin-O staining was carried out. Rehydrated slides were stained in haematoxylin for 5 minutes and then washed in running water until clear. The stain was differentiated in 1% acid-alcohol for 2 seconds and then rinsed in distilled water. Slides were then counterstained in 0.02% Fast Green solution for 1 minute and placed in 1% acetic acid for 30 seconds. Slides were immediately stained in 1% safranin-O solution for 30 minutes and cleared in 95% ethanol. Samples were dehydrated in graded alcohols and cleared in 2 changes of xylene before mounting in DPX under a cover slip.

2.21.4 Alizarin red

To detect mineralisation alizarin red staining was carried out. Slides were rehydrated and cells were fixed in 10% NBFS for 20 minutes then washed in PBS. Samples were stained in 2% Alizarin redpH4.22 solution for 30 seconds. Excess stain was removed and samples blotted. Samples were dehydrated in acetone for 20 seconds, then acetone: xylene (1:1) for 20 seconds before clearing in xylene. Samples were mounted using DPX under a cover slip.

2.21.5 Von Kossa

To detect mineralisation von Kossa staining was carried out. Rehydrated sections were washed for a further 2 minutes to allow the von Kossa silver impregnation technique to be performed. Sections were stained with fresh 5% aqueous silver nitrate for 30 minutes under bright light, and then rinsed 3 times in distilled water. The stain was developed using 5% sodium carbonate in 10% NBFS for 5 minutes. Sections were then rinsed in distilled water before fixation in 5% sodium thiosulphate for 2 minutes. Samples were mounted using DPX under a cover slip.

2.21.6 Oil red –O

To detect lipid deposits oil red -O staining was carried out. Cells were fixed in

10% NBFS for 20 minutes and washed in PBS. Fresh Oil red-O was prepared from a stock solution of 0.5% Oil red-O in 100% isopropanol by diluting 30ml stock solution in 20ml distilled water. Cells were rinsed in 60% isopropanol and stained with Oil red-O working solution for 15 minutes at room temperature. Cells were rinsed in 60% isopropanol before nuclei staining with haematoxylin for 20 seconds. Cells were washed with distilled water and mounted in glycerol.

2.21.7 Crystal violet

Crystal violet staining was used to visualise cell membranes. Cells were fixed in 10% NBFS for 5 minutes and washed in PBS. Samples were stained in 0.05% crystal violet solution for 30 minutes and washed 2 times in tap water. Cells were mounted in glycerol under a cover slip.

2.22 Statistics

Statistical analyses are outlined in each individual Chapter.

CHAPTER 3:

WHOLE TRANSCRIPTOME NEXT GENERATION SEQUENCING OF CARTILAGE STEM CELLS

3.1 Introduction

Articular cartilage is classically believed to comprise of a single cell type, the chondrocyte, which is embedded within a complex extracellular matrix. Distinctive chondrocyte subpopulation phenotypes are identifiable within the superficial, radial, deep and calcified zones of articular cartilage. Chondrocytes are a differentiated cell type derived from multipotent progenitors, the mesenchymal stem cells (MSCs) (Alsalameh et al., 2004). Friedenstein and colleagues first identified MSCs in bone marrow in the 1970s (Friedenstein et al., 1976). MSCs can differentiate into multiple lineages including chondrocytes, osteocytes, adipocytes tenocytes and myocytes (Caplan, 1991, Phinney and Prockop, 2007). MSCs can be characterised, identified and isolated through the expression of particular cell-surface antigens including CD29, CD44, CD45e, CD90, CD73, CD105, CD166 and STRO-1 (Barry et al., 1999, Bruder et al., 1998a, Bruder et al., 1998b, Lv et al., 2014, Majumdar et al., 2003).

It has been shown that articular cartilage grows by appositional growth from the articular surface and therefore, a population of progenitor cells must reside within the tissue to generate growth (Hayes et al., 2001). Progenitor cells were first reported to reside in the surface zone of bovine articular cartilage after isolation through adhesion to fibronectin *in vitro;* challenging the notion of the single cell phenotype within articular cartilage (Dowthwaite et al., 2004). Recent studies by multiple groups have demonstrated the presence of progenitor cells *in vivo* and *in vitro* (Alsalameh et al., 2004, Dowthwaite et al., 2004, Fickert et al., 2004, Grogan et al., 2009, Pretzel et al., 2011, Williams et al., 2010, Nelson et al., 2014). These studies demonstrated that a sub-population of cells expressing various combinations of CD105/CD166/CD90, Notch-1, Stro-1 and VCAM-1 are present within human articular cartilage and that these cells can differentiate into chondrocytes, adipocytes and osteoblasts.

CD166 is widely expressed by both hematopoietic and non- haematopoietic cells including mesenchymal stem cells and bone marrow stromal cells where it may act to support both hematopoietic and mesenchymal progenitor cells by inhibiting stem cell differentiation (Nelissen et al., 2000, Ohneda et al., 2001). Mesenchymal stem cells lose CD166 expression when alkaline phosphatase

expression begins during osteogenic differentiation (Bruder et al., 1998a). CD105 (Endoglin) is a membrane glycoprotein that forms part of the TGF receptor complex and plays an important role in angiogenesis (Duff et al., 2003). Although frequently used as a surface antigen for identification of MSCs, in cartilage, the majority of differentiated chondrocytes express CD105 (Alsalameh et al., 2004). CD90 expression is highest during proliferation, with greater expression seen in culture-expanded chondrocytes than *in vivo* (Diaz-Romero et al., 2005). Notch and its transmembrane ligands are cell surface proteins that regulate cell differentiation during development and have been suggested as potential progenitor markers (Hayes et al., 2003). Stro-1 is a cell surface protein expressed by bone marrow stromal cells (Simmons and Torok-Storb, 1991). A subset of human bone marrow cells expressing Stro-1 was found to be multipotent, capable of differentiating into several mesenchymal lineages including, haematopoiesis-supportive stromal cells with a vascular smooth muscle-like phenotype, adipocytes, osteocytes and chondrocytes (Dennis et al., 2002).

The suitability of the MSC surface antigens for identification of articular cartilage-derived stem cells is ambiguous. A large and variable percentage of cells are isolated utilising these markers (2-45%) and, therefore, the specificity of such markers for isolation of stem cells within articular cartilage could be deemed insufficient. It has also been reported that enzymatic digestion of cartilage can alter the expression of mesenchymal stem cell surface antigens and that freshly isolated cells and cell cultured for 24hrs have highly variable expression levels (Richardson, 2011). Therefore, the aim of this study is to identify a novel panel of candidate stem cell markers, which are suitable for the identification and isolation of articular cartilage-derived stem cells, both *in vitro* and *in vivo* using next generation transcriptomic sequencing.

The transcriptome is the complete gene transcript complement of a cell or tissue, at a specific developmental stage or physiological condition. Transcriptomics allows analyses of mRNAs, non-coding RNAs and small RNAs to determine the transcriptional structure of genes and to quantify changes in gene expression levels at different times or conditions.

Many methodologies exist for analyses and quantification of the transcriptome, including hybridisation- and sequence-based approaches. Hybridisation-based approaches involve incubating fluorescently labelled cDNA with microarrays. Hybridisation-based approaches are high throughput and relatively inexpensive, however, these methods have several limitations. These include reliance upon prior knowledge about the genome, high background levels, a limited dynamic range for detection and, finally, cross comparison between different experiments is difficult requiring complicated normalisation methods (Wang et al., 2009).

Sequence-based approaches directly determine the cDNA sequence. In 1977, a technique faster and less hazardous than previous methods of sequencing was published by Sanger and Coulson (Sanger et al., 1977). Sanger sequencing is sequencing by termination; this technique uses di-deoxynucleotides to terminate the polymerization of the DNA at specific nucleotides. These nucleotides are then separated on a gel by size; it is relatively low throughput, expensive and not quantitative. Improvements, such as the inclusion of Taq polymerase, dye labelled oligonucleotides and parallel capillary electrophoresis allow up to 750bp read lengths and increase the speed of Sanger sequencing (Schuster, 2008). Sanger sequencing can only analyse a portion of the transcript and isoforms are generally indistinguishable, therefore, the information on the structure of transcriptome is limited (Mak, 2011).

Recently, the development of novel high-throughput DNA sequencing methods has provided a new method for both mapping and quantifying transcriptomes. This second generation of sequencing included development of pyrosequencing; this technique detects pyrophosphate release from oligonucleotides when incorporated by polymerase (Schuster, 2008). This is sequencing by synthesis; this technique allows parallel analysis, increased efficiency by 50 times and decreased costs by ~80% of that of Sanger sequencing (Schuster, 2008). The improvements have allowed for RNA sequencing RNA-seq to revolutionise the way in which eukaryotic transcriptomes are analysed (Wang et al., 2009).

RNA-seq can be achieved in 2 ways; either RNA is converted to a library of cDNA fragments with adaptors attached to one or both ends or sequencing can be performed directly from RNA (Ozsolak et al., 2009). If a cDNA library is produced, the library can be amplified if quantity is low. The sequencing occurs

in a high-throughput manner to obtain short sequences from one end (single-end sequencing) or both ends (pair-end sequencing) of the templates. The reads can be between 30–400bp, depending on the sequencing platform used. The sequence reads are then aligned to a reference genome/transcripts, or assembled *de novo* without the genomic sequence to create a transcription map that contains both the transcriptional structure and level of gene expression (Wang et al., 2009, Mak, 2011).

Next generation sequencing offers numerous advantages, firstly, unlike microarray, RNA-Seq is not reliant on sequences from prior known genomic information. This makes RNA-Seq particularly attractive for non-model organisms with genomic sequences that are yet to be determined. RNA-Seq has a high resolution and transcription boundaries can be located to a single base. In addition, RNA-Seq can also reveal sequence mutations (for example, SNPs) in the transcribed regions. RNA-Seq has next to no background signal and does not have an upper limit for quantification. There is a huge dynamic range with fold-changes of tens of thousands being detected and the range of over five orders of magnitude in transcript expression that is detectable. By contrast, DNA microarrays lack sensitivity for genes with low or very high levels and, therefore, the dynamic range is just a few-hundred-fold. RNA-Seq has also been shown to be highly accurate, correlating with qPCR and spike in RNA controls of known concentrations (Wang et al., 2009). The technique is highly reproducible and offers a greater array of information than classical transcriptomic methods.

RNA-seq as a technique is challenging, the library construction is complex, the purity and quantity of RNA essential to ensure high-quality data; the cost of sequencing is still expensive and, finally, there are bioinformatics challenges including the development of efficient methods to store, retrieve and process large amounts of data. With development of third generation sequencing methods, costs are decreasing and read-lengths are increasing reducing the bioinformatic strain.

In this Chapter, whole transcriptome sequencing will be utilised to identify molecular differences between cartilage cells of different phenotypes. This technique will be used to identify novel specific markers for articular cartilage-

derived stem cells (ACSC). Articular cartilage-derived stem cells will be isolated using differential adhesion to fibronectin and expanded in culture. The gene expression profiles of ACSC will be compared to de-differentiated full-depth chondrocytes using the SOLiD S4s NGS platform. Differential gene expression analyses will be performed using open source bio-informatics packages and the 'R' statistical platform.

3.2 Methodology

Material	Catalogue number	Supplier
40µm mesh cell strainer	352340	BD FalconTM, UK
Dulbecco's modified Eagle's medium	41965-062	Gibco, UK
Trypsin-EDTA 0.05%	25300-062	Gibco, UK
Foetal calf serum	10106-169 1	Gibco, UK
L-glutamine 200mM	25030-081	Gibco, UK
Hepes buffer	15630-056	Gibco, UK
Steriflip® filter unit	GCGP00525	Millipore, UK
CellTrics 30 µm filters	04-004-2326	Partec, UK
Human FGF - basic	00 - 18B	Peprotech, UK
Human TGF - β2	100 – 35B	Peprotech, UK
Pronase from Streptomyces griseus	11 459 643 001	Roche, UK
Collagenase from clostridium histolyticum	C0130	Sigma Aldrich, UK
L-Ascorbic acid 2-phosphate	A8960	Sigma Aldrich, UK
Cloning rings	C7983	Sigma Aldrich, UK
Phosphate buffered saline	P4417	Sigma Aldrich, UK
Fibronectin from bovine plasma	F1141	Sigma Aldrich, UK
D-(+)-Glucose	G6152	Sigma Aldrich, UK
Ethanol	E/0650DF/17	Thermo Fisher Scientific, UK
RNeasy Mini Kit	74104	Qiagen, UK
RNase-free DNase set	79254	Qiagen, UK
RNA analysis kit	5067-1511	Agilent Technologies, UK

Table 3.1 – Materials and suppliers

3.2.1 Cell isolation and culture

Full-depth chondrocytes and articular cartilage-derived stem cells were isolated from healthy and osteoarthritic donors as previously described (Sections 2.1-2.5). In brief, tissue was dissected and digested in sequential pronase and collagenase enzymes. Full-depth chondrocytes were pelleted through centrifugation (2000 rpm, 5 minutes), re-suspended in DMEM+ plus TGF-β2 and FGF-2 (Section 2.4), plated and expanded in culture. Stem cells were selected through differential adhesion to fibronectin and colonies isolated after 14 days using cloning rings (Section 2.3). Monoclonal cells lines were expanded and cultured in DMEM+ plus (1ng/µl) TGF-β2 and (5ng/µl) FGF-2.

3.2.2 RNA extraction and purification

RNA was isolated from a full-depth chondrocyte cell line, a normal articular cartilage-derived stem cell line and two OA articular cartilage-derived stem cell lines. Cell lines were grown in culture as described in Section 3.2.1 until population doublings of 25 had been achieved. Cells were trypsinised at 70% confluence, counted and frozen in buffer RLT in one million cell aliquots at -80^{o}C until needed. RNA was extracted from monoclonal cell lines using RNeasy kit and a DNase1 column digest (Qiagen, UK). RNA was purified by 2 rounds of polyA-magnetic bead isolation (Invitrogen, UK). Isolated RNA was quality checked and quantified using the Agilent 2100 bioanalyzer. RNA integrity values and nanodrop results are included in the Appendix (Figure S1.1).

3.2.3 Next generation transcriptomic sequencing (NGS)

No RNA amplification strategies were employed during the NGS sequencing experiment. This experiment was undertaken as a direct RNA single strand sequencing, no strand-specific information was generated that would induce a 3' bias. The minimal standard and guidelines for publication of RNA sequencing data states that in order to ensure that the data are reproducible, experiments should be performed with at least two biological replicates, unless there is a compelling reason indicating that this is impractical (ENCODE, 2011). In this study, a single replicate for each sample was used due to financial constraints, which is covered under the guidelines. Whole transcriptome direct RNA NGS was

performed in collaboration with the centre for genomic research at the University of Liverpool using the SOLiD S4s sequencer with 99.94% accuracy and read lengths of 50-100bps (Liu et al., 2012).

3.2.4 Pipeline

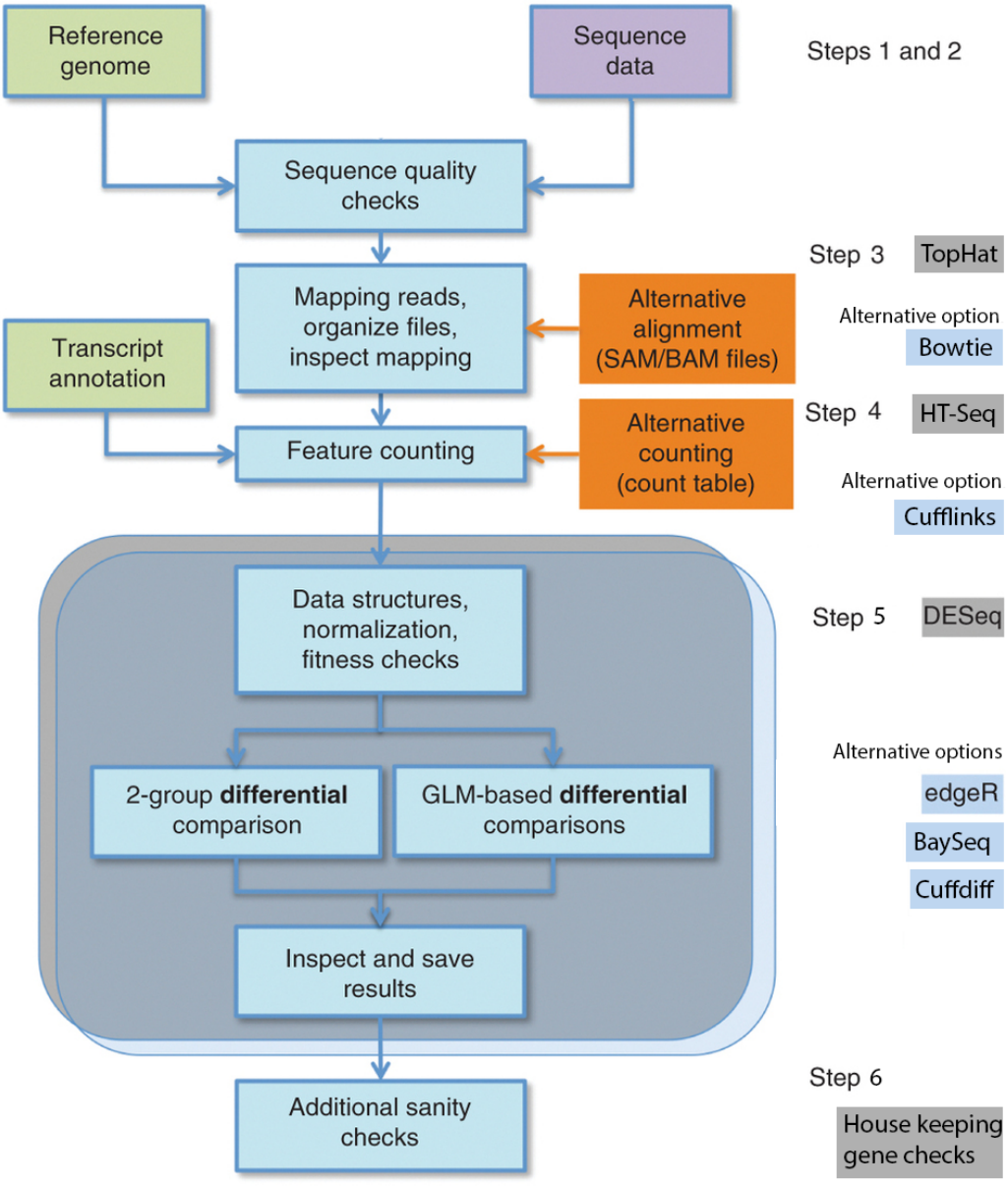


Figure 3.1 – RNA-seq pipeline and workflow

Pipeline for next generation RNA sequencing analysis employed in this study. Programs and methodologies used are show in grey. Sequencing was performed using the SOLiD sequencing platform and reads were aligned to the HG19 human genome using TopHat. Independent mapped reads were counted using the HT-Seq python package and differential expression analysis was performed using the DESeq package for the 'R' statistical software. Figure adapted from (Anders et al., 2013)

3.2.5 Sequence alignment

To be able to quantify the gene expression in the RNA-Seq samples, the reads need to first be aligned and then assembled into transcripts.

3.2.5.1 'Tophat' alignment

RNA-Seq reads were aligned to the HG19 human genome using 'Tophat' to identify splice junctions mapping between exons in RNA-Seq-reads. 'Tophat' aligns RNA-Seq reads to the HG19 human genome using the ultra-high-throughput short read aligner 'Bowtie' and then analyses the mapping results to identify splice junctions between exons. RNA-Seq read FASTA files are the input data, which are processed and aligned to HG19 producing the SAM/BAM file format. 'Bowtie' is an, memory-efficient aligner designed for quickly aligning large sets of short reads to large genomes. The genome is indexed and to reduce memory requirements. For single-end alignment of the human genome memory requirement are as small as 2.2 GB or 2.9 GB for paired-end alignment. In this study 'Tophat' alignment of sequence data was used as it is capable of aligning both single-and paired-end sequencing and is optimal for read lengths of 75bp or longer (range = 50 - 1024bp).

3.2.5.2 'Cufflinks' alignment

For a comparative analysis the alternative aligner 'Cufflinks' was utilised. 'Cufflinks' was required for downstream differential expression analysis using 'Cuffdiff'. Cufflinks assembles transcripts, estimates their abundances, and tests for differential expression and regulation in RNA-Seq samples. The input data are raw RNA-Seq read FASTA files, which are assembled into a set of alignment of SAM/BAM files. Cufflinks then estimates the relative abundances of these transcripts based on how many reads comprise each one.

3.2.6 Normalisation

Aligned counts were normalised to External RNA Controls Consortium (ERCC) spiked RNA internal controls; these provided a ladder of RNA spike-ins to calibrate quantification, sensitivity, coverage and linearity of the sequencing.

3.2.7 'HTSeq' – Generating transcript counts

'HTSeq' is a Python package that provides infrastructure to process data from high-throughput sequencing assays (Anders et al., 2014). Given a SAM/BAM file and an ensembl gene transfer file (GTF) or GFF file with gene structure information. It counts how many aligned reads overlap each exon for every given gene. These counts are then utilised in differential gene expression analyses through 'DESeq' or 'Bayseq'. Only reads mapping unequivocally to a single gene are counted. A read that maps to more than one gene or to multiple positions is discarded; this prevents extra reads from differentially expressed genes causing anomalous differential expression being detected in the other genes (Anders et al., 2014).

3.2.8 Differentiation gene expression analysis

When different condition, time points or sample groups are being compared differentially expressed genes/isoforms can be calculated. 'DESeq', 'edgeR' and 'Bayseq' are widely used tools for differential expression both available through the 'Bioconductor' 'R' package, that all use a negative binomial distribution to model the variance in read counts across replicates. 'Cuffdiff' is part of the 'Cufflinks' alignment software; it offers a non-parametric methodology for analysis of differentiation expression.

3.2.8.1 Gene count based methods

3.2.8.1.1 Negative binomial modals

3.2.8.1.1.1 'DESeq'

The 'DESeq' algorithm was used within the 'R' statistical software to perform the differential expression analysis. Normalized counts form 'HTSeq' were analysed using the 'DESeq' package for the 'R' Statistical software, to identify statistically significant differentially expressed genes. 'DESeq' allows for statistical analysis to be performed without biological replicates, as described by (Anders and Huber, 2010). The numbers of reads *per* sample assigned to each gene were modelled using a negative binomial (NB) distribution and false discovery rate of 10%. The false discovery rate (FDR) is a statistical control method used to correct for multiple comparisons in multiple hypothesis testing by compensating

for an expected proportion of incorrectly rejected null-hypotheses. 'DESeq' was chosen over other methodologies as normalisation and error processing can be performed for each individual sample rather than across an entire group, which is not possible within 'Bayseq' and 'edgeR'. This allowed for variation within individual donors to be controlled. 'DESeq' also allowed for individual samples to be grouped and compared as a cohort rather than individual pair-wise comparisons alone. This then allowed the stem cells samples to be combined into a group for the analysis.

3.2.8.1.1.2 'edgeR'

Like 'DESeq', the input data for 'edgeR' is the normalised reads from 'HTSeq' (Robinson et al., 2010). The numbers of reads *per* sample assigned to each gene are again fitted to a negative binomial (NB) modelled distribution. The false discovery rate was set to 10%. The alternative algorithm employed by 'edgeR' was used as a substitute analysis to confirm the results seen through 'DESeq' analysis and to identify the effect of normalisation within a group rather than within each individual sample. The 'edgeR' algorithm was used within the 'R' statistical software to perform this analysis.

3.2.8.1.2 Bayesian model

3.2.8.1.2.1 'Bayseq'

The 'Bayseq' algorithm assumes a negative binomial distribution and derives a Bayesian prior distribution for the entire dataset. The algorithm takes an empirical Bayesian approach that is able to increase the accuracy of predictions by borrowing information across the dataset (Hardcastle and Kelly, 2010). The false discovery rate was set to 10% and normalisation was performed across the whole group and not within individual samples and statistical probability is calculated at 'log' likelihood. The 'Bayseq' algorithm was used as a substitute analysis to compare to the results seen through 'DESeq' analysis and to identify the effect of normalisation within a group rather than within each individual sample. The 'Bayseq' algorithm was used within the 'R' statistical software to perform this analysis.

3.2.8.2 Transformation-based method

3.2.8.2.1 'Cuffdiff'

The other differential expression packages count reads at a gene level and looks for direct differences in these counts. This approach can be inaccurate for genes with multiple isoforms as relative abundance of an isoform can change overall gene abundance without large changes in the number of reads for that gene. 'Cuffdiff' assesses for differentially expressed genes by estimating how many fragments came from each isoform and then converting the counts into isoform expression levels. To find differentially expressed genes, 'Cuffdiff' calculates expression levels in each condition for each gene by adding-up the expression levels for each gene's splice isoforms (Trapnell et al., 2013). The starting data for the 'Cuffdiff' analysis is the aligned reads generated through 'Cufflinks'. 'Cufflinks' does not produce an array of count data like 'HTseq', but rather generates Reads *per* kilobase of exon model *per* million mapped reads (RPKM) values. The RPKM values were analysed for significant differential expression using 'Cuffdiff' of paired samples to confirm the results of the original analysis and to identify any variation in the original analyses due to isoform variants. A major disadvantage of the 'Cuffdiff' analysis is that it only allows pair-wise comparisons between 2 individual samples, rather than allowing multiple samples to be compared to one another as a group. Unlike the previous methods, 'Cuffdiff' transforms the data before estimating differential expression and before employing a negative binomial model.

3.3 Results

The ability of adult stem cells to undergo self-renewal allows for their identification by a standard colony-forming assay. Articular cartilage-derived stem cells (ACSC) from healthy and OA donors were successfully enriched from their differentiated progeny using differential adhesion to fibronectin, cloned and expanded in culture for 25 population doublings. Colonies were stained by crystal violet for visualisation (Figure 3.2). Full-depth differentiated chondrocyte (FD) populations without differential stem cell selection were grown in parallel to the same number of population doublings. High quality RNA was isolated and purified (Figure S1.1) and sent for whole transcriptome sequencing.

Two different sample groups were analysed in this study, full-depth de-differentiated chondrocytes (FD) and articular cartilage-derived stem cells (ACSC) using the RNA-seq pipeline. The FD set comprises a RNA-Seq dataset from a cell line from an individual donor. The ACSC set consisted of RNA-seq datasets for each of the 3 individual monoclonal cell lines isolated from the cartilage from 3 separate donors. The reads from each sample were aligned to the HG19 human genome using 'Tophat'. The aligned raw reads from the RNA-seq were used to generate gene counts using the 'HTseq' bioinformatics software; this identified 23,228 genes that are expressed across both groups of cartilage-derived cells. The expression counts from RNA-Seq were then compared and differential gene expression calculated between the experimental groups.

3.3.1 Quality and normalisation control

RNA sequence reads were quality vetted and low quality base reads and non-uniquely mapped reads removed to avoid contaminating the results. Data were normalised to ERCC spike-in controls and gene expression counts fitted to a negative binomial distribution with a false discovery rate set at 10% using 'DESeq'. Twenty-two house-keeping gene were selected to assess the normalisation and reliability of the RNA-Seq data sets. These house-keeping genes were divided into 3 groups; commonly used cartilage house-keeping genes, commonly used NGS house-keeping genes and house-keeping genes

commonly utilised in other tissues (Table 3.2). The fold-change observed between the FD and ACSC groups across all house-keeping genes had an average of -0.13 (range -0.49-0.40). The panel of commonly used RNA-Seq house-keeping genes had the lowest variation (mean = -0.064), then the panel of common cartilage house-keeping genes (mean = -0.16) and finally the panel of other house-keeping genes (mean= -0.20). None of the house-keeping genes tested had a statistically significant change in expression between FD and ACSC (p-value = 0.20-0.99, p-adj-value = 1), validating the integrity of RNA-Seq pipeline employed (Table 3.2).

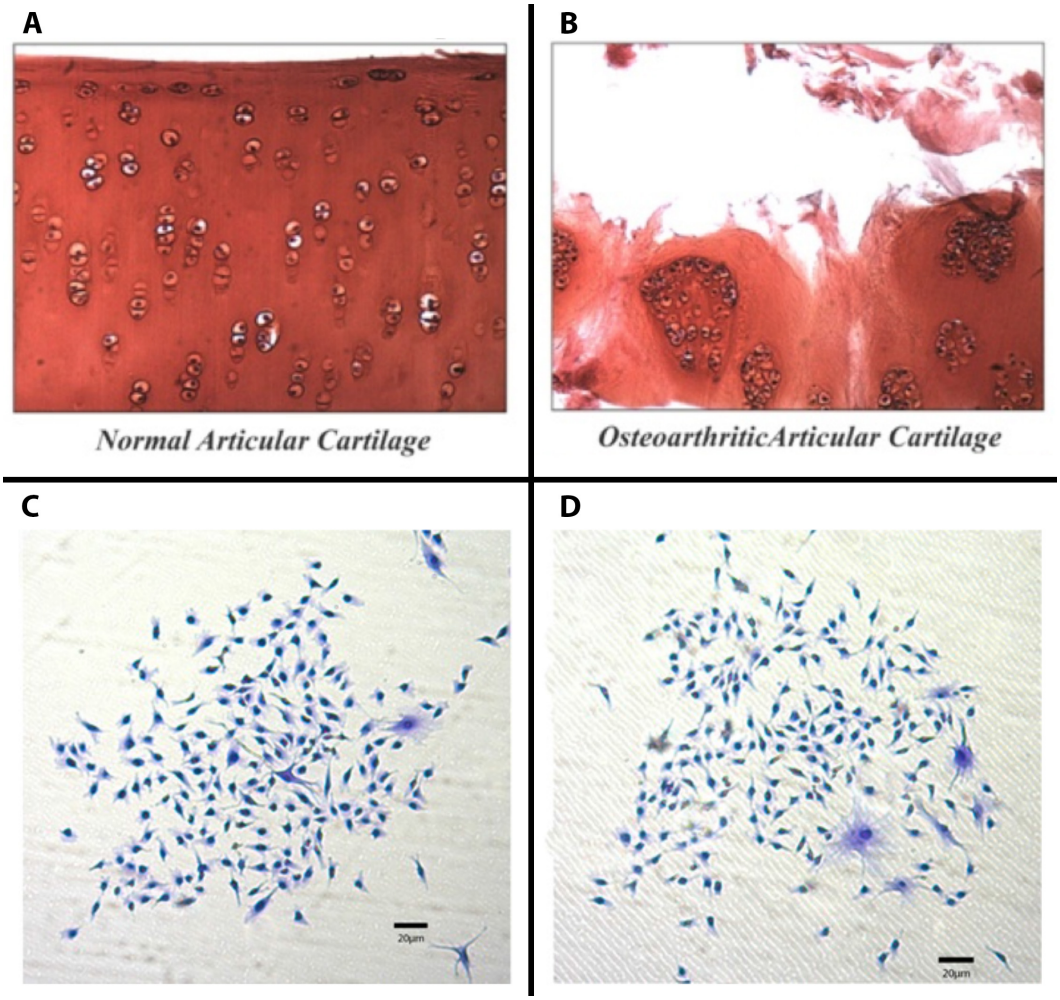


Figure 3.2 – Representative images of normal and osteoarthritic cartilage and stem cell colonies.

A) Safranin-O stained healthy normal human articular cartilage. There is an abundance of proteoglycan with a smooth flat surface. The chondrocytes in the superficial zone are flattened and smaller than the cells deeper in the matrix, which are in the classical columnar arrangement. **B)** Safranin-O stained osteoarthritic human articular cartilage. There is a reduction in proteoglycan and major delamination and loss of the surface. The surface is rough and torn and no flattened chondrocytes are remaining in the superficial zone. Cluster of chondrocytes have developed, a classical phenotype of osteoarthritis. **C)** Cartilage stem cell colony derived from normal healthy cartilage and stained with crystal violet. **D)** Cartilage stem cell colony derived from osteoarthritic cartilage and stained with crystal violet. Colonies are tight, derived from a simple precursor, the cells exhibit a fibroblastic shape. Scale bar 20µm

	Gene symbol	Mean expression in FD	Mean expression in ACSCs	Fold-change	p-value	p-adj-value
Cartilage house-keeping gene panel	RPS18	7104.15	7750.13	0.13	0.80	1
	B2M	50589.83	39872.66	-0.34	0.48	1
	RPL13a	504.44	401.08	-0.33	0.54	1
	PMP31 (RP11)	3895.05	3876.23	-0.01	0.94	1
	HPRT1	1272.56	1061.07	-0.26	0.56	1
NGS house-keeping gene panel	C1orf43	7730.87	7204.67	-0.10	0.77	1
	CHMP2A	2347.35	2399.51	0.03	0.98	1
	GPI	8641.34	8198.59	-0.08	0.83	1
	PSMB2	5086.40	4619.21	-0.14	0.69	1
	PSMB4	4974.62	4564.60	-0.12	0.72	1
	RAB7A	17021.87	17832.60	0.07	0.93	1
	REEP5	7685.01	6897.88	-0.16	0.66	1
	SNRPD3	1937.49	1784.40	-0.12	0.75	1
	VCP	21920.06	22408.47	0.03	0.99	1
	VPS29	3399.21	3285.22	-0.05	0.86	1
Common house-keeping genes in other tissues panel	PPIA	3446.03	2665.44	-0.37	0.34	1
	TUBB	44763.01	58963.87	0.40	0.56	1
	UBC	26726.54	23826.48	-0.17	0.68	1
	TBP	904.74	793.23	-0.19	0.67	1
	GUSB	3306.54	2350.94	-0.49	0.22	1
	ACTB	195594.31	161801.25	-0.27	0.68	1
	GAPDH	51371.32	42260.42	-0.28	0.57	1

Table 3.2 – Table showing uniform expression of house-keeping genes in RNA-seq experiment.

Panel of house-keeping genes was produced from a pre-existing panel of cartilage house-keeping genes and a NGS sequencing house-keeping gene panel previously published by Eisenberg and colleagues (Eisenberg and Levanon, 2013). No significant variation was observed in any of the 22 house-keeping genes observed. p-adj-value corresponds to the p-value adjusted for multiple testing using the Benjamini-Hochberg method. Statistical significance is defined as p-adj<0.1.

3.3.2 Differential expression

3.3.2.1 'DESeq' analysis

Approximately 1100 genes were found to be statistically significantly differentially regulated between the FD and ACSC groups ($p<0.05$) (Figure 3.3), however, this number was reduced to 410 after correction for multiple testing using the Benjamini-Hochberg method at 10% FDR (p-adj<0.1). The distribution of statistical significant genes after correction for multiple testing is shown in Figure 3.4. There is a slight skew towards genes that are down-regulated especially with genes of low base level expression; however the distribution of statistically significant genes is fairly evenly divided between up-regulated and down-regulated genes (Figure 3.4).

To allow for differential gene expression analysis to be performed and samples to be clustered based on expression profiles, fold-change was transformed to modified log ratios to provide a finite range for investigation (Figure 3.5).

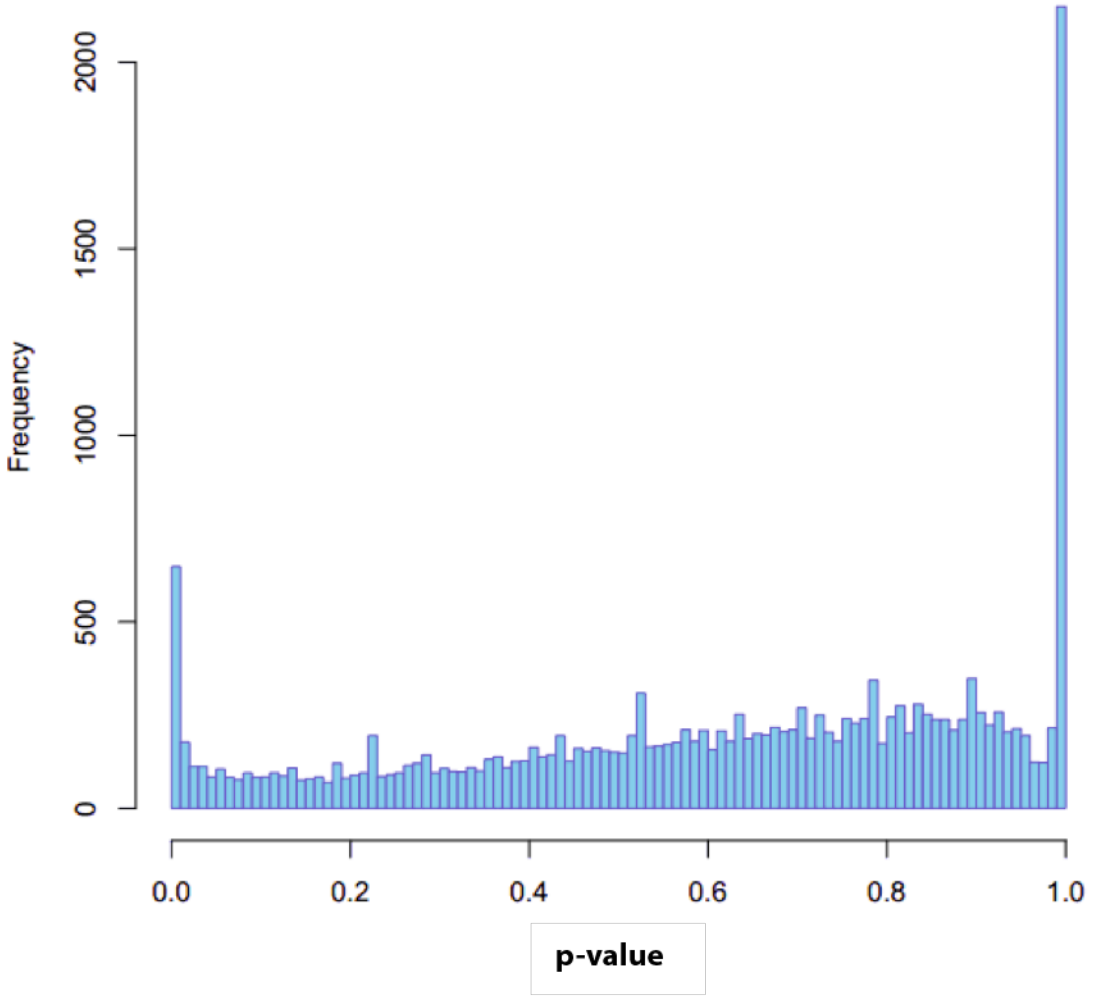


Figure 3.3 – Histogram showing the distribution of p-values for differentially expressed genes.

Approximately 1100 genes were found to be statistically significant in the negative binomial model. Calculated p-values are prior to correction for multiple testing using the Benjamini-Hochberg method.

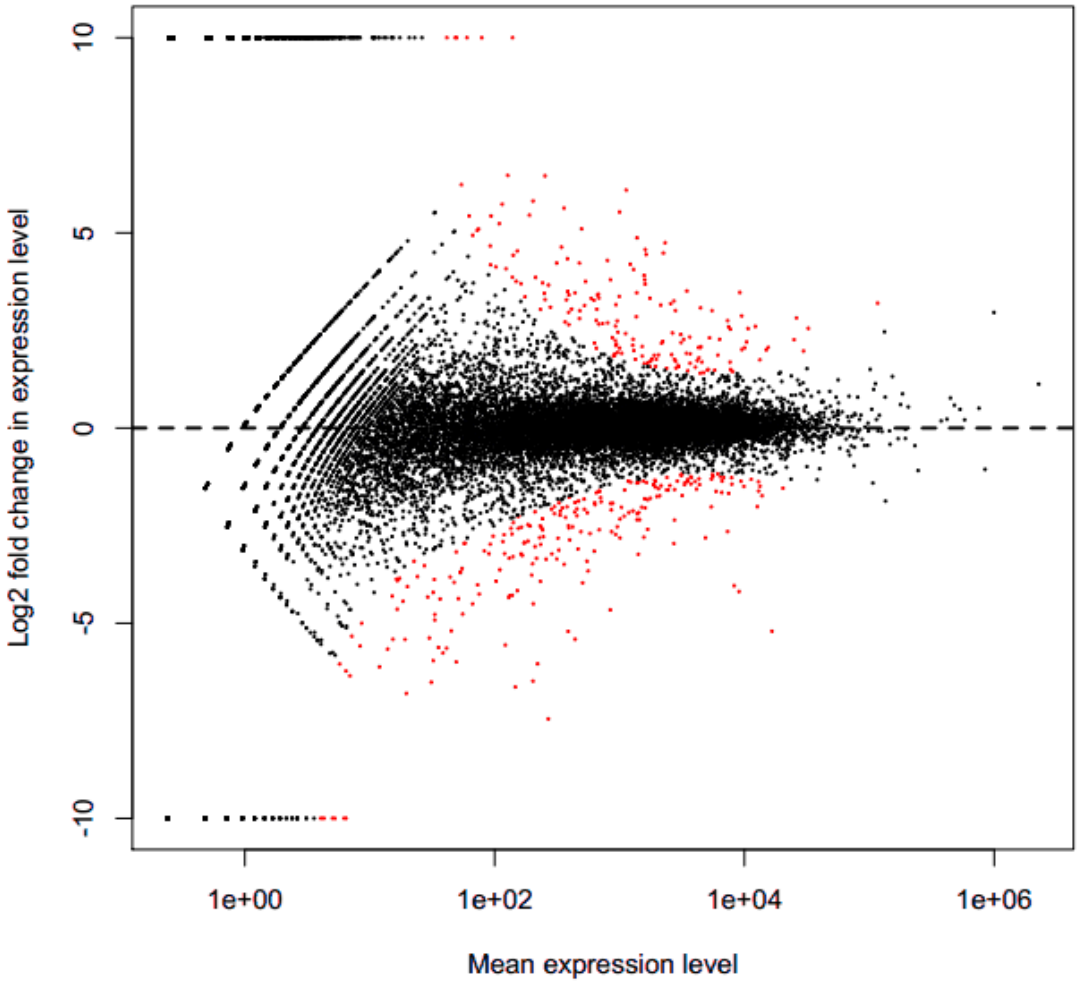


Figure 3.4 – Scatter plot of changes in gene expression between full-depth chondrocytes (FD) and the average expression across all articular cartilage stem cells.

Genes with an infinite fold-change are plotted at ±10 $\log_2$ fold-change. Statistically significant genes at a 10% false discovery rate are shown in red (p-adj<0.1). Data show a light skew towards down-regulated genes.

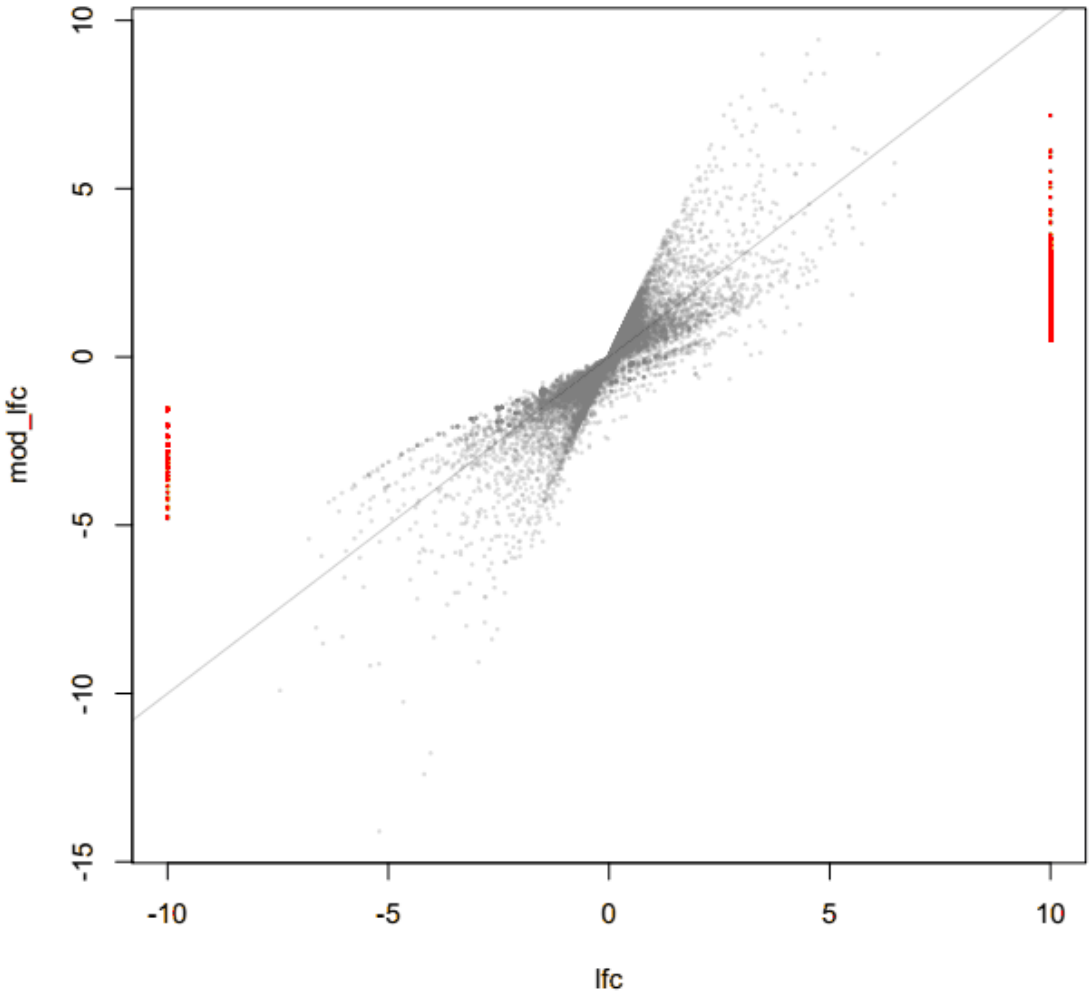


Figure 3.5 – Scatterplot of direct log fold-change (lfc) versus moderated log-ratios (mod_lfc).

Gene expression data were transformed to produce moderated log-ratios to provide variance stabilisation. The points close to the solid diagonal line represent the strongly expressed genes. The red points correspond to values that were infinite in lfc and were set to ±10 for the purpose of plotting. Moderated log-ratios values vary within a finite range unlike the original log fold-change, this allows for subsequent data clustering analysis and plotting to be performed.

The top 50 significant differentially expressed genes were plotted in a heatmap (Figure 3.6). During analysis the full-depth-derived population was treated as the control group against which the articular cartilage-derived stem cell lines that were analysed. Hierarchical clustering of the samples using gene expression levels clustered all the samples as cartilage-derived cells, and then clustered a sub-set containing the ACSC samples as a stem cell cohort and finally the OA tissue derived ACSC samples were grouped together as an osteoarthritic cluster.

The top 50 statistically significant up-regulated genes identified in the 'DESeq' analysis are shown in Table 3.3 and the top 50 statistically significant down-regulated genes identified in the 'DESeq' analysis are shown in Table 3.4. Genes that were up-regulated in ACSC were considered to be candidate stem cell markers and genes that were down-regulated in ACSC were considered potential markers of differentiated chondrocytes or possible negative markers of ACSC. There were numerous cartilage-associated genes that were strongly expressed in the differentiated chondrocytes shown in Table 3.4. These FD specific cartilaginous genes included Collagen Type II, Aggrecan and lubricin, which were all significantly down-regulated in the ACSC ($p\text{-adj}<0.1$) supporting the notion that the ACSC are an immature phenotype.

3.3.2.2 'edgeR' analysis

A parallel analysis was performed using the 'edgeR' algorithm, approximately 1700 genes were found to be statistically significantly differentially regulated between the FD and ACSC groups ($p<0.05$), which was reduced to 733 after correction for multiple testing using the Benjamini-Hochberg method at 10% FDR ($p\text{-adj}<0.1$). 'EdgeR' produced a larger number of statistically significant genes than 'DESeq', which is due to less stringent normalisation in the algorithm that can be largely affected by outliers in small sample sets. The top 50 statistically significant up-regulated genes identified in the 'edgeR' analysis are shown in Table 3.6 and the top 50 statistically significant down-regulated genes identified in the 'edgeR' analysis are shown in Table 3.7. Twenty-three of the top 50 significant up-regulated genes were also in the top 50 genes in the 'DESeq' analysis and 25 of the top 50 significant up-regulated genes were also in the top 50 genes in the 'DESeq' analysis.

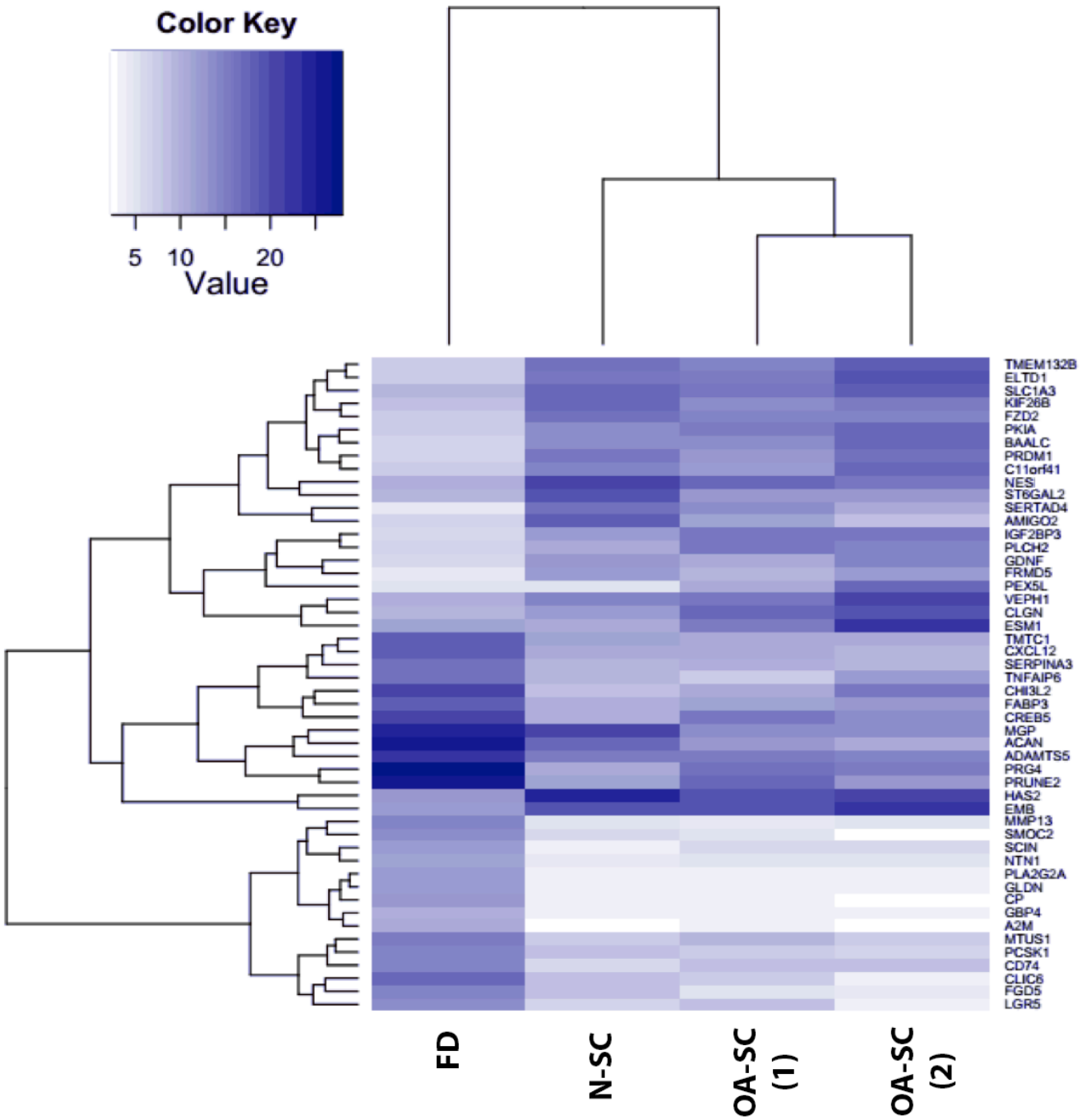


Figure 3.6 – Heatmap of next generation sequencing (NGS) of normal and osteoarthritic cartilage cell lines.

Heatmap showing the top 50 significant differentially expressed genes between FD, N-SCs and both OA-SC**.** The heatmap demonstrates that articular cartilage-derived stem cell specific genes can be identified. Hierarchical clustering analysis of the samples based on gene expression profiles shows the OA-SC cell lines are first grouped together as on OA cohort, then all the articular cartilage-derived stem cells are grouped as a stem cell cohort, before finally grouping all the cell lines as cartilage-derived. Key shows the modified log-ratios, white indicates a low or down-regulated gene while dark blue indicated a high or up-regulated gene with relation to the control group (FD)

FD compared to all ACSC lines					
Gene symbol	**Mean expression in FD**	**Mean expression in ACSCs**	**Fold-change**	**p-value**	**p-adj-value**
SERTAD4	21.97	1502.08	68.36	1.99E-16	4.22E-13
TMEM132B	113.69	3052.85	26.85	1.46E-15	2.52E-12
ELTD1	131.84	2947.68	22.36	2.41E-14	2.87E-11
PEX5L	28.66	1327.29	46.31	8.44E-14	9.46E-11
IGF2BP3	62.10	1818.26	29.28	1.09E-13	1.15E-10
PRDM1	88.85	2113.58	23.79	2.40E-13	2.29E-10
BAALC	98.40	2145.09	21.80	6.51E-13	5.90E-10
NES	81.21	859.94	10.59	1.78E-11	1.36E-08
HAS2	1070.02	11892.36	11.11	4.01E-11	2.94E-08
PLCH2	86.94	1596.17	18.36	6.36E-11	4.46E-08
C11ORF41	136.62	2053.40	15.03	7.95E-11	4.96E-08
AMIGO2	101.27	1693.48	16.72	8.07E-11	4.96E-08
PKIA	149.04	2074.63	13.92	1.63E-10	9.40E-08
FZD2	161.46	2082.62	12.90	3.29E-10	1.74E-07
CLGN	367.82	3512.23	9.55	8.45E-10	4.12E-07
ESM1	676.40	5716.20	8.45	1.61E-09	7.67E-07
SLC1A3	362.09	3296.15	9.10	1.81E-09	8.42E-07
EMB	876.08	7045.60	8.04	2.10E-09	9.39E-07
GDNF	53.50	1050.50	19.64	2.12E-09	9.39E-07
FRMD5	19.11	656.00	34.33	3.67E-09	1.55E-06
KIF26B	225.47	2259.96	10.02	3.81E-09	1.58E-06
ST6GAL2	309.54	2749.94	8.88	4.59E-09	1.82E-06
VEPH1	447.11	3596.08	8.04	7.86E-09	2.99E-06
EREG	160.50	1776.28	11.07	8.67E-09	3.24E-06
PTGS2	1653.75	12108.14	7.32	1.41E-08	5.06E-06
NTSR1	9.55	475.24	49.74	1.61E-08	5.68E-06
NRG1	79.30	1102.28	13.90	2.03E-08	6.78E-06
CAMK2N1	1386.25	9330.57	6.73	2.97E-08	9.41E-06
TFAP2D	3.82	336.29	88.00	8.36E-08	2.38E-05
FZD1	1563.94	9446.59	6.04	1.04E-07	2.86E-05
OPCML	124.20	1285.29	10.35	1.34E-07	3.53E-05
NKD1	33.44	624.98	18.69	2.32E-07	5.51E-05
CLDN11	1680.50	9725.32	5.79	2.87E-07	6.51E-05
RAB3B	2546.07	15457.04	6.07	3.43E-07	7.60E-05
MTRNR2L1	2306.27	13489.20	5.85	5.90E-07	0.00012
CTHRC1	240.75	1735.31	7.21	7.54E-07	0.00015
RNF128	18.15	450.46	24.82	8.66E-07	0.00017
NR2F1	24.84	502.65	20.24	9.23E-07	0.00017
WWC1	51.59	696.13	13.49	1.03E-06	0.00019
HOXD10	134.71	1201.53	8.92	1.05E-06	0.00019
DNER	81.21	876.42	10.79	1.22E-06	0.00022
ST8SIA1	737.55	3879.72	5.26	1.28E-06	0.00023
NTM	392.66	4478.59	11.41	1.29E-06	0.00023
PAPPA	1321.28	6565.46	4.97	1.32E-06	0.00023
NPR3	906.65	4564.20	5.03	1.36E-06	0.00024
FGF5	617.17	3333.38	5.40	1.43E-06	0.00025
HHIP	87.89	882.12	10.04	1.52E-06	0.00025
FLRT2	4706.16	33274.70	7.07	1.59E-06	0.00026
NTRK3	4.78	268.99	56.31	2.07E-06	0.00034
FIBIN	1636.55	7893.11	4.82	2.23E-06	0.00036

Table 3.3 – The 50 most significantly up-regulated genes between full-depth differentiated chondrocytes and articular cartilage derived stem cells lines using 'DESeq' analysis.

p-adj-value corresponds to p-value adjusted for multiple testing using Benjamini-Hochberg method at 10% FDR. Statistical significance is defined as p-adj<0.1.

FD compared to all ACSC lines					
Gene symbol	**Mean expression in FD**	**Mean expression in ACSCs**	**Fold-change**	**p-value**	**p-adj-value**
PRG4	61456.23	1665.01	-36.91	3.37E-36	6.41E-32
ACAN	31078.26	1703.66	-18.24	3.16E-28	3.01E-24
PRUNE2	28057.37	1704.40	-16.46	8.43E-27	5.35E-23
CP	1057.60	6.04	-175.17	1.22E-23	5.83E-20
CLIC6	3013.24	119.28	-25.26	4.06E-22	1.54E-18
MMP13	1647.06	38.71	-42.55	1.36E-20	4.33E-17
SMOC2	1435.92	38.79	-37.02	5.53E-18	1.50E-14
GLDN	784.36	8.77	-89.41	4.07E-17	9.70E-14
PLA2G2A	843.59	12.80	-65.89	2.25E-16	4.28E-13
CHI3L2	7862.71	1011.27	-7.78	2.78E-15	4.41E-12
A2M	568.45	5.72	-99.35	8.79E-15	1.29E-11
CXCL12	4282.93	455.13	-9.41	1.48E-14	2.01E-11
ADAMTS5	13691.44	1949.11	-7.02	2.09E-14	2.65E-11
FGD5	1702.47	108.85	-15.64	2.19E-13	2.19E-10
MGP	19891.81	3159.82	-6.30	1.06E-12	9.21E-10
PCSK1	1809.48	142.72	-12.68	2.55E-12	2.11E-09
TMTC1	4381.34	629.62	-6.96	1.03E-11	8.16E-09
CD74	1710.12	160.65	-10.64	6.56E-11	4.46E-08
GBP4	458.58	9.71	-47.22	7.77E-11	4.96E-08
FABP3	4484.52	740.99	-6.05	1.42E-10	8.43E-08
TNFAIP6	2831.72	402.90	-7.03	2.27E-10	1.27E-07
NTN1	720.35	31.75	-22.69	2.48E-10	1.35E-07
MTUS1	1878.26	210.73	-8.91	4.46E-10	2.30E-07
CREB5	6950.33	1354.16	-5.13	6.00E-10	3.01E-07
SERPINA3	2565.17	387.58	-6.62	2.64E-09	1.14E-06
LGR5	1139.76	101.28	-11.25	4.27E-09	1.73E-06
SCIN	776.72	51.04	-15.22	5.56E-09	2.16E-06
RGS16	2340.66	370.82	-6.31	1.29E-08	4.73E-06
AK4	1377.65	160.62	-8.58	1.66E-08	5.75E-06
VCAM1	3650.48	716.89	-5.09	1.82E-08	6.18E-06
IL26	188.21	2.96	-63.65	2.74E-08	9.00E-06
CRISPLD2	3468.00	680.70	-5.09	2.79E-08	9.02E-06
LOC100134229	972.57	94.97	-10.24	4.04E-08	1.26E-05
PEG3	2523.14	437.09	-5.77	4.55E-08	1.40E-05
SERPING1	12506.78	3083.48	-4.06	5.50E-08	1.66E-05
ELMO1	520.68	29.00	-17.95	5.63E-08	1.67E-05
SLC19A3	479.60	24.56	-19.52	5.71E-08	1.67E-05
SDK2	451.89	22.25	-20.31	7.55E-08	2.18E-05
KCNA6	456.67	23.17	-19.71	9.04E-08	2.53E-05
BAMBI	647.74	47.59	-13.61	1.12E-07	3.03E-05
CRTAC1	120.38	1.32	-91.21	1.25E-07	3.37E-05
ADAMTSL3	1589.74	243.69	-6.52	1.59E-07	4.14E-05
FXYD6	1843.87	302.35	-6.10	1.63E-07	4.19E-05
SLC7A2	3351.45	729.24	-4.60	1.86E-07	4.73E-05
CIITA	155.73	3.11	-50.03	2.15E-07	5.36E-05
VGLL3	2528.87	502.59	-5.03	2.18E-07	5.36E-05
GALNT12	797.74	77.59	-10.28	2.19E-07	5.36E-05
ADAMTS1	29133.12	7203.24	-4.04	2.24E-07	5.41E-05
ITGB8	3411.63	759.56	-4.49	2.46E-07	5.71E-05
HLA-DRA	146.17	2.69	-54.43	2.47E-07	5.71E-05

Table 3.4 – The 50 most significantly down-regulated genes between full-depth differentiated chondrocytes and articular cartilage derived stem cell lines using 'DESeq'.

p-adj-value corresponds to p-value adjusted for multiple testing using Benjamini-Hochberg method at 10% FDR. Statistical significance is defined as p-adj<0.1.

FD compared to all ACSC lines					
Gene symbol	**Mean expression in FD**	**Mean expression in ACSCs**	**Fold-change**	**p-value**	**p-adj-value**
PRG4	61456.23	1665.01	-36.91	3.37E-36	6.41E-32
ACAN	31078.26	1703.66	-18.24	3.16E-28	3.01E-24
COL2a1	508.26	52.95	-9.60	9.724E-06	0.0013
COL9a1	21.97	2.33	-9.44	0.029	0.60
COL9a2	154.77	96.72	-1.6	0.40	1
COL9a3	126.11	22.61	-5.58	0.010	0.30
COL11a1	6473.602311	15533.09124	2.4	0.0072	0.23
COL11a2	230.24	64.41	-3.57	0.027	0.56
SOX9	2675.04	2466.89	-1.08	0.72	1

Table 3.5 – Gene expression of cartilaginous genes between full-depth differentiated chondrocytes and articular cartilage derived stem cells.

Articular cartilage-derived stem cells down regulate expression of differentiated cartilage specific genes compared to full-depth differentiated chondrocyte cells. Fold-change and p-values were generated using the 'DESeq' algorithm. Statistical significance is defined as p-adj<0.1.

FD compared to all ACSC lines			
Gene symbol	**Fold-change**	**p-value**	**p-adj-value**
SERTAD4	69.03	7.67E-11	4.05E-08
CXADR	1455.36	1.37E-10	6.94E-08
TFAP2D	81.65	6.75E-10	3.02E-07
PEX5L	44.46	1.07E-09	4.30E-07
NTSR1	48.74	2.08E-09	7.66E-07
RFPL4B	862.24	7.32E-09	2.33E-06
NTRK3	54.28	8.09E-09	2.51E-06
C1orf133	84.50	9.53E-09	2.80E-06
FRMD5	33.94	1.27E-08	3.69E-06
IGF2BP3	29.07	1.64E-08	4.59E-06
TMEM132B	26.52	2.56E-08	6.63E-06
ADAMTS16	43.75	2.85E-08	7.18E-06
IP6K3	656.41	4.79E-08	1.15E-05
PRDM1	23.56	6.45E-08	1.48E-05
CCDC141	52.30	6.61E-08	1.51E-05
ELTD1	22.05	9.01E-08	1.98E-05
BAALC	21.43	1.12E-07	2.38E-05
RNF128	24.33	1.33E-07	2.79E-05
RP1	534.54	1.79E-07	3.68E-05
ELFN2	512.87	2.05E-07	4.13E-05
SERPINB7	36.64	2.64E-07	5.03E-05
PDE11A	42.01	2.76E-07	5.17E-05
GDNF	19.30	2.82E-07	5.19E-05
PLCH2	18.35	4.01E-07	7.06E-05
NR2F1	20.32	4.30E-07	7.34E-05
NKD1	19.01	5.16E-07	8.76E-05
ANKRD30BL	439.75	5.68E-07	9.36E-05
AMIGO2	17.02	7.17E-07	0.00011
UNC5D	65.26	7.83E-07	0.00012
KRT19	18.55	8.09E-07	0.00012
FAM196B	22.36	9.39E-07	0.00013
NKD2	41.12	1.30E-06	0.00018
TMEM155	33.19	1.32E-06	0.00018
C11ORF41	14.78	1.38E-06	0.00019
CASS4	32.62	1.54E-06	0.00020
DKK2	21.00	1.56E-06	0.00020
KRT17	25.22	2.00E-06	0.00025
PKIA	13.79	2.38E-06	0.00029
NRG1	14.15	2.73E-06	0.00033
TTLL6	29.34	2.74E-06	0.00033
WWC1	13.46	3.77E-06	0.00044
FZD2	12.94	3.88E-06	0.00045
THNSL2	16.02	3.91E-06	0.00045
SCN3A	13.83	5.12E-06	0.00056
B4GALNT4	14.33	7.51E-06	0.00079
IGSF5	31.14	7.58E-06	0.00079
NTF3	17.18	7.83E-06	0.00081
TMEM130	18.15	7.99E-06	0.00082
NES	11.53	8.17E-06	0.00083
RASGRP3	10.66	8.24E-06	0.00083

Table 3.6 – The 50 most significantly up-regulated genes between full-depth differentiated chondrocytes and articular cartilage derived stem cells lines using 'edgeR' analysis.

p-adj-value corresponds to p-value adjusted for multiple testing using a 10% FDR. Statistical significance is defined as p-adj<0.1.

FD compared to all ACSC lines			
Gene symbol	**Fold-change**	**p-value**	**p-adj-value**
CP	-170.18	5.78E-30	1.34E-25
GLDN	-87.93	7.02E-25	8.15E-21
A2M	-96.75	1.49E-24	1.15E-20
PLA2G2A	-64.99	9.04E-23	5.25E-19
MMP13	-42.57	2.11E-20	9.80E-17
PRG4	-36.89	6.18E-20	2.39E-16
GBP4	-46.16	2.26E-19	7.51E-16
SMOC2	-36.16	3.96E-19	1.15E-15
IL26	-59.41	5.16E-18	1.33E-14
CRTAC1	-81.51	4.08E-17	9.48E-14
CIITA	-49.16	2.02E-16	3.72E-13
CLIC6	-24.71	2.05E-16	3.72E-13
HLA-DRA	-51.66	2.08E-16	3.72E-13
L3MBTL4	-57.25	4.50E-16	7.46E-13
SHE	-47.28	1.17E-15	1.81E-12
ITIH5L	-95.50	4.71E-15	6.83E-12
LBP	-36.78	5.35E-15	7.30E-12
NTN1	-22.56	6.62E-15	8.55E-12
SLC37A1	-39.52	3.05E-14	3.73E-11
GPRC5C	-26.40	4.17E-14	4.85E-11
ACAN	-17.96	5.64E-14	6.24E-11
SDK2	-19.83	1.24E-13	1.31E-10
SLC19A3	-19.32	2.00E-13	1.88E-10
EYA4	-22.15	2.02E-13	1.88E-10
KCNA6	-19.19	2.02E-13	1.88E-10
TSHZ2	-28.79	3.43E-13	3.07E-10
PRUNE2	-16.22	3.63E-13	3.12E-10
ELMO1	-17.82	5.97E-13	4.95E-10
PGR	-26.43	8.91E-13	7.14E-10
FGD5	-15.37	1.59E-12	1.20E-09
APCDD1	-18.57	1.60E-12	1.20E-09
FAM84B	-39.51	1.82E-12	1.32E-09
RBP4	-20.04	2.44E-12	1.72E-09
SCIN	-15.27	4.65E-12	3.18E-09
CES1	-46.20	1.51E-11	1.00E-08
IRX3	-38.86	1.60E-11	1.04E-08
GCNT4	-20.62	1.75E-11	1.10E-08
SYT13	-15.72	1.92E-11	1.17E-08
ALDH1A2	-15.05	1.98E-11	1.18E-08
LONRF2	-57.36	2.54E-11	1.48E-08
BAMBI	-13.36	3.56E-11	2.01E-08
PCSK1	-12.51	5.36E-11	2.96E-08
ZBTB7C	-19.50	5.88E-11	3.18E-08
TRIM29	-17.85	1.00E-10	5.18E-08
ITGA9	-14.95	1.60E-10	7.91E-08
KCND3	-12.28	3.47E-10	1.65E-07
KIAA2022	-23.81	3.48E-10	1.65E-07
LGR5	-10.96	4.41E-10	2.05E-07
KIF21B	-13.69	6.27E-10	2.86E-07
LMO2	-20.53	6.93E-10	3.04E-07

Table 3.7 – The 50 most significantly down-regulated genes between full-depth differentiated chondrocytes and articular cartilage derived stem cells lines using 'edgeR' analysis.

p-adj-value corresponds to p-value adjusted for multiple testing using a 10% FDR. Statistical significance is defined as p-adj<0.1.

3.3.2.3 'Bayseq' analysis

A parallel analysis was performed using the 'Bayseq' algorithm, approximately 300 genes were found to be statistically significantly and differentially regulated between the FD and ACSC groups ($p<0.05$), with 134 remaining after correction for multiple testing using the Benjamini-Hochberg method at 10% FDR (p-adj<0.1). 'Bayseq' produced a lower number of statistically significant genes than 'DESeq' and the lowest of all the analyses. The top 50 statistically significantly up-regulated genes identified in the 'Bayseq' analysis are shown in Table 3.8 and the top 50 statistically significantly down-regulated genes identified in the 'Bayseq' analysis are shown in Table 3.9. Thirteen of the top 50 significantly up-regulated genes were also in the top 50 genes in the 'DESeq' analysis and 27 of the top 50 significantly down-regulated genes were also in the top 50 genes in the 'DESeq' analysis.

3.3.2.4 'Cuffdiff' analysis

A alternative transformation based analysis was employed utilising the 'Cuffdiff' software, approximately 1000 genes were found to be statistically significantly and differentially regulated between the FD and ACSC groups ($p<0.05$), with 343 remaining after correction for multiple testing using the Benjamini-Hochberg method at 10% FDR (p-adj<0.1). Previous researchers have reported that 'DESeq' and 'Cuffdiff' produce consistent results and we found 'Cuffdiff' produced a similar number of statistically significant genes to 'DESeq' (Nookaew et al., 2012). The 'Cuffdiff' analysis was employed in a pair-wise manor, only comparing the FD and the normal articular cartilage stem cell (N-SC) samples, this may account for some of the differences between the genes identified with other methodologies. The top 50 statistically significantly up-regulated genes identified in the 'Cuffdiff' analysis are shown in Table 3.10 and the top 50 statistically significantly down-regulated genes identified in the 'Cuffdiff' analysis are shown in Table 3.11. Twenty-one of the top 50 significantly up-regulated genes were also in the top 50 genes in the 'DESeq' analysis and 19 of the top 50 significantly up-regulated genes were also in the top 50 genes in the 'DESeq' analysis.

FD compared to all ACSC lines					
Gene symbol	**Mean expression in FD**	**Mean expression in SCs**	**Fold-change**	**Log-likelihood**	**p-adj-value**
GREM1	17124	148716.00	8.68	1.00	0.0003
WLS	3952	8641.67	2.19	0.98	0.01
FZD2	169	2059.67	12.19	0.97	0.01
RFTN1	2632	5477.67	2.08	0.94	0.02
ADAMTS14	201	1157.00	5.76	0.92	0.03
MALAT1	601519	801562.67	1.33	0.91	0.03
IGSF5	2	62.33	31.17	0.90	0.03
C1orf133	2	169.33	84.67	0.90	0.04
RAB3B	2665	15334.67	5.75	0.89	0.04
FRMD5	20	643.00	32.15	0.83	0.07
LOC646324	31	317.33	10.24	0.82	0.07
NKD2	2	82.33	41.17	0.81	0.07
KRT19	23	403.67	17.55	0.80	0.08
MIAT	144	581.67	4.04	0.79	0.09
LOC643723	1	15.33	15.33	0.79	0.09
F2RL1	46	488.67	10.62	0.78	0.09
PAPPA	1383	6449.67	4.66	0.77	0.10
NTRK3	5	262.00	52.40	0.76	0.10
FLJ42709	80	604.33	7.55	0.76	0.10
DUSP6	3257	7305.67	2.24	0.76	0.10
SLC1A3	379	3227.33	8.52	0.76	0.10
TMEM51	38	295.00	7.76	0.75	0.11
STX1B	317	1072.00	3.38	0.75	0.11
NR2F1	26	499.67	19.22	0.74	0.11
PLXDC1	4295	10117.67	2.36	0.74	0.11
NTF4	1	26.00	26.00	0.73	0.12
LPCAT2	1471	2947.00	2.00	0.73	0.12
SERTAD4	23	1502.67	65.33	0.73	0.12
PDZRN3	4602	10250.67	2.23	0.71	0.13
LRRC4	82	316.67	3.86	0.71	0.13
SEC1	2	19.67	9.83	0.71	0.13
LOC149773	253	626.33	2.48	0.71	0.13
MERTK	423	1585.00	3.75	0.68	0.14
UNC5D	1	69.33	69.33	0.68	0.14
NTF3	8	131.33	16.42	0.67	0.15
C8orf34	1	21.33	21.33	0.65	0.16
PRDM1	93	2064.67	22.20	0.64	0.17
NTSR1	10	464.67	46.47	0.63	0.17
MEX3A	276	1152.33	4.18	0.63	0.17
SEMA6A	67	494.33	7.38	0.61	0.18
TIMP3	31563	163388.33	5.18	0.59	0.19
TMEM132B	119	2973.00	24.98	0.59	0.19
COL7A1	1036	3314.00	3.20	0.58	0.20
WWTR1	24657	44146.67	1.79	0.58	0.20
MYLK	16032	34055.67	2.12	0.58	0.20
MYB	1	42.67	42.67	0.58	0.20
KIF26B	236	2228.67	9.44	0.57	0.20
SNORD116-2	2	20.33	10.17	0.57	0.21
PKIA	156	2026.67	12.99	0.56	0.21
IGF2BP1	275	1382.33	5.03	0.55	0.21

Table 3.8 – The 50 most significantly up-regulated genes between full-depth differentiated chondrocytes and articular cartilage derived stem cells lines using ''Bayseq' analysis.

p-adj-value corresponds to p-value adjusted for multiple testing using a 10% FDR. Statistical significance is defined as p-adj<0.1.

FD compared to all ACSC lines					
Gene symbol	**Mean expression in FD**	**Mean expression in SCs**	**Fold-change**	**Log-likelihood**	**p-adj-value**
CP	1107	6.00	-184.50	1.00	0.000
GLDN	821	8.67	-94.73	1.00	0.000
PLA2G2A	883	12.67	-69.71	1.00	0.000
A2M	595	5.67	-105.00	1.00	0.000
MMP13	1724	38.00	-45.37	1.00	0.000
GBP4	480	9.67	-49.66	1.00	0.000
SMOC2	1503	39.00	-38.54	1.00	0.000
NTN1	754	31.33	-24.06	1.00	0.001
PRUNE2	29368	1703.67	-17.24	1.00	0.001
TMTC1	4586	621.33	-7.38	1.00	0.001
HLA-DRA	153	2.67	-57.38	1.00	0.001
SHE	140	2.67	-52.50	1.00	0.002
ELMO1	545	28.67	-19.01	0.99	0.002
PRG4	64327	1641.33	-39.19	0.99	0.002
CXCL12	4483	451.67	-9.93	0.99	0.002
SERPINA3	2685	383.33	-7.00	0.99	0.003
SLC19A3	502	24.33	-20.63	0.99	0.003
PGR	125	4.33	-28.85	0.99	0.003
SLC37A1	117	2.67	-43.88	0.99	0.004
PCSK1	1894	142.33	-13.31	0.99	0.004
CLIC6	3154	120.00	-26.28	0.99	0.004
FGF7	4255	1368.33	-3.11	0.99	0.005
SDK2	473	22.33	-21.18	0.98	0.01
FAM134B	2495	577.33	-4.32	0.98	0.01
VGLL3	2647	494.33	-5.35	0.98	0.01
CRTAC1	126	1.33	-94.50	0.98	0.01
COL15A1	1184	153.00	-7.74	0.98	0.01
LBP	174	4.33	-40.15	0.98	0.01
FGD5	1782	109.00	-16.35	0.98	0.01
ITIH5L	80	0.67	-120.00	0.98	0.01
RGS16	2450	368.33	-6.65	0.98	0.01
PDGFD	1017	110.33	-9.22	0.98	0.01
TSHZ2	126	4.00	-31.50	0.98	0.01
EYA4	246	10.33	-23.81	0.97	0.01
ADAMTS5	14331	1933.67	-7.41	0.97	0.01
IL26	197	3.00	-65.67	0.97	0.01
LOC100134229	1018	93.33	-10.91	0.97	0.01
GCNT4	134	6.00	-22.33	0.97	0.01
CACNB4	2977	623.67	-4.77	0.96	0.01
ALDH1A2	359	22.33	-16.07	0.96	0.01
ADCY1	181	13.33	-13.58	0.96	0.02
CIITA	163	3.00	-54.33	0.96	0.02
GPRC5C	209	7.33	-28.50	0.96	0.02
DMKN	1162	189.33	-6.14	0.96	0.02
L3MBTL4	129	2.00	-64.50	0.95	0.02
LONRF2	48	0.67	-72.00	0.95	0.02
IRX3	60	1.33	-45.00	0.94	0.02
ABI3BP	44672	17009.67	-2.63	0.94	0.02
RASD1	452	73.33	-6.16	0.94	0.02
FAM84B	75	1.67	-45.00	0.94	0.02

Table 3.9 – The 50 most significantly down-regulated genes between full-depth differentiated chondrocytes and articular cartilage derived stem cells lines using ''Bayseq' analysis.

p-adj-value corresponds to p-value adjusted for multiple testing using a 10% FDR. Statistical significance is defined as p-adj<0.1.

FD compared to N-SC					
Gene symbol	**Mean expression in FD**	**Mean expression in NSC**	**Fold-change**	**p-value**	**p-adj-value**
NRG1	1.07929	20.07	18.60	0	0
NTM	3.31112	60.39	18.24	2.22E-16	3.43E-13
NES	0.267485	2.23	10.56	2.27E-15	3.87E-12
COL8A1	36.1238	225.07	6.23	3.12E-13	2.20E-10
PRDM1	0.401853	7.44	18.51	3.05E-11	1.34E-08
SERTAD4	0.450182	24.21	53.77	7.67E-11	3.04E-08
TCF4	37.7621	130.48	3.46	2.57E-10	9.01E-08
ELN	51.1748	589.96	11.53	6.06E-10	1.92E-07
AMIGO2	0.85003	22.43	26.38	7.06E-10	2.19E-07
MATN2	14.2143	89.65	6.31	1.03E-09	3.05E-07
POSTN	977.597	10842.10	11.09	2.32E-09	6.12E-07
PMEPA1	7.70988	33.52	4.35	3.86E-08	7.45E-06
ADAMTS16	0.0324503	2.35	72.53	6.16E-08	1.12E-05
NPR3	2.82337	21.18	7.50	6.54E-08	1.18E-05
ST6GAL2	1.08708	17.35	15.96	7.61E-08	1.35E-05
PTGS2	8.11076	101.54	12.52	1.04E-07	1.78E-05
SLC1A3	2.02865	16.18	7.98	1.14E-07	1.91E-05
HAS2	6.2782	93.16	14.84	1.92E-07	3.03E-05
FRMD5	0.170719	6.37	37.29	3.08E-07	4.58E-05
GREM1	81.3635	967.78	11.89	3.37E-07	4.88E-05
LTBP1	165.814	411.35	2.48	6.11E-07	8.13E-05
PDE11A	0.0211485	0.80	37.72	9.33E-07	0.00012
CLEC18A	0.190398	6.64	34.89	1.05E-06	0.00013
KRT17	0.169316	6.46	38.17	1.21E-06	0.00015
TRIB2	28.6094	98.25	3.43	1.24E-06	0.00015
FZD1	8.75127	84.37	9.64	1.29E-06	0.00016
TMEM132B	0.393634	6.80	17.29	1.73E-06	0.00020
MME	25.2954	77.43	3.06	2.03E-06	0.00022
FLRT2	14.1989	138.70	9.77	2.04E-06	0.00022
TMEM155	0.0549409	1.96	35.60	2.20E-06	0.00024
SNORD27	1460.51	29515.40	20.21	2.36E-06	0.00025
NKD1	0.0863915	1.92	22.18	2.53E-06	0.00027
CLEC18C	0.136863	4.46	32.56	3.69E-06	0.00038
NR2F1	0.232672	4.97	21.37	4.29E-06	0.00042
CLEC18B	0.134538	4.25	31.61	4.45E-06	0.00044
MYLK	56.8439	131.11	2.31	4.53E-06	0.00044
SNORD5	159.259	4615.43	28.98	9.23E-06	0.00082
PGBD5	0.0260789	1.15	43.94	1.14E-05	0.00099
NTRK3	0.0493417	1.15	23.36	1.15E-05	0.00099
FZD2	1.32364	16.55	12.50	1.23E-05	0.0011
KIF26B	0.786821	9.26	11.77	1.56E-05	0.0013
GXYLT2	17.0793	137.25	8.04	1.76E-05	0.0014
SERPINB7	0.116591	2.52	21.60	1.86E-05	0.0015
RASGRP3	0.112376	1.57	13.99	1.94E-05	0.0016
IL1RAP	5.82766	17.16	2.95	2.37E-05	0.0018
TPM1	236.248	636.52	2.69	2.65E-05	0.0020
TEK	0.135925	2.41	17.72	2.82E-05	0.0021
ELTD1	0.997018	11.86	11.90	3.38E-05	0.0024
MMP11	1.01536	13.20	13.00	3.41E-05	0.0025
NKD2	0.0485165	1.60	33.08	5.41E-05	0.0036

Table 3.10 – The 50 most significantly up-regulated genes between full-depth differentiated chondrocytes and articular cartilage derived stem cells lines using ''Cuffdiff' analysis.

p-adj-value corresponds to p-value adjusted for multiple testing using a 10% FDR. Unlike previous analysis, this is a pairwise comparison between FD and normal cartilage-derived stem cells (N-SC) alone, as grouping of samples is not possible in 'Cuffdiff'. Some genes may be incorrectly included or excluded from this analysis, as stem cell replicates could not be included. Statistical significance is defined as p-adj<0.1.

FD compared to N-SC					
Gene symbol	**Mean expression in FD**	**Mean expression in NSC**	**Fold-change**	**p-value**	**p-adj-value**
CHI3L2	129.00	3.31	-39.03	0	0
PRG4	282.41	2.61	-108.38	0	0
MTUS1	7.02	0.49	-14.42	2.44E-15	2.85E-12
ACAN	76.21	8.33	-9.15	2.09E-14	2.02E-11
APOL3	12.32	0.92	-13.39	1.60E-12	9.32E-10
PRUNE2	39.71	0.86	-46.27	2.46E-12	1.35E-09
CSF1	55.78	7.88	-7.08	4.35E-12	2.30E-09
CD74	28.03	0.94	-29.85	5.26E-11	2.20E-08
FGFR2	30.03	7.14	-4.20	1.88E-10	6.78E-08
CP	5.74	0.06	-102.45	9.96E-10	2.95E-07
FAM20A	3.77	0.16	-23.30	1.45E-09	4.08E-07
SCIN	4.73	0.11	-43.70	1.63E-09	4.46E-07
NEDD4L	13.98	4.62	-3.02	3.76E-09	9.54E-07
MMP13	11.21	0.28	-40.60	5.05E-09	1.21E-06
PPARG	7.99	0.22	-36.44	7.65E-09	1.76E-06
PLA2G2A	22.26	0.21	-104.47	1.38E-08	2.95E-06
GLDN	2.98	0.06	-49.73	3.61E-08	7.01E-06
GBP4	1.87	0.03	-69.97	6.42E-08	1.16E-05
HAS3	16.77	1.31	-12.80	9.35E-08	1.62E-05
SERPINA1	15.13	0.74	-20.40	1.00E-07	1.72E-05
CXCL12	55.79	8.01	-6.96	1.39E-07	2.28E-05
CYP3A5	3.69	0.46	-8.03	2.56E-07	3.89E-05
MRAP2	4.87	0.09	-53.45	2.68E-07	4.04E-05
FST	151.38	24.42	-6.20	3.24E-07	4.75E-05
PTPN20B	2.06	0.13	-15.87	3.35E-07	4.88E-05
A2M	2.19	0.01	-266.70	3.40E-07	4.91E-05
SEPP1	67.42	4.34	-15.55	5.36E-07	7.26E-05
PRIMA1	2.49	0.05	-46.98	7.67E-07	9.88E-05
SMAD3	39.79	12.58	-3.16	8.59E-07	0.00011
VCAM1	22.94	4.82	-4.76	9.86E-07	0.00012
GALNT12	6.71	0.27	-24.45	1.25E-06	0.00015
DOCK8	1.87	0.12	-15.39	1.77E-06	0.00020
VIT	8.95	1.36	-6.58	1.79E-06	0.00020
OAS2	5.22	0.66	-7.92	1.85E-06	0.00021
SMOC2	9.67	0.50	-19.25	1.90E-06	0.00021
DLX4	6.80	0.50	-13.63	1.99E-06	0.00022
SEMA3E	1.74	0.07	-23.51	2.07E-06	0.00023
OAS1	8.76	0.40	-21.85	2.66E-06	0.00028
PDE5A	8.24	2.07	-3.99	3.56E-06	0.00037
MX1	25.87	6.13	-4.22	3.82E-06	0.00039
SLC7A8	117.92	31.73	-3.72	4.06E-06	0.00041
CSGALNACT1	10.32	0.91	-11.38	4.27E-06	0.00042
IFIT3	31.65	6.41	-4.94	5.38E-06	0.00051
RBP4	5.06	0.10	-50.26	5.43E-06	0.00052
ELMO1	2.44	0.18	-13.36	5.69E-06	0.00054
LAMA3	5.25	0.94	-5.56	6.38E-06	0.00060
DCN	2131.32	533.73	-3.99	6.64E-06	0.00062
MYPN	1.03	0.03	-39.15	6.64E-06	0.00062
DLX3	3.45206	0.137198	-25.1610461	9.28E-06	0.00082
NTN1	2.52388	0.133567	-18.89601356	9.45E-06	0.00084

Table 3.11 – The 50 most significantly down-regulated genes between full-depth differentiated chondrocytes and articular cartilage derived stem cells lines using ''Cuffdiff' analysis.

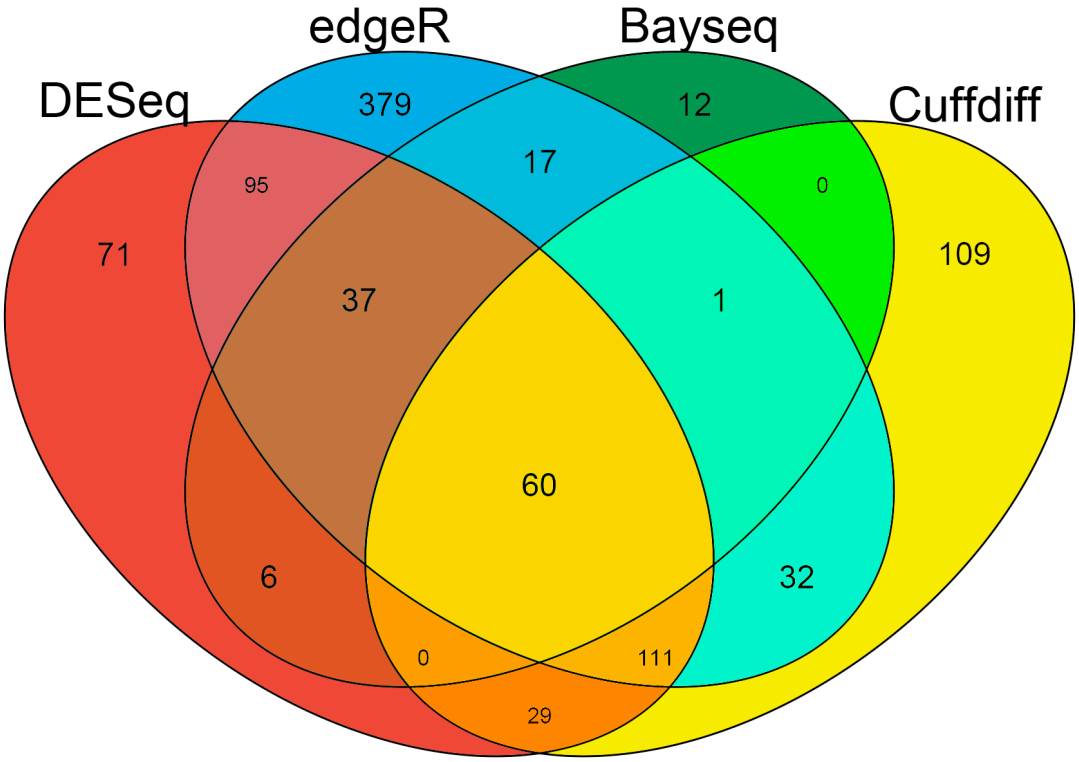
p-adj-value corresponds to p-value adjusted for multiple testing using a 10% FDR. Unlike previous analysis, this is a pairwise comparison between FD and normal cartilage-derived stem cells (N-SC) alone, as grouping of samples is not possible in 'Cuffdiff'. Some genes may be incorrectly included or excluded from this analysis, as stem cell replicates could not be included. Statistical significance is defined as p-adj<0.1.

3.3.2.5 Comparative analysis

We compared the number of differentially expressed genes found by each method (Figure 3.7). The highest number of differentially expressed genes was found by 'edgeR, while 'Bayseq' returned relatively fewer. As can be seen in Figure 3.7, 'DESeq' and 'Cuffdiff' found similar numbers of differentially expressed genes. The overlap between the sets of differentially expressed genes identified by different methods was analysed in the venn diagram (Figure3.7). Figure 3.7 shows the overlap between the sets of differentially expressed genes found by 'DESeq', 'edgeR' 'Bayseq' and 'Cuffdiff'. The differentially expressed genes found by 'DESeq' were to a large extent found also by 'edgeR' and 'Bayseq'. In contrast, both 'edgeR' and 'Cuffdiff' had a large quantity of 'unique' differentially expressed genes, which were not shared with the other methods. The fold-change between FD and ACSC of individual gene expression counts stayed relatively constant between each method as shown in Table 3.12.

3.3.3 Candidate stem cells markers

A panel of potential stem cell marker genes were selected for further investigation shown in Table 3.12. Genes selected were statistically significant in at least 3 of the 4 separate analyses, providing validity to the selection. The genes were selected based on a large statistical significant up-regulation within the RNA-seq experiments in the ACSC compared to FD populations. Genes were also chosen that had previous association to stem cells in the literature, including *NESTIN, PRDM1, FRMD5 and SLC1a3 (EAAT1)*. A set of genes was also selected that had extracellular membrane protein localisation, to facilitate live cell isolation. Cell surface genes included *FRMD5, EMBIGIN, SLC1a3 (EAAT1), ST6GAL2* and *TMEM132B*. All candidate genes from Table 3.12 are further validated and analysed in the subsequent Chapters of this thesis.



Methodology	Total number of significant genes (10%FDR) (p-adj-value <0.1)
'DESeq'	410
'edgeR'	733
'Bayseq'	134
'Cuffdiff'	343

Figure 3.7 – Venn diagram showing a comparison in differentially regulated genes between 'DESeq', 'edgeR', 'Bayseq' and 'Cuffdiff'

Venn diagram of significant gene with a p-adj-value of less than 0.1 (10%FDR) identified through the 4 different algorithms. 'edgeR' generated the most significant genes while 'Bayseq' the least. The difference between 'DESeq', and 'edgeR' can be attributed to the more stringent normalisation within each individual sample possible with the 'DESeq' algorithm.

	FD compared to all SC lines						FD compared to all SC lines	
Gene symbol	**Fold-change 'DESeq'**	**p–adj-value 'DESeq'**	**Fold-change 'edgeR'**	**p– adj-value 'edgeR'**	**Fold-change 'Bayseq'**	**p–adj-value 'Bayseq'**	**Fold-change 'Cuffdiff'**	**p–adj-value 'Cuffdiff'**
Potential stem cell marker genes								
NES	10.59	1.36E-8	10.66	0.00083	10.05	0.49	10.56	3.87E-12
C11ORF41	15.03	4.96E-8	14.78	0.00019	13.92	0.45	11.13	0.00011
FRMD5	34.33	1.55E-6	33.94	3.69E-6	32.15	0.07	37.29	4.58E-5
PRDM1	23.79	2.29E-10	23.56	1.48E-5	22.20	0.17	18.51	1.34E-8
EMB	8.04	9.39E-7	7.75	0.0054	2.90	0.57	4.46	0.07
SLC1a3 (EAAT1)	9.10	8.42E-7	9.04	0.0029	8.52	0.10	7.98	1.91E-5
TMEM132B	26.85	2.52E-12	26.52	6.63E-6	24.98	0.19	17.29	0.00020
ST6GAL2	8.88	1.82E-6	8.99	0.0033	8.47	0.75	15.96	1.35E-05
KIF26B	10.02	1.58E-9	10.02	0.0017	9.44	0.20	11.77	0.0013
Chondrogenic genes								
ACAN	-18.24	6.41E-32	-17.96	6.24E-11	-19.08	0.16	-9.15	2.02E-11
COL2a1	-9.60	0.0013	-9.49	2.58E-6	-10.10	0.11	-1.69	1.00
COL9A1	-9.44	0.60	-8.86	0.11	-9.86	0.54	-13.79	1.00
COL9A2	-1.60	0.40	-1.58	1.00	-1.68	0.93	-1.08	1.00
COL9A3	-5.58	0.30	-5.46	0.0027	-5.82	0.61	-2.62	1.00
COL11A1	2.39	0.23	2.43	0.81	2.29	0.97	4.45	0.038
COL11a2	-3.57	0.56	-3.52	0.055	-3.75	0.69	-4.42	1.00
PRG4	-36.91	6.41E-32	-36.89	2.39E-16	-39.19	0.002	-108.38	0

Table 3.12 – Comparison of expression levels of genes selected as potential stem cell markers or full-depth differentiated chondrocyte markers using 'DESeq', 'edgeR', 'Bayseq' and 'Cuffdiff'.

'DESeq', 'edgeR' and 'Bayseq' fold-change and statistical significance is calculated using all stem cell lines as a cohort. 'Cuffdiff' analysis is calculated as a pair-wise comparison between a single full-depth chondrocyte cell line and a single normal articular cartilage-derived stem cell line. Therefore, 'Cuffdiff' values are more prone to variation caused by anomalous or erroneous data, an obvious example of this is with the expression of Collagen Type II. Statistical significance is defined as p-adj<0.1.

Fold-change was found to be relatively constant irrespective of the analysis algorithm employed. The statistical significance was found to be extremely dependent on the model and normalisation method used. 'Bayseq' analysis returned a lot fewer statically significant genes to the other methodologies.

3.4 Discussion

In this Chapter, experiments were carried out using full-depth differentiated chondrocytes (FD) and articular cartilage-derived stem cells (ACSC) isolated from full-thickness knee articular cartilage of both healthy and osteoarthritic donors. Cell lines were expanded in culture prior to transcriptome analysis.

The presence of articular cartilage stem/progenitor cells has now become a widely accepted concept with various research groups reporting their discovery (Alsalameh et al., 2004, Dowthwaite et al., 2004, Fickert et al., 2004, Grogan et al., 2009, Pretzel et al., 2011, Williams et al., 2010, Nelson et al., 2014). Previously, within our laboratory, these cells have been isolated from immature and mature bovine, mature equine and healthy and osteoarthritic human cartilage through differential selection to fibronectin, mediated by α5β1 integrin interactions (Dowthwaite et al., 2004, McCarthy et al., 2012, Nelson et al., 2014, Williams et al., 2010). Our previous studies have shown that clonogenic cells from human articular cartilage express cell surface markers CD105 and CD166 and undergo multipotential differentiation into adipogenic, osteogenic and chondrogenic lineages, and therefore, fulfill the criteria for classification as mesenchymal stem cells (Williams et al., 2010). Other research groups have identified tissue-specific progenitor cells using other methods of identification including mesenchymal surface antigen markers (CD29, CD44, CD49e, CD90, CD105, CD117 and CD166) and migratory capacities to demonstrate the existence of progenitor cells in normal and osteoarthritic human tissue (Alsalameh et al., 2004). Studies utilising these surface antigens have reported highly variable results; extracting between 2-45% of the total cells (Pretzel et al., 2011, Grogan et al., 2009). It has also been reported that enzymatic digestion of cartilage can alter the expression of cell surface markers (Richardson, 2011). Therefore, these current procedures utilizing classical MSC markers are insufficient for use in selection of tissue specific stem cells within articular cartilage.

Advances in next generation sequencing technologies allow high-throughput sequencing to be applied in transcriptomic studies, in particular for identifying differentially expressed genes between sample groups. RNA-Seq has revolutionised the understanding and complexity of the eukaryotic

transcriptome. Reductions in cost, increased speed and improved sensitivity and precision over other methodologies means RNA-Seq is increasingly popular (Wang et al., 2009). Compared to microarray techniques, RNA-Seq can be performed without prior knowledge of a reference sequence, enabling *de novo* assembly (Grabherr et al., 2011, Robertson et al., 2010), abundance estimation (Anders and Huber, 2010, Anders et al., 2013, Oshlack et al., 2010), and the detection of alternative splicing (Pan et al., 2008).

3.4.1 Identification of potential stem cell markers

In this study, we successfully isolated ACSC cell populations from healthy and osteoarthritic articular cartilage using differential adhesion to fibronectin. Each cell line was passaged to 25 population doublings and processed for RNA for transcriptomic analysis. We demonstrated that it is possible to distinguish different cell populations from articular cartilage based on their transcriptional profile, successfully identifying differentially expressed genes between the FD sample and the ACSC samples. A panel of candidate stem cell specific genes and a panel of differentiated chondrocyte specific genes were isolated.

The total number of genes expressed by either FD or ACSC was 23228 and 410 genes were found to be statistically significantly differentially expressed ('DESeq") between FD and ACSC. Of the 410 genes identified, a panel of 9 candidate stem cell markers were selected based on protein localisation, previous associations to stem cells and statistical significance within the RNA-Seq study. These genes included *NESTIN, FRMD5, C11ORF41, SLC1a3 (EAAT1), EMBIGIN, PRDM1, TMEM132B, ST6GAL2* and *KIF26B.* Genes that were down-regulated in ACSC included genes that are associated with differentiated chondrocyte. These included Collagen Type II, Aggrecan and lubricin; this supports evidence that ACSC are an immature phenotype. Hierarchical clustering showed that samples could be identified based on their gene expression profiles. All ACSC, samples were clustered together with the FD sample in a separate group. Within the ACSC samples we were further able to distinguish between N-SC and OA-SC, indicating that the data set contain OA specific genes that were not analysed in this study.

NESTIN showed approximately an 11-fold increase in expression within the ACSC. NESTIN is an intermediate filament protein expressed in dividing cells during early development. Upon differentiation, NESTIN is down-regulated and replaced by tissue-specific intermediate filament proteins (Eriksson et al., 1992b). In adult organisms, NESTIN expressing cells are restricted to defined niches, where they may function as a quiescent stem cell reserve capable of proliferation, differentiation and migration once activated. NESTIN is widely utilised as a marker of proliferating and migrating adult stem cells (Michalczyk and Ziman, 2005).

PRDM1 showed approximately a 23-fold increase in ACSC. PRDM1 is a zinc finger transcription factor with multiple functions reported in immunity and embryonic stem cell development (Chu et al., 2011). PRDM1 has not, previously been reported in adult stem cells of the mesenchymal lineage, however, Robertson and colleagues showed PRDM1 was essential in multipotent progenitor cell populations within the developing forelimb and pharayngeal arches (Robertson et al., 2007). A PRDM1-positive tissue specific progenitor has been reported in the epidermis (Blanpain and Fuchs, 2009). Recently it has been shown that PRDM1 is involved in pluripotency, and that it can be used in conjunction with or in replacement of Yamanaka factors for formation of iPS cells (Nagamatsu et al., 2011). PRDM1 was selected due to its associations to pluripotency in the literature.

FRMD5 showed an approximate 34-fold increase in ACSC. The specific role for FRMD5 is yet to be identified, however, FRMD5 was one of the most significant genes in the transcriptome sequencing experiment and it has also been identified as a gene that is up-regulated 15-30 fold in MSCs in microarray studies (Kubo et al., 2009). FRMD5 was selected as it has been shown to have role in cell adhesion and localises to the cell membrane facilitating live cell isolation (Wang et al.).

Excitatory Amino Acid Transporter 1 (EAAT1) showed an approximate 9-fold increase in ACSC. EAAT1 was selected as it is predominantly expressed in the plasma membrane, allowing it to remove glutamate from the extracellular space (Divac, 1977) as cited in (Knut, 1995). This approach allows EAAT1 to be used for live cell isolation. Previous studies have shown EAAT1 expression in NESTIN-

positive neural stem cells, which is up-regulated during brain injury (Gilley and Kernie, 2011, Mich et al., 2014).

EMBIGIN showed an approximate 8-fold increase in ACSC. EMBIGIN is a developmentally expressed protein that is a member of the immunoglobulin superfamily (IgSF) class of cell adhesion molecules (Guenette et al., 1997). Previous studies have not identified EMBIGIN specifically within adult stem cells however, it is reported to be involved in wound healing and tissue remodelling as well as being strongly expressed in cancer cell lines *in vitro* (Tachikui et al., 1999). Two studies have identified EMBIGIN expression within embryonic stem cells, where it function to enhance cell-substratum adhesion (Huang and Wu, 2008, Muramatsu and Muramatsu, 2004). EMBIGIN was selected for its extracellular localisation and expression in pluripotent stem cells.

Transmembrane protein 132b (TMEM132B) is a transmembrane protein of unknown function, which showed an approximate 27-fold increase in ACSC. TMEM132B was selected for its membrane localisation and a microarray study identifying markers for neural progenitors found TMEM132B as one of the most significant genes (Obayashi et al., 2009).

ST6 beta-galactosamide alpha-2,6-sialyltranferase 2 (ST6GAL2) showed an approximate 34-fold increase in ACSC. Sialyltransferases catalyses the synthesis of sialylglycoconjugates by transferring a sialic acid molecule (Takashima and Tsuji, 2014). The protein is localised to the cell membrane with extracellular epitopes and, therefore, selected to facilitate live cell isolation.

Chromosome 11 open-reading frame 41 (C11ORF41) showed an approximate 15-fold increase in ACSC. No known function is reported for C11ORF41, the protein sequence predicts localisation within the cytoplasmic membrane. C11ORF41 was one of the most significant genes in the transcriptome sequencing experiment and selected for further study on this basis.

Kinesin family gene 26b (KIF26B) showed an approximate 10-fold increase in ACSC. Kinesins are widely involved in development, stem cell phenotype and tumour progression (Wang et al., 2013). Specifically, kinesins are responsible for

asymmetric division giving rise to a self-renewed stem cell and a differentiated daughter cell (Knoblich, 2008). Kinesin family member 26B has been shown to have an important role in the embryonic development but no previous function has been reported in adult stem cells (Uchiyama et al., 2010). KIF26B was selected as one of the most significantly up-regulated genes in the RNA-Seq study as well as previous family member connections to stem cells.

Other genes were considered as candidates for stem cell markers but were rejected following further validation (Chapter 3). The panel of stem cell marker genes and the panel of differentiated chondrocyte-specific genes are further investigated and validated in the subsequent Chapters of this thesis.

3.4.2 Comparison of differential expression methods

Many software packages have been developed for isolating differentially expressed genes between treatment groups based on RNA-Seq data (Zhang et al., 2014). However, there is a lack of consensus on which is the most suitable software for the analysis, with no single method optimal under all circumstances; therefore, the method of choice is dependent on the experimental conditions (Soneson and Delorenzi, 2013). This study utilised 4 of the most frequently used software tools: 'DESeq', 'edgeR', Bayseq' and 'Cuffdiff' and compares the differentially expressed genes identified by each to identify novel markers for ACSC.

'DESeq', 'edgeR' and 'Bayseq' are 3 widely used gene count-based tools that analysed differential expression. 'Cuffdiff' is a transformation-based alternative that transforms the alignment results to RPKM values before calculating statistical significance. 'DESeq', 'edgeR' and 'Cuffdiff' use a negative binomial model to calculate statistical significance while 'Bayseq' utilises a Bayesian based model.

'DESeq' performed the most effectively for our data set based on the number of differentially expressed genes and the overlap with other methodologies. One or more of the other algorithms also found the majority of genes identified by 'DESeq'. 'Bayseq' also had the majority of the genes produced identified by other

methods, however, due to the vastly lower number of differentially expressed genes it was deemed overly stringent with our dataset.

Although both 'DESeq' and 'edgeR' both use negative binomial models, algorithms with same input data, many genes were identified solely by 'edgeR'. Further investigation showed these genes often had a high-fold-change but a low absolute expression or were variable between ACSC samples. This indicates 'DESeq' is more conservative than 'edgeR' in identifying differentially expressed genes, which has been found in numerous previous studies (Kvam et al., 2012, Soneson and Delorenzi, 2013, Zhang et al., 2014). One possible explanation for the large differences in the numbers of differentially expressed genes is the differences in the method of estimating the dispersion parameters with 'edgeR having poor FDR controls with small sample sets (Soneson and Delorenzi, 2013).

'BaySeq' uses a different Bayesian model based approach to calculate the probability of a gene being differentially expressed. 'Bayseq' was highly conservative only identifying 134 genes. It has been reported that 'BaySeq' requires a higher-fold-change than the other methods to call a gene differentially expressed (Soneson and Delorenzi, 2013). In this study, we found the distribution of differentially expressed genes with small and large fold-changes using 'Bayseq' to be similar and comparable to the distribution found by the other methods. Soneson and Delorenzi (2013) also found that when differential expression of genes are skewed in one direction 'Bayseq' is highly variable in this study the 'Bayseq' analysis had considerably more down-regulated genes than up-regulated genes and this could have affected the statistical analysis.

The overall performance of Cuffdiff for differential expression was not as good as the count based negative binomial methods but showed an improvement on 'Bayseq'. Fewer differentially expressed genes were identified than 'DESeq' and 'edgeR', with 32% of the genes identified unique to this analysis. A possible explanation is that Cuffdiff transforms the alignment reads to RPKM values rather than to raw count values. This study was employed as direct RNA, single strand, sequencing, it has previously been reported that RPKM values when a single-end sequencing strategy is applied, may not be an appropriate way to normalize RNA-Seq data and that RPKM normalisation has been shown to cause

a conservative bias in 'Cuffdiff' (Li et al., 2012, Zhang et al., 2014). Finally, 'Cuffdiff' analysis was performed as a pair-wise analysis between FD and a normal articular cartilage stem cell (N-SC) line, reducing accuracy due to a reduction in experimental replicates.

In this study, 60 differentially expressed genes were identified by all 4 methodologies. With the majority of differentially expressed genes being identified by at least 2 techniques. The highest number of differentially expressed genes was found by 'edgeR, while 'Bayseq' returned the least, 'DESeq' and 'Cuffdiff' found similar numbers of differentially expressed genes. 'edgeR' detected far more differentially expressed genes than the other tools, with over 50% of these differentially expressed genes identified exclusively by 'edgeR'. Identification of more differentially expressed genes is not always beneficial as this can increase false positives making future validation difficult. A previous study by Zhang and colleague's also found 'edgeR' to produce the most differentially expressed genes but of these were 108 false positives compared with 77 in 'Cuffdiff' and 8 with 'DESeq' (Zhang et al., 2014).

3.4.3 Limitations

Budgetary constraints are common with NGS; therefore, optimal experimental designs need to be a balance between cost, sequencing depth and the number of replicates in each group. Including sufficient biological replicates should be the prime consideration in study design as the overall impact of the sequencing depth is not as critical as replicates (Liu et al., 2014). In this study, budgetary constraints limited the number of biological replicates, the FD group contained only 1 sample and the ACSC contained 3 samples; this reduces the accuracy of the results, resulting in more validation requirements. The minimal standard and guidelines for publication of RNA sequencing data states that single biological replicates can be used if there is a compelling reason, including financial constraints (ENCODE, 2011). No technical replicates were employed in this study, although RNA-Seq is highly reproducible, therefore, the need for technical replicates is low. The negative binomial model has been used to tolerate the low number of biological replicates, because of its ability to deal with the over dispersion problem that can occur.

3.4.4 Conclusions

Transcriptomics has successfully identified mRNA differences between FD and ACSC populations. This has provided potential novel markers of cartilage-specific stem cells. These markers offer new targets to identify, localise, characterize and isolate ACSC, which will be explored in the subsequent Chapters of this thesis.

CHAPTER 4:

AN IMMUNOHISTOCHEMICAL AND QUANTITATIVE ANALYSIS OF NOVEL STEM CELL MARKERS IN PRIMARY MONOLAYER CUTURES

4.1 Introduction

There is a widely held assumption that osteoarthritis is a progressive and terminal disease of joints, predicated on the belief that articular cartilage has a poor innate capability for repair. In many, if not all tissues, stem cells drive the reparative response; therefore, the discovery of tissue specific stem cells within articular cartilage has obvious and important implications for understanding the role of endogenous repair processes (Alsalameh et al., 2004, Dowthwaite et al., 2004, Williams et al., 2010). One fundamental property of stem cells is their ability to replicate, and in the first instance, their capacity to replace cells and tissues lost due to injury and/or disease.

The challenge we face is to understand the precise role of tissue-specific stem cells during disease, specifically to investigate the numbers and location of stem cells remaining in diseased tissue and their replicative and reparative capacity. In order to achieve this, reliable and specific markers are required to distinguish articular cartilage stem cells from their differentiated progeny.

Cell therapies for articular cartilage repair use culture-expanded chondrocytes and/or MSCs. However, chondrocytes pose certain problems due to the limitations in harvestable cell numbers, donor site morbidity and de-differentiation upon *in-vitro* expansion (Saha, 2012, Mobasheri et al., 2014). Mesenchymal stem cells represent a multipotent adult stem cell with a reduced differentiation and proliferative potential than embryonic stem cells. MSCs are a plastic adherent, colony forming, multipotential cell with a Hayflick limit for *in vitro* expansion of 30-50PDs (Wagner et al., 2008, Stenderup et al., 2003). MSCs offer a promising alternative therapeutic cell source that does not require harvesting of healthy cartilage and greater cell numbers that can be achieved through extended proliferation *in vitro*. However, treatments using bone marrow derived MSCs often results in a fibrocartilage repair tissue with poor integration to the native hyaline cartilage (Carey, 2012). Additionally, bone marrow MSCs produce Type X collagen during *in vitro* chondrogenesis (Barry et al., 2001). Up-regulation of Type X collagen during *in vitro* chondrogenesis has been shown to result in matrix calcification accompanied by vascularization; this process is similar to endochondral ossification which ultimately leads to the development

of new bone (Pelttari et al., 2006). Therefore, the predisposition of bone marrow-derived MSCs towards osteogenesis may make them unsuitable for hyaline-like repair in articular cartilage defects. A stem cell population with a predisposition towards the chondrogenic phenotype should produce more favourable results.

As mentioned in Chapter 3, stem cell populations have been identified through differential adhesion assays or expression of MSC surface antigens in healthy and osteoarthritic cartilage across multiple species (Alsalameh et al., 2004, Dowthwaite et al., 2004, Fickert et al., 2004, Grogan et al., 2009, Pretzel et al., 2011, Williams et al., 2010, Nelson et al., 2014, McCarthy et al., 2012). These cells have been shown to be superior to MSCs in producing a functional repair tissue. ACSC have a pre-disposition towards chondrogenesis and chondrogenic induction of ACSC that does not result in Collagen Type X and alkaline phosphatase production unlike MSCs (McCarthy et al., 2012). In order to allow for rapid isolation and screening of ACSC for use in therapeutics, markers of this stem cell population are essential. As previously mentioned, mesenchymal stem cells surface antigens have highly variable expression levels (2-45% of cells) within articular cartilage and are deemed unsuitable for reliable isolation of a stem cell population. The purpose of this study is to identify specific markers of ACSC that can be used to isolate a cell source that can be used for repair of articular cartilage.

By analysing the proliferative properties of articular cartilage-derived stem cells (ACSC) from normal and osteoarthritic (OA) human cartilage, it should be possible to understand quantitatively, and to a greater degree than previously, the potential for repair that exists in injured or diseased joints. In this study, ACSCs were cultured as single clonal isolates from normal or osteoarthritic joints using colony forming assays, a well-established method for the identification of mesenchymal stem cells (Dowthwaite et al., 2004). Their replicative efficiency was measured by population doublings and bromodeoxyuridine (BrdU) incorporation and, there phenotypic plasticity was assessed through differentiation in chondrogenic, osteogenic and adipogenic lineages. In this Chapter, novel NGS-generated stem cell markers were investigated, building on the work in Chapter 3. Differentially expressed genes identified in the transcriptomic study were validated through both gene and protein expression in *in vitro* expanded ACSC and FD cell lines.

4.2 Methodology

Material	Catalogue number	Supplier
40µm mesh cell strainer	352340	BD FalconTM, UK
Dako pen	S2002	Dako, UK
Mouse immunoglobulins	X0931	Dako, UK
Dulbecco's modified Eagle's medium	41965-062	Gibco, UK
Trypsin-EDTA 0.05%	25300-062	Gibco, UK
Foetal calf serum	10106-169 1	Gibco, UK
L-glutamine 200mM	25030-081	Gibco, UK
Hepes buffer	15630-056	Gibco, UK
Insulin-transferrin-selenium (ITS)	41400-045	Gibco, UK
SafeView Nucleic Acid Stain	NBS-SV1	NBS Biologicals Ltd, UK
Low Molecular Weight DNA Ladder	N0468	New England Biolabs, UK
Steriflip® filter unit	SCGP00525	Millipore, UK
CellTrics 30 µm filters	04-004-2326	Partec, UK
Human FGF - basic	00 - 18B	Peprotech, UK
Human TGF - β2	100 – 35B	Peprotech, UK
Human TGF – β1	100 – 21	Peprotech, UK
GoTaq® G2 Hot start DNA Polymerase	M7405	Promega, USA
AMV Reverse Transcriptase, RNase H Minus	M5108	Promega, USA
Random primers	C1181	Promega, USA
Recombinant RNasin Ribonuclease Inhibitor	N2511	Promega, USA
Set of dATP, dCTP, dGTP, dTTP	U1240	Promega, USA
TBE Buffer	V4251	Promega, USA
Agarose	V3125	Promega, USA
GoTaq® qPCR Master Mix	A6002	Promega, USA
DPX mounting medium	RAYKKAMB/DPX	Raymond A Lamb Medical, UK
Goat immunoglobulin	AB-108-C	R&D systems, UK
Rabbit immunoglobulin	AB-105-C	R&D systems, UK
Pronase from Streptomyces griseus	11 459 643 001	Roche, UK
Hydrogen peroxide, 30% (w/w)	H1009	Sigma Aldrich, UK
Phosphate buffered saline	P4417	Sigma Aldrich, UK

Toluidine blue	89640	Sigma Aldrich, UK
Tween-20	P1379	Sigma Aldrich, UK
Triton-X-100	T8787	Sigma Aldrich, UK
Collagenase from clostridium histolyticum	C0130	Sigma Aldrich, UK
L-Ascorbic acid 2-phosphate	A8960	Sigma Aldrich, UK
Cloning rings	C7983	Sigma Aldrich, UK
Dexamethasone	D8893	Sigma Aldrich, UK
Dimethyl sulfoxide	D5879	Sigma Aldrich, UK
Fibronectin from bovine plasma	F1141	Sigma Aldrich, UK
D-(+)-Glucose	G6152	Sigma Aldrich, UK
β-Glycerophosphate disodium salt hydrate	G9422	Sigma Aldrich, UK
Indomethacin	I7378	Sigma Aldrich, UK
Insulin solution, human	I9278	Sigma Aldrich, UK
3-Isobutyl-1-methylxanthine	I7018	Sigma Aldrich, UK
β -Mercaptoethanol	M3148	Sigma Aldrich, UK
Silver nitrate	S6506	Sigma Aldrich, UK
Methanol	322415	Sigma Aldrich, UK
Oil-red-O	O1391	Sigma Aldrich, UK
10 % Formalin solution, neutral buffered	HT501128	Sigma Aldrich, UK
Ethanol	E/0650DF/17	Thermo Fisher Scientific, UK
Sodium hydroxide	S/4920/60	Thermo Fisher Scientific, UK
Polylysine adhesion glass slides	MNJ-800-010F	Thermo Fisher Scientific, UK
RNase Mini Kit	74104	Qiagen, UK
RNase-free DNase set	79254	Qiagen, UK
Antigen unmasking solutions	H-3300	Vector Laboratories, UK
R.T.U Vectastain Universal Quick Kit	PK-7800	Vector Laboratories, UK
DAB Peroxidase Substrate Kit, 3,3'-diaminobenzidine	SK4100	Vector Laboratories, UK
Safranin O Gurr 'Certistain'	343122N	VWR, UK

Table 4.1– Materials and suppliers

4.2.1 Cell isolation and culture

Full-depth chondrocytes and articular cartilage adult stem cells were isolated from healthy and osteoarthritic donors as previously described (Sections 2.1-2.5). In brief, tissue was dissected and digested in sequential pronase and collagenase enzymes. Full-depth chondrocytes were pelleted through centrifugation (2000 rpm, 5 minutes), re-suspended in DMEM+ plus TGF-β2 and FGF-2 (Section 2.4), and then plated and expanded in culture. Stem cells were selected through differential adhesion to fibronectin and colonies isolated after 14 days using cloning rings (Section 2.3). Monoclonal cells lines were expanded and cultured in DMEM+ plus TGF-β2 and FGF-2.

4.2.2 RNA extraction and purification

RNA was isolated from one million cell aliquots of each cell lines using the Qiagen RNeasy kit as outlined in Section 2.7. Purity and concentration was checked using a nano-drop DNA quantifier.

4.2.3 cDNA synthesis

One microgram of RNA was used *per* sample for cDNA synthesis for each reaction. Reactions were performed in 50µl containing, 400µM dNTPs, 0.4µg of random hexameric primers (Promega), 0.2U/µl AMV RT enzyme (Promega) and 0.5U/µl RNasein (Promega). Samples were incubated at 25^{o}C for 10 minutes, 48^{o}C for 1 hour and then 95^{o}C for 2 minutes in a thermocycler. (Section 2.8)

4.2.4 qPCR analysis

Quantitative polymerase chain reaction (qPCR) was completed using the ABI 7700 and the Biorad CFX96 detection systems as outlined in Section 2.12. Plasmids were cloned from PCR products (Section 2.9-2.11) and sequenced to confirm the identity of the insert. Gene expression was quantified against a standard curve of serial diluted plasmid and normalised to the house-keeping genes beta-2 microglobulin (*B2M)* and ribosomal protein S18 (*RPS18),* after the NormFinder algorithm identified this combination as optimal from the panel of candidate genes (Table 4.2). Primer sequences and annealing temperatures are shown in Table 4.3. Melt curves and standard curves for each gene are provided in the Appendix (Figure S1.2 & S1.3).

Gene name	Gene symbol	Forward primer sequence	Reverse primer sequence	Annealing temp (°C)	NormFinder coefficient of variance	NormFinder M - value
Beta-2 microglobulin	B2M	AGA-TGA-GTA-TGC-CTG-CCG-TG	TCA-TCC-AAT-CCA-AAT-GCG-GC	56	0.0130	0.1352
Ribosomal protein S18	RPS18	CAC-AGG-AGG-CCT-ACA-CGC-CG	AGG-CTA-TTT-TCC-GCC-GCC-CA	56	0.0013	0.1352
Hyperparathyroidism 1	HRPT1	GAG-ACA-GGA-CCA-CTC-ATG-AAG-T	TCG-AGC-AAG-ACG-TTC-AGT-CC	56	0.1388	0.2679
Pre-mRNA processing factor 31	PMP31 (RP11)	GTG-CGG-CTG-CTT-CCA-TAA-G	CCC-TGG-CGT-CGT-GAT-TAG-TG	56	0.1272	0.2453
60S ribosomal protein L13a	RPL13a	CGT-GGC-TAA-ACA-GGT-ACT-GC	GTT-TGG-TGT-TCA-TCC-GCT-TGC	56	0.1580	0.4798
Beta actin	ACTB	CAA-GTC-CAC-ACA-GGG-GAG-GT	AGA-CCA-AAA-GCC-TTC-ATA-CAT-CTC-A	56	0.2568	0.7707
Combination of ribosomal protein S18 and beta-2 microglobulin	**RPS18 + B2M**				**0.0072**	**0.0207**

Table 4.2 – NormFinder results and primer sequences for house-keeping genes.

A coefficient of variance of <0.25 and a M-value of <0.5 shows gene homogenous gene expression across all cDNA samples. All house-keeping genes considered with the exception of beta actin were found to be suitable candidates. House-keeping genes were considered and tested both individually and in combinations (all possible iterations were processed using the NormFinder algorithm). The combination of the beta-2microglobulin and ribosomal protein S18 was found to provide the optimum normalisation and therefore chosen as the house-keeping genes for all qPCR experiments in this study.

Gene name	Gene symbol	Forward primer sequence	Reverse primer sequence	Annealing temp (°C)
NESTIN	NES	ATG-AAC-GGG-CTG-GAG-CAG-TCT-GAG-GAA-GT	CTG-AGG-ACC-AGG-ACT-CTC-TA	55
FERM domain containing 5	FRMD5	TCC-GCC-AGA-CCC-CCG-AGT-TT	CCG-ATG-GTT-CCG-CGA-TGG-GT	56
Chromosome 11 open reading frame 41	C11ORF41	CGT-GTC-CCA-GGC-CCG-AAG-GA	GGC-GGG-TTC-TTC-ACC-ACG-GG	56
EMBIGIN	EMB	TGA-ATC-CCT-GCT-CCT-TTG-ACC	AGC-CAC-GCA-AAA-GAG-GGA-TT	57
Excitatory amino acid transporter 1 (solute carrier family 1 member 3)	EAAT1 (SLC1A3)	CTG-TGG-CTG-TGA-TGC-TGA-TTG-T	CGT-GAC-CAG-CGT-GCT-CC	56
Transmembrane protein 132B	TMEM132B	AAG-GCG-GCA-GCA-GGT-GTG-AAG	CTC-TGC-GTG-TCC-GGG-CGA-TG	58
PR domain containing 1 with ZNF domain	PRDM1 (BLIMP-1)	TCC-AGC-ACT-GTG-AGG-TTT-CA	TCA-AAC-TCA-GCC-TCT-GTC-CA	57
Kinesin family member 26B	KIF26B	AAG-GGG-GTC-CTG-CCG-TCT-CG	GGC-TCA-TTC-CAA-CCG-GGG-GC	55
ST6 beta-galactosamide alpha-2, 6-sialytranferase 2	ST6GAL2	AAG-GGG-AAC-GTC-TCT-TCC-AAA	CTT-GTT-GGC-GGT-CAG-GTA-ATC	55
Notch-1	Notch-1	GAG-GCG-TGG-CAG-ACT-ATG-C	CTT-GTA-CTC-CGT-CAG-CGT-GA	56
Jagged-1	JAG1	GTC-CAT-GCA-GAA-CGT-GAA-CG	GCG-GGA-CTG-ATA-CTC-CTT-GA	56
Collagen II alpha 1	COL2A1	CCA-GAT-GAC-CTT-CCT-ACG-CC	TTC-AGG-GCA-GTG-TAC-GTG-AAC	56
Aggrecan	ACAN	ACT-CTG-GGT-TTT-CGT-GAC-TCT	ACA-CTC-AC-CAG-TTG-TCA-TGG	56
Collagen IX alpha 1	COL9A1	GAG-CAC-CGA-CAG-ATC-ACC-AC	AGT-GGC-ACC-TCA-GTC-TGG-A	56
Collagen XI alpha 2	COL11A2	TCT-TTG-GTC-CCC-GTA-TTC-TGG	TGG-GGT-TCC-TGA-TTT-TGT-GGC	56
Proteoglycan 4 (Articular superficial zone protein) (Lubricin)	PRG4	GGG-AGT-TGT-GGG-GAA-GGG-TA	CCT-CCC-TCT-CTC-GAA-GAA-CT	56
SRY (sex determining region Y) – box 9	SOX9	GCC-AGG-TGC-TCA-AGG-GCT-A	TCT-CGT-TCA-GCA-GTC-TCC-AGA-G	56

Table 4.3 – Primer sequences and annealing temperature for primers used in this study.

4.2.5 Immunocytochemistry

Immunofluorescence detection of stem cell markers was performed on culture-expanded cell lines as described in Section 2.20.1. In brief, cells were fixed in 95% ethanol for 10 minutes and then samples were washed 3 times in PBS/0.1% Tween 20 (PBST) and blocked in 10% relevant sera for 1 hour. All antibodies and immunoglobulin matched (IgG-matched) controls were prepared in PBS (Sigma-Aldrich) containing 0.2% Triton-X100 (Sigma-Aldrich) and 5% blocking serum (serum was species matched to the secondary antibody). Excess serum was removed and cells were incubated with primary antibodies for 1 hour at room temperature. The slides were washed 3 times in PBST and then incubated with 10μg ml^{-1} fluorescence conjugated secondary antibodies for 1 hour at room

temperature. Samples were washed a further 3 times in PBST before being mounted in Vector shield ™ containing DAPI. Antibody concentrations are shown in Table 4.4.

Antigen	Antibody	Host species	Supplier	Concentration
A recombinant 150 amino acid fragment from human NESTIN conjugated to glutathione S transferase.	Anti-NESTIN [10C2]	Mouse monoclonal	Abcam (ab22035)	10µg ml^{-1}
Epitope mapping within an internal region of FRMD5 of human origin	Anti-FRMD5 (G-12)	Goat polyclonal	Santa Cruz (sc-137483)	10µg ml^{-1}
Epitope mapping within an internal region of C11ORF41 of human origin	Anti-C11ORF41 (D-19)	Goat polyclonal	Santa Cruz (sc-242004)	10µg ml^{-1}
Recombinant fragment, corresponding to a region within amino acids 122-315 of Human EMBIGIN homolog	Anti-EMBIGIN	Rabbit polyclonal	Abcam (ab127692)	1:200
Synthetic peptide, corresponding to 20 residues from the C-terminus of RAT EAAT1	Anti-EAAT1	Rabbit polyclonal	Abcam (ab416)	1:50

Table 4.4 – Primary antibody optimal concentrations.

Primary antibodies were titrated using 10µg ml^{-1} fluorescent conjugated secondary antibody to ensure optimum labelling.

Secondary antibody		Supplier	Concentration
Donkey anti goat – Alexa Fluor 488	(DαG-488)	Abcam (ab150133)	1:400
Goat anti mouse – Alexa Fluor 594	(GαM-594)	Abcam (ab150120)	10µg ml^{-1}
Donkey anti goat – Alexa Fluor 647	(DαG-647)	Abcam (ab150135)	10µg ml^{-1}
Donkey anti rabbit – Alexa Fluor 633	(DαR-633)	Life technologies (A-21070)	1:200
Goat anti rabbit –FITC	(GαR-FITC)	Sigma Aldrich (F6005)	1:200
Rabbit anti mouse –FITC	(RαM-FITC)	Sigma Aldrich (F9137)	1:400

Table 4.5 – Secondary antibody optimal concentrations.

Secondary antibodies were titrated using the optimised primary antibody concentrations the antibody that exhibited the strongest cellular labelling was chosen to optimise the respective secondary antibody. NESTIN was used to optimise DαM-594 and RαM-FITC, FRMD5 was chosen to optimise (DαG-647) and (DαG-488) while EMBIGIN was chosen to optimise (DαR-633) and (GαR-FITC).

4.2.6 Quantification of positive labelling through immunocytochemistry

The percentage of cells exhibiting positive labelling was quantified by counting the total number of DAPI stained nuclei and the number of cells displaying antibody labelling. Five fields of view were counted for 3 separate normal and 3 separate osteoarthritic donors, using x20 magnification on a fluorescence microscope. Minimums of 35 cells were present in each field of view.

4.2.7 Bromodeoxyuridine labelling (BrdU)

BrdU incorporation into cellular DNA occurs during cell proliferation in place of thymidine. As such, a BrdU assay was carried out in order to elucidate the extent of proliferation within the monoclonal cell lines from normal and osteoarthritic cartilage. Briefly, cells were seeded at 1.0 x 10^5 in 12 well plates and cultured for 24 hours. After 24 hours, 10μM BrdU was added to each well and incubated for a further 24 hours. The cells were then washed several times in PBS and fixed in ice-cold 95% ethanol for 10 minutes. BrdU incorporation was detected using a specific G3G4 anti-BrdU mouse monoclonal antibody (at 3μg ml^{-1} for 1 hour at room temperature). After several washes in PBS-T, cells were incubated in 3% H_2O_2 diluted in distilled water for 5 minutes. Following this procedure, cells were incubated in 4M HCl for 10 minutes. Cells were rinsed and the following steps utilised the R.T.U Vectastain Universal Quick Kit. Cells were incubated in pre-diluted normal horse serum for 20 minutes Excess serum was removed and cells were washed in PBS (three changes of 5 minutes) and then incubated for 15 minutes in pre-diluted biotinylated pan-specific universal secondary antibody at room temperature. Following 3 further 5-minute washes in PBS, each well was incubated in a streptavidin/peroxidase complex for 5 minutes. Cells were washed again and developed using a 3,3'Diaminobenzidine (DAB) substrate kit, for 2 to 3 minutes to visualize staining. Subsequently, each well was rinsed in distilled H_20 before being imaged.

Nine images were taken at random using a x20 objective. The numbers of positively stained and unstained cells were counted. The percentage of proliferating cells was calculated from these values.

4.2.8 Phenotype plasticity

Differentiation studies were undertaken to determine phenotypic plasticity. Chondrogenic and osteogenic differentiation were performed in pellet culture as described in Section 2.6.3 and adipogenic differentiation was performed on monolayer as described in Section 2.6.2. In brief, pellet cultures were set up at $5x10^5$ ml^{-1} in a sterile Eppendorf tube in either chondrogenic (Section 2.6.1.1) or osteogenic media (Section 2.6.1.2). Pellets were cultured for 3 weeks and media changed every 2 days. Cells for adipogenic differentiation were plated at 50,000

cells *per* well in a 6-well plate and cultured until 70% confluence, at this point media was changed to either control (Section 2.4) or adipogenic media (Section 2.6.1.3) for 10 days, media was changed every 2 days.

4.2.9 Histology

Safranin-O and toluidine blue staining were used to show proteoglycan incorporation during articular cartilage and during chondrogenic differentiation as described in Sections 2.21.2 and 2.21.3. Alizarin red and Von- Kossa staining were performed to identify mineral deposits in the osteogenic differentiated pellets as described in Sections 2.21.4 and 2.21.5. Oil red-O staining was performed to identify vacuoles of triglycerides within adipogenic-differentiated cells as described in Section 2.21.6. Crystal violet was used as a cytoplasmic counter stain as described in Section 2.21.7.

4.2.10 Statistics

All statistics were performed using the 'R' statistical software. Statistical significance was confirmed using a parametric analysis of generalised linear mixed models, Anova and Student T-tests where appropriate. Data that did not fit into the Gaussian distribution was 'normalised' by data transformations to allow for parametric analysis where possible. If data could not be normalised non-parametric alternatives were performed where stated. Statistical significance was defined as $p<0.05$.

Principal components analysis was performed to convert a multiple variable into two linear variables allowing visualisation of variables, which have similar effects. Samples were clustered using K-means.

Correlation analysis was performed using Pearson's product moment correlation coefficient after data was 'normalised' and linearised using a log-base 2 transformations. A correlation coefficient of +1 implies strong positive correlation while the inverse is true of a coefficient of -1, implying a strong negative correlation.

4.3 Results

Articular cartilage-derived stem cells were successfully isolated from healthy and osteoarthritic tibial plateaux and culture-expanded. The number of days required for colonies to form ranged from 7 days up to 14 days. Colonies were isolated using cloning rings to enable clonal cell lines to be expanded independently.

4.3.1 Percentage stem cells

There was a ~2-fold statistically significant increase (T_{16} = -4.58; $p<0.0005$) in the mean percentage of fibronectin-adhered cell colonies derived from osteoarthritic cartilage (2.90±0.87%; n = 9) when compared to normal cartilage (1.47±0.47%; n = 9) (Figure 4.1A).

4.3.2 Proliferation analysis

Growth kinetics (population doublings) of the clonally-derived stem cells and full-depth articular cartilage cell lines from 6 normal and 6 OA donor tibial plateaux were investigated (Figure 4.1B). The initial growth rates of ACSC were found to be linear until approximately 30PD after which the rate of proliferation started to slow, FD populations had a linear rate of growth until PD20 at which time the rate of proliferation slowed until senescence (Figure 4.1B). It was observed that within ACSC from healthy tissue that there was a slight degree of heterogeneity between cell lines from the different patients; however, cell lines from the same patient appeared to adopt similar proliferation rates; this was more apparent in OA derived cell lines. The most distinguishing feature in the growth kinetics is that OA-derived cell lines can be sub-divided into two populations, early senescent (ES-OA-SC) and late senescent (LS-OA-SC). Of the eleven OA stem cell (OA-SC) lines, 45% senesced before surpassing 30PD, the remainder displayed growth kinetics comparable to stem cells from normal cartilage (N-SC) (Figure 4.1B and Figure 4.2A-D). The initial rate of proliferation of ES-OA-SC lines initially appeared to be proliferating normally before a sudden arrest in their proliferation (Figure 4.1B). The normal ACSC were expanded to a maximum of 56.36 PDs and this was achieved in 210 days. The OA ACSC expanded to a maximum of 58.4 PDs and this was achieved in 245 days. The FD cell lines from

both normal and OA cartilage senesced around 30 population doublings; one N-FD cell line did proliferate to 40PD before senescence.

No significant difference in the average time taken to reach 10 and 20PD were found between normal and both OA ACSC sub-populations. However heterogeneity in proliferation rate between clonal cell lines was observed within OA-SC samples, while N-SC lines exhibited a more uniform rate of proliferation (Figure 4.2A-B), the variation with the OA-SC samples was observed both between donors and between clonal cell lines from the same donor. Additionally no significant difference in the average times taken to reach 30 and 40PD were found between N-SC and LS-OA-SC lines were observed. Again there was more heterogeneity in growth rates in the OA-SC populations than N-SC populations (Figure 4.2C-D). The initial rate of growth of both normal full-depth chondrocytes (N-FD) and OA full-depth chondrocytes (OA-FD) was significantly slower than the ACSC lines ($p<0.05$), with individual FD cell lines found to be highly heterogeneous in the proliferative rates from both normal and OA donors (Figure 4.1B and Figure 4.2A-B). The time taken to reach 20 PDs ranged between 38 and 52 days for N-SC populations and ranged between 33 and 64 days for OA-SC populations and this significant difference highlights the heterogeneity in the cells isolated. The time taken to reach 20 PDs ranged between 60 and 121 days for N-FD populations and ranged between 67 and 129 days for OA-FD populations and this significant difference highlights the heterogeneity in cells isolated (Figure 4.2B).

The proliferative dynamics of ACSC was further investigated through BrdU incorporation, representative images of positive and negative staining nuclei of ES-OA-SC and LS-OA-SC lines are shown in Figure 4.3A. Early senescing OA-derived isolates display a statistically significant ($F_{2,17} = 4.773$; $p<0.05$) lower proliferative index, measured through BrdU incorporation, than either normal or late-senescent OA cell isolates (Figure 4.3C). N-SC and LS-OA-SC display a uniform proliferative index whereas the ES-OA-SC cells show variation between clonal cell lines (Figure 4.3D). A linear regression was plotted in order to establish the relationship between population doublings at senescence and BrdU incorporation at 25PD. It was found that there was a strong statistically significant positive correlation, indicating that BrdU labelling at an early PD is a good indicator for proliferative longevity of the cell line ($R^2 = 0.8099$) (Figure

4.3E). Pearson's correlation test demonstrated a positive relationship (correlation coefficient = 0.90, p-value = $7.8x10^{-8}$). Linear regressions were also plotted in order to establish whether or not there was a relationship between population doubling at senescence and donor age (Figure 4.4A) and BrdU incorporation at 25PD and donor age (Figure 4.4D). The slight negative correlation indicates that ageing may have a negative effect on proliferative potential, however, neither regression was statistically significant and both had a low R^2 value indicating that this may not be a true relationship.

4.3.3 Phenotype plasticity

Williams and colleagues (2010) and Nelson and colleagues (2014) have previously shown that ACSC derived through differential adhesion to fibronectin are capable of tri-lineage differentiation into chondrogenic, osteogenic and adipogenic lineages; to confirm this finding, I assessed the phenotypic plasticity of both normal and OA cell lines.

4.3.3.1 Chondrogenic pellet differentiation

ACSC and FD cell lines were chondrogenically induced into 3D-pellets containing $5x10^5$ cells at 22-25PD (Figures 4.5A-D). These pellets were smooth and opalescent, resembling a typical hyaline cartilage surface. The pellets formed varied in size between clonal cell lines and between patients but were typically between 500μm and 1.0mm. The size and gross morphology of the pellets were consistent within the clonal cell lines. All cell lines both ACSC and FD cell lines were capable of chondrogenic differentiation. The ECM present in pellets was visualised by toluidine blue staining (Figure 4.5). Figure 4.5B represents a pellet formed from a N-SC line, Figure 4.5A represents a pellet formed from a N-FD cell line, Figure 4.5D shows a pellet formed from an OA-SC line and Figure 4.5C illustrated a pellet formed from an OA-FD cell line. In all cases, GAG deposition was evident, however, varying amounts of GAG were observed in pellets from different cell lines and cell types. Detectable GAG was particularly evident around the periphery of the pellet.

4.3.3.2 Osteogenic pellet differentiation

Osteogenic differentiation was induced in a 3D-pellet culture system using $5x10^5$ cells at 22-25PD (Figures 4.6A-H). Gross morphology of the osteogenic pellets

after 3 weeks closely resembled that of the chondrogenic pellet, with a smooth white surface. Sectioned pellets were stained using Alizarin red and the Von Kossa technique to demonstrate deposits of calcium and mineral rich matrix. Figures 4.6B & D represents a N-SC cell line while Figures 4.6A & C demonstrates an N-FD cell line. Figures 4.6F & H depicts an OA-SC line while Figure 4.6E & G shows an OA-FD cell line. All normal and OA ACSC cell lines were found to be capable of osteogenic differentiation signified by strong positive labelling with both Alizarin red and Von Kossa (Figure 4.6). Full-depth chondrocytes from both normal and OA cartilage were not found to be capable of differentiation into the osteogenic lineage. Full-depth chondrocyte pellets survived in culture and had a similar size and morphology to ACSC pellets; however, mineralisation was not present with no staining found for both Alizarin red and Von Kossa in FD pellets (Figure 4.6).

4.3.3.3 Adipogenic differentiation

Following 10 days of adipogenic induction, the ACSC adopted a different morphology, cells developed a granular appearance and were more dendritic compared to the controls (Figure 4.7A-F). Histological examination using Oil red-O revealed accumulation of lipid deposits within the cells. This was consistent between all the ACSC lines (Figure 4.7C-D). No lipid vacuoles formed in the corresponding controls (Figure 4.7E-F).

Articular cartilage-derived stem cells were found to be capable of multipotent tri-lineage differentiation into chondrogenic, osteogenic and adipogenic lineages.

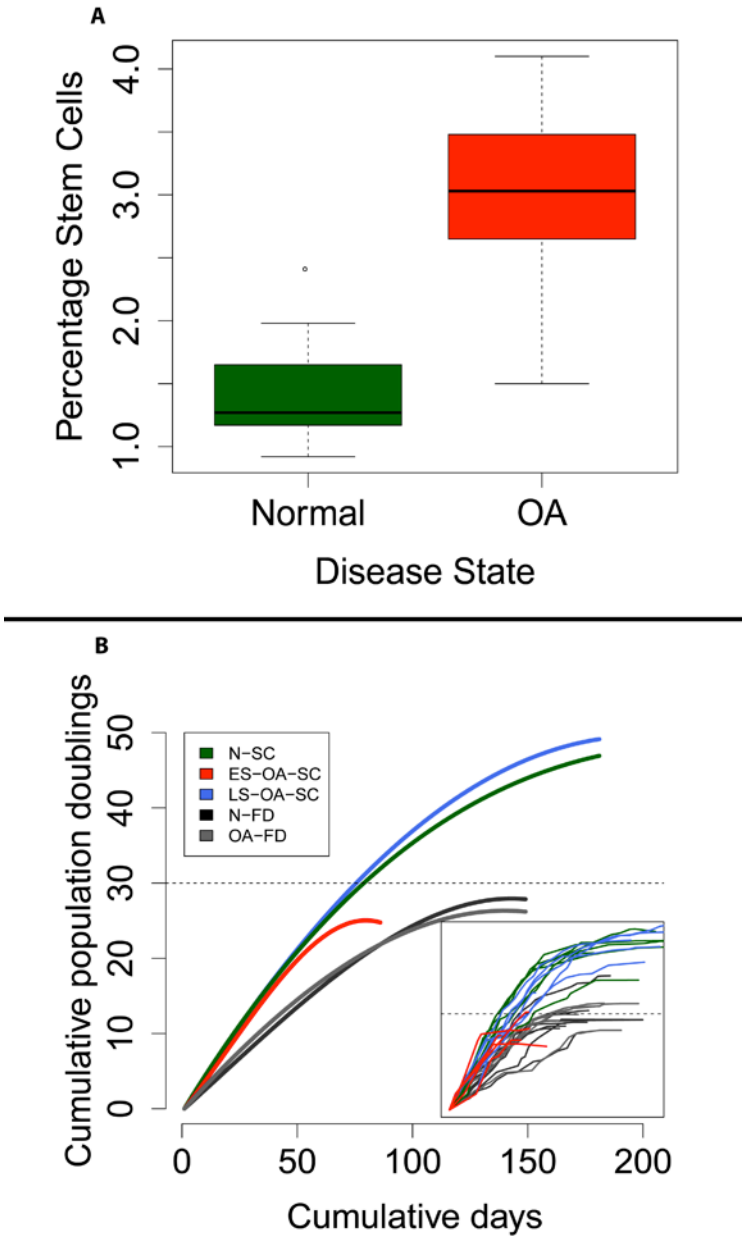


Figure 4.1 – Percentage stem cells within healthy normal and osteoarthritic cartilage and growth kinetics of articular cartilage-derived cells lines.

A) Number of colonies were quantified based on initial seeding density, box plots demonstrate the percentage mean of clonogenic cells from OA cartilage digests (n = 9) was 2.90 (±0.29%) compared to 1.47 (±0.16%) for normal cartilage digests (n = 9). A 2-fold statistically significant increase was found using the T-test ($T_{16} = -4.58$, $p<0.0005$).

B) Normal (n = 8) and OA-derived (n = 11) clonogenic stem cell lines and normal (n = 8) and OA (N = 5) full-depth chondrocytes were maintained in culture with population doublings (PD) calculated at each passage. OA- stem cell lines diverged into two groups, senescent (red line) and non-senescent (blue line). Normal articular cartilage-derived stem cells (N-SC) are shown in green, OA late senescent articular cartilage-derived stem cells (OA-LS-SC) are shown in blue, OA senescent articular cartilage-derived stem cells (OA-ES-SC) are shown in red, Normal full-depth chondrocytes (N-FD) are shown in dark grey and OA full-depth chondrocytes (OA-FD) are shown in light grey. The normal and late senescent osteoarthritic stem cells lines proliferate past 50 population doublings, while differentiated chondrocytes and OA early senescent stem cells senesce before 30 population doublings. Average growth curves were calculated from the non-linear regression equations from individual cell lines within each group. *Inset*; Individual clonal cell line growth kinetics.

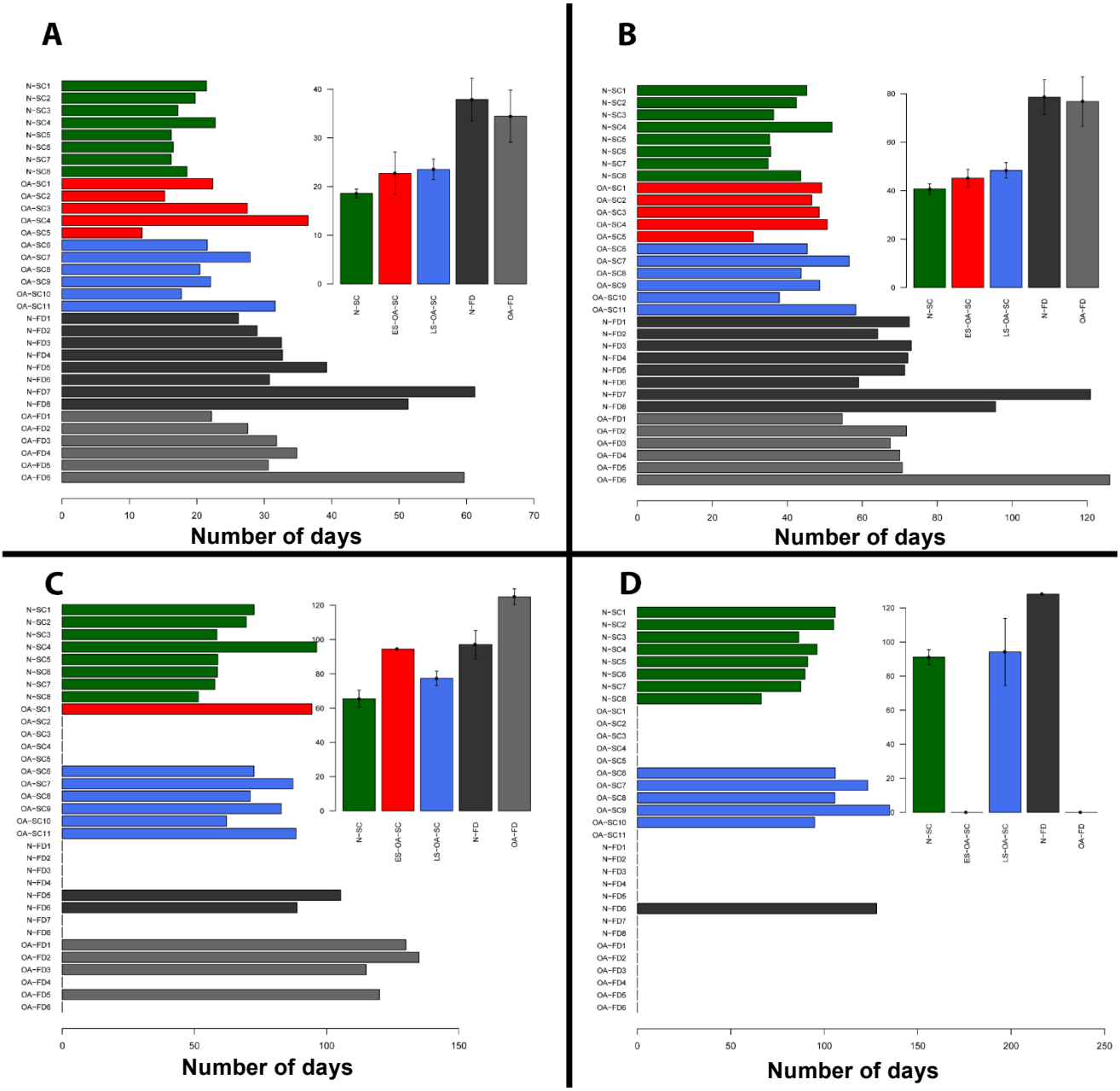


Figure 4.2 – Number of day to reach 10, 20, 30 and 40 population doublings (PD) of articular cartilage-derived cell lines.

A) Bar chart representing the range of number of days in culture before clonally derived stem cell lines and full-depth chondrocyte lines reached 10 population doublings. **Figure B.** Days in culture to reached 20 population doublings. **Figure C**. Days in culture to reached 30 population doublings. **Figure D.** Days in culture to reached 40 population doublings. *Inset*; Average number of days taken for each group.

A one-way Anova confirmed statistical a statistically significant ($p<0.005$) difference in time taken to reach 10 and to reach 20 and 30 population doublings between different osteoarthritic donors, however no statistical significant difference was found between donors of healthy cartilage. After 40 population doublings no statistical significant difference was found between donors (in the remaining non senescent cell lines). No statistical difference was found between the average times for N-SC, OA-ES-SC and OS-LS-SC to reach 10 or 20 or 30 population doublings. A Students T-test confirmed a statistically significant difference ($p<0.001$) between the times for articular cartilage-derived stem cells and full-depth chondrocytes to reach 10, 20 and 30 population doublings; with full-depth chondrocytes taking longer. Only 1 full-depth line was fond to proliferate to 40 population doublings.

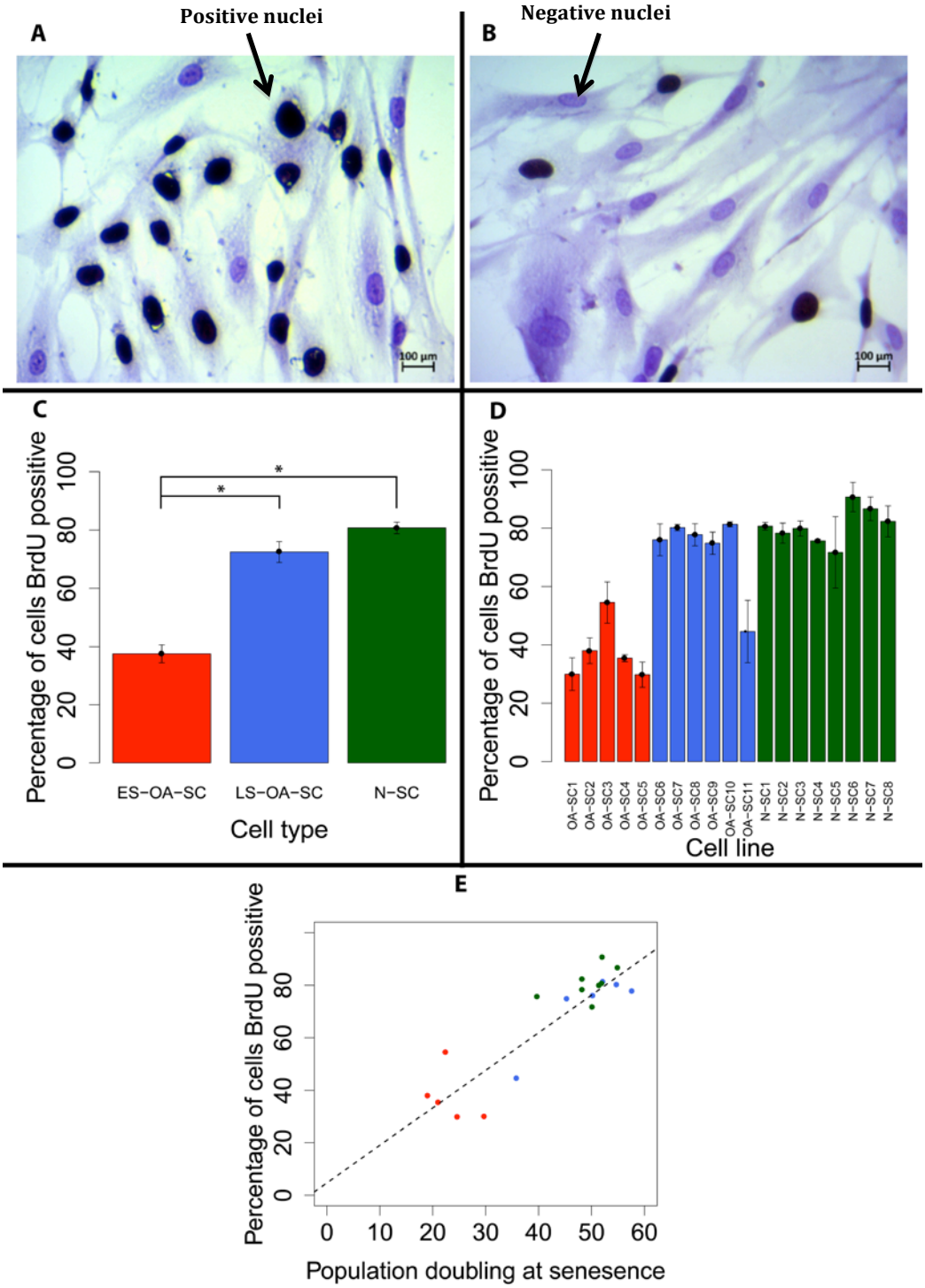


Figure 4.3 – Bromodeoxyuridine (BrdU) labelling of normal and osteoarthritic articular cartilage-derived stem cell lines.

A) & B) Representative images of positive and negative BrdU labelling counter stained with crystal violet. **A)** A late senescent OA derived stem cell line (LS-OA-SC). **B)** An early senescent OA derived stem cell line (LS-OA-SC), BrdU incorporation was analysed at PD25.

C) & D) ES-OA-SC lines (n = 5) analysed by BrdU incorporation demonstrated a significantly reduced proliferative index (*) ($F_{2,17}$ = 4.773; p = 0.02) compared to normal clonogenic cells (N-SC) (n = 8) and LS-OA-SC (n = 6) (Anova with Tukey's pair wise comparisons). **D)** N-SC and LS-OA-SC display a uniform proliferative index whereas the OA-ES-SC cells show variation between clonal cell lines.

E) BrdU incorporation at PD25 strongly correlates to number of population doublings at senescence (R^2 = 0.8099). Pearson's correlation test demonstrated a positive relationship (correlation coefficient = 0.90, p-value = 7.8×10^{-8}). Red– ES-OA-SC, Blue– LS-OA-SC, Green– N-SC.

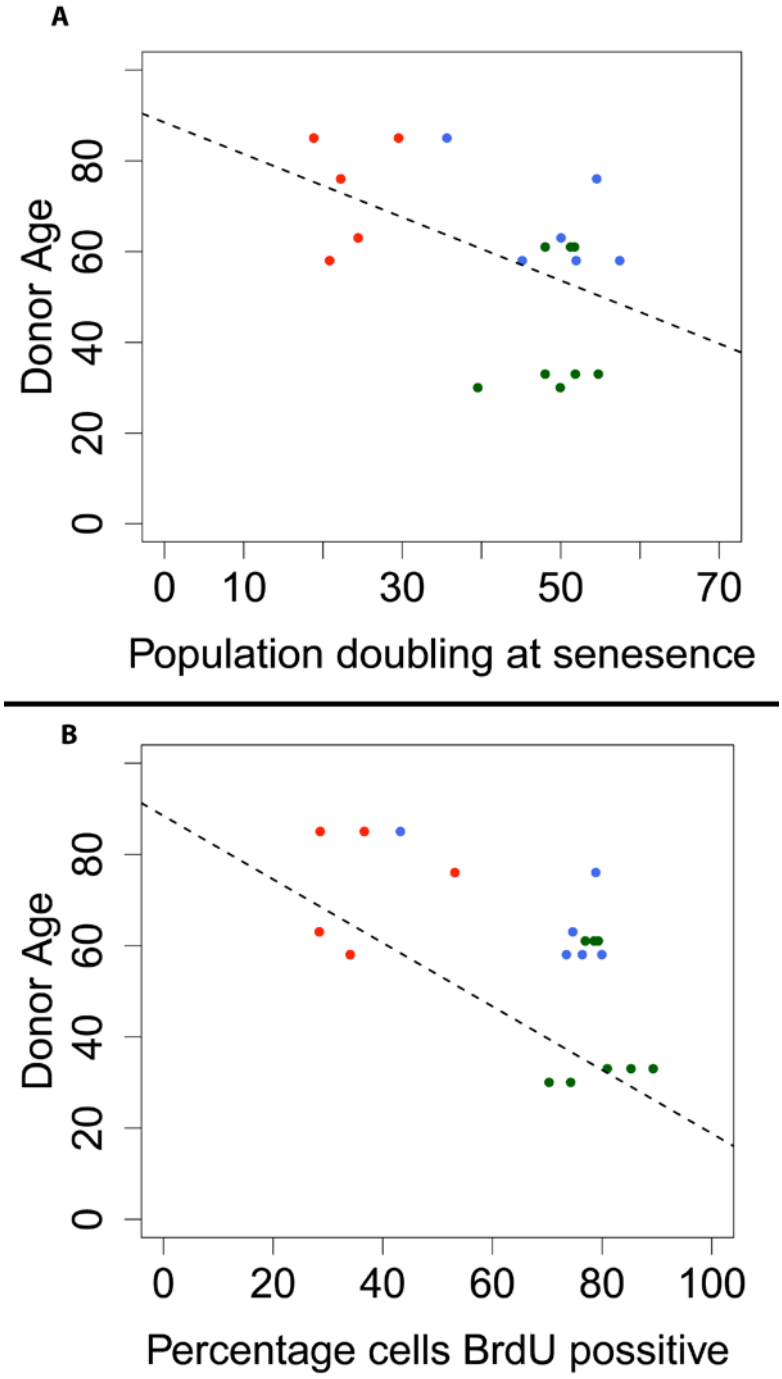


Figure 4.4 – Donor age does not correlate with proliferative capacity of cartilage stem cells.

A) Scatter plot demonstrating the relationship between donor age and population doublings at time of senescence (R^2 = 0.2309). The correlation was found to be non-significant using Pearson's correlation test (correlation coefficient -0.48, p-value = 0.98). Red– ES-OA-SC, Blue– LS-OA-SC, Green– N-SC.

B) Scatter plot demonstrating the relationship between donor age and BrdU positive cells at PD 25 (R^2 = 0.37). The correlation was found to be non-significant using Pearson's correlation test (correlation coefficient -061, p-value = 1.0). Red– ES-OA-SC, Blue– LS-OA-SC, Green– N-SC.

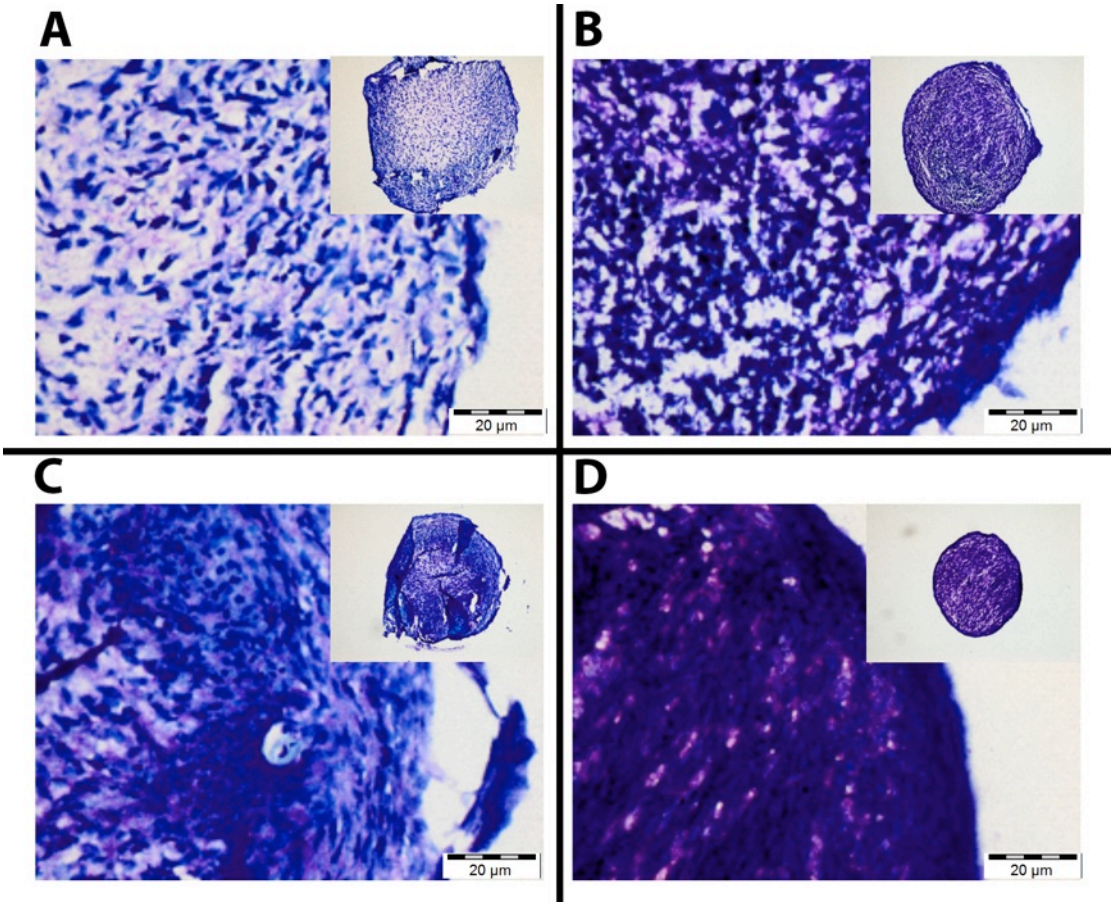


Figure 4.5 – Representative images of toluidine blue stained chondrogenic differentiated pellet cultures showing glycosaminoglycan accumulation.

A). Glycosaminoglycan within chondrogenic pellets from normal cartilage-derived full-depth chondrocytes. **B)** Glycosaminoglycan within chondrogenic pellets from normal cartilage-derived stem cells. **C)** Glycosaminoglycan within chondrogenic pellets from OA cartilage-derived full-depth chondrocytes. **D)** Glycosaminoglycan within chondrogenic pellets from OA cartilage-derived stem cells. Varying amounts of GAG were observed in pellets from different cell lines and cell types at PD 22-25 (A-D). Detectable GAG was particularly evident around the periphery of the pellet. Scale bars: A-D = 20µm.

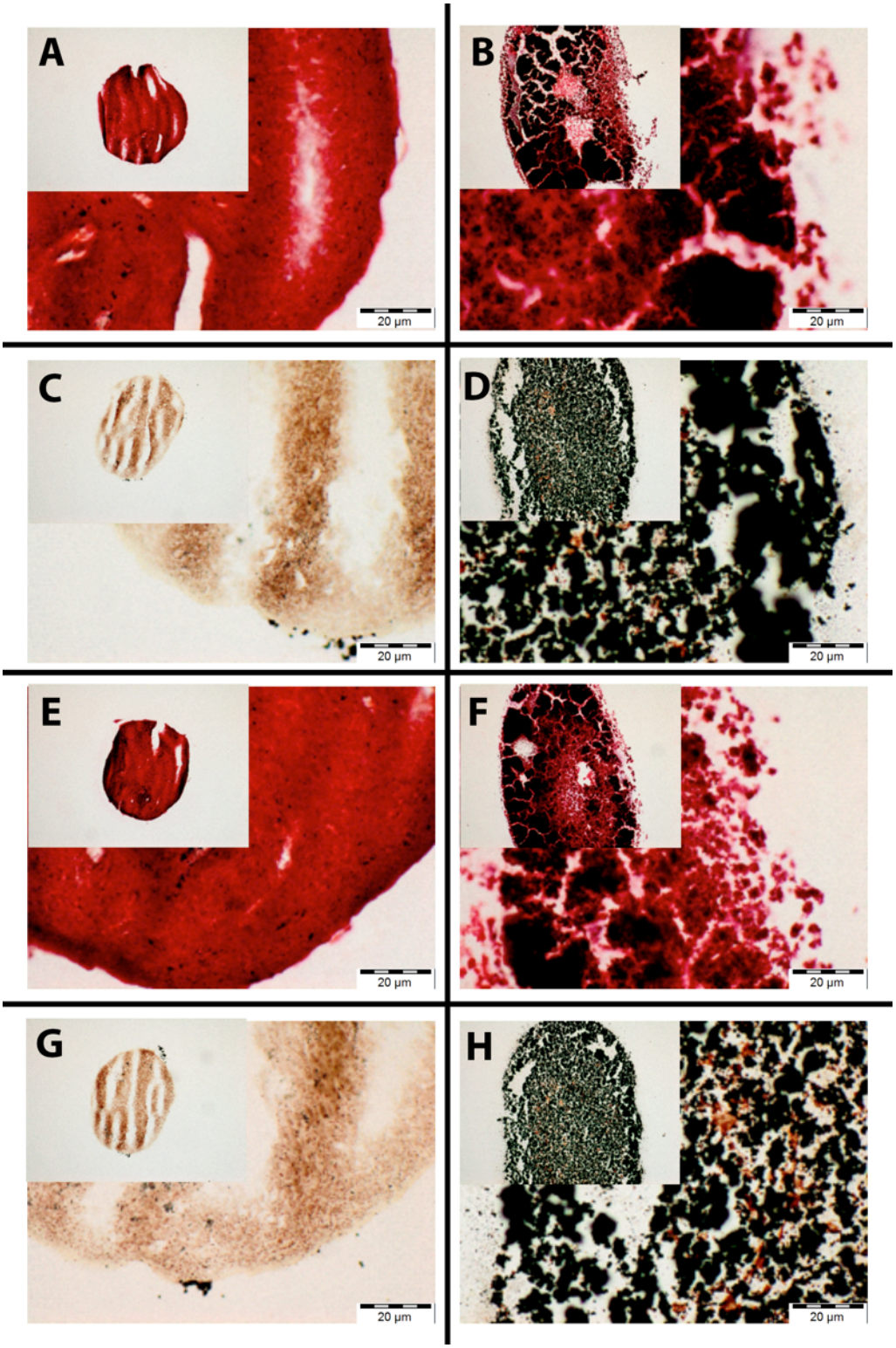


Figure 4.6 – Representative images of Alizarin red(A,B,D,E,F) and Von Kossa (C,D,G,H) stained osteogenic differentiated pellet cultures, showing mineral deposits.

A-D) Osteogenic pellets from normal cartilage-derived cell lines. **A,C) P**ellets from full-depth chondrocytes, showing little or no mineralisation or osteogenic differentiation, **B,D)** Pellets from normal cartilage-derived stem cells, extensive mineralisation and osteogenic differentiation is evident. Scale bars: A-D = 20µm. **E-H)** Osteogenic pellets from OA cartilage-derived cell lines. **E,G)** Pellets from full-depth chondrocytes, showing little or no mineralisation or osteogenic differentiation, **F,H)** Pellets from OA cartilage-derived stem cells, extensive mineralisation and osteogenic differentiation is evident. Scale bars: E-H = 20µm.

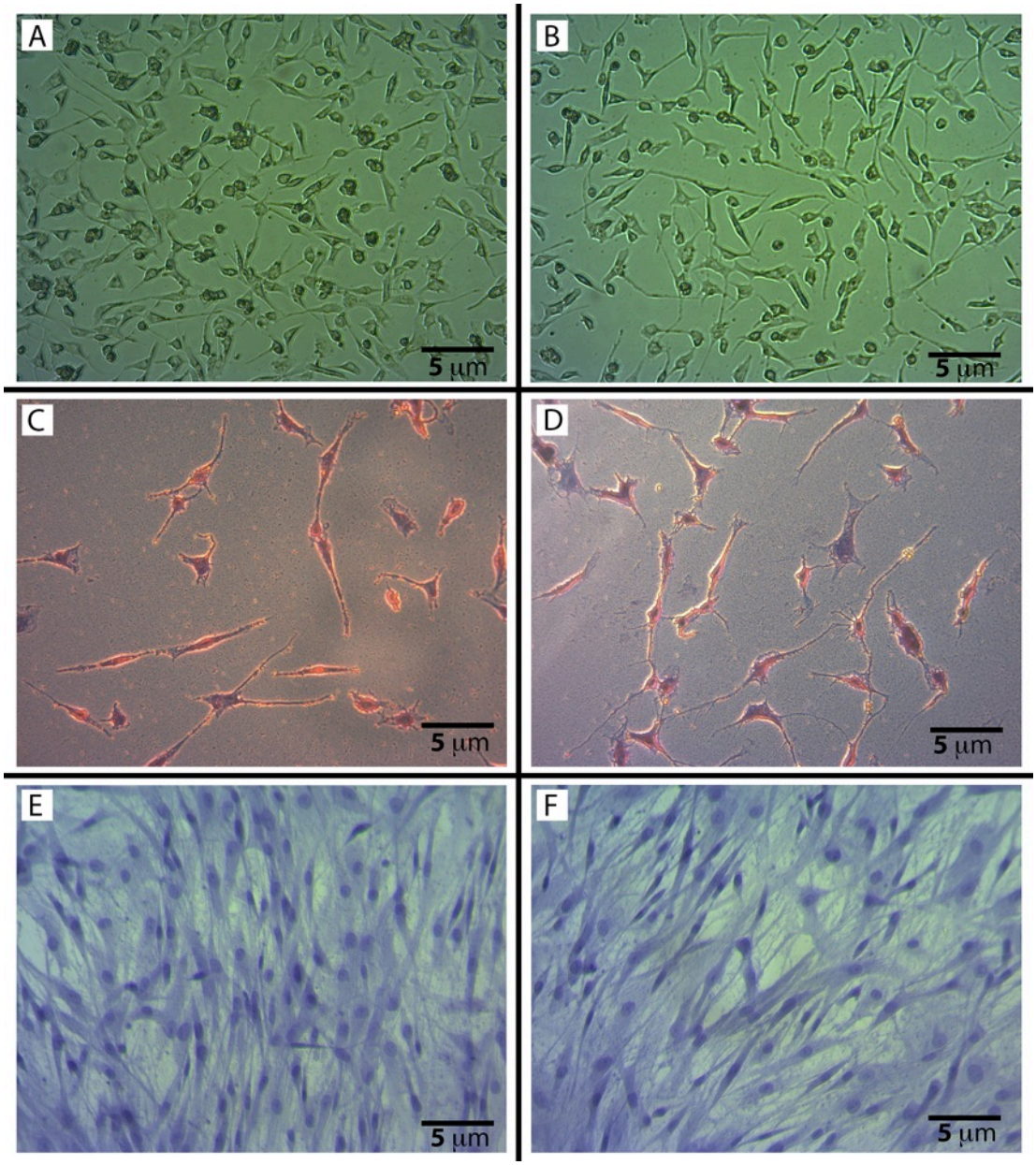


Figure 4.7 – Adipogenic differentiation of cartilage stem cells.

A, B). Normal cartilage (A) and osteoarthritic cartilage (B) derived stem cells after 7 days in adipogenic media start to acquire a granular morphology. **C, D)** Normal cartilage (C) and osteoarthritic cartilage (D) derived stem cells after 10 days in adipogenic, stained using oil red O to highlight lipid vacuoles. Cells are counter stained with crystal violet. **E, F)** Normal cartilage (E) and osteoarthritic cartilage (F) derived stem cells after 10 days in control, stained using oil red O and counter stained with crystal violet. No lipid vacuole formation can be seen.

4.3.4 Identification of ACSC markers

4.3.4.1 qPCR analysis

Differentially expressed genes identified through transcriptomics in Chapter 3 were validated using quantitative polymerase chain reaction. Twenty-one N-SC lines were analysed from 7 different donors, 32 OA-SC lines were used from 7 separate donors and 12 individual FD chondrocyte cell lines were analysed from 7 discrete donors. Candidate stem cell markers that were analysed were *NESTIN*, *FRMD5, C11ORF41, SLC1a3 (EAAT1), EMBIGIN, TMEM132B, ST6GAL2* and *KIF26B*. All candidate markers showed a statistically significant ($p<0.005$) up-regulation in gene expression between both N-SC/OA-SC and the FD chondrocyte cell lines, with no difference in expression between N-SC and OA-SC cohorts (Figure 4.8A-I). Figure 4.8A shows *NESTIN* gene expression N-SC had a 7.5-fold increase and OA-SC had a 7.6-fold increase over the FD chondrocytes. Figure 4.8B shows *FRMD5* gene expression N-SC had a 13.0-fold increase and OA-SC had a higher 20.5-fold increase over the FD chondrocytes. Figure 4.8C shows *C11ORF41* gene expression N-SC had a 7.9-fold increase and OA-SC had a 6.9-fold increase over the FD chondrocytes. Figure 4.8D shows *EMB* gene expression N-SC had a 3.8-fold increase and OA-SC had a 3.2-fold increase over the FD chondrocytes. Figure 4.8E shows *EAAT1* gene expression N-SC had a 6.0-fold increase while OA-SC had a slightly lower 3.6-fold increase over the FD chondrocytes. Figure 4.8F shows *TMEM132B* gene expression N-SC had a 13.0-fold increase and OA-SC had a lower 8.6-fold increase over the FD chondrocytes. Figure 4.8G shows *PRDM1* gene expression N-SC had a 3.9-fold increase and OA-SC had larger a 5.4-fold increase over the FD chondrocytes. Figure 4.8H shows *KIF26B* gene expression N-SC had a 3.1-fold increase and OA-SC had a 3.5-fold increase over the FD chondrocytes. Finally Figure 4.8I shows *ST6GAL2* gene expression N-SC had a 3.0-fold increase and OA-SC had a 3.2-fold increase over the FD chondrocytes.

Gene expression of differentiated cartilage genes was also explored; expression of cartilage specific genes was found to be down-regulated in both N-SC and OA-SC compared to FD chondrocytes. Aggrecan, Collagen Type II, Collagen Type IX and lubricin were all had statistically significant down-regulation in both N-SC and OA-SC ($p<0.05$) (Figure 4.9A-D). Collagen Type XI was down-regulated in both N-SC and OA-SC, however, was only significant in OA-SC ($p<0.05$) (Figure

4.9E). The chondrogenic regulator SOX-9 gene expression was consistent between all three cell types (Figure 4.9F). Figure 4.9A shows *ACAN* gene expression, FD chondrocytes had a 6.1-fold higher expression than N-SC and an 8.0-fold higher than OA-SC. Figure 4.9B shows *COL2A1* gene expression, FD chondrocytes had a 20.7-fold higher expression than N-SC and 162.3-fold higher than OA-SC. Figure 4.9C shows *PRG4* gene expression, FD chondrocytes had a 41.0-fold higher expression than N-SC and a 270.0-fold higher than OA-SC. Figure 4.9D shows *COL9A1* gene expression, FD chondrocytes had a 320.1-fold higher expression than N-SC and 319.5-fold higher than OA-SC. Figure 4.9E shows *COL11A2* gene expression, FD chondrocytes had a 1.3-fold higher expression than N-SC and a 3.4-fold higher than OA-SC. Expression of chondrogenic gene was slightly higher in N-SC than OA-SC lines however this was non-significant.

The development markers Notch-1 and Jagged-1 have been suggested as potential markers of ACSC (Dowthwaite et al., 2004). Gene expression analysis showed no difference in Notch-1 expression between N-SC, OA-SC and FD cell lines (Figure 4.10A). Jagged-1 expression was slightly higher in OA-SC lines than in N-SC or FD cell lines, however, this was not a significant increase (Figure 4.10B). Neither Notch-1 nor Jagged were found to be a suitable marker for culture-expanded ACSC.

Principal components analysis of gene expression data for ACSC (N-SC, n = 8; OA-SC, n = 8) and FD cells (n = 8) was employed to identify whether different cell populations could be distinguished based on expression profiles (Figure 4.11). Figure 4.11A shows that principal components analysis (PCA) using both cartilaginous and the ACSC specific genes. K-means clustering formed 3 groups. Group 1 contained the full-depth chondrocyte cell lines; Group 2 predominantly contained the ES-OA-SC lines, while group 3 contained N-SC and LS-OA-SC lines stem cells. This shows that the gene expression profiles are sufficient to distinguish ACSC for FD cells and that expression of certain genes are sufficient to identify an ES-OA-SC from LS-OA-SC. To further explore which genes may be indicators of proliferative potency, PCA was employed using only the ACSC specific genes (Figure 4.11B). K-means clustering again found 3 groups. Group 1 contained the N-SC and the LS-OA-SC cells. Group 2 predominantly contained the ES-OA-SC and some FD chondrocyte cell lines, while group 3 contained the

majority of the FD chondrocyte cell lines. Figure 4.11B shows that separation between groups 1 and 2 was predominantly based on *NESTIN, FRMD5, C110RF41, PRDM1* and *KIF26B* gene expression. These data indicate that expression of these 5 genes may predict longevity in culture. Figure 4.11C shows PCA analysis using only chondrogenic genes, 2 clusters were identified, group 1 contained all the ACSC lines and group 2 contain all the FD cell lines. Figure 4.12 shows a heatmap presenting the gene expression data for stem cell specific and cartilage specific gene expression. The stem cell lines were found to cluster together with similar patterns of gene expression and full-depth cartilage chondrocyte cell lines formed a separate cluster of samples with similar gene expression profiles. Both the heatmap and PCA analyses confirm that ACSC marker and chondrogenic gene expression profiles are sufficient to identify different cell populations.

To analyse the effect that ACSC marker genes have on proliferative potency linear regression were plotted to show the relationship between gene expression and number of population doublings at senescence (Figure 4.13A-J). *NESTIN* gene expression has a strong positive correlation to population doublings at senescence (correlation coefficient = 0.89, R^2 = 0.79, p = $2.4e^{-7}$) (Figure 4.13A). *PRDM1* gene expression also exhibits a strong positive correlation to population doublings at senescence (correlation coefficient = 0.67, R^2 = 0.45, p = 0.002), however, to a lesser degree than NESTIN (Figure 4.13B). *C11ORF41* gene expression shows positive correlation to population doublings at senescence (correlation coefficient = 0.48, R^2 = 0.232, p = 0.03) (Figure 4.13C), as does *FRMD5* (correlation coefficient = 0.427, R^2 = 0.175, p = 0.05) (Figure 4.13D). *C11ORF41* and *FRMD5* have a low correlation coefficient and R^2 value so the validity of this correlation may be questionable, therefore *NESTIN and PRDM1* expression are the best predictors of proliferative potency *in vitro*. *TMEM132B, ST6GAL2, KIF26B, EMB and EAAT1* gene expression was found to have a non-significant effect on population doublings at senescence (Figure 4.13E-I)

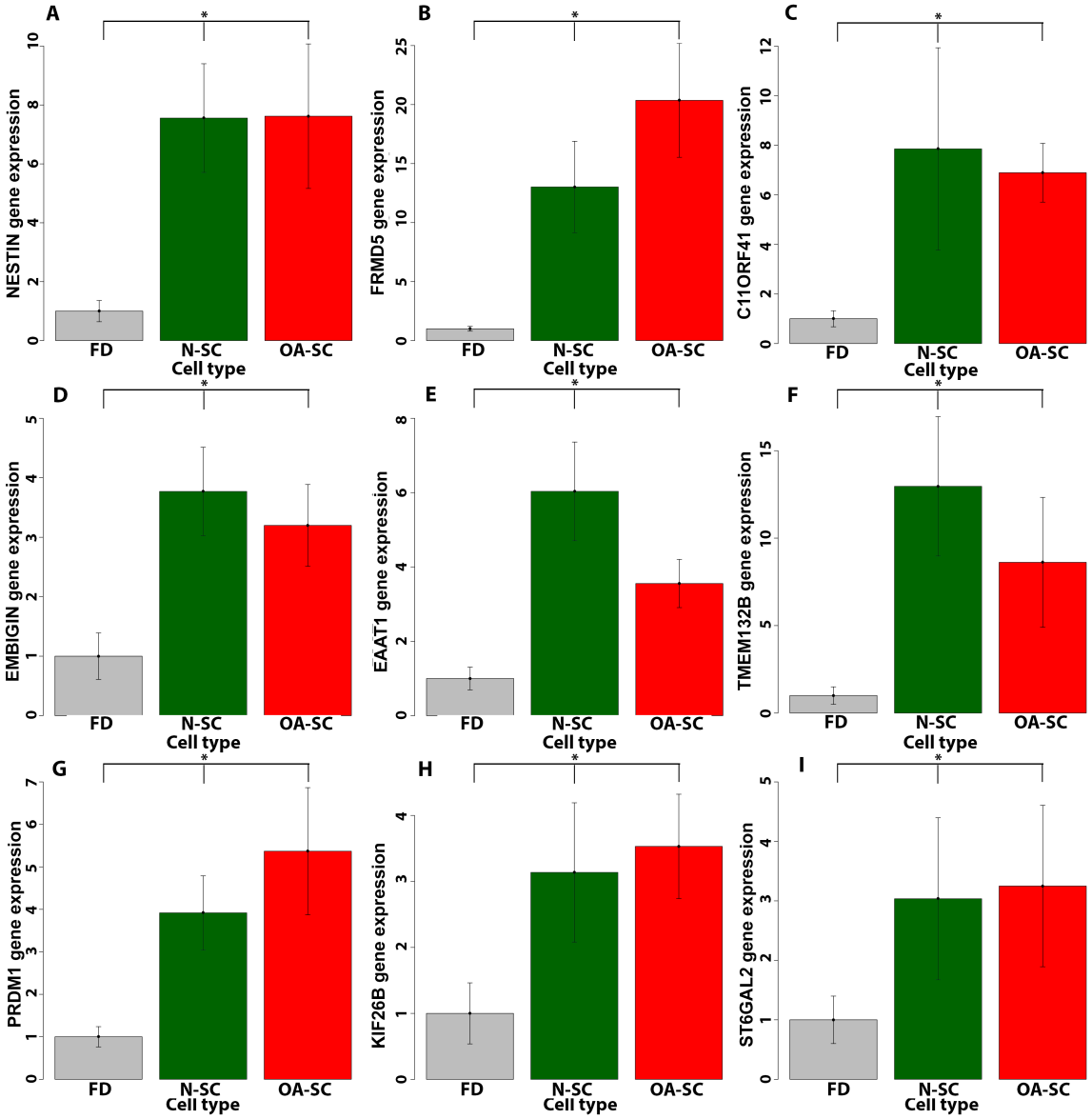


Figure 4.8 – Gene expression of novel cartilage stem cell specific genes in full-depth chondrocytes, normal cartilage-derived stem cells and osteoarthritic cartilage-derived stem cells.

Data show stem cell specific expression of multiple genes through qPCR analysis; genes were identified from the next generation sequencing transcriptomics study. Gene expression is displayed as fold-change. All genes investigated were found to be statistically significant ($p<0.005$) between both normal stem cells (N-SC) (n = 21) and full-depth chondrocytes (FD) (n = 12) and between OA derived stem cells (OA-SC) (n = 32) and FD chondrocytes ($p<-0.005$) using Anova with Tukey's pair wise comparisons. No significant differences were observed between N-SC and OA-SC for any gene. **A)** *NESTIN*, **B)** *FRMD5*, **C)** *C11ORF41*, **D)** *EMBIGIN*, **E)** *EAAT1*, **F)** *TMEM132B*, **G)** *PRDM1*, **H)** *KIF26B*, **I)** *ST6GAL2*.

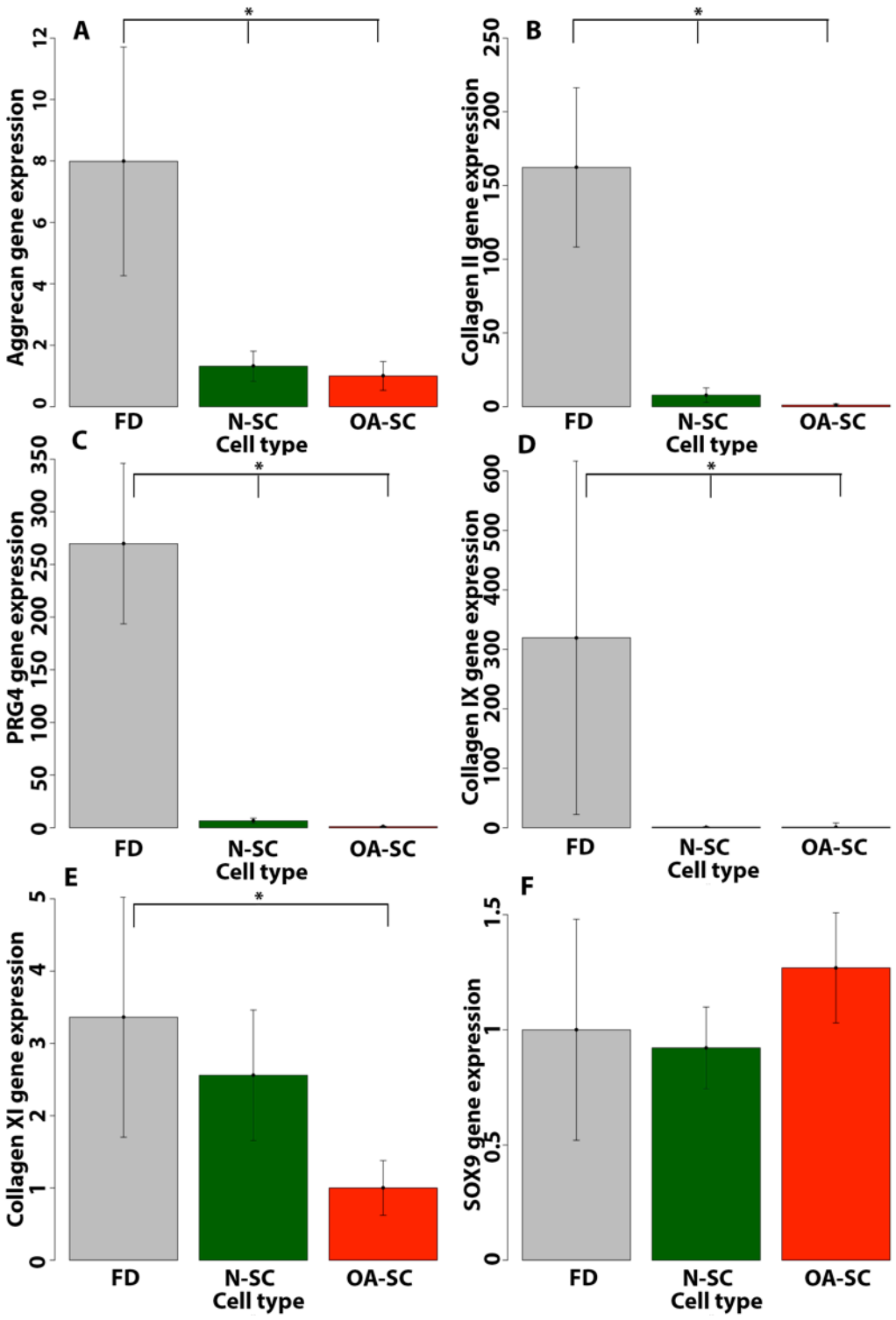


Figure 4.9 – Gene expression of cartilage specific genes in full-depth chondrocytes, normal cartilage-derived stem cells and osteoarthritic cartilage-derived stem cells.

Data show full-depth chondrocyte (FD) (n = 12) specific expression of cartilage genes through qPCR analysis. Gene expression is displayed as fold-change. Aggrecan, Collagen Type II, PRG4 and Collagen Type IX were found to be significantly unregulated in full-depth chondrocytes compared to the other sample grouped ($p<0.005$). Collagen Type XI was found to be significantly increased in FD compared with OA derived stem cells (n = 32) ($P<0.05$) but not compared to normal cartilage-derived stem cells. SOX-9 expression was uniform across all 3-cell types, showing they all maintain chondrogenic potential. No significant differences were observed between N-SC (n = 21) and OA-SC for any gene. Statistical analysis performed using Anova with Tukey's pair wise comparisons. **A)** *ACAN*, **B)** *COL2A1*, **C)** *PRG4*, **D)** *COL9A1* **E)** *COL11A2*, **F)** *SOX9*.

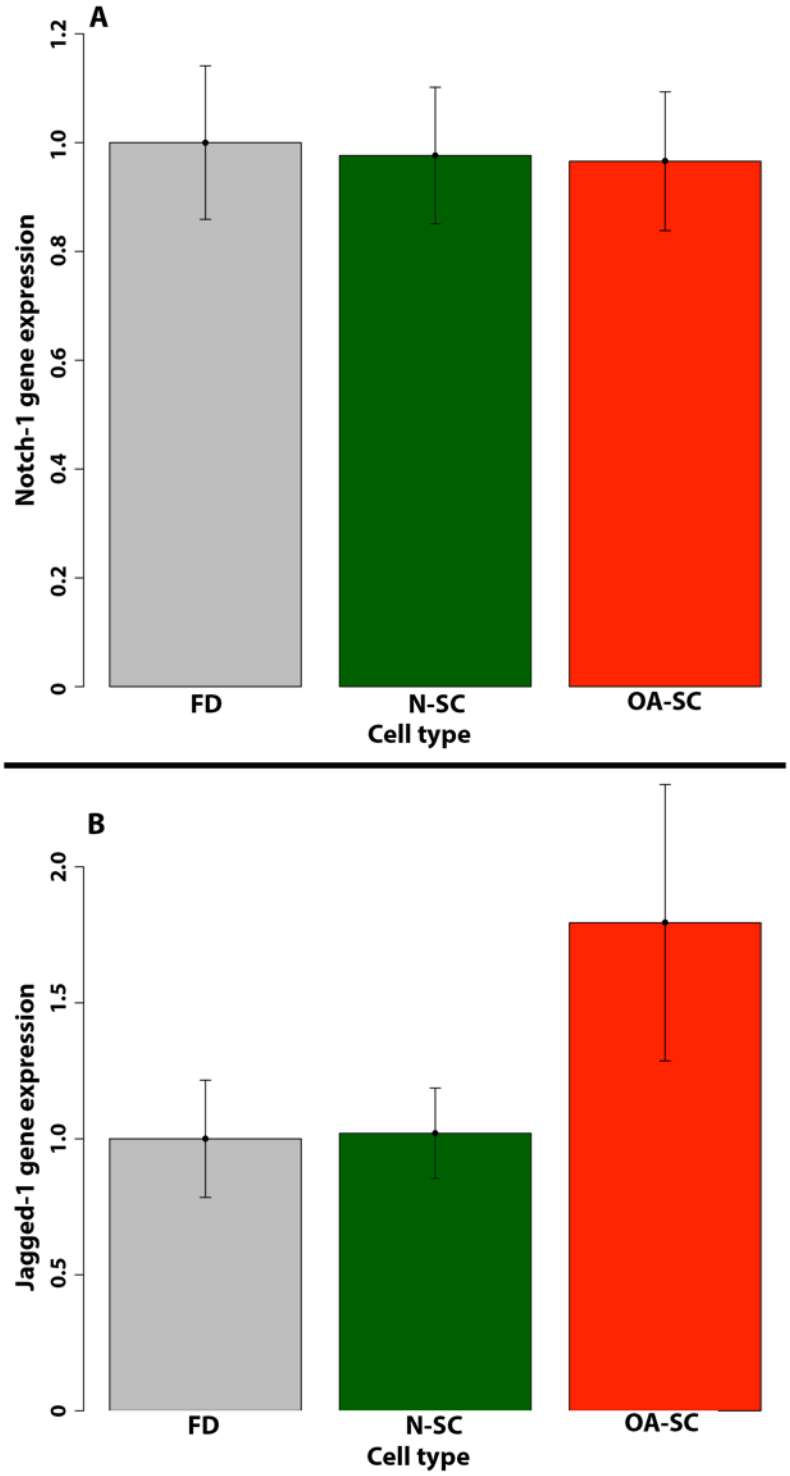


Figure 4.10 – Gene expression of the progenitor cell markers Notch-1 and Jagged-1 in full-depth chondrocytes, normal cartilage-derived stem cells and osteoarthritic cartilage-derived stem cells.

No statistically significant increase was found in the progenitor cell markers Notch-1 or Jagged-1 in either normal stem cells (N-SC) (n = 21) or OA stem cells (OA-SC) (n = 32) compared to full-depth chondrocytes (FD) (n = 12). **A)** *NOTCH1*, **B)** *JAG1.*

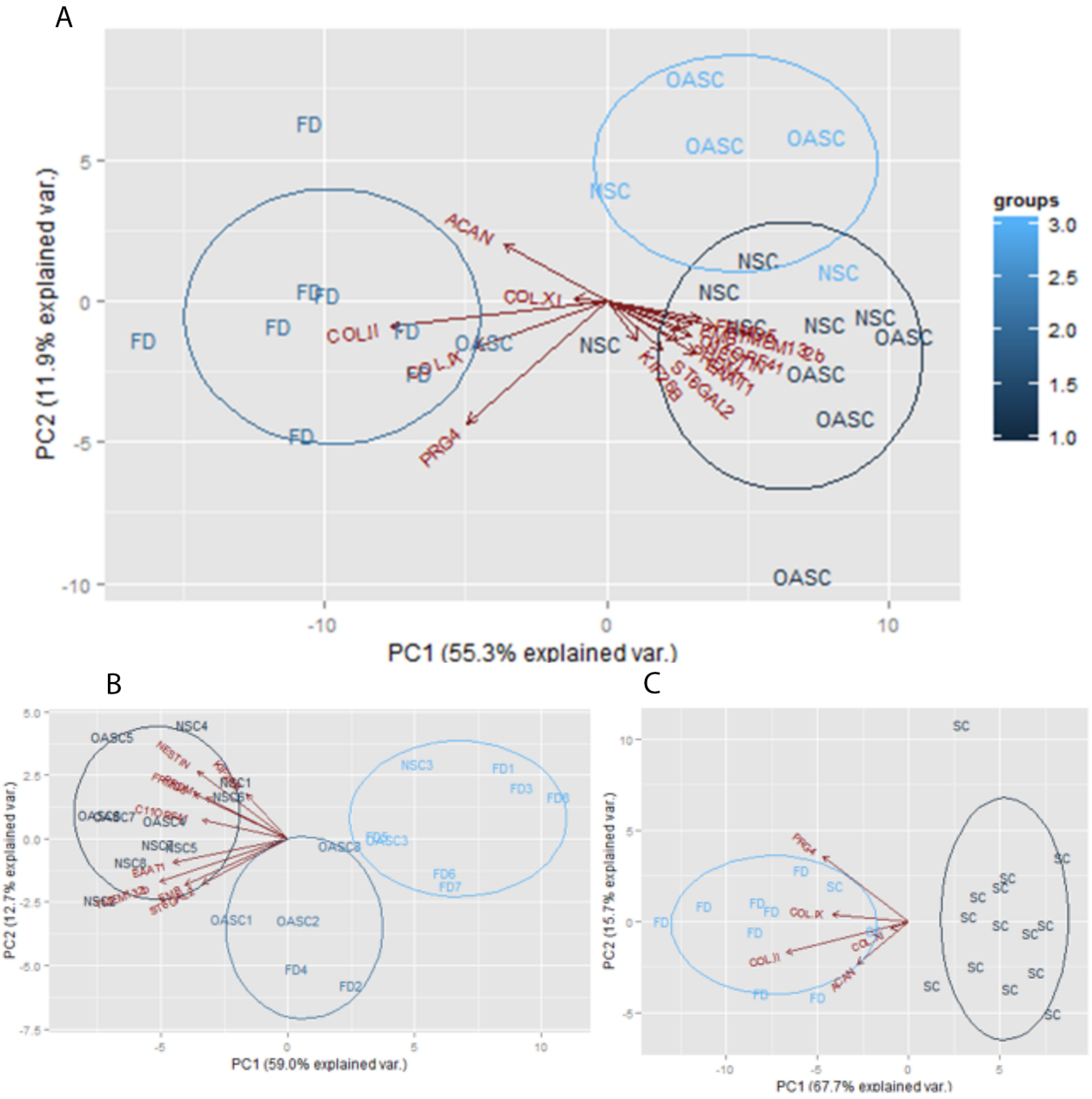


Figure 4.11 – Principal components analysis (PCA) of gene expression within full-depth chondrocytes, normal cartilage-derived stem cells and osteoarthritic cartilage-derived stem cells.

A) Principal components analysis (PCA) of the cartilage cell specific and the stem cell specific genes. K-means clustering formed 3 groups. Group 1 contained the full-depth chondrocyte cell lines. Group 2 predominantly contained the early sensing stem cells lines; while group 3 contained the normal stem cells and the late senescing OA stem cells. Showing gene expression profiles genes are sufficient to different cell populations. **B)** Principal components analysis (PCA) of the stem cell specific genes, *NESTIN*, *FRMD5*, *C11ORF41*, *EMB*, *EAAT1*, *PRDM1*, *ST6GAL2*, *KIF26B* and *TMEM132B*. Cells were separated based on expression of each of these genes, K-means clustering formed 3 groups. Group 1 contained the normal stem cells and the late senescing OA stem cells. Group 2 predominantly contained the early sensing stem cells and some full-depth chondrocyte cell lines; while group 3 contained the majority of the full-depth chondrocyte cell lines. Showing stem specific genes are sufficient to distinguish the different populations. **C)** Principal components analysis (PCA) of the cartilage cell specific genes, *ACAN*, *COL2A1*, *COL9A1*, *COL11A1* and *PRG4*. K-means clustering formed 2 groups; group 1 contained the stem cells lines while group 2 contained the full-depth chondrocyte cell lines. Showing cartilage specific genes are sufficient to distinguish the 2 populations.

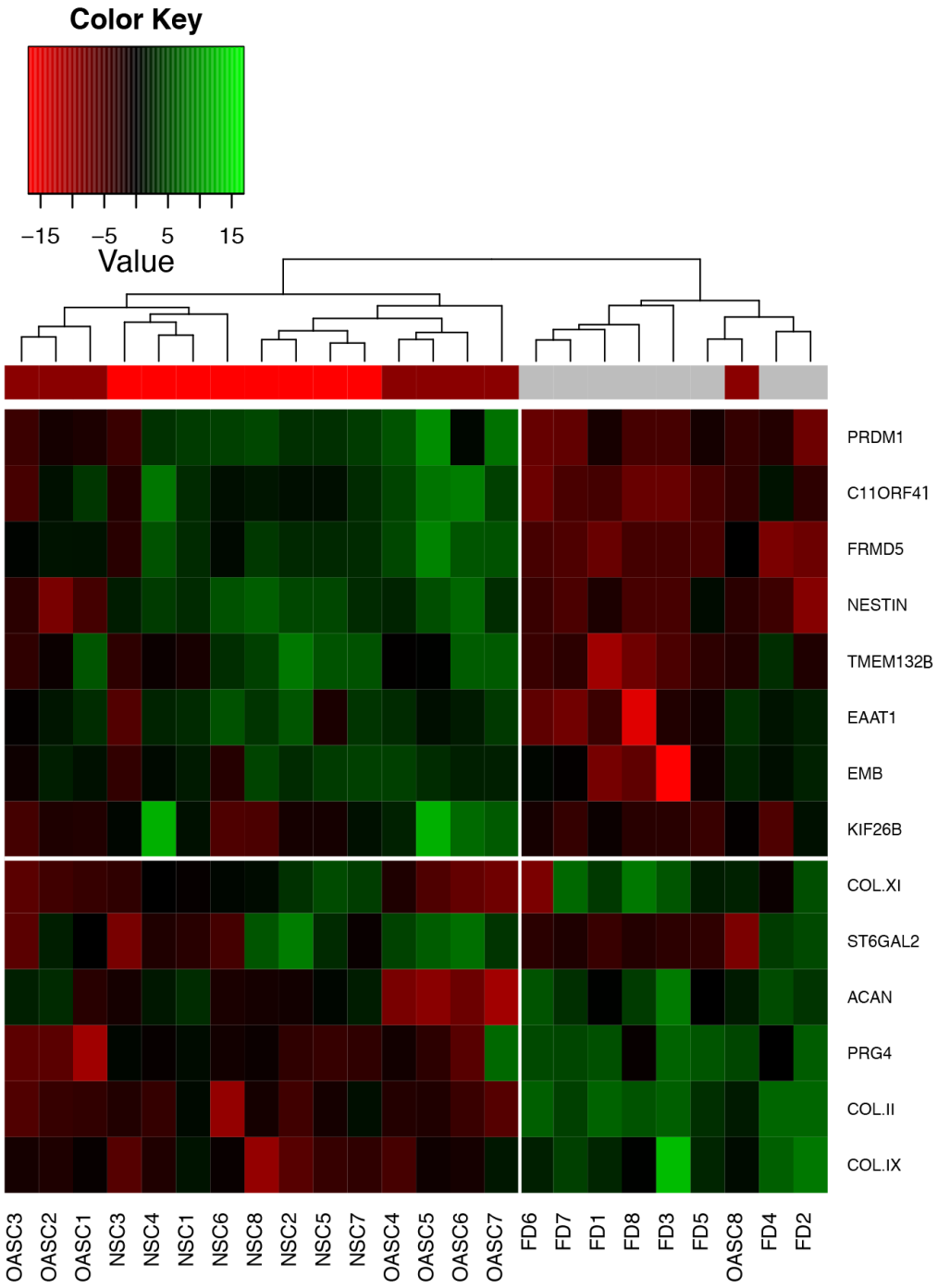


Figure 4.12 – Heatmap of gene expression within full-depth chondrocytes, normal cartilage-derived stem cells and osteoarthritic cartilage-derived stem cells.

A heatmap showing the gene expression data for stem cell specific and cartilage specific gene expression. The stem cell lines were found to cluster together with similar patterns of gene expression. The full-depth cartilage chondrocyte cell lines formed a separate cluster of samples with similar gene expression profiles.

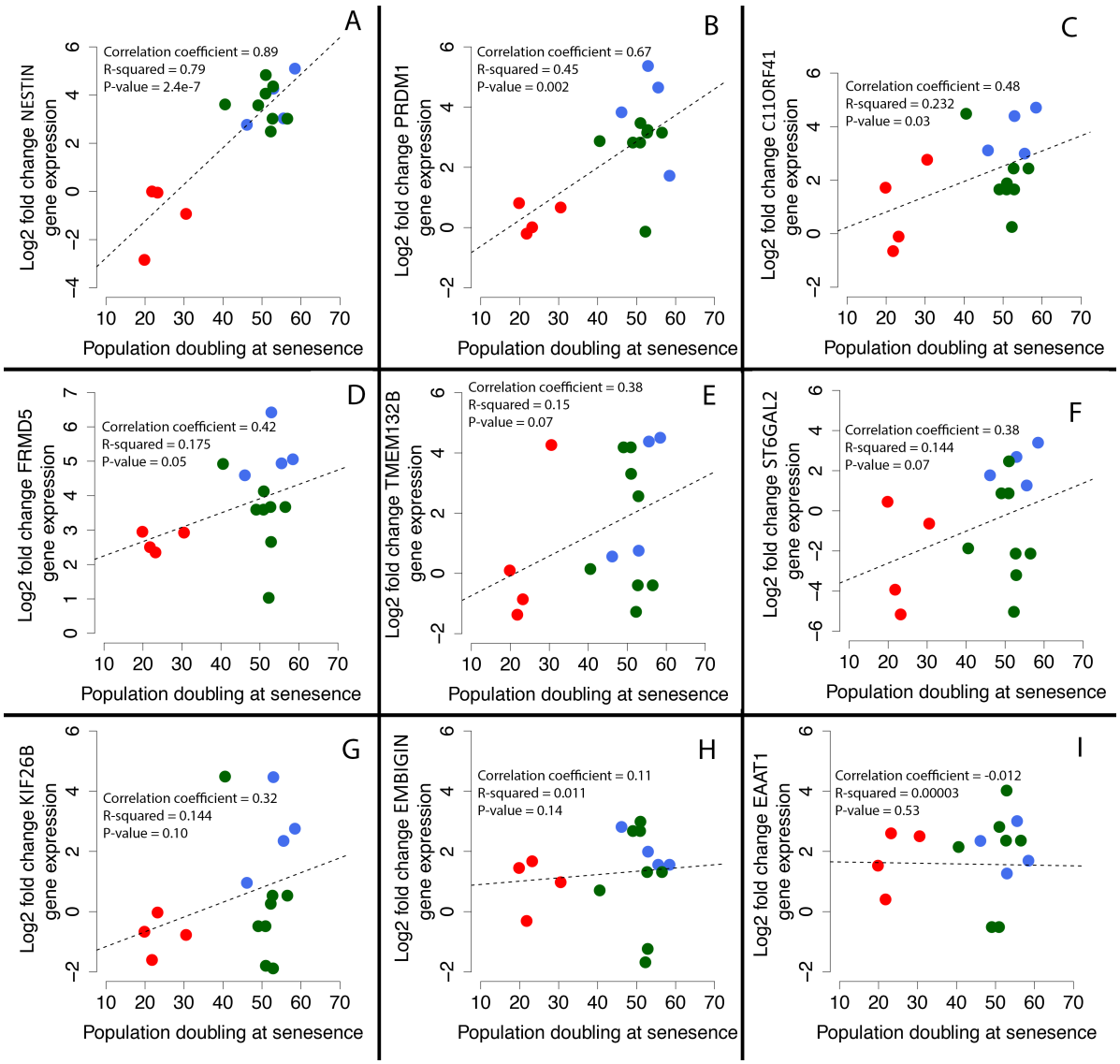


Figure 4.13 –Scatter graphs showing correlations between proliferative capacity and stem cell marker gene expression in normal cartilage-derived and osteoarthritic cartilage-derived cartilage stem cells.

Scatter plots to investigate the relationship between stem cell marker expression and proliferative capacity. *NESTIN*, *PRDM1*, *C11ORF41* and *FRMD5* were all found to have a statistically significant correlation with proliferative capacity ($P<0.05$), with higher gene expression being an indication of later senescence. The strongest correlation was found to be *NESTIN* with a correlation coefficient of 0.89 and highly statistically significant p-value = 2.4×10^{-7}. *TMEM132B*, *ST6GAL2*, *KIF26B*, *EMB* and *EAAT1* were found to have no significant effect on proliferative longevity. Correlation analysis was performed using Pearson's product moment correlation coefficient. Red – ES-OA-SC, Blue – LS-OA-SC, Green – N-SC.

4.3.4.2 Immunocytochemical analyses of potential stem cell markers

To confirm the panel of stem cell markers were viable for identification and isolation of ACSC, protein labelling was examined through immunocytochemistry for both ACSC and FD cell lines from normal and OA donors. Protein labelling of NESTIN, FRMD5, C11ORF41, EMBIGIN and EAAT1 were investigated.

NESTIN exhibited positive cytoskeletal labelling in ACSC lines from both normal and OA donors; no labelling was present in either FD populations (Figure 4.14A-D). More than 80% of cells from clonogenic isolates derived from normal or osteoarthritic cartilage expressed NESTIN protein; within N-SC lines (n = 3) the average percentage of cells positively labelling was 99%, there was a significant reduction in positive labelling in OA-SC lines (n = 3) with an average of 81.4% ($p = 6.5e^{-6}$) (Figure 4.19A). No antibody labelling was present in the no primary or isotype matched controls (Figure 4.14E-F).

FRMD5 labelling was found in cell membrane of the ACSC lines from both normal and OA donors; again no labelling was observed in FD populations (Figure 4.15A-D). More than 90% of cells from clonogenic isolates derived from normal or osteoarthritic cartilage expressed FRMD5 protein; within N-SC lines (n = 3) the average percentage of cells positively labelling was 92% and within OA-SC lines (n = 3) an average of 99% of cells were positive. No significant difference was observed between N-SC and OA-SC percentage labelling ($p>0.05$) (Figure 4.19B). No antibody labelling was present in the no primary or isotype matched controls (Figure 4.15E-F).

C11ORF41 membrane labelling was found in the ACSC lines from both normal and OA donors; with no labelling was observed in FD populations (Figure 4.16A-D). More than 98% of cells from clonogenic isolates derived from normal or osteoarthritic cartilage expressed FRMD5 protein; within N-SC lines (n = 3) the average percentage of cells positively labelling was 99% and within OA-SC lines (n = 3) an average of 98% of cells were positive. No significant difference was observed between N-SC and OA-SC percentage labelling ($p>0.05$) (Figure 4.19C). No antibody labelling was present in the controls (Figure.4.16E-F).

EMBIGIN protein was strongly expressed in the cell membrane of ACSC lines from both normal and OA donors (Figure 4.17B,D). No protein labelling was observed in N-FD population, however, some OA-FD cells lines showed low-level labelling (Figure 4.17A,C). One hundred percent of the cells in both normal and OA cell lines were found to have positive labelling for EMBIGIN protein (Figure 4.19D). No antibody labelling was present in the no primary or isotype matched controls (Figure 4.17E-F).

EAAT1 protein labelling was localised to the cell membrane in the ACSC lines from both normal and OA donors; no labelling was observed in FD populations (Figure 4.18A-D). One hundred percent of the cells in both normal and OA cell lines were found to positively labelling EMBIGIN protein (Figure 4.19E). No antibody labelling was present in the controls (Figure 4.18E-F).

Candidate stem cell marker labelling was also investigated within bone marrow-derived MSCs. NESTIN, FRMD5, C11ORF41, EMBIGIN and EAAT1 were all expressed by MSCs (Figure 4.20A-E). No antibody labelling was present in the controls (Figure 4.20F-H).

Protein labelling was explored within the initial adhesion colonies prior to cloning and extended expansion. Figure 4.21A-B shows EMBIGIN labelling in initial adhesion colonies, labelling was present in both normal of OA colonies. Figure 4.21C-D shows EAAT1 labelling in initial adhesion colonies, strong labelling is only present in normal cartilage-derived colony, weak labelling can be seen in some of the OA colony derived cells. FRMD5 labelling was positive in initial adhesion colonies from both normal and OA colonies (Figure 4.21E-F). Figures 4.21G-H shows positive C11ORF41 labelling in initial adhesion colonies from both normal of OA colonies. NESTIN labelling in initial adhesion colonies was absent in colonies derived from normal cartilage and is only present in a subset of cells within OA derived colonies (Figure 4.21I-J).

Protein labelling of candidate stem cell markers was found to be specific to ACSC cell lines with no labelling identified in FD chondrocytes.

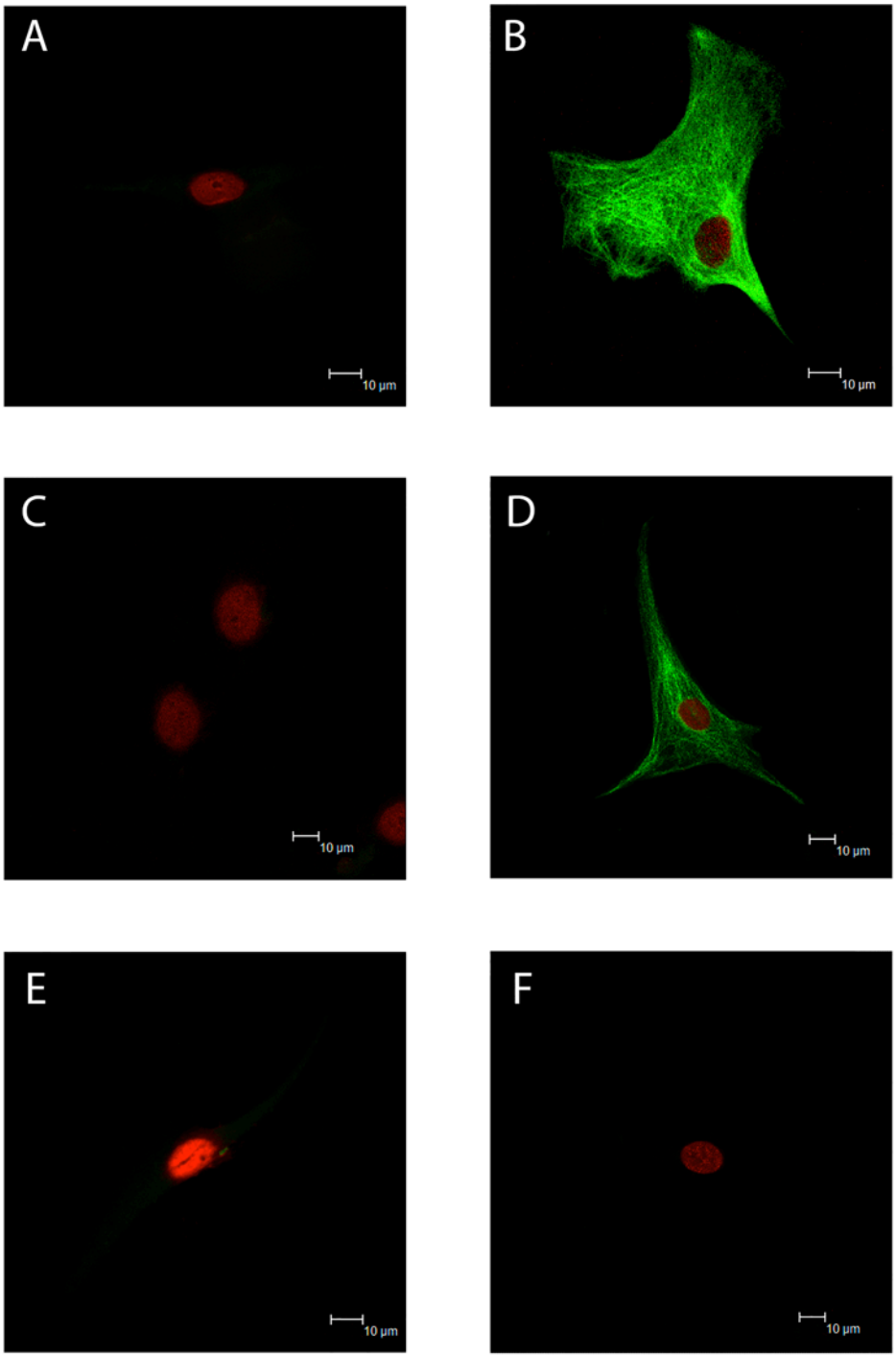


Figure 4.14 – Immunocytochemistry of NESTIN protein labelling within culture-expanded full-depth chondrocytes, normal cartilage-derived stem cells and osteoarthritic cartilage-derived stem cells.

A, C) NESTIN protein labelling is not evident in full-depth chondrocyte derived cell lines. **Figure A -** shows a representative image of a normal cartilage full-depth cell line, **Figure C -** shows a representative image of an OA cartilage full-depth cell line. **B, D)** NESTIN protein labelling shows cytoskeletal labelling in cartilage-derived stem cell lines. **Figure B -** shows a representative image of a normal cartilage full-depth cell line, **Figure D -** shows a representative image of an OA cartilage full-depth cell line. **E, F)** Controls using normal cartilage-derived stem cells. Figure E- an isotype matched IgG control and Figure F- a no primary antibody control.

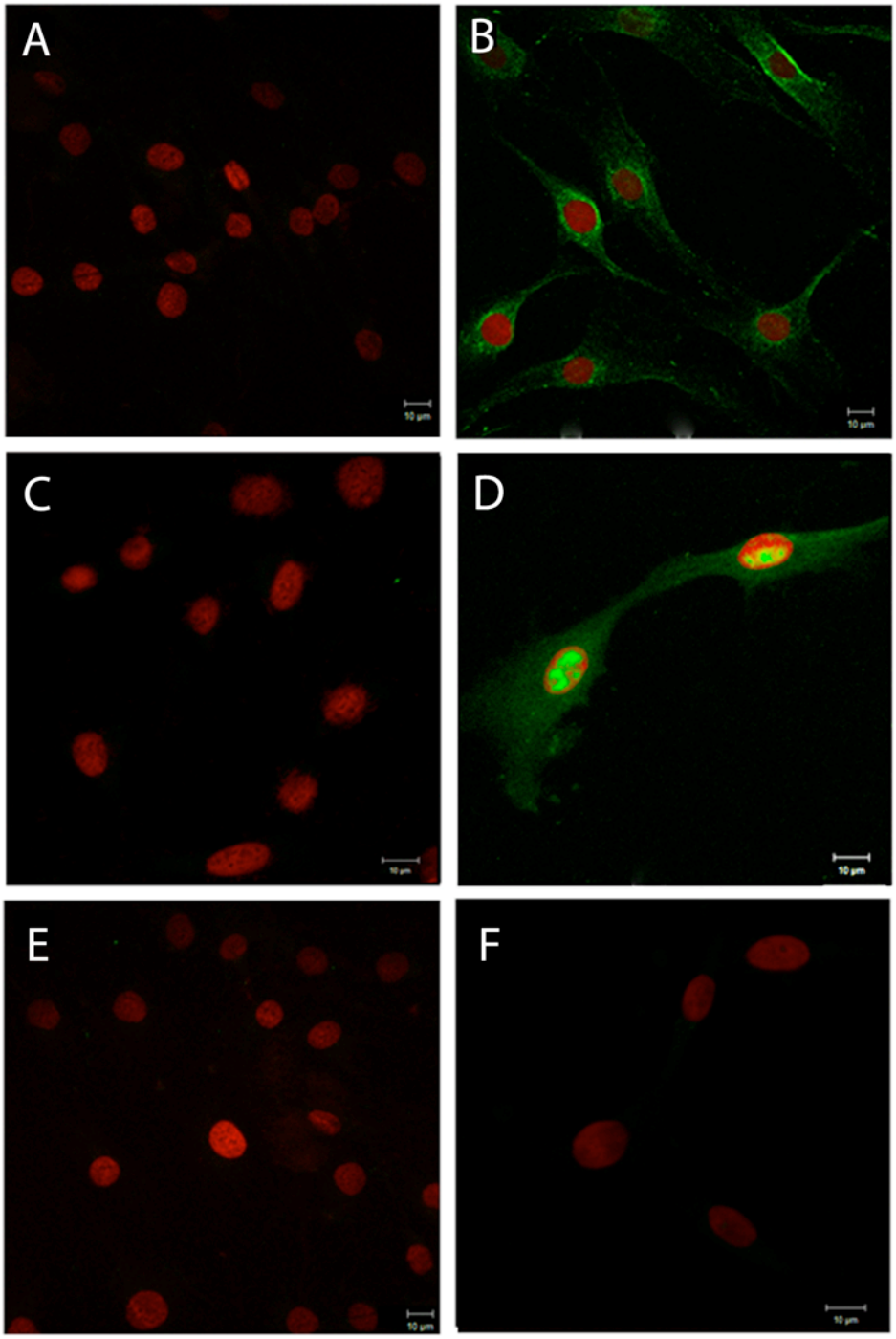


Figure 4.15 –Immunocytochemistry of FRMD5 protein labelling within culture-expanded full-depth chondrocytes, normal cartilage-derived stem cells and osteoarthritic cartilage-derived stem cells.

A, C) FRMD5 protein labelling is not evident in full-depth chondrocyte derived cell lines. **Figure A -** shows a representative image of a normal cartilage full-depth cell line, **Figure C -** shows a representative image of an OA cartilage full-depth cell line. **B, D)** FRMD5 protein labelling shows cytoplasmic labelling in cartilage-derived stem cell lines. **Figure B -** shows a representative image of a normal cartilage full-depth cell line, **Figure D -** shows a representative image of an OA cartilage full-depth cell line. **E, F)** Controls using normal cartilage-derived stem cells. Figure E- an isotype matched IgG control and Figure F- a no primary antibody control.

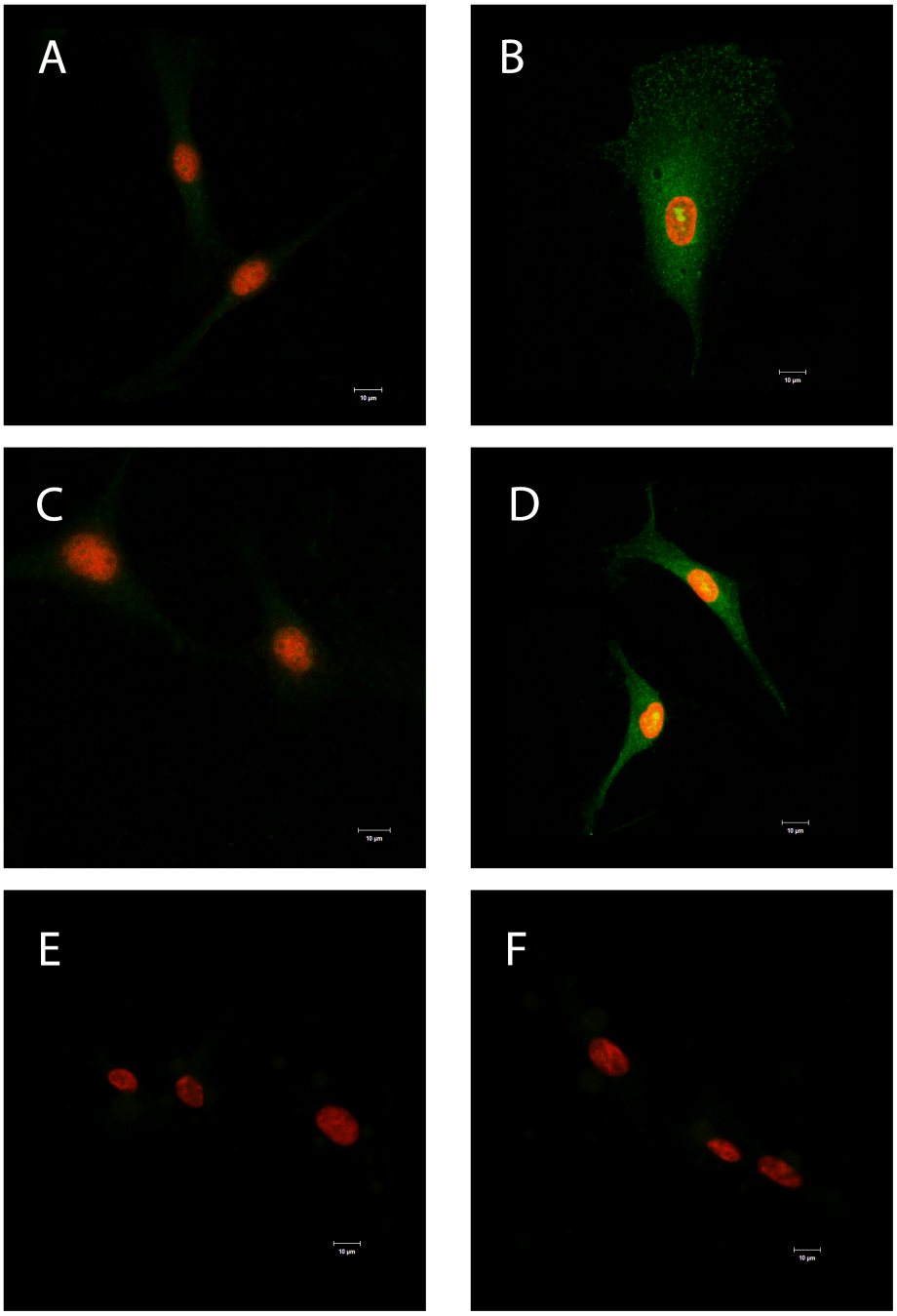


Figure 4.16 –Immunocytochemistry of C11ORF41 protein labelling within culture-expanded full-depth chondrocytes, normal cartilage-derived stem cells and osteoarthritic cartilage-derived stem cells.

A, C) C11ORF41 protein labelling is not evident in full-depth chondrocyte derived cell lines. **Figure A -** shows a representative image of a normal cartilage full-depth cell line, **Figure C -** shows a representative image of an OA cartilage full-depth cell line. **B, D)** C11ORF41 protein labelling shows cytoplasmic labelling in cartilage-derived stem cell lines. **Figure B -** shows a representative image of a normal cartilage full-depth cell line, **Figure D -** shows a representative image of an OA cartilage full-depth cell line. **E, F)** Controls using normal cartilage-derived stem cells. Figure E- an isotype matched IgG control and Figure F- a no primary antibody control.

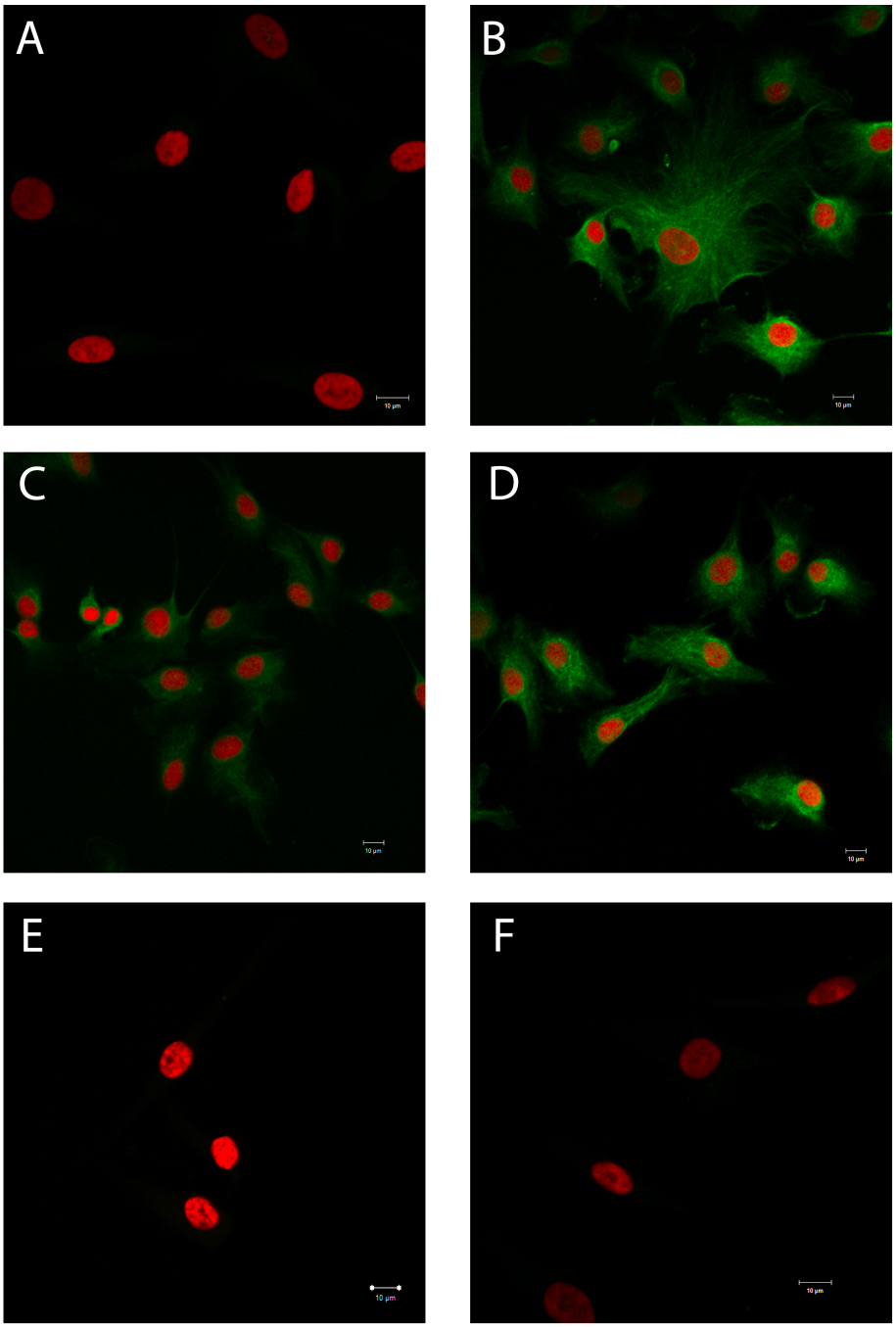


Figure 4.17 –Immunocytochemistry of EMBIGIN protein labelling within culture-expanded full-depth chondrocytes, normal cartilage-derived stem cells and osteoarthritic cartilage-derived stem cells.

A, C) EMBIGIN protein labelling is not evident in full-depth chondrocyte derived cell lines. **Figure A -** shows a representative image of a normal cartilage full-depth cell line, **Figure C -** shows a representative image of an OA cartilage full-depth cell line. **B, D)** EMBIGIN protein labelling shows cytoplasmic labelling in cartilage-derived stem cell lines. **Figure B -** shows a representative image of a normal cartilage full-depth cell line, **Figure D -** shows a representative image of an OA cartilage full-depth cell line. **E, F)** Controls using normal cartilage-derived stem cells. Figure E- an isotype matched IgG control and Figure F- a no primary antibody control.

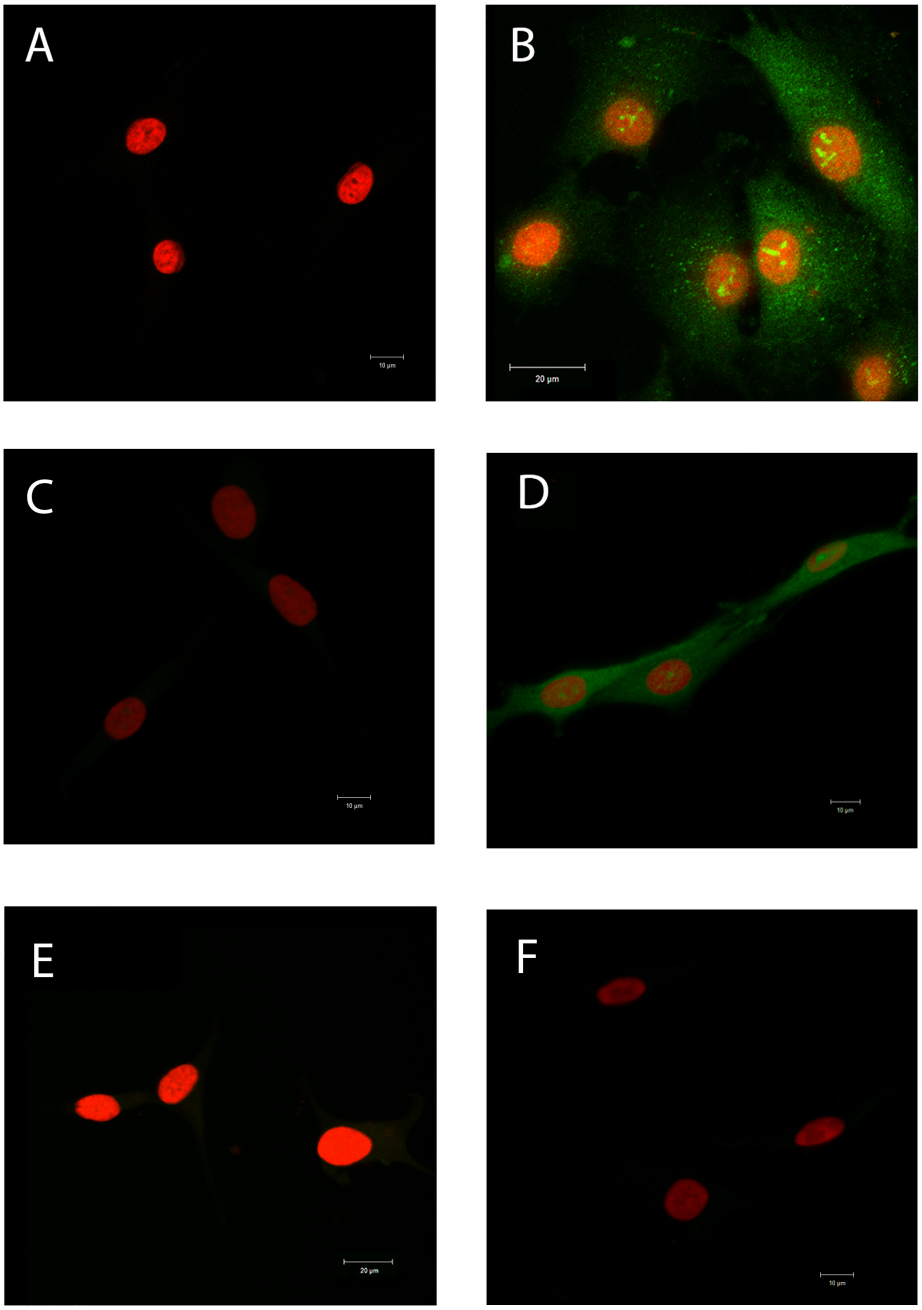


Figure 4.18 –Immunocytochemistry of EAAT1 protein labelling within culture-expanded full-depth chondrocytes, normal cartilage-derived stem cells and osteoarthritic cartilage-derived stem cells.

A, C) EAAT1 protein labelling is not evident in full-depth chondrocyte derived cell lines. **Figure A -** shows a representative image of a normal cartilage full-depth cell line, **Figure C -** shows a representative image of an OA cartilage full-depth cell line. **B, D)** EAAT1 protein labelling shows cytoplasmic labelling in cartilage-derived stem cell lines. **Figure B -** shows a representative image of a normal cartilage full-depth cell line, **Figure D -** shows a representative image of an OA cartilage full-depth cell line. **E, F)** Controls using normal cartilage-derived stem cells. Figure E- an isotype matched IgG control and Figure F- a no primary antibody control.

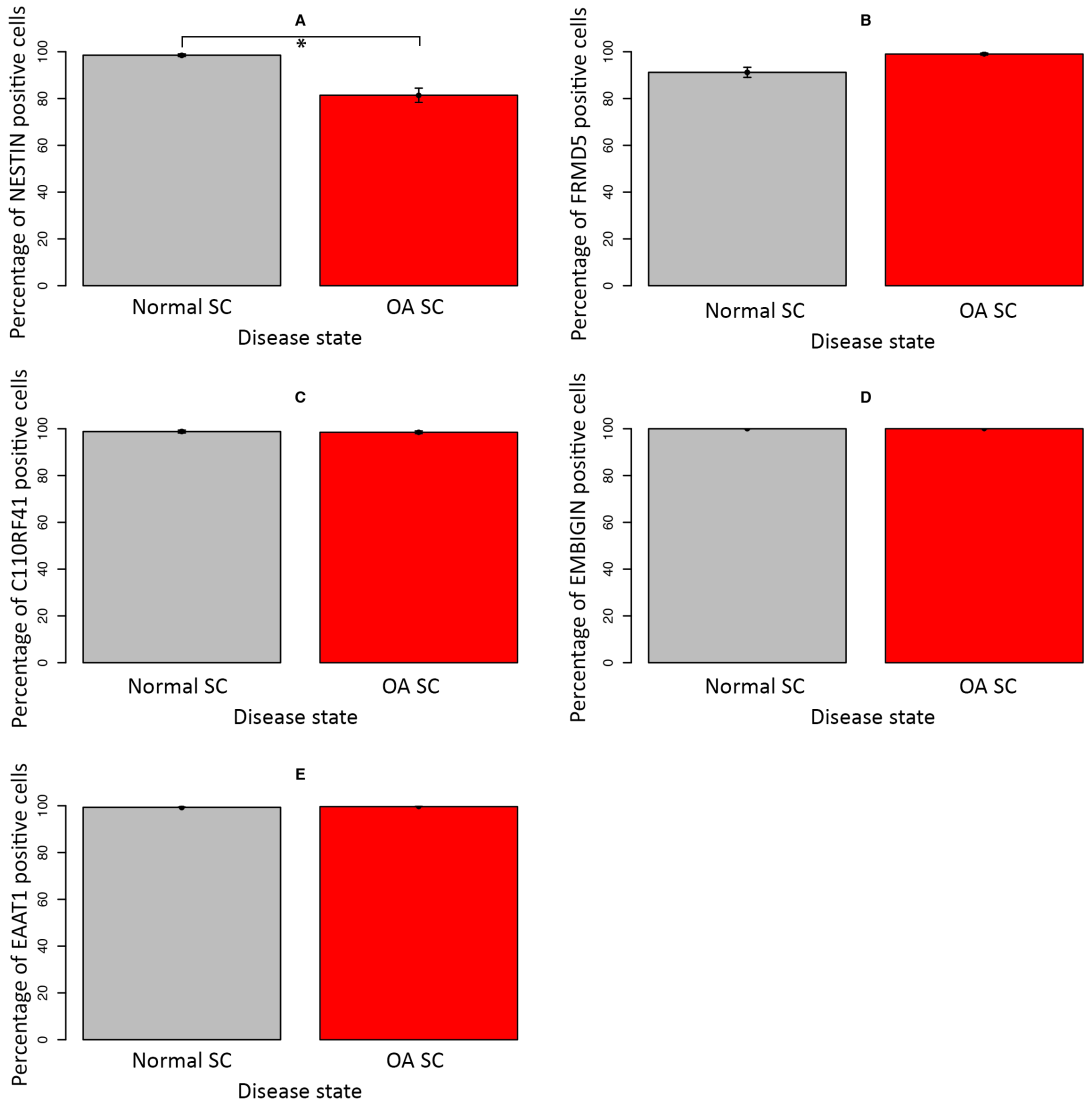


Figure 4.19 –Bar graphs showing the percentage cells exhibiting positive antibody labelling for stem cell markers in culture-expanded normal and osteoarthritic cartilage-derived stem cells.

Percentage of cells exhibiting antibody labelling was quantifies for 5 fields of view for 3 separate donors in each group. In most cases all the cells counted were found to be positive. However, in osteoarthritic cartilage approximately 20% fewer cells were positive for NESTIN protein labelling than in normal cartilage-derived cell lines ($p = 6.5e^{-6}$, Student's T-test). No significant differences were found between normal of OA derived cell lines for C11ORF41, FRMD5, EMBIGIN and EAAT1 protein labelling. **A -** *NESTIN,* **B -** *FRMD5,* **C -** *C11ORF41,* **D -** *EMBIGIN*, **E -** *EAAT1*.

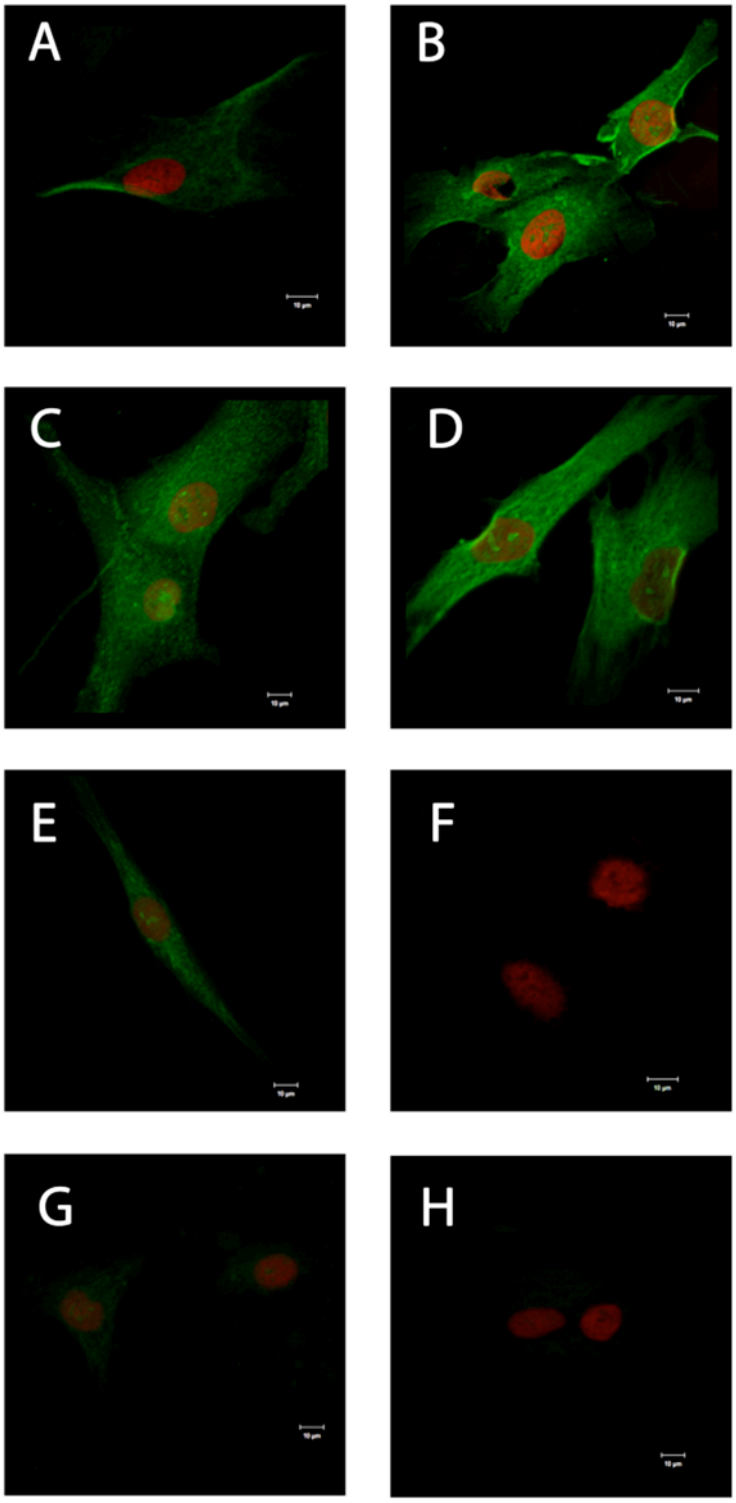


Figure 4.20 –Immunocytochemistry of stem cell marker protein labelling within human bone marrow stromal cells (mesenchymal stem cells) (MSCs).

MCSs were found to positively label for the stem cell marker proteins. **A -** NESTIN labelling, **B -** FRMD5 labelling, **C -** C11ORF41 labelling, **D -** EMBIGIN labelling, **E -** EAAT1 labelling. Figures F, D, H- Are isotype matched IgG controls.

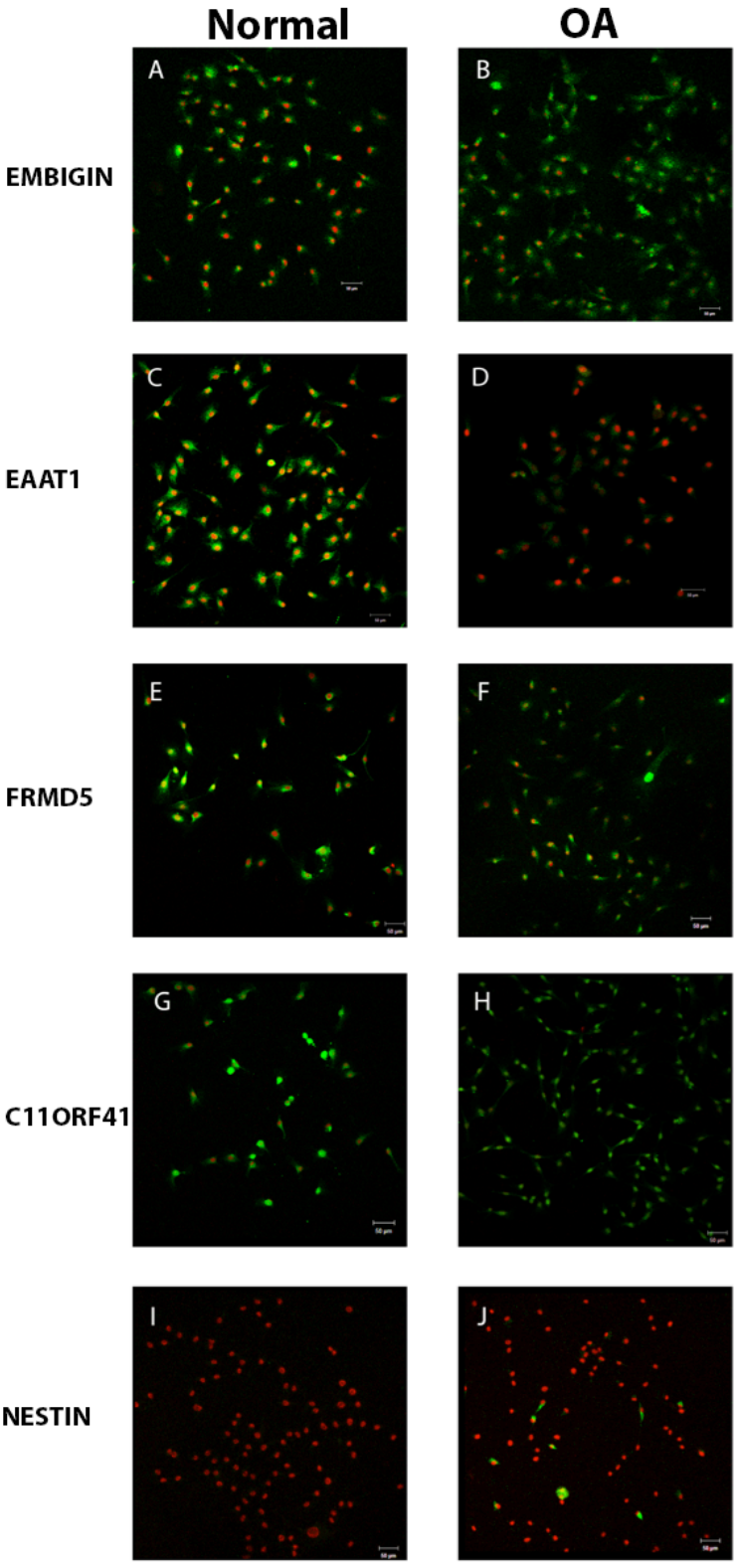


Figure 4.21 – Immunocytochemistry of stem cell marker protein labelling within initial colonies of cartilage-derived stem cells.

A, B) EMBIGIN labelling in initial adhesion colonies, labelling present in both normal of OA colonies. **C, D)** EAAT1 labelling in initial adhesion colonies, strong labelling is only present in normal cartilage-derived colony, weak labelling can be seen in some of the OA colony derived cells. **E, F)** FRMD5 labelling in initial adhesion colonies, labelling present in both normal of OA colonies. **G, H)** C11ORF41 labelling in initial adhesion colonies, labelling present in both normal of OA colonies. **I, J**) NESTIN labelling in initial adhesion colonies, labelling is absent in normal cartilage-derived colonies and is only present in a subset of the cells within the osteoarthritic colony.

4.4 Discussion

In this study, we focused on the isolation and quantification of articular cartilage-specific adult stem cells from normal and OA human knee joints and compared their characteristics with particular focus on proliferative kinetics. Using differential adhesion to fibronectin, first described by Jones and Watt, ACSC were successfully enriched from their differentiated progeny (Jones and Watt, 1993). ACSC were shown to have multipotent differentiation capacity, differentiating into chondrogenic, osteogenic and adipogenic lineages. This study has identified novel stem cell markers that are specific to ACSC and not expressed by FD chondrocytes.

4.4.1 Characterisation of ACSC

Percentage stem cells were calculated using a colony forming efficiency assay (CFEs). CFEs were calculated using the percentage of colonies formed as a proportion of the initial seeding density, giving an indication of the number of clonal cells within the entire population from digested tissue (Jones and Watt, 1993). Within normal tissue, this number was ~1.5% of the total cells and in OA ~3% of the total cells. These data are greater to that of Dowthwaite et al., (2004) who reported a mean CFE of 0.27% in cells digested from 7-day-old bovine articular cartilage. The increase in CFE in human tissue could be due to species variation or difference between an immature infantile tissue and a mature adult tissue. It is also worth noting, that results from previous papers isolating stem/progenitor cell within articular cartilage specifically targeted clonogenic cells residing in the surface zone of articular cartilage. This study has used full-thickness biopsies and, therefore, may contain progenitors from other regions of articular cartilage (Dowthwaite et al., 2004, McCarthy et al., 2012, Williams et al., 2010). CFEs determined that OA cartilage has approximately a 2-fold higher percentage of clonogenic stem cells compared to normal cartilage. Using cell surface markers CD105 and CD166, three other studies have found a similar increase in stem cell number in OA tissue. Alsalameh and colleagues identified a doubling in $CD166^{+}/CD105^{+}$ cells from ~3.5% in normal tissue to ~7.5% in OA tissue (Alsalameh et al., 2004). Pretzel and colleagues identified a small increase in $CD166^{+}/CD105^{+}$ cell in OA from 15.3% in normal cartilage to 16.7% in OA cartilage (Pretzel et al., 2011). Finally, Chang and colleagues found that 4.9% of

cells in normal cartilage were $CD166^+/CD105^+$, which increased to 6.3% in OA tissue (Chang et al., 2011). The up-regulation of stem cell markers in OA tissue has been reported in multiple studies and thus, it would be expected that, CFEs would be higher in the diseased state (Alsalameh et al., 2004, Grogan et al., 2009, Pretzel et al., 2011). It is reported that blunt force injury to articular cartilage stimulates a migratory and proliferative progenitor population mediated through HMGB-1 release and RAGE-mediated chemotaxis. This population is multipotent, clonogenic and expresses putative stem cell markers while being morphologically distinct from native chondrocytes *in situ* (Seol et al., 2012). An increase in stem cells within disease tissue could be due to a proliferative or migratory response to injury.

Upon culture expansion of normal ACSC and OA-SC cell lines, a clear difference in overall growth kinetics of OA-SCs was observed; most significantly, OA-SC could be separated into two groups. The initial growth kinetics of all ACSC was found to be comparable, with FD chondrocyte initially proliferating at slower rate. N-SC cell lines from the same patient appear to proliferate at similar rates with a small degree of heterogeneity between donors. OA-SC displayed a large degree of heterogeneity in the growth kinetics from the same donor. An explanation for this could be that there are different cohorts of cells within OA tissue and, as such, the highly proliferative, late senescing cohort behave in a similar way to each other, yet differently to the cohort of cells which are less viable. Understanding the differences between these cell sub-populations is essential, it will greatly impact cell screening and selection for regenerative strategies.

After the initial exponential and linear phases of growth, the rate proliferation of ES-OA-SC abruptly decreases before senescence by 30PD. It was interesting to note that in FD cell lines, although senescing at a similar PD to ES-OA-SC, the reduction in proliferative rate is more gradual that the ES-OA-SC. Only 45% of the cell lines cultured from OA cartilage surpassed 30 PDs, approximately half of the ACSC isolated have the capacity to be cultured long term. A study by Nelson and colleagues (2014) recently isolate a progenitor population from OA articular cartilage, and this study also identifies that 50% of the cell lines established failed to reach 30PD. In this study, population doubling data was corroborated by proliferative index, examined using BrdU, that correlates with growth kinetics. BrdU incorporation identified no notable differences between N-SC and

LS-OA-SC cultures; however there was a significant reduction in dividing cells between both N-SC/LS-OA-SC and the ES-OA-SC sub-population. Within individual cohorts there was significant variation between samples of the ES-OA-SC group, while the N-SC and LS-OA-SC exhibited a heterogeneous proliferative index across samples. The sub-populations identified within the OA-SC were not due to variation between donors, multiple cell lines established from the same donor showed this variation. This implies that the divergence in proliferative capacity of ACSC is due to disease and not due to donor variations such as age. In fact, in this study, age was not found to have a significant effect on time of senescence or BrdU incorporation. These data suggest that although there is an increase in the number of ACSC in diseased tissue, possibly as a reparative response; OA-SCs become dysfunctional as a facet of the disease. A degenerate stem/progenitor population has previously been suggested by (Dealy, 2012), this editorial stated that "the presence of disease may alter endogenous progenitor populations and compromise their ability to accomplish self-repair".

We do not see ACSC with divergent cell properties from normal cartilage therefore, the question arises as to how clonogenic cell lines with divergent characteristics emerge within diseased cartilage? One possible mechanism is as a result of telomere shortening; the replicative lifespan of somatic cells is restricted by telomere erosion and the presence of short telomeres correlates with ageing and the progression of OA (Martin and Buckwalter, 2001). Williams and colleagues have previously shown that ACSC from healthy cartilage have a uniform high average telomere length and that telemore length is maintained by telomerase enzyme activity *in vitro* (Williams et al., 2010). A reduction in telomerase activity or telomere shortening within the ES-OA-SC cohort could be responsible for the reduced proliferation capacity of these cells. Recently, work within our group has identified that individual ACSC populations isolated from OA cartilage have 2 populations with divergence in average telomere length. Both high and low average telomere sizes have been observed (unpublished observations), supporting the notion that telomere shortening is one mechanism behind the appearance of ACSC sub-populations in OA. Replicative exhaustion through telomere shortening during *in vitro* culture, whilst being an identifying feature of a divergent sub-population of adult stem cells does not explain its emergence within diseased tissue. One possible mechanism for the appearance

of clonal sub-populations is episodic exposure to acute oxidative stress during OA inflammatory flares. Inflammatory activity over a prolonged period of time affects not only the stem cell phenotype but also the stem cell niche due to loss of specific proteoglycans (Hayes et al., 2008). OA cartilage *in situ* has heterogeneous cells types compared to healthy cartilage; structural studies have identified three different cell types. Type 1 cells are single or clustered chondrocyte-like cells, type 2 cells are elongated secretory cells and type 3 cells are irregularly shaped cells undergoing degeneration (Kouri et al., 1996). These cellular changes prior to ACSC extraction may be in part responsible for the different sub-populations observed in ACSC. Finally, abnormal or incomplete differentiation of daughter cells produced in response to tissue injury could result in retention of adult stem cell characteristics, such as clonogenic potential and stem cell marker expression but without an extended proliferative capacity. We hypothesise that aberrant daughter cells are unable to promote productive repair of damaged cartilage and contribute to disease progression; further work including lineage tracing would be required to confirm this hypothesis.

Previous studies within our laboratory have shown that clonogenic cells from human articular cartilage express cell surface markers CD105 and CD166 and undergo multipotential differentiation into adipogenic, osteogenic and chondrogenic lineages, and therefore, fulfil the criteria for classification as mesenchymal stem cells (Williams et al., 2010). We confirmed the multipotential phenotype of both normal and OA ACSC using the chondrogenic 3D-pellet culture, osteogenic 3D-pellet culture and monolayer adipogenic differentiation.

Pellet cultures were established using the ACSC and FD cell-lines isolated and expanded from normal and OA tibial plateaux. Morphologically, the pellets were consistent in terms of appearance; presenting a smooth, iridescent white surface. The size of pellets from different cell lines was variable. Morphologically, the cells within the 3D-pellets adopted a rounded phenotype, characteristic of articular cartilage *in situ* (Archer and Francis-West, 2003). The ACSC and FD chondrocyte capacity for chondrogenic differentiation was examined histologically using toluidine blue staining to demonstrate the level of sulphated GAG production within the matrix. Toluidine blue staining demonstrated the accumulation of GAGs, particularly around the outer edges of the pellets. The outer edges of the pellets had higher cell densities and direct exposure to the

chondrogenic media, therefore, it is understandable that this area had the largest deposition of matrix. Within the centre of the pellets, all pellets displayed GAG deposition, however, there was variability between the levels of GAG between pellets of the same cohort. The variability in chondrogenic capacity of ACSC was not explored in this study, however, Nelson et al., (2014) found large heterogeneity in OA clonogenic cell response to chondrogenic stimuli. All N-SC and both ES-OA-SC and LS-OA-SC lines examined were found to be capable of chondrogenic differentiation and all FD cell lines from both normal and OA donors were also found have chondrogenic capacity.

The ability for the ACSC to produce multi-lineage progeny was examined through induction into adipogenic and osteogenic lineages. The results from our study demonstrate that all ACSC lines have the capacity to differentiate into the adipogenic lineage, which is consistent with previous studies (Nelson et al., 2014, Williams et al., 2010). The cartilage ACSC pellets cultured in osteogenic differentiation media showed gross morphology and size that was comparable to FD osteogenic-induced pellets. When stained for mineralisation, cartilage progenitor pellets showed extensive regions of calcium deposition as indicated by both Von Kossa and Alizarin red stain. The full-depth chondrocyte pellets displayed no evidence of mineralisation. This confirms that all ACSC, regardless of proliferative capacity, can undergo tri-lineage differentiation; whereas, the FD chondrocytes displayed limited differentiation potentials. As such, ACSCs enriched by differential adhesion meet the multi-lineage criterion for classification of a mesenchymal stem cell population (Wagner et al., 2008). Early senescent OA-SC lines while maintaining multi-lineage potential are unable to meet the Hayflick limit for classification of an MSC. It has been documented that hair follicle transit-amplifying cells are capable of differential adhesion (to Collagen Type VI) and are clonogenic, although to a lesser degree than true hair follicle stem cells, the transit-amplifying cells were only capable of growth to passage 3 while the stem cells reached passage 7 (Roh et al., 2005). Nakagawa and colleagues 2007 previously reported that transit-amplifying cells of the testis, under regenerative stresses, were able to regain characteristics of stemness, returning to a stem cell like phenotype. It is possible that the ES-OA-SC population represent a transit-amplifying population that has re-acquired multipotency through OA induced reprogramming (Nakagawa et al., 2007).

However, contrary to this, some bone marrow derived MSC cell lines have been reported to undergo replicative senescence as early as 20PD. It is, therefore, possible the ES-OA-SC cohort are true stem cells that have a reduced proliferative capacity for the reasons discussed previously (Estrada et al., 2013).

4.4.2 Characterisation of potential stem cell markers

This study has validated the finding from the NGS transcriptomic sequencing experiments of Chapter 3. From the panel of potential stem cell markers selected in Chapter 3, all were found to be significantly up-regulated in gene expression between FD chondrocytes and both normal and OA-derived ACSC lines. Articular cartilage specific genes were found to be expressed significantly higher in the FD population that the ACSC cohorts again correlating with the finding in Chapter 3. We have shown that it is possible to identify different cell populations using gene expression data alone; FD chondrocytes were separated from ACSC, and within ACSC it was possible to distinguish ES-OA-SC from N-SC/LS-OA-SC lines. The separation of early senescent cells from the proliferative cohort implies that certain genes within this panel are having a functional effect on the proliferative capacity of ACSCs.

The adult stem cell phenotype of clonogenic cells was further corroborated by the discovery that both populations from normal and OA-derived cartilage express *NESTIN* gene transcripts and NESTIN protein at higher levels than full-depth culture-expanded chondrocytes derived from normal and OA cartilage. NESTIN is an intermediate filament protein expressed in dividing cells during early development. Upon differentiation, NESTIN is down-regulated and replaced by tissue-specific intermediate filament proteins such as vimentin (Eriksson et al., 1992b). During embryogenesis, NESTIN expression can also be found in multiple tissues, especially the developing central nervous system and muscle (Kachinsky et al., 1994, Park et al., 2010). Most NESTIN-positive cells in early development are stem/progenitor populations engaged in active proliferation (Wiese et al., 2004). In adult organisms, NESTIN-positive cells are restricted to defined niches, where they may function as a quiescent stem cell reserve capable of proliferation, differentiation and migration once activated (Park et al., 2010). NESTIN is widely utilised as a marker of proliferating and

migrating adult stem cells (Michalczyk and Ziman, 2005). In this study we found that cell lines with the strongest *NESTIN* gene expression had the greatest proliferative capacity. Screening for high *NESTIN* expression may allow for selection of ACSC with a potent proliferative capacity, allowing early detection of ES-OA-SC lines. The correlation of NESTIN expression with cell proliferation is also observed in neoplasms, abundant NESTIN expression was found in several cancers such as neuroblastoma, glioma, and melanoma and higher levels of expression correlated with an increased malignancy (Dahlstrand et al., 1992, Yang et al., 2008). *In vitro* knock down of *NESTIN* in neuroblastoma and astrocytoma cells have also been shown to reduce cell growth (Thomas et al., 2004, Wei et al., 2008). Previous studies in multiple tissue types have shown that injury or pathology induce cells to re-express or up-regulate NESTIN (Namiki and Tator, 1999), indicating a move towards an immature phenotype to facilitate remodelling or induction of a reparative process. NESTIN protein labelling was absent in initial adhesion colonies derived from normal cartilage and only present in a subset of cell in colonies derived from OA cartilage. Previous studies have shown the removal of growth factors such as of EGF and FGF-2 results in the suppression of NESTIN expression in neural stem cells (Sun et al., 2008); initial adhesion colonies cultured in the absence of growth factors, with FGF-2 and TGF-β2 supplements added post cloning. The lack of growth factor stimuli during the culture of initial colonies may explain the absence of NESTIN labelling. This is the first study to identify NESTIN-positive cells from articular cartilage, however, previous work has suggested the presence of NESTIN-positive cells in lung cartilage (Ortega-Martínez et al., 2013).

Proteins containing a FERM domain are ubiquitous components of the cell membrane and the cytocortex of eukaryotic cells where they are engaged in structural, transport, and signalling functions, with several FERM protein-encoding genes being associated with human diseases (Tepass, 2009). *FRMD5* showed the largest increase in gene expression between ACSC and FD cells. Immunocytochemistry showed clear strong labelling of FRMD5 at the cell membrane of ACSC, labelling was highly specific and exclusive to the stem cells with no labelling seen in the full-depth or controls. The specific function of FRMD5 is yet to be identified with only one function study previously published. Wang and colleagues showed FRMD5 has a role in cell adhesion through

interaction with p120-catenin. FRMD5 enhanced the binding of p120-catenin with E-cadherin, to form a FRMD5–p120-catenin–E-cadherin complex that stabilise adherens junctions (Wang et al., 2012). Knock-down of FRMD5 down-regulated E-cadherin and up-regulated vimentin (Wang et al., 2012); therefore, FRMD5 may play a role regulating cytoskeletal composition of ACSC, potentially regulating NESTIN. Further work would require over-expression and knock-down studies in ACSC to confirm this hypothesis. Like *NESTIN, FRMD5* gene expression was also found to correlate with proliferative potential of ACSC, that supports the possibility that FRMD5 and NESTIN may function within a common pathway. Screening for FRMD5 has potential for isolation of highly proliferative stem cells.

Chromosome 11 open reading frame 41 (C11ORF41) is a single transmembrane domain protein; no previous publications exist and the protein function is currently unknown. *C11ORF41* gene expression was significantly increased in ACSC and immunocytochemistry for C11ORF41 protein showed diffuse labelling within the cell membrane of the chondroprogenitor stem cells while no labelling is seen in the full-depth cells. Like *FRMD5* and *NESTIN*, *C11ORF41* correlates with proliferative longevity of ACSC, indicating it may have a functional role in self-renewal and offers a screening target during stem cell selection. Further study is required to identify the functional role of C11ORF41 in ACSC.

EMBIGIN gene expression was found to be significantly higher in ACSC and immunocytochemistry identified the protein was specifically expressed within ACSC, localising to the cell membrane. EMBIGIN is a developmentally expressed cell adhesion molecule that is a member of the immunoglobulin superfamily (IgSF) class of cell adhesion molecules (Guenette et al., 1997). Cell adhesion molecules are involved in multiple cellular processes, including development, proliferation, apoptosis and differentiation (Guenette et al., 1997). The function of EMBIGIN within embryonic stem cells has been shown to enhance cell adhesion to the extracellular matrix (Huang et al., 1993). Muramatsu (2004), identified a mechanism by with EMBIGIN increases adhesion through enhanced integrin activity. ACSC were isolated through differential adhesion to the ECM molecule fibronectin, mediated through alpha5 and beta1 integrins; it is, therefore, reasonable that a molecule enhancing integrin activity is significantly

increased within this cell population. Protein complex immunoprecipitation (CO-IP) of EMBIGIN will be required to identify whether EMBIGIN is directly interacting with integrins within ACSC. Additionally, many types of stem cells, including MSCs reside in a hypoxic niche and are heavily reliant on anaerobic glycolysis to maintain the low oxygen tension required to maintain an undifferentiated state and allow self-renewal (Ito and Suda, 2014). Anaerobic glycolysis produces lactate as the end product; monocarboxylate transporters (MCT) move lactate out of the cell through the cell membrane. EMBIGIN is a co-factor required to localise MCT to the cell membrane (Halestrap and Price, 1999). EMBIGIN has been shown to specifically interact with MCT2, while MCT1, 3 and 4 interact with Basigin (Halestrap and Price, 1999). The MCT2 isoform has a 10-fold higher affinity for substrates than the other isoforms and is found in cells that heavily rely of anaerobic respiration (Halestrap and Price, 1999). EMBIGIN may be functioning within ACSC to facilitate anaerobic respiration; maintaining the capacity for self-renewal. More insight into the interaction between EMBIGIN, Basigin and MCT isoforms is provided in Chapter 6.

EAAT1 gene expression was also found to be significantly higher in ACSC and immunocytochemistry identified the protein was specifically expressed within ACSC, localising to the cell membrane. EAAT1 is predominantly expressed in the plasma membrane, allowing it to remove glutamate from the extracellular space (Divac, 1977) as cited in (Knut, 1995). Multiple studies have reported that EAAT1, like NESTIN, is expressed within neural stem cells, however is also highly expressed within differentiated astrocytes (Conti et al., 2005, Sirko et al., 2007). This is the first study to identify EAAT1 expression in cells derived from human cartilage; previous studies have shown EAAT1 is expressed by cells of the mesenchymal lineage, with expression identified in bone cells (Laketic-Ljubojevic et al., 1999, Mason et al., 1997). Jean and colleagues have shown that EAAT1 expression increases in rabbit cartilage following anterior cruciate ligament transection, this suggests a potential role in OA pathogenesis or in attempted repair (Jean et al., 2008). Expression of glutamate transporters with ACSC indicates that excitatory amino acids may be involved in paracrine intercellular communication between stem cells.

4.4.3 Conclusions

In conclusion, our data has confirmed the presence of ACSC in healthy and diseased human articular cartilage and has shown that OA tissue has a 2-fold increase in stem cell number. Novel markers for ACSC populations have been identified that will allow the identification and isolation of stem cells from their differentiated progeny. Within this cohort of novel markers there is the potential for separation of stem cells with a high proliferative capacity, however further work is required to validate these findings and ascertain the functional mechanisms. OA-derived ACSC are composed of two distinct and divergent populations in regards to proliferative capacity. Divergence can potentially be explained on the basis that the early-senescing clonogenic cells are the product of aberrant or incomplete differentiation of the resident adult stem cell population. Whether incomplete differentiation is an inherent property of OA adult stem cells or, in part, due to changes in the stem cell niche requires experimental verification. These experiments will also have to test the possibility that divergent sub-populations are not derived from migrating MSCs from either subchondral bone or synovium. From the perspective of endogenous repair capacity of OA cartilage, it is encouraging to note that a viable adult stem cell population is present in significant quantity. To mobilise these cells and initiate productive repair of osteoarthritic lesions, a combination of cellular reprogramming and recapitulation of the normal stem cell niche may be necessary. If we can resolve these issues in future research, the potential for endogenous repair of osteoarthritic lesions will be a realistic goal.

CHAPTER 5:

GENE EXPRESSION ANALYSIS AND LOCALISATION OF NOVEL STEM CELL MARKERS IN NORMAL AND OSTEOARTHRITIC CARTILAGE

5.1 Introduction

Articular cartilage has a structural organization that has been highly conserved during evolution. Cartilage is divided into four distinct cellular zones: superficial, middle, deep and calcified. The chondrocytes in each layer differ morphologically and in mechanical properties. The superficial zone is characterized by discoid cells, oriented parallel to the surface. The cells are surrounded by densely packed fine collagen fibrils aligned parallel to the surface. The transitional zone has spheroid cells and thicker collagen fibrils with a predominant oblique direction, forming an arch-like organization. Within the deep zone the chondrocytes typically arrange in columns perpendicular to the articular surface. Here, collagen fibrils are thickest, with a predominant vertical orientation. Finally, the calcified zone anchors articular cartilage to the subchondral bone, the deep zone collagen fibres extend into the calcified zone reinforcing the attachment (Eyre, 2002, Hunziker, 2010).

Osteoarthritis (OA), the most common joint disorder worldwide; by 65 years of age, the majority of people have radiographic evidence of OA that affects the knee, hip, hand or spine, and less commonly, the wrists and ankles (Arden and Nevitt, 2006). OA is a heterogeneous disorder that affect all joint tissues, although articular cartilage and the subchondral bone show the most degeneration (Herrero-Beaumont et al., 2009). On gross examination, normal articular cartilage is firm, smooth and opalescent in young healthy individuals. With normal ageing, cartilage becomes more opaque and later yellowish. In OA, the cartilage becomes softer and irregular, with formation of fibrillations and ulcerations (Lotz and Loeser, 2012). OA lesions are progressive and located to areas of high load, there are often lesions of varying severity in the same joint. Initially, lesions are superficial fibrillations running parallel to the articular surface. Gradually, lesions progress into deeper fibrillations of vertical fissures. Further deterioration results in horizontal splitting between the un-mineralized and mineralized cartilage occurs that results in shedding of mineralized cartilage. In advanced OA, the subchondral bone is exposed (Horton et al., 2006, Lotz and Loeser, 2012). In areas close to lesions there is a reduced cell density due to apoptosis, while adjacent sites show chondrocyte clustering and proliferation (Poole, 1997, Rothwell and Bentley, 1973). There are also parallel

changes in the subchondral bone such as sclerosis, osteonecrosis and fractures. Osteophyte formation at the joint margins is another prominent feature of OA. There are also biochemical changes such as decreased proteoglycan content, altered proteoglycan structure and increases in proteolytic enzymes (Pearle et al., 2005). There is an increase in non-aggregating proteoglycans combined with degradation of Aggrecan orchestrated by aggrecanases and metalloproteinases. This reduces the negative charge within the cartilage and, consequently, the hydrostatic pressure decreases, compromising the mechanical structure. Finally, the collagen network is broken down by metalloproteinases reducing the tensile stiffness and strength of the cartilage (Horton et al., 2006).

As cited in Chapter 1, articular cartilage grows by appositional growth from the articular surface therefore a population of progenitor cells must reside within the tissue (Hayes et al., 2001). Progenitor cells were first reported to reside in the surface zone of immature bovine articular cartilage after isolation through adhesion to fibronectin *in vitro* (Dowthwaite et al., 2004). Pretzel et al., (2011) immunolocalised $CD166^{+}$ cells both in OA and normal cartilage to the superficial and middle cartilage zones; this study identified that normal cartilage had 22.1 ± 1.7% and OA cartilage had 23.6 ± 1.4% positive for CD166 expression (Pretzel et al., 2011). Grogan and colleagues (2009), using Notch-1, Stro-1 and VCAM-1 as stem cell markers, immunologically quantified the positive cells in normal, OA non-fibrillated and OA fibrillated cartilage. Within normal cartilage, around 80% of the superficial zone cells, 45% of transitional zone cells and 35% of deep zone cells were positive. There was a slight increase in OA non-fibrillated cartilage and a further increase was observed in OA fibrillated cartilage. Osteoarthritic chondrocyte clusters were also found to be positive for stem cell markers (Grogan et al., 2009). Both these studies have found very high numbers of positively labelled cells.

As previously mentioned, MSC surface markers are unsuitable for identification of stem cells in articular cartilage. Therefore, the localisation of ACSC in both a healthy and diseased mature human tissue has not been identified. This Chapter aims to identify the zonal distribution, localisation and quantification of stem cells in normal and OA articular cartilage. The wide array of structural changes that occurs during OA may alter the quantity and distribution of ACSC. The novel

ACSC markers identified in earlier Chapters of this thesis will be utilised to achieve this goal.

5.2 Methodology

Material	Catalogue number	Supplier
Dako pen	S2002	Dako, UK
Mouse immunoglobulins	X0931	Dako, UK
SafeView Nucleic Acid Stain	NBS-SV1	NBS Biologicals Ltd, UK
Low Molecular Weight DNA Ladder	N0468	New England Biolabs, UK
GoTaq® G2 Hot start DNA Polymerase	M7405	Promega, USA
AMV Reverse Transcriptase, RNase H Minus	M5108	Promega, USA
Random primers	C1181	Promega, USA
Recombinant RNasin Ribonuclease Inhibitor	N2511	Promega, USA
Set of dATP, dCTP, dGTP, dTTP	U1240	Promega, USA
TBE Buffer	V4251	Promega, USA
Agarose	V3125	Promega, USA
GoTaq® qPCR Master Mix	A6002	Promega, USA
DPX mounting medium	RAYLLAMB/DPX	Raymond A Lamb Medical, UK
Goat immunoglobulin	AB-108-C	R&D systems, UK
Rabbit immunoglobulin	AB-105-C	R&D systems, UK
Hyaluronidase, from bovine testis	H4272	Sigma Aldrich, UK
Chondroitinase ABC, from Proteus vulgaris	C3667	Sigma Aldrich, UK
N-Hexane	296090	Sigma Aldrich, UK
10 % Formalin solution, neutral buffered	HT501128	Sigma Aldrich, UK
Phosphate buffered saline	P4417	Sigma Aldrich, UK
6mm Biopsy punch	BI2000	Stiefel, UK
Ethanol	E/0650DF/17	Thermo Fisher Scientific, UK
Sodium hydroxide	S/4920/60	Thermo Fisher Scientific, UK
Polylysine adhesion glass slides	MNJ-800-010F	Thermo Fisher Scientific, UK
RNeasy Mini Kit	74104	Qiagen, UK
RNase-free DNase set	79254	Qiagen, UK
Antigen unmasking solutions	H-3300	Vector Laboratories, UK

Table 5.1 – Materials and suppliers

5.2.1 Tissue processing

Cartilage explants were prepared from normal and OA donors using 6mm biopsy punches (Stiefel) as previously described in Sections 2.1-2.5. Cartilage explants were excised under sterile conditions from tibial plateaux of males and females for both the normal donors (n = 6; mean age 47.8yrs, range 25-75) and OA donors (n = 6; mean age 52.7yrs, range 50-85). Only tissues from the tibial plateaux were used for this study; cartilage and bone obtained from the femoral condyles were omitted in this analysis in order to maintain consistency. Explants from OA donors were taken from a region adjacent to the lesion site that showed macroscopic roughening but not degraded cartilage Tissue was immediately snap-frozen in N-hexane using dry ice and ethanol for RNA extraction or fixed in 10% NBFS at 4^{o}C overnight for histology.

5.2.2 RNA extraction and purification

RNA was isolated from 100mg of snap-frozen tissue aliquots of each donor. Tissue was homogenised in TRI reagent by shaking at 2000 rpm for 1 minute using a micro-dismembranator (B. Braun Biotech) as described in Section 2.7.2. RNA was purified using the Qiagen RNeasy kit as outlined in Section 2.7. Purity and concentration was checked using a nano-drop spectrophotometer.

5.2.3 cDNA synthesis

One microgram of RNA was used *per* sample for cDNA synthesis for each reaction. Reactions were performed in 50µl containing, 400µM dNTPs, 0.4µg of random hexameric primers (Promega), 0.2U/µl AMV RT enzyme (Promega) and 0.5U/µl RNasein (Promega). Samples were incubated at 25^{o}C for 10 minutes, 48^{o}C for 1 hour and then 95^{o}C for 2 minutes in a thermocycler. (Section 2.8)

5.2.4 qPCR analysis

Quantitative polymerase chain reaction (qPCR) was completed using the Biorad CFX96 detection systems as outlined in Section 2.12. Plasmids were cloned from PCR products (Section 2.9-2.11) and sequenced to confirm the identity of the insert. Gene expression was quantified against a standard curve of serial diluted plasmid and normalised to the house-keeping genes beta-2 microglobulin (*B2M)* and ribosomal protein S18 (*RPS18),* after the NormFinder algorithm identified

this combination as optimal from the panel of candidate genes (Table 5.2). Primer sequences and annealing temperatures are shown in Table 4.3 (Chapter 4). Melt curves and standard curves for each gene are provided in the Appendix (Figure S1.3 and Figure S1.4).

Gene name	Gene symbol	Forward primer sequence	Reverse primer sequence	Annealing temp (°C)	NormFinder coefficient of variance	NormFinder M - value
Beta-2 microglobulin	B2M	AGA-TGA-GTA-TGC-CTG-CCG-TG	TCA-TCC-AAT-CCA-AAT-GCG-GC	56	0.1916	0.4104
Ribosomal protein S18	RPS18	CAC-AGG-AGG-CCT-ACA-CGC-CG	AGG-CTA-TTT-TCC-GCC-GCC-CA	56	0.1331	0.3399
Hyperparathyroidism 1	HRPT1	GAG-ACA-GGA-CCA-CTC-ATG-AAG-T	TCG-AGC-AAG-ACG-TTC-AGT-CC	56	0.1388	0.2679
Pre-mRNA processing factor 31	PMP31 (RP11)	GTG-CGG-CTG-CTT-CCA-TAA-G	CCC-TGG-CGT-CGT-GAT-TAG-TG	56	0.2056	0.4320
60S ribosomal protein L13a	RPL13a	CGT-GGC-TAA-ACA-GGT-ACT-GC	GTT-TGG-TGT-TCA-TCC-GCT-TGC	56	0.1566	0.3646
Beta actin	ACTB	CAA-GTC-CAC-ACA-GGG-GAG-GT	AGA-CCA-AAA-GCC-TTC-ATA-CAT-CTC-A	56	0.6078	0.9954
Combination of Beta-2 microglobulin and Ribosomal protein S18	**RPS18 + B2M**				**0.1294**	**0.3746**

Table 5.2– NormFinder results and primer sequences for house-keeping genes.

A coefficient of variance of <0.25 and a M-value of <0.5 shows gene homogenous gene expression across all cDNA samples. All house-keeping genes considered with the exception of beta actin were found to be suitable candidates. House-keeping genes were considered and tested both individually and in combinations (all possible iterations were processed using the NormFinder algorithm). The combination of the beta-2microglobulin and ribosomal protein S18 was found to provide the optimum normalisation and, therefore, chosen as the house-keeping genes for all qPCR experiments in this study.

5.2.5 Immunofluorescence

Immunofluorescence detection of stem cell markers were performed on paraffin wax embedded sectioned articular cartilage tissue as described in Section 2.20.2. In brief, tissues were fixed in 10% NBFS for 30 minutes and processed for wax embedding as described in Section 2.15. Ten-micron thick sections were cut using a microtome and rehydrated through xylenes and graded alcohols (Section 2.16). Antigen unmasking was performed by boiling for 1 minute in antigen unmasking solution (Vectorlab). Sections were washed and incubated with hyaluronidase (2U ml^{-1}) and chondroitinase ABC (0.1U ml^{-1}) in PBS 0.2% Triton-X-100 for 1 hour at 37°C. Sections were washed before proceeding to block with relevant sera (Section 2.19). All antibodies and immunoglobulin matched (IgG-matched) controls were prepared in PBS (Sigma-Aldrich) containing 0.2%

Triton-X-100 (Sigma-Aldrich) and 5% blocking serum (serum was species matched to the secondary antibody). Primary antibodies were incubated for 1 hour at room temperature, and then slides were washed 3 times in PBST before incubation with 10μg ml^{-1} fluorescence-conjugated secondary antibodies for 1 hour at room temperature. Samples were washed a further 3 times in PBST before being mounted in Vector shield ™ containing DAPI. Antibody concentrations are shown in Tables 4.4 and 4.5 (Chapter 4). Due to the autofluorescent nature of articular cartilage far-red (Alexa Fluor 633, 647) secondary antibodies were chosen to reduce background fluorescence.

5.2.6 Quantification of positive labelling in tissue through immunofluorescence

The percentage of cells exhibiting positive labelling was quantified for each zone of normal and OA articular cartilage. The total number of DAPI stained nuclei were recorded for each field of view and the number of cells displaying antibody labelling were counted. Three fields of view were counted for each zone of articular cartilage (superficial, upper transitional, lower transitional and deep zones) for 3 separate normal and 3 separate osteoarthritic donors, using x40 magnification on a fluorescence microscope.

5.2.7 Statistics

All statistics were performed using the 'R' statistical software. Statistical significance was confirmed using a parametric analysis of generalised linear mixed models, Anova and Student T-tests where appropriate. Data that did not fit into the Gaussian distribution was 'normalised' by data transformations to allow for parametric analysis where possible. If data could not be normalised non-parametric alternatives were performed where stated. Statistical significance was defined as $p<0.05$.

5.3 Results

Optimisation of immunofluorescence protocols allowed for the maximum signal to noise ratio to be achieved. Many factors were examined, including tissue preparation, fixation, antibody concentration and antigen unmasking. In this study, cryosections and paraffin wax embedded sections were used. Antibodies were titrated with and without antigen unmasking procedures to determine the optimum tissue processing procedure. Antigen preservation and detection was found to be optimal in formalin fixed, paraffin wax embedded tissue after antigen unmasking with all antibodies. However, a worse general matrix autofluorescence was observed with wax sections using Alexa Fluor 488 and 594 secondary antibodies. Tissue autofluorescence was overcome using far-red secondary antibodies (Alexa Fluor 633 and 647). All images shown in the Chapter, are of paraffin wax embedded human articular cartilage fixed in NBFS and pre-treated with hyaluronidase, chondroitinase ABC and antigen unmasking solution prior to antibody labelling.

5.3.1 NESTIN

NESTIN gene expression was significantly up-regulated 9-fold between normal and OA cartilage ($p<0.05$) (Figure 5.1A). In healthy cartilage, NESTIN labelling was observed in a small number of cells within the superficial and upper transitional zones (Figure 5.2A and B), no labelling was apparent in the rest of the tissue (Figure 5.2 C and D). Immunologically, in normal cartilage, the average number of cells with protein labelling observed within the superficial zone was 2.5 ± 1.3%, upper transitional zone 3.2 ± 1.0%, lower transitional zone 0.8 ± 1.0% and deep zone 0.1 ± 0.3%. The total NESTIN-positive cells within normal articular cartilage was 2.3 ± 0.5% (Figure 5.18A). In OA cartilage, there was a large increase in NESTIN-positive cells localised to the superficial and upper transitional zones (Figure 5.3A and B), no labelling was apparent in the rest of the tissue (Figure 5.3C and D). The average number of positive cells observed within the superficial zone increased to 23.0 ± 3.1%, upper transitional zone 20.3 ± 2.6%, lower transitional zone 1.4 ± 2.1% and deep zone 0.1 ± 0.3%. The total NESTIN-positive cells within OA articular cartilage had a statistically significant increase ($p<0.005$) to 10.9 ± 2.3% (Figure 5.18A). Labelling was specific with no positive cells identifiable in the controls (Figures 5.4 and 5.5).

5.3.2 FRMD5

FRMD5 gene expression showed a small but significant 1.4-fold up-regulation between normal and OA cartilage ($p<0.05$) (Figure 5.1B). In healthy cartilage, FRMD5 protein labelling was sparse in the superficial and deep zones and observed in very few cells (Figure 5.6A and D). Staining was more abundant in upper and lower transitional zones (Figure 5.6B and C). Immunologically, in normal cartilage, the average percentage of cells with protein labelling observed within the superficial zone was 2.1 ± 2.2%, upper transitional zone 6.3 ± 3.1%, lower transitional zone 3.9 ± 2.8% and deep zone 0.8 ± 1.8%. The total, FRMD5-positive cells within normal articular cartilage was 3.6 ± 2.1% (Figure 5.18B). In OA cartilage, there was a large increase in FRMD5 protein labelling especially within the superficial zone (Figure 5.7A). Staining also increased though, to a lesser degree, in upper and lower transitional zones (Figure 5.7B and C). No change in labelling was observed in the deep zone (Figure 5.7D). Immunologically, in OA cartilage, the average number of positive cells observed within the superficial zone was 10.4 ± 4.9%, upper transitional zone 11.0 ± 2.7%, lower transitional zone 10.3 ± 2.0% and deep zone 0.5 ± 1.4%. The total FRMD5-positive cells within OA articular cartilage was 13.3 ± 2.7% (Figure 5.18B). Labelling was specific with no positive cells identifiable in the controls (Figures 5.10 and 5.11).

5.3.3 C11ORF41

C11ORF41 gene expression showed a significant 5.4-fold up-regulation between normal and OA cartilage ($p<0.05$) (Figure 5.1C). In healthy cartilage, C11ORF41 protein labelling was expressed in a sub-population of cells residing in the superficial zone and both the upper and lower transitional zones (Figure 5.8A, B and C). No labelling was present in the deep zone (Figure 5.8D). Immunologically, in normal cartilage, the average number of cells with protein labelling observed within the superficial zone was 6.6 ± 3.1%, upper transitional zone 6.7 ± 2.0%, lower transitional zone 9.3 ± 2.1% and deep zone 0.4 ± 1.3%. The total C11ORF41-positive cells within normal articular cartilage was 5.7 ± 1.0% (Figure 5.18C). In OA cartilage, there was a large increase in C11ORF41-positive cells within the superficial zone and upper radial zones (Figure 5.9A and B). The percentage of cell labelling in the lower transitional zone decreases, often

with no cells labelling at all (Figure 5.9C). No change in labelling was observed in the deep zone (Figure 5.9D). Immunologically, in OA cartilage, the average number of positive cells observed within the superficial zone was 16.1 ± 2.2%, upper transitional zone 13.3 ± 3.8%, lower transitional zone 3.2 ± 3.9% and deep zone 0.6 ± 1.0%. The total C11ORF41-positive cells increases in OA articular cartilage to 10.1 ± 2.6% (Figure 5.18C). Labelling was specific with no positive cells being identifiable in the controls (Figures 5.10 and 5.11).

5.3.4 EMBIGIN

EMBIGIN gene expression had a small non-significant 1.25-fold increase in OA tissue ($p>0.05$) (Figure 5.1E). In healthy cartilage, cells labelling EMBIGIN protein were a sub-population residing in upper and lower transitional zones (Figure 5.12B and C). There was occasionally a low number of positive cells within the superficial but, often, no cells labelled at all (Figure 5.12A). No labelling was present in the deep zone (Figure 5.12D). Immunologically, in normal cartilage, the average number of cells with positive protein labelling observed within the superficial zone was 2.1 ± 2.2%, upper transitional zone 8.1 ± 1.6%, lower transitional zone 11.4 ± 2.2% and deep zone 1.4 ± 2.3%. The total EMBIGIN-positive cells within normal articular cartilage was 5.9 ± 1.9% (Figure 5.18D). In OA cartilage, there was a large increase in EMBIGIN-positive cells within the superficial zone and upper radial zones (Figure 5.13A and B). The percentage of cell labelling in the lower transitional zone decreases, often with no cells labelling at all (Figure 5.13C). No change in labelling was observed in the deep zone (Figure 5.13D). Immunologically, in OA cartilage, the average percentage of cells with EMBIGIN protein labelling within the superficial zone was 17.1 ± 6.0%, upper transitional zone 17.2 ± 7.0%, lower transitional zone 3.7 ± 4.3% and deep zone 1.5 ± 2.4%. The total number of EMBIGIN-positive cells increases in OA articular cartilage to 11.3 ± 1.7% (Figure 5.18D). Labelling was specific with no positive cells identifiable in the controls (Figures 5.16 and 5.17).

5.3.5 EAAT1

EAAT1 gene expression has a small non-significant 1.82-fold increase in OA tissue ($p>0.05$) (Figure 5.1F). In healthy cartilage, cells labelling for EAAT1 protein were a sub-population residing in upper and lower transitional zones

(Figure 5.14B and C). There were occasionally, a low number of positive cells within the superficial zone but often, no cells labelled at all (Figure 5.14A). No labelling was present in the deep zone (Figure 5.14D). Immunologically, in normal cartilage, the average number of cells with positive protein labelling observed within the superficial zone was 1.8 ± 1.6%, upper transitional zone 13.3 ± 6.4%, lower transitional zone 5.6 ± 3.9% and deep zone 1.1 ± 1.8%. The total EAAT1-positive cells within normal articular cartilage was 6.2 ± 1.1% (Figure 5.18E). In OA cartilage, there was a large increase in EAAT1-positive cells within the superficial zone and upper transitional zones (Figure 5.15A and B). The percentage of cell labelling in the lower transitional zone decreases, often with no cells labelling at all (Figure 5.15C). No change in labelling was observed in the deep zone (Figure 5.15D). Immunologically, in OA cartilage, the average percentage of cells with EAAT1 protein labelling within the superficial zone was 27.7 ± 8.2%, upper transitional zone 20.8 ± 2.4%, lower transitional zone 4.3 ± 4.3% and deep zone 1.1 ± 1.8%. The total EAAT1-positive cells increased in OA articular cartilage to 11.6 ± 1.9% (Figure 5.18D). Labelling was specific with no positive cells identifiable in the controls (Figures 5.16 and 5.17).

5.3.6 Other markers

PRDM1, ST6GAL2, TMEM132B and KIF26B were not examined for protein labelling. Gene expression for these markers was analysed by qPCR in normal and OA tissue. All genes displayed an increase in expression in OA cartilage. *PRDM1* gene expression showed a 2.4-fold statistically significant increase in gene expression between healthy and OA cartilage ($p<0.05$) (Figure 5.1D). *ST6GAL2* gene expression had a statistically significant 4.4-fold increase in OA cartilage compared to normal cartilage ($p<0.05$) (Figure 5.1G). *TMEM132B* gene expression showed a statistically significant 5.6-fold increase in OA cartilage compared to normal cartilage ($p<0.05$) (Figure 5.1H). *KIF26B* gene expression was statistically significantly increased 7.9-fold in OA cartilage compared to normal cartilage ($p<0.05$) (Figure 5.1I).

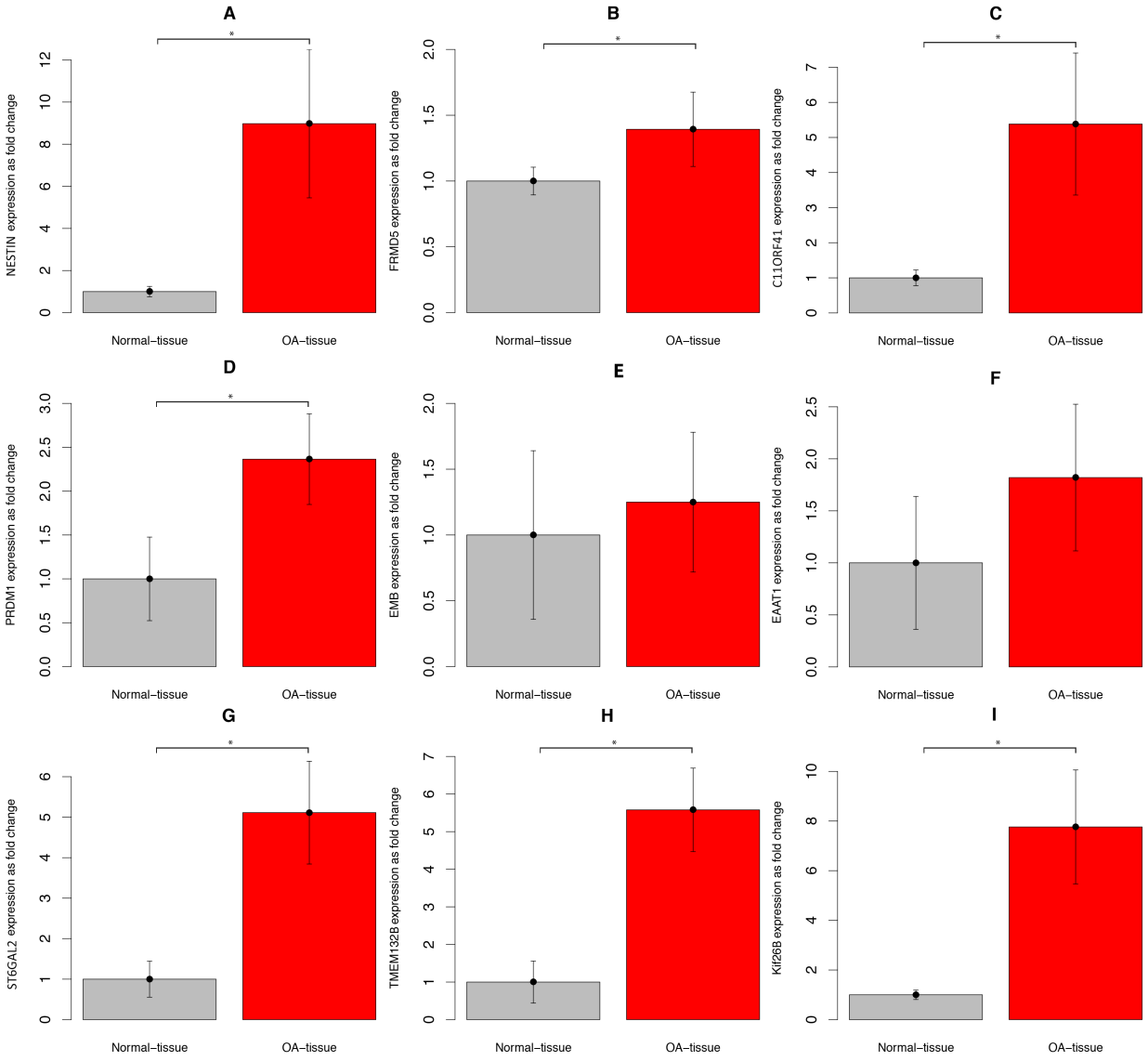


Figure 5.1– Gene expression of cartilage stem cell specific genes in normal and osteoarthritic tissue.

Data show an up-regulation in expression in stem cell specific genes in osteoarthritic cartilage compared to healthy cartilage. The increase observed in *EMBIGIN* and *EAAT1* expression was not found to have statistical significance (p.0.05). Gene expression of *NESTIN*, *FRMD5*, *C11ORF41*, *PRDM1*, *ST6GAL2*, *TEME132B* and *KIF26B* were all found to be statistically significant ($p<0.05$) between normal and OA cartilage using Student's T-test. **A)** *NESTIN*, **B)** *FRMD5*, **C)** *C11ORF41*, **D)** *PRDM1*, **E)** *EMGIGIN*, **F)** *EAAT1*, **G)** *ST6GAL2*, **H)** *TMEM132B*, **I)** *KIF26B*.

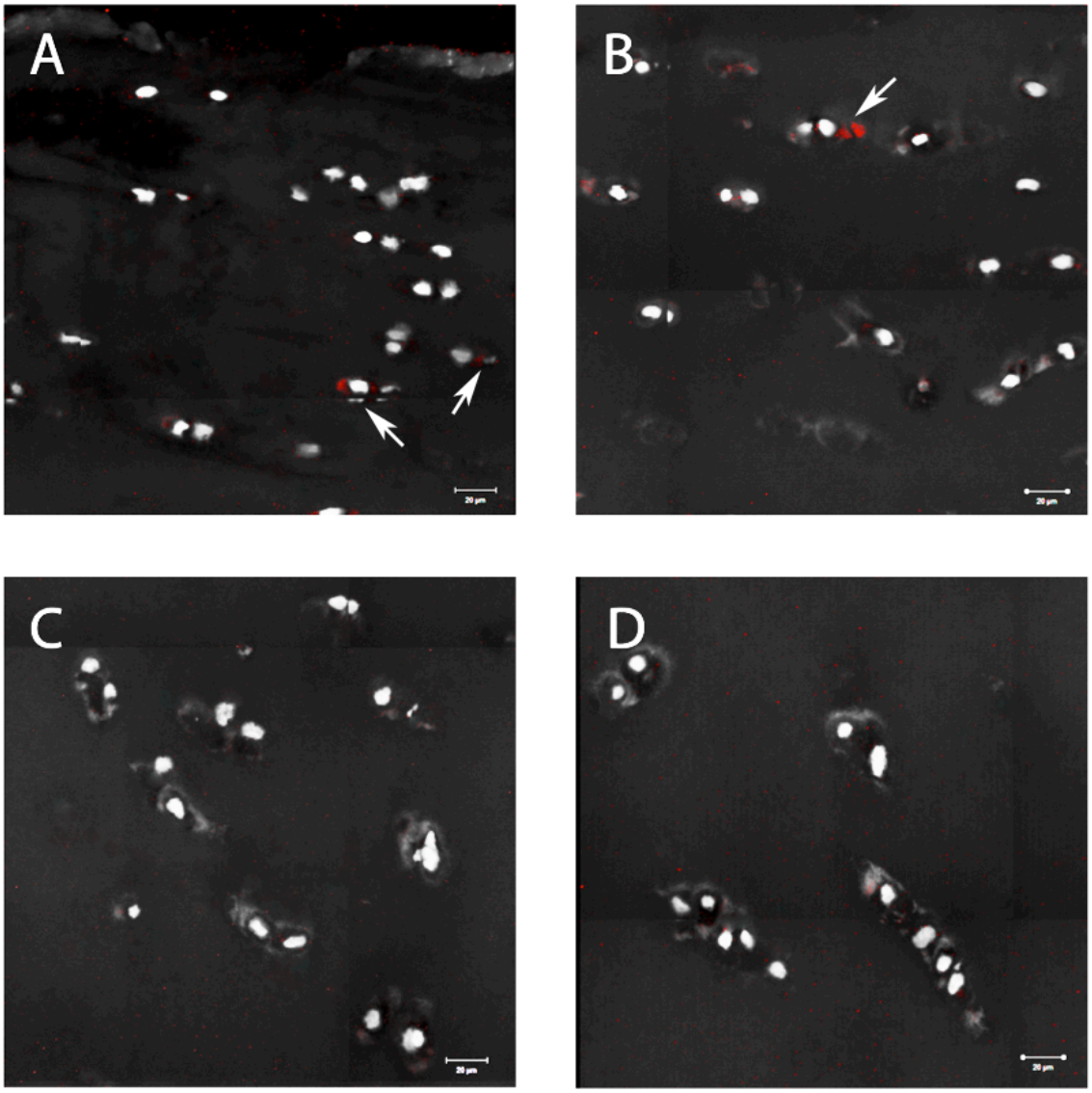


Figure 5.2–Immunofluorescence of NESTIN in normal articular cartilage

A) Superficial zone, **B)** Upper transitional zone, **C)** Lower transitional zone and **D)** Deep zone. NESTIN-positive cells were found in the superficial and upper transitional zones, positive cells are labelled in red and representative cells marked with an arrow. Nuclei are stained with DAPI and shown in white.

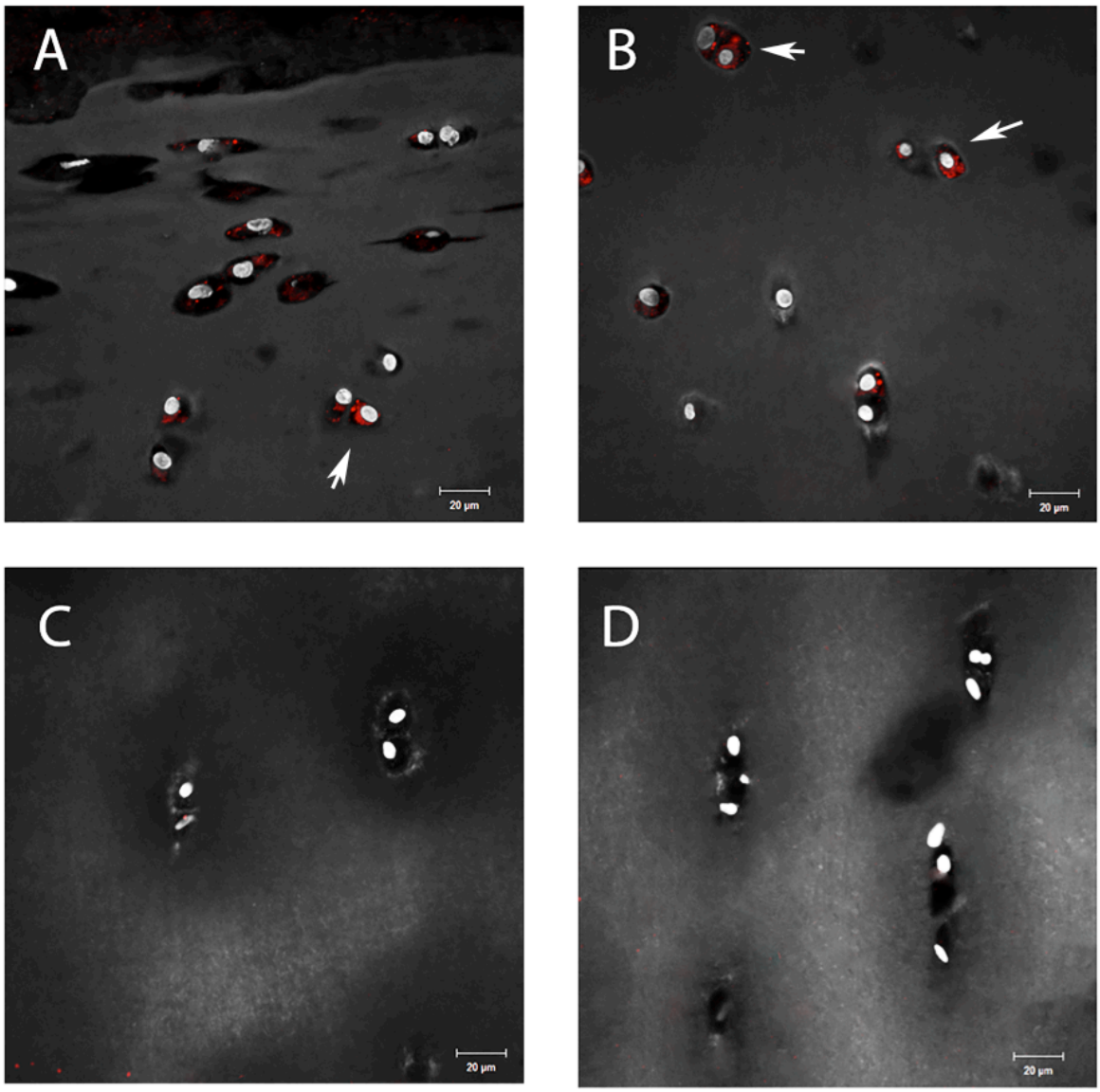


Figure 5.3–Immunofluorescence of NESTIN in OA articular cartilage

A) Superficial zone, **B)** Upper transitional zone, **C)** Lower transitional zone and **D)** Deep zone. NESTIN-positive cells were found in the superficial and upper transitional zones, positive cells are labelled in red and representative cells marked with an arrow. Nuclei are stained with DAPI and shown in white.

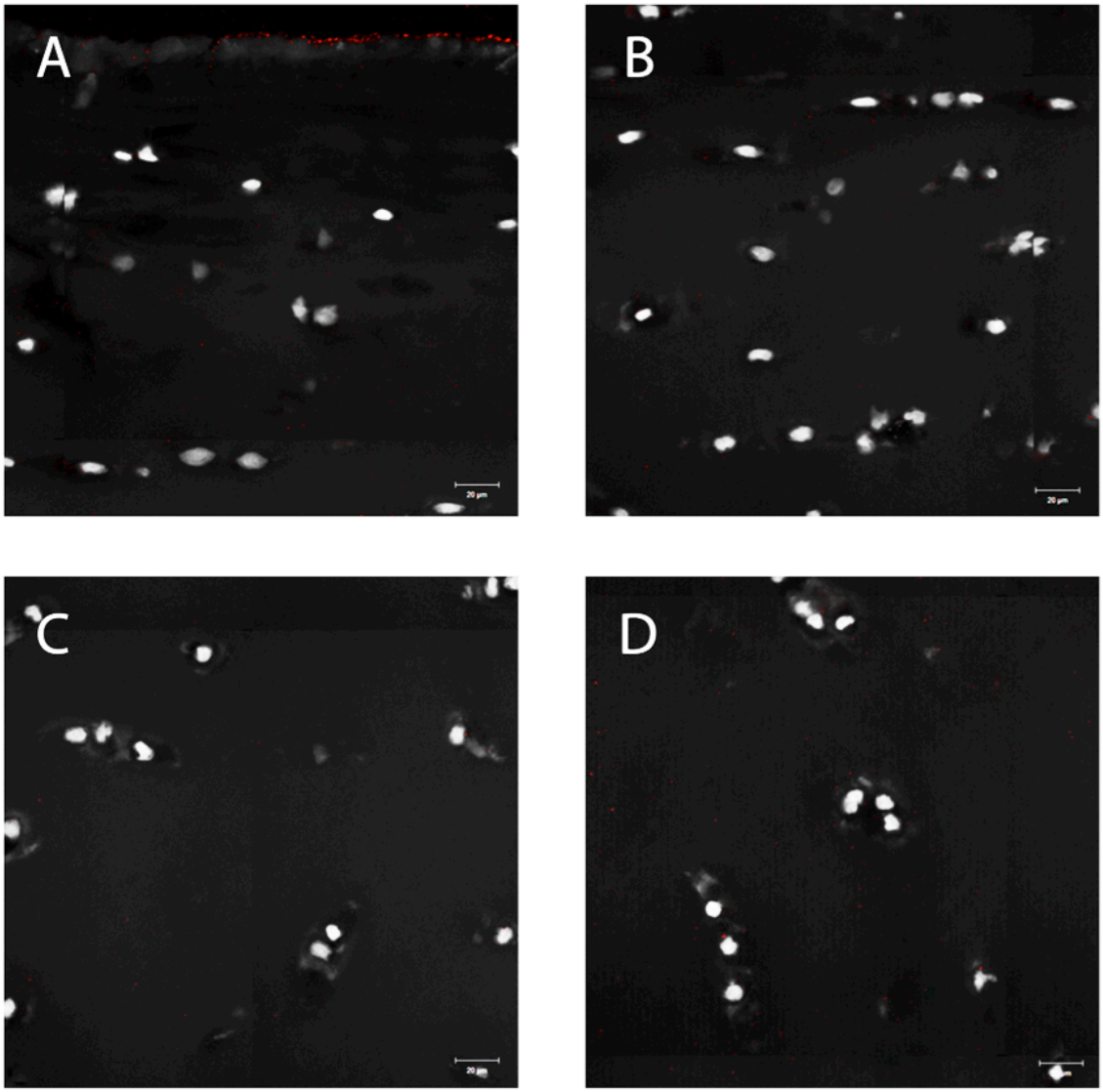


Figure 5.4–No primary control for NESTIN in normal articular cartilage

A) Superficial zone, **B)** Upper transitional zone, **C)** Lower transitional zone and **D)** Deep zone. No positive labelling is present**.** Nuclei are stained with DAPI and shown in white.

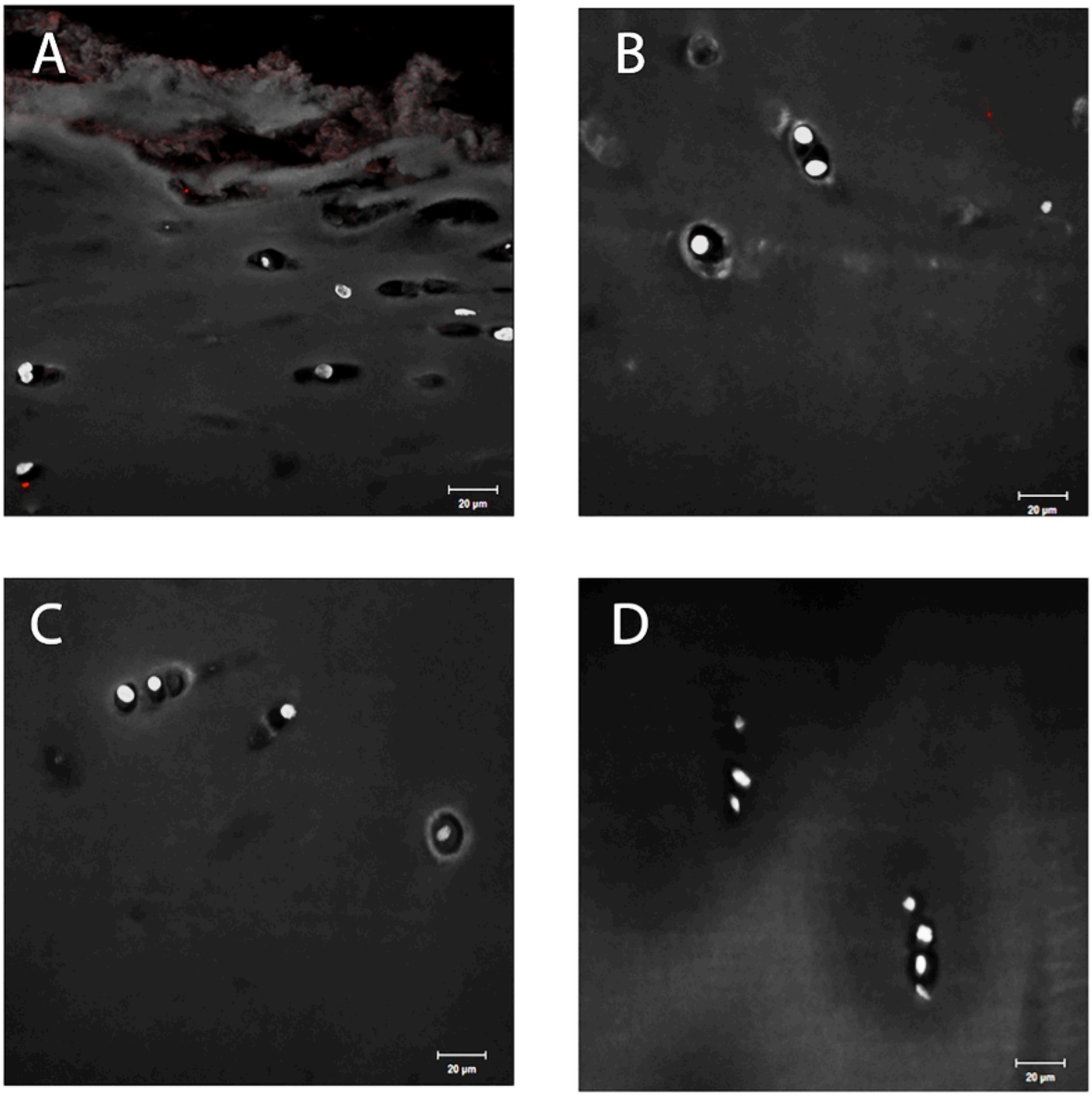


Figure 5.5–No primary control for NESTIN in OA articular cartilage

A) Superficial zone, **B)** Upper transitional zone, **C)** Lower transitional zone and **D)** Deep zone. No positive labelling is present**.** Nuclei are stained with DAPI and shown in white.

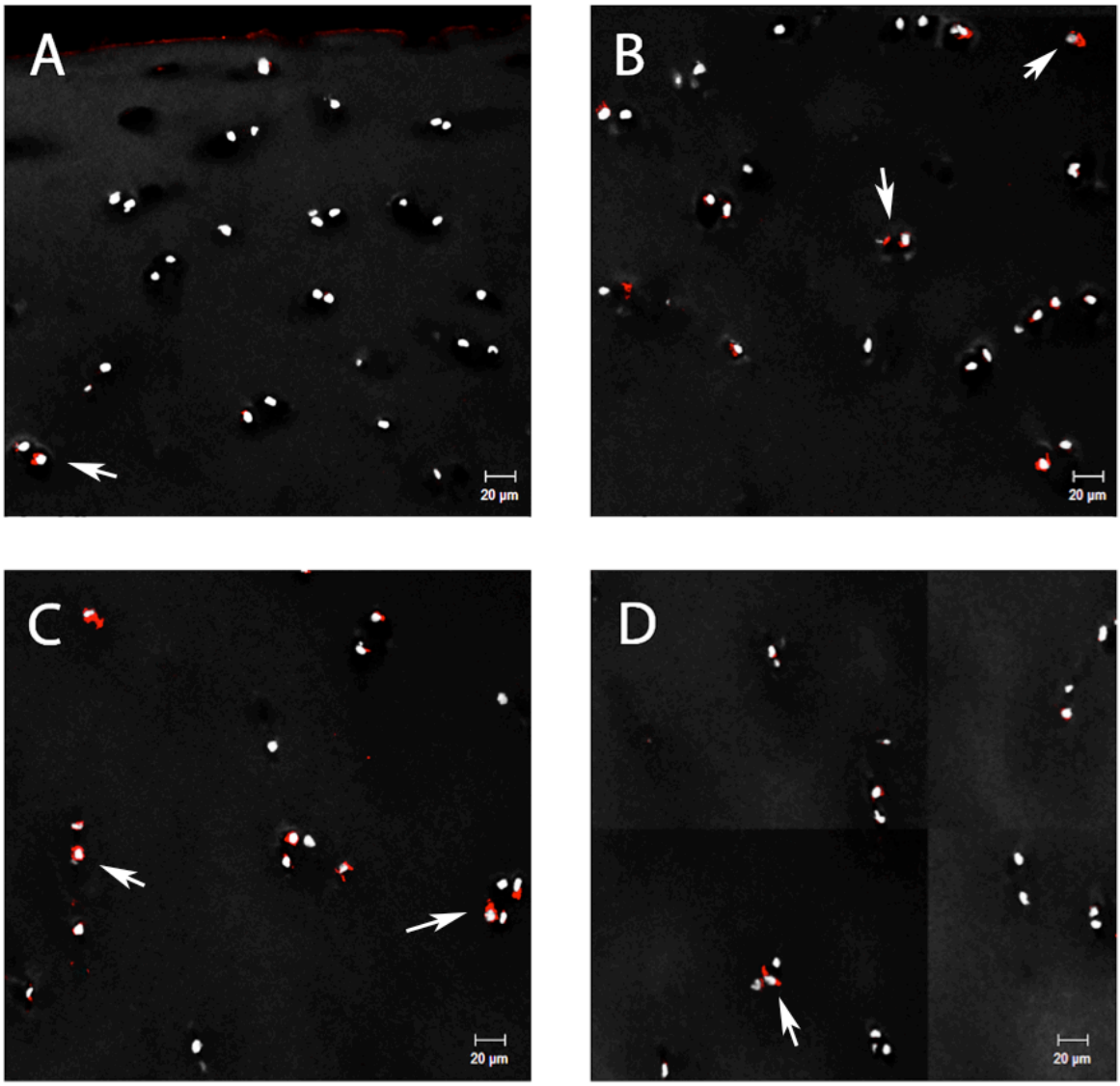


Figure 5.6–Immunofluorescence of FRMD5 in normal articular cartilage

A) Superficial zone, **B)** Upper transitional zone, **C)** Lower transitional zone and **D)** Deep zone. FRDM5-positive cells, shown in red, are predominantly localised to the transitional zone, representative positive cells are marked with an arrow. Nuclei are stained with DAPI and shown in white.

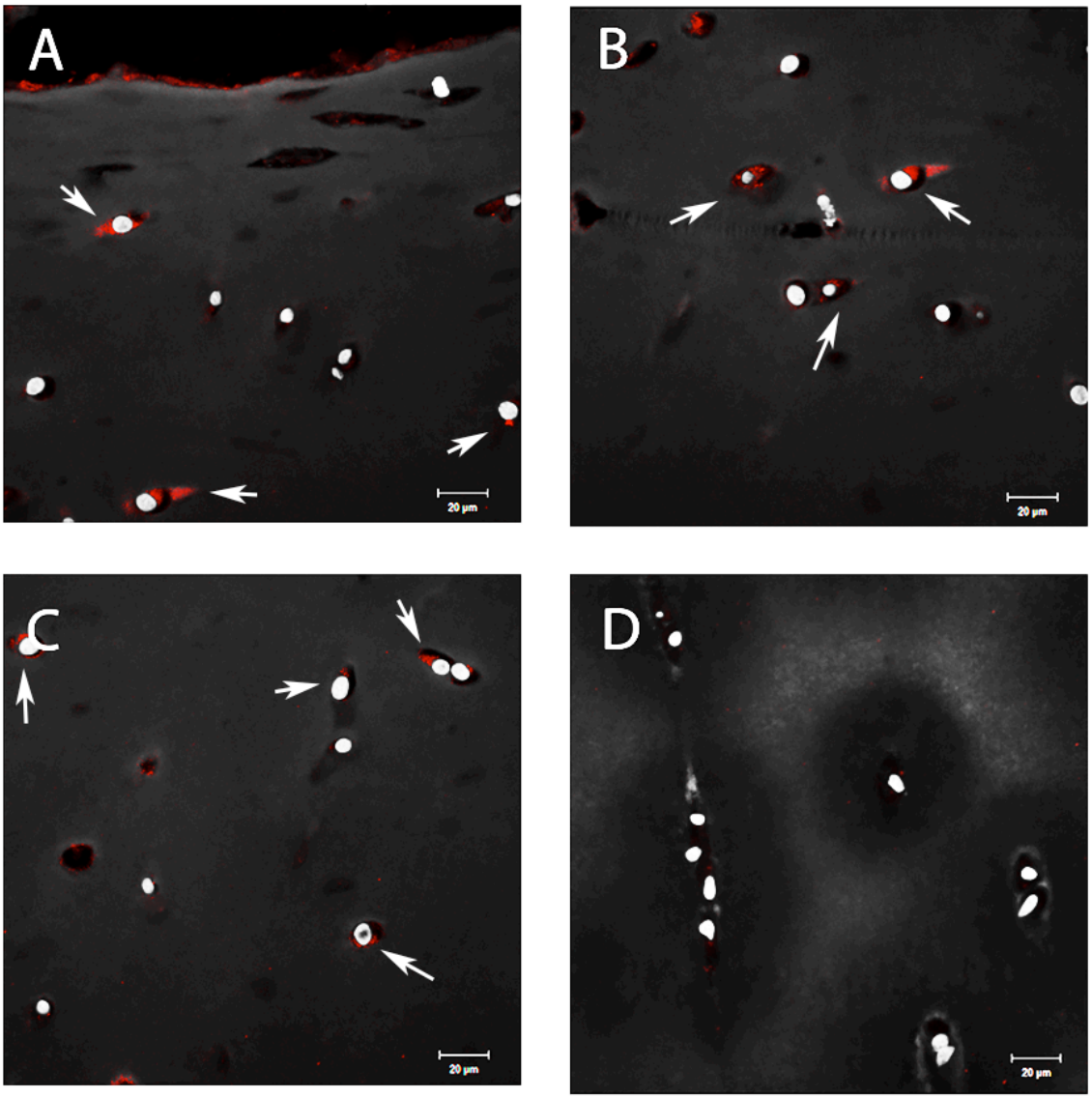


Figure 5.7–Immunofluorescence of FRMD5 in OA articular cartilage

A) Superficial zone, **B)** Upper transitional zone, **C)** Lower transitional zone and **D)** Deep zone. FRDM5-positive cells, shown in red, are predominantly localised to the transitional zone and superficial zones. Positive cells can now clearly be identified within the superficial zone unlike in normal cartilage. Representative positive cells are marked with an arrow. Nuclei are stained with DAPI and shown in white.

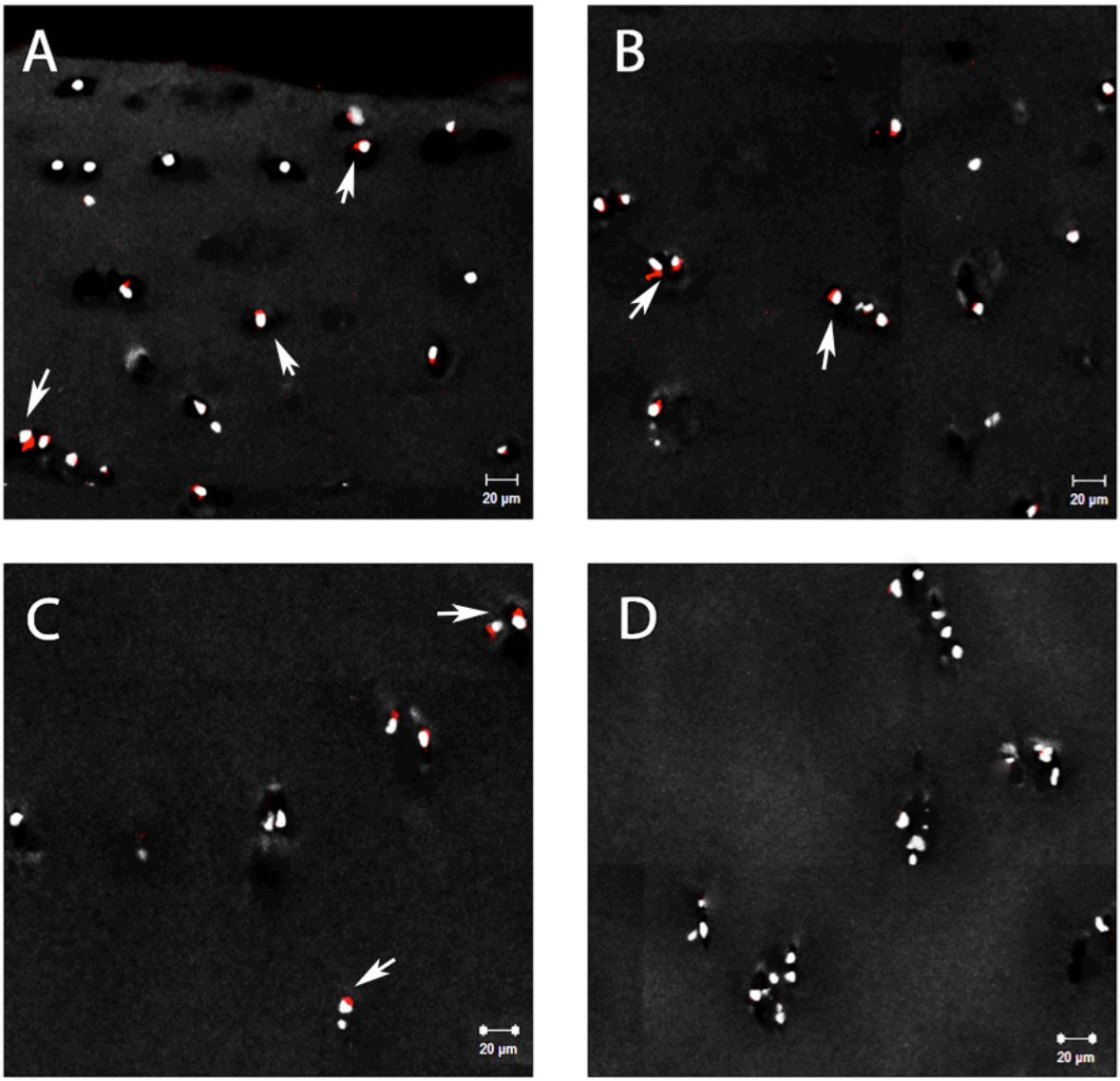


Figure 5.8–Immunofluorescence of C11ORF41 in normal articular cartilage

A) Superficial zone, **B)** Upper transitional zone, **C)** Lower transitional zone and **D)** Deep zone. C11ORF41-positive cells, shown in red, are predominantly localised within the superficial zone, and the transitional zone. Representative positive cells are marked with an arrow. Nuclei are stained with DAPI and shown in white.

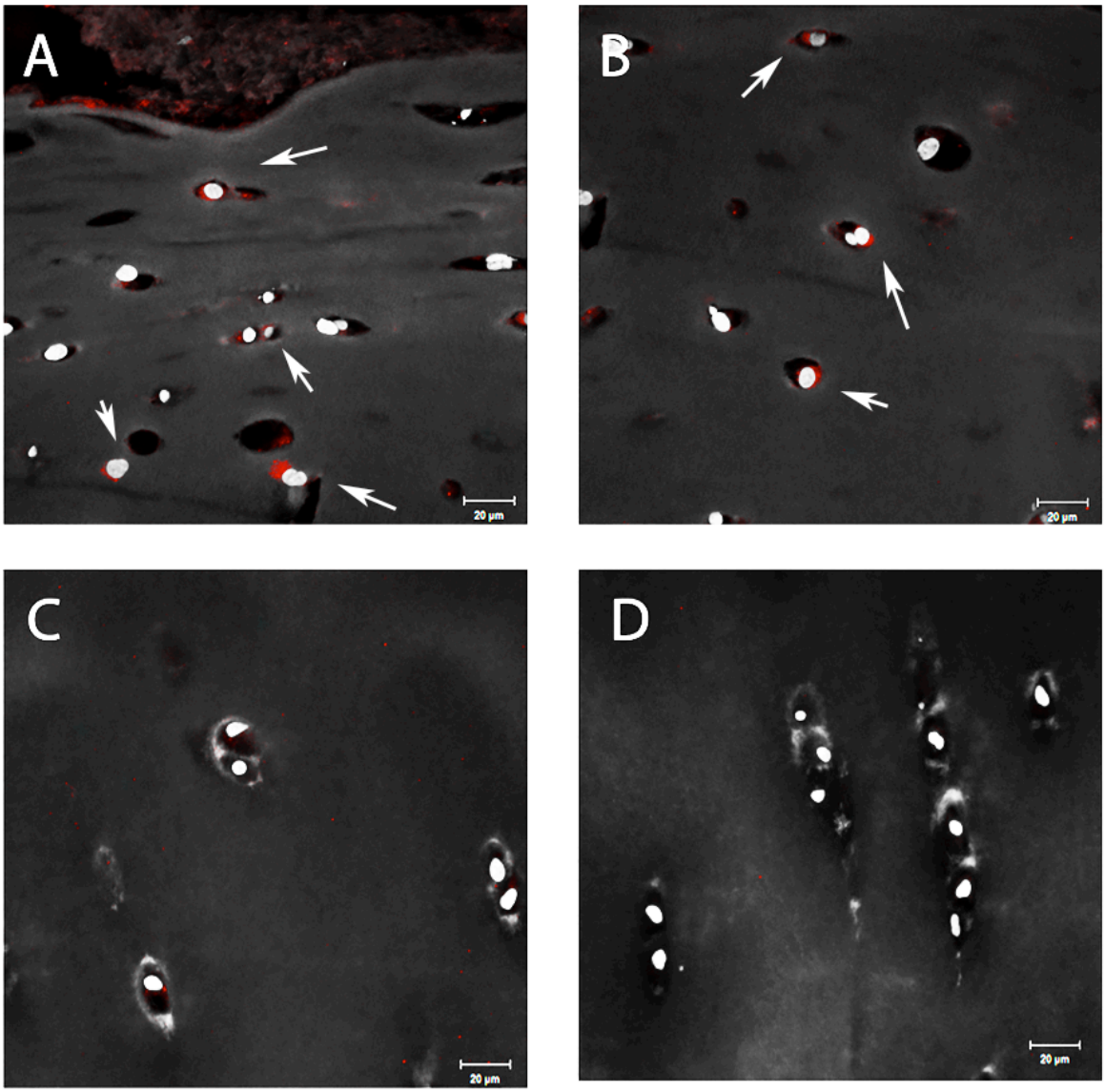


Figure 5.9–Immunofluorescence of C11ORF41 in OA articular cartilage

A) Superficial zone, **B)** Upper transitional zone, **C)** Lower transitional zone and **D)** Deep zone. C11ORF41-positive cells, shown in red, are exclusively localised within the superficial zone, and the upper transitional zone. No labelling is seen in the lower transitional zone unlike normal cartilage. Representative positive cells are marked with an arrow. Nuclei are stained with DAPI and shown in white.

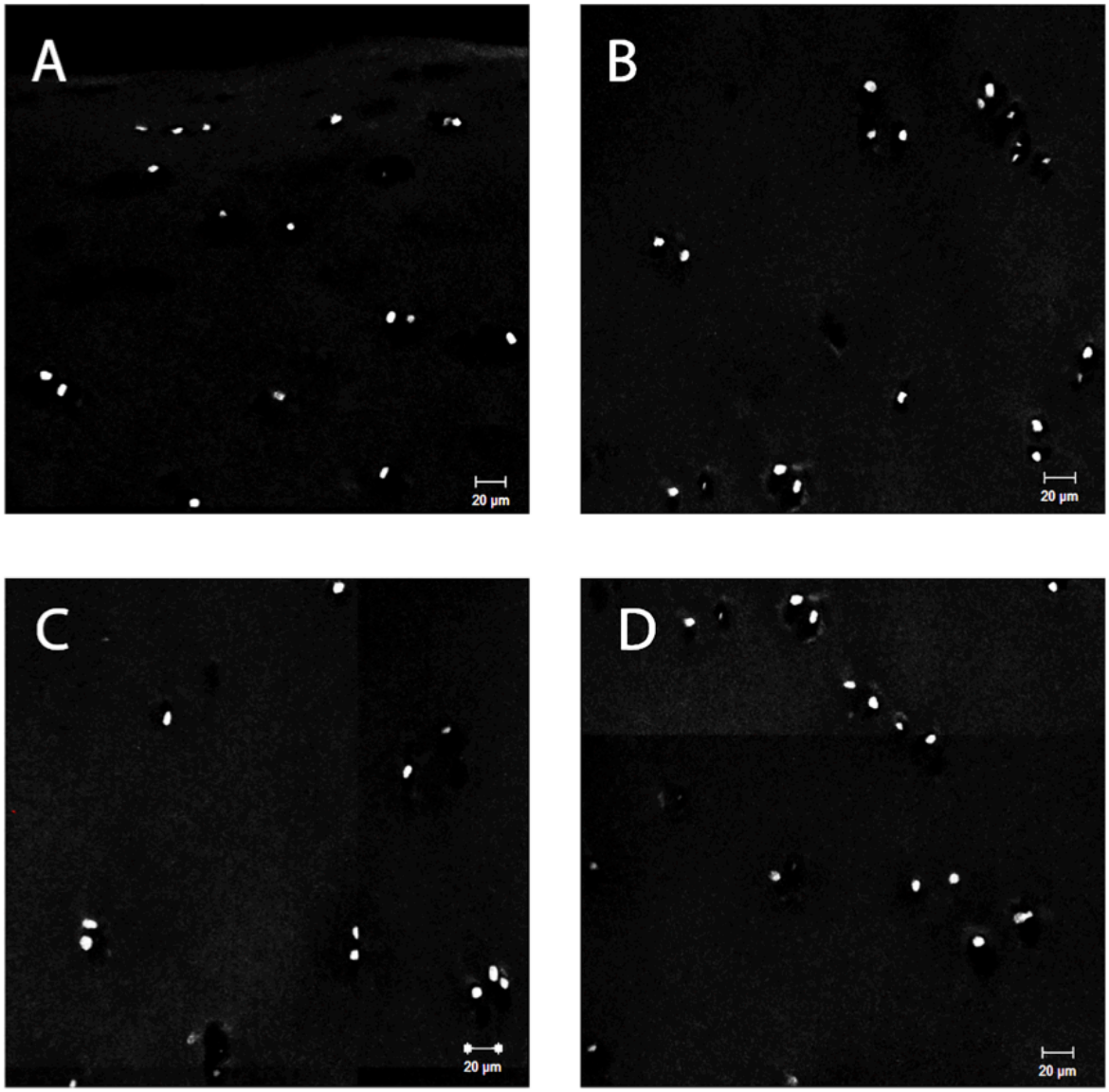


Figure 5.10– No primary antibody control for FRMD5 and C11ORF41 in normal articular cartilage

A) Superficial zone, **B)** Upper transitional zone, **C)** Lower transitional zone and **D)** Deep zone. No positive staining can be seen. Nuclei are stained with DAPI and shown in white.

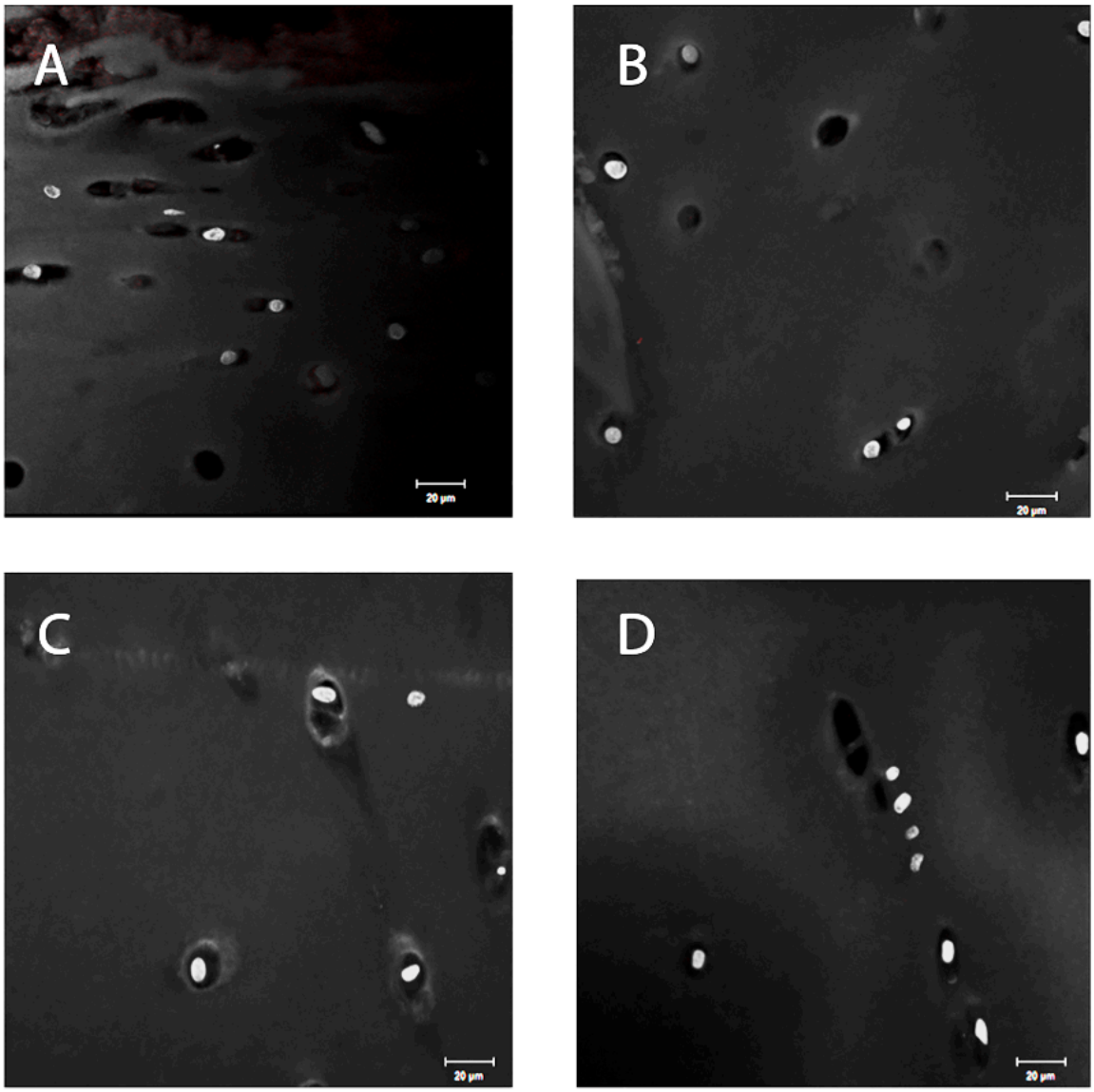


Figure 5.11– No primary antibody control for FRMD5 and C11ORF41 in OA articular cartilage

A) Superficial zone, **B)** Upper transitional zone, **C)** Lower transitional zone and **D)** Deep zone. No positive staining can be seen. Nuclei are stained with DAPI and shown in white.

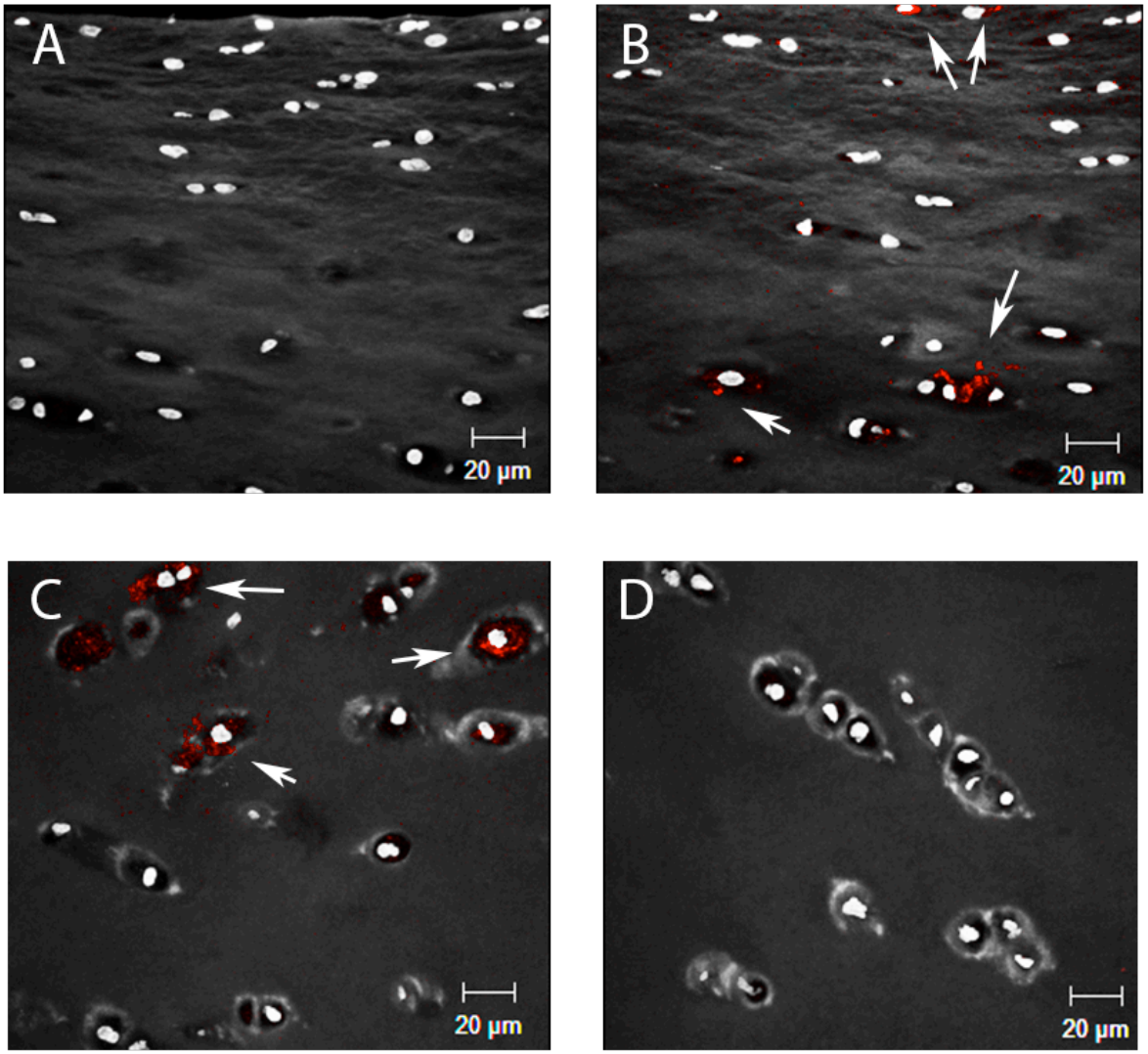


Figure 5.12– Immunofluorescence of EMBIGIN in normal articular cartilage

A) Superficial zone, **B)** Upper transitional zone, **C.)**Lower transitional zone and **D)** Deep zone. Positively stained cells, shown in red, are localised to the transitional zones. No staining is seen in the superficial zone. Nuclei are stained with DAPI and shown in white.

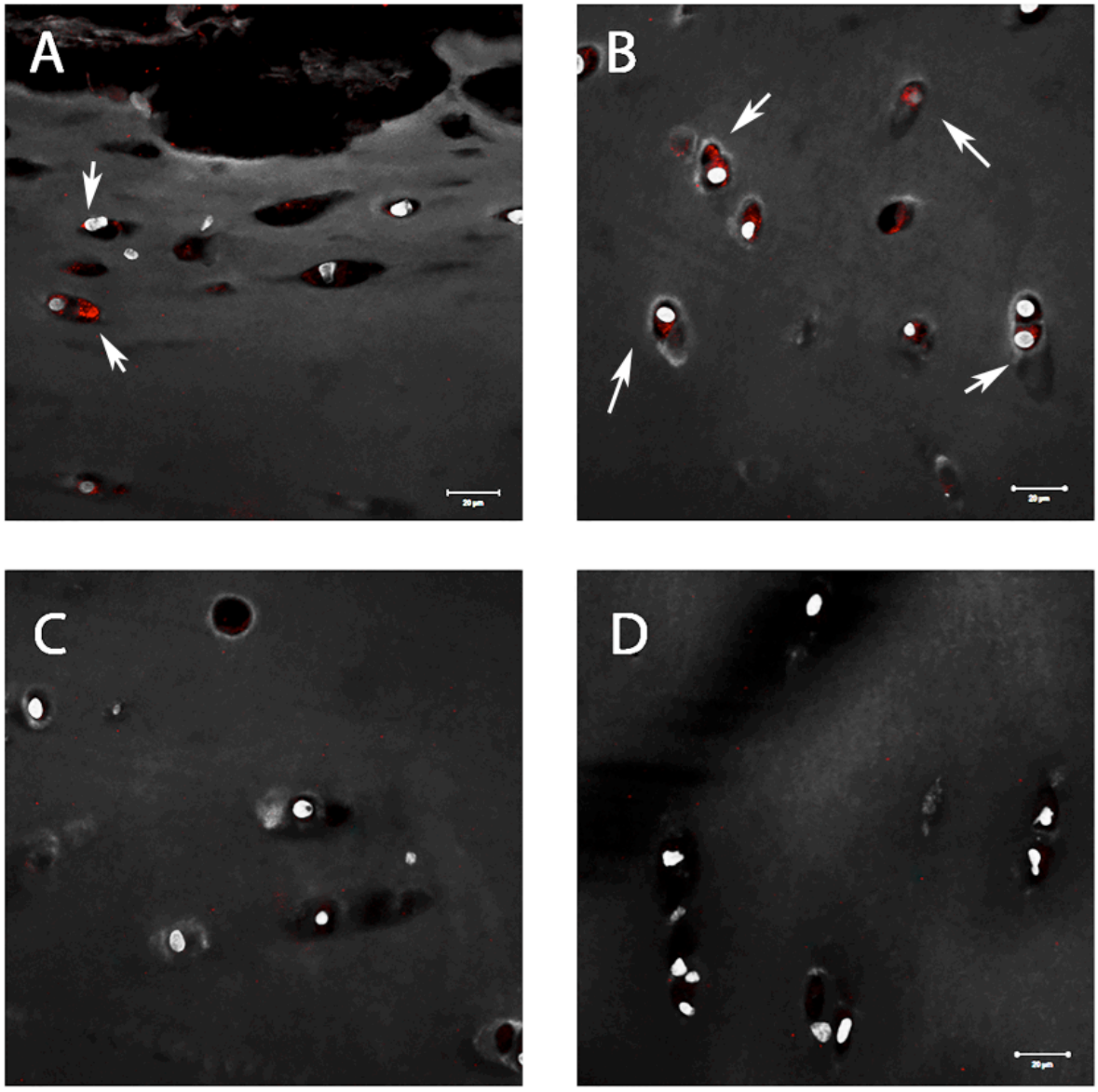


Figure 5.13– Immunofluorescence of EMBIGIN in OA articular cartilage

A) Superficial zone, **B)** Upper transitional zone, **C)** Lower transitional zone and **D)** Deep zone. EMBIGIN-positive cells, shown in red, are exclusively localised within the superficial zone, and the upper transitional zone. No labelling is seen in the lower transitional zone unlike normal cartilage. Representative positive cells are marked with an arrow. Nuclei are stained with DAPI shown in white.

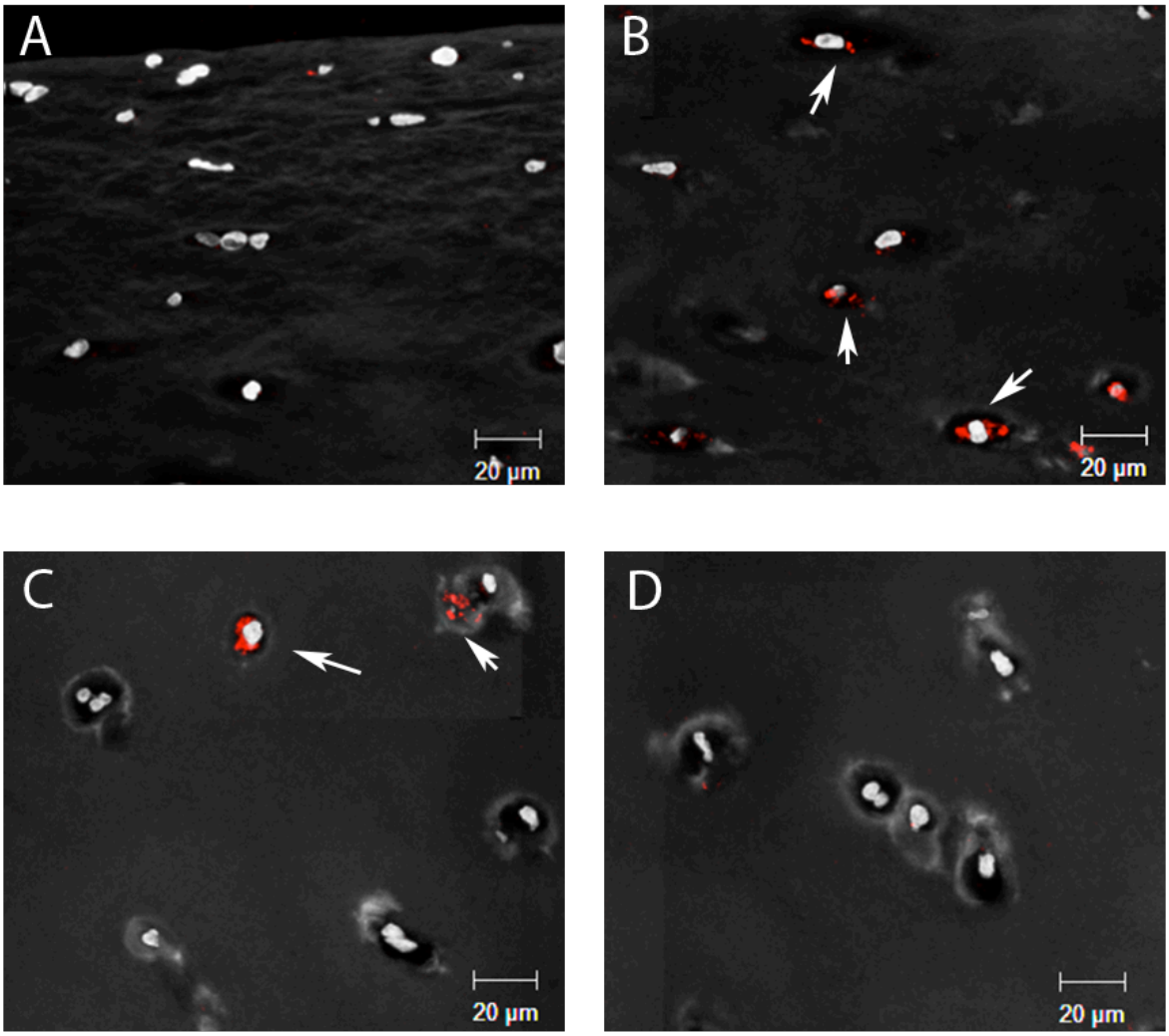


Figure 5.14– Immunofluorescence of EAAT1 in normal articular cartilage

A) Superficial zone, **B)** Upper transitional zone, **C)** Lower transitional zone and **D)** Deep zone. EAAT1-positive cells, shown in red, are exclusively localised within the transitional zones. No labelling is seen in the surface zone unlike OA cartilage. Representative positive cells are marked with an arrow. Nuclei stained with DAPI.

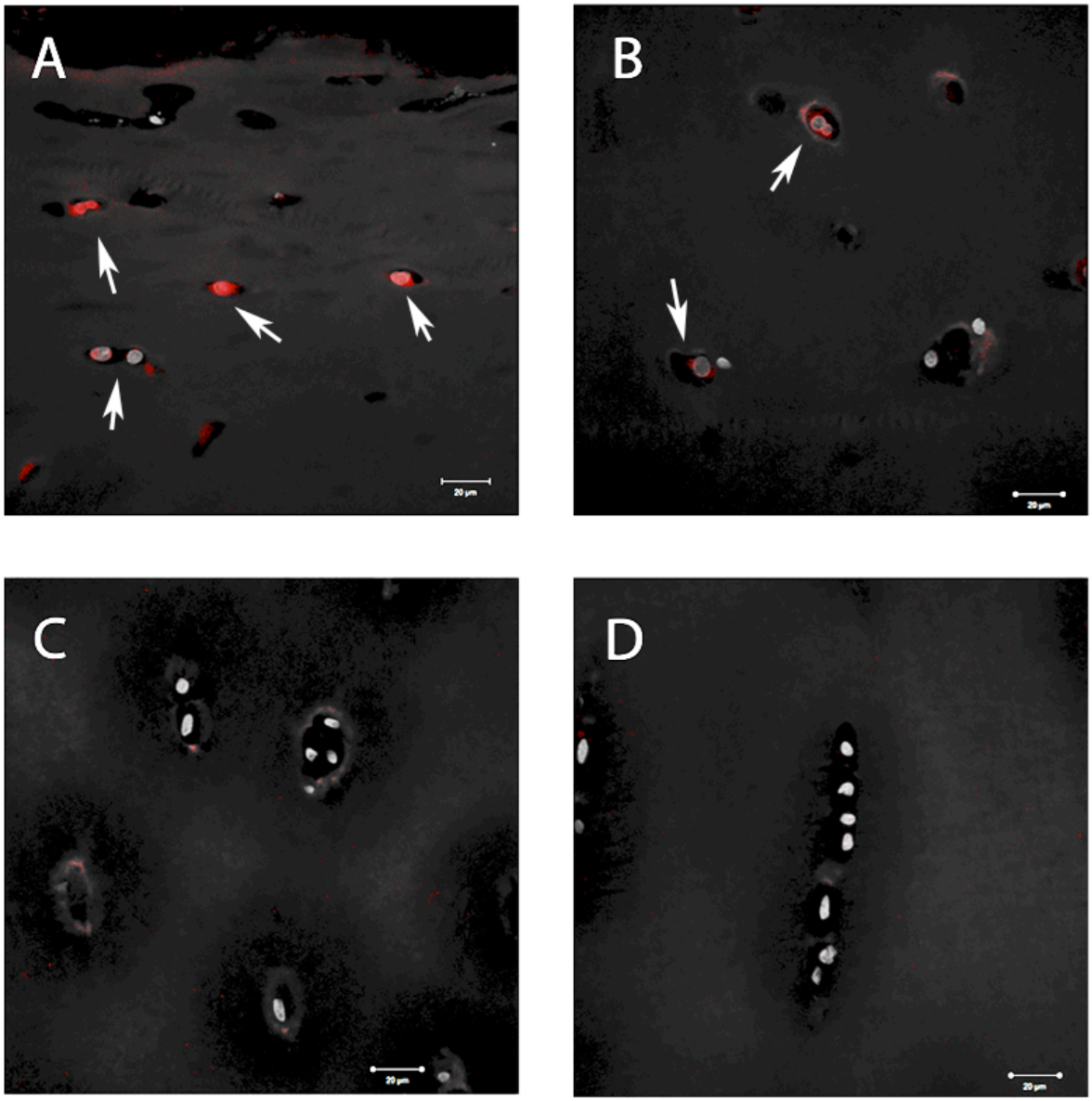


Figure 5.15– Immunofluorescence of EAAT1 in OA articular cartilage

A) Superficial zone, **B)** Upper transitional zone, **C)** Lower transitional zone and **D)** Deep zone. EAAT1-positive cells, shown in red, are exclusively localised within the superficial zone, and the upper transitional zone. No labelling is seen in the lower transitional zone unlike normal cartilage. Representative positive cells are marked with an arrow. Nuclei are stained with DAPI and shown in white.

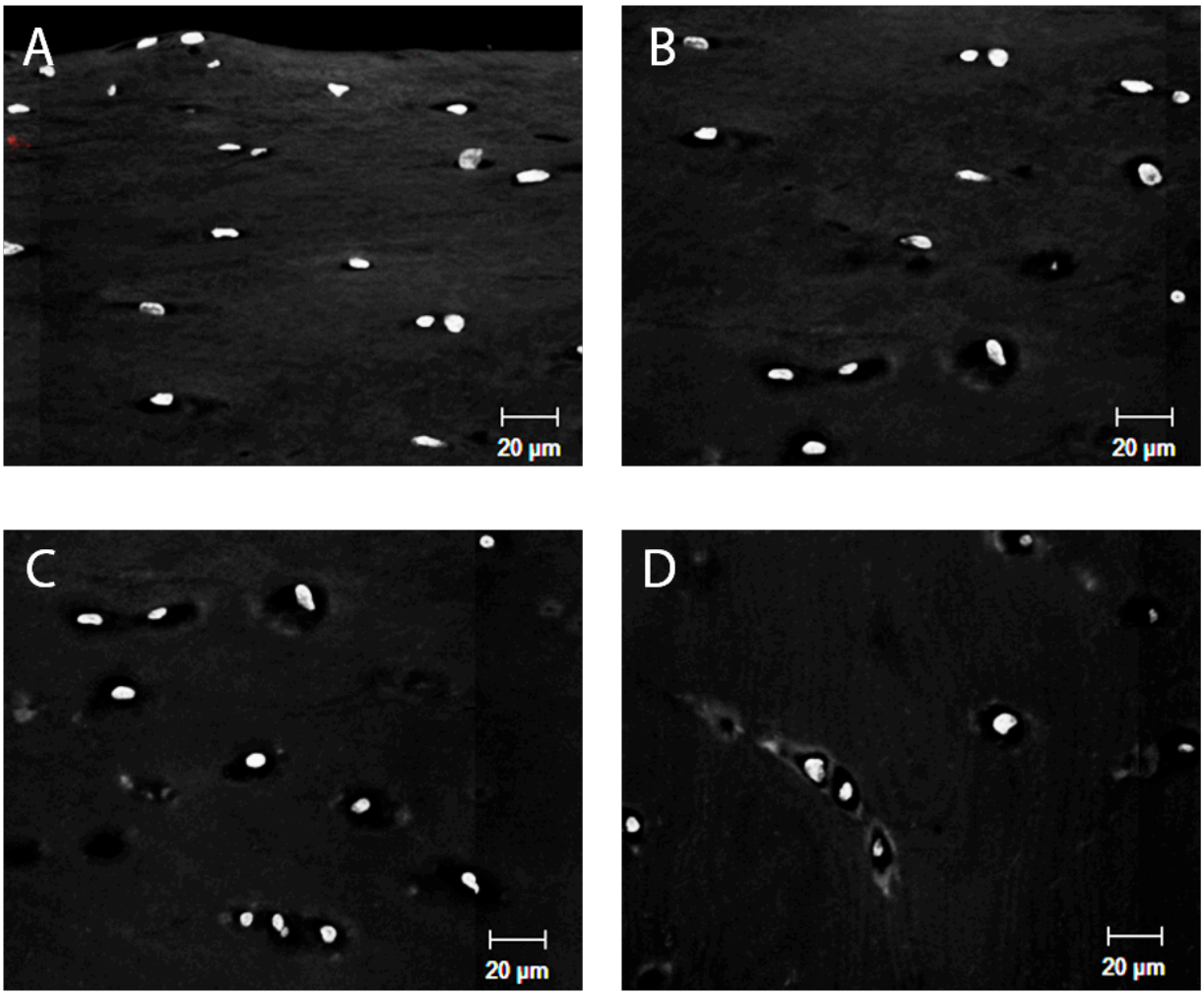


Figure 5.16– No primary control from EMBIGIN and EAAT1 in normal articular cartilage

A) Superficial zone, **B)** Upper transitional zone, **C)** Lower transitional zone and **D)** Deep zone. No positive labelling can be seen. Nuclei are stained with DAPI and shown in white.

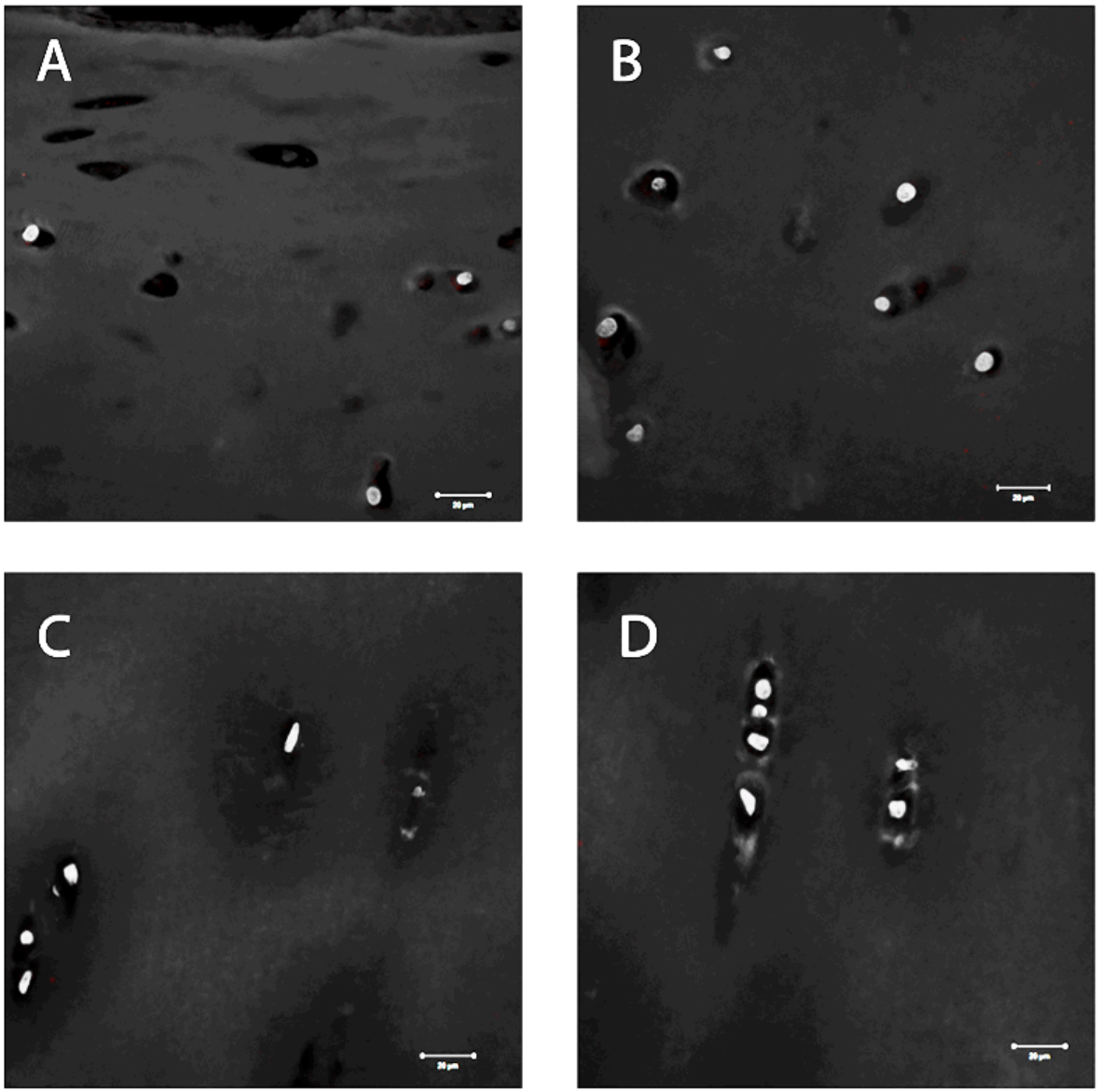


Figure 5.17– No primary control from EMBIGIN and EAAT1 in OA articular cartilage

A) Superficial zone, **B)** Upper transitional zone, **C)** Lower transitional zone and **D)** Deep zone. No positive labelling can be seen. Nuclei are stained with DAPI and shown in white.

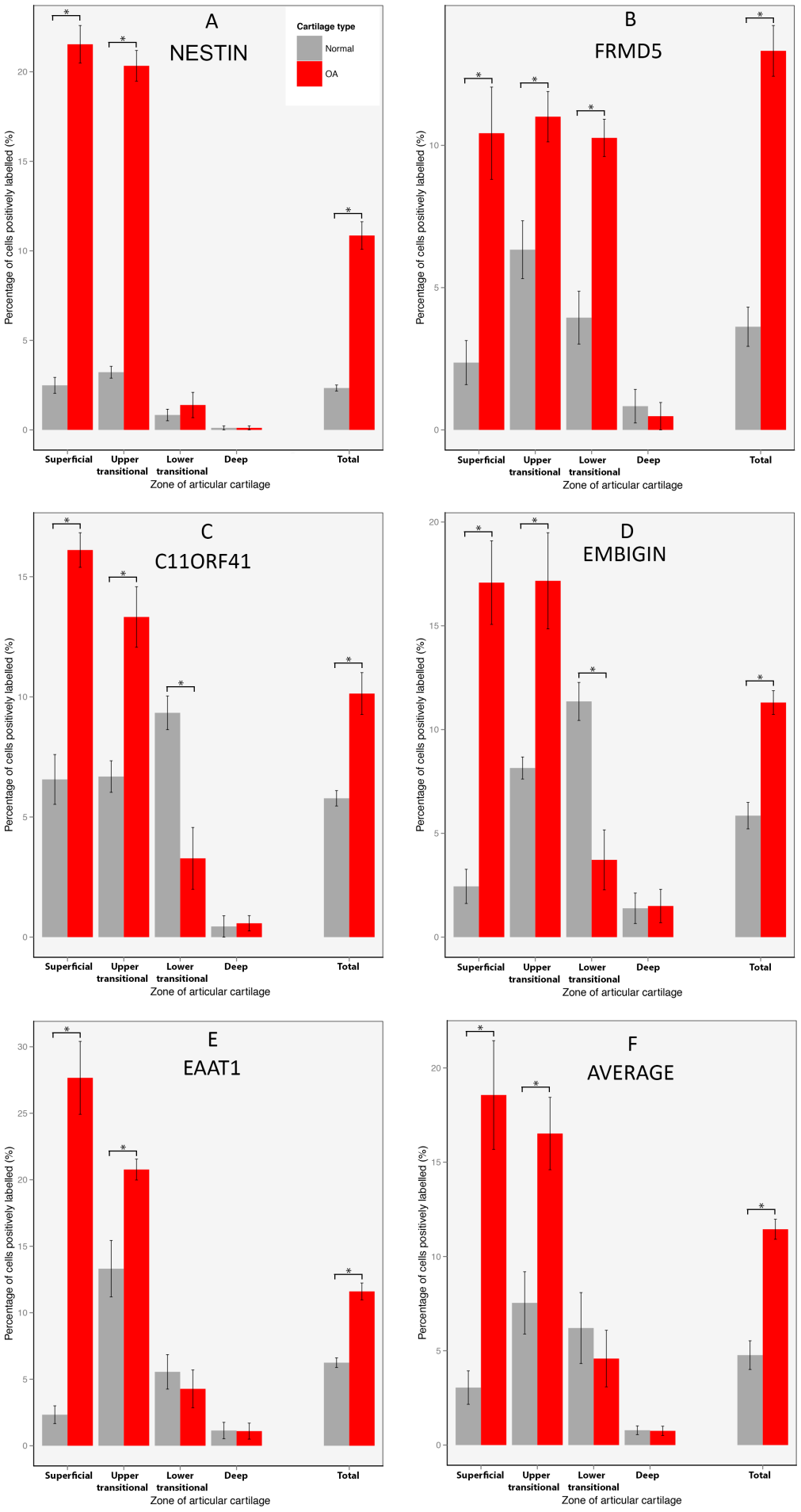

A
NESTIN
Cartilage type
Normal
OA
B
FRMD5
C
C11ORF41
D
EMBIGIN
E
EAAT1
F
AVERAGE
Percentage of cells positively labelled (%)
Superficial
Upper transitional
Lower transitional
Deep
Total
Zone of articular cartilage

Figure 5.18– Percentage positively labelled cells within each zone of normal and OA articular cartilage.

A) Percentage of cells labelling for NESTIN *per* zone of normal an OA articular cartilage. **B)** Percentage of cells labelling for FRMD5 *per* zone of normal an OA articular cartilage. **C)** Percentage of cells labelling for C11ORF41 *per* zone of normal an OA articular cartilage. **D)** Percentage of cells labelling for EMBIGIN *per* zone of normal an OA articular cartilage. **E)** Percentage of cells labelling for EAAT1 *per* zone of normal an OA articular cartilage. **F)** Average percentage of cells labelling for any of the stem cell markers *per* zone of normal an OA articular cartilage.

With all stem cell markers, an overall increase in the number of cells labelling was increased in osteoarthritis. There is a large up-regulation of stem cell marker protein labelling within the superficial and upper transitional zones of articular cartilage in OA. This increase is accompanied by a reduction in labelling within the lower transitional zone, suggesting there is a migration to the sight of injury. The total number of positive cells was shown to increase overall in osteoarthritis with the mean-fold increase of 2.4. Statistical significance is denoted by (*) ($p<0.05$, Anova with Tukey's HSD pairwise comparisons).

5.4 Discussion

In this study, novel stem cell markers were localised to either the superficial and/or the transitional zones of articular cartilage. In general, the abundance of positively labelled cells was found to increase in osteoarthritic cartilage and more positive cells were localised within the superficial zone. In normal cartilage, NESTIN, FRMD5, EMBIGIN and EAAT1-positive cells were predominantly localised to the upper transitional zone. C11ORF41 was localised within both the superficial and upper transitional zones. In osteoarthritic cartilage, all stem cell markers were localised to the superficial and upper transitional zones and often accompanied with a decrease in labelling within the lower transitional zone. Gene expression for stem cell marker genes increased in OA, which is consistent with the increase in stem cells identified in Chapter 4 and by previous studies (Chang et al., 2011, Grogan et al., 2009, Pretzel et al., 2011).

Wax embedded sections preferentially preserved the tissue structure compared with frozen sections; this is comparable with previous findings (Chevrier et al., 2005). Alcohol fixation has been shown to have reduced immuno-reactivity compared to formalin fixation or frozen cartilage (Bos et al., 2000). In this study, we also observed a reduced labelling intensity using alcohol fixation, compared to the other preparation procedures. No reduction in labelling was observed between formalin-fixed wax embedded samples and frozen tissue. Human articular cartilage is prone to autofluorescence, this is exacerbated by paraformaldehyde fixation and wax embedding (Ahrens and Dudley, 2011, Bos et al., 2000, Pretzel et al., 2011). Ahrens and colleagues (2011) were able to reduce autofluorescence using the autofluorescence quencher sodium borohydride; in this study this was not required, as autofluorescence was not observed using far-red secondary antibodies. In order to improve labelling intensity, a combination of hyaluronidase, chondroitinase and antigen unmasking solutions were tested for formalin and alcohol fixed wax sections. Frozen sections were enzyme treated without antigen unmasking solution due to no fixation. No differences in localisation were seen after enzymatic treatments, therefore, the dense ECM was not preventing antibody penetration; however, enzyme digestion did increase labelling intensity. Formalin fixed wax embedded tissue showed the highest intensity of antibody labelling after enzymatic pre-

treatment and antibody unmasking. This combination was comparable to the optimum conditions previously described by Ahrens and Dudley (2011).

In normal articular cartilage, the number of cells positive for NESTIN was lower than the other stem cell markers. A dramatic increase in positively labelled cells predominantly within the superficial zone and upper transitional zone was observed in OA cartilage. NESTIN has widely been used as a stem cell marker in multiple tissues, but predominantly with neural stem cells. A recent study by Codega and colleagues (2014), showed that *in vivo* quiescent neural stem cells were negative for NESTIN expression; however, upon activation, there is an up-regulation of NESTIN and the cells become highly proliferative (Codega et al., 2014). It is possible that many ACSC in normal tissue are quiescent due to the post-mitotic nature of cartilage and do not express NESTIN until they are activated during a reparative response to OA or other damage. An increase or re-expression of NESTIN in response to injury is widely reported in the literature across multiple tissue types, whether this is due to activation of quiescent stem cells or de-differentiation of adult cells to a more immature phenotype is unknown (Holmin et al., 1997, Luna et al., 2010, Namiki and Tator, 1999). As previously mentioned, NESTIN is widely utilised as a marker of proliferating and migrating adult stem cells (Michalczyk and Ziman, 2005) and we have shown in Chapter 4 that *in vitro NESTIN*-positive ACSC have the highest proliferative capacity. The increase in NESTIN-positive cells in OA may not only be due to activation, but may also be an increase in ACSC number after proliferative attempts to repair the tissue.

FRMD5, EAAT1 and EMBIGIN-positive cells had similar tissue localisation and abundance. Cells were primarily in the transitional zone in normal cartilage but positive cells in OA tissue were located in the superficial zone and upper transitional zone with a decrease in the lower transitional zone. The shift in localisation suggests a migratory response of ACSC to the sight of injury. Work by Koelling et al., (2009) supports the hypothesis that ACSC are migrating to the surface in OA tissue; this study showed a population of progenitor cells from OA cartilage, when placed on an OA joint *ex vivo,* migrate to the sight of injury and proliferate in an attempt to repopulate the cartilage; (Koelling et al., 2009). The overall increase in cells labelling for FRMD5, EMBIGIN and EAAT1 cells in OA

cartilage shows there must be both a proliferative and a possible migratory stem cell response. C11ORF41-positive cells were distributed evenly throughout the superficial zone and transitional zone of normal cartilage and were more abundant than positive cells for the other markers. Like the other stem cell markers, the C11ORF41-positive population increased in OA especially within the superficial zone, while decreasing in the lower radial zone. It is possible that NESTIN, EMBIGIN, EAAT1 and FRMD5 are a sub-population within the overall C11ORF41-positive fraction. It was not possible to identify whether this was the case as many antibodies used in this study were raised in the same species.

Previous studies have localised stem/progenitor cells in articular cartilage to the superficial zone and upper transitional zone in both normal and OA cartilage (Dowthwaite et al., 2004, Grogan et al., 2009, Koelling et al., 2009, Pretzel et al., 2011). In this study, we have found that the majority of ACSC, as distinguished by antibody labelling of novel markers, are within healthy tissue are located in the transitional zone and not within the superficial zone. ACSC being located below the surface zone would ensure that they are away from the area of continual loading and potential damage, guaranteeing the viability of the stem cell population. Protein labelling experiments suggest that in OA patients, ACSCs migrate from the lower transition zone in response to damage and populate the superficial zone. The overall increase in ACSCs in OA cartilage suggests that OA pathology invokes a proliferative and potential migratory response in these cells.

The average number of positive cells labelling across all stem cell markers *in situ* in normal articular cartilage was 4.8 ± 1.7%, which increased to 11.4 ± 1.2% in OA tissue. This increase is of similar magnitude to the increase in stem cell number identified by colony forming efficiency in Chapter 4. The percentage of stem cells observed (normal = 4.8%, OA = 11.4%) was lower than described by Pretzel et al., (2011), whom, using of $CD105^{+}/CD166^{+}$ identified 22.1 ± 1.7% of normal cartilage and 23.6 ± 1.4% OA cartilage cells were stem cells. Grogan et al., (2009) also reported far higher stem cell numbers. The stem cell numbers identified through the use of these novel markers are more reasonable than previous studies and comparable to the stem cell number identified through flow-cytometry by Alsalameh et al., (2004).

CHAPTER 6:

FLUORESCENCE ACTIVATED CELL SORTING OF EMBIGIN AND FERM DOMAIN CONTAINING 5-positive CELLS – ISOLATION OF A SPECIFIC CHONDROCYTE SUB-POPULATION WITH STEM CELL PROPERTIES

6.1 Introduction

In the previous Chapters, we have identified novel markers of ACSCs *in vitro* and localised the marker labelling cells predominantly within the upper transitional zone and the superficial zone of articular cartilage. Both *in vitro* colony forming efficiency values and, immunohistochemical analysis *in situ* have shown an increase in ACSC in osteoarthritic cartilage. Following on from this work, we aimed to further quantify the expression of our stem cell markers in normal and osteoarthritic cartilage using flow-cytometry and to isolate cells based on protein labelling using fluorescence activated cell sorting (FACS).

Cell surface proteins are ideal for use as biomarkers because they perform numerous essential biological functions, including mediation of cell-cell communication, cell attachment and responses to external signals. Antibodies that recognize cell surface antigens are widely used as research tools, for diagnostics, therapeutics and live cell isolation (Gedye et al., 2014). Flow-cytometry is increasingly recognized as an invaluable technology in biomarker research. It can provide highly detailed information on any single cell in a heterogeneous population because multiple parameters can be investigated simultaneously (Barnard, 2012). Cells can be scanned at several thousand cells per-second allowing high throughput automated individual cell enumeration and characterisation (Collier, 2000).

Cytometry refers to the measurement of physical or chemical characteristics of cells or biological particles. The characteristics measured can be intrinsic, such as light scatter and electrical conductivity or extrinsic, primarily using fluorescence probes to DNA/RNA or protein (Fu, 2002). Flow-cytometry is the method of analysing these characteristics as cells or particles pass through an excitatory laser, one at a time, in a fluid stream. Lasers illuminate the cell and optical systems collect the light scattered or emitted by the sample. Light scattered in a forward direction, is collected by a lens known as the forward scatter detector and light deflected by organelles is detected perpendicular to the laser and is measured by the side scatter detector (Collier, 2000). Forward scattered light is indicative of cell size and can distinguish between viable cells and cellular debris. Side scattered light provides information on the cytoplasmic

complexity or granularity of a cell (Black et al., 2011). Fluorescence channels known as photomultiplier tubes detect emitted light, optical filters that only allow passage of specific bandwidths of light control the specificity of detection. The flow chamber consists of a central core containing the sample surrounded by an outer core of sheath fluid, which creates a laminar flow (Brown and Wittwer, 2000). The pressure of the sheath fluid against the cell maintains a stream of single cells at a constant flow velocity, which allows for single cell excitation by one or more lasers. If the cell that passes through the laser beam has been labelled with a fluorochrome, it emits fluorescence. Autofluorescence may also occur naturally and must be compensated for by using controls. Fluorochromes coupled to antibodies allow detection of both intracellular and extracellular molecules; however, for live cell analysis, extracellular antibodies are required. The fluorescence of a cell is proportional to the amount of the molecule to which the antibody has bound (Herzenberg et al., 2002).

Sorting devices break-up the jet of cells into charged droplets and deflect their pathway through a pair of high voltage deflection plates. During a sample run, as each cell passes through lasers, photodetectors collect the fluorescence and scattered light through the optics. These photodetectors convert light signals into electrical signals and the computer analyses and stores these data. The fluorescence activated cell sorter has a charging ring that is built into the flow chamber. A charge is placed on the cell droplet based on the immediately prior fluorescence intensity. The droplet is deflected in a desired direction when biased under a high-voltage from the deflection plates, collecting cells into test tubes of 2 or more population; this is called electrostatic deflection (Galbraith, 2010). A schematic image of a fluorescence activated cell sorting flow cytometer is shown in Figure 6.1.

The majority of studies investigating antigen expression of isolated or cultured chondrocytes and stem/progenitors use flow-cytometry; this method enables rapid analysis and quantification of a large number of cells. Previously, Alsalameh (2004), Grogan (2009), Chang (2011) and Pretzel (2011) used flow-cytometry to analyse the proportion of cells labelling for mesenchymal stem cell markers within articular cartilage and to examine cultured populations isolated through immuno-magnetic separation of specific MSC surface antigen expressing cells. Fickert (2004) used FACS to directly isolate cell populations expressing

mesenchymal stem cell surface antigens from articular cartilage. The purpose of this Chapter is to quantify the labelling of EMBIGIN and FRMD5 in normal and osteoarthritic cartilage and to isolate two cell populations, cells that are positive for both proteins and cells that are negative for both proteins. These cell populations will be analysed to examine whether FRMD5 and EMBIGIN expression does truly represent a stem cell population within articular cartilage.

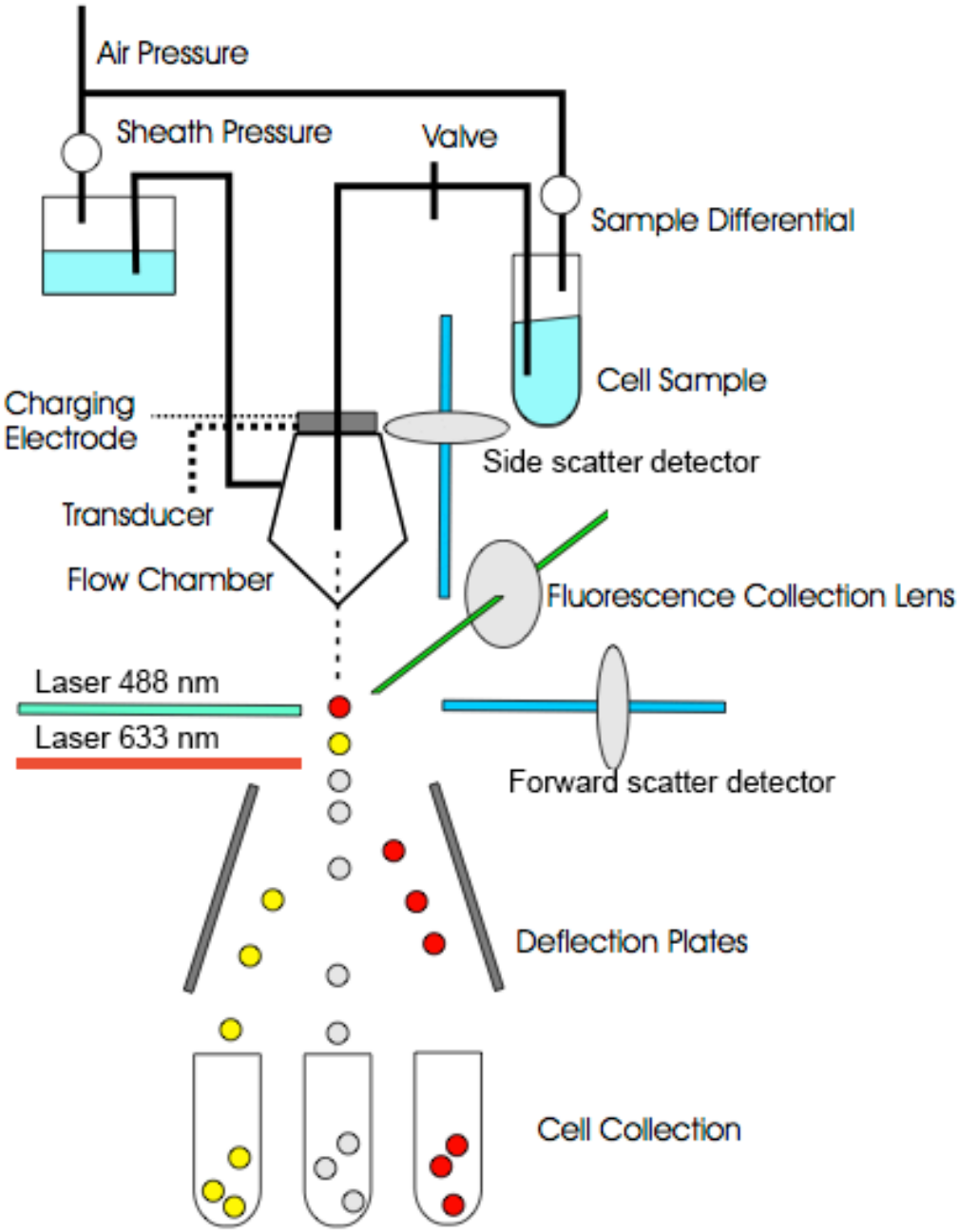


Figure 6. 1 – A schematic of conventional fluorescence activated cell-sorting (FACS)

Cells are hydrodynamically focussed within the flow chamber to produce a single cell stream. Excitation by one or more lasers provides fluorescence intensity data, side scatter (cytoplasmic complexity) and forward scatter (size). Adapted from (Fu, 2002)

6.2 Methodology

Material	Catalogue number	Supplier
Antibody concentration kit	Ab102778	Abcam, UK
Antibody conjugation kit – Cy5	Ab188288	Abcam, UK
Antibody conjugation kit – APC/Cy7	Ab102859	Abcam, UK
40µm mesh cell strainer	352340	BD FalconTM, UK
12mm FACS tubes	352002	BD FalconTM, UK
Dako pen	S2002	Dako, UK
Mouse immunoglobulins	X0931	Dako, UK
Dulbecco's modified eagles medium	41965-062	Gibco, UK
Trypsin-EDTA 0.05%	25300-062	Gibco, UK
Foetal calf serum	10106-169 1	Gibco, UK
L-glutamine 200mM	25030-081	Gibco, UK
Hepes buffer	15630-056	Gibco, UK
Insulin-transferrin-selenium (ITS)	41400-045	Gibco, UK
SafeView Nucleic Acid Stain	NBS-SV1	NBS Biologicals Ltd, UK
Low Molecular Weight DNA Ladder	N0468	New England Biolabs, UK
Steriflip® filter unit	SCGP00525	Millipore, UK
CellTrics 30 µm filters	04-004-2326	Partec, UK
Human FGF - basic	00 - 18B	Peprotech, UK
Human TGF - β2	100 – 35B	Peprotech, UK
Human TGF – β1	100 – 21	Peprotech, UK
GoTaq® G2 Hot start DNA Polymerase	M7405	Promega, USA
AMV Reverse Transcriptase, RNase H Minus	M5108	Promega, USA
Random primers	C1181	Promega, USA
Recombinant RNasin Ribonuclease Inhibitor	N2511	Promega, USA
Set of dATP, dCTP, dGTP, dTTP	U1240	Promega, USA
TBE Buffer	V4251	Promega, USA
Agarose	V3125	Promega, USA
GoTaq® qPCR Master Mix	A6002	Promega, USA
DPX mounting medium	RAYLLAMB/DPX	Raymond A Lamb Medical, UK
Goat immunoglobulin	AB-108-C	R&D systems, UK

Rabbit immunoglobulin	AB-105-C	R&D systems, UK
Pronase from Streptomyces griseus	11 459 643 001	Roche, UK
Phosphate buffered saline	P4417	Sigma Aldrich, UK
Toluidine blue	89640	Sigma Aldrich, UK
Tween-20	P1379	Sigma Aldrich, UK
Triton-X-100	T8787	Sigma Aldrich, UK
Collagenase from clostridium histolyticum	C0130	Sigma Aldrich, UK
L-Ascorbic acid 2-phosphate	A8960	Sigma Aldrich, UK
Dexamethasone	D8893	Sigma Aldrich, UK
Dimethyl sulfoxide	D5879	Sigma Aldrich, UK
Fibronectin from bovine plasma	F1141	Sigma Aldrich, UK
D-(+)-Glucose	G6152	Sigma Aldrich, UK
β-Glycerophosphate disodium salt hydrate	G9422	Sigma Aldrich, UK
Indomethacin	I7378	Sigma Aldrich, UK
Insulin solution, human	I9278	Sigma Aldrich, UK
3-Isobutyl-1-methylxanthine	I7018	Sigma Aldrich, UK
β -Mercaptoethanol	M3148	Sigma Aldrich, UK
Methanol	322415	Sigma Aldrich, UK
Oil-red-O	O1391	Sigma Aldrich, UK
10 % Formalin solution, neutral buffered	HT501128	Sigma Aldrich, UK
Ethanol	E/0650DF/17	Thermo Fisher Scientific, UK
Sodium hydroxide	S/4920/60	Thermo Fisher Scientific, UK
Polylysine adhesion glass slides	MNJ-800-010F	Thermo Fisher Scientific, UK
RNeasy Mini Kit	74104	Qiagen, UK
RNase-free DNase set	79254	Qiagen, UK
Antigen unmasking solutions	H-3300	Vector Laboratories, UK
Safranin O Gurr 'Certistain'	343122N	VWR, UK

Table 6.1 – Materials and suppliers

6.2.1 Cell isolation

Tissue was dissected from healthy (n = 4, mean age = 54; range 51-60) and osteoarthritic (n = 3 mean age = 65; range 60-73) donors and digested in sequential pronase and collagenase enzymes as described in Sections 2.1 and 2.2. The enzymatic digestion was carried out on a shaking-platform to ensure uniform digestion of the tissue. The resultant full-depth cell suspension was filtered through a 40µm cell strainer and the filtered cell suspension was centrifuged for 5 minutes at 2000 rpm. The supernatant was removed and the cell pellet re-suspended in PBS + 0.1% BSA. The cells were re-suspended at 1.0 x 10^6 cells ml^{-1} and passed through a CellTrics 30µm filters to ensure a single cell suspension, without clumping to allow accurate fluorescence activated cell sorting (FACS) analysis.

6.2.2 Antibody purification and conjugation

Commercially available conjugated antibodies against external epitopes of FRMD5 and EMBIGIN were not available. In order to allow for analysis by flow-cytometry, unconjugated antibodies were conjugated in-house. Antibodies were purified and concentrated using an antibody concentration kit (Abcam, UK), this removed glycine, tris and sodium azide that may inhibit the conjugation reactions. One hundred micrograms of antibody was added to the spin column and centrifuged at 15000 rpm for 1-3 minutes until the buffer volume was reduced to 50µl. Flow-through was discarded and 400µl of conjugation buffer added to the column and centrifuged at 15000 rpm for 1-3 minutes until buffer volume was reduced to 50µl, conjugation buffer wash was repeated 5 times. Antibody was eluted in 10µl. One microliter of Modifier reagent was added for each 10µl of antibody to be labelled and gently mixed. Antibody plus modifier was then added directly to APC/Cy7 or Cy5 lyophilised conjugation material. Conjugation mix was re-suspended gently by withdrawing and re-dispensing the liquid once or twice using a pipette and then incubated for 3 hours in the dark at room temperature. After incubation 1µl of Quencher reagent was added for every 10µl of antibody used. The conjugate can be used after 30 minutes.

6.2.3 FACS – directly conjugated antibodies

All centrifugation steps were performed at 2000 rpm for 3 minutes unless otherwise stated. One million cells from the single cell suspensions were transferred to 1.5ml microcentrifuge tubes. Cells were centrifuged and the supernatant aspirated. Conjugated primary antibodies or no primary controls were added to each tube (dilutions shown in Table 6.2), re-suspended and incubated for 30 minutes at 4˚C (in the dark). Following incubation, the cells were centrifuged and washed twice in PBS/BSA. Finally, cells were re-suspended in 0.5ml PBS/BSA filtered through Celltrics 30µm filters to ensure a single cell suspension without clumping and transferred into 12mm FACS tubes. Fluorescence activated cell sorting was performed using a BD FACS Aria flow cytometer (BD Biosciences). FACS was performed with antibodies in combination, individually and with no primary controls.

Antigen	Antibody	Fluorophore	Host species	Supplier	Concentration
Epitope mapping within an internal region of FRMD5 of human origin	Anti-FRMD5 Cy5 (G-12)	Cy5	Goat polyclonal	Santa Cruz (sc-137483)	10µg ml^{-1}
Recombinant fragment, corresponding to a region within amino acids 122-315 of Human EMBIGIN homolog	Anti-EMBIGIN – APC/Cy7	APC/Cy7	Rabbit polyclonal	Abcam (ab127692)	1:500
The antibody is specific for an extracellular epitope EAAT1.	Anti-GLAST1-PE	PE	Mouse monoclonal	MACS 130-098-804	1:11

Table 6.2 – Table showing conjugated antibodies used in flow-cytometry experiments

* APC – Allophycocynanin
** Cy - Cyandye
*** PE - Phycoerythrin

Anti-GLAST1-PE was only used for the preliminary experiments, no positive labelling was found possibly due to epitope degradation during the pronase digestion. All subsequent experiments utilised dual labelling of anti-FRDM5-CY5 and anti-EMBIGIN-APC/Cy7. Antibody concentrations were initially used at the optimum concentration determined for immunocytochemistry in Chapter 4 or at manufactures recommendations. Final antibody concentrations for FACS are shown in Table 6.2. This was achieved through titration after preliminary experimentation.

6.2.4 Flow-cytometry analysis

Flow-cytometry was performed using a BD Aria bench top flow cytometer, equipped with 633nm and 488nm lasers and BD FACS Diva software (v 5.0.3). Multi-colour analysis was performed using primary antibodies conjugated to PE, Cy5 or APC-Cy7 excitation and emission spectra for these fluorophores can be seen in Figure 6.2. Data analyses were performed using the FlowJo software.

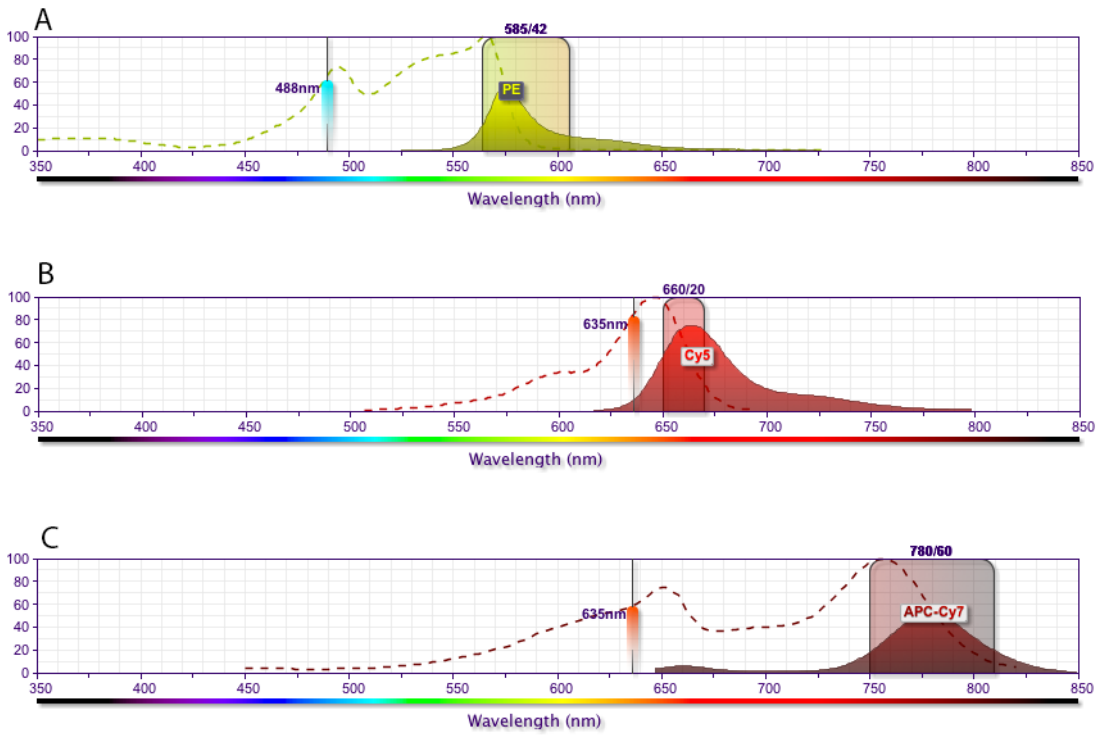


Figure 6.2 – Fluorophore spectra

Spectra illustrating the excitation spectra (dotted lines) and emission spectra (solid filled histogram) of PE (yellow), Cy5 (red) and APC-Cy7 (brown). The highlighted rectangular area on each graph demonstrates the band pass filter used for each fluorophore. (BD.Biosciences, 2014).

Cells were initially analysed for forward scatter (FSC) and side scatter (SSC). FSC is a measure of cell size and SSC is a measure of granularity. Density dot-plots were used to show the distribution of cells using the FSC and SSC parameters; voltages were adjusted to ensure optimal alignment of cells (Figure 6.3). Analysis was gated on an area of concentrated live, single cells shown if Figure 6.3. This is essential to reduce the error associated with contaminating dead cells and cell doublets. Dead cells are prone to non-specific antibody binding, leading to false positives and cell doublets would increase the level of fluorescence observed. During analysis, the whole, un-gated population data are recorded to ensure no sub-populations were omitted. Voltages were adjusted for individual fluorophores so that the negative controls were set to the second logarithmic (log) decade (Figure 6.3). If voltages are set incorrectly, control samples could be set too low to analyse or labelled cells could be above the level of detection by the flow cytometer. Instrument settings were adjusted using unstained cell samples. Labelling of cells was assessed though the geometric mean fluorescent intensity (MFI) and percentage of dual-labelled cells compared to control cells populations.

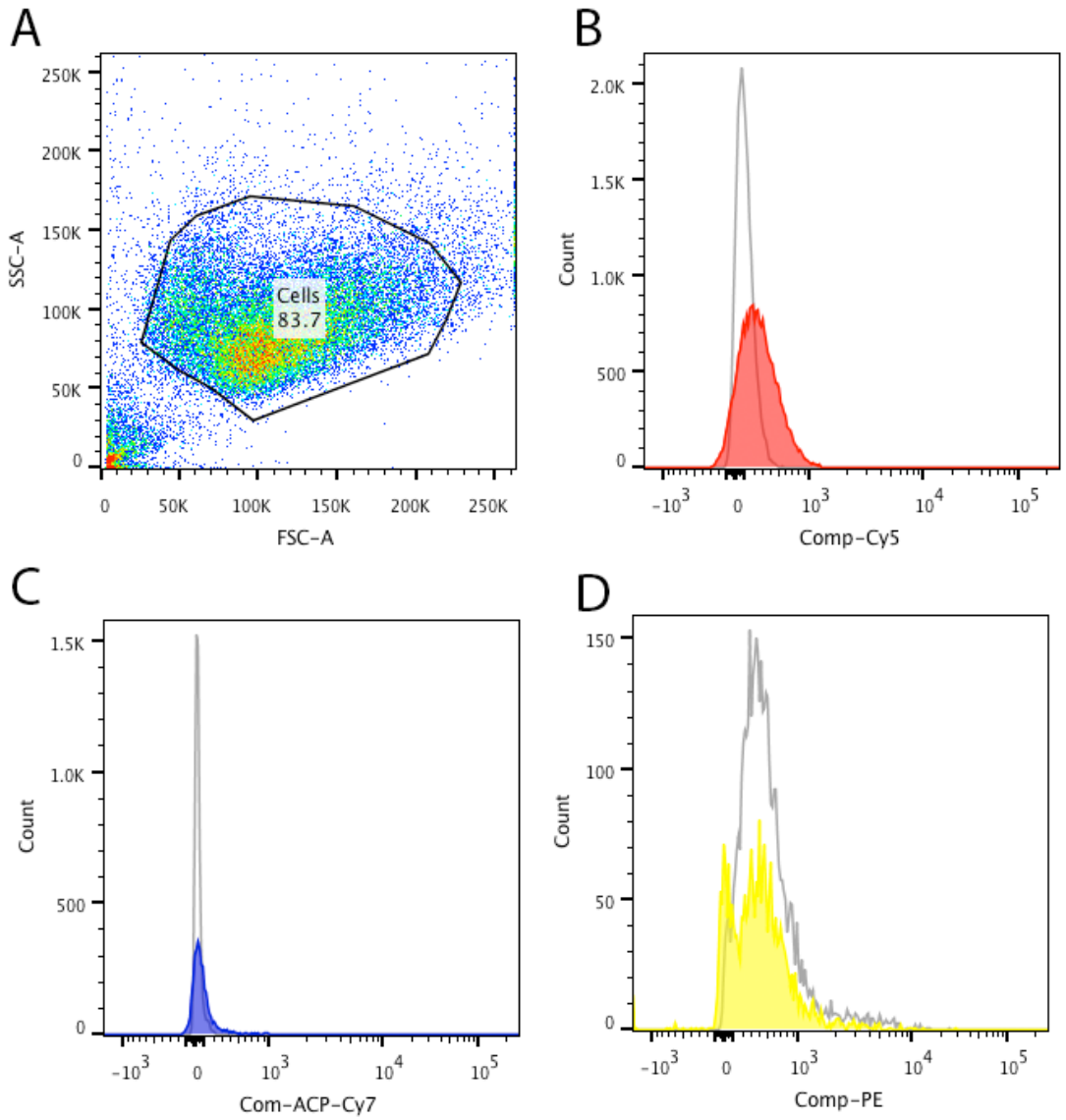


Figure 6.3 – Diagram illustrating gating and voltage adjustments

A) The dot-plot illustrates a position of the live single cell population and gating used. Highest density cells are displayed as red pixels and lowest density cells are displayed as blue pixels. The cells were positioned away from the axes and cell debris. **B, C, D)** The gated population from the negative control sample was set so that the median fluorescence was close to the second logarithmic decade (grey line), the distribution of labelled cells (blue) was then overlaid and compared. **B)** FRMD5-Cy5, **C)** EMBIGIN-APC-Cy7 and **D)** EAAT1-PE. No difference was observed in PE fluorescence between labelled and unlabelled and, therefore, the EAAT1-PE antibody was not used in the FACS analysis.

6.2.5 Cell culture

Dual-labelled positive cells for FRMD5 and EMBIGIN protein expression and dual-negative cells from FACS were cultured and expanded. Immediately following sorting, cell populations were re-suspended in DMEM+ plus TGF-β2 and FGF-2 (Section 2.4), and plated in a T25 culture flask. Cell lines were grown

as polyclonal populations and expanded and cultured in DMEM+ plus TGF-β2 and FGF-2, cell lines were passaged at 70% confluence and cultured until senescence (Section 2.4.1). Population doublings were calculated at each passage as described in Section 2.4.2.

Dual-labelled and dual-negative cells were also plated at low density in the DMEM+ in the absence TGF-β2 and FGF-2 to allow for calculation of colony forming efficiencies. The total number of cells surviving was counted after 24hrs and the number of colonies (>32 cells) was counted after 14 days (Section 2.3).

6.2.6 RNA extraction and purification

RNA was isolated from one million cell aliquots of each cell line using the Qiagen RNeasy kit as outlined in Section 2.7. Purity and concentration was checked using a nano-drop spectrophotometer.

6.2.7 cDNA synthesis

One microgram of RNA was used *per* sample for cDNA synthesis for each reaction. Reactions were performed in 50µl containing, 400µM dNTPs, 0.4µg of random hexameric primers (Promega), 0.2U/µl AMV RT enzyme (Promega) and 0.5U/µl RNaseIn (Promega). Samples were incubated at 25^{o}C for 10 minutes, 48^{o}C for 1 hour and then 95^{o}C for 2 minutes in a thermocycler. (Section 2.8)

6.2.8 qPCR analysis

Quantitative polymerase chain reaction (qPCR) was completed using the ABI 7700 and the Biorad CFX96 detection systems as outlined in Section 2.12. Plasmids were cloned from PCR products (Section 2.9-2.11) and sequenced to confirm the identity of the insert. Gene expression was quantified against a standard curve of serial diluted plasmid and normalised to the house-keeping genes hyperparathyroidism 1 (*HRPT1)* and ribosomal protein S18 (*RPS18),* after the NormFinder algorithm identified this combination as optimal from the panel of candidate genes (Table 6.3). Primer sequences and annealing temperatures are shown in Table 4.3 (Chapter 4) and Table 6.4. Melt curves and standard curves for each gene are provided in the Appendix (Figure S1.2 &S1.3).

Gene name	Gene symbol	Forward primer sequence	Reverse primer sequence	Annealing temp (°C)	NormFinder coefficient of variance	NormFinder M - value
Beta-2 microglobulin	B2M	AGA-TGA-GTA-TGC-CTG-CCG-TG	TCA-TCC-AAT-CCA-AAT-GCG-GC	56	0.6222	1.0844
Ribosomal protein S18	RPS18	CAC-AGG-AGG-CCT-ACA-CGC-CG	AGG-CTA-TTT-TCC-GCC-GCC-CA	56	0.1232	0.3226
Hyperparathyroidism 1	HRPT1	GAG-ACA-GGA-CCA-CTC-ATG-AAG-T	TCG-AGC-AAG-ACG-TTC-AGT-CC	56	0.1916	0.3646
Pre-mRNA processing factor 31	PMP31 (RP11)	GTG-CGG-CTG-CTT-CCA-TAA-G	CCC-TGG-CGT-CGT-GAT-TAG-TG	56	0.2118	0.3069
60S ribosomal protein L13a	RPL13a	CGT-GGC-TAA-ACA-GGT-ACT-GC	GTT-TGG-TGT-TCA-TCC-GCT-TGC	56	0.1097	0.3069
Combination of Ribosomal protein S18 and hyperparathyroidism 1	**RPS18 + HRPT1**				**0.0587**	**0.1694**

Table 6.3 – NormFinder results and primer sequences for house-keeping genes.

A coefficient of variance of <0.25 and a M-value of <0.5 shows gene homogenous gene expression across all cDNA samples. All house-keeping genes considered with the exception of B2M were found to be suitable candidates. House-keeping genes were considered and tested both individually and in combinations (all possible iterations were processed using the NormFinder algorithm). The combination of the Hyperparathyroidism 1 and ribosomal protein S18 was found to provide the optimum normalisation and, therefore, chosen as the house-keeping genes for all qPCR experiments in this study.

Gene name	Gene symbol	Forward primer sequence	Reverse primer sequence	Annealing temp (°C)
Collagen X	COL10A1	CAT-AAA-AGG-CCC-ACT-ACC-CAA-C	ACC-TTG-CTC-TCC-TCT-TAC-TGC	56
Alkaline phosphatase	ALPL	ACT-GGT-ACT-CAG-ACA-ACG-AGA-T	ACG-TCA-ATG-TCC-CTG-ATG-TTA-TG	56
Runt related transcription factor 2	RUNX2	TGG-TTA-CTG-TCA-TGG-CGG-GTC	TCT-CAG-ATC-GTT-GAA-CCT-TGC-TA	56
Osteocalcin	BGLAP	CAC-TCC-TCG-CCC-TAT-TGG-C	CCC-TCCC-TGC-TTG-GAC-ACA-AAG	56
Collagen I	COL1A1	GTG-CGA-TGA-CGT-CAT-CTG-TGA	CGG-TGG-TTT-CTT-GGT-CGG-T	56
Lipoprotein lipase	LPL	TCA-TTC-CCG-GAG-TAG-CAG-AGT	GGC-CAC-AAG-TTT-TGG-CAC-C	56
Fatty acid binding protein 4	FABP4	ACT-GGG-CCA-GGA-ATT-TGA-CG	CTC-GTG-GAA-GTG-ACG-CCT-T	56
Peroxisome proliferator activated receptor gamma coactivator – related protein 1	PPRC1	GAG-CAG-GTT-ATC-TCT-GGA-GGA	AGC-AGC-TCC-GAA-TCA-GGA-ATG	56
Basigin	BAS	GAA-GTC-GTC-AGA-ACA-CAT-CAA-CG	CCC-TGC-GAG-GAA-CTC-ACG-AA	56
Monocarboxylate transporter 1	MCT1	CGT-GGA-GGC-TTC-TCT-CAC-AG	CGT-AGG-ACA-GCC-CGT-TTA-TCG	56
Monocarboxylate transporter 2	MCT2	GCA-ACC-CGC-CTT-AAC-CAT-AAT	AGG-TAC-TGA-TTG-AAA-GGA-GCC-A	56
Monocarboxylate transporter 3	MCT3	GTG-GGC-TTC-GTG-GAC-ATC-G	CAG-GCT-GAA-CAG-ATA-CGG-GAC	56
Monocarboxylate transporter 4	MCT4	CGG-CTT-TGT-GCT-TTA-CGC-C	GCT-GAA-GAG-GTA-GAC-GGA-GTA	56

Table 6.4 – Primer sequences and annealing temperature for primers used in this study.

6.2.9 Immunocytochemistry

Immunofluorescence detection of stem cell markers was performed on culture-expanded cell lines as described in Section 2.20.1. In brief, cells were fixed in 95% ethanol for 10 minutes and then, samples were washed 3 times in PBS/0.1% Tween 20 (PBST) and blocked in 10% relevant sera for 1 hour. All antibodies and immunoglobulin-matched (IgG-matched) controls were prepared in PBS (Sigma-Aldrich) containing 0.2% Triton-X-100 (Sigma-Aldrich) and 5% blocking serum (serum was species matched to the secondary antibody). Excess serum was removed and cells were incubated with primary antibodies for 1 hour at room temperature. The slides were washed 3 times in PBST and then incubated with fluorescence 10μg ml^{-1} conjugated secondary antibodies for 1 hour at room temperature. Samples were washed a further 3 times in PBST before being mounted in Vector shield ™ containing DAPI. Antibody concentrations are shown in Tables 4.5 and Table 4.6 (Chapter 4).

6.2.10 Phenotypic plasticity

Differentiation studies were undertaken to determine phenotypic plasticity. Chondrogenic and osteogenic differentiation were performed in pellet culture as described in Section 2.6.3 and adipogenic differentiation was performed in monolayer as described in Section 2.6.2. In brief, pellet cultures were set up at $5x10^5$ ml^{-1} in a sterile Eppendorf tube in either chondrogenic (Section 2.6.1.1) or osteogenic media (Section 2.6.1.2). Pellets were cultured for 3 weeks and media changed every 2 days. Cells for adipogenic differentiation were plated at 50,000 cells *per* well in a 6-well plate and cultured until 70% confluence, at this point media was changed to either control (Section 2.4) or adipogenic media (Section 2.6.1.3) for 10 days, media was changed every 2 days.

6.2.11 Papain digestion

Pellets were lysed by adding 1 ml of papain digestion buffer consisting of 300μg ml^{-1} papain, 20mM sodium phosphate at pH6.8, 1mM EDTA and 2mM DL-Dithiothreitol (DTT) to each pellet. These were incubated at 60˚C for one hour or until the pellet had fully lysed, after which 5μl of idoacetamide (at 100μg $μl^{-1}$) was added to each Eppendorf tube to inhibit further digestion. Aliquots of this digest were assayed for glycosaminoglycan (GAG) content. Samples were either

taken directly for analysis or frozen at -20°C until required.

6.2.12 DMMB

A dimethylmethylene blue (DMMB) assay was used for the quantification of GAGs within the digest. Standards were prepared using stock chondroitin-6-sulphate (CS) at 0µg ml^{-1}, 10µg ml^{-1}, 20µg ml^{-1}, 30µg ml^{-1}, and 40µg ml^{-1}. DMMB reagent contained 16mg L^{-1} DMMB dissolved in 1 litre dH_2O containing 10ml ethanol, 29ml of 1M sodium hydroxide and 3.5ml formic acid (98%). Forty microlitres of standard or samples were pipetted in duplicate onto a 96-well plate, and 200µl of DMMB was added to each well. The absorbances of the samples were read immediately at 525nm on a FLUOstar OPTIMA plate reader using the OPTIMA software. Absorbances were quantified using the standard curve and normalized to the wet weight of each pellet.

6.2.13 Histology

Safranin-O and toluidine blue staining were used to show proteoglycan present in articular cartilage and during chondrogenic differentiation as described in Sections 2.21.2 and 2.21.3. Alizarin red staining was performed to identify mineral deposits in the osteogenic differentiated pellets as described in Sections 2.21.4 and 2.21.5. Oil red-O staining was performed to identify vacuoles of triglycerides within adipogenic-differentiated cells as described in Section 2.21.6. Crystal violet was used as a cytoplasmic counter-stain as described in Section 2.21.7.

6.2.14 Statistics

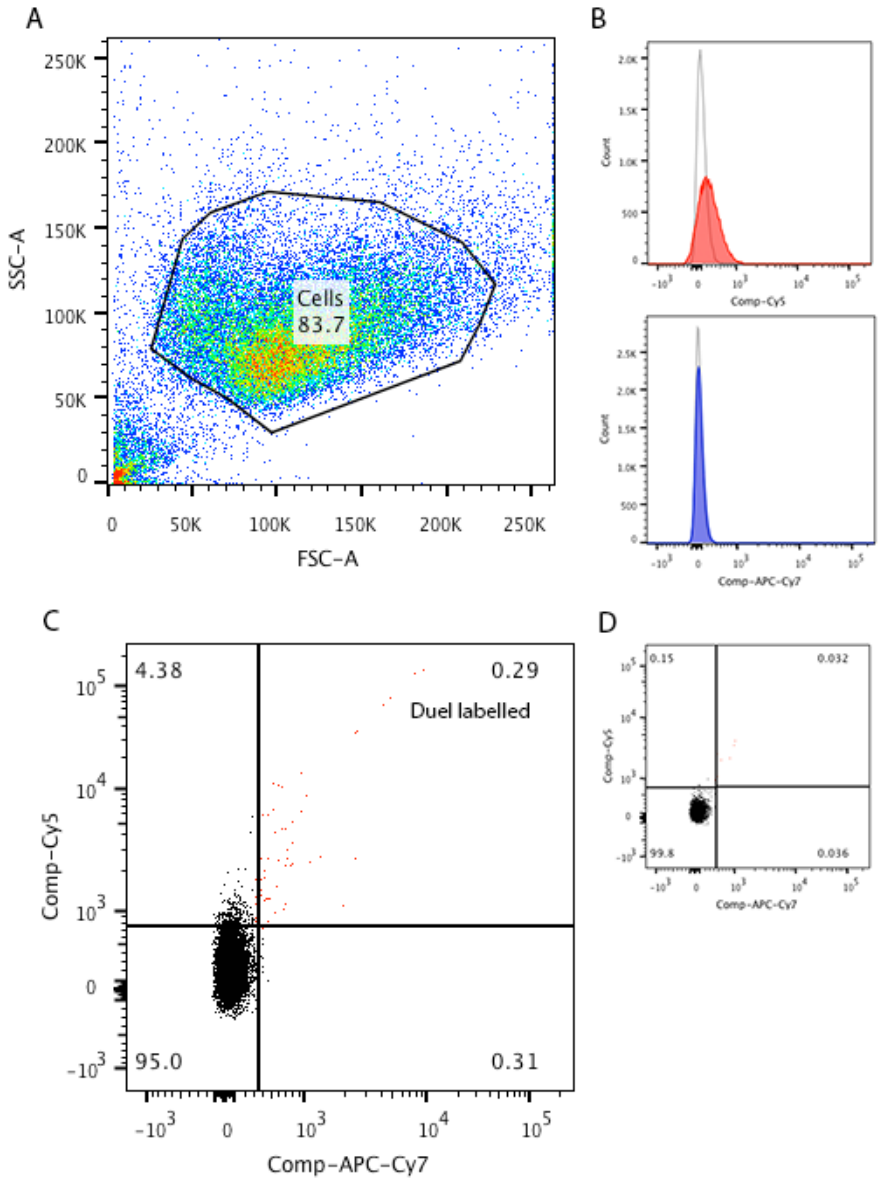
All statistics were performed using the 'R' statistical software. Statistical significance was confirmed using a parametric analysis of generalised linear mixed models, Anova and Student T-tests where appropriate. Data that did not fit into the Gaussian distribution were 'normalised' by data transformations to allow for parametric analysis where possible. If data could not be normalised, non-parametric alternatives were performed where stated. Statistical significance was defined as $p<0.05$.

6.3 Results

Full-thickness cartilage biopsies were digested using pronase and collagenase enzymes to release cells from the matrix. Cells were immediately labelled with fluorescently conjugated antibodies to FRMD5 and EMBIGIN and analysed using a BD Aria flow cytometer. All data were acquired using BD FACS Diva software and further analyses were completed using FlowJo (version 10.0, Tree Star, Inc., Oregon, USA) from data stored in FCS 3.0 format. Cells were manually gated based on size and granularity to isolate live single cell events. Gated populations were analysed for fluorescence intensity, using mean fluorescence intensity (MFI) and percentage labelled values. The percentage of labelled cells was defined by placing a delineator at the limit of the control sample fluorescence; any cells above this level were designated as positively labelled.

6.3.1 Flow-cytometry

No increase in MFI was observed in the labelled cells for EAAT1-PE compared to controls so EAAT1 was not used during cell sorting. The MFI increased for both FRMD5-Cy5 and EMBIGIN-APC-Cy7 relative to controls (Figures. 6.4E-6.10E). The MFI for cells incubated with FRMD5 was 2.13-fold higher than controls in normal tissue and 8.63-fold higher than control in OA tissue. The increase in geometric mean fluorescence between normal and OA derived cells was statistically significant (Normal = 211.5, OA = 471.0, $P<0.005$). The MFI for cells incubated with EMBIGIN was 1.60-fold higher than controls in normal tissue and 11.97-fold higher than control in OA tissue. The increase in geometric mean fluorescence between normal and OA derived cells was also statistically significant (Normal = 38.7, OA = 132.7, $P<0.0005$). The percentage of cells dual labelling for both FRMD5 and EMBIGIN in normal articular cartilage was 0.37% (0.29-0.43%) (Figures 6.4C-6.7C and Figure 6.11A). The number of dual-labelled cells significantly increased in OA cartilage to 5.43% (4.20-7.35%) ($p<0.005$). In normal cartilage, 94.2% (93.1-95.4%) of cells were negative for both FRMD5 and EMBIGIN and in OA 82.8% (75.7-89.3%) of cells were dual-negative (Figures 6.4C-6.10C). The dual-positive and dual-negative cells were sorted into 2 separate populations and expanded in culture for further analysis. Dual-positive cells from normal cartilage were termed N+ve and from OA cartilage OA+ve. The negative fractions are referred to as N-ve and OA-ve.

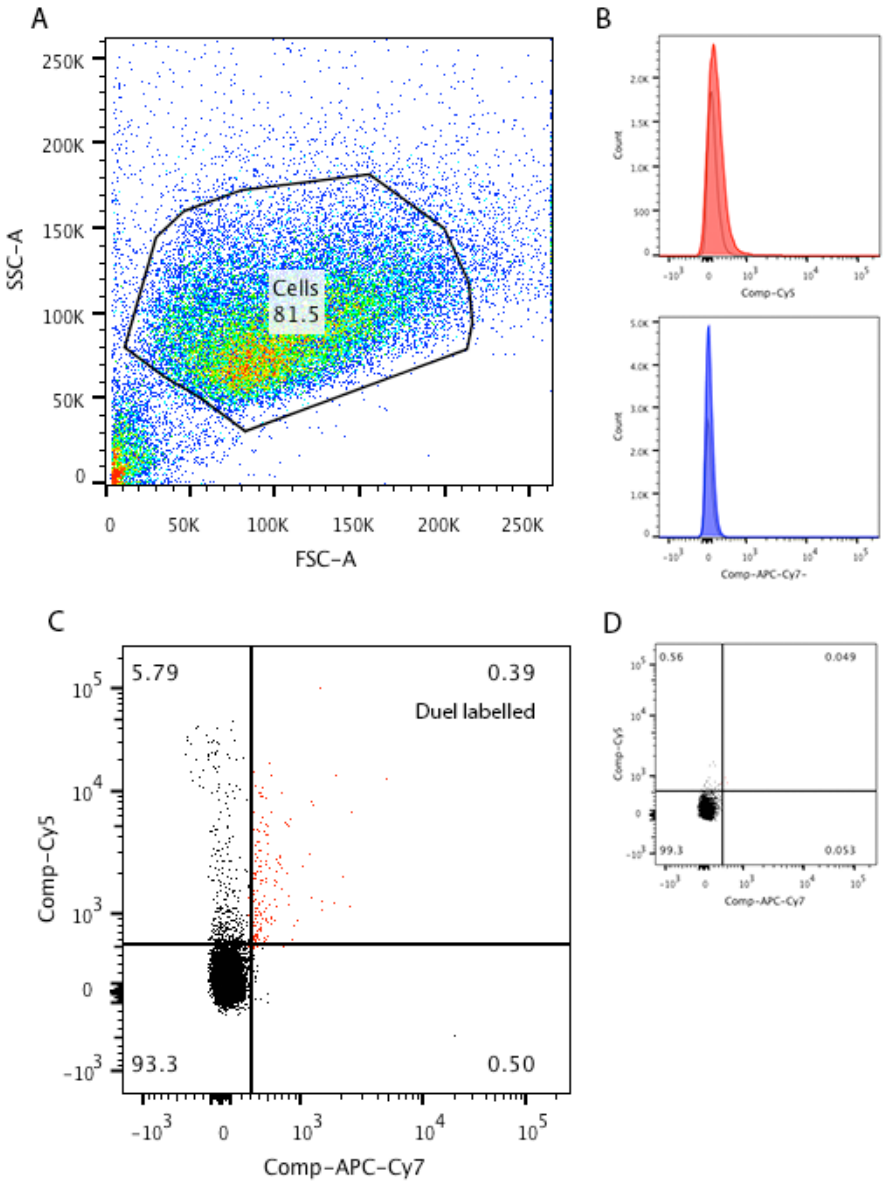


E

	Fluorescence intensity					
	Geometric mean		Median		MFI ratio	
	Cy5	APC-Cy7	Cy5	APC-Cy7	Cy5	APC-Cy7
Control	92.4	26.8	77.1	18	2.89	1.67
FRMD5 and EMBIGIN labelled	267	44.8	244	34.7		

Figure 6.4 – Flow-cytometry analysis of normal sample 1 (CF01N)

Cells were gated, excluding dead cells, clumped cells and debris **(A)** this gate accounted for 83.7% of the total population. The gated control (grey line) and FRMD5 (red) and EMB (blue) labelled cells were analysed for fluorescent intensity **(B)**. A quadrant gate was placed on the unlabelled control population **(D)**, this allowed identification of the dual-labelled population **(C)**. FRMD5 and EMB dual-positive cells accounted for 0.24% of the total population. **E)** Contains a table displaying the average fluorescence intensity of the controlled and labelled cells and the mean fluorescence intensity ratio (MFI), which is the ratio between labelled and control.

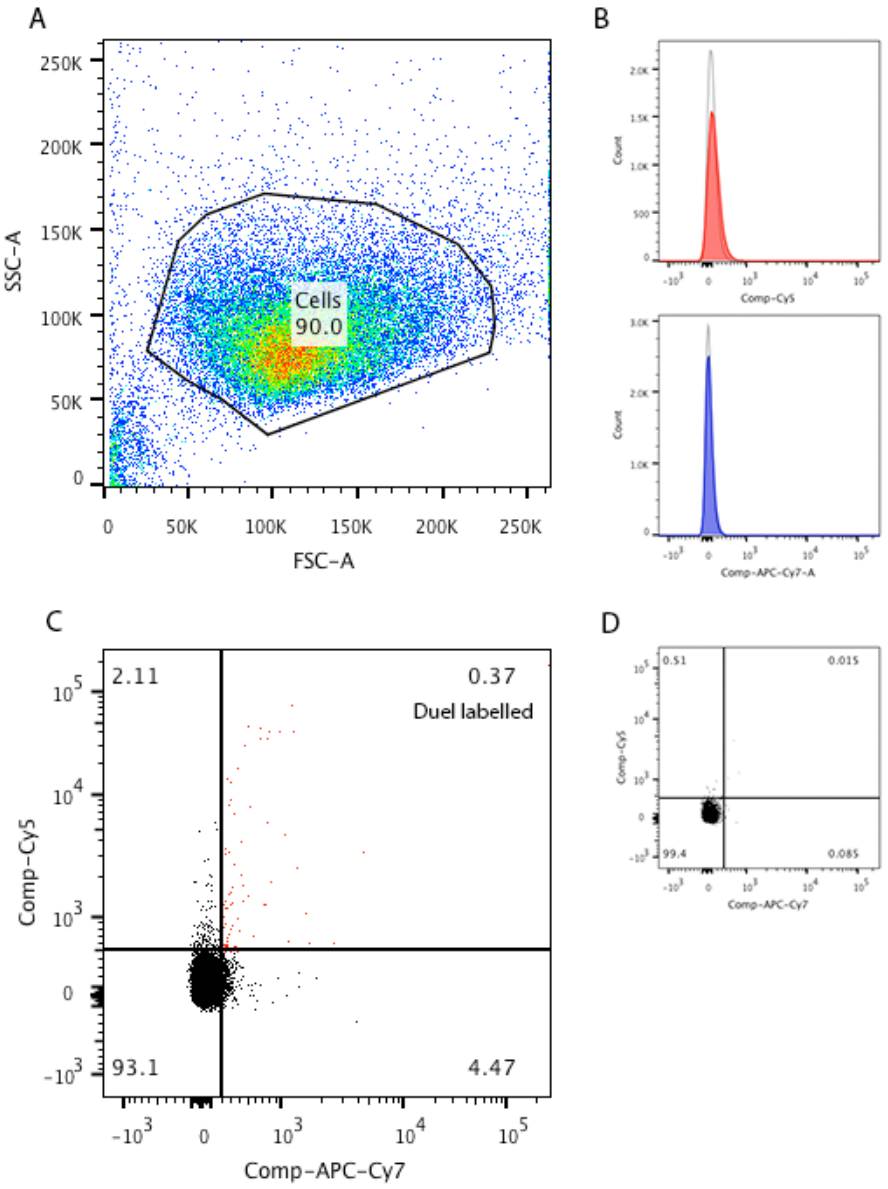


E

	Fluorescence intensity					
	Geometric mean		Median		MFI ratio	
	Cy5	APC-Cy7	Cy5	APC-Cy7	Cy5	APC-Cy7
Control	101	19.5	83.5	10.3	2.03	1.56
FRMD5 and EMBIGIN labelled	205	30.5	155	19.3		

Figure 6.5 – Flow-cytometry analysis of normal sample 2 (CF02N)

Cells were gated, excluding dead cells, clumped cells and debris **(A)** this gate accounted for 81.5% of the total population. The gated control (grey line) and FRMD5 (red) and EMB (blue) labelled cells were analysed for fluorescent intensity **(B)**. A quadrant gate was placed on the unlabelled control population **(D)**, this allowed identification of the dual-labelled population **(C)**. FRMD5 and EMB dual-positive cells accounted for 0.39% of the total population. **E)** Contains a table displaying the average fluorescence intensity of the controlled and labelled cells and the mean fluorescence intensity ratio (MFI), which is the ratio between labelled and control.

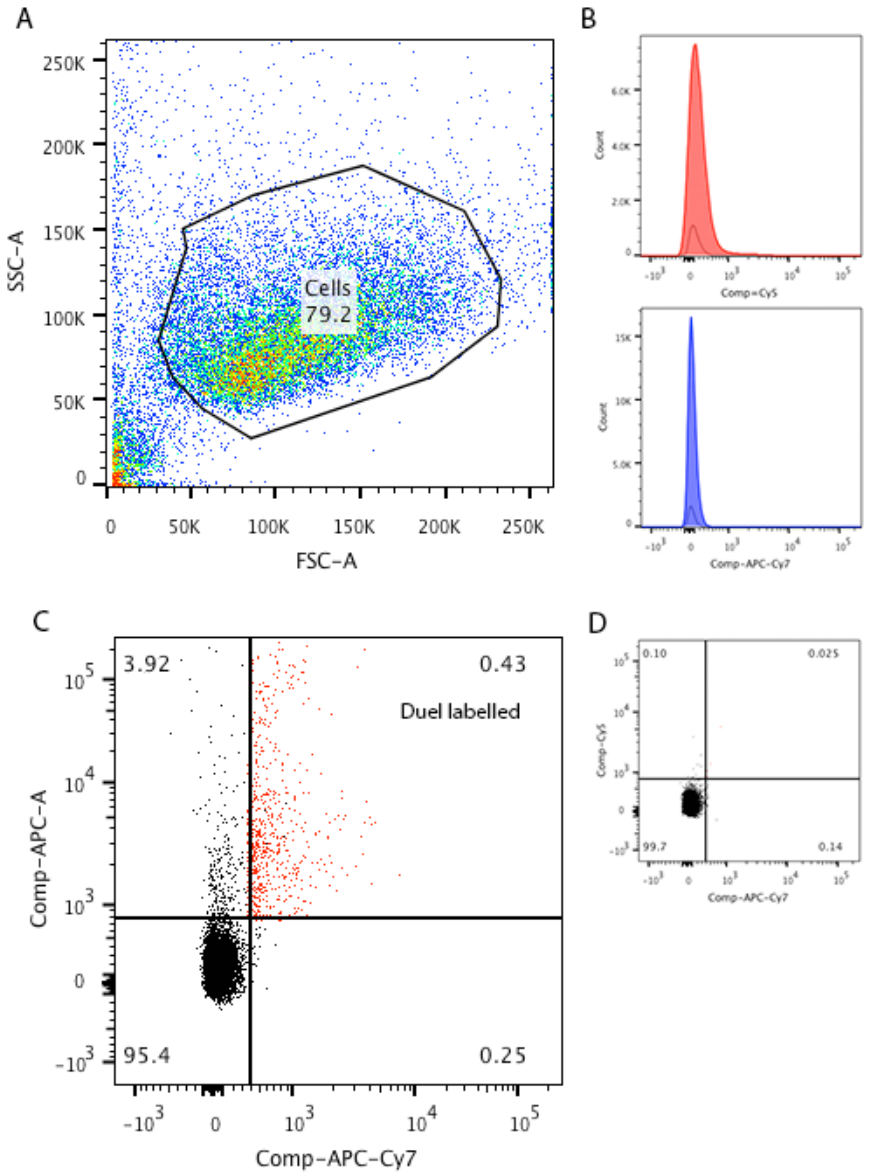


E

	Fluorescence intensity					
	Geometric mean		Median		MFI ratio	
	Cy5	APC-Cy7	Cy5	APC-Cy7	Cy5	APC-Cy7
Control	87.1	20	75.8	11.6	1.68	1.80
FRMD5 and EMBIGIN labelled	146	36.1	122	23.1		

Figure 6.6 – Flow-cytometry analysis of normal sample 3 (CF03N)

Cells were gated, excluding dead cells, clumped cells and debris **(A)** this gate accounted for 90% of the total population. The gated control (grey line) and FRMD5 (red) and EMB (blue) labelled cells were analysed for fluorescent intensity **(B)**. A quadrant gate was placed on the unlabelled control population **(D)**, this allowed identification of the dual-labelled population **(C)**. FRMD5 and EMB dual-positive cells accounted for 0.37% of the total population. **E)** Contains a table displaying the average fluorescence intensity of the controlled and labelled cells and the mean fluorescence intensity ratio (MFI), which is the ratio between labelled and control.

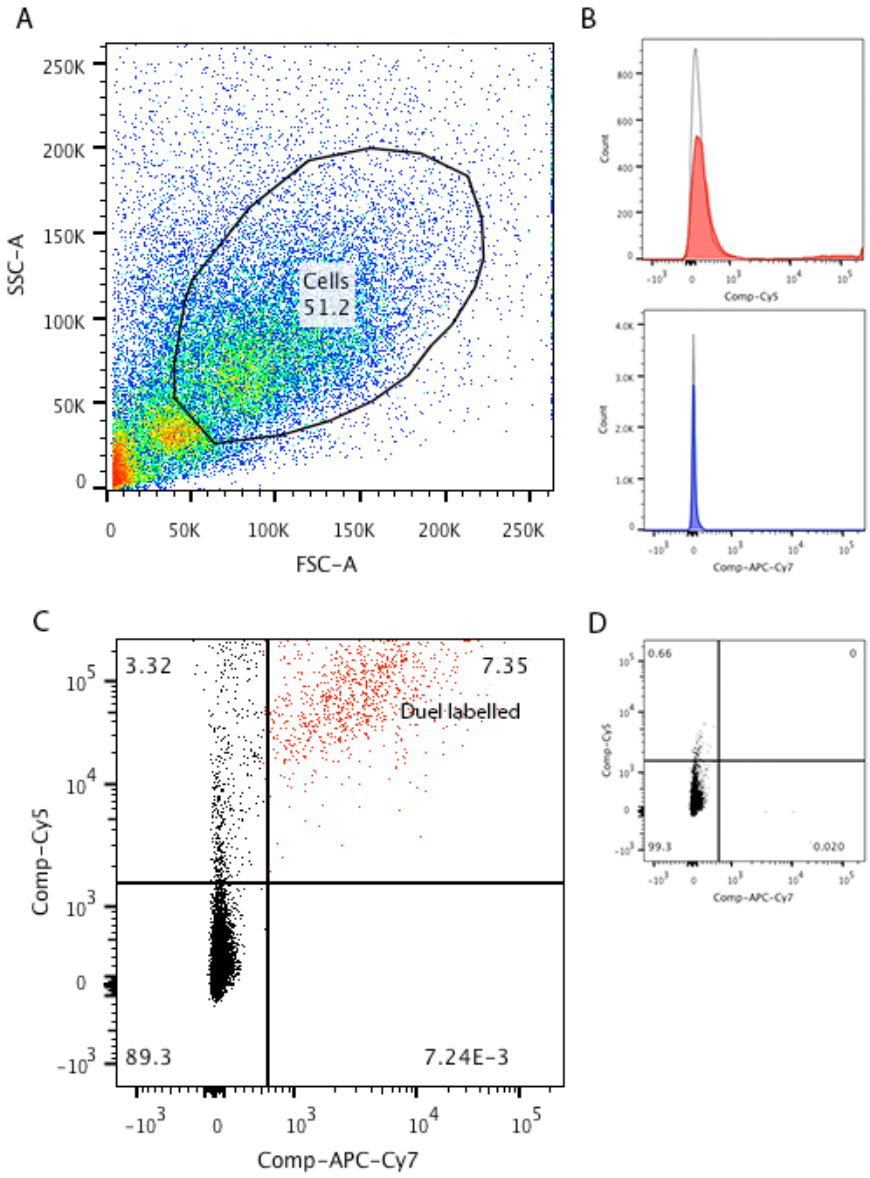


E

	Fluorescence intensity					
	Geometric mean		Median		MFI ratio	
	Cy5	APC-Cy7	Cy5	APC-Cy7	Cy5	APC-Cy7
Control	119	31.8	100	20.5	1.92	1.36
FRMD5 and EMBIGIN labelled	228	43.4	164	30.8		

Figure 6.7 – Flow-cytometry analysis of normal sample 4 (CF04N)

Cells were gated, excluding dead cells, clumped cells and debris **(A)** this gate accounted for 79.2% of the total population. The gated control (grey line) and FRMD5 (red) and EMB (blue) labelled cells were analysed for fluorescent intensity **(B)**. A quadrant gate was placed on the unlabelled control population **(D)**, this allowed identification of the dual-labelled population **(C)**. FRMD5 and EMB dual-positive cells accounted for 0.43% of the total population. **E)** Contains a table displaying the average fluorescence intensity of the controlled and labelled cells and the mean fluorescence intensity ratio (MFI), which is the ratio between labelled and control.

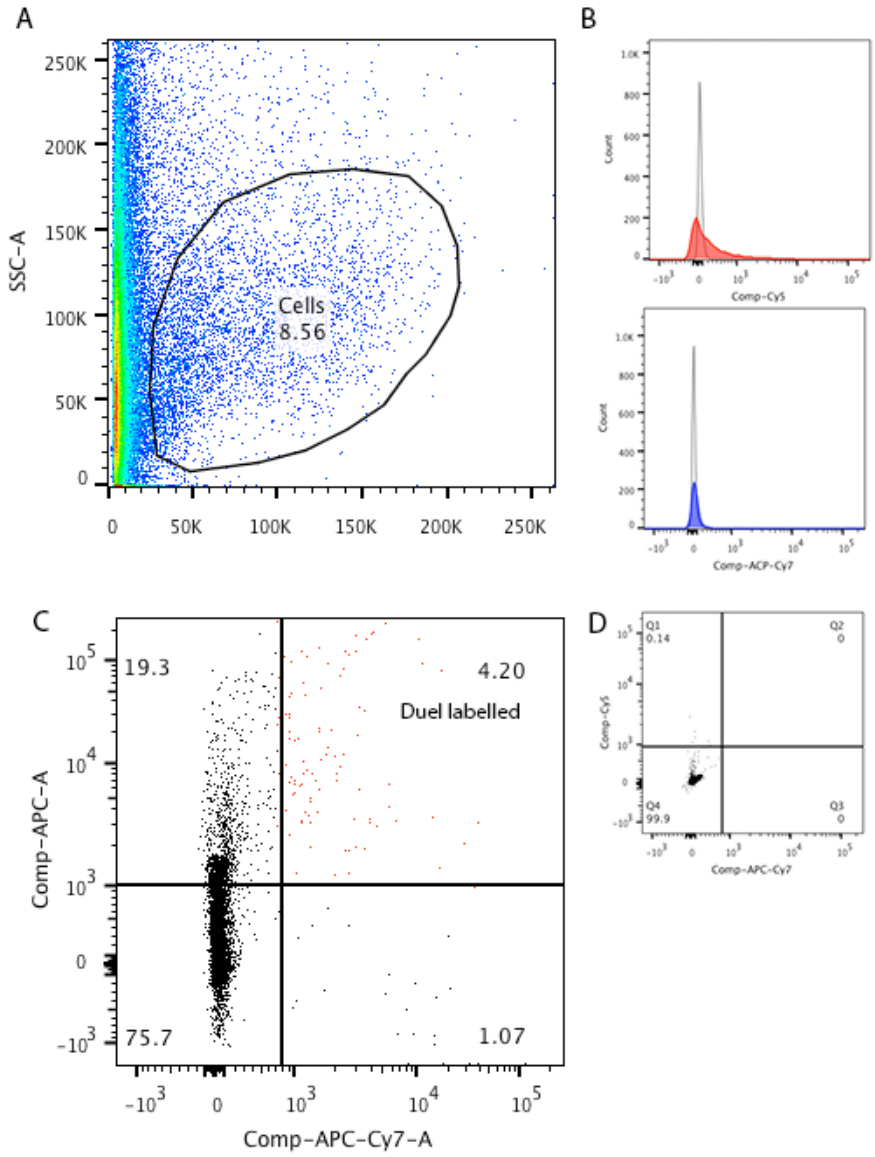


E

	Fluorescence intensity					
	Geometric mean		Median		MFI ratio	
	Cy5	APC-Cy7	Cy5	APC-Cy7	Cy5	APC-Cy7
Control	188	9.44	139	0	3.04	14.83
FRMD5 and EMBIGIN labelled	571	140	232	8.98		

Figure 6.8 – Flow-cytometry analysis of OA sample 1 (CF01OA)

Cells were gated, excluding dead cells, clumped cells and debris **(A)** this gate accounted for 51.2% of the total population. The gated control (grey line) and FRMD5 (red) and EMB (blue) labelled cells were analysed for fluorescent intensity **(B)**. A quadrant gate was placed on the unlabelled control population **(D)**, this allowed identification of the dual-labelled population **(C)**. FRMD5 and EMB dual-positive cells accounted for 7.35% of the total population. **E)** Contains a table displaying the average fluorescence intensity of the controlled and labelled cells and the mean fluorescence intensity ratio (MFI), which is the ratio between labelled and control.

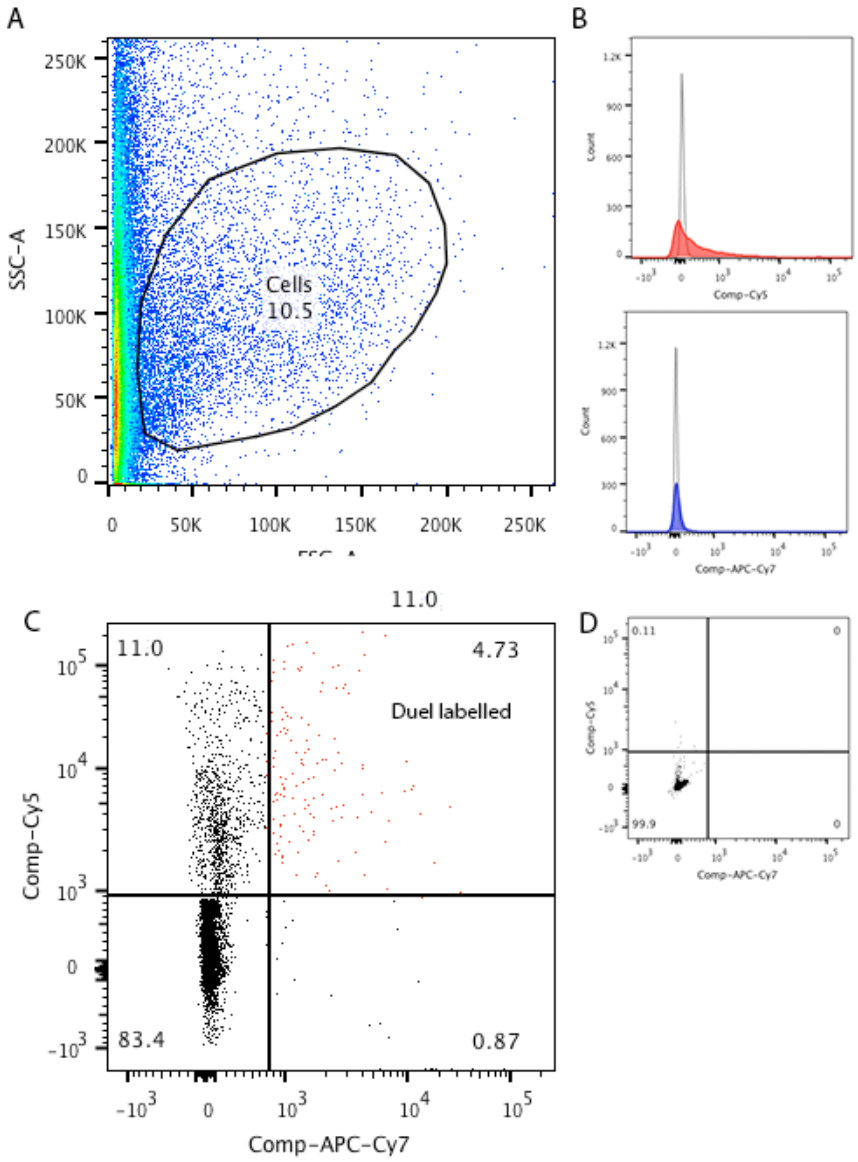


E

	Fluorescence intensity					
	Geometric mean		Median		MFI ratio	
	Cy5	APC-Cy7	Cy5	APC-Cy7	Cy5	APC-Cy7
Control	38.2	13.0	25.7	5.13	9.84	9.61
FRMD5 and EMBIGIN labelled	376	125	133	37.2		

Figure 6.9 – Flow-cytometry analysis of OA sample 2 (CF02OA)

Cells were gated, excluding dead cells, clumped cells and debris **(A)** this gate accounted for 8.56% of the total population. The gated control (grey line) and FRMD5 (red) and EMB (blue) labelled cells were analysed for fluorescent intensity **(B)**. A quadrant gate was placed on the unlabelled control population **(D)**, this allowed identification of the dual-labelled population **(C)**. FRMD5 and EMB dual-positive cells accounted for 4.20% of the total population. **E)** Contains a table displaying the average fluorescence intensity of the controlled and labelled cells and control.



E

	Fluorescence intensity					
	Geometric mean		Median		MFI ratio	
	Cy5	APC-Cy7	Cy5	APC-Cy7	Cy5	APC-Cy7
Control	35.8	11.6	23.1	3.85	13.01	11.47
FRMD5 and EMBIGIN labelled	466	133	191	42.4		

Figure 6.10 – Flow-cytometry analysis of OA sample 3 (CF03OA)

Cells were gated, excluding dead cells, clumped cells and debris **(A)** this gate accounted for 10.5% of the total population. The gated control (grey line) and FRMD5 (red) and EMB (blue) labelled cells were analysed for fluorescent intensity **(B)**. A quadrant gate was placed on the unlabelled control population **(D)**, this allowed identification of the dual-labelled population **(C)**. FRMD5 and EMB dual-positive cells accounted for 4.73% of the total population. **E)** Contains a table displaying the average fluorescence intensity of the controlled and labelled cells and control.

6.3.2 Percentage colony forming cells

The N+ve cells and OA+ve cells were analysed for colony-forming efficiency (CFE). CFE values were calculated as a percentage of colony forming cells *per* total number of cells that survived 24hrs initial culture. The flow-cytometry and labelling procedures were found to affect cell viability and hence calculation of CFEs as a percentage of initial seeding density were not possible due to cell death occurring within the first 24 hours. Both normal and OA dual-positive cells had greater than 87% colony forming efficiencies (Figure 6.11B). No difference was observed in CFE between normal and OA cartilage-derived dual-positive cells.

6.3.3 Proliferation analysis

Dual-positive and dual-negative cell lines were cultured as polyclonal populations. Growth kinetics (population doublings), of 12 polyclonal N+ve and 4 polyclonal N-ve cell lines from 4 individual normal donors and 9 polyclonal OA+ve and 3 OA-ve cell lines from 3 individual OA donor tibial plateaux were investigated (Figure 6.12). The initial growth rates of dual-positives were found to be linear until approximately 30PD after which the rate of proliferation started to slow, dual-negative populations had a linear rate of growth until PD20 at which time the rate of proliferation slowed until senescence (Figure 6.12). It was observed that dual-positive cells from both healthy and OA tissue appeared to adopt similar proliferation rates, with very little heterogeneity observed both between cell lines from the same donor and, between cell lines of different donors (Figure 6.12-*inset*). The N+ve cells were expanded to a maximum of 58.78 PDs and this was achieved in 150 days. The OA+ve cells expanded to a maximum of 55.1 PDs and this was achieved in 161 days. The dual-negative cell lines from both normal and OA cartilage senesced at around 30 population doublings.

Articular cartilage-derived FRMD5/EMBIGIN dual-positive cells were found to be highly clonogenic and capable of extended proliferation *in vitro* i.e. past the Hayflick limit of 30PD for MSCs.

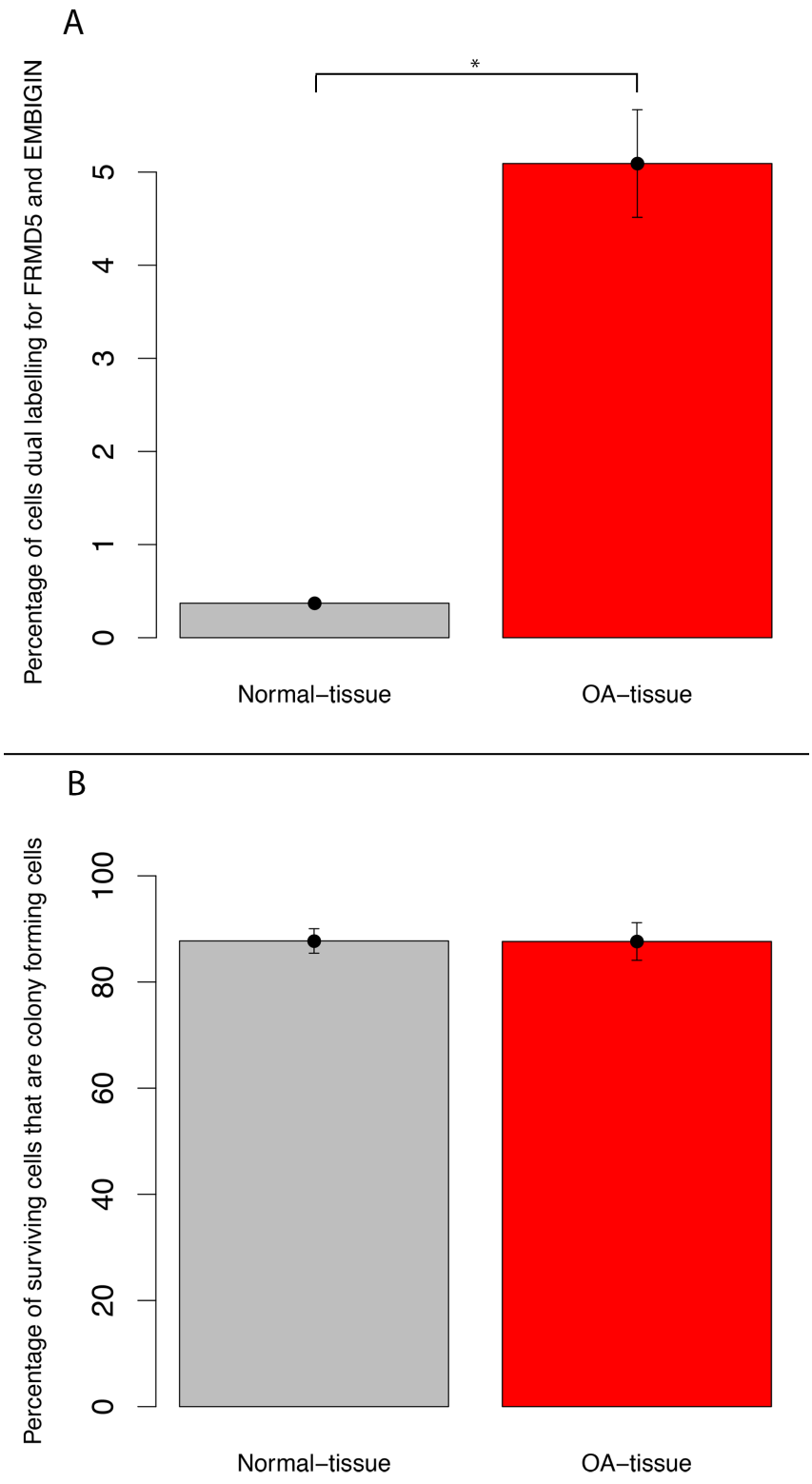


Figure 6.11 – Percentage dual-labelled and colony forming cells in normal and OA cartilage

A. Percentage of dual-labelled FRMD5 and EMBIGIN-positive cells in normal (n = 4) and OA (n = 3) articular cartilage. There is a statistically significant 13.7-fold increase in the number of dual-labelled cells in OA cartilage (mean = 5.43%) compared to normal cartilage (mean = 0.37%), ($p<0.001$, Student's T-test). **B.** Percentage colony-forming cells in dual-labelled population. Of cells that survive 24 hours post FACS, both normal and OA cartilage had 88% (mean normal = 87.73%, Mean OA = 87.63%) of these cells that formed colonies of greater than 32 cells within 14 days.

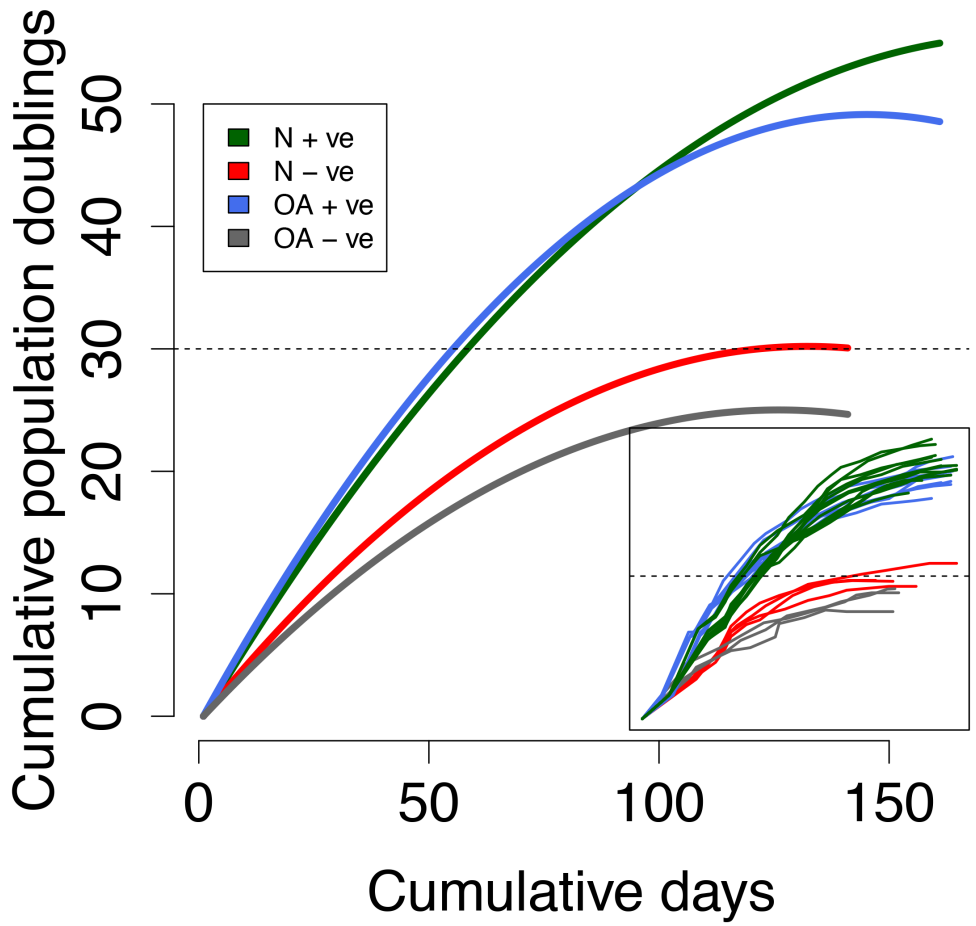


Figure 6.12 – Growth kinetics of dual FRDM5 and EMBIGIN-positive and dual FRDM5 and EMBIGIN-negative cells.

Normal dual-positive cells (n = 12) proliferated past 50 population doublings in culture. OA dual-positive cell lines (n = 9) proliferated to approximately 50 population doublings, where some cells lines senesced while others continued to proliferate. Both normal (n = 4) and OA (n = 3) dual-negative cells senesced before 30 population doublings. Inset shows the individual cell line growth kinetics.

6.3.3.1 Immunocytochemical analyses of ACSC markers

Dual-positive and dual-negative cell lines were analysed for protein labelling of the ACSC markers identified earlier in this thesis. Protein labelling of NESTIN, FRMD5, C11ORF41, EMBIGIN and EAAT1 were investigated.

NESTIN exhibited positive cytoskeletal labelling in dual-positive cell lines from both normal and OA donors; no labelling was present in either dual-negative populations (Figure 6.13A-D. No antibody labelling was present in the no primary or isotype matched controls (Figure 6.13E-F).

FRMD5 labelling was found in the cell membrane of the dual-positive cell lines from both normal and OA donors; again no labelling was observed in dual-negative populations (Figure 6.14A-D). No antibody labelling was present in the no primary or isotype matched controls (Figure 6.14E-F).

C11ORF41 membrane labelling was found in the dual-positive cell lines from both normal and OA donors; with no labelling observed in dual-negative populations (Figure 6.15A-D). No antibody labelling was present in the no primary or isotype matched controls (Figure.6.15E-F).

EMBIGIN protein was expressed in the cell membrane of dual-positive cell lines from both normal and OA donors (Figure 6.16B,D). No protein labelling was observed in either of the dual-negative populations (Figure 6.16A,C). No antibody labelling was present in the no primary or isotype matched controls (Figure 6.16E-F).

EAAT1 protein labelling was localised to the cell membrane in the dual-positive cell lines from both normal and OA donors; no labelling was observed in dual-negative populations (Figure 4.17A-D). No antibody labelling was present in the no primary or isotype matched controls (Figure 4.17E-F).

Protein labelling of ACSC markers identified through transcriptomics in Chapter 3 and validated through qPCR and protein labelling in Chapter 4 were found to

be specific to the dual-positive cell lines with no labelling identified in dual-negative chondrocytes.

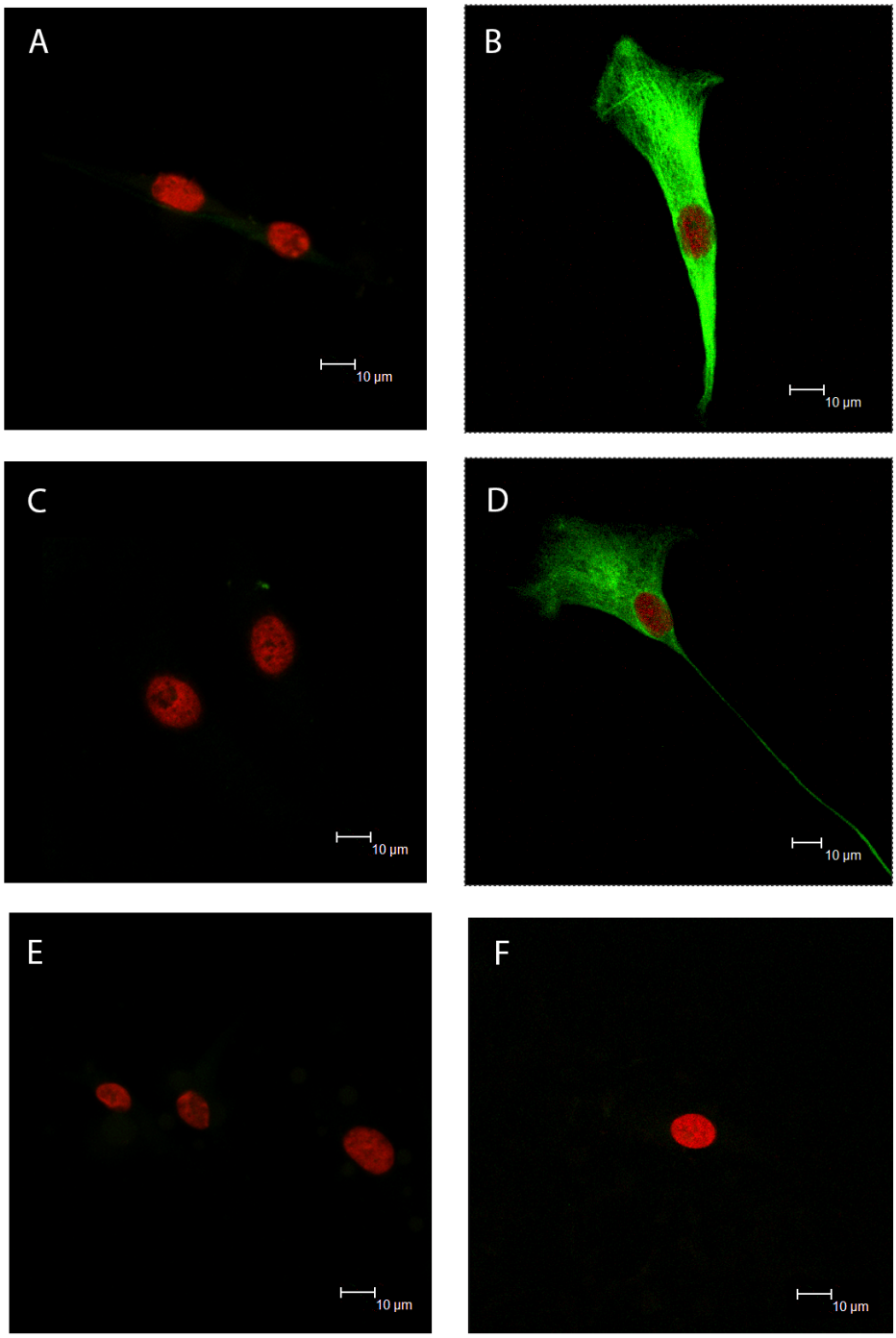


Figure 6.13 – Immunocytochemistry of NESTIN in FACS cells

A, C) NESTIN protein labelling was not evident in the culture-expanded cell lines derived from the dual-negative sorted cells. **Figure A-** A representative image of a normal cartilage-derived cell line, **Figure C-** A representative image of an OA cartilage-derived cell line. **B, D)** NESTIN protein labelling shows cytoskeletal labelling in culture-expanded cell lines derived from the dual-positive sorted cells. **Figure B-** A representative image of a normal derived cell line, **Figure D-** A representative image of an OA cartilage-derived cell line. **E, F)** Controls using normal cartilage-derived dual-positive cells. Figure E- an isotype matched IgG control and Figure F- a no primary antibody control.

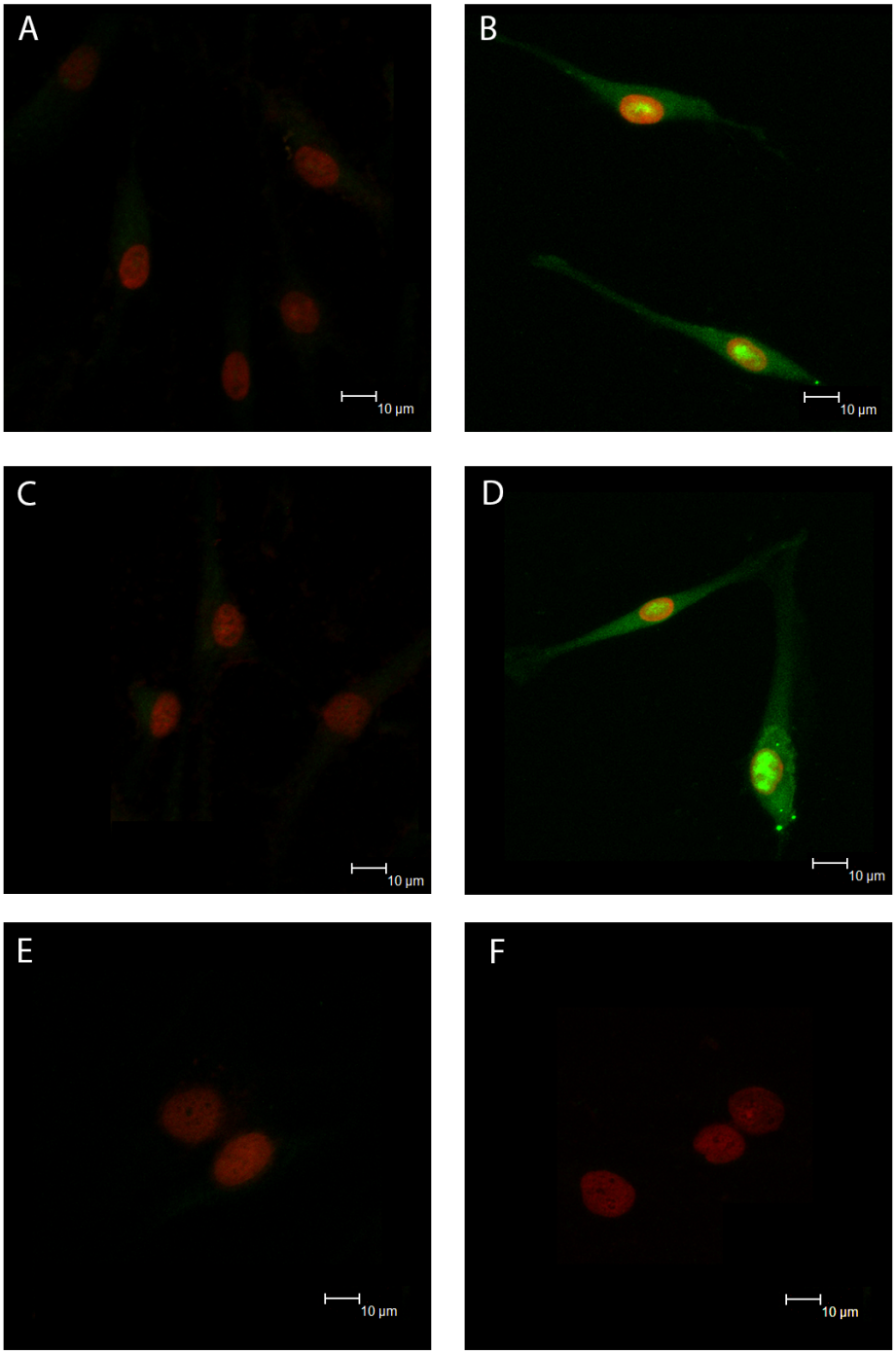


Figure 6.14 – Immunocytochemistry of FRMD5 in FACS cells

A, C) FRMD5 protein labelling was not evident in the culture-expanded cell lines derived from the dual-negative sorted cells. **Figure A-** A representative image of a normal cartilage-derived cell line, **Figure C-** A representative image of an OA cartilage-derived cell line. **B, D)** FRMD5 protein labelling shows cytoplasmic labelling in culture-expanded cell lines derived from the dual-positive sorted cells. **Figure B-** A representative image of a normal derived cell line, **Figure D-** A representative image of an OA cartilage-derived cell line. **E, F)** Controls using normal cartilage-derived dual-positive cells. Figure E- an isotype matched IgG control and Figure F- a no primary antibody control.

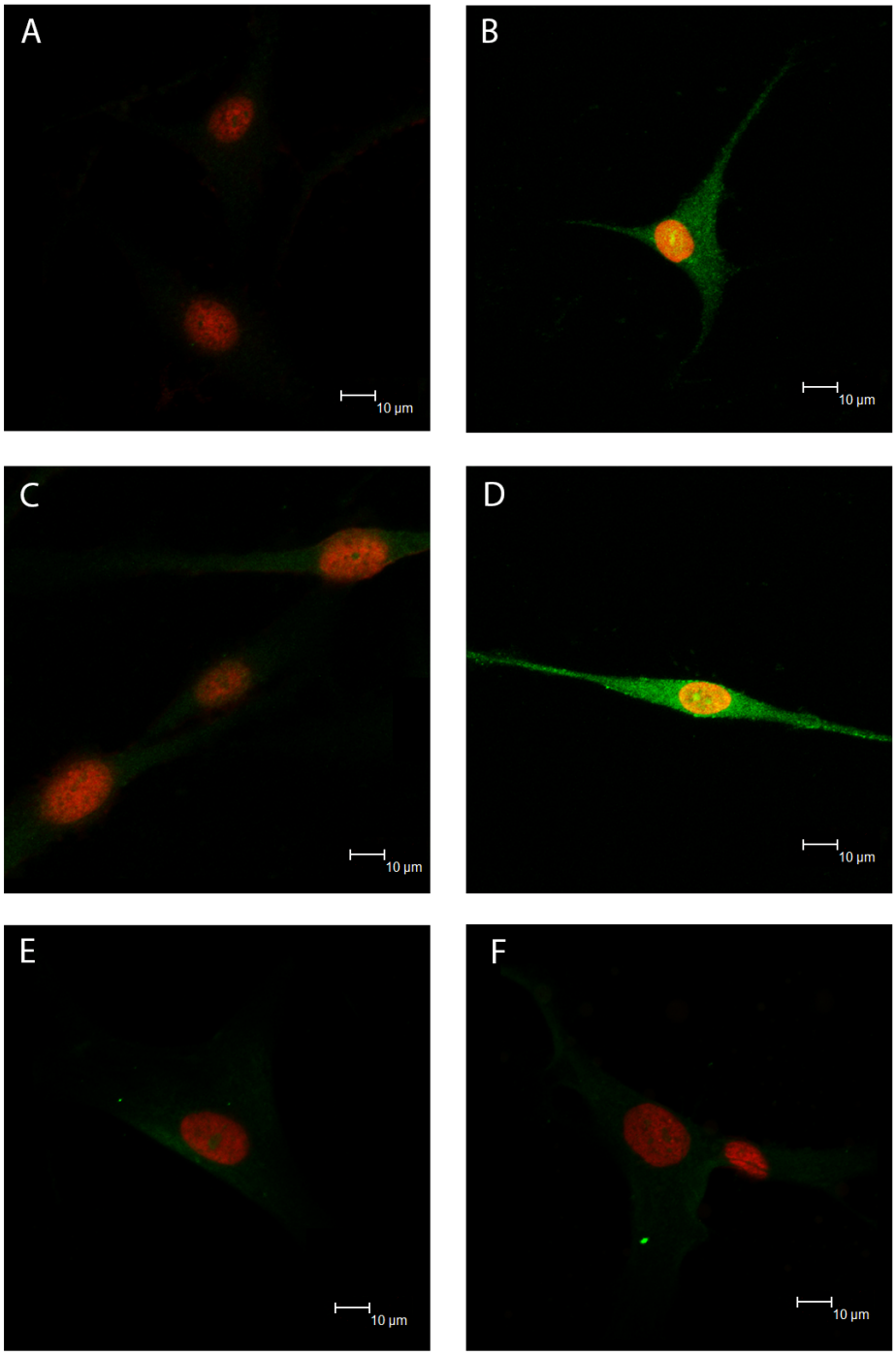


Figure 6.15 – Immunocytochemistry of C11ORF41 in FACS cells

A, C) C11ORF41 protein labelling was not evident in the culture-expanded cell lines derived from the dual-negative sorted cells. **Figure A-** A representative image of a normal cartilage-derived cell line, **Figure C-** A representative image of an OA cartilage-derived cell line. **B, D)** C11ORF41 protein labelling shows cytoplasmic labelling in culture-expanded cell lines derived from the dual-positive sorted cells. **Figure B-** A representative image of a normal derived cell line, **Figure D-** A representative image of an OA cartilage-derived cell line. **E, F)** Controls using normal cartilage-derived dual-positive cells. Figure E- an isotype matched IgG control and Figure F- a no primary antibody control.

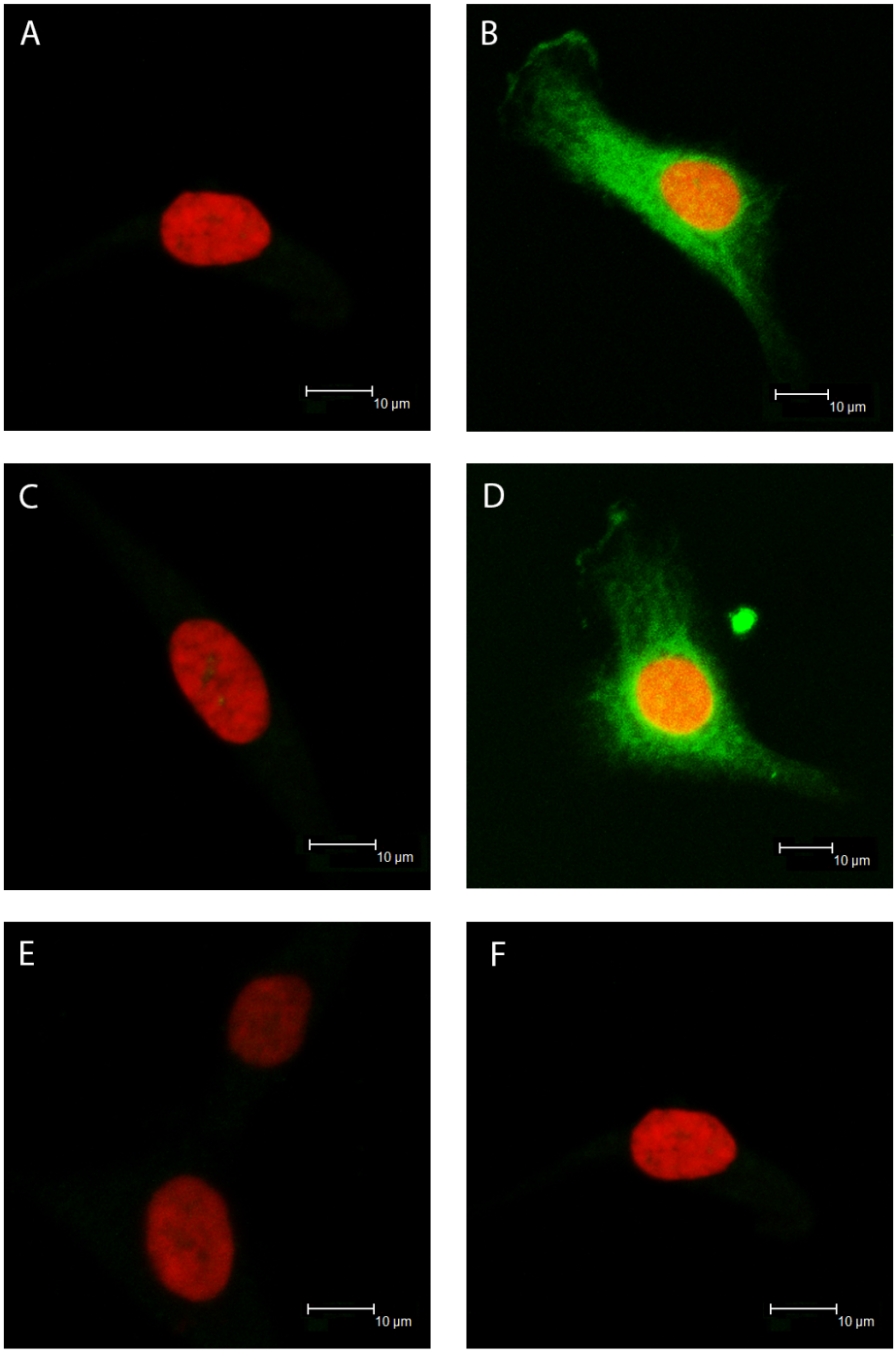


Figure 6.16 – Immunocytochemistry of EMBIGIN in FACS cells

A, C) EMBIGIN protein labelling was not evident in the culture-expanded cell lines derived from the dual-negative sorted cells. **Figure A-** A representative image of a normal cartilage-derived cell line, **Figure C-** A representative image of an OA cartilage-derived cell line. **B, D)** EMBIGIN protein labelling shows cytoplasmic labelling in culture-expanded cell lines derived from the dual-positive sorted cells. **Figure B-** A representative image of a normal derived cell line, **Figure D-** A representative image of an OA cartilage-derived cell line. **E, F)** Controls using normal cartilage-derived dual-positive cells. Figure E- an isotype matched IgG control and Figure F- a no primary antibody control.

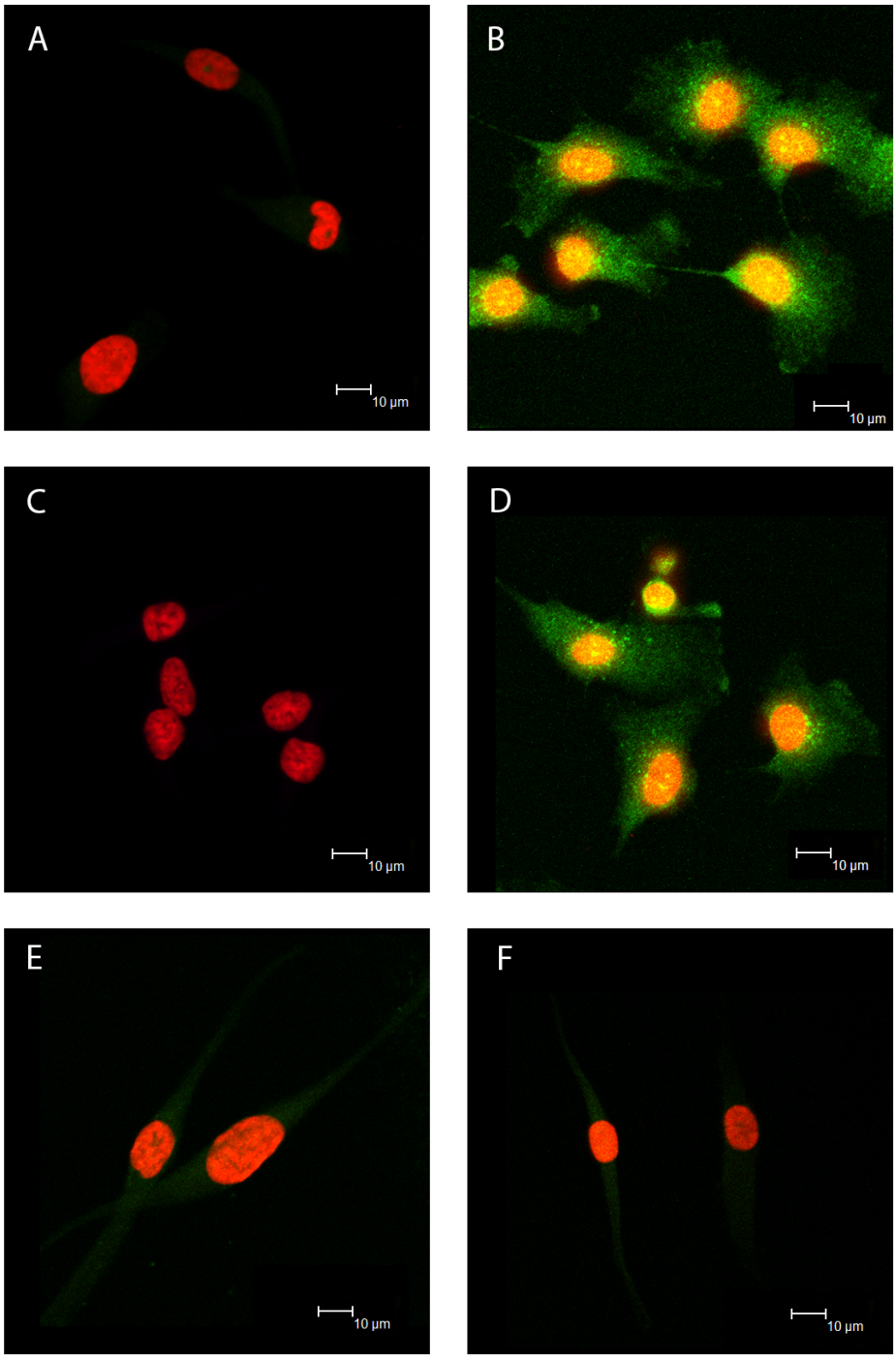


Figure 6.17 – Immunocytochemistry of EAAT1 in FACS cells

A, C) EAAT1 protein labelling was not evident in the culture-expanded cell lines derived from the dual-negative sorted cells. **Figure A-** A representative image of a normal cartilage-derived cell line, **Figure C-** A representative image of an OA cartilage-derived cell line. **B, D)** EAAT1 protein labelling shows cytoplasmic labelling in culture-expanded cell lines derived from the dual-positive sorted cells. **Figure B-** A representative image of a normal derived cell line, **Figure D-** A representative image of an OA cartilage-derived cell line. **E, F)** Controls using normal cartilage-derived dual-positive cells. Figure E- an isotype matched IgG control and Figure F- a no primary antibody control.

6.3.3.2 qPCR analysis

ACSC marker gene expression was examined through qPCR. Eight N+ve cell lines and 8 N-ve cell lines were analysed from 4 different donors; 8 OA+ve cell lines and 8 OA-ve cell lines were used from 3 separate donors. ACSC markers that were analysed were *NESTIN, FRMD5, C11ORF41, SLC1a3 (EAAT1), EMBIGIN, TMEM132B, ST6GAL2* and *KIF26B*. All ACSC markers showed a statistically significant ($p<0.005$) up-regulation in gene expression between N+ve and N-ve cohorts (Figure 6.18A-I). In OA cartilage-derived cell lines, all ACSC markers, with the exception of *ST6GAL2* showed a statistically significant ($p<0.005$) up-regulation in gene expression between OA+ve and OA-ve populations (Figure 6.19A-I). Figures 6.18A and 6.19A shows *NESTIN* gene expression in N+ve cells had a 5.0-fold increase and OA+ve cells had a 4.5-fold increase over the respective dual-negative cells. Figures 6.18B and 6.19B show *FRMD5* gene expression in the N+ve group had a 7.0-fold increase and the OA+ve cohort had a 4.8-fold increase over the respective dual-negative cells. Figures 6.18C and 6.19C show *C11ORF41* gene expression, N+ve cells had a 4.4-fold increase and OA+ve cells had a 5.8-fold increase over the respective dual-negative cells. Figures 6.18D and 6.19D shows *EMBIGIN* gene expression. N+ve had an 11.7-fold increase and OA+ve had a 6.0-fold increase over the respective dual-negative cells. Figures 6.18E and 6.19E show *EAAT1* gene expression, N+ve had a 10.4-fold increase and OA+ve had a 7.4-fold increase over the respective dual-negative cells. Figures 6.18F and 6.19F show *TMEM132B* gene expression, N+ve had a 24.9-fold increase and OA+ve had a 48.1-fold increase over the respective dual-negative cells. Figures 6.18G 6.19G and show *PRDM1* gene expression N+ve, had a 4.1-fold increase and OA+ve had a 2.3-fold increase over the respective dual-negative cells. Figures 6.18H and 6.19H show *KIF26B* gene expression N+ve had a 14.75-fold increase and OA+ve cells had a 2.6-fold increase over the respective dual-negative cells. Figures 6.18I 6.19I and show *ST6GAL2* gene expression, N+ve had a 2.8-fold increase and OA+ve had a 0.57-fold decrease over the respective dual-negative cells.

Gene expression of differentiated cartilage genes was also explored; expression of cartilage-specific genes was found to be down-regulated in both N+ve and OA+ve compared to N-ve and OA-ve chondrocytes. Aggrecan, Collagen Type II

both had statistically significant down-regulation in OA+ve ($p<0.05$) (Figure 6.19J-K). Aggrecan was significantly decreased in N+ve cells compared to N-ve cells ($p<0.05$), the decrease in Collagen Type II expression in N+ve cells was found to be non-significant (Figures 6.18J-K). SOX9 gene expression was significantly up-regulated in N+ve cell lines, but down regulate in OA+ve cell lines compared to the dual-negative populations (Figure 6.18L and 6.19L). Figures 6.18J and 6.19J show *ACAN* gene expression N+ve had a 2.8-fold decrease and OA+ve had a 92.4-fold decrease over the respective dual-negative cells. Figures 6.18K and 6.19K show *COL2A1* gene expression N+ve had a 1.6-fold decrease and OA+ve had a 3.2-fold decrease over the respective dual-negative cells. Figures 6.18L and 6.19L show *SOX9* gene expression N+ve had a 2.4-fold increase and OA+ve had a 2.0-fold decrease over the respective dual-negative cells.

To explore a possible mechanism for EMBIGIN expression specifically within ACSC the gene expression of other family members and, co-factors were investigated. No difference was observed in immunoglobulin family member *BASIGIN* gene expression between N+ve, OA+ve, N-ve and OA-ve cell lines (Figure 6.20A); whilst *EMBIGIN* gene expression was significantly up-regulated in both N+ve and OA+ve populations ($p<0.05$) (Figure 6.20B). Gene expression of monocarboxylate transporter (MCT) 1,2,3 and 4, cofactors of Basigin and EMBIGIN, were investigated. *MCT1* was not expressed in any of the cell lines used (Figure 6.20C). *MCT2* gene expression was significantly up-regulated in both N+ve and OA+ve cell cohorts ($p<0.05$), following the same pattern of expression as *EMBIGIN* (Figure 6.20D). No difference in gene expression was identified for *MCT3 or MCT4* (Figure 6.20E-F).

In summary, Dual FRMD5/EMBIGIN-positive cell lines had an increased expression of articular cartilage-derived stem cell marker genes and a reduction in genes associated with differentiated cartilage.

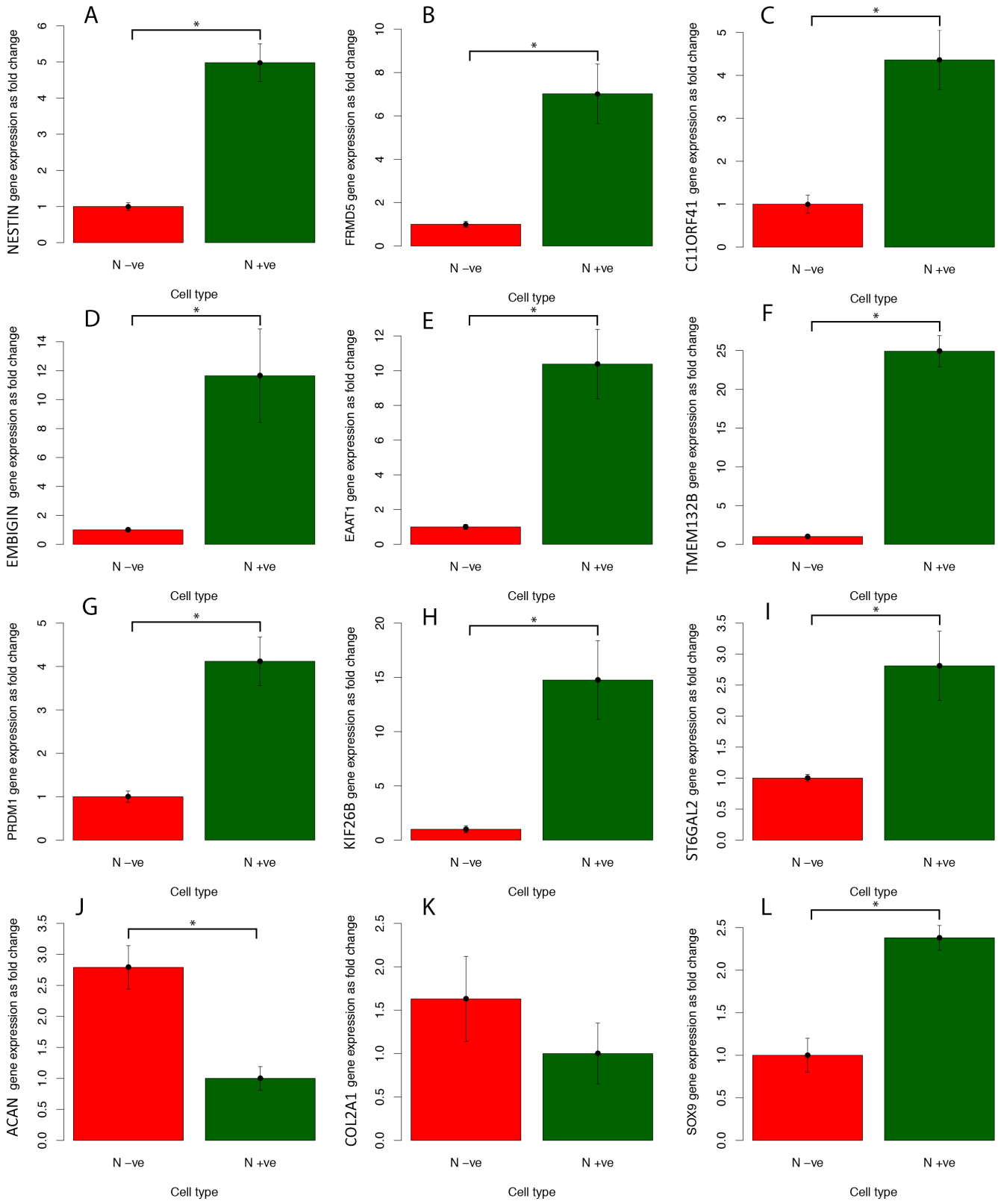


Figure 6.18 – qPCR of stem cell markers in FAC sorted cells isolated from normal cartilage

Data show that dual-positive FACS isolated cells have significantly higher gene expression of stem cell marker genes. All stem cell specific genes were found to have statistical significance ($p<0.005$) between dual-positive (N +ve) (n = 8) and dual-negative (N –ve) (n = 8) cell lines; statistical significance is denoted by (*) (Students T-test). Dual-negative cell lines had higher Aggrecan and Collagen Type II expression. **A)** *NESTIN*, **B)** *FRMD5*, **C)** *C11ORF41*, **D)** *EMBIGIN*, **E)** *EAAT1*, **F)** *TMEM132B*, **G)** *PRDM1*, **H)** *KIF26B*, **I)** *ST6GAL2*, **J)** *ACAN*, **K)** *COL2A1*, **L)** *SOX9*

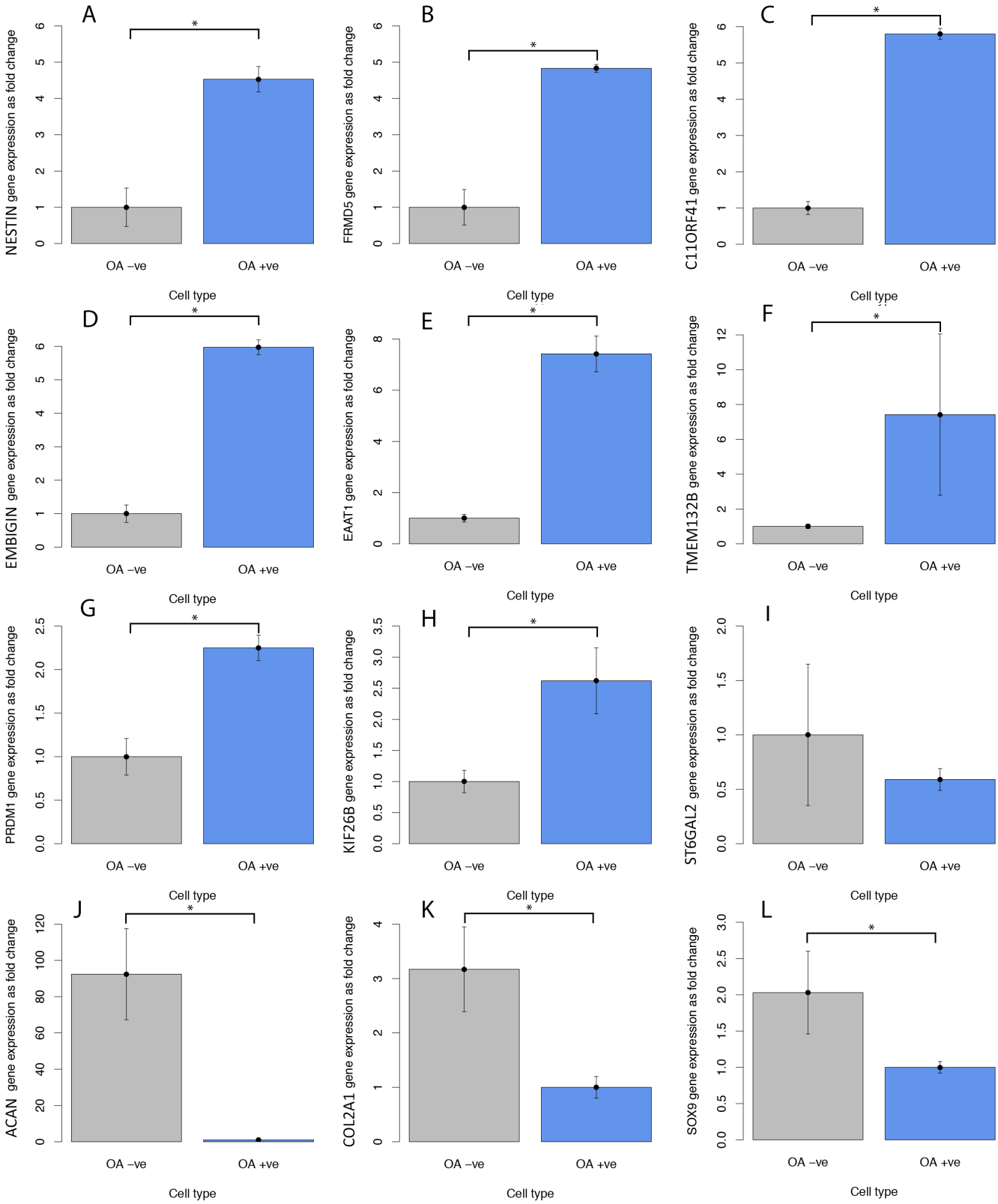


Figure 6.19 – qPCR of stem cell markers in FAC sorted cells isolated from OA cartilage

Data show that dual-positive FACS isolated cells have significantly higher gene expression of stem cell marker genes. With the exception of ST6GAL2, all stem cell specific genes were found to be statistically significant ($p<0.005$) between dual-positive (OA +ve) (n = 8) and dual-negative (OA –ve) (n = 8) cell lines; statistical significance is denoted by (*) (Students T-test). Dual-negative cell lines had higher Aggrecan and Collagen Type II expression. **A)** *NESTIN*, **B)** *FRMD5*, **C)** C11ORF41, **D)** *EMBIGIN*, **E)** *EAAT1*, **F)** *TMEM132B*, **G)** *PRDM1*, **H)** *KIF26B*, **I)** *ST6GAL2*, **J)** *ACAN*, **K)** *COL2A1*, **L)** *SOX9*

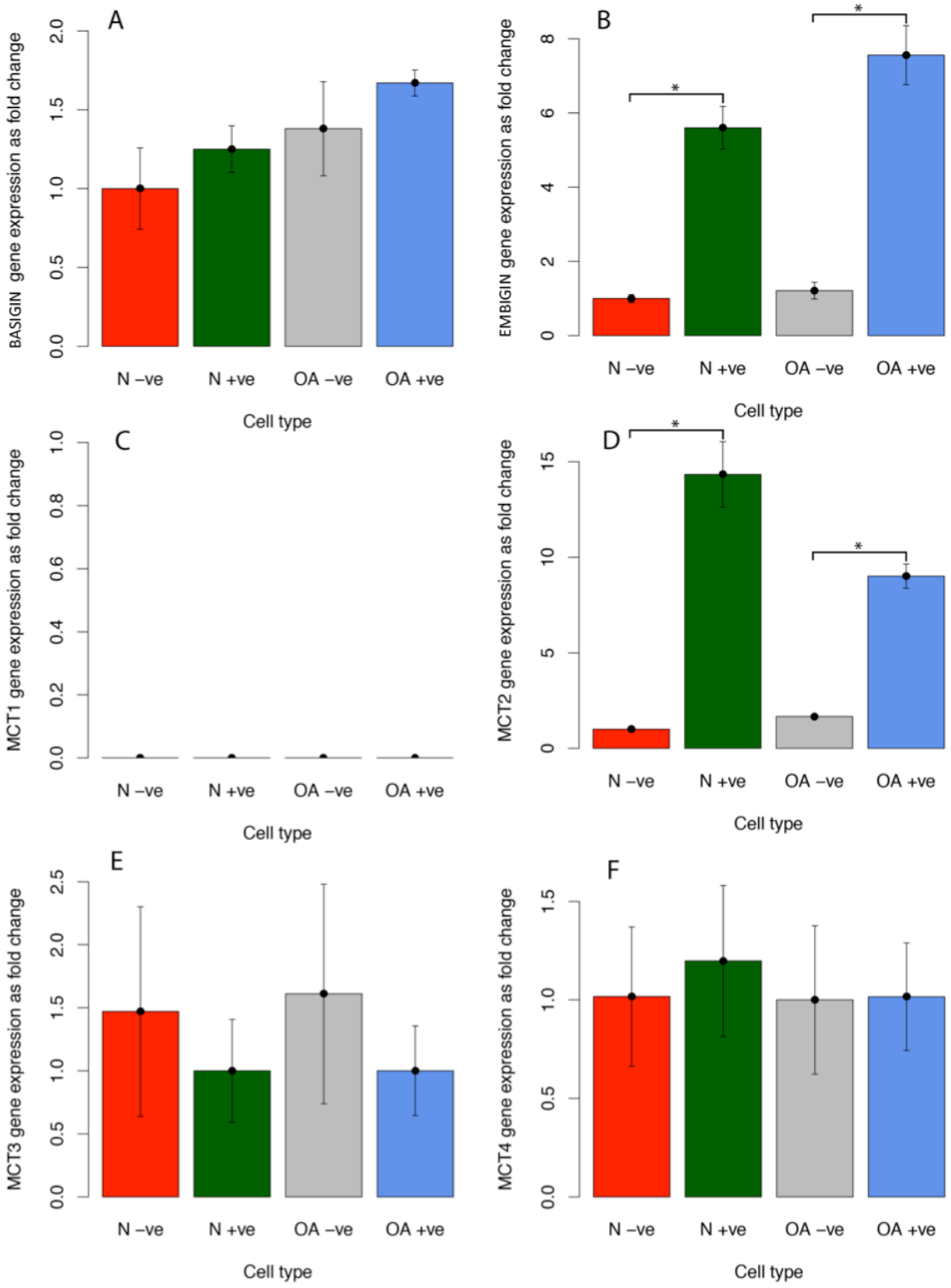


Figure 6.20 – qPCR of Basigin, EMBIGIN and Monocarboxylate transporter (MCT) -1, -2, -3 and -4 in FAC sorted cells

Data show that dual-positive FACS isolated cells have significantly higher gene expression of EMBIGIN and Monocarboxylate transporter (MCT) -2. No expression of MCT1 was observed in any of the cells lines. No difference was found in gene expression of Basigin, MCT3 and MCT4. Statistical significance ($p<0.05$) is denoted by (*) (Anova with Tukey's pair wise comparisons). **A)** *BASIGIN*, **B)** *EMBIGIN*, **C)** *MCT1*, **D)** *MCT2*, **E)** *MCT3*, **F)** *MCT4*. (n = 8 for all sample groups)

6.3.4 Phenotype plasticity

To confirm a stem cell identity for the FRMF5/EMBIGIN dual-positive cells differentiation into the chondrogenic, osteogenic and adipogenic lineages were explored

6.3.4.1 Monolayer differentiation

6.3.4.1.1 Chondrogenic differentiation

Fifty thousand N+ve and OA+ve cells from each cell line were cultured until 70-80% confluence and then induced to undergo chondrogenic differentiation for 10 days. All N+ve and OA+ve cell lines were capable of chondrogenic differentiation in monolayer. After chondrogenic induction, cell lines were stained with Alcian blue for GAG content, 3 representative cell lines from the normal and OA dual-positive populations are shown in Figure 6.21. Strong blue staining is seen in the differentiated samples, which is absent in the controls.

6.3.4.1.2 Osteogenic differentiation

Fifty thousand N+ve and OA+ve cells from each cell line were cultured until 70-80% confluence and then induced to undergo osteogenic differentiation for 10 days. All N+ve and OA+ve cell lines were capable of osteogenic differentiation in monolayer. After osteogenic induction, cell lines were stained with Alizarin red for mineralisation, 3 representative cell lines from the normal and OA dual-positive populations are shown in Figure 6.22. Strong 'brick red' staining was seen in the differentiated samples, which was absent in the controls.

6.3.4.1.3 Adipogenic differentiation

Following 10 days of adipogenic induction, the N+ve and OA+ve cell lines adopted a different morphology, cells developed a granular appearance and were more dendritic compared to the controls (Figure 6.23A-F). Histological examination using Oil red-O revealed accumulation of lipid deposits within the cells. This was consistent between all the dual-positive lines (Figure 6.23C-D). No lipid vacuoles formed in the corresponding controls (Figure 6.23E-F).

To confirm adipogenic induction, PCR of adippogenic genes was employed.

Lipoprotein lipase, fatty acid binding protein 4 and peroxisome proliferator-activator receptor 1 were all expressed in the adipogenic differentiated populations and absent in the control (Figure 6.24). The house-keeping gene ribosomal protein S18 was consistent across the control and adipogenic samples. No bands were present in the negative controls. Strong bands were evident in the adipocyte positive control for *LPL, FABP4* and *PPAR1*.

6.3.4.2 3D-pellet culture differentiation

6.3.4.2.1 3D chondrogenic differentiation

Dual-positive cells ($5x10^5$ cells at 25PD) were chondrogenically induced into 3D-pellets for 3 weeks (Figures 6.25.5A-G and 6.26A-G). These pellets were smooth and opalescent, resembling a typical hyaline cartilage surface. The pellets formed were fairly consistent in size between polycolonal cell lines of different donors, typically about 1.0mm. All FACS dual-labelled cell lines were capable of chondrogenic differentiation. The ECM present in pellets was visualised by toluidine blue staining (Figure 6.25) and safranin-O staining (Figure 6.26). Figure 6.25A-D and Figure 6.26A-D represent pellets formed from N+ve cell lines, Figure 6.25E-F and 6.26E-F represent pellets formed from OA+ve cell lines. GAG deposition was evident with both toluidine blue and safranin-O staining; however safranin-O staining provided better detection. Varying amounts of GAG were observed in pellets from different cell lines. The most abundant detection of GAG was evident around the periphery of the pellet. For N+ve pellets, pellet A (N+ve1, donor CF01N) had the strongest touldine blue and safranin-O staining, especially around the edges of the pellet. In pellet B (N+ve2, donor CF02N), it can be seen that there are areas that lack GAG deposition particularly in the centre of the pellet. The pellets C (N+ve3, donor CF03N) and pellet D (N+ve4, donor CF04N) had comparable GAG content, again, the largest deposition of GAG was at the pellet edge. For OA+ve pellets, pellet F (OA+ve2, donor CF02OA) had the strongest touldine blue and safranin-O staining, with very high deposition at the periphery of the pellet. In pellet E (OA+ve2, donor CF01OA), it can be seen that there is a large accumulation of GAG at the periphery in the safranin-O staining that is not apparent in the toluidine blue staining. Pellets G (OA+ve3, donor CF03OA) had more uniform GAG deposition throughout the pellet.

The level of GAG in the pellet was quantified using DMMB and normalised to wet

weight (Figure 6.27). The variability in GAG content between individual cell lines seen histologically was again identified (Figure 6.27A). No difference in average GAG content was observed between normal cartilage-derived dual-positive cell lines and OA cartilage-derived dual-positive cell lines (normal derived = 118.0 μg ml^{-1} g^{-1}, OA = 119.9 μg ml^{-1} g^{-1}) (Figure 6.27B). The cell lines whose pellets had the strongest histological staining were the pellets with the highest GAG content when quantified through DMMB. All dual-labelled cell lines had GAG content that was evident.

The expression of chondrogenic genes were analysed through qPCR. Aggrecan, Collagen Type II, Collagen Type IX and lubricin were all significantly increased in the chondrogenic pellets compared to undifferentiated controls ($p<0.05$) (Figures 6.28 and 6.29). Collagen Type XI was found only significantly increased in N+ve cell line pellets not in OA+ve cell line pellets compare to undifferentiated controls. *COL2A1* gene expression had the largest increase after differentiation, increasing 398.0-fold in N+ve pellets and 308.9-fold in OA+ve pellets compared to undifferentiated controls (Figures 6.28B and 6.29B). *ACAN* gene expression increased 7.5-fold in N+ve pellets and 35.7-fold in OA+ve pellets (Figures 6.28A and 6.29A). *COL9A1* gene expression increased 11.5-fold in N+ve pellets and 2.0-fold in OA+ve pellets (Figures 6.28C and 6.29C). *COL11A2* gene expression increased 6.81-fold in N+ve pellets and 2.1-fold in OA+ve pellets (Figures 6.28A and 6.29A). *PRG4* gene expression increased 3.2-fold in N+ve pellets and 4.0-fold in OA+ve pellets (Figures 6.28A and 6.29A). No change in *SOX9* gene expression was observed after differentiation of N+ve cell lines (Figure 6.28F); however, *SOX9* significantly decreased 2.7-fold after differentiation in the OA pellets ($p<0.05$) (Figure 6.29F).

Protein labelling of Collagen Type II and Aggrecan within dual-labelled cell line chondrogenic pellets was analysed by Immunofluorescence. All cell lines showed Collagen Type II labelling within the pellets with the strongest labelling at the periphery (Figure 6.30). In the normal cartilage-derived cell lines, pellet A (N+ve1, donor CF01N) had the strongest labelling, then pellet D (N+ve4, donor CF04N). The weakest labelling was pellet B (N+ve2, donor CF02N), which also had the least GAG. In the OA cartilage-derived cell lines pellet F (OA+ve2, donor CF02OA) had the strongest labelling at the periphery, however, pellets E (OA+ve1, donor CF01OA) and G (OA+ve3, donor CF03OA) had greater labelling

throughout the pellets. All cell lines showed Aggrecan labelling within the pellets again, the strongest labelling was often at the edges (Figure 6.31). In the normal cartilage-derived cell lines pellet A (N+ve1, donor CF01N) had the strongest labelling, concentrated around the edges. Pellet D also had strong peripheral labelling (N+ve4, donor CF04N). Once more the weakest labelling was pellet B (N+ve2, donor CF02N), with only the outer edge of the pellet showing Aggrecan antibody labelling. In OA derived dual-positive cell lines, all pellets had similar Aggrecan antibody labelling throughout the pellet. Pellets with the greatest GAG content were also found to have the largest Collagen Type II and Aggrecan protein labelling, showing a superior differentiation has occurred.

Dual-negative cells were also found to be capable of forming chondrogenic pellets that histologically and through DMMB showed GAG deposition (data not shown).

After 3 weeks of chondrogenic differentiation, gene expression for ACSC marker genes was investigated. Stem cell marker genes were all significantly down-regulated in both normal cartilage-derived dual-positive pellets and OA cartilage-derived dual-positive pellets compared to undifferentiated controls ($P<0.005$) (Figures 6.32 and 6.33). The exception was *PRDM1* in N+ve pellets which was reduced but found to be non-significant ($p>0.05$) (Figure 6.32G); it was, however, significant in OA+ve pellets ($p<0.05$) (Figure 6.33G).

6.3.4.2.2 Osteogenic differentiation

Osteogenic differentiation was induced in a 3D-pellet culture system using $5x10^5$ cells at 25PD (Figures 6.34A-G). Gross morphology of the osteogenic pellets after 3 weeks closely resembled that of the chondrogenic pellet, with a smooth white surface. Sectioned pellets were stained using Alizarin red to demonstrate deposits of calcium and mineral-rich matrix. Figure 6.34A-D represents pellets formed from N+ve cell lines, Figure 6.34E-F represent pellets formed from OA+ve cell lines. All normal and OA dual-positive cell lines were found to be capable of osteogenic differentiation to a greater or lesser extent, signified by brick red staining with Alizarin red (Figure 6.34). Dual-negative chondrocytes from both normal and OA cartilage were not able to form osteogenic pellets, the pellets disintegrated after 1-2 weeks for all cell lines. Normal pellet A (N+ve1, donor CF01N) and pellet C (N+ve3, donor CF03N) were found to be capable of

complete osteogenesis with the whole pellet staining with alizarin red. Normal pellet B (N+ve2, donor CF02N) and pellet D (N+ve4, donor CF04N) were only partially differentiated with a section of the pellet staining with alizarin red. OA pellet G (OA+ve2, donor CF02OA) was capable of complete osteogenesis, while OA pellet E (OA+ve1, donor CF01OA) and pellet F (OA+ve3, donor CF03OA) were only partially differentiated. Whether partial differentiation is due to insufficient time for complete osteogenic differentiation of osteogenic capacity is unknown.

Upon osteogenic differentiation, even partial differentiation, osteogenic genes were significantly up-regulated. In normal cartilage-derived dual-labelled osteogenic pellets, alkaline phosphatase, Collagen Type I, Collagen Type X, osteocalcin and RUNX2 were all significantly increased compared to undifferentiated controls ($p<0.05$) (Figure 6.35). In OA cartilage-derived dual-labelled osteogenic pellets, alkaline phosphatase, Collagen Type I and osteocalcin significantly increased compared to undifferentiated controls ($p<0.05$) (Figure 6.35A, B, D). No significant increase was observed in Collagen Type X or RUNX2 in the OA+ve osteogenic samples (Figure 6.35C, D) The largest increase was observed in alkaline phosphatase which was increased 1623.8-fold in N+ve osteogenic pellets and 411.2-fold in OA+ve osteogenic pellets compared to undifferentiated controls (Figures 6.35A and 6.36A). Collagen Type I was increased by 6.1-fold in N+ve osteogenic samples and 3.1-fold in OA+ve osteogenic samples (Figures 6.35B and 6.36B). Collagen Type X was increased by 3.9-fold in N+ve osteogenic samples and 1.3-fold in OA+ve osteogenic samples (Figures 6.35C and 6.36C). Osteocalcin was increased by 7.1-fold in N+ve osteogenic samples and 3.2-fold in OA+ve osteogenic samples (Figures 6.35D and 6.36D). Finally, RUNX2 was increased by 12.9-fold in N+ve osteogenic samples and 1.3-fold in OA+ve osteogenic samples (Figures 6.35E and 6.36E).

Articular cartilage-derived FRMD5/EMBIGIN dual-positive cells were found to be capable of multipotent tri-lineage differentiation into chondrogenic, osteogenic and adipogenic lineages.

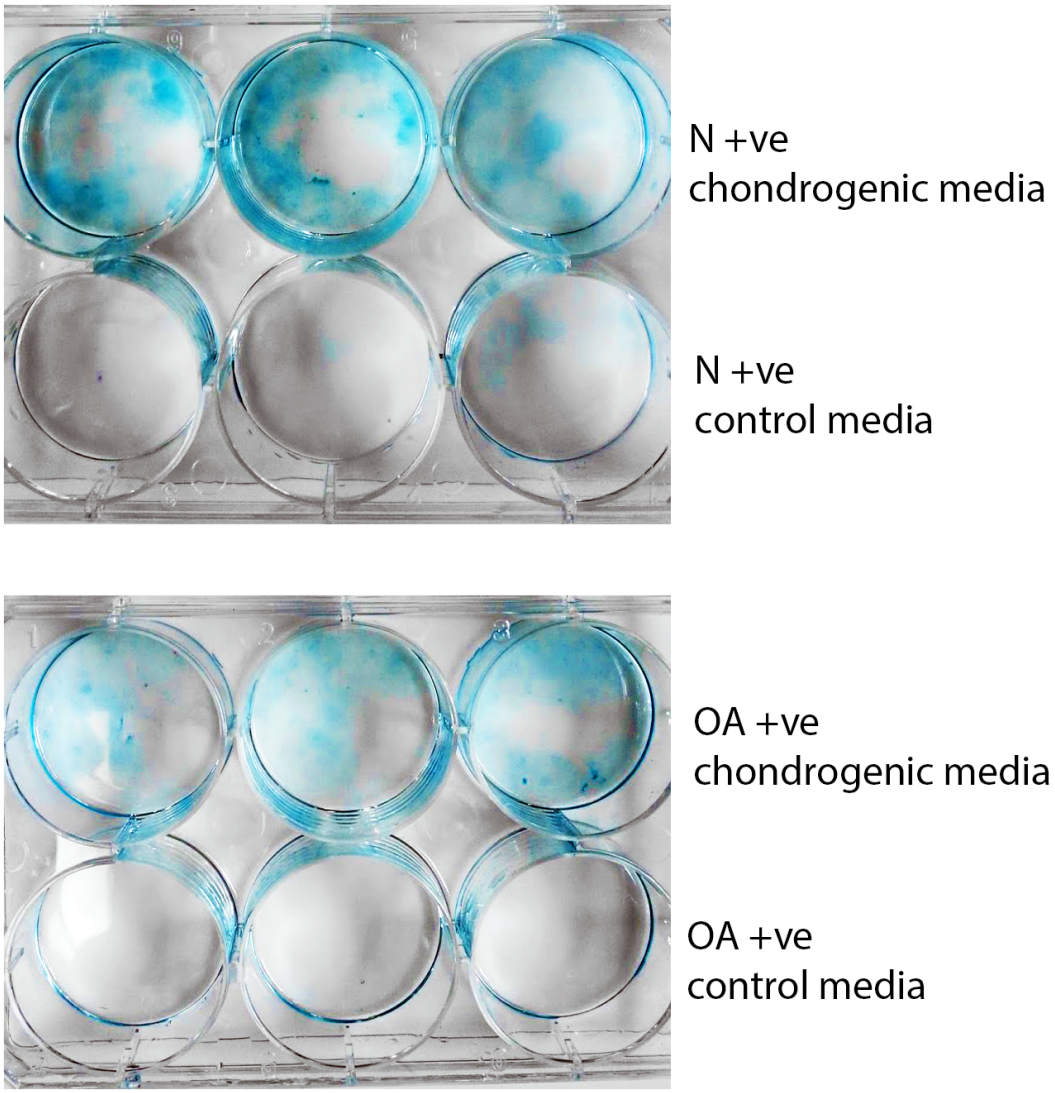


Figure 6.21 – Monolayer chondrogenic differentiation of FACS cells.

Alcian blue staining for proteoglycan can clearly be seen in both the normal and OA cells that have been culture in the chondrogenic differentiation media.

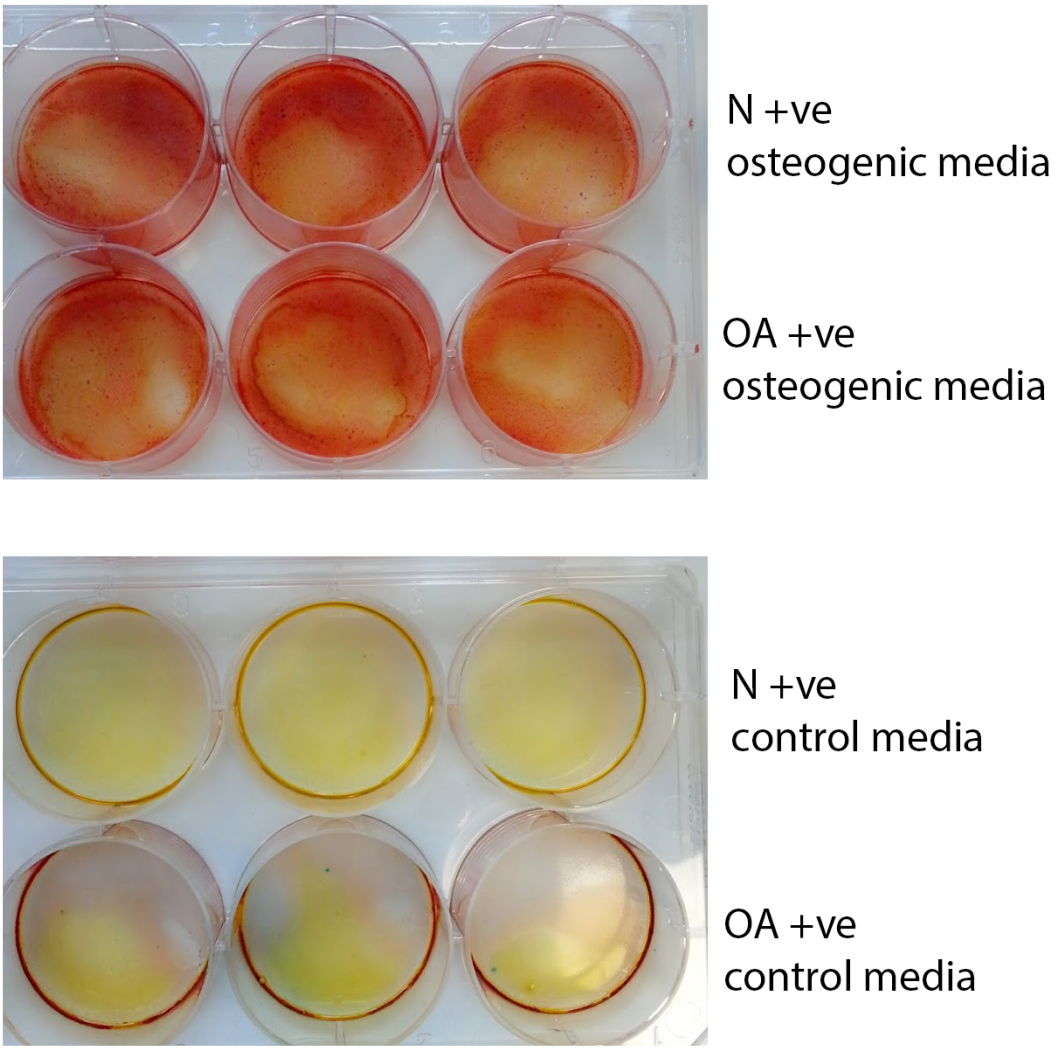


Figure 6.22 – Monolayer osteogenic differentiation of FACS cells.

Alizarin red staining for mineralisation can clearly be seen in both the normal and OA cells that have been culture in the osteogenic differentiation media.

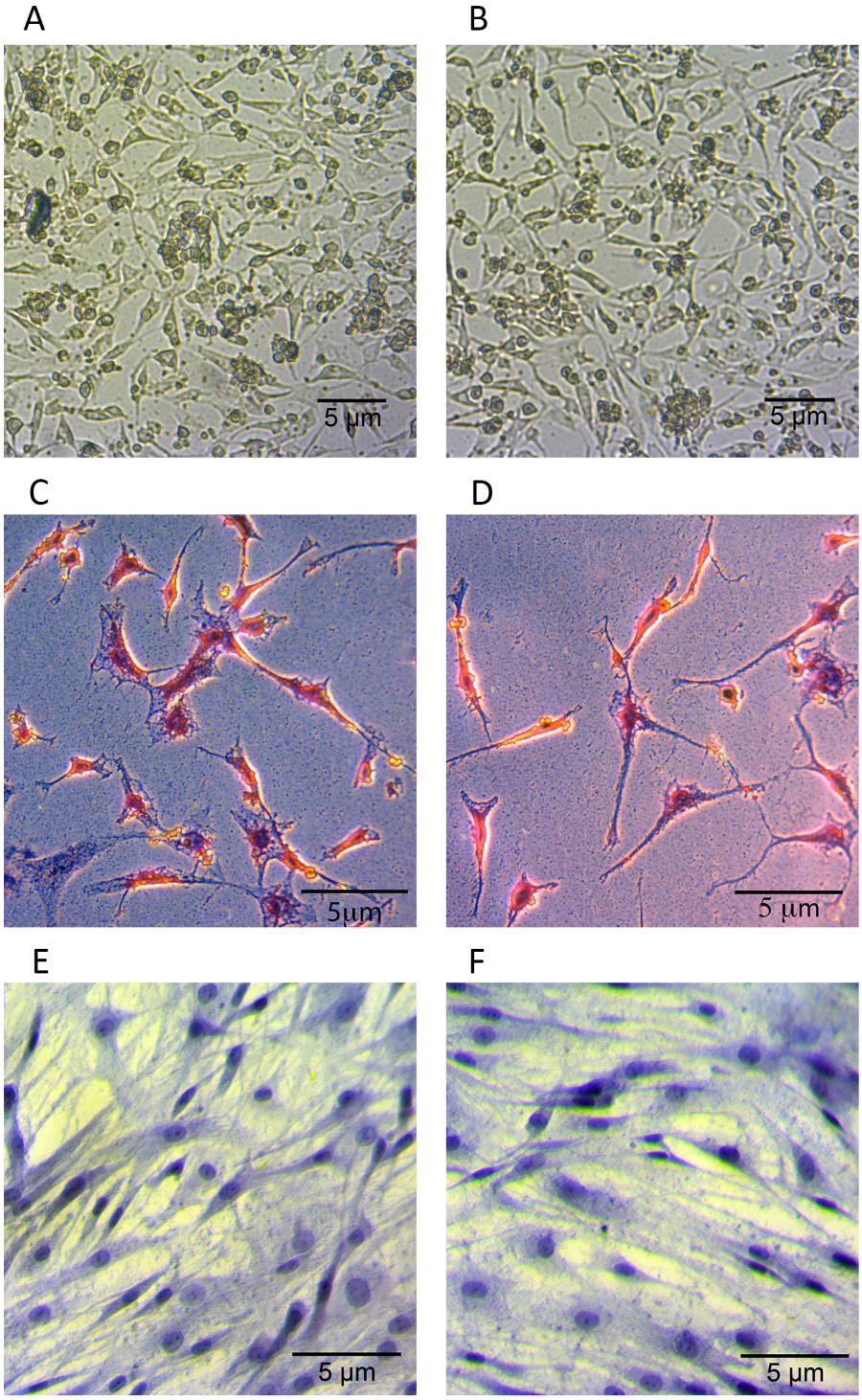


Figure 6.23 – Monolayer adipogenic differentiation of FACS cells.

A, B) Normal cartilage **(A)** and osteoarthritic cartilage **(B)** derived dual-positive cells after 7 days in adipogenic media start to acquire a granular morphology. Representative images **C, D)** Normal cartilage **(C)** and osteoarthritic cartilage **(D)** derived dual-positive cells after 10 days in adipogenic media, stained using oil red O to highlight lipid vacuoles. Cells are counter-stained with crystal violet. Representative images. **E, F)** Normal cartilage **(E)** and osteoarthritic cartilage **(F)** derived dual-positive cells after 10 days in control media, stained using oil red O and counter stained with crystal violet. No lipid vacuole formation can be seen.

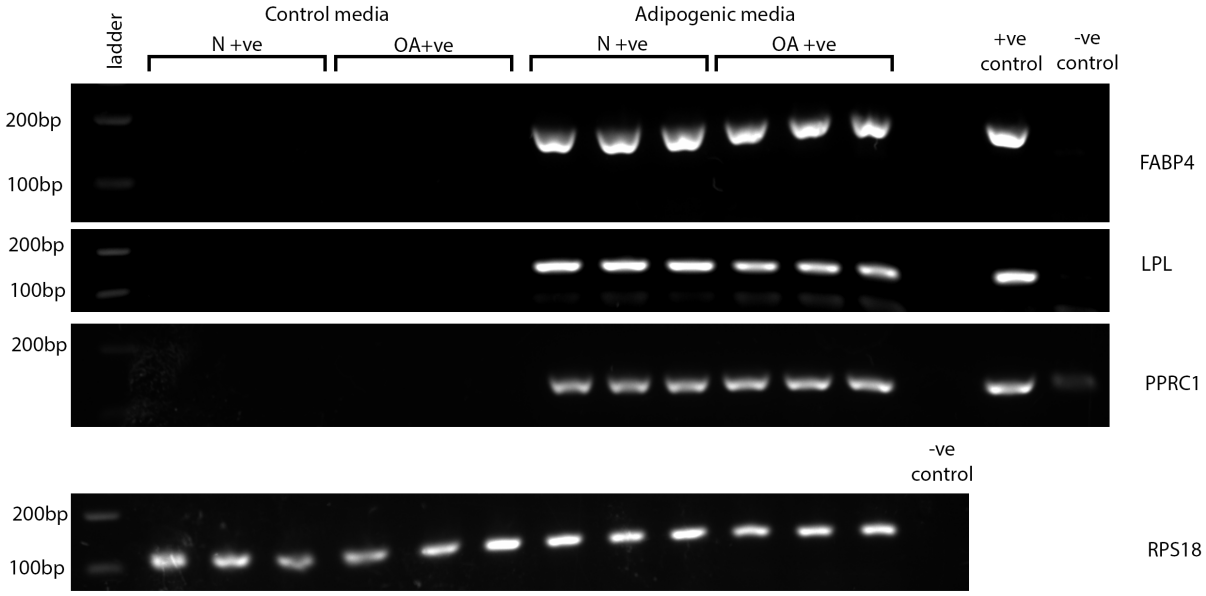


Figure 6.24 – PCR for adipogenic genes in adipogenic induced cultures.

All normal and osteoarthritic dual-positive cell lines were capable of adipogenic differentiation. Cells cultured in control media do not express adipogenic genes. Cells cultured in adipogenic differentiation media exhibit strong expression of fatty acid binding protein 4 (FABP4), lipoprotein lipase (LPL) and peroxisome proliferator activated receptor gamma coactivator-related protein 1 (PPRC1). Ribosomal protein S18 (RPS18) as used as a house-keeping gene, expression can be seen in both the control and the adipogenic cultures.

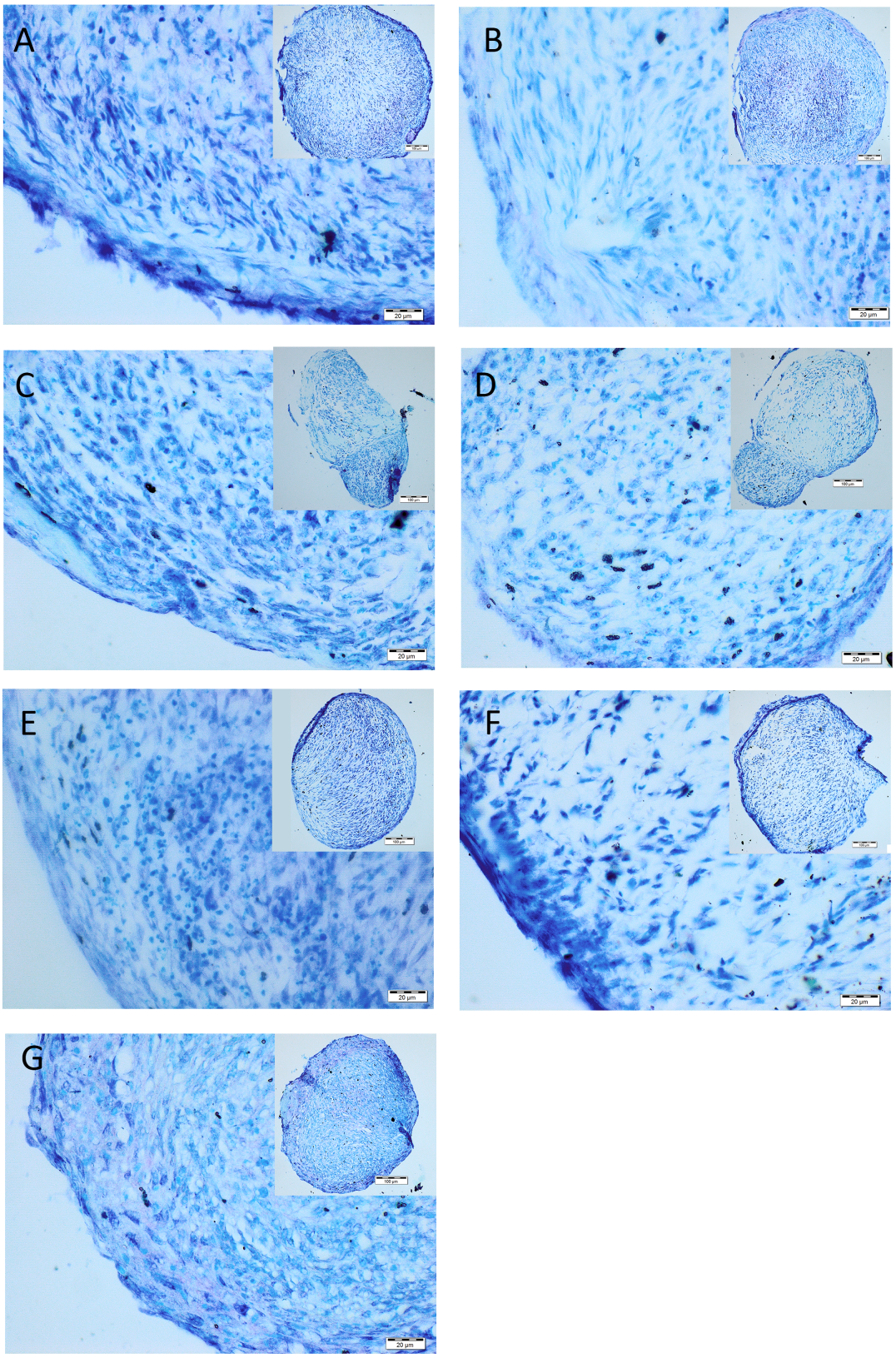


Figure 6.25 – Three dimensional chondrogenic differentiation of FACS cells.

Metachromatic Toluidine blue staining for proteoglycan in 3-week chondrogenic induced pellet cultures. Varying amounts of proteoglycan can be seen between each cells line. **A, B, C and D)** Pellets formed from normal cartilage-derived dual-positive cells. **E, F, and G)** Pellets formed from OA cartilage-derived dual-positive cells. All dual-positive cell lines were capable of chondrogenic differentiation. **A)** N+ve1 (CF01N) **B)** N+ve2 (CF02N) **C)** N+ve3 (CF03N) **D)** N+ve4 (CF04N) **E)** OA+ve1 (CF01OA) **F)** OA+ve2 (CF02OA) **G)** OA+ve3 (CF03OA).

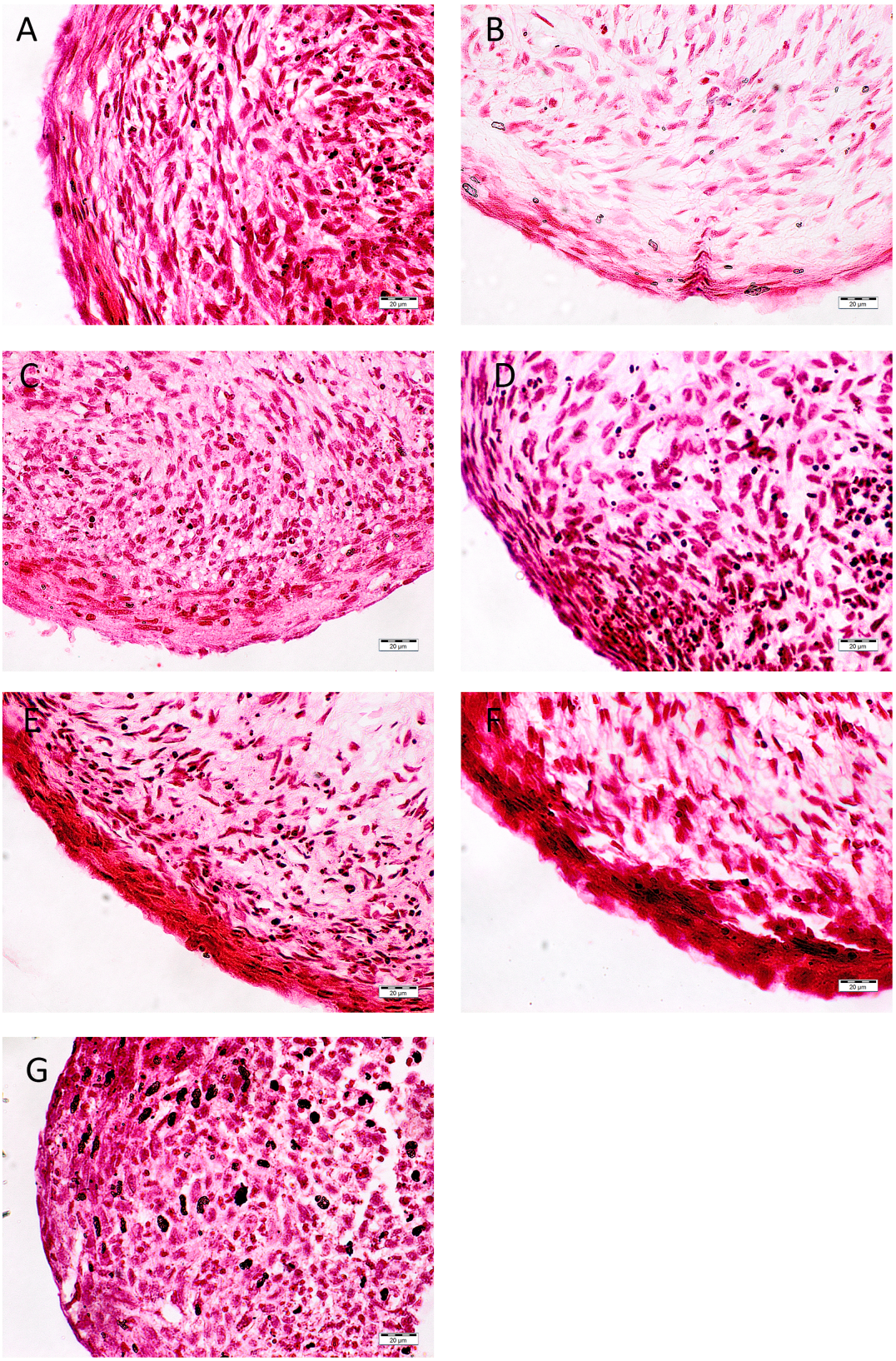


Figure 6.26 – Three dimensional chondrogenic differentiation of FAC sorted cells.

Safranin-O staining for proteoglycan in 3-week chondrogenic induced pellet cultures. Varying amounts of proteoglycan can be seen between each cells line**. A, B, C and D)** Pellets formed from normal cartilage-derived dual-positive cells. **E, F, and G)** Pellets formed from OA cartilage-derived dual-positive cells. All dual-positive cell lines were capable of chondrogenic differentiation. The strongest staining can be seen at the edges of the pellet when the most differentiation has occurred. **A)** N+ve1 (CF01N) **B)** N+ve2 (CF02N) **C)** N+ve3 (CF03N) **D)** N+ve4 (CF04N) **E)** OA+ve1 (CF01OA) **F)** OA+ve2 (CF02OA) **G)** OA+ve3 (CF03OA)**.**

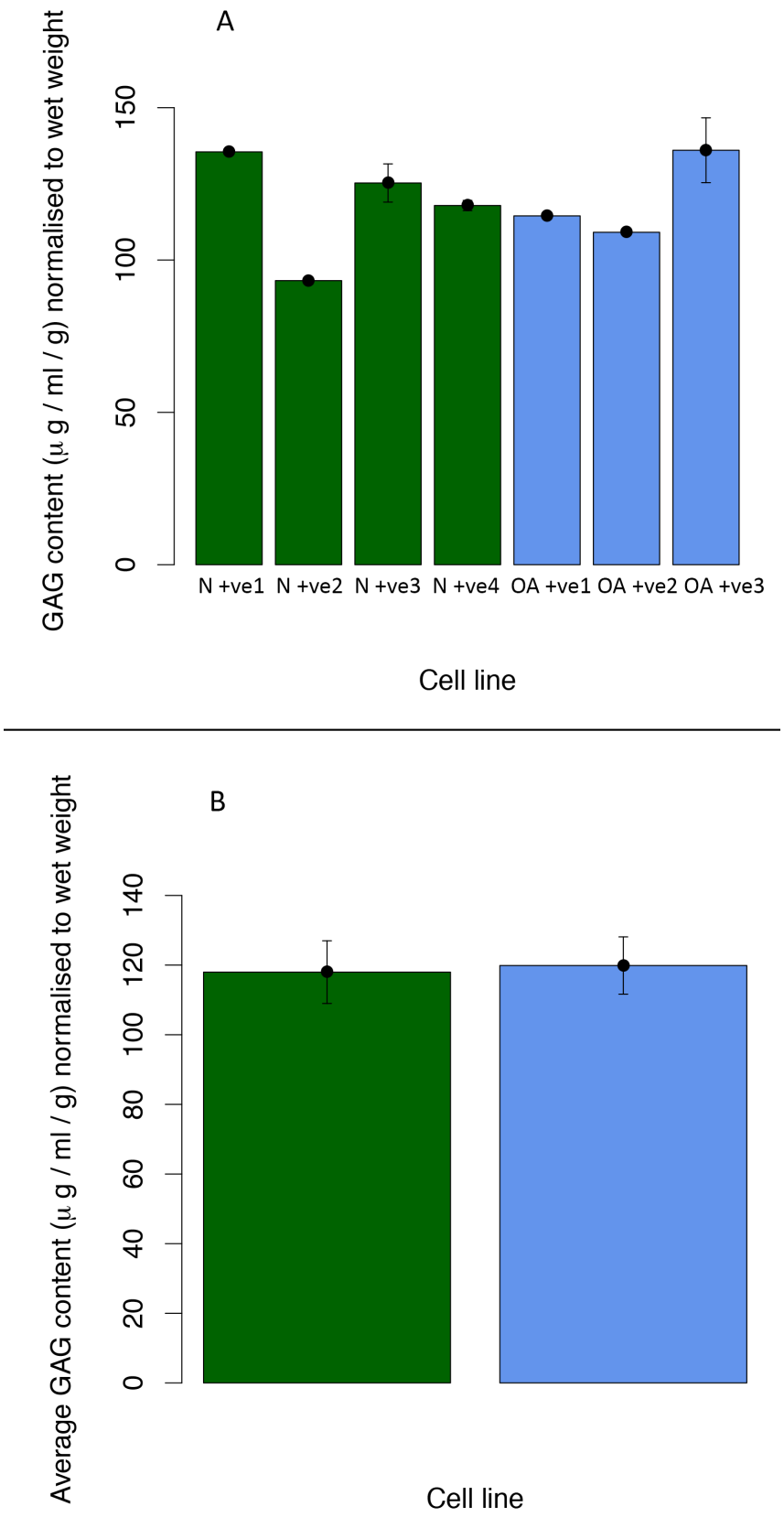


Figure 6. 27 – DMMB assay quantifying glycosaminoglycan (GAG) content of chondrogenic pellets.

A) Variation in the quantity of GAG content was observed between cell lines. **B)** No difference in the average quantity of GAG was observed between normal and OA derived cell lines.

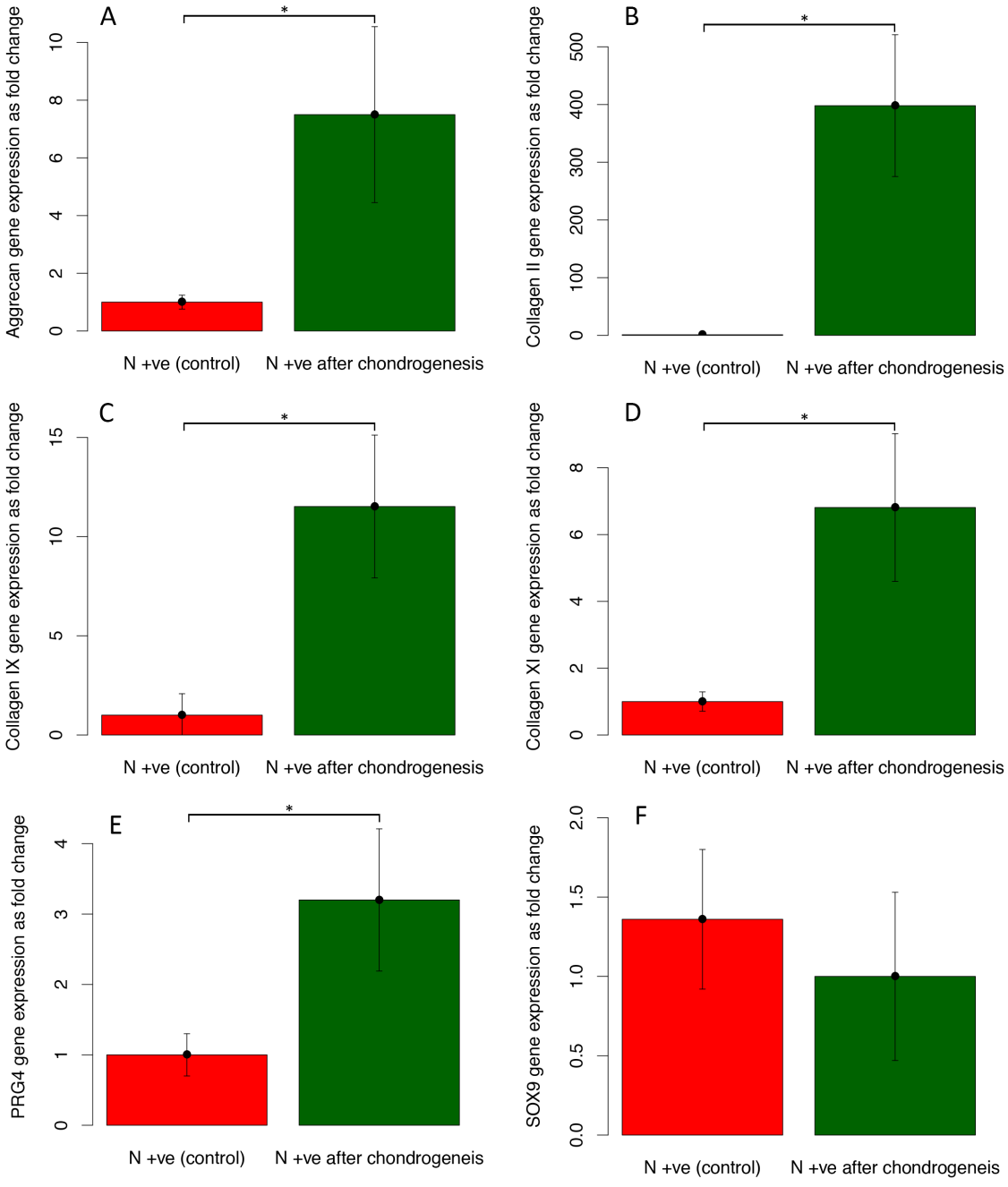


Figure 6.28 – qPCR for chondrogenic genes in 3D chondrogenic pellet culture differentiation of FACS cells from normal tissue.

Genes associated with differentiated articular cartilage were all significantly ($p<0.05$) up-regulated after culture in chondrogenic media for 3 weeks in pellet culture. *SOX9* gene expression stayed constant. **A)** *ACAN*, **B)** *COL2A1*, **C)** *COL9A1*, **D)** *COL11A2*, **E)** PRG4, **F)** *SOX9*. (n = 8 for both sample groups).

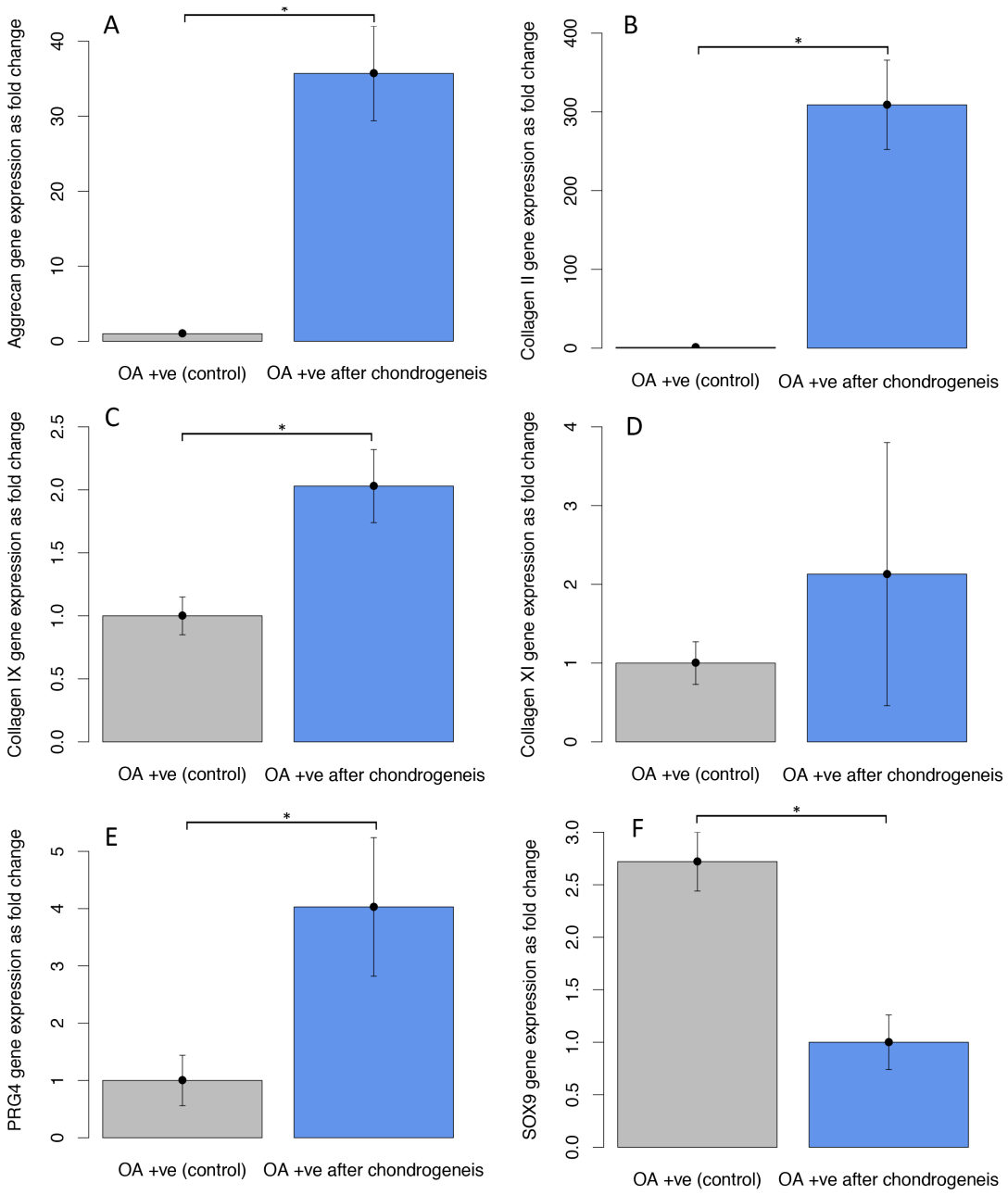


Figure 6.29 – qPCR for chondrogenic genes in 3D chondrogenic pellet culture differentiation of FACS cells from OA tissue.

Genes associated with differentiated articular cartilage were significantly ($p<0.05$) up-regulated after culture in chondrogenic media for 3 weeks in pellet culture. No significant change was found in Collagen Type XI gene expression. **A)** *ACAN*, **B)** *COL2A1*, **C)** *COL9A1*, **D)** *COL11A2*, **E)** *PRG4*, **F)** *SOX9*. (n = 8 for both sample groups).

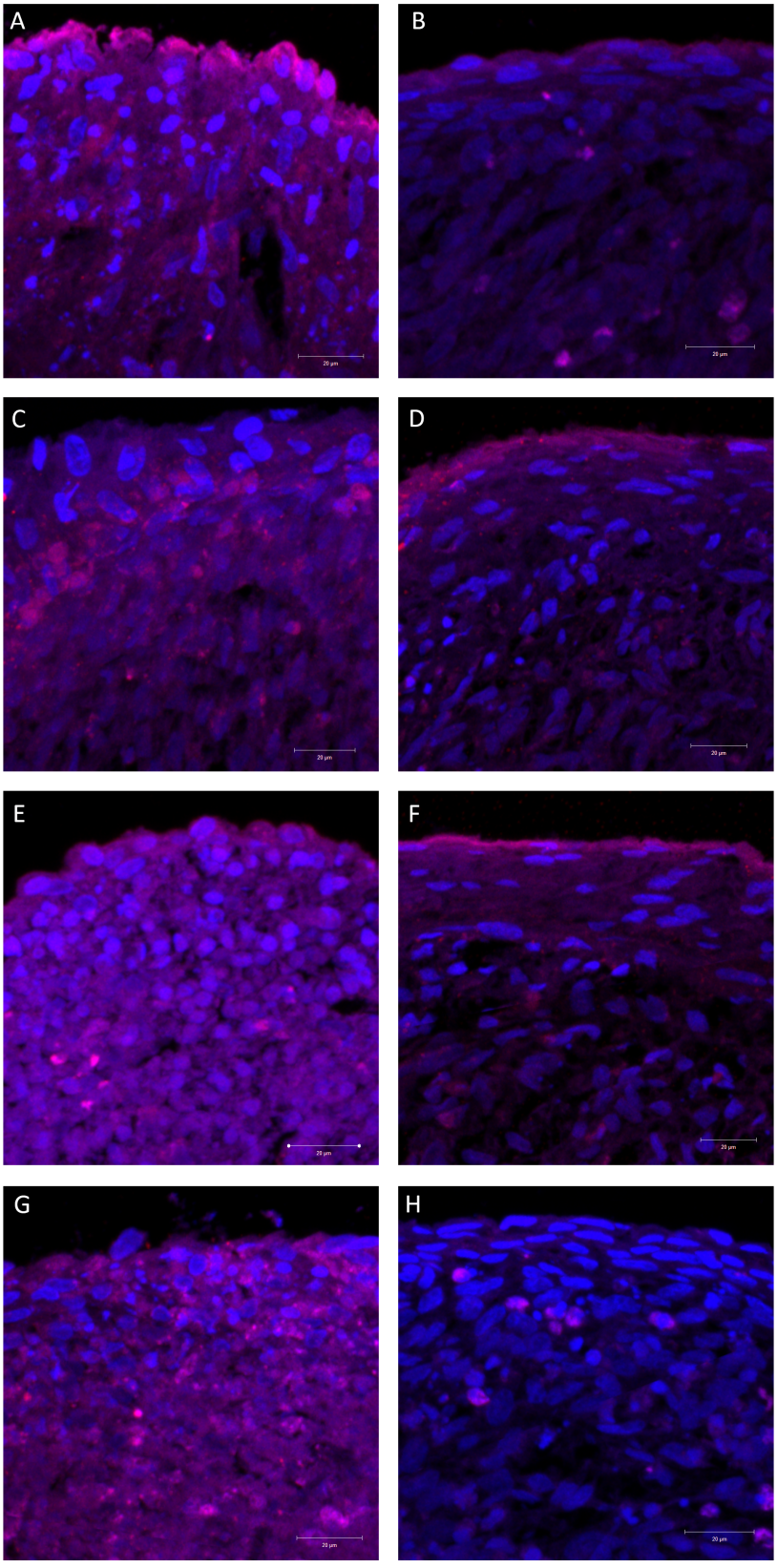


Figure 6.30 – Immunofluorescence for Collagen Type II in 3D chondrogenic pellet culture differentiation of FACS cells.

Collagen Type II is expressed in varying amounts in the chondrogenic pellets with the strongest labelling at the edges of the pellets. **A, B, C and D**) Chondrogenic pellets derived from normal cartilage. **E, F, G)** Chondrogenic pellets derived from OA cartilage. **H**) No primary control. **A)** N+ve1 (CF01N) **B)** N+ve2 (CF02N) **C)** N+ve3 (CF03N) **D)** N+ve4 (CF04N) **E)** OA+ve1 (CF01OA) **F)** OA+ve2 (CF02OA) **G)** OA+ve3 (CF03OA).

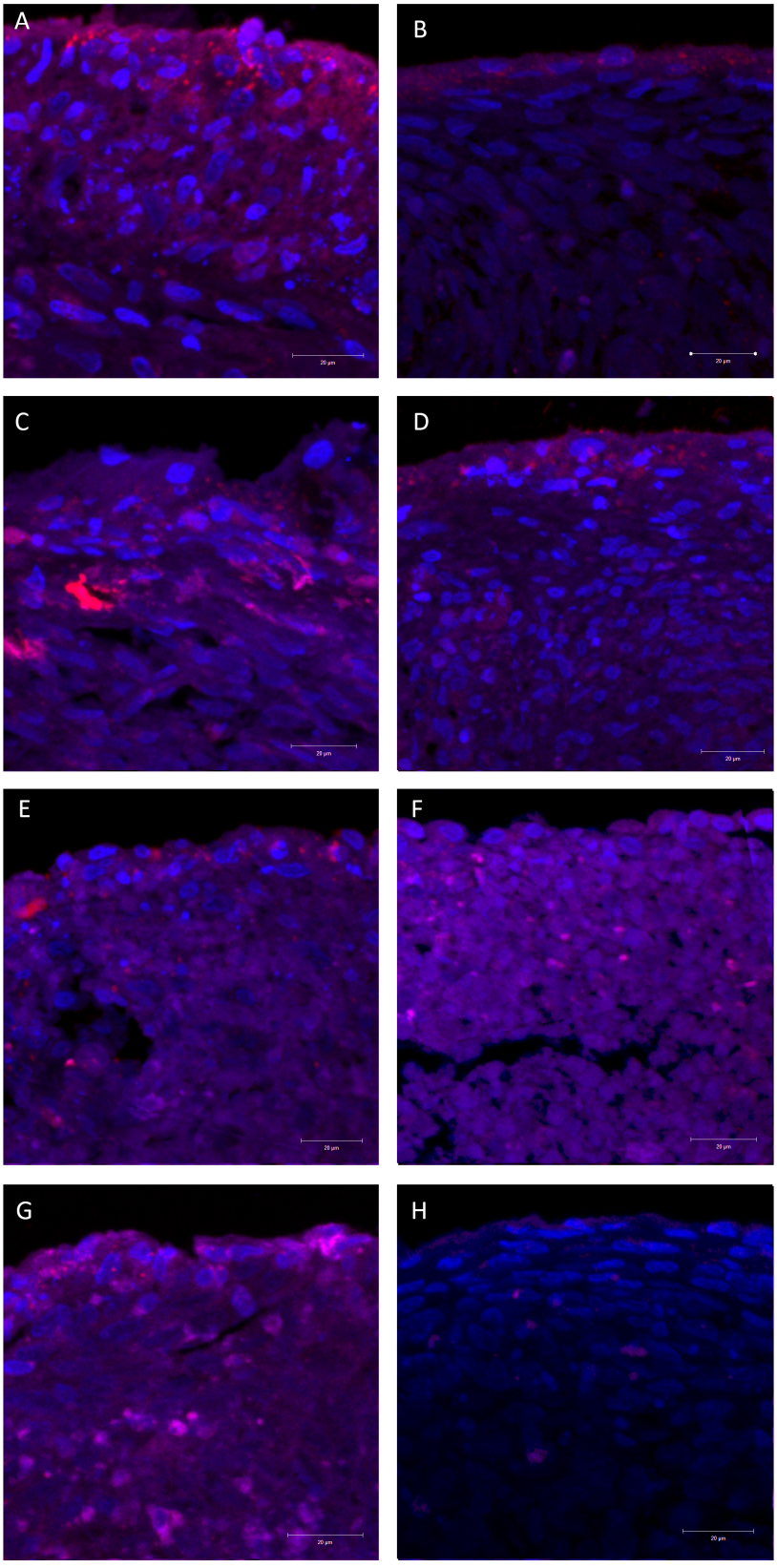


Figure 6.31 – Immunofluorescence for Aggrecan in 3D chondrogenic pellet culture differentiation of FACS cells.

Aggrecan is expressed in varying amounts in the chondrogenic pellets with the strongest labelling at the edges of the pellets. **A, B, C and D)** Chondrogenic pellets derived from normal cartilage. **E, F, G)** Chondrogenic pellets derived from OA cartilage. **H**) No primary control. **A)** N+ve1 (CF01N) **B)** N+ve2 (CF02N) **C)** N+ve3 (CF03N) **D)** N+ve4 (CF04N) **E)** OA+ve1 (CF01OA) **F)** OA+ve2 (CF02OA) **G)** OA+ve3 (CF03OA)**.**

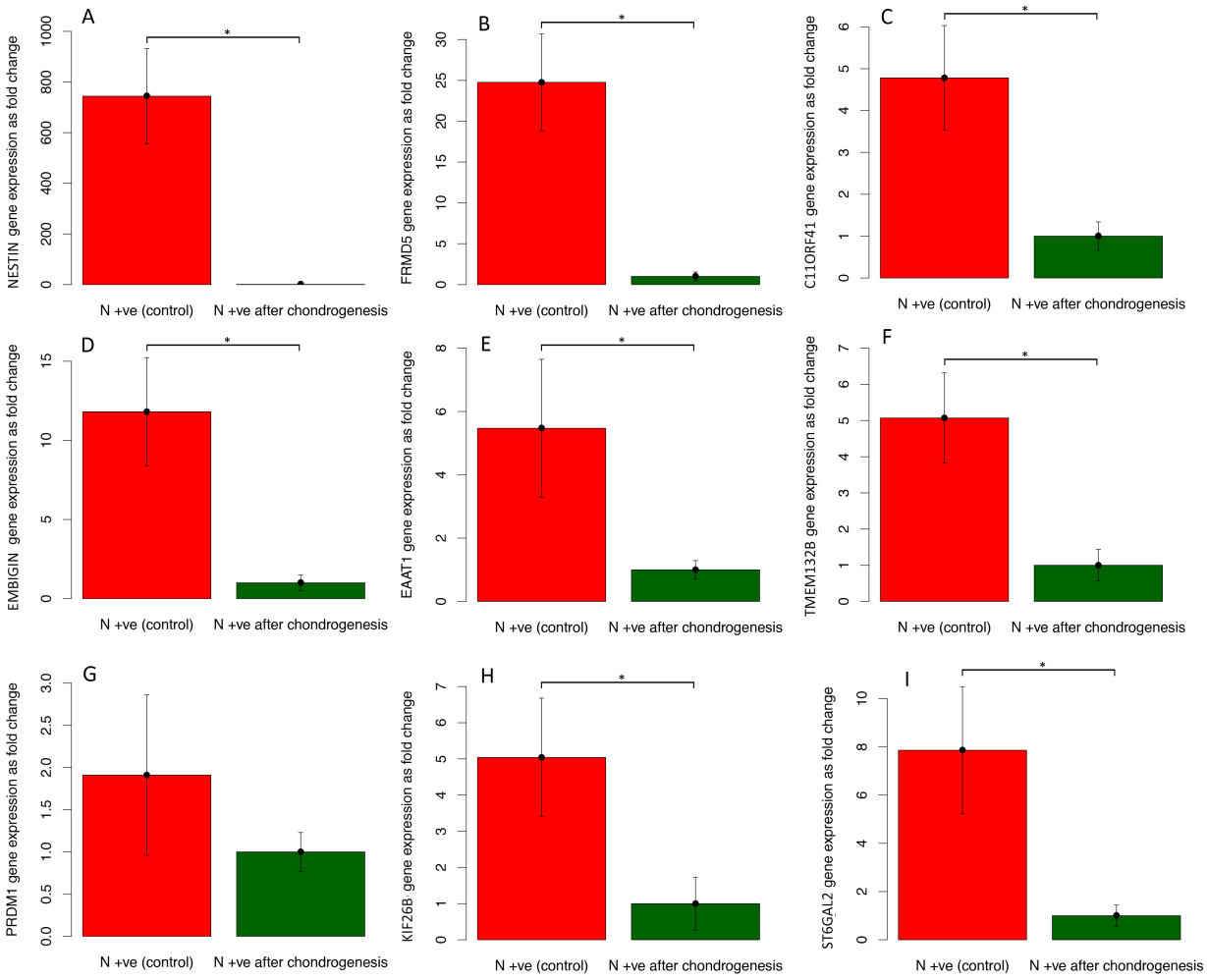


Figure 6.32 – qPCR for stem cell marker genes in 3D chondrogenic pellet culture differentiation of FACS cells from normal tissue.

Stem cell marker gene expression is down-regulated upon chondrogenic differentiation. Statistical significance is down by (*), (P<0.005, Student's T-test). **A)** NESTIN, **B)** FRMD5, **C)** C11ORF41, **D)** EMBIGIN, **E)** EAAT1, **F)** TMEM132B, **G)** PRDM1, **H)** KIF26B, **I)** ST6GAL2.(n = 8 for both sample groups).

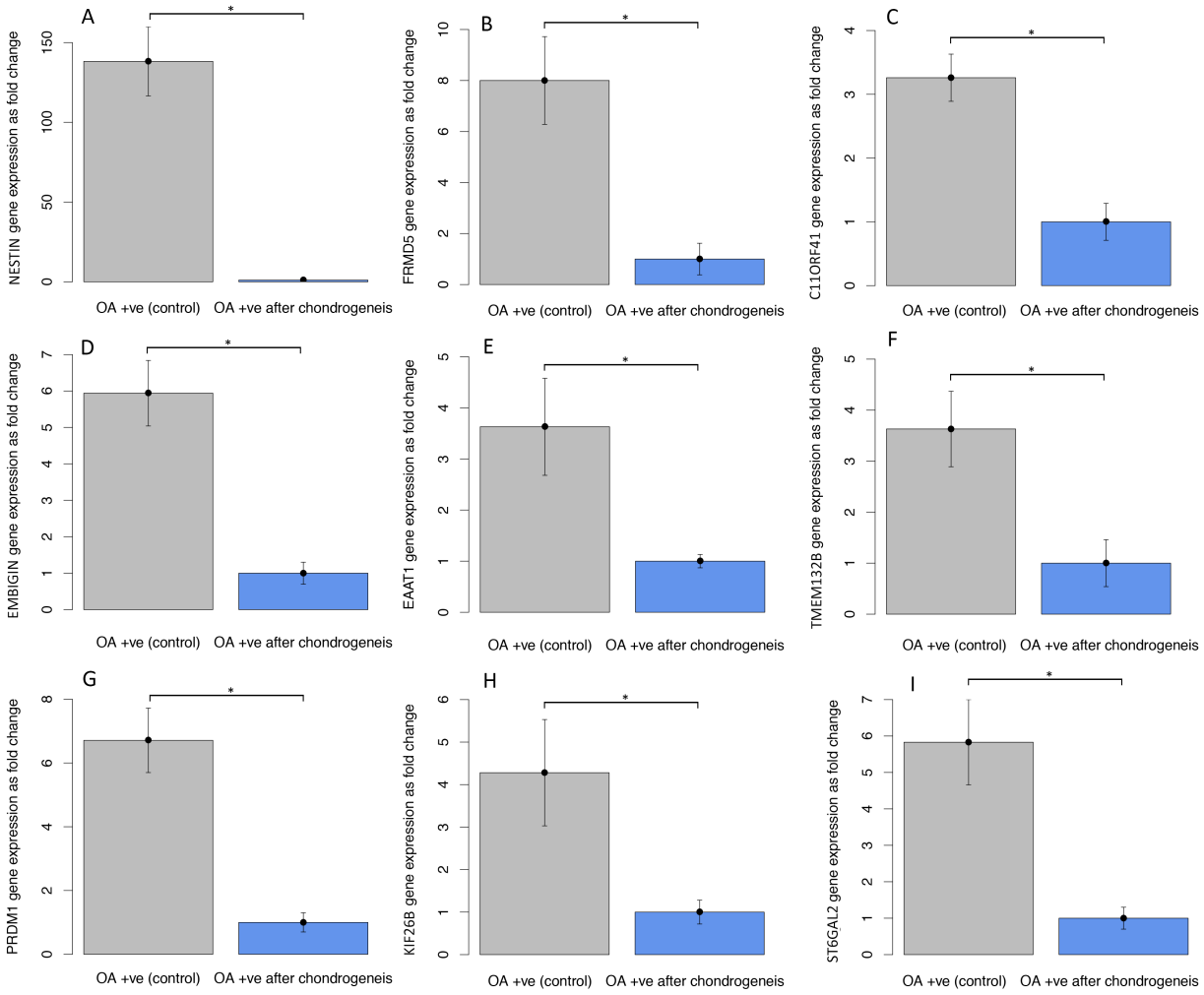


Figure 6.33 – qPCR for stem cell marker genes in 3D chondrogenic pellet culture differentiation of FACS cells from OA tissue.

Stem cell marker gene expression is down-regulated upon chondrogenic differentiation. Statistical significance is down by (*), ($P<0.005$, Student's T-test). **A)** NESTIN, **B)** FRMD5, **C)** C11ORF41, **D)** EMBIGIN, **E)** EAAT1, **F)** TMEM132B, **G)** PRDM1, **H)** KIF26B, **I)** ST6GAL2. (n = 8 for both sample groups).

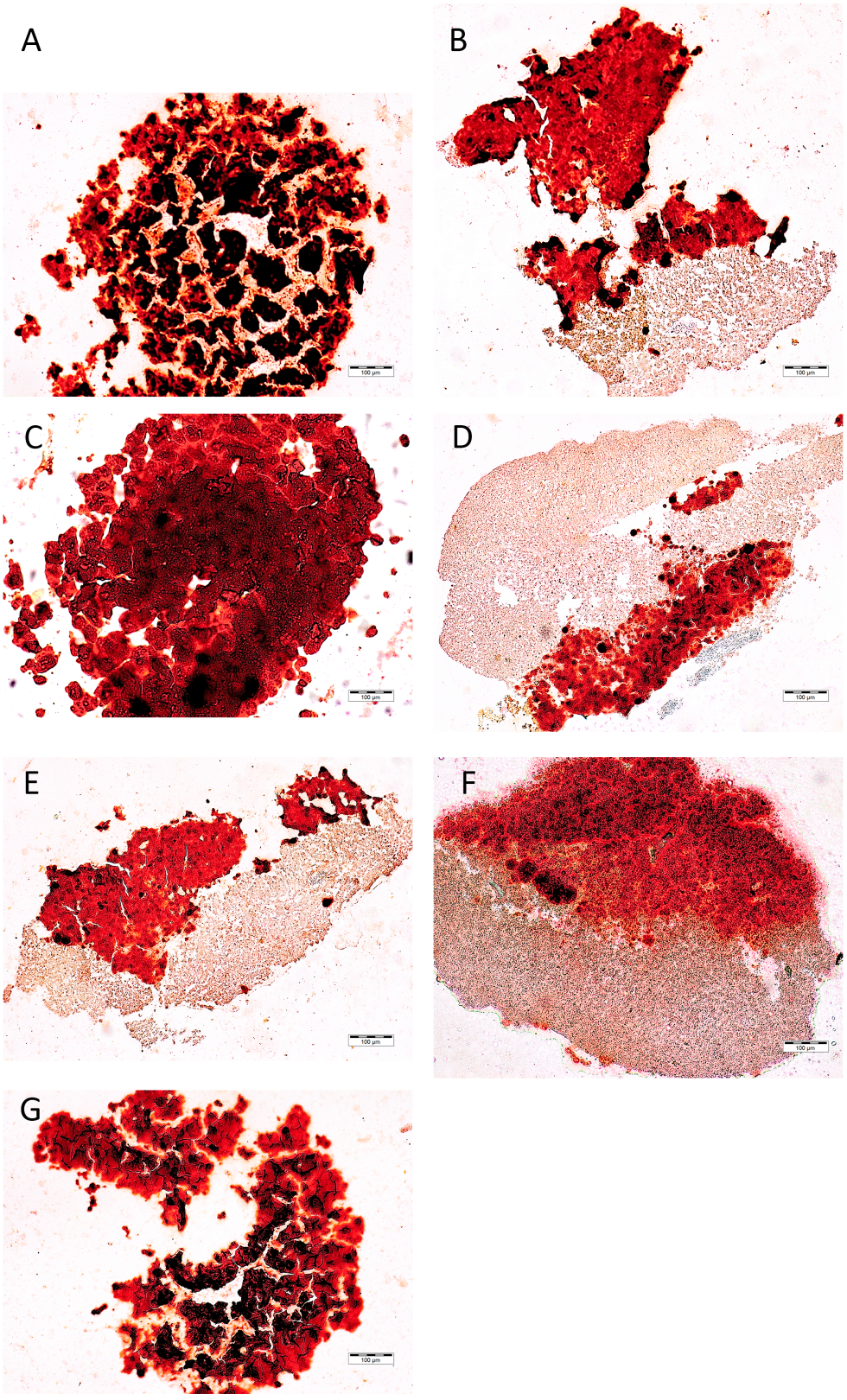


Figure 6.34 – Three dimensional osteogenic differentiation of FAC sorted cells.

Alizarin red showing mineral deposits in 3-week osteogenic pellet cultures. **A-D)** Osteogenic pellets from normal cartilage-derived dual-positive cells. **E-G)** Osteogenic pellets from OA cartilage-derived dual-positive cells. Varying degrees of mineralisation can been seen. **Figures A, C and G** show complete mineralisation while **Figures B, D, E and F** have degrees of partial mineralisation. All cell lines have started to undergo osteogenic differentiation after 3 weeks, the degree and speed of differentiation is varied. Scale bar 100µm. **A)** N+ve1 (CF01N) **B)** N+ve2 (CF02N) **C)** N+ve3 (CF03N) **D)** N+ve4 (CF04N) **E)** OA+ve1 (CF01OA) **F)** OA+ve2 (CF02OA) **G)** OA+ve3 (CF03OA).

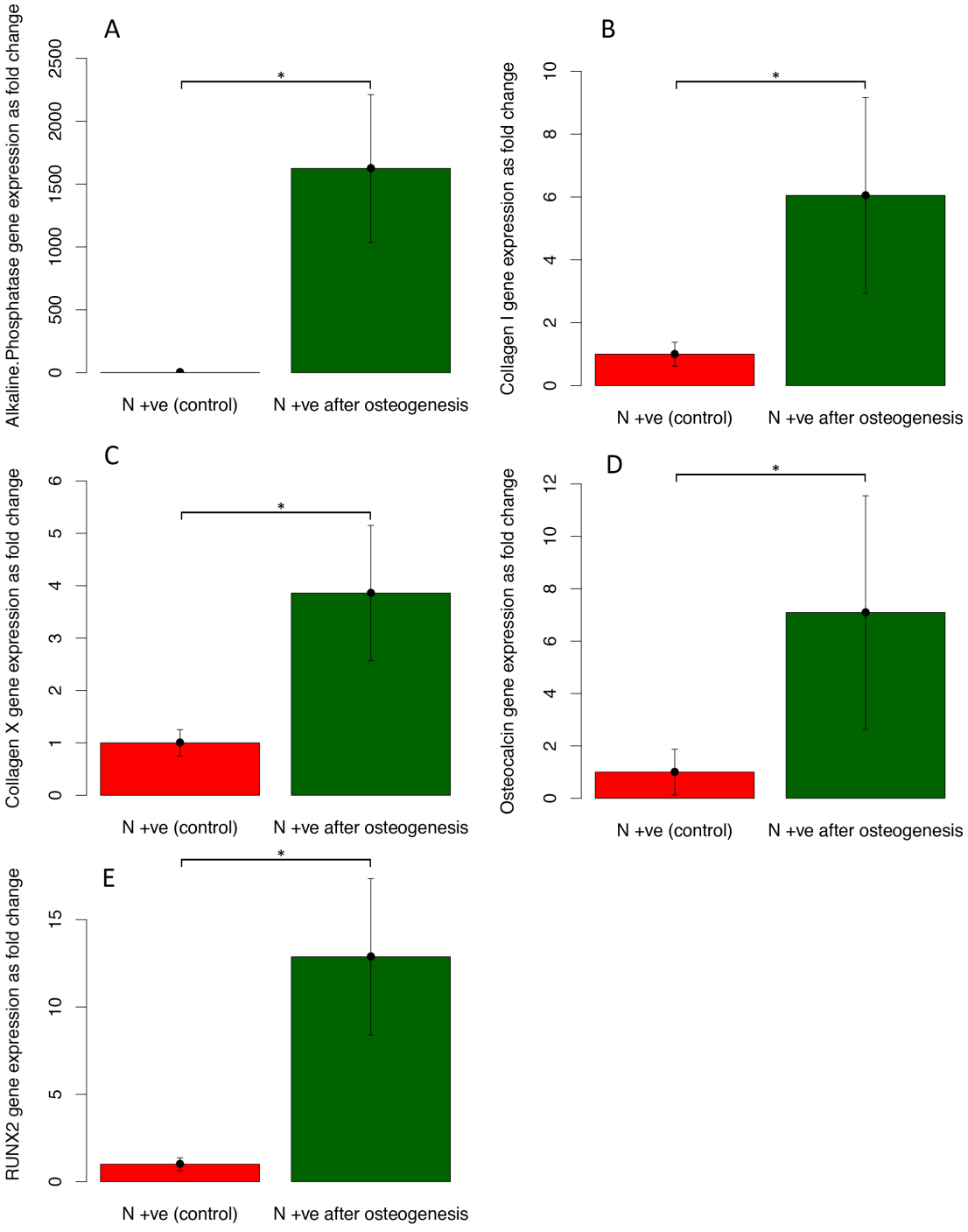


Figure 6.35 – qPCR for osteogenic genes in 3D chondrogenic pellet culture differentiation of FACS cells from normal tissue.

Alkaline phosphatase, Collagen Type I, Collagen Type X, osteocalcin and RUNX2 were all found to be significantly increased in the osteogenic cultures. ($P<0.05$, Student's T-test). **A)** *ALPL*, **B)** *COL1A1*, **C)** *COL10A1*, **D)** *BGLAP*, **E)** *RUNX2*. (n = 8 for both sample groups).

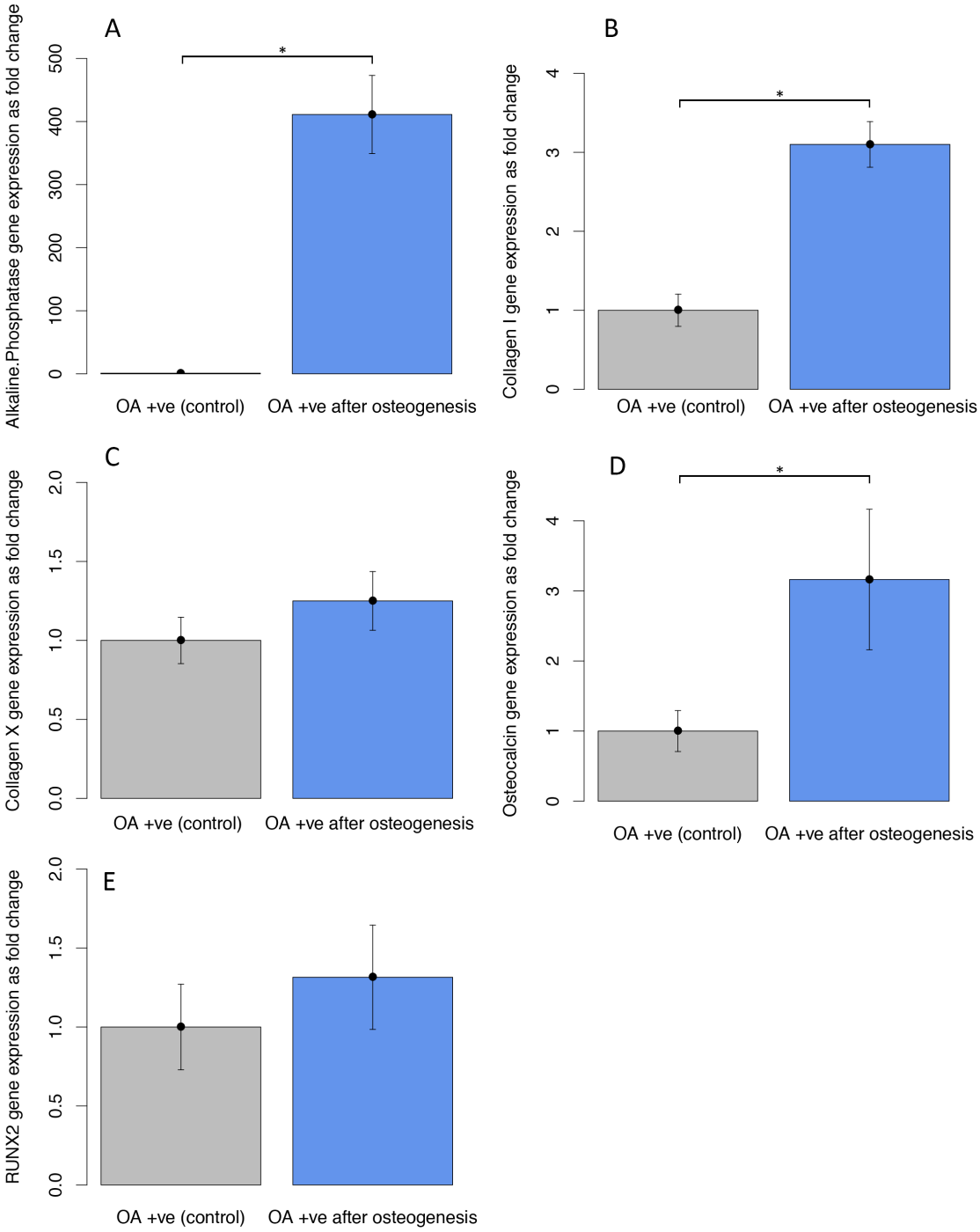


Figure 6.36 – qPCR for osteogenic genes in 3D chondrogenic pellet culture differentiation of FAC sorted cells from normal tissue.

Alkaline phosphatase, Collagen Type I and, osteocalcin were found to be significantly increased in the osteogenic cultures. ($P<0.05$, Student's T-test). No increase in Collagen Type X or RUNX2 was observed in the OA derived osteogenic cultures. **A)** *ALPL*, **B)** *COL1A1*, **C)** *COL10A1*, **D)** *BGLAP*, **E)** *RUNX2*. (n = 8 for both sample groups).

6.4 Discussion

In this Chapter, chondrocytes were isolated from full-thickness cartilage biopsies of normal and osteoarthritic articular cartilage. Cells were immunolabelled immediately following isolation and analysed for the expression of FRMD5, EAAT1 and EMBIGIN through flow-cytometry. Analyses were immediately conducted following digestion in an attempt to quantify expression levels *in vivo*. However, during enzymatic digestion, cell surface markers or transmembrane receptors may be cleaved resulting in reduced labelling or absence of these markers (Diaz-Romero et al., 2005). The absence of EAAT1 labelling after digestion could be due to pronase digestion of the epitope; therefore, only FRMD5 and EMBIGIN were used for subsequent analyses.

A small sub-population of cells was found to be both FRMD5 and EMBIGIN-positive within normal articular cartilage, and this cell fraction was increased in OA cartilage. This increase correlates with data from Chapter 4 and Chapter 5 and previous studies discussed earlier, that also show an increase in stem cell presence in osteoarthritic cartilage (Alsalameh et al., 2004, Chang et al., 2011, Pretzel et al., 2011). The number of positive cells in normal cartilage (0.37%) and in OA cartilage (5.43%) is lower than observed through Immunofluorescence in Chapter 5. Whether the reduction is because of partial epitope degradation during digestion of cartilage or, in fact, a more accurate representation of the number of stem cells in articular cartilage than quantification using immunostained tissue is not certain. The number of FRMD5-positive cells identified by flow-cytometry is comparable to the Immunofluorescence results (Chapter 5), with a reduction found in EMBIGIN-positive cells. It is, therefore, probable that partial degradation of the EMBIGIN epitope has occurred. As mentioned in previous Chapters, the up-regulation of stem cells in OA cartilage could be due to migration, proliferation or a dedifferentiation as a result of disease or injury (Seol et al., 2012, Alsalameh et al., 2004).

6.4.1 Characterisation of FRMD5/EMBIGIN dual-positive cells

Cells expressing both of the ACSC markers FRMD5 and EMBIGIN and cells expressing neither marker were isolated into 2 separate populations by FACS. Colony forming efficiencies showed that dual-positive cells from both healthy

and osteoarthritic cartilage were highly clonogenic with CFEs close to 90%. CFE is a standard *in vitro* assay for mesenchymal stem cells, quantified by scoring individual colonies presumed to be derived from a single precursor. Using this assay, several groups have estimated the number of mesenchymal stem cells in bone marrow and other tissues (Deans and Moseley, 2000, Pittenger et al., 1999, Zuk et al., 2002). The extremely high colony forming values suggest we have isolated a very pure population of adult stem cells.

During culture expansion of N+ve and OA+ve cell lines, the growth kinetic were comparable. All dual-positive cell lines were capable of extended proliferation *in vitro* past 50 population doublings. There was very little variation in growth kinetics observed both between cell lines from the same donor and from different donors. The growth kinetics of both normal and OA cartilage-derived dual-positive cells were comparable to the growth kinetics of normal and late-senescent OA ACSC in Chapter 4. The initial rate of growth of the dual-negative cells was slower than dual-positive cells, with the dual-negative cells senescing before 30PD. The growth kinetics of dual-negative cells were comparable for normal and OA cartilage-derived cells and showed the same proliferative dynamics as FD chondrocytes from Chapter 4. The divergent ACSC populations observed from OA donors (ES-OA-SC and LS-OA-SC) in Chapter 4 were not found in OA+ve cell lines. This could be due to polyclonal expansion of dual-positive cell lines rather than monoclonal expansion of ACSC in Chapter 4. During expansion, cells with the greatest proliferative capacity will dominate the culture producing more uniform growth kinetics, possibly masking the divergent sub-population. A study by Jones and colleagues (2008) supports this notion, polyclonal bone marrow-derived MSCs and synovial fluid-derived MSCs were found to proliferate faster and with less variation in growth kinetics than monoclonal expansion. Bone marrow-derived MSCs during polyclonal expansion displayed a doubling time of 2.1±0.2 days, while monoclonal cell lines took 4.1±1.0 days (Jones et al., 2008). In our study, we also found that polyclonal dual-positive cells proliferated faster than the monoclonal ACSC lines from Chapter 4, reaching 50PDs after approximately 130 days compared to 165 days for ACSC. To identify whether polyclonal culture is resulting in uniform growth kinetics, culture of dual-positive cells as clonal cell lines would be required to provide a direct comparison. Isolation of cells using FRMD5 provides an alternate

explanation for the uniform growth kinetics of OA dual-positive cells. In Chapter 4, we showed that proliferative longevity in culture correlated with level of *FRMD5* gene expression, it is possible that by selecting for FRMD5-positive cell lines we have isolated only cells with a high proliferative capacity.

Dual-positive cells and ACSC isolated by differential adhesion have comparable growth kinetics, both exhibiting extended proliferative capacity *in vitro,* surpassing a Hayflick limit of 30PD. Therefore, FRMD5/EMBIGIN-positive cells meet this criterion for classification as an articular cartilage-derived stem cell population (Hayflick, 1965, Stenderup et al., 2003).

The ability of dual-positive cells to produce multilineage progeny was examined through induction into the chondrogenic, adipogenic and osteogenic lineages. Initially, multilineage potential was tested through monolayer differentiation; all normal cartilage-derived dual-positive and OA cartilage-derived dual-positive cell lines were found to be capable of multipotent differentiation. Alcian blue staining showed clear GAG deposition in the chondrogenic induction monolayer cultures, which was absent in the controls. No obvious differences between individual polyclonal cell lines from the same cohort or between normal and OA cohorts were apparent. Osteogenic monolayer culture had large deposition of mineralised matrix identified by strong Alizarin red staining. Again, no differences were observed in monolayer osteogenic capacity between individual polyclonal cell lines of the same cohort or between normal and OA sample groups. After adipogenic induction, all dual-positive cell lines tested produced lipid vacuoles in monolayer cultures and stained positively with Oil red-O. The consistent adipogenic differentiation capacity of dual-positive cells is equivalent to ACSC in Chapter 4 and to previous studies in our group (Nelson et al., 2014, Williams et al., 2010). The adipogenic genes *LPL, FABP4* and *PPAR1* were all expressed after 10 days of adipogenic differentiation and absent in the controls. Many previous studies have used monolayer differentiation assays alone to show multipotency of mesenchymal stem cells isolated from various tissues sources (Barry and Murphy, 2004, Bruder et al., 1998b, Muraglia et al., 2000, Portron et al., 2013, Suzawa et al., 2003, Winter et al., 2003). Based on the monolayer differentiation potential, both normal and OA-derived FRMD5/EMBIGIN dual-positive cells meet this condition for classification as a mesenchymal stem cell population.

To further explore the differentiation capacity of dual-positive cell lines, 3D-pellet culture systems were used for chondrogenic and osteogenic induction. Morphologically, the chondrogenic pellets were consistent, exhibiting a smooth, opalescent white surface. Unlike the pellet cultures in Chapter 4, the size of pellets from different cell lines was consistent across both the normal and OA cohorts. The reduced variability in pellet size may be due to the polyclonal expansion of the dual-positive cells. It has previously been shown that MSC chondrogenic pellets from clonal cell lines have a large variation in size and weight, while polyclonal cell lines produce consistently sized pellets (Jones et al., 2008). Morphologically, the cells within the 3D-pellets adopted a rounded phenotype, characteristic of articular cartilage *in situ* (Archer and Francis-West, 2003). The capacity for chondrogenic differentiation was examined histologically using toluidine blue and safranin-O staining to demonstrate the level of sulphated GAG production within the matrix. Safranin-O provided better detection of GAG than toluidine blue.

Histological staining demonstrated the accumulation of GAGs, particularly around the outer edges of the pellets. The outer edges of the pellets had higher cell densities and direct exposure to the chondrogenic media; therefore, it is expected to contain the greatest amount of matrix. All pellets displayed GAG deposition, however, there was variability in the levels of GAG between pellets of the same cohort. The variability in chondrogenic capacity is consistent with the variability identified in ACSC in Chapter 4 and by Nelson et al., (2014). Variability in GAG content was observed both in normal and OA cartilage-derived dual-positive cells and, therefore, is not thought to be due to disease. The variation is likely due to differences in chondrogenic potential between different donors, whether this is due to age or other factors could not be determined with this sample size. Although it wasn't possible to certify the cause of variation, donor age has been shown to negatively impact the differentiation potential of both adipose-derived and bone marrow-derived MSCs (Choudhery et al., 2014, Sethe et al., 2006). The level of GAG following 21 days in pellet culture was accessed by DMMB, no overall difference was observed between normal and OA pellets in terms of biochemical composition. The variation in GAG content identified histologically was also evident quantitatively. DMMB results correlated to histological analyses; the pellets that quantitatively contained lowest GAG were

also the cell lines with the least toluidine blue and safranin-O staining. The overall levels of GAG observed in this study are comparable to previous studies using MSCs in pellet culture (Barry et al., 2001).

To confirm the production of cartilaginous matrix Collagen Type II and Aggrecan (5C5) content was investigated immunologically. Collagen Type II and Aggrecan labelling was evident in all the chondrogenic pellets, with staining more abundant in some pellets than others. The pellets that exhibited the strongest Collagen Type II and Aggrecan content were also the pellets that contained the greatest amount of GAG. This emphasises the heterogeneity in chondrogenic capacity, showing that certain cell lines have a superior cartilaginous differentiation.

Chondrogenic differentiation of dual-positive cell line pellets was confirmed through chondrogenic gene expression. *COL2A1, COL9A1, COL11A2, ACAN* and *PRG4* were all up-regulated in chondrogenic pellets compared to controls. Combined, these results supply evidence that dual-positive cells excised from both normal and osteoarthritic tissue do have the potential to produce a cartilage-like, hyaline matrix rich in GAGs, Aggrecan and Collagen Type II.

Osteogenic differentiation was further explored using osteogenic 3D-pellet culture. Like the chondrogenic pellets, there was variability in the extent of osteogenic differentiation that occurred. Upon Alizarin red staining, evidence of mineralisation was intense in some pellets, and partially absent in other pellets. It was apparent that in certain cases, only a portion of the pellet had undergone osteogenic differentiation. It is possible that 3 weeks was insufficient time for some pellets to completely differentiate. Unpublished work from our laboratory has revealed that the rate of osteogenic differentiation of OA cartilage-derived articular cartilage stem cells varies between cell lines; certain cell lines have been shown to have no mineralisation after 3 weeks, however, deposits were abundant after 6 weeks. As such, the variable results may be a result of variable osteogenic differentiation capability or differences in the rate of osteogenic differentiation of a cell line. The variation in mineralization further highlights the heterogeneity between donors observed in this study. Heterogeneity in differentiation capacity is not a phenomenon specific to cartilage stem cells;

Pittenger et al., (1999) was the first to reported heterogeneity in multi-lineage potential of expanded mesenchymal stem cells. Further work is required to identify the cause of this variation and to determine appropriate cell lines for use in regenerative therapies.

Osteogenic differentiation of 3D-pellet cultures was confirmed through analyses of osteogenic gene expression. *ALPL, COL1A1, COL10A1, BGLAP* and *RUNX2* were up-regulated in osteogenic pellets. It was interesting that osteogenic genes were highly expressed even in pellets that had only achieved partial differentiation. Dual-negative cell were not capable of osteogenic differentiation, osteogenic pellet disintegrated in culture after 1-2 weeks.

FRMD5/EMBIGIN dual-positive cells were found to be capable of both monolayer and three-dimensional differentiation into the adipogenic, chondrogenic and osteogenic lineages. Therefore, dual-positive cells were found to be multipotent and meet the criteria for classification as a mesenchymal stem cell population.

6.4.2 ACSC stem cell marker labelling in FRMD5/EMBIGIN dual-positive cells

After *in vitro* culture expansion of dual-positive cells, the expression for ACSC markers, identified throughout this thesis, were analysed. Our data show that dual-positive cells express ACSC markers at both the genetic and protein level, and that these markers are absent in the dual-negative populations. Protein immunocytochemistry produced consistent results with strong positive labelling for NESTIN, FRMD5, C11ORF41, EMBIGIN and EAAT1 in all dual-positive cell lines. The staining was found to be comparable to ACSC samples investigated in Chapter 4. Dual-negative cell lines were found to be comparable to FD chondrocytes with no labelling observed. At the genetic level, all ACSC markers were significantly up-regulated in both normal and OA-derived dual-positive samples, with the exception of *ST6GAL2* in the OA+ve cohort. Gene expression of *ACAN* and *COL2A1* were decreased in the dual-positive cells compared to the dual-negative populations, confirming an immature phenotype in these cells. The expression of marker specific to ACSC provides further evidence that isolation of cells using FRMD5/EMBIGIN represents an adult stem cell population.

As mentioned in Chapter 4, EMBIGIN is a developmentally expressed cell adhesion molecule that is a member of the immunoglobulin superfamily (IgSF) class of cell adhesion molecules (Guenette et al., 1997). EMBIGIN may function to enhance integrin activity and/or facilitate anaerobic respiration through monocarboxylate transporters (Halestrap and Price, 1999, Muramatsu and Muramatsu, 2004). To explore the functional mechanism of EMBIGIN in articular cartilage stem cells, gene expression of immunoglobulin super-family members and MCT co-factors were investigated. The immunoglobulin super-family member *BASIGIN* was not found to have differential expression between dual-positive and dual-negative cell lines. Basigin was first identified on the surface of tumour cells, where it promotes the production of matrix metalloproteinases in neighbouring mesenchymal cells, leading to enhanced tumour invasion (Biswas et al., 1995, Muramatsu and Miyauchi, 2003). It has been identified that BASIGIN specifically interacts with MCT1, 3 and 4 while EMBIGIN is the specific co-factor for MCT2 (Halestrap and Price, 1999, Muramatsu and Miyauchi, 2003). In the FACS sorted cells *MCT1* was not expressed in either cohort, while *MCT3* and *4,* like BASIGIN, had consistent expression in both dual-positive and negative cell lines. *MCT2* gene expression was found to be specifically up-regulated in the dual-positive cell lines, mirroring *EMBIGIN* expression. These data support the previous studies, suggesting that EMBIGIN is the cofactor specifically for MCT2. These data suggest that in articular cartilage-derived stem cells, EMBIGIN functions as a co-factor required to localise MCT2 to the cell membrane, allowing the transport of lactate across the cell membrane, facilitating anaerobic respiration, a major component for self-renewal *in vivo* (Halestrap and Price, 1999, Ito and Suda, 2014).

The specificity of stem cell marker genes was confirmed using the chondrogenic pellet cultures. Upon differentiation dual-positive cell pellets down-regulate gene expression of all stem cell marker genes. The largest reduction was in *NESTIN* gene expression with many samples that have no expression after chondrogenic differentiation. These data confirm the specificity of the panel of markers for identification of articular cartilage stem cells.

In conclusion, we have shown that cartilage cells isolated using FACS for FRMD5 and EMBIGIN protein represent an articular cartilage-derived stem cell

population. Mesenchymal stem cells are a multipotent adult stem cell defined by: a) plastic adherent, b) colony forming, c) immunophenotype, d) multipotential *in vitro* differentiation and e) extended proliferative capacity *in vitro* (Wagner et al., 2008).

Dual-positive cells are plastic adherent and highly clonogenic with a proliferative capacity greater than 50 population doublings. We have shown they are capable of both monolayer and three-dimensional tri-lineage differentiation. As discussed throughout this thesis, conventional MSC surface antigens are not suitable for identification of specific sub-populations of chondrocytes in cartilage; dual-positive cells have been shown to express all novel ACSC markers identified in this study. Therefore, dual-positive cells meet all the criteria required for definition as a specific adult mesenchymal stem cell population.

CHAPTER 7:

GENERAL DISCUSSION

7.1 General discussion

Articular cartilage has a poor intrinsic repair capacity; due to its avascular nature, lack of nerve supply and low cellularity. Focal damage progresses from the articular surface to the subchondral bone resulting in degradation of the matrix, a loss of organization and structure, reduced motion and a painful joint. These focal defects can progress to osteoarthritis. It is widely considered that osteoarthritis is a progressive and terminal disease of the joint. The majority of current repair strategies rely on infiltration of autologous chondrocyte or stem cells from the bone marrow (Brittberg et al., 1994, Yen et al., 2008). ACI cannot treat large lesions and mesenchymal stem cell repair strategies result in an inferior, less robust, fibrocartilaginous tissue (Carey, 2012). In many, if not all tissues, stem cells drive repair and tissue homeostasis; therefore, the discovery of tissue specific stem cells within articular cartilage has important implications for understanding the potential for endogenous repair (Alsalameh et al., 2004, Dowthwaite et al., 2004, Williams et al., 2010). If resident stem cells can be reliably identified and isolated from within articular cartilage, these cells, once expanded *in vitro,* offer a novel therapeutic avenue, that would ultimately produce a superior hyaline-like repair tissue when re-implanted into the joint.

The cellular component of articular cartilage is classically believed to be exclusively the chondrocyte. Chondrocytes are a differentiated cell type derived from multipotent progenitors, mesenchymal stem cells (Alsalameh et al., 2004). Friedenstein and colleagues first identified MSCs in bone marrow in the 1970s, since then, MSCs have been identified in virtually all post-natal organs and tissues (Friedenstein et al., 1976, da Silva Meirelles et al., 2006). MSCs can differentiate into multiple lineages including chondrocytes, osteoblasts, adipocytes tendon cells and myocytes (Caplan, 1991, Phinney and Prockop, 2007). For classification, MSCs have been defined by: plastic adherence, clonogenicity, immunophenotype, multi-lineage potential and an extended proliferative capacity *in vitro* (Wagner et al., 2008). Classically, MSCs are characterised and isolated using cell-surface antigens including CD29, CD44, CD45e, CD90, CD73, CD105, CD166 and STRO-1 (Barry et al., 1999, Bruder et al., 1998a, Bruder et al., 1998b, Lv et al., 2014, Majumdar et al., 2003, Simmons and Torok-Storb, 1991). Cells expressing MSC surface antigens have been reported

within both healthy and osteoarthritic adult articular cartilage by multiple groups (Alsalameh et al., 2004, Chang et al., 2011, Fickert et al., 2004, Grogan et al., 2009, Pretzel et al., 2011, Williams et al., 2010). MSC markers for identification and isolation of articular cartilage-derived stem cells has proven unreliable with large variability reported in the abundance and reproducibility of results. Identification of new, reliable and specific markers will allow for greater insight into the role of tissue-specific stem cells during disease, specifically allowing analyses of the numbers of stem cells remaining in diseased tissue, the localisation and their replicative and reparative capacity.

Within this study, the main focus was directed towards identification of reliable markers for ACSC, to isolate cells using these markers and to evaluate the phenotype of these cells *in vitro.* This was with the aim of understanding the potential for hyaline-like cartilage repair using ACSC from normal and osteoarthritic donors. In parallel to these studies, we have analysed the stem cell number in normal and OA cartilage and discovered their location within adult tissue.

Using transcriptomics we have, for the first time, complete gene expression profiles for full-depth chondrocytes and articular cartilage stem cells. We were successfully able to identify a panel of genes specific to cartilage-derived stem cells that were not present in the differentiated progeny. These genes included *NESTIN, FRMD5, C11ORF41, PRDM1, SLC1a3 (EAAT1), EMBIGIN, TMEM132B, ST6GAL2* and *KIF26B*. *NESTIN, FRMD5, EAAT1, PRDM1* and *EMBIGIN* have previous connections to stem cells in the literature (Chu et al., 2011, Eriksson et al., 1992a, Gilley and Kernie, 2011, Kubo et al., 2009, Mich et al., 2014). However, this is the first time the other genes have been reported in a stem cell population. Transcriptomic data were validated using qPCR; all genes identified as stem cell specific were strongly up-regulated within the ACSC cohorts compared to FD chondrocytes. Protein labelling of NESTIN, FRMD5, C11ORF41, EAAT1 and EMBIGIN confirmed ACSC specific expression *in vitro* with no labelling identified in differentiated cells. This panel of markers was highly specific for ACSC and provided a reliable alternative to mesenchymal stem cell markers for identification of articular cartilage-derived stem cells.

Using the panel of novel stem cell markers, a stem cell population was isolated from both healthy and osteoarthritic cartilage using FACS for FRMD5/EMBIGIN dual-positive cells. This population was plastic adherent, highly clonogenic, multipotent and proliferated past 50 population doublings *in vitro*. Therefore, this population met the criteria for classification as a mesenchymal stem cell. This stem cell population had consistent growth kinetics across all cell lines, however, heterogenetity was observed in the differentiation capacity of cell lines from different donors. We successfully differentiated FRMD5/EMBIGIN dual-positive stem cells into the chondrogenic, osteogenic and adipogenic lineages. Dual-negative cell lines were found to be capable of chondrogenic differentiation but were not able to undergo osteogenic or adipogenic differentiation. No heterogeneity was observed in monolayer differentiation capacity but, variation was observed in 3D culture. Whether this was due to the rate of differentiation or the lineage potential of the cell line cannot be determined. Extended differentiation culture of 6-8 weeks will allow for clarification of the potential cause of the variation. All dual-positive cell lines isolated using flow-cytometry had gene and protein expression for the other stem cell markers; expression was not found in the dual-negative fraction.

Previous studies have reported an increase in MSC marker expressing cells in osteoarthritic cartilage (Alsalameh et al., 2004, Chang et al., 2011, Grogan et al., 2009, Pretzel et al., 2011). We identified that the percentage of stem cells, calculated using a colony forming efficiency assay, doubled in osteoarthritic cartilage compared to normal cartilage. This increase was corroborated using immunofluorescence of the novel ACSC marker; again we observed an approximately 2-fold increase in stem cell marker positive cells for all markers. The labelling of NESTIN in OA cartilage was found to increase dramatically, indicating that in normal tissue, stem cells may be in a quiescent state that does not express NESTIN (Codega et al., 2014). Tissue-specific adult stem cells persist in the quiescent state for prolonged periods of time, with both quiescent and active stem cells sub-populations coexisting in the same tissue (Li and Clevers, 2010). Although quiescence is not an essential characteristic of a stem cell, dysregulation and loss of quiescence often results in an imbalance in stem/progenitor cell populations, possibly explaining the increase observed in OA (Cheung and Rando, 2013). Gene expression of ACSC markers in OA tissue

also increases supporting the evidence for an increase in stem cells in diseased tissue. Isolation of stem cells using FACS of FRMD5/EMBIGIN dual-positive cells also identified a significant increase in stem cells in osteoarthritic tissue, although this was of a larger magnitude than in previous methodologies. These data show that there are a significant number of stem cells within the OA joint; however, these cells are not sufficient for achieving endogenous repair. The question remains as to whether these cells are capable of producing hyaline-like cartilaginous repair if used for regenerative therapies.

Previous studies have localised stem/progenitor cells in articular cartilage to the superficial zone and upper transitional zone in both normal and OA cartilage (Dowthwaite et al., 2004, Grogan et al., 2009, Koelling et al., 2009, Pretzel et al., 2011). In this study, we have found that the majority of ACSC in healthy tissue are located in the transitional zone and not within the superficial zone. Situating a stem cell population below the surface zone would ensure that they are away from the area of high mechanical strain and damage, protecting the stem cell population. In OA, the ACSC migrate from the lower transition zone into the superficial zone, doubtlessly in an endeavour to orchestrate repair. The overall increase in ACSC in OA cartilage suggests that OA also invokes a proliferative response in the ACSC, potentially, in an attempt to repopulate the tissue; or due to, dysregulation of stem cell proliferation and differentiation because of loss of the stem cell niche.

Culture expansion of differential adhesion isolated normal ACSC and OA-SC cell lines showed clear differences in growth kinetics and BrdU incorporation. OA-SC contained 2 sub-populations, an early senescent population and a late senescent population, with only 45% of the cell lines cultured from OA cartilage surpassing 30PD. N-SC cell lines contain a single population, all with a consistent proliferative capacity. After the initial phases of growth, the rate of proliferation of ES-OA-SC abruptly decreased before senescence by 30PD. This finding was consistent with previous work by Nelson and colleagues (2014) who also identified that only 50% of stem cells from the arthritic joint are capable of long-term expansion. The sub-populations identified within the OA-SC were not due to variation between donors, multiple cell lines established from the same donor showed this variation. This implies that the divergence in proliferative capacity

of ACSC is due to disease and not due to donor variations, such as age. These data suggest that although there is an increase in the number of ACSC in diseased tissue, possibly as a reparative response; proliferation of OA-SCs become dysfunctional as a facet of the disease. The replicative potential of somatic cells is dependent on telomere length (Martin and Buckwalter, 2001). The divergent populations observed in OA-SC may be due to telomere shortening; our group has identified that ACSC derived from normal cartilage have a uniform high telomere length, while 60% of the ACSC cell lines from OA cartilage have short telomeres (Williams et al., 2010). Another possible mechanism for the appearance of the sub-populations is episodic exposure to acute oxidative stress during OA inflammatory flares. Inflammatory activity over a prolonged period of time has been shown to affect the stem cell phenotype and their niche (Hayes et al., 2008). Pre-isolation cellular changes may be responsible for the different sub-populations observed in ACSC. The ACSC marker gene expression of *NESTIN* *PRDM1*, *C11ORF41* and *FRMD5* were found to correlate with proliferative potential of the cell line. NESTIN expression has previously been reported to correlate with the proliferation of cancer cell lines and knock-down studies reduced the cell growth (Dahlstrand et al., 1992, Yang et al., 2008, Thomas et al., 2004, Wei et al., 2008). No prior relationship to proliferation had previously been identified for *PRDM1*, *FRMD5* and *C11ORF41*. We observed that isolation of stem cells using FRMD5/EMBIGIN labelling resulted in a uniform growth kinetic of both normal cartilage-derived and OA cartilage-derived stem cell lines. It is possible that by isolating stem cells using FRMD5, we have preferentially selected for the OA stem cell sub-population with the normal proliferative dynamics. It cannot, however, be excluded that the uniform population observed in FACS-isolated cells is due to polyclonal expansion; growth kinetics of monoclonal cell lines will be required to identify whether preferential selection for highly proliferative cohort has been achieved.

7.2 Future work

In terms of future work, it would be interesting to identify the functional role for each of the ACSC markers have in the stem cells. With a view to achieving this aim, gain and loss of function constructs would provide insight into the phenotypic changes that occur when marker expression is increased or

decreased. This may provide insight into the emergence of proliferative sub-population in OA-SC. In view of understanding the sub-populations in OA, isolation and culture of FRMD5/EMBIGIN dual-positive cells as monoclonal cell lines is essential to identify whether selection of highly proliferative cells has occurred. Experiments will also have to test the possibility that divergent sub-populations are not derived from migrating MSCs from either the subchondral bone or synovium.

We have identified that gene expression of *MCT2*, a co-factor for EMBIGIN has the same gene expression profile as *EMBIGIN.* CO-IP would provide evidence that EMBIGIN is directly interacting with MCT2 and provide information on other binding partners such as integrins, indicating the functional role in ACSC.

With regard to FACS, EAAT1 labelling was not found and we also experienced a reduction in EMBIGIN labelling compared to immunofluorescence *in situ*. These reductions in labelling were assumed to be due to enzymatic degradation of the epitope. It would be interesting to extract cells from tissue using collagenase alone in order to see if labelling is detectable in the absence of pronase. It would also be useful to look at the protein labelling after plating the cells overnight to allow for extracellular proteins to be restored. Cells could be detached using accutase, which has been shown to preserve extracellular epitopes. This would provide an understanding of any epitope degradation occurring during the cartilage digestion.

We found heterogeneity in the chondrogenic and osteogenic pellet culture differentiation. It was not possible in this study to ascertain whether the differences were due to the rate of differentiation or donor differences in lineage potentials. Donor age has previously been shown to reduce the differentiation potential of mesenchymal stem cells, increasing the sample size will allow examination of the effect that donor age has on ACSC differentiation. Differentiation cultures should also be maintained for a longer time-period to establish whether the rate of differentiation produces the variation observed.

Finally, transgenic ACSC reporter constructs could provide information on the function of adult stem cells in cartilage homeostasis and information on the stem

cell response to injury and disease. This would offer new insight into OA disease mechanisms and, possibly, identify novel therapeutic windows and targets. This would also help identify the origin of the increase in stem cell number in disease. *In vitro* reporter constructs could also provide information on the dynamics of differentiation and stem cell maintenance.

7.3 Conclusion

In conclusion, we have identified novel markers that are specific for human articular cartilage-derived stem cells. These markers have been used to identify and isolate stem cell populations both *in vitro* and *in situ*.

We discovered that stem cell number increases in osteoarthritic tissue with the stem cells relocating from the transitional to the superficial zone in response to OA. OA-derived monoclonal ACSC cell lines isolated by differential adhesion contain two distinct and divergent populations differentiated by early or late senescence. We were able to distinguish between these divergent populations based on stem cell marker gene expression, with high *NESTIN*, *FRMD5*, *PRDM1* and *C11ORF41* gene expression predicting an extended proliferative capacity *in vitro*.

We have shown that cartilage cells isolated using FACS for FRMD5 and EMBIGIN protein labelling represent a stem cell population that is plastic adherent, highly clonogenic, has multi-lineage potential and proliferate past a 50PD. Therefore, dual-positive cells meet the criteria required for definition as an adult mesenchymal stem cell population.

CHAPTER 8:

BIBLIOGRAPHY

AGRAWAL, C. M. & RAY, R. B. 2001. Biodegradable polymeric scaffolds for musculoskeletal tissue engineering. *J Biomed Mater Res,* 55**,** 141-50.

AHRENS, M. J. & DUDLEY, A. T. 2011. Chemical pretreatment of growth plate cartilage increases immunofluorescence sensitivity. *J Histochem Cytochem,* 59**,** 408-18.

AIGNER, T., ZHU, Y., CHANSKY, H. H., MATSEN, F. A., 3RD, MALONEY, W. J. & SANDELL, L. J. 1999. Reexpression of type IIA procollagen by adult articular chondrocytes in osteoarthritic cartilage. *Arthritis Rheum,* 42**,** 1443-50.

ALSALAMEH, S., AMIN, R., GEMBA, T. & LOTZ, M. 2004. Identification of mesenchymal progenitor cells in normal and osteoarthritic human articular cartilage. *Arthritis Rheum,* 50**,** 1522-32.

ANDERS, S. & HUBER, W. 2010. Differential expression analysis for sequence count data. *Genome Biology,* 11**,** 1-12.

ANDERS, S., MCCARTHY, D. J., CHEN, Y., OKONIEWSKI, M., SMYTH, G. K., HUBER, W. & ROBINSON, M. D. 2013. Count-based differential expression analysis of RNA sequencing data using R and Bioconductor. *Nat. Protocols,* 8**,** 1765-1786.

ANDERS, S., PYL, P. T. & HUBER, W. 2014. *HTSeq – A Python framework to work with high-throughput sequencing data*.

ARCHER, C. W. 1994. Skeletal development and osteoathritis. *Annal of the Rheumatic Diseases,* 53**,** 624-630.

ARCHER, C. W., DOWTHWAITE, G. P. & FRANCIS-WEST, P. 2003. Development of synovial joints. *Birth Defects Research Part C: Embryo Today: Reviews,* 69**,** 144-155.

ARCHER, C. W. & FRANCIS-WEST, P. 2003. The chondrocyte. *The International Journal of Biochemistry & Cell Biology,* 35**,** 401-404.

ARCHER, C. W., MORRISON, H. & PITSILLIDES, A. A. 1994. Cellular aspects of the development of diarthrodial joints and articular cartilage. *J. Anat,* 1984**,** 447-456.

ARDEN, N. & NEVITT, M. C. 2006. Osteoarthritis: Epidemiology. *Best Practice & Research Clinical Rheumatology,* 20**,** 3-25.

ARMSTRONG, C. G. & MOW, V. C. 1982. Variations in the intrinsic mechanical properties of human articular cartilage with age, degeneration, and water content. *J Bone Joint Surg Am,* 64**,** 88-94.

ASADA, S., FUKUDA, K., NISHISAKA, F., MATSUKAWA, M. & HAMANISI, C. 2001. Hydrogen peroxide induces apoptosis of chondrocytes; involvement of calcium ion and extracellular signal-regulated protein kinase. *Inflammation Research,* 50**,** 19-23.

ASPDEN, R. M. & HUKINS, D. W. 1979. The lamina splendens of articular cartilage is an artefact of phase contrast microscopy. *Proc R Soc Lond B Biol Sci,* 206**,** 109-13.

ATKINS, E. D. & SHEEHAN, J. K. 1971. The molecular structure of hyaluronic acid. *Biochem J,* 125**,** 92P.

BADER, D. L., SALTER, D. M. & CHOWDHURY, T. T. 2011. Biomechanical influence of cartilage homeostasis in health and disease. *Arthritis,* 2011**,** 979032.

BARBERO, A., PLOEGERT, S., HEBERER, M. & MARTIN, I. 2003. Plasticity of clonal populations of dedifferentiated adult human articular chondrocytes. *Arthritis Rheum,* 48**,** 1315-25.

BARNARD, R. M. 2012. Flow cytometry: a flexible tool for biomarker research. *Bioanalysis,* 4**,** 2471-83.

BARRY, F., BOYNTON, R. E., LIU, B. & MURPHY, J. M. 2001. Chondrogenic differentiation of mesenchymal stem cells from bone marrow: differentiation-dependent gene expression of matrix components. *Exp Cell Res,* 268**,** 189-200.

BARRY, F. & MURPHY, M. 2013. Mesenchymal stem cells in joint disease and repair. *Nat Rev Rheumatol,* 9**,** 584-594.

BARRY, F. P., BOYNTON, R. E., HAYNESWORTH, S., MURPHY, J. M. & ZAIA, J. 1999. The Monoclonal Antibody SH-2, Raised against Human Mesenchymal Stem Cells, Recognizes an Epitope on Endoglin (CD105). *Biochemical and Biophysical Research Communications,* 265**,** 134-139.

BARRY, F. P. & MURPHY, J. M. 2004. Mesenchymal stem cells: clinical applications and biological characterization. *The International Journal of Biochemistry & Cell Biology,* 36**,** 568-584.

BARTLETT, W., SKINNER, J. A., GOODING, C. R., CARRINGTON, R. W. J., FLANAGAN, A. M., BRIGGS, T. W. R. & BENTLEY, G. 2005. Autologous chondrocyte implantation versus matrix-induced autologous chondrocyte implantation for osteochondral defects of the knee: A PROSPECTIVE, RANDOMISED STUDY. *Journal of Bone & Joint Surgery, British Volume,* 87-B**,** 640-645.

BATES, E. J., JOHNSON, C. C. & LOWTHER, D. A. 1985. Inhibition of proteoglycan synthesis by hydrogen peroxide in cultured bovine articular cartilage. *Biochimica et Biophysica Acta (BBA) - General Subjects,* 838**,** 221-228.

BAYLISS, M. T., VENN, M., MAROUDAS, A. & ALI, S. Y. 1983. STRUCTURE OF PROTEOGLYCANS FROM DIFFERENT LAYERS OF HUMAN ARTICULAR-CARTILAGE. *Biochemical Journal,* 209**,** 387-400.

BD.BIOSCIENCES. 2014. *BD Biosciences fluorescence spectrum viewer* [Online]. BD Biosciences. Available: http://www.bdbiosciences.com/ca/research/multicolor/spectrum_viewer/index.jsp [Accessed 21/08/14 2014].

BECERRA, J., ANDRADES, J. A., GUERADO, E., ZAMORA-NAVAS, P., LOPEZ-PUERTAS, J. M. & REDDI, A. H. 2010. Articular cartilage: structure and regeneration. *Tissue Eng Part B Rev,* 16**,** 617-27.

BENJAMIN, M. 1999. An introduction to synovial joints. *In:* ARCHER, C. W., CATERSON, B., BENJAMIN, M. & RALPHS, J. R. (eds.) *Biology of the synovial joint.* Amsterdam: Harwood publishers.

BENJAMIN, M. & RALPHS, J. R. 1998. Fibrocartilage in tendons and ligamentsÐan adaptation to compressive load. *J. Anat,* 193**,** 481-494.

BENNINGHOFF, A. 1925. Form und Bau der Gelenkknorpel in ihren Beziehungen zur Funktion. *Zeitschrift für Zellforschung und Mikroskopische Anatomie,* 2**,** 783-862.

BENYA, P. D. & SHAFFER, J. D. 1982. Dedifferentiated chondrocytes reexpress the differentiated collagen phenotype when cultured in agarose gels. *Cell,* 30**,** 215-224.

BERTHIAUME, M. J., RAYNAULD, J. P., MARTEL-PELLETIER, J., LABONTE, F., BEAUDOIN, G., BLOCH, D. A., CHOQUETTE, D., HARAOUI, B., ALTMAN, R. D., HOCHBERG, M., MEYER, J. M., CLINE, G. A. & PELLETIER, J. P. 2005. Meniscal tear and extrusion are strongly associated with progression of symptomatic knee osteoarthritis as assessed by quantitative magnetic resonance imaging. *Ann Rheum Dis,* 64**,** 556-63.

BHOSALE, A. M. & RICHARDSON, J. B. 2008. Articular cartilage: structure, injuries and review of management. *British Medical Bulletin,* 87**,** 77-95.

BISWAS, C., ZHANG, Y., DECASTRO, R., GUO, H., NAKAMURA, T., KATAOKA, H. & NABESHIMA, K. 1995. The human tumor cell-derived collagenase stimulatory factor (renamed EMMPRIN) is a member of the immunoglobulin superfamily. *Cancer Res,* 55**,** 434-9.

BITTON, R. 2009. The economic burden of osteoarthritis. *Am J Manag Care,* 15**,** S230-5.

BLACK, C., B, DUESING, T., D, TRINKLE, L., S & DUNLAY, T., R 2011. Cell-Based Screening Using High-Throughput Flow Cytometry. *ASSAY and Drug Development Technologies,* 9**,** 13-20.

BLANPAIN, C. & FUCHS, E. 2009. Epidermal homeostasis: a balancing act of stem cells in the skin. *Nat Rev Mol Cell Biol,* 10**,** 207-217.

BLOM, A. B., BROCKBANK, S. M., VAN LENT, P. L., VAN BEUNINGEN, H. M., GEURTS, J., TAKAHASHI, N., VAN DER KRAAN, P. M., VAN DE LOO, F. A., SCHREURS, B. W., CLEMENTS, K., NEWHAM, P. & VAN DEN BERG, W. B. 2009. Involvement of the Wnt signaling pathway in experimental and human osteoarthritis: prominent role of Wnt-induced signaling protein 1. *Arthritis Rheum,* 60**,** 501-12.

BOLLET, A. J. & NANCE, J. L. 1966. Biochemical Findings in Normal and Osteoarthritic Articular Cartilage. II. Chondroitin Sulfate Concentration and Chain Length, Water, and Ash Content. *J Clin Invest,* 45**,** 1170-7.

BONDESON, J., WAINWRIGHT, S., HUGHES, C. & CATERSON, B. 2008. The regulation of the ADAMTS4 and ADAMTS5 aggrecanases in osteoarthritis: a review. *Clin Exp Rheumatol,* 26**,** 139-45.

BONNET, C. S. & WALSH, D. A. 2005. Osteoarthritis, angiogenesis and inflammation. *Rheumatology,* 44**,** 7-16.

BOS, P. K., VAN OSCH, G. V. M., VAN DER KWAST, T., VERWOERD-VERHOEF, H. & VERHAAR, J. N. 2000. Fixation-dependent Immunolocalization Shift and Immunoreactivity of Intracellular Growth Factors in Cartilage. *The Histochemical Journal,* 32**,** 391-396.

BRISMAR, B. H., WREDMARK, T., MOVIN, T., LEANDERSSON, J. & SVENSSON, O. 2002. Observer reliability in the arthroscopic classification of osteoarthritis of the knee. *J Bone Joint Surg Br,* 84**,** 42-7.

BRITTBERG, M., LINDAHL, A., NILSSON, A., OHLSSON, C., ISAKSSON, O. & PETERSON, L. 1994. Treatment of deep cartilage defects in the knee with autologous chondrocyte transplantation. *N Engl J Med,* 331**,** 889-95.

BRITTBERG, M., PETERSON, L., SJOGREN-JANSSON, E., TALLHEDEN, T. & LINDAHL, A. 2003. Articular cartilage engineering with autologous chondrocyte transplantation. A review of recent developments. *J Bone Joint Surg Am,* 3**,** 109-15.

BROWN, M. & WITTWER, C. 2000. Flow Cytometry: Principles and Clinical Applications in Hematology. *Clinical Chemistry,* 46**,** 1221-1229.

BRUDER, S. P., HOROWITZ, M. C., MOSCA, J. D. & HAYNESWORTH, S. E. 1998a. Monoclonal antibodies reactive with human osteogenic cell surface antigens. *Bone,* 21**,** 225-235.

BRUDER, S. P., RICALTON, N. S., BOYNTON, R. E., CONNOLLY, T. J., JAISWAL, N., ZAIA, J. & BARRY, F. P. 1998b. Mesenchymal Stem Cell Surface Antigen SB-10 Corresponds to Activated Leukocyte Cell Adhesion Molecule and Is Involved in Osteogenic Differentiation. *Journal of Bone and Mineral Research,* 13**,** 655-663.

BUCKWALTER, J. A. 1999. New approaches to articular cartilage repair and regeneration. *In:* ARCHER, C. W., CATERSON, B., BENJAMIN, M. & RALPHS, J. R. (eds.) *Biology of the synovial joint.* Amsterdam: Harwood Academic.

BUCKWALTER, J. A. & HUNZIKER, E. B. 1999. Articular Cartilage Morphology and Biology. *In:* ARCHER, C. W., CATERSON, B., BENJAMIN, M. & RALPHS, J. R. (eds.) *Biology of the synovial joint.* Amsterdam: Harwood Academic.

BUCKWALTER, J. A., HUNZIKER, E. B., ROSENBERG, L. C., COUTTS, R. D., ADAMS, M. E. & EYRE, D. R. 1988. Articular cartilage: composition and structure. *In:* WOO, S. L. & BUCKWALTER, J. A. (eds.) *Injury and repair of the musculoskeletal soft tissue.* Park Ridge: American Acadamy of Orthapaedic Surgeons.

BUCKWALTER, J. A. & LANE, N. E. 1996. Aging, Sports, and Osteoarthritis. *Sports Medicine and Arthroscopy Review,* 4**,** 276-287.

BUCKWALTER, J. A. & MANKIN, H. J. 1997. Articular cartilage I. Tissue design and chondrocyte matrix interactions. *J. Bone Joint Surg,* 79A.

BUCKWALTER, J. A. & MARTIN, J. A. 2006. Osteoarthritis. *Adv Drug Deliv Rev,* 58**,** 150-67.

CAPLAN, A. I. 1991. Mesenchymal stem cells. *Journal of Orthopaedic Research,* 9**,** 641-650.

CAPLAN, A. I. 2007. Adult mesenchymal stem cells for tissue engineering versus regenerative medicine. *Journal of Cellular Physiology,* 213**,** 341-347.

CAPLAN, A. I. 2009. Why are MSCs therapeutic? New data: new insight. *The Journal of Pathology,* 217**,** 318-324.

CAREY, J. L. 2012. Fibrocartilage Following Microfracture Is Not as Robust as Native Articular Cartilage. *J Bone Joint Surg Am.,* 94**,** e80.

CATERSON, E. J., NESTI, L. J., LI, W. J., DANIELSON, K. G., ALBERT, T. J., VACCARO, A. R. & TUAN, R. S. 2001. Three-dimensional cartilage formation by bone marrow-derived cells seeded in polylactide/alginate amalgam. *J Biomed Mater Res,* 57**,** 394-403.

CHANG, H. X., YANG, L., LI, Z., CHEN, G. & DAI, G. 2011. Age-related biological characterization of mesenchymal progenitor cells in human articular cartilage. *Orthopedics,* 34**,** e382-8.

CHANG, J. & POOLE, C. A. 1996. Sequestration of type VI collagen in the pericellular microenvironment of adult chrondrocytes cultured in agarose. *Osteoarthritis and Cartilage,* 4**,** 275-85.

CHANG, R. W., FALCONER, J., STULBERG, S. D., ARNOLD, W. J., MANHEIM, L. M. & DYER, A. R. 1993. A randomized, controlled trial of arthroscopic surgery versus closed-needle joint lavage for patients with osteoarthritis of the knee. *Arthritis Rheum,* 36**,** 289-96.

CHAPEKAR, M. S. 2000. Tissue engineering: challenges and opportunities. *J Biomed Mater Res,* 53**,** 617-20.

CHEUNG, T. H. & RANDO, T. A. 2013. Molecular regulation of stem cell quiescence. *Nat Rev Mol Cell Biol,* 14**,** 329-340.

CHEVRIER, A., ROSSOMACHA, E., BUSCHMANN, M. D. & HOEMANN, C. D. 2005. Optimization of Histoprocessing Methods to Detect Glycosaminoglycan, Collagen Type II, and Collagen Type I in Decalcified Rabbit Osteochondral Sections. *Journal of Histotechnology,* 28**,** 165-175.

CHIA, S. L., SAWAJI, Y., BURLEIGH, A., MCLEAN, C., INGLIS, J., SAKLATVALA, J. & VINCENT, T. 2009. Fibroblast growth factor 2 is an intrinsic chondroprotective agent that suppresses ADAMTS-5 and delays cartilage degradation in murine osteoarthritis. *Arthritis Rheum,* 60**,** 2019-27.

CHIANG, C., LITINGTUNG, Y., LEE, E., YOUNG, K. E., CORDEN, J. L., WESTPHAL, H. & BEACHY, P. A. 1996. Cyclopia and defective axial patterning in mice lacking Sonic hedgehog gene function. *Nature,* 383**,** 407-13.

CHIDGEY, A. P. & BOYD, R. L. 2008. Immune Privilege for Stem Cells: Not as Simple as It Looked. *Cell stem cell,* 3**,** 357-358.

CHIQUET-EHRISMANN, R., KALLA, P., PEARSON, C. A., BECK, K. & CHIQUET, M. 1988. Tenascin interferes with fibronectin action. *Cell,* 53**,** 383-390.

CHOUDHERY, M., BADOWSKI, M., MUISE, A., PIERCE, J. & HARRIS, D. 2014. Donor age negatively impacts adipose tissue-derived mesenchymal stem cell expansion and differentiation. *Journal of Translational Medicine,* 12**,** 8.

CHU, L. F., SURANI, M. A., JAENISCH, R. & ZWAKA, T. P. 2011. Blimp1 expression predicts embryonic stem cell development in vitro. *Curr Biol,* 21**,** 1759-65.

CHU, Q., LOPEZ, M., HAYASHI, K., IONESCU, M., BILLINGHURST, R. C., JOHNSON, K. A., POOLE, A. R. & MARKEL, M. D. 2002. Elevation of a collagenase generated type II collagen neoepitope and proteoglycan epitopes in synovial fluid following induction of joint instability in the dog. *Osteoarthritis and Cartilage,* 10**,** 662-9.

CILLA, S., INGO, M., TAMARA, K., FRANZ, R., JORGE, E.-G., MARGITTA, W., CHRISTOPH, G., GABRIELE, M., MARIO, A., KLAUS, R., HERBERT, S., ULRICH, W., NORBERT, H. & YOUNG-AE, L. 2007. Variants in a Novel Epidermal Collagen Gene (COL29A1) Are Associated with Atopic Dermatitis. *PLoS Biology,* 5**,** 1952-1961.

CODEGA, P., SILVA-VARGAS, V., PAUL, A., MALDONADO-SOTO, ANGEL R., DELEO, ANNINA M., PASTRANA, E. & DOETSCH, F. 2014. Prospective Identification and Purification of Quiescent Adult Neural Stem Cells from Their In Vivo Niche. *Neuron,* 82**,** 545-559.

COLLIER, J. L. 2000. FLOW CYTOMETRY AND THE SINGLE CELL IN PHYCOLOGY. *Journal of Phycology,* 36**,** 628-644.

CONTI, L., POLLARD, S. M., GORBA, T., REITANO, E., TOSELLI, M., BIELLA, G., SUN, Y., SANZONE, S., YING, Q.-L., CATTANEO, E. & SMITH, A. 2005. Niche-Independent Symmetrical Self-Renewal of a Mammalian Tissue Stem Cell. *PLoS Biol,* 3**,** e283.

COURNIL-HENRIONNET, C., HUSELSTEIN, C., WANG, Y., GALOIS, L., MAINARD, D., DECOT, V., NETTER, P., STOLTZ, J. F., MULLER, S., GILLET, P. & WATRIN-PINZANO, A. 2008. Phenotypic analysis of cell surface markers and gene expression of human mesenchymal stem cells and chondrocytes during monolayer expansion. *Biorheology,* 45**,** 513-26.

CRAIG, F. M., BENTLEY, G. & ARCHER, C. W. 1987. The spatial and temporal pattern of collagens I and II and keratan sulphate in the developing chick metatarsophalangeal joint. *Development,* 99**,** 383-391.

DA SILVA MEIRELLES, L., CHAGASTELLES, P. C. & NARDI, N. B. 2006. Mesenchymal stem cells reside in virtually all post-natal organs and tissues. *J Cell Sci,* 119**,** 2204-13.

DAHLSTRAND, J., COLLINS, V. P. & LENDAHL, U. 1992. Expression of the class VI intermediate filament nestin in human central nervous system tumors. *Cancer Res,* 52**,** 5334-41.

DEALY, C. N. 2012. Chondrogenic Progenitors for Cartilage Repair and Osteoarthritis Treatment. *Rheumatology: Current Research,* S3**,** 1-4.

DEANS, R. J. & MOSELEY, A. B. 2000. Mesenchymal stem cells: Biology and potential clinical uses. *Experimental Hematology,* 28**,** 875-884.

DELL'ACCIO, F., DE BARI, C., EL TAWIL, N. M., BARONE, F., MITSIADIS, T. A., O'DOWD, J. & PITZALIS, C. 2006. Activation of WNT and BMP signaling in adult human articular cartilage following mechanical injury. *Arthritis Res Ther,* 8**,** R139.

DENNIS, J. E., CARBILLET, J. P., CAPLAN, A. I. & CHARBORD, P. 2002. The STRO-1+ marrow cell population is multipotential. *Cells Tissues Organs,* 170**,** 73-82.

DIAZ-ROMERO, J., GAILLARD, J. P., GROGAN, S. P., NESIC, D., TRUB, T. & MAINIL-VARLET, P. 2005. Immunophenotypic analysis of human articular chondrocytes: Changes in surface markers associated with cell expansion in monolayer culture. *Journal of Cellular Physiology,* 202**,** 731-742.

DIEZ VILLANUEVA, P., SANZ-RUIZ, R., NUNEZ GARCIA, A., FERNANDEZ SANTOS, M. E., SANCHEZ, P. L. & FERNANDEZ-AVILES, F. 2012. Functional multipotency of stem cells: what do we need from them in the heart? *Stem Cells Int,* 2012**,** 1-12.

DIVAC, I. F., F. STORM-MATHISEN, J 1977. High affinity uptake of glutamate in terminals of corticostriatal axons. *Nature,* 266**,** 377-378.

DOWTHWAITE, G. P., BISHOP, J. C., REDMAN, S. N., KHAN, I. M., ROONEY, P., EVANS, D. J. R., HAUGHTON, L., BAYRAM, Z., BOYER, S., THOMSON, B., WOLFE, M. S. & ARCHER, C. W. 2004. The surface of articular cartilage contains a progenitor cell population. *J Cell Sci,* 117**,** 889-897.

DOWTHWAITE, G. P., FLANNERY, C. R., FLANNELLY, J., LEWTHWAITE, J. C., ARCHER, C. W. & PITSILLIDES, A. A. 2003. A mechanism underlying the movement requirement for synovial joint cavitation. *Matrix Biology,* 22**,** 311-322.

DOWTHWAITE, G. P., WARD, A. C., FLANNELY, J., SUSWILLO, R. F., FLANNERY, C. R., ARCHER, C. W. & PITSILLIDES, A. A. 1999. The effect of mechanical strain on hyaluronan metabolism in embryonic fibrocartilage cells. *Matrix Biol,* 18**,** 523-32.

DUANCE V. C., V.-T. A., WARDALE R. J., WOTTON S. F. 1999. The collagens of articular and meniscal cartilages. *In:* ARCHER, C. W., CATERSON, B., BENJAMIN, M. & RALPHS, J. R. (eds.) *Biology of the synovial joint.* Amsterdam: Harwood publishers.

DUFF, S. E., LI, C., M., G. J. & KUMAR, S. 2003. CD105 is important for angiogenesis: evidence and potential applications. *The FASEB Journal,* 17**,** 984-992.

DY, P., SMITS, P., SILVESTER, A., PENZO-MÉNDEZ, A., DUMITRIU, B., HAN, Y., LA MOTTE, C. A. D., KINGSLEY, D. M. & LEFEBVRE, V. 2010. Synovial joint morphogenesis requires the chondrogenic action of Sox5 and Sox6 in growth plate and articular cartilage. *Developmental Biology,* 341**,** 346-359.

EDWARDS, J. C., WILKINSON, L. S., H M JONES, P. S., HENDERSON, K. J., WORRALL, J. G. & PITSILLIDES, A. A. 1994. The formation of human synovial joint cavities: a possible role for hyaluronan and CD44 in altered interzone cohesion. *J. Anat,* 185**,** 355-367.

EISENBERG, E. & LEVANON, E. Y. 2013. Human housekeeping genes, revisited. *Trends Genet,* 29**,** 569-74.

EMONS, J., CHAGIN, A. S., SÄVENDAHL, L., KARPERIEN, M. & WIT, J. M. 2011. Mechanisms of Growth Plate Maturation and Epiphyseal Fusion. *Hormone Research in Paediatrics,* 75**,** 383-391.

ENCODE 2011. Standards, Guidelines and Best Practices for RNA-Seq. *The ENCODE Consortium.*

ERIKSSON, J. E., BRAUTIGAN, D. L., VALLEE, R., OLMSTED, J., FUJIKI, H. & GOLDMAN, R. D. 1992a. Cytoskeletal integrity in interphase cells requires protein phosphatase activity. *Proc Natl Acad Sci U S A,* 89**,** 11093-7.

ERIKSSON, J. E., OPAL, P. & GOLDMAN, R. D. 1992b. Intermediate filament dynamics. *Curr Opin Cell Biol,* 4**,** 99-104.

ESTRADA, J. C., TORRES, Y., BENGURIA, A., DOPAZO, A., ROCHE, E., CARRERA-QUINTANAR, L., PEREZ, R. A., ENRIQUEZ, J. A., TORRES, R., RAMIREZ, J. C., SAMPER, E. & BERNAD, A. 2013. Human mesenchymal stem cell-replicative senescence and oxidative stress are closely linked to aneuploidy. *Cell Death Dis,* 4**,** e691.

EYRE, D. 2002. Collagen of articular cartilage. *Arthritis Research,* 4**,** 30-35.

EYRE, D., WEIS, M. & WU, J. 2006. Articular cartilage collagen: an irreplaceable framework? *European Cells and Materials,* 12**,** 57-63.

EYRE, D. R. 1991. The collagens of articular cartilage. *Semin Arthritis Rheum,* 21**,** 2-11.

EYRE, D. R., APON, S., WU, J. J., ERICSSON, L. H. & WALSH, K. A. 1987. Collagen type IX: evidence for covalent linkages to type II collagen in cartilage. *FEBS Lett,* 220**,** 337-41.

EYRE, D. R., DICKSON, I. R. & VAN NESS, K. 1988. Collagen cross-linking in human bone and articular cartilage. Age-related changes in the content of mature hydroxypyridinium residues. *The Biochemical journal,* 252**,** 495-500.

FICKERT, S., FIEDLER, J. & BRENNER, R. E. 2004. Identification of subpopulations with characteristics of mesenchymal progenitor cells from human osteoarthritic cartilage using triple staining for cell surface markers. *Arthritis Res Ther,* 6**,** R422-32.

FINKEL, T. & HOLBROOK, N. J. 2000. Oxidants, oxidative stress and the biology of ageing. *Nature,* 408**,** 239-247.

FLANNERY, C. R., HUGHES, C. E., SCHUMACHER, B. L., TUDOR, D., AYDELOTTE, M. B., KUETTNER, K. E. & CATERSON, B. 1999. Articular cartilage superficial zone protein (SZP) is homologous to megakaryocyte stimulating factor precursor and Is a multifunctional proteoglycan with potential growth-promoting, cytoprotective, and lubricating properties in cartilage metabolism. *Biochem Biophys Res Commun,* 254**,** 535-41.

FRANCIS-WEST, P. H., ABDELFATTAH, A., CHEN, P., ALLEN, C., PARISH, J., LADHER, R., ALLEN, S., MACPHERSON, S., LUYTEN, F. P. & ARCHER, C. W. 1999. Mechanisms of GDF-5 action during skeletal development. *Development,* 126**,** 1305-1315.

FRIEDENSTEIN, A. J., GORSKAJA, J. F. & KULAGINA, N. N. 1976. Fibroblast precursors in normal and irradiated mouse hematopoietic organs. *Exp Hematol,* 4**,** 267-74.

FU, A. Y.-C. 2002. *Microfabricated Fluorescence-Activated Cell Sorters for Screening Bacterial Cells.* PhD, California Istitute of Technology.

GALBRAITH, D. W. 2010. Flow cytometry and fluorescence-activated cell sorting in plants: the past, present, and future. *Biomedica,* 30**,** 65-70.

GARCÍA-CARVAJAL, Z. Y., GARCIADIEGO-CÁZARES, D., PARRA-CID, C., AGUILAR-GAYTÁN, R., VELASQUILLO, C., IBARRA, C. & CARMONA, J. S. C. 2013. Cartilage Tissue Engineering: The Role of Extracellular Matrix (ECM) and Novel Strategies. *In:* ANDRADES, J. A. (ed.). Regenerative Medicine and Tissue Engineering.

GEDYE, C. A., HUSSAIN, A., PATERSON, J., SMRKE, A., SAINI, H., SIRSKYJ, D., PEREIRA, K., LOBO, N., STEWART, J., GO, C., HO, J., MEDRANO, M., HYATT, E., YUAN, J., LAURIAULT, S., KONDRATYEV, M., VAN DEN BEUCKEN, T., JEWETT, M., DIRKS, P., GUIDOS, C. J., DANSKA, J., WANG, J., WOUTERS, B., NEEL, B., ROTTAPEL, R. & AILLES, L. E. 2014. Cell Surface Profiling Using High-Throughput Flow Cytometry: A Platform for Biomarker Discovery and Analysis of Cellular Heterogeneity. *PLoS ONE,* 9**,** e105602.

GELSE, K., POSCHL, E. & AIGNER, T. 2003. Collagens - structure, function, and biosynthesis. *Advanced Drug Delivery Reviews,* 55**,** 1531-1546.

GILLEY, J. A. & KERNIE, S. G. 2011. Excitatory amino acid transporter 2 and excitatory amino acid transporter 1 negatively regulate calcium-dependent proliferation of hippocampal neural progenitor cells and are persistently upregulated after injury. *Eur J Neurosci,* 34**,** 1712-23.

GLUHAK, J., MAIS, A. & MINA, M. 1996. Tenascin-C is associated with early stages of chondrogenesis by chick mandibular ectomesenchymal cells in vivo and in vitro. *Dev Dyn,* 205**,** 24-40.

GOLDRING, M. B., BIRKHEAD, J., SANDELL, L. J., KIMURA, T. & KRANE, S. M. 1988. Interleukin 1 suppresses expression of cartilage-specific types II and IX collagens and increases types I and III collagens in human chondrocytes. *J Clin Invest,* 82**,** 2026-37.

GOLDRING, M. B. & MARCU, K. B. 2009. Cartilage homeostasis in health and rheumatic diseases. *Arthritis Research & Therapy,* 11**,** 224-224.

GOLDRING, M. B., OTERO, M., TSUCHIMOCHI, K., IJIRI, K. & LI, Y. 2008. Defining the roles of inflammatory and anabolic cytokines in cartilage metabolism. *Ann Rheum Dis,* 67**,** 098764.

GOMOLL, A. H., FILARDO, G., ALMQVIST, F. K., BUGBEE, W. D., JELIC, M., MONLLAU, J. C., PUDDU, G., RODKEY, W. G., VERDONK, P., VERDONK, R., ZAFFAGNINI, S. & MARCACCI, M. 2012. Surgical treatment for early osteoarthritis. Part II: allografts and concurrent procedures. *Knee Surg Sports Traumatol Arthrosc,* 20**,** 468-86.

GRABHERR, M. G., HAAS, B. J., YASSOUR, M., LEVIN, J. Z., THOMPSON, D. A., AMIT, I., ADICONIS, X., FAN, L., RAYCHOWDHURY, R., ZENG, Q., CHEN, Z., MAUCELI, E., HACOHEN, N., GNIRKE, A., RHIND, N., DI PALMA, F., BIRREN, B. W., NUSBAUM, C., LINDBLAD-TOH, K., FRIEDMAN, N. & REGEV, A. 2011. Full-length transcriptome assembly from RNA-Seq data without a reference genome. *Nat Biotech,* 29**,** 644-652.

GRAY, H. 1989. *Grays's Anatomy,* London, Churchill Livingstone.

GRODZINSKY, A. J., LEVENSTON, M. E., JIN, M. & FRANK, E. H. 2000. CARTILAGE TISSUE REMODELING IN RESPONSE TO MECHANICAL FORCES. *Annual Review of Biomedical Engineering,* 2**,** 691-713.

GROGAN, S. P., MIYAKI, S., ASAHARA, H., D'LIMA, D. D. & LOTZ, M. K. 2009. Mesenchymal progenitor cell markers in human articular cartilage: normal distribution and changes in osteoarthritis. *Arthritis Res Ther,* 11**,** R85.

GUENETTE, R. S., SRIDHAR, S., HERLEY, M., MOOIBROEK, M., WONG, P. & TENNISWOOD, M. 1997. Embigin, a developmentally expressed member of the immunoglobulin super family, is also expressed during regression of prostate and mammary gland. *Developmental Genetics,* 21**,** 268-278.

GUILAK, F., ALEXOPOULOS, L. G., UPTON, M. L., YOUN, I., CHOI, J. B., CAO, L. I., SETTON, L. A. & HAIDER, M. A. 2006. The Pericellular Matrix as a Transducer of Biomechanical and Biochemical Signals in Articular Cartilage. *Annals of the New York Academy of Sciences,* 1068**,** 498-512.

HALESTRAP, A. P. & PRICE, N. T. 1999. The proton-linked monocarboxylate transporter (MCT) family: structure, function and regulation. *Biochem J,* 343 Pt 2**,** 281-99.

HALFON, S., ABRAMOV, N., GRINBLAT, B. & GINIS, I. 2011. Markers distinguishing mesenchymal stem cells from fibroblasts are downregulated with passaging. *Stem Cells Dev,* 20**,** 53-66.

HANGODY, L., KISH, G., KARPATI, Z., UDVARHELYI, I., SZIGETI, I. & BELY, M. 1998. Mosaicplasty for the treatment of articular cartilage defects: application in clinical practice. *Orthopedics,* 21**,** 751-6.

HANGODY, L., RATHONYI, G. K., DUSKA, Z., VASARHELYI, G., FULES, P. & MODIS, L. 2004. Autologous osteochondral mosaicplasty. Surgical technique. *J Bone Joint Surg Am,* 1**,** 65-72.

HARDCASTLE, T. & KELLY, K. 2010. baySeq: Empirical Bayesian methods for identifying differential expression in sequence count data. *BMC Bioinformatics,* 11**,** 422.

HARDINGHAM, T. E., OLDERSHAW, R. A. & TEW, S. R. 2006. Cartilage, SOX9 and Notch signals in chondrogenesis. *Journal of Anatomy,* 209**,** 469-480.

HAYASHI, T., ABE, E. & JASIN, H. E. 1996. Fibronectin synthesis in superficial and deep layers of normal articular cartilage. *Arthritis Rheum,* 39**,** 567-73.

HAYES, A. J., DOWTHWAITE, G. P., WEBSTER, S. V. & ARCHER, C. W. 2003. The distribution of Notch receptors and their ligands during articular cartilage development. *Journal of Anatomy,* 202**,** 495-502.

HAYES, A. J., HALL, A., BROWN, L., TUBO, R. & CATERSON, B. 2007. Macromolecular Organization and In Vitro Growth Characteristics of Scaffold-free Neocartilage Grafts. *Journal of Histochemistry & Cytochemistry,* 55**,** 853-866.

HAYES, A. J., MACPHERSON, S., MORRISON, H., DOWTHWAITE, G. & ARCHER, C. W. 2001. The development of articular cartilage: evidence for an appositional growth mechanism. *Anatomy and Embryology,* 203**,** 469-479.

HAYES, A. J., TUDOR, D., NOWELL, M. A., CATERSON, B. & HUGHES, C. E. 2008. Chondroitin sulfate sulfation motifs as putative biomarkers for isolation of articular cartilage progenitor cells. *J Histochem Cytochem,* 56**,** 125-38.

HAYFLICK, L. 1965. THE LIMITED IN VITRO LIFETIME OF HUMAN DIPLOID CELL STRAINS. *Exp Cell Res,* 37**,** 614-36.

HEINEGARD, D. & OLDBERG, A. 1989. Structure and biology of cartilage and bone matrix noncollagenous macromolecules. *Faseb J,* 3**,** 2042-51.

HEINO, J., HUHTALA, M., KAPYLA, J. & JOHNSON, M. S. 2009. Evolution of collagen-based adhesion systems. *International Journal of Biochemistry & Cell Biology,* 41**,** 341-348.

HELLEMANS, J., COUCKE, P. J., GIEDION, A., PAEPE, A. D., KRAMER, P., BEEMER, F. & MORTIER, G. R. 2003. Homozygous Mutations in IHH Cause Acrocapitofemoral Dysplasia, an Autosomal Recessive Disorder with Cone-Shaped Epiphyses in Hands and Hips. *American journal of human genetics,* 72**,** 1040-1046.

HENDREN, L. & BEESON, P. 2009. A review of the differences between normal and osteoarthritis articular cartilage in human knee and ankle joints. *The Foot,* 19**,** 171-176.

HERRERO-BEAUMONT, G., ROMAN-BLAS, J. A., CASTAÑEDA, S. & JIMENEZ, S. A. 2009. Primary Osteoarthritis No Longer Primary: Three Subsets with Distinct Etiological, Clinical, and Therapeutic Characteristics. *Seminars in Arthritis and Rheumatism,* 39**,** 71-80.

HERZENBERG, L. A., PARKS, D., SAHAF, B., PEREZ, O., ROEDERER, M. & HERZENBERG, L. A. 2002. The History and Future of the Fluorescence Activated Cell Sorter and Flow Cytometry: A View from Stanford. *Clinical Chemistry,* 48**,** 1819-1827.

HOCHEDLINGER, K. & PLATH, K. 2009. Epigenetic reprogramming and induced pluripotency. *Development,* 136**,** 509-523.

HOLMIN, S., ALMQVIST, P., LENDAHL, U. & MATHIESEN, T. 1997. Adult nestin-expressing subependymal cells differentiate to astrocytes in response to brain injury. *Eur J Neurosci,* 9**,** 65-75.

HOLMVALL, K., CAMPER, L., JOHANSSON, S., KIMURA, J. H. & LUNDGREN-AKERLUND, E. 1995. Chondrocyte and chondrosarcoma cell integrins with affinity for collagen type II and their response to mechanical stress. *Exp Cell Res,* 221**,** 496-503.

HOMANDBERG, G. A., WEN, C. & HUI, F. 1998. Cartilage damaging activities of fibronectin fragments derived from cartilage and synovial fluid. *Osteoarthritis and Cartilage,* 6**,** 231-44.

HORTON, W. E., JR., BENNION, P. & YANG, L. 2006. Cellular, molecular, and matrix changes in cartilage during aging and osteoarthritis. *J Musculoskelet Neuronal Interact,* 6**,** 379-81.

HORWITZ, E. M., LE BLANC, K., DOMINICI, M., MUELLER, I., SLAPER-CORTENBACH, I., MARINI, F. C., DEANS, R. J., KRAUSE, D. S. & KEATING, A. 2005. Clarification of the nomenclature for MSC: The International Society for Cellular Therapy position statement. *Cytotherapy,* 7**,** 393-395.

HOWLETT, C. R. 1979. The fine structure of the proximal growth plate of the avian tibia. *J Anat,* 128**,** 377-99.

HUANG, K. & WU, L. 2008. Aggrecanase and Aggrecan Degradation in Osteoarthritis: A Review. *Journal of International Medical Research,* 36**,** 1149-1160.

HUANG, R.-P., OZAWA, M., KADOMATSU, K. & MURAMATSU, T. 1993. Embigin, a Member of the Immunoglobulin Superfamily Expressed in Embryonic Cells, Enhances Cell-Substratum Adhesion. *Developmental Biology,* 155**,** 307-314.

HUNZIKER, E. B. 2002. Articular cartilage repair: basic science and clinical progress. A review of the current status and prospects. *Osteoarthritis and Cartilage,* 10**,** 432-63.

HUNZIKER, E. B. 2009. The Elusive Path to Cartilage Regeneration. *Advanced Materials,* 21**,** 3419-3424.

HUNZIKER, E. B. 2010. The structure of articular cartilage. *In:* ARCHER, C. W. & RALPHS, J. R. (eds.) *Regenerative medicine and biomaterials for the repair of connective tissues.* Oxford, Cambridge, New Delhi: Woodhead publishing limited.

HUNZIKER, E. B., KAPFINGER, E. & GEISS, J. 2007. The structural architecture of adult mammalian articular cartilage evolves by a synchronized process of tissue resorption and neoformation during postnatal development. *Osteoarthritis and Cartilage,* 15**,** 403-413.

HUTMACHER, D. W. 2000. Scaffolds in tissue engineering bone and cartilage. *Biomaterials,* 21**,** 2529-2543.

IOZZO, R. V. 1998. Matrix proteoglycans: From molecular design to cellular function. *Annual Review of Biochemistry,* 67**,** 609-652.

ISHIDA, O., TANAKA, Y., MORIMOTO, I., TAKIGAWA, M. & ETO, S. 1997. Chondrocytes are regulated by cellular adhesion through CD44 and hyaluronic acid pathway. *J Bone Miner Res,* 12**,** 1657-63.

ITO, K. & SUDA, T. 2014. Metabolic requirements for the maintenance of self-renewing stem cells. *Nat Rev Mol Cell Biol,* 15**,** 243-256.

ITO, T., SAWADA, R., FUJIWARA, Y. & TSUCHIYA, T. 2008. FGF-2 increases osteogenic and chondrogenic differentiation potentials of human mesenchymal stem cells by inactivation of TGF-beta signaling. *Cytotechnology,* 56**,** 1-7.

JACKSON, D. W., LALOR, P. A., ABERMAN, H. M. & SIMON, T. M. 2001. Spontaneous repair of full-thickness defects of articular cartilage in a goat model. A preliminary study. *J Bone Joint Surg Am,* 83-a**,** 53-64.

JAKOB, R. P., FRANZ, T., GAUTIER, E. & MAINIL-VARLET, P. 2002. Autologous osteochondral grafting in the knee: indication, results, and reflections. *Clin Orthop Relat Res,* 401**,** 170-84.

JEAN, Y. H., WEN, Z. H., CHANG, Y. C., HSIEH, S. P., LIN, J. D., TANG, C. C., CHEN, W. F., CHOU, A. K. & WONG, C. S. 2008. Increase in excitatory amino acid concentration and transporters expression in osteoarthritic knees of anterior cruciate ligament transected rabbits. *Osteoarthritis Cartilage,* 16**,** 1442-9.

JEFFERY, A. K., BLUNN, G. W., ARCHER, C. W. & BENTLEY, G. 1991. 3-DIMENSIONAL COLLAGEN ARCHITECTURE IN BOVINE ARTICULAR-CARTILAGE. *Journal of Bone and Joint Surgery-British Volume,* 73**,** 795-801.

JEFFREY, J. E., GREGORY, D. W. & ASPDEN, R. M. 1995. Matrix Damage and Chondrocyte Viability Following a Single Impact Load on Articular-Cartilage. *Archives of Biochemistry and Biophysics,* 322**,** 87-96.

JOBERT, A. S., ZHANG, P., COUVINEAU, A., BONAVENTURE, J., ROUME, J., LE MERRER, M. & SILVE, C. 1998. Absence of functional receptors for parathyroid hormone and parathyroid hormone-related peptide in Blomstrand chondrodysplasia. *The Journal of Clinical Investigation,* 102**,** 34-40.

JOHNSTONE, B., HERING, T. M., CAPLAN, A. I., GOLDBERG, V. M. & YOO, J. U. 1998. In vitro chondrogenesis of bone marrow-derived mesenchymal progenitor cells. *Exp Cell Res,* 238**,** 265-72.

JONES, E. A., CRAWFORD, A., ENGLISH, A., HENSHAW, K., MUNDY, J., CORSCADDEN, D., CHAPMAN, T., EMERY, P., HATTON, P. & MCGONAGLE, D. 2008. Synovial fluid mesenchymal stem cells in health and early osteoarthritis: detection and functional evaluation at the single-cell level. *Arthritis Rheum,* 58**,** 1731-40.

JONES, P. H. & WATT, F. M. 1993. Separation of human epidermal stem cells from transit amplifying cells on the basis of differences in integrin function and expression. *Cell,* 73**,** 713-724.

KACHINSKY, A. M., DOMINOV, J. A. & MILLER, J. B. 1994. Myogenesis and the intermediate filament protein, nestin. *Dev Biol,* 165**,** 216-28.

KANDEL, R. A., CHEN, H., CLARK, J. & RENLUND, R. 1995. Transplantation of cartilagenous tissue generated in vitro into articular joint defects. *Artif Cells Blood Substit Immobil Biotechnol,* 23**,** 565-77.

KARLSSON, C., THORNEMO, M., HENRIKSSON, H. B. & LINDAHL, A. 2009. Identification of a stem cell niche in the zone of Ranvier within the knee joint. *J Anat,* 215**,** 355-63.

KARP, G. 2008. *Cellular and molecular biology concepts and experiments,* , Wiley & Sons.

KHAN, I. M., EVANS, S. L., YOUNG, R. D., BLAIN, E. J., QUANTOCK, A. J., AVERY, N. & ARCHER, C. W. 2011. Fibroblast growth factor 2 and transforming growth factor β1 induce precocious maturation of articular cartilage. *Arthritis & Rheumatism,* 63**,** 3417-3427.

KHAN, I. M., FRANCIS, L., THEOBALD, P. S., PERNI, S., YOUNG, R. D., PROKOPOVICH, P., CONLAN, R. S. & ARCHER, C. W. 2013. In vitro growth factor-induced bio engineering of mature articular cartilage. *Biomaterials,* 34**,** 1478-1487.

KHAN, I. M., GILBERT, S. J., CATERSON, B., SANDELL, L. J. & ARCHER, C. W. 2008a. Oxidative stress induces expression of osteoarthritis markers procollagen IIA and 3B3(-) in adult bovine articular cartilage. *Osteoarthritis and Cartilage,* 16**,** 698-707.

KHAN, I. M., PALMER, E. A. & ARCHER, C. W. 2010. Fibroblast growth factor-2 induced chondrocyte cluster formation in experimentally wounded articular cartilage is blocked by soluble Jagged-1. *Osteoarthritis and Cartilage,* 18**,** 208-19.

KHAN, I. M., REDMAN, S. N., WILLIAMS, R., DOWTHWAITE, G. P., OLDFIELD, S. F. & ARCHER, C. W. 2007. The Development of Synovial Joints. *In:* GERALD, P. S. (ed.) *Current Topics in Developmental Biology.* Academic Press.

KHAN, W. S., TEW, S. R., ADESIDA, A. B. & HARDINGHAM, T. E. 2008b. Human infrapatellar fat pad-derived stem cells express the pericyte marker 3G5 and show enhanced chondrogenesis after expansion in fibroblast growth factor-2. *Arthritis Res Ther,* 10**,** 3.

KIM, S. J., KIM, E. J., KIM, Y. H., HAHN, S. B. & LEE, J. W. 2003. The modulation of integrin expression by the extracellular matrix in articular chondrocytes. *Yonsei Med J,* 44**,** 493-501.

KIM, Y.-J., GRODZINSKY, A. J. & PLAAS, A. H. K. 1996. Compression of Cartilage Results in Differential Effects on Biosynthetic Pathways for Aggrecan, Link Protein, and Hyaluronan. *Archives of Biochemistry and Biophysics,* 328**,** 331-340.

KNOBLICH, J. A. 2008. Mechanisms of Asymmetric Stem Cell Division. *Cell,* 132**,** 583-597.

KNUDSON, C. B. & KNUDSON, W. 2001. Cartilage proteoglycans. *Seminars in Cell & Developmental Biology,* 12**,** 69-78.

KNUT, P. L., M. OTTERSON, OLE P, STORM-MATHISEN, J. DANBOLD, NIELS C 1995. Differential Expression of Two Glial Glutamate Transporters in the Rat Brain: Quantitative and lmmunocytochemical Observations *Journal of Neuriscience,* 15**,** 1835-1853.

KNUTSEN, G., DROGSET, J. O., ENGEBRETSEN, L., GRONTVEDT, T., ISAKSEN, V., LUDVIGSEN, T. C., ROBERTS, S., SOLHEIM, E., STRAND, T. & JOHANSEN, O. 2007. A randomized trial comparing autologous chondrocyte implantation with microfracture. Findings at five years. *J Bone Joint Surg Am,* 89**,** 2105-12.

KOELLING, S., KRUEGEL, J., IRMER, M., PATH, J. R., SADOWSKI, B., MIRO, X. & MIOSGE, N. 2009. Migratory chondrogenic progenitor cells from repair tissue during the later stages of human osteoarthritis. *Cell Stem Cell,* 4**,** 324-35.

KOURI, J. B., JIMÉNEZ, S. A., QUINTERO, M. & CHICO, A. 1996. Ultrastructural study of chondrocytes from fibrillated and non-fibrillated human osteoarthritic cartilage. *Osteoarthritis and Cartilage,* 4**,** 111-125.

KOYAMA, E., LEATHERMAN, J. L., SHIMAZU, A., NAH, H.-D. & PACIFICI, M. 1995. Syndecan-3, tenascin-C, and the development of cartilaginous skeletal elements and joints in chick limbs. *Developmental Dynamics,* 203**,** 152-162.

KRONENBERG, H. M. 2003. Developmental regulation of the growth plate. *Nature,* 423**,** 332-6.

KUBO, H., SHIMIZU, M., TAYA, Y., KAWAMOTO, T., MICHIDA, M., KANEKO, E., IGARASHI, A., NISHIMURA, M., SEGOSHI, K., SHIMAZU, Y., TSUJI, K., AOBA, T. & KATO, Y. 2009. Identification of mesenchymal stem cell (MSC)-transcription factors by microarray and knockdown analyses, and

signature molecule-marked MSC in bone marrow by immunohistochemistry. *Genes Cells,* 14**,** 407-24.
KURTH, T. B., DELL'ACCIO, F., CROUCH, V., AUGELLO, A., SHARPE, P. T. & DE BARI, C. 2011. Functional mesenchymal stem cell niches in adult mouse knee joint synovium in vivo. *Arthritis Rheum,* 63**,** 1289-300.
KVAM, V. M., LIU, P. & SI, Y. 2012. A comparison of statistical methods for detecting differentially expressed genes from RNA-seq data. *American Journal of Botany,* 99**,** 248-256.
KWAN, A. P., CUMMINGS, C. E., CHAPMAN, J. A. & GRANT, M. E. 1991. Macromolecular organization of chicken type X collagen in vitro. *The Journal of Cell Biology,* 114**,** 597-604.
LAJEUNESSE, D., MASSICOTTE, F., PELLETIER, J. P. & MARTEL-PELLETIER, J. 2003. Subchondral bone sclerosis in osteoarthritis: not just an innocent bystander. *Modern Rheumatology,* 13**,** 0007-0014.
LAJEUNESSE, D. & REBOUL, P. 2003. Subchondral bone in osteoarthritis: a biologic link with articular cartilage leading to abnormal remodeling. *Curr Opin Rheumatol,* 15**,** 628-33.
LAKETIC-LJUBOJEVIC, I., SUVA, L. J., MAATHUIS, F. J., SANDERS, D. & SKERRY, T. M. 1999. Functional characterization of N-methyl-D-aspartic acid-gated channels in bone cells. *Bone,* 25**,** 631-7.
LE GRAVERAND, M. P., BUCK, R. J., WYMAN, B. T., VIGNON, E., MAZZUCA, S. A., BRANDT, K. D., PIPERNO, M., CHARLES, H. C., HUDELMAIER, M., HUNTER, D. J., JACKSON, C., KRAUS, V. B., LINK, T. M., MAJUMDAR, S., PRASAD, P. V., SCHNITZER, T. J., VAZ, A., WIRTH, W. & ECKSTEIN, F. 2010. Change in regional cartilage morphology and joint space width in osteoarthritis participants versus healthy controls: a multicentre study using 3.0 Tesla MRI and Lyon-Schuss radiography. *Ann Rheum Dis,* 69**,** 155-62.
LEBARON, R. G. & ATHANASIOU, K. A. 2000. Ex vivo synthesis of articular cartilage. *Biomaterials,* 21**,** 2575-87.
LI, J., WITTEN, D. M., JOHNSTONE, I. M. & TIBSHIRANI, R. 2012. Normalization, testing, and false discovery rate estimation for RNA-sequencing data. *Biostatistics,* 13**,** 523-538.
LI, L. & CLEVERS, H. 2010. Coexistence of Quiescent and Active Adult Stem Cells in Mammals. *Science,* 327**,** 542-545.
LI, N. G., SHI, Z. H., TANG, Y. P., WANG, Z. J., SONG, S. L., QIAN, L. H., QIAN, D. W. & DUAN, J. A. 2011. New hope for the treatment of osteoarthritis through selective inhibition of MMP-13. *Curr Med Chem,* 18**,** 977-1001.
LIU, L., LI, Y., LI, S., HU, N., HE, Y., PONG, R., LIN, D., LU, L. & LAW, M. 2012. Comparison of Next-Generation Sequencing Systems. *Journal of Biomedicine and Biotechnology,* 2012**,** 1-11.
LIU, Y., ZHOU, J. & WHITE, K. P. 2014. RNA-seq differential expression studies: more sequence or more replication? *Bioinformatics,* 30**,** 301-304.
LIVESLEY, P. J., DOHERTY, M., NEEDOFF, M. & MOULTON, A. 1991. Arthroscopic lavage of osteoarthritic knees. *J Bone Joint Surg Br,* 73**,** 922-6.
LOESER, R. F. 2002. Integrins and cell signaling in chondrocytes. *Biorheology,* 39**,** 119-24.
LONGOBARDI, L., O'REAR, L., AAKULA, S., JOHNSTONE, B., SHIMER, K., CHYTIL, A., HORTON, W. A., MOSES, H. L. & SPAGNOLI, A. 2006. Effect of IGF-I in the chondrogenesis of bone marrow mesenchymal stem cells in the presence or absence of TGF-beta signaling. *J Bone Miner Res,* 21**,** 626-36.
LORENZ, H. & RICHTER, W. 2006. Osteoarthritis: cellular and molecular changes in degenerating cartilage. *Prog Histochem Cytochem,* 40**,** 135-63.

LOTZ, M. & LOESER, R. F. 2012. Effects of aging on articular cartilage homeostasis. *Bone,* 51**,** 241-248.

LUNA, G., LEWIS, G. P., BANNA, C. D., SKALLI, O. & FISHER, S. K. 2010. Expression profiles of nestin and synemin in reactive astrocytes and Muller cells following retinal injury: a comparison with glial fibrillar acidic protein and vimentin. *Mol Vis,* 16**,** 2511-23.

LV, F.-J., TUAN, R. S., CHEUNG, K. M. C. & LEUNG, V. Y. L. 2014. Concise Review: The Surface Markers and Identity of Human Mesenchymal Stem Cells. *STEM CELLS,* 32**,** 1408-1419.

MACKIE, E. J., AHMED, Y. A., TATARCZUCH, L., CHEN, K. S. & MIRAMS, M. 2008. Endochondral ossification: How cartilage is converted into bone in the developing skeleton. *The International Journal of Biochemistry & Cell Biology,* 40**,** 46-62.

MACKIE, E. J. & RAMSEY, S. 1996. Expression of tenascin in joint-associated tissues during development and postnatal growth. *J Anat,* 188**,** 157-65.

MACKIE, E. J., THESLEFF, I. & CHIQUET-EHRISMANN, R. 1987. Tenascin is associated with chondrogenic and osteogenic differentiation in vivo and promotes chondrogenesis in vitro. *The Journal of Cell Biology,* 105**,** 2569-2579.

MAJUMDAR, M., KEANE-MOORE, M., BUYANER, D., HARDY, W., MOORMAN, M., MCINTOSH, K. & MOSCA, J. 2003. Characterization and functionality of cell surface molecules on human mesenchymal stem cells. *Journal of Biomedical Science,* 10**,** 228-241.

MAK, H. C. 2011. Next-generation sequence analysis. *Nat Biotech,* 29**,** 45-46.

MANKIN, H. J. 1962a. Localization of Tritiated Thymidine in Articular Cartilage of Rabbits I. Growth In Immature Cartilage. *The Journal of Bone & Joint Surgery,* 44**,** 682-688.

MANKIN, H. J. 1962b. Localization of Tritiated Thymidine in Articular Cartilage of Rabbits II. Repair in Immature Cartilage. *The Journal of Bone & Joint Surgery,* 44**,** 688-698.

MANKIN, H. J. 1963. Localization of Tritiated Thymidine in Articular Cartilage of Rabbits III. MATURE ARTICULAR CARTILAGE. *The Journal of Bone & Joint Surgery,* 45**,** 529-540.

MARTEL-PELLETIER, J. & PELLETIER, J. P. 2010. Is osteoarthritis a disease involving only cartilage or other articular tissues? *Eklem Hastalik Cerrahisi,* 21**,** 2-14.

MARTIN, J. A. & BUCKWALTER, J. A. 2000. The role of chondrocyte-matrix interactions in maintaining and repairing articular cartilage. *Biorheology,* 37**,** 129-40.

MARTIN, J. A. & BUCKWALTER, J. A. 2001. Telomere Erosion and Senescence in Human Articular Cartilage Chondrocytes. *The Journals of Gerontology Series A: Biological Sciences and Medical Sciences,* 56**,** B172-B179.

MARTIN, J. A. & BUCKWALTER, J. A. 2002. Aging, articular cartilage chondrocyte senescence and osteoarthritis. *Biogerontology,* 3**,** 257-64.

MARTIN, R., BRUCE., BURR, D. B. & SHARKEY, N. A. 1998. *Skeletal Tissue Mechanics,* United Kingdom, Springer.

MARTINI, F. H. 2006. *Fundamentals of Anatomy & Physiology,* United States of America, Persons.

MASON, D. J., SUVA, L. J., GENEVER, P. G., PATTON, A. J., STEUCKLE, S., HILLAM, R. A. & SKERRY, T. M. 1997. Mechanically regulated expression of a neural glutamate transporter in bone: a role for excitatory amino acids as osteotropic agents? *Bone,* 20**,** 199-205.

MASUHARA, K., NAKAI, T., YAMAGUCHI, K., YAMASAKI, S. & SASAGURI, Y. 2002. Significant increases in serum and plasma concentrations of matrix metalloproteinases 3 and 9 in patients with rapidly destructive osteoarthritis of the hip. *Arthritis Rheum,* 46**,** 2625-31.

MCCARTHY, H. E., BARA, J. J., BRAKSPEAR, K., SINGHRAO, S. K. & ARCHER, C. W. 2012. The comparison of equine articular cartilage progenitor cells and bone marrow-derived stromal cells as potential cell sources for cartilage repair in the horse. *The Veterinary Journal,* 192**,** 345-351.

MENGSHOL, J. A., VINCENTI, M. P. & BRINCKERHOFF, C. E. 2001. IL-1 induces collagenase-3 (MMP-13) promoter activity in stably transfected chondrocytic cells: requirement for Runx-2 and activation by p38 MAPK and JNK pathways. *Nucleic Acids Res,* 29**,** 4361-72.

MICH, J. K., SIGNER, R. A., NAKADA, D., PINEDA, A., BURGESS, R. J., VUE, T. Y., JOHNSON, J. E. & MORRISON, S. J. 2014. Prospective identification of functionally distinct stem cells and neurosphere-initiating cells in adult mouse forebrain. *Elife,* 3**,** e02669.

MICHALCZYK, K. & ZIMAN, M. 2005. Nestin structure and predicted function in cellular cytoskeletal organisation. *Histol Histopathol,* 20**,** 665-71.

MIOSGE, N., HARTMANN, M., MAELICKE, C. & HERKEN, R. 2004. Expression of collagen type I and type II in consecutive stages of human osteoarthritis. *Histochem Cell Biol,* 122**,** 229-36.

MIOSGE, N., WALETZKO, K., BODE, C., QUONDAMATTEO, F., SCHULTZ, W. & HERKEN, R. 1998. Light and electron microscopic in-situ hybridization of collagen type I and type II mRNA in the fibrocartilaginous tissue of late-stage osteoarthritis. *Osteoarthritis and Cartilage,* 6**,** 278-85.

MITROVIC, D. R. 1977. Development of the metatarsophalangeal joint of the chick embryo: Morphological, ultrastructural and histochemical studies. *American Journal of Anatomy,* 150**,** 333-347.

MOBASHERI, A., KALAMEGAM, G., MUSUMECI, G. & BATT, M. E. 2014. Chondrocyte and mesenchymal stem cell-based therapies for cartilage repair in osteoarthritis and related orthopaedic conditions. *Maturitas,* 78**,** 188-198.

MOLLENHAUER, J., MOK, M. T., KING, K. B., GUPTA, M., CHUBINSKAYA, S., KOEPP, H. & COLE, A. A. 1999. Expression of Anchorin CII (Cartilage Annexin V) in Human Young, Normal Adult, and Osteoarthritic Cartilage. *Journal of Histochemistry & Cytochemistry,* 47**,** 209-220.

MORRISON, E. H., FERGUSON, M. W., BAYLISS, M. T. & ARCHER, C. W. 1996. The development of articular cartilage: I. The spatial and temporal patterns of collagen types. *J Anat,* 189 (Pt 1)**,** 9-22.

MUIR, H. 1995. The chondrocyte, architect of cartilage. Biomechanics, structure, function and molecular biology of cartilage matrix macromolecules. *Bioessays,* 17**,** 1039-1048.

MURAGLIA, A., CANCEDDA, R. & QUARTO, R. 2000. Clonal mesenchymal progenitors from human bone marrow differentiate in vitro according to a hierarchical model. *Journal of Cell Science,* 113**,** 1161-1166.

MURAMATSU, T. & MIYAUCHI, T. 2003. Basigin (CD147): a multifunctional transmembrane protein involved in reproduction, neural function, inflammation and tumor invasion. *Histol Histopathol,* 18**,** 981-7.

MURAMATSU, T. & MURAMATSU, H. 2004. Carbohydrate antigens expressed on stem cells and early embryonic cells. *Glycoconjugate Journal,* 21**,** 41-45.

MURDOCH, A. D., GRADY, L. M., ABLETT, M. P., KATOPODI, T., MEADOWS, R. S. & HARDINGHAM, T. E. 2007. Chondrogenic differentiation of human bone

marrow stem cells in transwell cultures: generation of scaffold-free cartilage. *Stem Cells,* 25**,** 2786-96.

MURRAY, R. C., SMITH, R. K., HENSON, F. M. & GOODSHIP, A. 2001. The distribution of cartilage oligomeric matrix protein (COMP) in equine carpal articular cartilage and its variation with exercise and cartilage deterioration. *Vet J,* 162**,** 121-8.

NAGAMATSU, G., KOSAKA, T., KAWASUMI, M., KINOSHITA, T., TAKUBO, K., AKIYAMA, H., SUDO, T., KOBAYASHI, T., OYA, M. & SUDA, T. 2011. A Germ Cell-specific Gene, Prmt5, Works in Somatic Cell Reprogramming. *Journal of Biological Chemistry,* 286**,** 10641-10648.

NAITO, K., TAKAHASHI, M., KUSHIDA, K., SUZUKI, M., OHISHI, T., MIURA, M., INOUE, T. & NAGANO, A. 1999. Measurement of matrix metalloproteinases (MMPs) and tissue inhibitor of metalloproteinases-1 (TIMP-1) in patients with knee osteoarthritis: comparison with generalized osteoarthritis. *Rheumatology,* 38**,** 510-5.

NAKAGAWA, T., NABESHIMA, Y.-I. & YOSHIDA, S. 2007. Functional Identification of the Actual and Potential Stem Cell Compartments in Mouse Spermatogenesis. *Developmental Cell,* 12**,** 195-206.

NAMIKI, J. & TATOR, C. H. 1999. Cell proliferation and nestin expression in the ependyma of the adult rat spinal cord after injury. *J Neuropathol Exp Neurol,* 58**,** 489-98.

NELISSEN, J. M., PETERS, I. M., DE GROOTH, B. G., VAN KOOYK, Y. & FIGDOR, C. G. 2000. Dynamic regulation of activated leukocyte cell adhesion molecule-mediated homotypic cell adhesion through the actin cytoskeleton. *Mol Biol Cell,* 11**,** 2057-68.

NELSON, L., MCCARTHY, H. E., FAIRCLOUGH, J., WILLIAMS, R. & ARCHER, C. W. 2014. Evidence of a Viable Pool of Stem Cells within Human Osteoarthritic Cartilage. *Cartilage,* 5**,** 203-214.

NEU, C. P., KOMVOPOULOS, K. & REDDI, H. A. 2009. The Interface of Functional Biotribology and Regenerative Medicine in Synovial Joints. *Tissue Engineering Part B: Reviews,* 14**,** 235-247.

NISHIDA, K., INOUE, H. & MURAKAMI, T. 1995. Immunohistochemical demonstration of fibronectin in the most superficial layer of normal rabbit articular cartilage. *Annals of the Rheumatic Diseases,* 54**,** 995-998.

NISWANDER, L. 2002. Interplay between the molecular signals that control vertebrate limb development. *Int. J. Dev. Biol,* 46**,** 877-881.

NOOKAEW, I., PAPINI, M., PORNPUTTAPONG, N., SCALCINATI, G., FAGERBERG, L., UHLEN, M. & NIELSEN, J. 2012. A comprehensive comparison of RNA-Seq-based transcriptome analysis from reads to differential gene expression and cross-comparison with microarrays: a case study in Saccharomyces cerevisiae. *Nucleic Acids Res,* 40**,** 10084-97.

OBAYASHI, S., TABUNOKI, H., KIM, S. & SATOH, J.-I. 2009. Gene Expression Profiling of Human Neural Progenitor Cells Following the Serum-Induced Astrocyte Differentiation. *Cellular and Molecular Neurobiology,* 29**,** 423-438.

OHNEDA, O., OHNEDA, K., ARAI, F., LEE, J., MIYAMOTO, T., FUKUSHIMA, Y., DOWBENKO, D., LASKY, L. A. & SUDA, T. 2001. ALCAM (CD166): its role in hematopoietic and endothelial development. *Blood,* 98**,** 2134-42.

ORTEGA-MARTÍNEZ, M., ROMERO-NÚÑEZ, E., NIDERHAUSER-GARCÍA, A., DE-LA-GARZA-GONZÁLEZ, C., ANCER-RODRÍGUEZ, J. & JARAMILLO-RANGEL, G. 2013. Evidence of chondrocyte turnover in lung cartilage, with the

probable participation of nestin-positive cells. *Cell Biology International,* 37**,** 239-241.
OSHLACK, A., ROBINSON, M. & YOUNG, M. 2010. From RNA-seq reads to differential expression results. *Genome Biology,* 11**,** 220.
OZSOLAK, F., PLATT, A. R., JONES, D. R., REIFENBERGER, J. G., SASS, L. E., MCINERNEY, P., THOMPSON, J. F., BOWERS, J., JAROSZ, M. & MILOS, P. M. 2009. Direct RNA sequencing. *Nature,* 461**,** 814-818.
PACIFICI, M. 1995. Tenascin-C and the development of articular cartilage. *Matrix Biol,* 14**,** 689-98.
PACIFICI, M., IWAMOTO, M., GOLDEN, E. B., LEATHERMAN, J. L., LEE, Y.-S. & CHUONG, C.-M. 1993. Tenascin is associated with articular cartilage development. *Developmental Dynamics,* 198**,** 123-134.
PACIFICI, M., KOYAMA, E. & IWAMOTO, M. 2005. Mechanisms of synovial joint and articular cartilage formation: Recent advances, but many lingering mysteries. *Birth Defects Research Part C: Embryo Today: Reviews,* 75**,** 237-248.
PACIFICI, M., KOYAMA, E., KIRSCH, T., LEATHERMAN, J. L. & GOLDEN, E. B. 1999. Involvement of tenascin-C and syndecan-3 in the development of chick limb diarthrodial joints. *In:* ARCHER, C. W., CATERSON, B., BENJAMIN, M. & RALPHS, J. R. (eds.) *Biology of the synovial joint.* Amsterdam: Harwood academic publishers.
PALMOSKI, M., PERRICONE, E. & BRANDT, K. D. 1979. Development and reversal of a proteoglycan aggregation defect in normal canine knee cartilage after immobilization. *Arthritis Rheum,* 22**,** 508-17.
PAN, Q., SHAI, O., LEE, L. J., FREY, B. J. & BLENCOWE, B. J. 2008. Deep surveying of alternative splicing complexity in the human transcriptome by high-throughput sequencing. *Nat Genet,* 40**,** 1413-1415.
PARK, D., XIANG, A. P., MAO, F. F., ZHANG, L., DI, C.-G., LIU, X.-M., SHAO, Y., MA, B.-F., LEE, J.-H., HA, K.-S., WALTON, N. & LAHN, B. T. 2010. Nestin Is Required for the Proper Self-Renewal of Neural Stem Cells. *STEM CELLS,* 28**,** 2162-2171.
PATEL, L., SUN, W., GLASSON, S., MORRIS, E., FLANNERY, C. & CHOCKALINGAM, P. 2011. Tenascin-C induces inflammatory mediators and matrix degradation in osteoarthritic cartilage. *BMC Musculoskeletal Disorders,* 12**,** 164.
PEARLE, A. D., WARREN, R. F. & RODEO, S. A. 2005. Basic science of articular cartilage and osteoarthritis. *Clin Sports Med,* 24**,** 1-12.
PELTTARI, K., STECK, E. & RICHTER, W. 2008. The use of mesenchymal stem cells for chondrogenesis. *Injury,* 39**,** 58-65.
PELTTARI, K., WINTER, A., STECK, E., GOETZKE, K., HENNIG, T., OCHS, B. G., AIGNER, T. & RICHTER, W. 2006. Premature induction of hypertrophy during in vitro chondrogenesis of human mesenchymal stem cells correlates with calcification and vascular invasion after ectopic transplantation in SCID mice. *Arthritis & Rheumatism,* 54**,** 3254-3266.
PETERSON, L., VASILIADIS, H. S., BRITTBERG, M. & LINDAHL, A. 2010. Autologous chondrocyte implantation: a long-term follow-up. *Am J Sports Med,* 38**,** 1117-24.
PFANNKUCHE, K., HANNES, T., KHALIL, M., NOGHABI, M. S., MORSHEDI, A., HESCHELER, J. & DROGE, P. 2010. Induced Pluripotent Stem Cells: A New Approach for Physiological Research. *Cellular Physiology and Biochemistry,* 26**,** 105-124.

PHINNEY, D. G. & PROCKOP, D. J. 2007. Concise Review: Mesenchymal Stem/Multipotent Stromal Cells: The State of Transdifferentiation and Modes of Tissue Repair—Current Views. *Stem Cells,* 25**,** 2896-2902.

PITSILLIDES, A. A. 1999. The role of hyaluronan in joint cavitation. *In:* ARCHER, C. W., CATERSON, B., BENJAMIN, M. & RALPHS, J. R. (eds.) *Biology of the synovial joint.* Amsterdam: Harwood Academic.

PITSILLIDES, A. A., SKERRY, T. M. & EDWARDS, J. C. W. 1999. Joint immobilization reduces synovial fluid hyaluronan concentration and is accompanied by changes in the synovial intimal cell populations. *Rheumatology,* 38**,** 1108-1112.

PITTENGER, M. F., MACKAY, A. M., BECK, S. C., JAISWAL, R. K., DOUGLAS, R., MOSCA, J. D., MOORMAN, M. A., SIMONETTI, D. W., CRAIG, S. & MARSHAK, D. R. 1999. Multilineage Potential of Adult Human Mesenchymal Stem Cells. *Science,* 284**,** 143-147.

POOLE, C. A. 1997. Articular cartilage chondrons: form, function and failure. *J Anat,* 191 (Pt 1)**,** 1-13.

POOLE, C. A., AYAD, S. & GILBERT, R. T. 1992. Chondrons from articular cartilage. V. Immunohistochemical evaluation of type VI collagen organisation in isolated chondrons by light, confocal and electron microscopy. *J Cell Sci,* 103**,** 1101-10.

POOLE, C. A., FLINT, M. H. & BEAUMONT, B. W. 1987. Chondrons in cartilage: ultrastructural analysis of the pericellular microenvironment in adult human articular cartilages. *J Orthop Res,* 5**,** 509-22.

POOLE, C. A., MATSUOKA, A. & SCHOFIELD, J. R. 1991. Chondrons from articular cartilage. III. Morphologic changes in the cellular microenvironment of chondrons isolated from osteoarthritic cartilage. *Arthritis Rheum,* 34**,** 22-35.

PORTRON, S., MERCERON, C., GAUTHIER, O., LESOEUR, J., SOURICE, S., MASSON, M., FELLAH, B. H., GEFFROY, O., LALLEMAND, E., WEISS, P., GUICHEUX, J. & VINATIER, C. 2013. Effects of In Vitro Low Oxygen Tension Preconditioning of Adipose Stromal Cells on Their In Vivo Chondrogenic Potential: Application in Cartilage Tissue Repair. *PLoS ONE,* 8**,** e62368.

PRETZEL, D., LINSS, S., ROCHLER, S., ENDRES, M., KAPS, C., ALSALAMEH, S. & KINNE, R. W. 2011. Relative percentage and zonal distribution of mesenchymal progenitor cells in human osteoarthritic and normal cartilage. *Arthritis Res Ther,* 13**,** R64.

PRITZKER, K. P. H., GAY, S., JIMENEZ, S. A., OSTERGAARD, K., PELLETIER, J. P., REVELL, P. A., SALTER, D. & VAN DEN BERG, W. B. 2006. Osteoarthritis cartilage histopathology: grading and staging. *Osteoarthritis and cartilage / OARS, Osteoarthritis Research Society,* 14**,** 13-29.

PROCKOP, D. J. 1997. Marrow stromal cells as stem cells for nonhematopoietic tissues. *Science,* 276**,** 71-4.

REDMAN, S. N., OLDFIELD, S. F. & ARCHER, C. W. 2005. Current strategies for articular cartilage repair. *Eur Cell Mater,* 9**,** 23-32.

REID, D. L., AYDELOTTE, M. B. & MOLLENHAUER, J. 2000. Cell attachment, collagen binding, and receptor analysis on bovine articular chondrocytes. *J Orthop Res,* 18**,** 364-73.

REVELL, P. A., PIRIE, C., AMIR, G., RASHAD, S. & WALKER, F. 1990. Metabolic activity in the calcified zone of cartilage: Observations on tetracycline labelled articular cartilage in human osteoarthritic hips. *Rheumatology International,* 10**,** 143-147.

RHEE, D. K., MARCELINO, J., BAKER, M., GONG, Y., SMITS, P., LEFEBVRE, V., JAY, G. D., STEWART, M., WANG, H., WARMAN, M. L. & CARPTEN, J. D. 2005. The secreted glycoprotein lubricin protects cartilage surfaces and inhibits synovial cell overgrowth. *J Clin Invest,* 115**,** 622-31.

RICHARDSON, K. 2011. *Analysis of Cell Surface Markers within Immature Bovine Articular Cartilage.* PhD thesis, Cardiff University.

ROBERT, S. & URBAN, J. P. G. 2013. *Intervertebral disks* [Online]. Available: http://www.ilo.org/safework_bookshelf/english?content&nd=857170059 [Accessed 14/07/2012 2013].

ROBERTS, S., MCCALL, I., DARBY, A., MENAGE, J., EVANS, H., HARRISON, P. & RICHARDSON, J. 2002. Autologous chondrocyte implantation for cartilage repair: monitoring its success by magnetic resonance imaging and histology. *Arthritis Res Ther,* 5**,** 1-14.

ROBERTSON, E. J., CHARATSI, I., JOYNER, C. J., KOONCE, C. H., MORGAN, M., ISLAM, A., PATERSON, C., LEJSEK, E., ARNOLD, S. J., KALLIES, A., NUTT, S. L. & BIKOFF, E. K. 2007. Blimp1 regulates development of the posterior forelimb, caudal pharyngeal arches, heart and sensory vibrissae in mice. *Development,* 134**,** 4335-4345.

ROBERTSON, G., SCHEIN, J., CHIU, R., CORBETT, R., FIELD, M., JACKMAN, S. D., MUNGALL, K., LEE, S., OKADA, H. M., QIAN, J. Q., GRIFFITH, M., RAYMOND, A., THIESSEN, N., CEZARD, T., BUTTERFIELD, Y. S., NEWSOME, R., CHAN, S. K., SHE, R., VARHOL, R., KAMOH, B., PRABHU, A.-L., TAM, A., ZHAO, Y., MOORE, R. A., HIRST, M., MARRA, M. A., JONES, S. J. M., HOODLESS, P. A. & BIROL, I. 2010. De novo assembly and analysis of RNA-seq data. *Nat Meth,* 7**,** 909-912.

ROBINSON, M. D., MCCARTHY, D. J. & SMYTH, G. K. 2010. edgeR: a Bioconductor package for differential expression analysis of digital gene expression data. *Bioinformatics,* 26**,** 139-140.

ROH, C., TAO, Q., PHOTOPOULOS, C. & LYLE, S. 2005. In Vitro Differences Between Keratinocyte Stem Cells and Transit-Amplifying Cells of the Human Hair Follicle. *J Investig Dermatol,* 125**,** 1099-1105.

RONN, K., REISCHL, N., GAUTIER, E. & JACOBI, M. 2011. Current Surgical Treatment of Knee Osteoarthritis. *Arthritis,* 2011**,** 1-9.

ROTHWELL, A. G. & BENTLEY, G. 1973. Chondrocyte multiplication in osteoarthritic articular cartilage. *J Bone Joint Surg Br,* 55**,** 588-94.

ROUGHLEY, P. J. 2006. The structure and function of cartilage proteoglycans. *Eur Cell Mater,* 12**,** 92-101.

RYAN, M. C. & SANDELL, L. J. 1990. Differential expression of a cysteine-rich domain in the amino-terminal propeptide of type II (cartilage) procollagen by alternative splicing of mRNA. *J Biol Chem,* 265**,** 10334-9.

SAHA, S. K., J. WOOD ,D ,J. YANG, X, B 2012. *Progenitor and Stem Cell Technologies and Therapies*, Woodhead Publishing Limited.

SALMIVIRTA, M., ELENIUS, K., VAINIO, S., HOFER, U., CHIQUET-EHRISMANN, R., THESLEFF, I. & JALKANEN, M. 1991. Syndecan from embryonic tooth mesenchyme binds tenascin. *J Biol Chem,* 266**,** 7733-9.

SALTER, D. M., GODOLPHIN, J. L. & GOURLAY, M. S. 1995. Chondrocyte heterogeneity: immunohistologically defined variation of integrin expression at different sites in human fetal knees. *Journal of Histochemistry & Cytochemistry,* 43**,** 447-57.

SANGER, F., NICKLEN, S. & COULSON, A. R. 1977. DNA sequencing with chain-terminating inhibitors. *Proc Natl Acad Sci U S A,* 74**,** 5463-7.

SASISEKHARAN, R., RAMAN, R. & PRABHAKAR, V. 2006. GLYCOMICS APPROACH TO STRUCTURE-FUNCTION RELATIONSHIPS OF GLYCOSAMINOGLYCANS. *Annual Review of Biomedical Engineering,* 8**,** 181-231.

SCHMID, T. M. & LINSENMAYER, T. F. 1985. Developmental acquisition of type × collagen in the embryonic chick tibiotarsus. *Developmental Biology,* 107**,** 373-381.

SCHUMACHER, B. L., BLOCK, J. A., SCHMID, T. M., AYDELOTTE, M. B. & KUETTNER, K. E. 1994. A novel proteoglycan synthesized and secreted by chondrocytes of the superficial zone of articular cartilage. *Arch Biochem Biophys,* 311**,** 144-52.

SCHUSTER, S. C. 2008. Next-generation sequencing transforms today's biology. *Nat Meth,* 5**,** 16-18.

SEKIYA, I., KOOPMAN, P., TSUJI, K., MERTIN, S., HARLEY, V., YAMADA, Y., SHINOMIYA, K., NIFUJI, A. & NODA, M. 2001. Dexamethasone enhances SOX9 expression in chondrocytes. *J Endocrinol,* 169**,** 573-9.

SEO, H.-S. & SERRA, R. 2007. Deletion of Tgfbr2 in Prx1-cre expressing mesenchyme results in defects in development of the long bones and joints. *Developmental Biology,* 310**,** 304-316.

SEOL, D., MCCABE, D. J., CHOE, H., ZHENG, H., YU, Y., JANG, K., WALTER, M. W., LEHMAN, A. D., DING, L., BUCKWALTER, J. A. & MARTIN, J. A. 2012. Chondrogenic progenitor cells respond to cartilage injury. *Arthritis & Rheumatism,* 64**,** 3626-3637.

SERRA, R. & CHANG, C. 2003. TGF-β signaling in human skeletal and patterning disorders. *Birth Defects Research Part C: Embryo Today: Reviews,* 69**,** 333-351.

SETHE, S., SCUTT, A. & STOLZING, A. 2006. Aging of mesenchymal stem cells. *Ageing Research Reviews,* 5**,** 91-116.

SETTLE, S., H, JR., ROUNTREE, R. B., SINHA, A., THACKER, A., HIGGINS, K. & KINGSLEY, D. M. 2003. Multiple joint and skeletal patterning defects caused by single and double mutations in the mouse Gdf6 and Gdf5 genes. *Developmental Biology,* 254**,** 116-130.

SHAPIRO, F., KOIDE, S. & GLIMCHER, M. J. 1993. Cell origin and differentiation in the repair of full-thickness defects of articular cartilage. *J Bone Joint Surg Am,* 75**,** 532-53.

SHARIF, M., GEORGE, E. & DIEPPE, P. A. 1995. Correlation between synovial fluid markers of cartilage and bone turnover and scintigraphic scan abnormalities in osteoarthritis of the knee. *Arthritis Rheum,* 38**,** 78-81.

SHI, Y. 2009. Induced Pluripotent Stem Cells as a Model for Accelerated Patient and Disease-specific Drug Discovery. *Current Molecular Pharmacology,* 2**,** 15-18.

SHINTANI, N. & HUNZIKER, E. B. 2011. Differential effects of dexamethasone on the chondrogenesis of mesenchymal stromal cells: influence of microenvironment, tissue origin and growth factor. *Eur Cell Mater,* 22**,** 302-19; discussion 319-20.

SICZKOWSKI, M. & WATT, F. M. 1990. Subpopulations of chondrocytes from different zones of pig articular cartilage. Isolation, growth and proteoglycan synthesis in culture. *Journal of Cell Science,* 97**,** 349-360.

SIMMONS, P. J. & TOROK-STORB, B. 1991. Identification of stromal cell precursors in human bone marrow by a novel monoclonal antibody, STRO-1. *Blood,* 78**,** 55-62.

SIRKO, S., VON HOLST, A., WIZENMANN, A., GÖTZ, M. & FAISSNER, A. 2007. Chondroitin sulfate glycosaminoglycans control proliferation, radial glia cell differentiation and neurogenesis in neural stem/progenitor cells. *Development,* 134**,** 2727-2738.

SMITH, M. D., TRIANTAFILLOU, S., PARKER, A., YOUSSEF, P. P. & COLEMAN, M. 1997. Synovial membrane inflammation and cytokine production in patients with early osteoarthritis. *J Rheumatol,* 24**,** 365-71.

SMYTH, P. A., RIFKIN, R. E., JACKSON, R. L. & HANSON, R. R. 2012. A Surface Roughness Comparison of Cartilage in Different Types of Synovial Joints. *Journal of Biomechanical Engineering,* 134**,** 021006-021011.

SOFAT, N., ROBERTSON, S. D., HERMANSSON, M., JONES, J., MITCHELL, P. & WAIT, R. 2012. Tenascin-C fragments are endogenous inducers of cartilage matrix degradation. *Rheumatol Int,* 32**,** 2809-17.

SONESON, C. & DELORENZI, M. 2013. A comparison of methods for differential expression analysis of RNA-seq data. *BMC Bioinformatics,* 14**,** 91.

SPAGNOLI, A., O'REAR, L., CHANDLER, R. L., GRANERO-MOLTO, F., MORTLOCK, D. P., GORSKA, A. E., WEIS, J. A., LONGOBARDI, L., CHYTIL, A., SHIMER, K. & MOSES, H. L. 2007. TGF-β signaling is essential for joint morphogenesis. *The Journal of Cell Biology,* 177**,** 1105-1117.

SPRING, J., BECK, K. & CHIQUET-EHRISMANN, R. 1989. Two contrary functions of tenascin: dissection of the active sites by recombinant tenascin fragments. *Cell,* 59**,** 325-34.

STEADMAN, J. R., BRIGGS, K. K., RODRIGO, J. J., KOCHER, M. S., GILL, T. J. & RODKEY, W. G. 2003. Outcomes of microfracture for traumatic chondral defects of the knee: average 11-year follow-up. *Arthroscopy,* 19**,** 477-84.

STENDERUP, K., JUSTESEN, J., CLAUSEN, C. & KASSEM, M. 2003. Aging is associated with decreased maximal life span and accelerated senescence of bone marrow stromal cells. *Bone,* 33**,** 919-926.

STOCKWELL, R. A. 1978. Chondrocytes. *J Clin Pathol Suppl,* 12**,** 7-13.

STODDART, M. J., GRAD, S., EGLIN, D. & ALINI, M. 2009. Cells and biomaterials in cartilage tissue engineering. *Regen Med,* 4**,** 81-98.

STORM, E. E. & KINGSLEY, D. M. 1999. GDF5 Coordinates Bone and Joint Formation during Digit Development. *Developmental Biology,* 209**,** 11-27.

STRUH, S. 2013. *Arthroscopy Association of North America* [Online]. New York. Available: http://www.shouldersandknees.com/articular-cartilage-defect.html [Accessed 08/07/2013 2013].

SUN, Y., POLLARD, S., CONTI, L., TOSELLI, M., BIELLA, G., PARKIN, G., WILLATT, L., FALK, A., CATTANEO, E. & SMITH, A. 2008. Long-term tripotent differentiation capacity of human neural stem (NS) cells in adherent culture. *Mol Cell Neurosci,* 38**,** 245-58.

SUZAWA, M., TAKADA, I., YANAGISAWA, J., OHTAKE, F., OGAWA, S., YAMAUCHI, T., KADOWAKI, T., TAKEUCHI, Y., SHIBUYA, H., GOTOH, Y., MATSUMOTO, K. & KATO, S. 2003. Cytokines suppress adipogenesis and PPAR-[gamma] function through the TAK1/TAB1/NIK cascade. *Nat Cell Biol,* 5**,** 224-230.

TACHIKUI, H., KUROSAWA, N., KADOMATSU, K. & MURAMATSU, T. 1999. Genomic organization and promoter activity of embigin, a member of the immunoglobulin superfamily. *Gene,* 240**,** 325-332.

TAKASHIMA, S. & TSUJI, S. 2014. ST6 Beta-Galactoside Alpha-2,6-Sialyltranferase 2 (ST6GAL2). *In:* TANIGUCHI, N., HONKE, K., FUKUDA, M., NARIMATSU, H., YAMAGUCHI, Y. & ANGATA, T. (eds.) *Handbook of Glycosyltransferases and Related Genes.* Springer Japan.

TAKECHI, M. & ITAKURA, C. 1995. Ultrastructural and histochemical studies of the epiphyseal plate in normal chicks. *Anat Rec,* 242**,** 29-39.
TEPASS, U. 2009. FERM proteins in animal morphogenesis. *Curr Opin Genet Dev,* 19**,** 357-67.
TETLOW, L. C., ADLAM, D. J. & WOOLLEY, D. E. 2001. Matrix metalloproteinase and proinflammatory cytokine production by chondrocytes of human osteoarthritic cartilage: associations with degenerative changes. *Arthritis Rheum,* 44**,** 585-94.
THOMAS, S. K., MESSAM, C. A., SPENGLER, B. A., BIEDLER, J. L. & ROSS, R. A. 2004. Nestin is a potential mediator of malignancy in human neuroblastoma cells. *J Biol Chem,* 279**,** 27994-9.
THONAR, E. J., BUCKWALTER, J. A. & KUETTNER, K. E. 1986. Maturation-related differences in the structure and composition of proteoglycans synthesized by chondrocytes from bovine articular cartilage. *J Biol Chem,* 261**,** 2467-74.
TIKU, M. L., GUPTA, S. & DESHMUKH, D. R. 1999. Aggrecan degradation in chondrocytes is mediated by reactive oxygen species and protected by antioxidants. *Free Radical Research,* 30**,** 395-405.
TIKU, M. L., SHAH, R. & ALLISON, G. T. 2000. Evidence Linking Chondrocyte Lipid Peroxidation to Cartilage Matrix Protein Degradation. *Journal of Biological Chemistry,* 275**,** 20069-20076.
TORTORA, G. J. & GRABOWSKI, S. R. 1996. *Principles of anatomy and physiology,* New York, Harper Collins.
TRAPNELL, C., HENDRICKSON, D. G., SAUVAGEAU, M., GOFF, L., RINN, J. L. & PACHTER, L. 2013. Differential analysis of gene regulation at transcript resolution with RNA-seq. *Nat Biotech,* 31**,** 46-53.
TSENG, S., REDDI, A. H. & DI CESARE, P. E. 2009. Cartilage Oligomeric Matrix Protein (COMP): A Biomarker of Arthritis. *Biomark Insights,* 4**,** 33-44.
UCHIYAMA, Y., SAKAGUCHI, M., TERABAYASHI, T., INENAGA, T., INOUE, S., KOBAYASHI, C., OSHIMA, N., KIYONARI, H., NAKAGATA, N., SATO, Y., SEKIGUCHI, K., MIKI, H., ARAKI, E., FUJIMURA, S., TANAKA, S. S. & NISHINAKAMURA, R. 2010. Kif26b, a kinesin family gene, regulates adhesion of the embryonic kidney mesenchyme. *Proceedings of the National Academy of Sciences,* 107**,** 9240-9245.
VAN ASSCHE, D., STAES, F., VAN CASPEL, D., VANLAUWE, J., BELLEMANS, J., SARIS, D. B. & LUYTEN, F. P. 2010. Autologous chondrocyte implantation versus microfracture for knee cartilage injury: a prospective randomized trial, with 2-year follow-up. *Knee Surg Sports Traumatol Arthrosc,* 18**,** 486-95.
VAN DEN BERG, W. B. 1995. Growth factors in experimental osteoarthritis: transforming growth factor beta pathogenic? *J Rheumatol Suppl,* 43**,** 143-5.
VAN DER KRAAN, P. M., BUMA, P., VAN KUPPEVELT, T. & VAN DEN BERG, W. B. 2002. Interaction of chondrocytes, extracellular matrix and growth factors: relevance for articular cartilage tissue engineering. *Osteoarthritis and Cartilage,* 10**,** 631-637.
VAN DER KRAAN, P. M., STOOP, R., MEIJERS, T. H., POOLE, A. R. & VAN DEN BERG, W. B. 2001. Expression of type X collagen in young and old C57Bl/6 and Balb/c mice. Relation with articular cartilage degeneration. *Osteoarthritis and Cartilage,* 9**,** 92-100.
VAN OSCH, G. J., VAN DER VEEN, S. W., BUMA, P. & VERWOERD-VERHOEF, H. L. 1998. Effect of transforming growth factor-beta on proteoglycan

synthesis by chondrocytes in relation to differentiation stage and the presence of pericellular matrix. *Matrix Biol,* 17**,** 413-24.
VANDERREST, M. & GARRONE, R. 1991. Collagen family of proteins. *Faseb Journal,* 5**,** 2814-2823.
VAUGHAN-THOMAS, A., YOUNG, R. D., PHILLIPS, A. C. & DUANCE, V. C. 2001. Characterization of type XI collagen-glycosaminoglycan interactions. *J Biol Chem,* 276**,** 5303-9.
VISNA, P., PASA, L., CIZMAR, I., HART, R. & HOCH, J. 2004. Treatment of deep cartilage defects of the knee using autologous chondrograft transplantation and by abrasive techniques--a randomized controlled study. *Acta Chir Belg,* 104**,** 709-14.
VON DER MARK, K., VON DER MARK, H. & GAY, S. 1976. Study of differential collagen synthesis during development of the chick embryo by immunofluorescence: II. Localization of type I and type II collagen during long bone development. *Developmental Biology,* 53**,** 153-170.
WAGNER, W., HORN, P., CASTOLDI, M., DIEHLMANN, A., BORK, S., SAFFRICH, R., BENES, V., BLAKE, J., PFISTER, S., ECKSTEIN, V. & HO, A. D. 2008. Replicative Senescence of Mesenchymal Stem Cells: A Continuous and Organized Process. *PLoS ONE,* 3**,** e2213.
WANG, Q., ZHAO, Z.-B., WANG, G., HUI, Z., WANG, M.-H., PAN, J.-F. & ZHENG, H. 2013. High Expression of KIF26B in Breast Cancer Associates with Poor Prognosis. *PLoS ONE,* 8**,** e61640.
WANG, T., PEI, X., ZHAN, J., HU, J., YU, Y. & ZHANG, H. FERM-containing protein FRMD5 is a p120-catenin interacting protein that regulates tumor progression. *FEBS Letters,* 586**,** 3044-3050.
WANG, Z., GERSTEIN, M. & SNYDER, M. 2009. RNA-Seq: a revolutionary tool for transcriptomics. *Nat Rev Genet,* 10**,** 57-63.
WATT, F. M. & HOGAN, B. L. M. 2000. Out of Eden - Stem cells and their niches. *Science,* 287**,** 1427-1430.
WEBB, S. 2009. iPS cell technology gains momentum in drug discovery. *Nat Rev Drug Discov,* 8**,** 263-264.
WEI, L. C., SHI, M., CAO, R., CHEN, L. W. & CHAN, Y. S. 2008. Nestin small interfering RNA (siRNA) reduces cell growth in cultured astrocytoma cells. *Brain Res,* 1196**,** 103-12.
WIESE, C., ROLLETSCHEK, A., KANIA, G., BLYSZCZUK, P., TARASOV, K. V., TARASOVA, Y., WERSTO, R. P., BOHELER, K. R. & WOBUS, A. M. 2004. Nestin expression – a property of multi-lineage progenitor cells? *Cellular and Molecular Life Sciences CMLS,* 61**,** 2510-2522.
WIJERATNE, S. S. K., CUPPETT, S. L. & SCHLEGEL, V. 2005. Hydrogen Peroxide Induced Oxidative Stress Damage and Antioxidant Enzyme Response in Caco-2 Human Colon Cells. *Journal of Agricultural and Food Chemistry,* 53**,** 8768-8774.
WILLIAMS, G. M., KLISCH, S. M. & SAH, R. L. 2008. Bioengineering cartilage growth, maturation, and form. *Pediatr Res,* 63**,** 527-34.
WILLIAMS, R., KHAN, I. M., RICHARDSON, K., NELSON, L., MCCARTHY, H. E., ANALBELSI, T., SINGHRAO, S. K., DOWTHWAITE, G. P., JONES, R. E., BAIRD, D. M., LEWIS, H., ROBERTS, S., SHAW, H. M., DUDHIA, J., FAIRCLOUGH, J., BRIGGS, T. & ARCHER, C. W. 2010. Identification and clonal characterisation of a progenitor cell sub-population in normal human articular cartilage. *PLoS One,* 5**,** e13246.
WINTER, A., BREIT, S., PARSCH, D., BENZ, K., STECK, E., HAUNER, H., WEBER, R. M., EWERBECK, V. & RICHTER, W. 2003. Cartilage-like gene expression in

differentiated human stem cell spheroids: a comparison of bone marrow-derived and adipose tissue-derived stromal cells. *Arthritis Rheum,* 48**,** 418-29.

WOODS, V. L., SCHRECK, P. J., GESINK, D. S., PACHECO, H. O., AMIEL, D., AKESON, W. H. & LOTZ, M. 1994. Integrin expression by human articular chondrocytes. *Arthritis & Rheumatism,* 37**,** 537-544.

WOOLEY, P. H., GRIMM, M. J. & RADIN, E. L. 2005. The structure and Function of Joints. *In:* KOOPMAN, W. J. & MORELAND, L. W. (eds.) *Arthritis & Aliied Conditions.* Philadelphia: Lippincott Williams & Wilkins.

WOTTON, S. F., DUANCE, V. C. & FRYER, P. R. 1988. Type IX collagen: a possible function in articular cartilage. *FEBS Lett,* 234**,** 79-82.

WU, J., KIRK, T. & ZHENG, M. 2008. Study of the collagen structure in the superficial zone and physiological state of articular cartilage using a 3D confocal imaging technique. *Journal of Orthopaedic Surgery and Research,* 3**,** 1-11.

YAMADA, K., HEALEY, R., AMIEL, D., LOTZ, M. & COUTTS, R. 2002. Subchondral bone of the human knee joint in aging and osteoarthritis. *Osteoarthritis and Cartilage,* 10**,** 360-9.

YAMANAKA, S. 2007. Strategies and new developments in the generation of patient-specific pluripotent stem cells. *Cell stem cell,* 1**,** 39-49.

YANG, X. H., WU, Q. L., YU, X. B., XU, C. X., MA, B. F., ZHANG, X. M., LI, S. N., LAHN, B. T. & XIANG, A. P. 2008. Nestin expression in different tumours and its relevance to malignant grade. *J Clin Pathol,* 61**,** 467-73.

YEN, Y. M., CASCIO, B., O'BRIEN, L., STALZER, S., MILLETT, P. J. & STEADMAN, J. R. 2008. Treatment of osteoarthritis of the knee with microfracture and rehabilitation. *Med Sci Sports Exerc,* 40**,** 200-5.

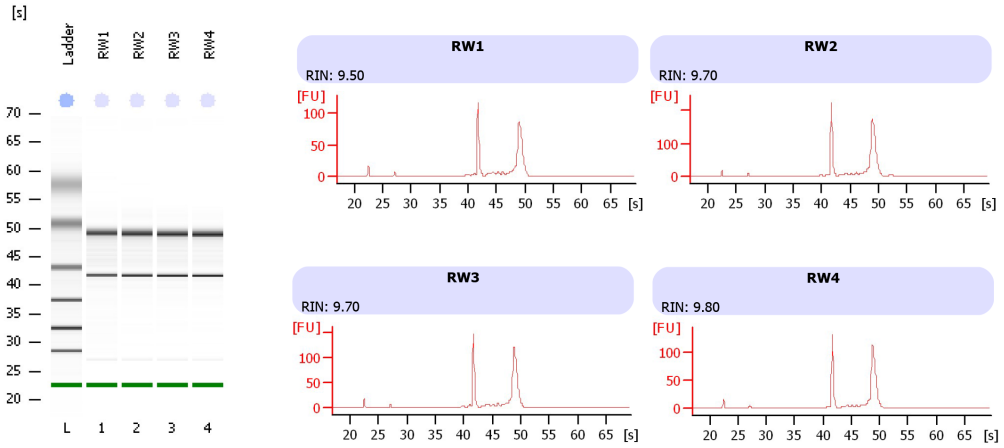
YOO, J. U., BARTHEL, T. S., NISHIMURA, K., SOLCHAGA, L., CAPLAN, A. I., GOLDBERG, V. M. & JOHNSTONE, B. 1998. The chondrogenic potential of human bone-marrow-derived mesenchymal progenitor cells. *J Bone Joint Surg Am,* 80**,** 1745-57.

ZHANG, Z. H., JHAVERI, D. J., MARSHALL, V. M., BAUER, D. C., EDSON, J., NARAYANAN, R. K., ROBINSON, G. J., LUNDBERG, A. E., BARTLETT, P. F., WRAY, N. R. & ZHAO, Q.-Y. 2014. A Comparative Study of Techniques for Differential Expression Analysis on RNA-Seq Data. *PLoS ONE,* 9**,** e103207.

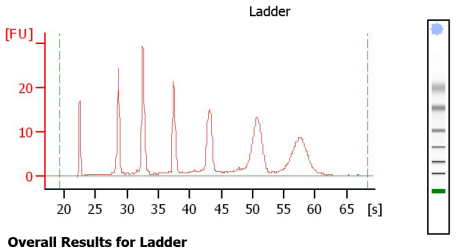
ZUK, P. A., ZHU, M., ASHJIAN, P., DE UGARTE, D. A., HUANG, J. I., MIZUNO, H., ALFONSO, Z. C., FRASER, J. K., BENHAIM, P. & HEDRICK, M. H. 2002. Human Adipose Tissue Is a Source of Multipotent Stem Cells. *Molecular Biology of the Cell,* 13**,** 4279-4295.

CHAPTER 9:

APPENDICES

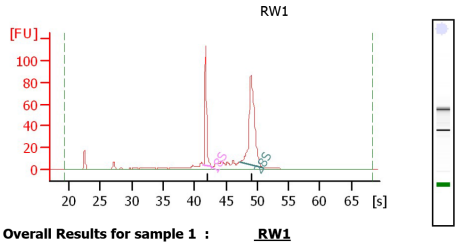


Electropherogram Summary



Overall Results for Ladder

RNA Area:	282.4
RNA Concentration:	150 ng/µl
Result Flagging Color:	
Result Flagging Label:	All Other Samples

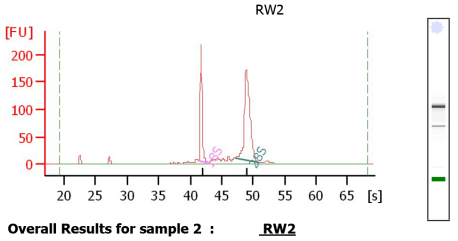


Overall Results for sample 1 : RW1

RNA Area:	416.8
RNA Concentration:	221 ng/µl
rRNA Ratio [28s / 18s]:	1.9
RNA Integrity Number (RIN):	9.5 (B.02.07)
Result Flagging Color:	
Result Flagging Label:	RIN: 9.50

Fragment table for sample 1 : RW1

Name	Start Time [s]	End Time [s]	Area	% of total Area
18S	41.43	42.72	92.7	22.2
28S	47.18	51.05	172.3	41.3

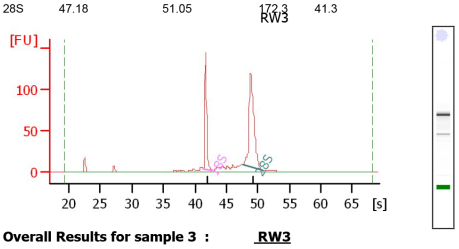


Overall Results for sample 2 : RW2

RNA Area:	743.4
RNA Concentration:	395 ng/µl
rRNA Ratio [28s / 18s]:	1.8
RNA Integrity Number (RIN):	9.7 (B.02.07)
Result Flagging Color:	
Result Flagging Label:	RIN: 9.70

Fragment table for sample 2 : RW2

Name	Start Time [s]	End Time [s]	Area	% of total Area
18S	41.39	42.68	188.4	25.3
28S	47.18	50.93	347.9	46.8

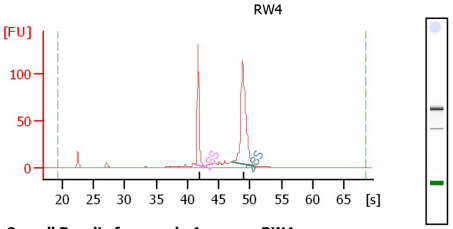


Overall Results for sample 3 : RW3

RNA Area:	492.0
RNA Concentration:	261 ng/µl
rRNA Ratio [28s / 18s]:	1.8
RNA Integrity Number (RIN):	9.7 (B.02.07)
Result Flagging Color:	
Result Flagging Label:	RIN: 9.70

Fragment table for sample 3 : RW3

Name	Start Time [s]	End Time [s]	Area	% of total Area
18S	41.34	42.73	121.2	24.6
28S	47.57	50.84	213.3	43.4



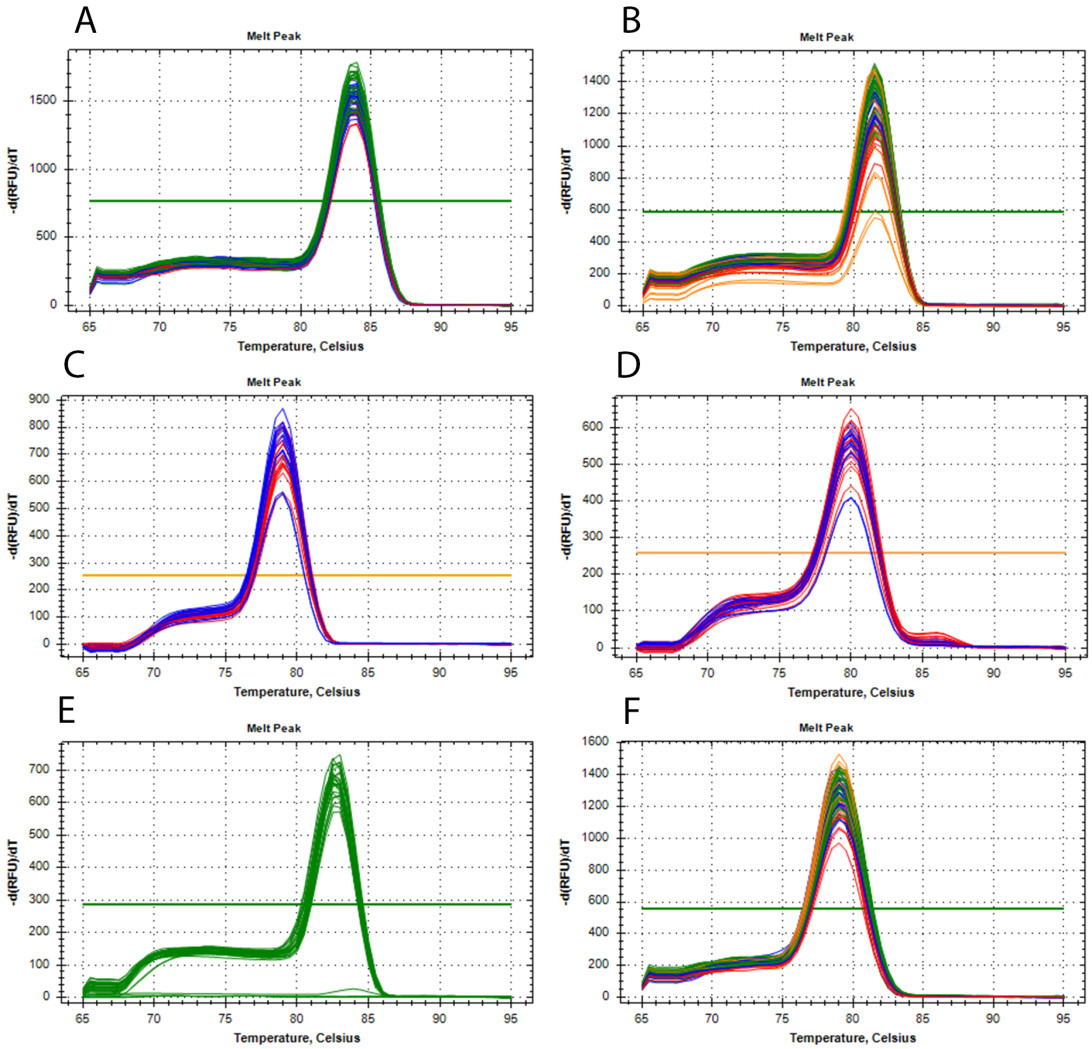
Overall Results for sample 4 : RW4

RNA Area:	429.2
RNA Concentration:	228 ng/µl
rRNA Ratio [28s / 18s]:	1.9
RNA Integrity Number (RIN):	9.8 (B.02.07)
Result Flagging Color:	
Result Flagging Label:	RIN: 9.80

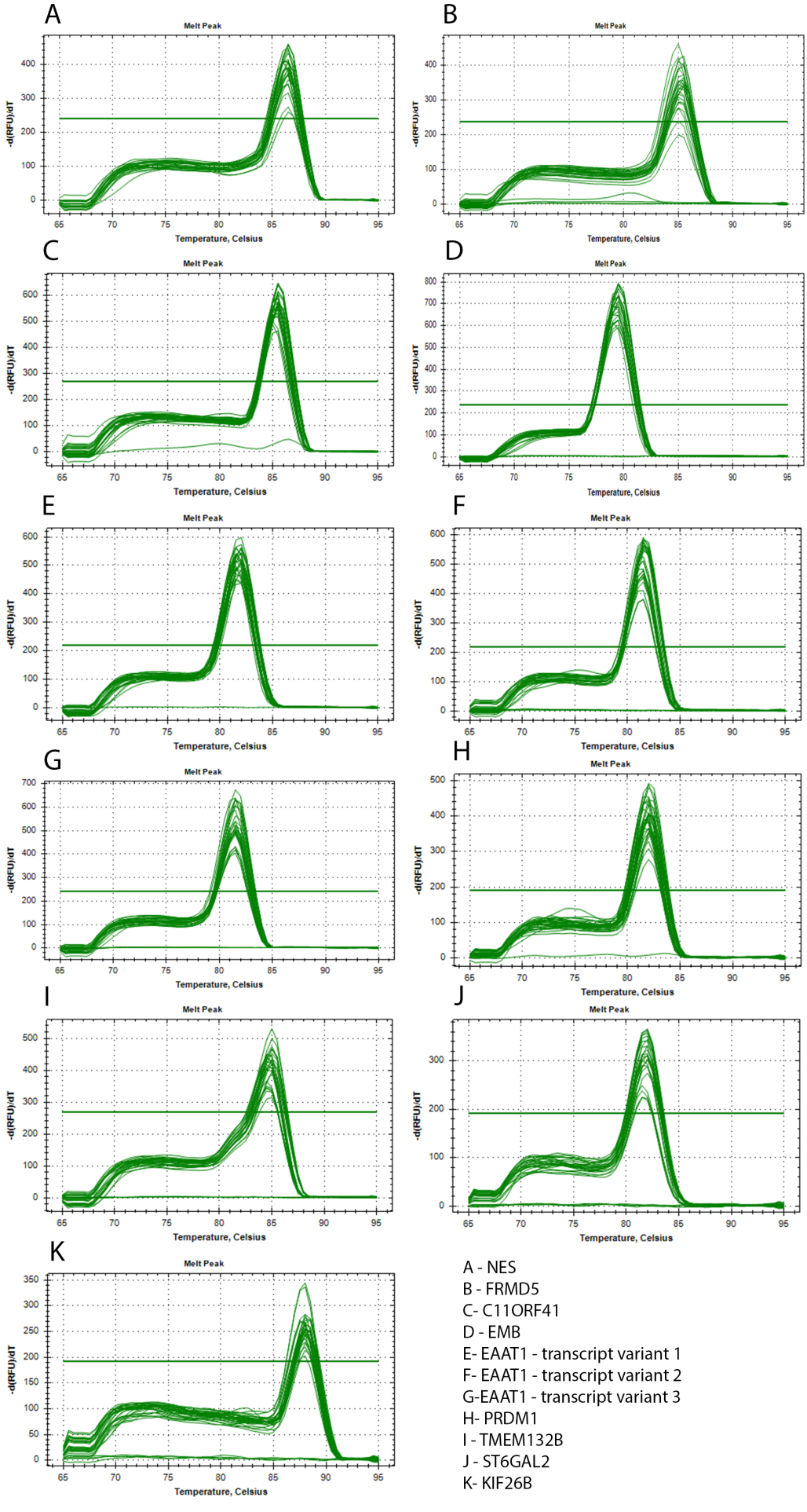
Fragment table for sample 4 : RW4

Name	Start Time [s]	End Time [s]	Area	% of total Area
18S	41.37	42.72	109.6	25.5
28S	47.04	50.96	208.9	48.7

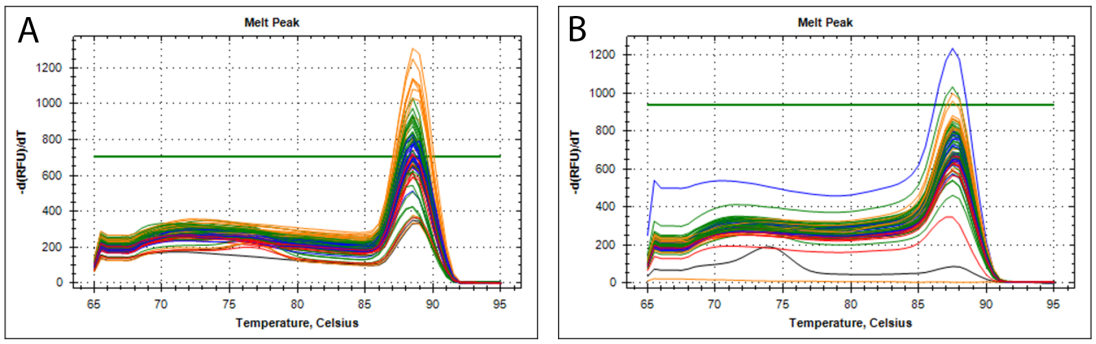
Figure S1.1 – NGS – Bio-analyser data



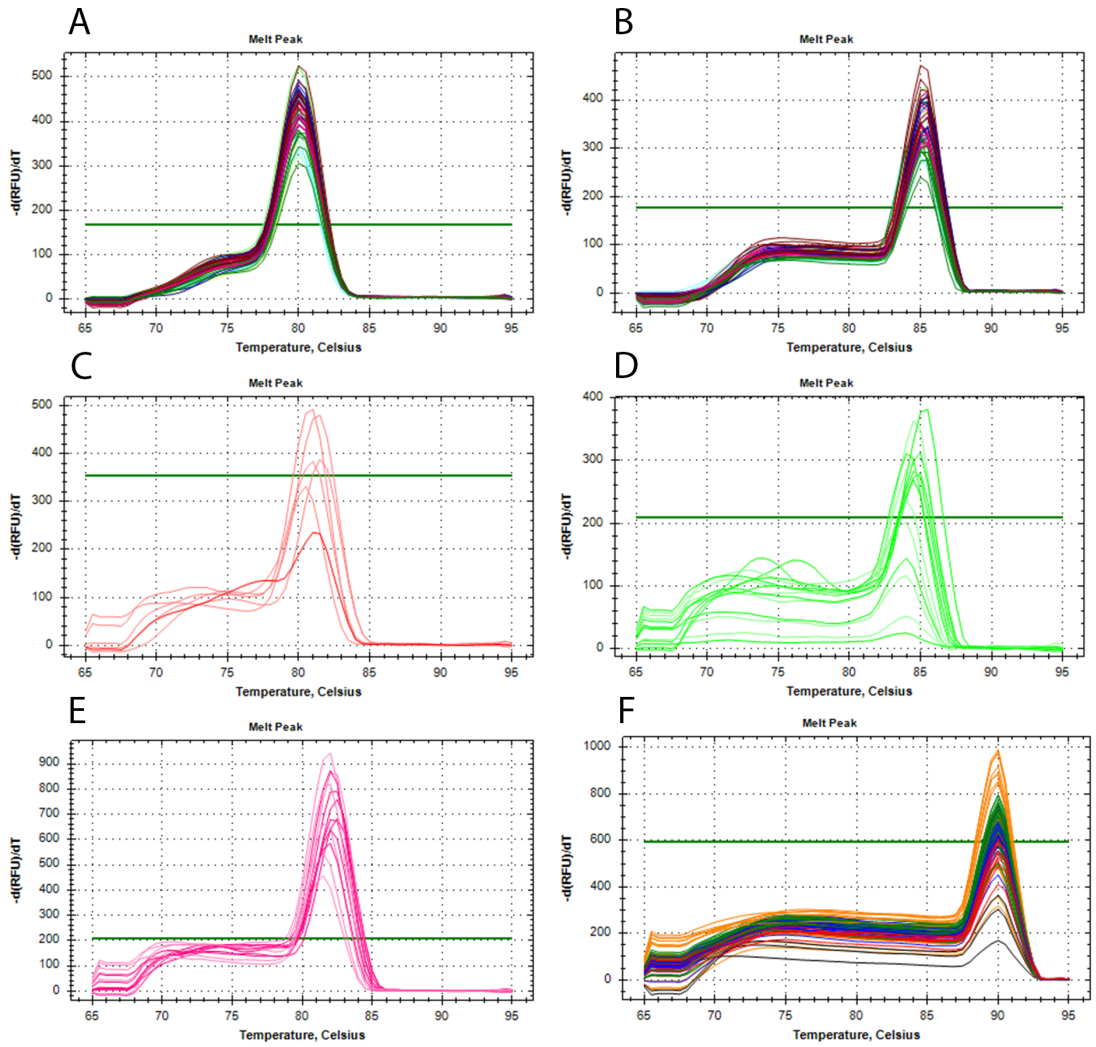
A- RPS18
B- B2M
C- HRPT1
D- PMP31 (RP11)
E- RPL13a
F- ACTB



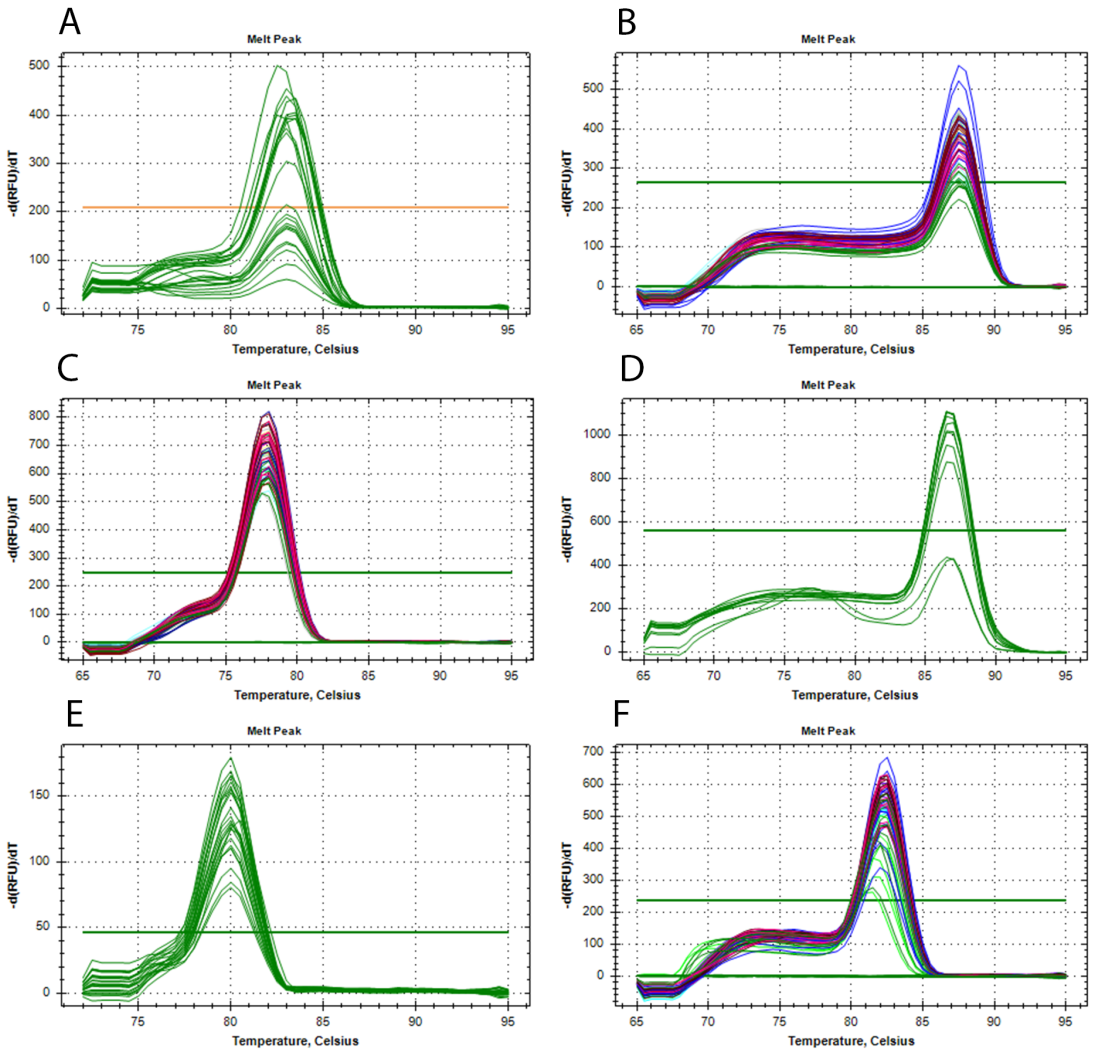
A - NES
B - FRMD5
C- C11ORF41
D - EMB
E- EAAT1 - transcript variant 1
F- EAAT1 - transcript variant 2
G-EAAT1 - transcript variant 3
H- PRDM1
I - TMEM132B
J - ST6GAL2
K- KIF26B



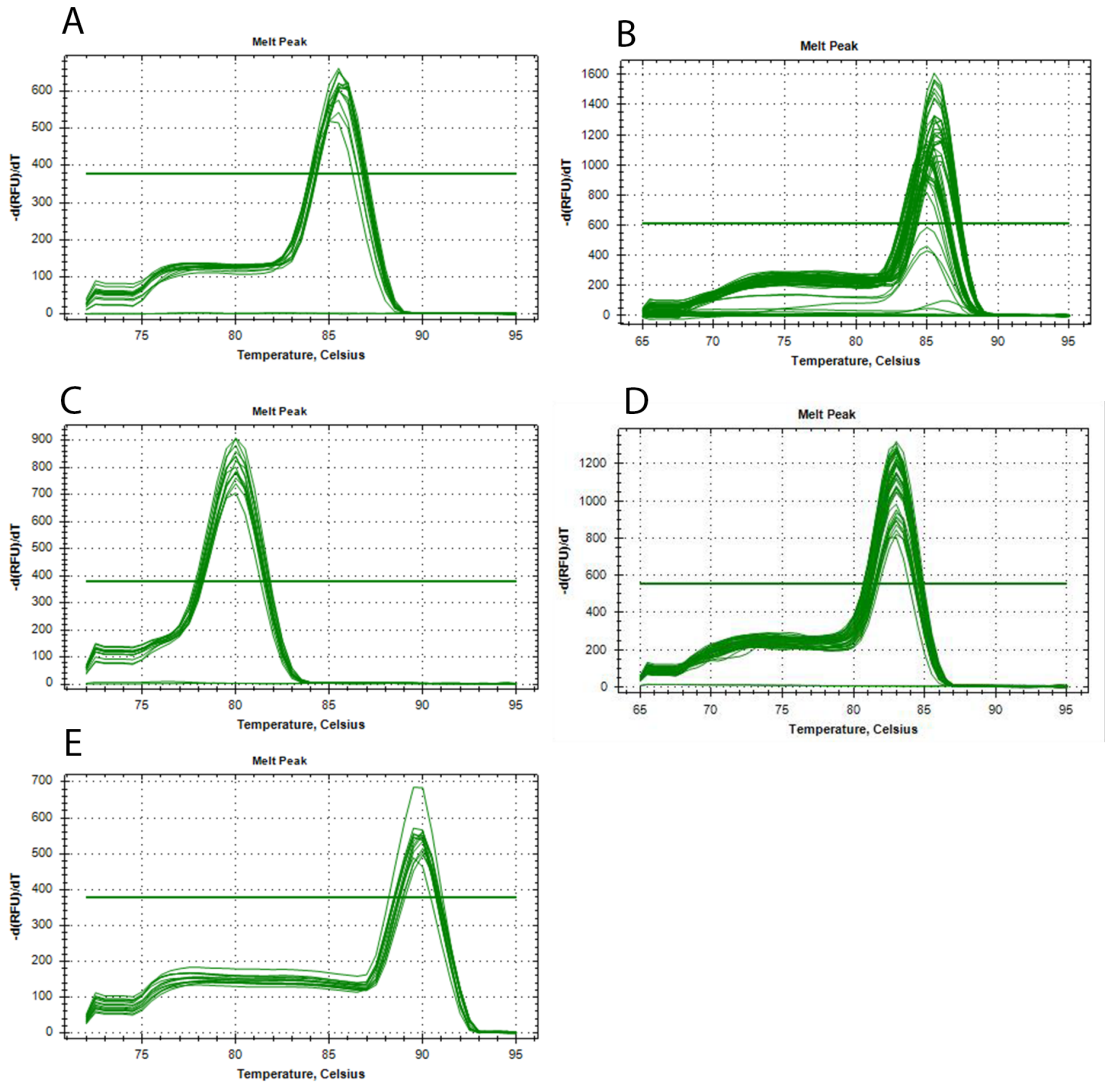
A- NOTCH-1
B- JAG-1



A- ACAN
B- COL2a1
C- COL9a1
D- COL11a1
E- PRG4
F- SOX9



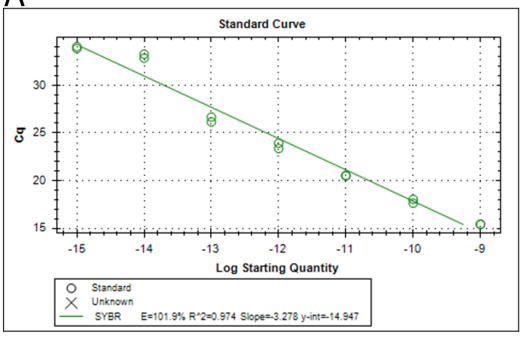
A- ALPL
B- COL1a1
C- COL10a1
D- BGLAP
E- RUNX2
F- MMP13



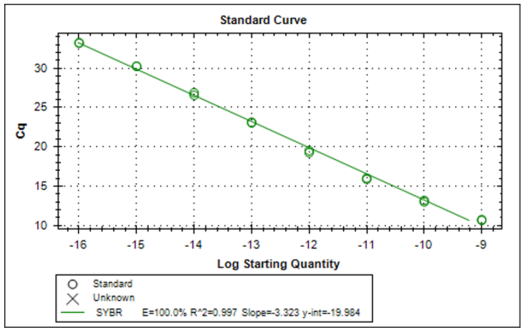
A- BAS
B- MTC1
C- MTC2
D- MTC3
E- MTC4

Figure S1.2 – qPCR melt curves

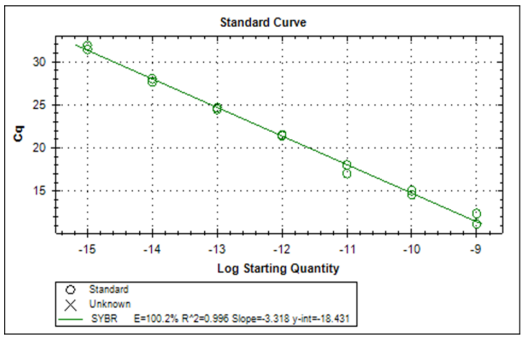
A



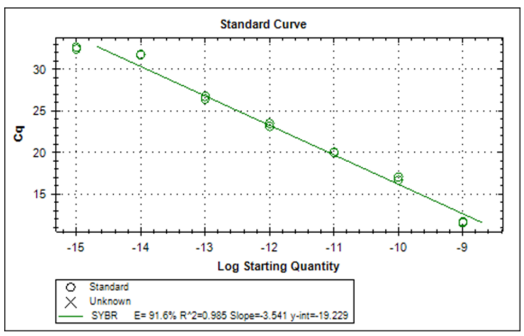
B



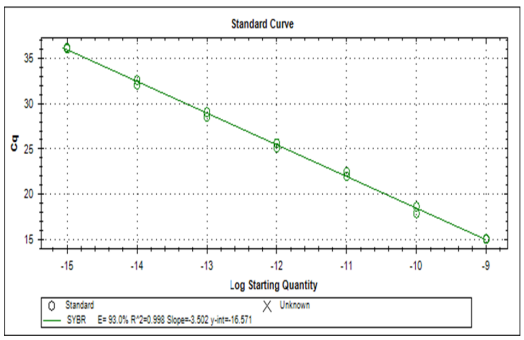
C



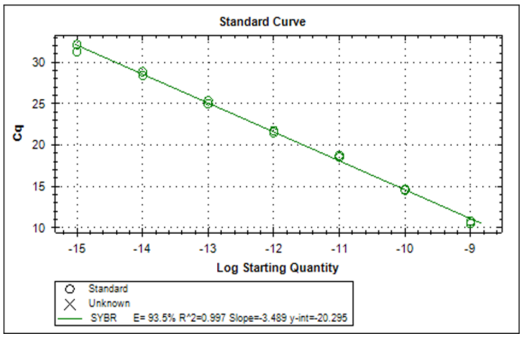
D



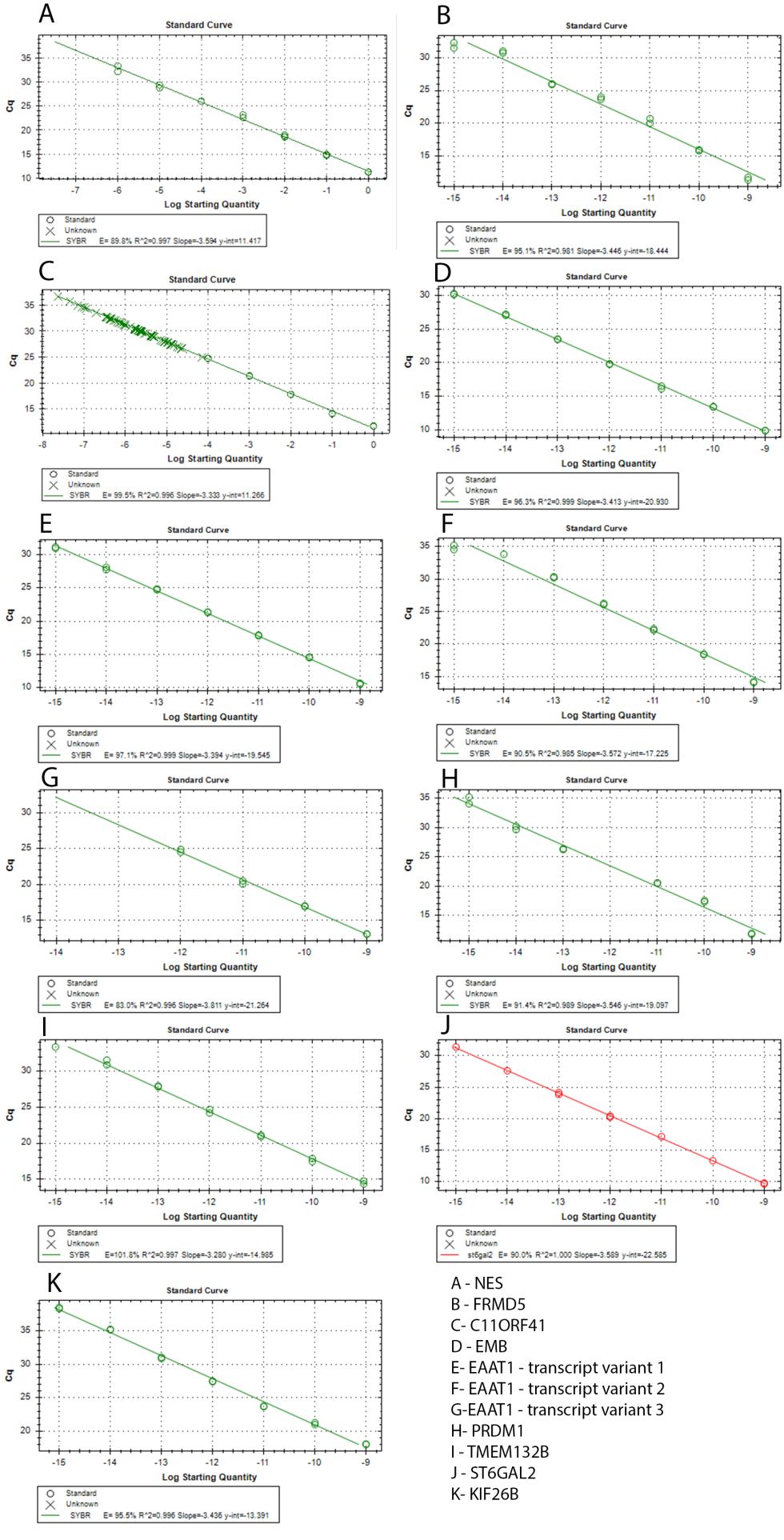
E



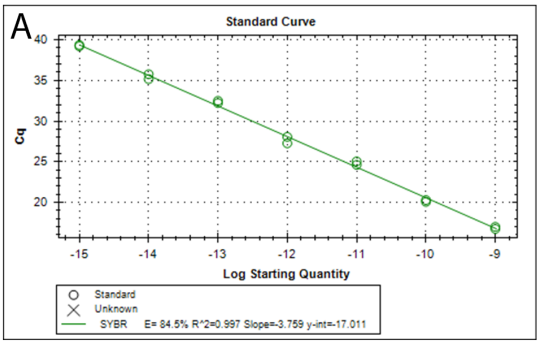
F

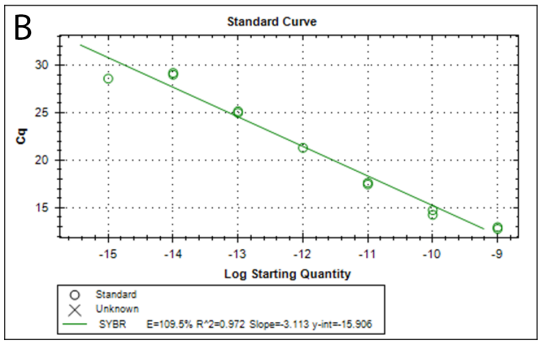


A- RPS18
B- B2M
C- HRPT1
D- PMP31 (RP11)
E- RPL13a
F- ACTB

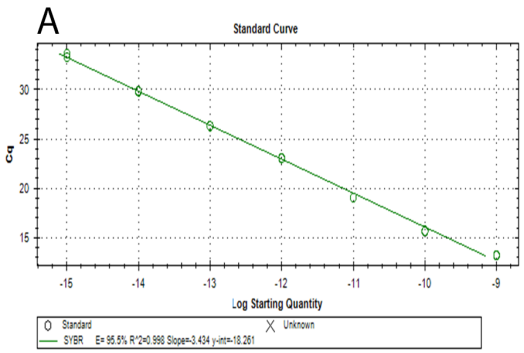


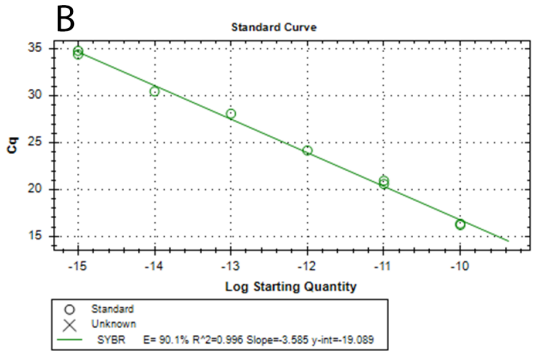
A - NES
B - FRMD5
C- C11ORF41
D - EMB
E- EAAT1 - transcript variant 1
F- EAAT1 - transcript variant 2
G-EAAT1 - transcript variant 3
H- PRDM1
I - TMEM132B
J - ST6GAL2
K- KIF26B

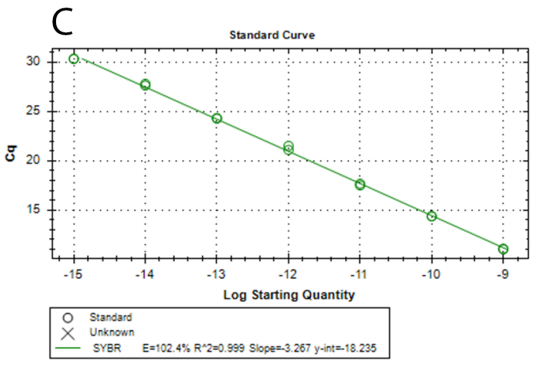


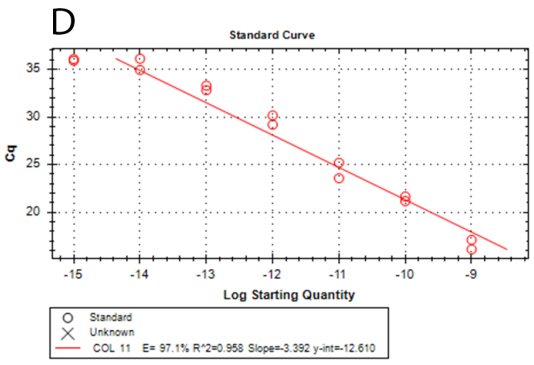


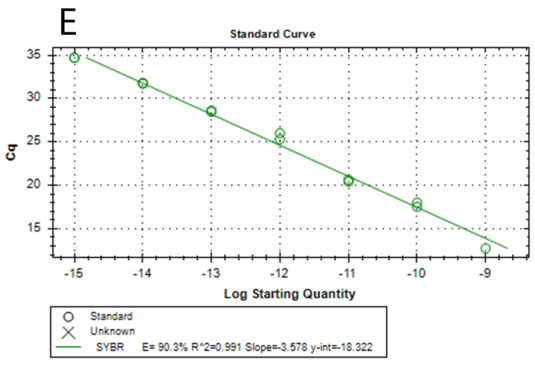
A- NOTCH-1
B- JAG-1

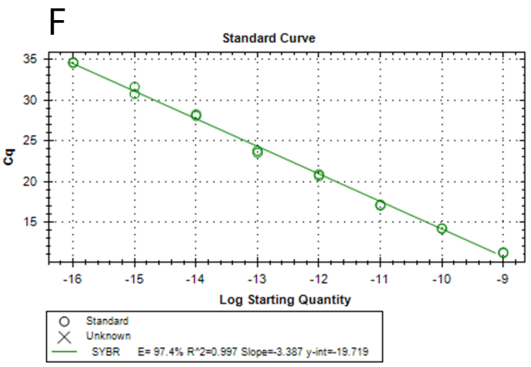




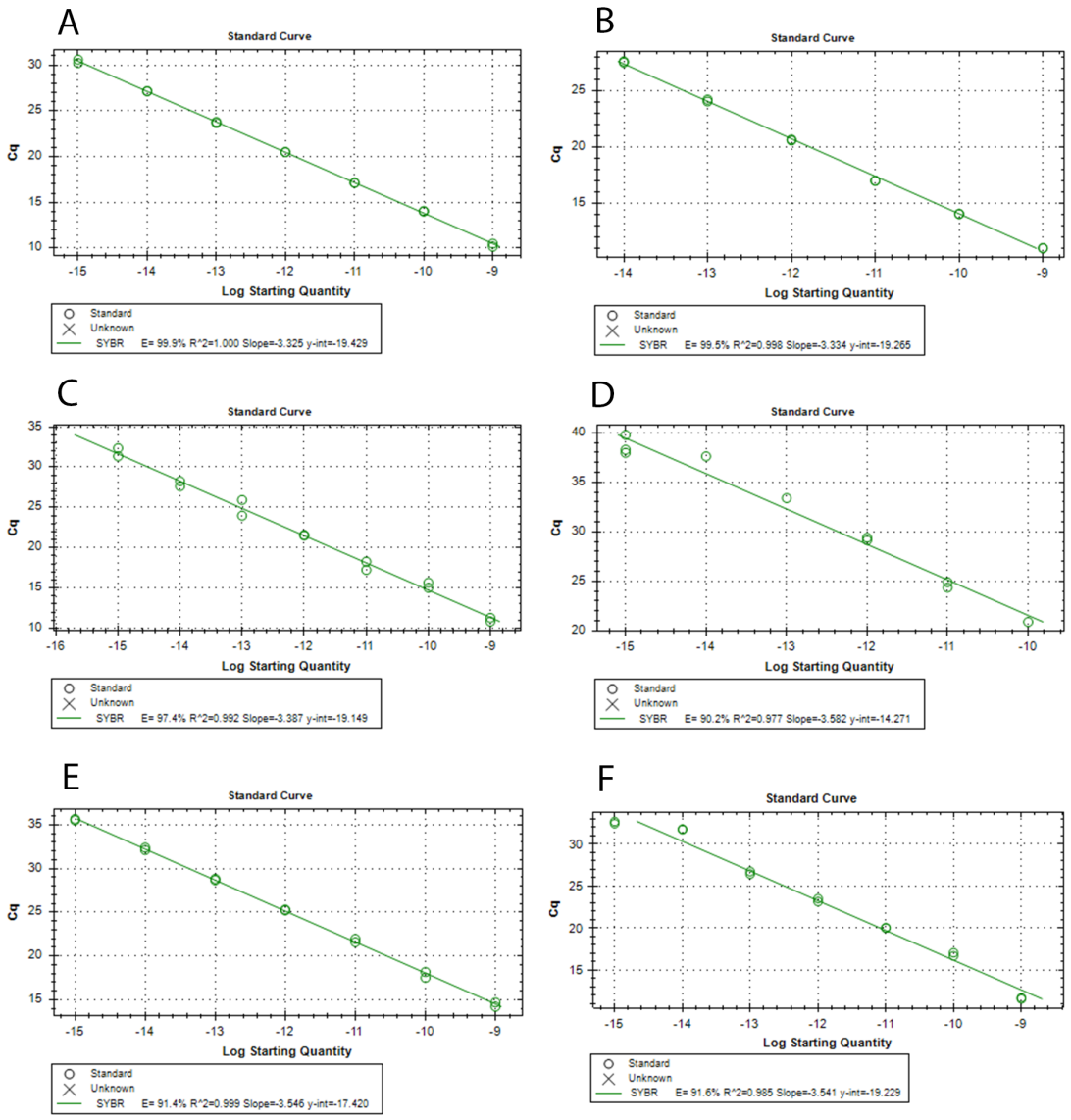








A- ACAN
B- COL2A1
C- COL9A1
D- COL11A2
E- PRG4
F- SOX9



A- ALPL
B- COL1A1
C- COL10A1
D- BGLAP
E- RUNX2
F- MMP13

Figure S1.3 – qPCR standard curves

Gene symbol	QPCR efficiency	R^2 value
NES	97.1%	0.999
FRMD5	95.1%	0.981
C11ORF41	99.5%	0.996
EMB	96.3%	0.999
EAAT1-TV1	97.1%	0.999
EAAT1-TV2	90.5%	0.985
EAAT1-TV3	83.0%	0.996
PRDM1	91.4%	0.989
ST6GAL2	101.8%	0.997
TMEM132B	90.0%	1.000
KIF26B	95.5%	0.996
ACAN	95.5%	0.998
COL2A1	99.1%	0.996
COL9A1	102.4%	0.999
COL11A2	97.1%	0.958
PRG4	90.3%	0.991
SOX9	97.4%	0.997
NOTCH1	84.5%	0.997
JAG1	109.5%	0.972
ALPL	99.9%	1.000
COL1A1	99.5%	0.998
COLXA1	97.4%	0.992
BGLAP	90.2%	0.977
RUNX2	91.4%	0.999
MMP13	91.6%	0.985
RPS18	101.9%	0.974
B2M	100.0%	0.997
HRPT1	100.2%	0.996
PMP31 (RP11)	91.6%	0.985
RPL13a	93.0	0.998
ACTB	93.5	0.997

Table S1.1 – qPCR efficiency and R^2 values